Synthesis of azobenzene glycoconjugates to control biological function

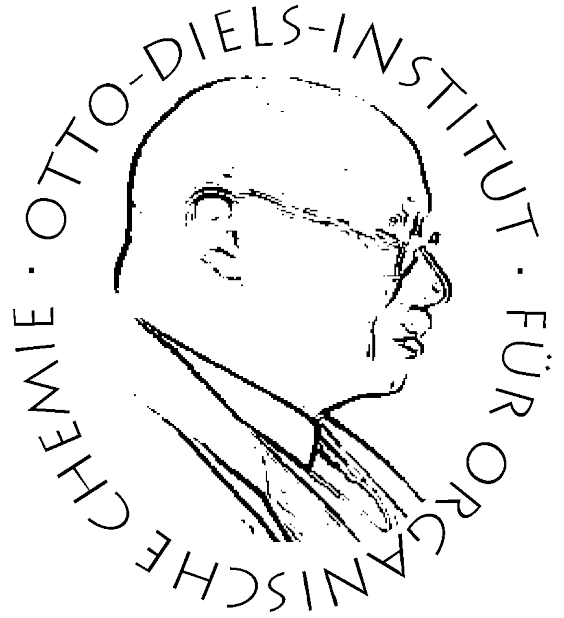

Dissertation

zur Erlangung des Doktorgrades
der Mathematisch-Naturwissenschaftlichen-Fakultät
der Christian-Albrechts-Universität
zu Kiel

vorgelegt von

Anne Heitmann

Otto Diels-Institut für Organische Chemie
Kiel 2016

Referentin: Prof. Dr. Thisbe K. Lindhorst
Koreferent: Prof. Dr. Frank D. Sönnichsen

Tag der mündlichen Prüfung: 07.11.2016
Zum Druck genehmigt: 06.12.2016

gez. Prof. Dr. N. Oppelt, Dekanin

Die vorliegende Arbeit wurde unter Anleitung von

Prof. Dr. Thisbe K. Lindhorst

am Otto Diels-Institut für Organische Chemie

der Christian-Albrechts-Universität zu Kiel

im Zeitraum von

April 2012 bis September 2016 angefertigt.

Hiermit erkläre ich, Anne Müller, an Eides statt, dass ich die vorliegende Arbeit selbstständig und nur mit den angegebenen Quellen und Hilfsmitteln angefertigt habe. Inhalt und Form dieser Arbeit sind eigenständig erarbeitet und verfasst worden. Die Arbeit enstand unter der Einhaltung der Regeln guter wissenschaftlicher Praxis der Deutschen Forschungsgemeinschaft. Teile dieser Arbeit wurden bereits wie folgt veröffentlicht:

A. Müller, H. Kobarg, V. Chandrasekaran, J. Gronow, F. D. Sönnichsen, T. K. Lindhorst, *Chem. Eur. J.* **2015**, *21*, 13723-13731.

A. Müller, T. K. Lindhorst, *Eur. J. Org. Chem.* **2016**, *2016*, 1669-1672.

L. Möckl, A. Müller, C. Bräuchle, T. K. Lindhorst, *Chem. Commun.* **2016**, *52*, 1254-1257.

Die Dissertation wird ausschließlich an dieser Stelle zur Promotion vorgelegt. Es handelt sich um meinen ersten Promotionsversuch.

Kiel, 11.09.2016

Anne Heitmann

Danksagung

An dieser Stelle möchte ich meinen besonderen Dank nachstehenden Personen entgegen bringen, ohne deren Mithilfe die Anfertigung dieser Promotionsschrift niemals zustande gekommen wäre:

Besonderer Dank gilt Frau Prof. Dr. Thisbe K. Lindhorst, meiner Doktormutter, für die Vergabe des hochinteressanten Themas, die Betreuung dieser Arbeit und die mannigfache Ideengebung. Die zahlreichen anregenden Gespräche und Diskussionen werden mir als bereichernder und konstruktiver Austausch in Erinnerung bleiben. Ich habe unsere Dialoge stets als Ermutigung und Motivation empfunden. Besonders bedanken will ich mich auch für die Freiheit und das Vertrauen, die sie mir während der gesamten Promotion gewährte, was maßgeblich zum Gelingen dieser Arbeit beitrug.

Weiterhin danke ich Herrn Prof. Dr. Frank D. Sönnichsen für die hilfsbereite und wissenschaftliche Betreuung als Zweitgutachter und Kooperationspartner. Danke für die hilfreichen Diskussionen und Ratschläge, welche zum Erstellen der Arbeit beigetragen haben.

Auch ohne meine zahlreichen Kooperationspartner: Prof. Dr. Laura Hartmann, Prof. Dr. Frank D. Sönnichsen, Claudia Fessele, Dr. Katharina Kolbe, Dr. Tobias-Elias Gloe, Dr. Leonhard Möckl, Daniel Pussack, S. Igde, Hauke Kobarg, Joana Gronow und Matthias Lipfert wären diese Ergebnisse nicht zustande gekommen. Ich bedanke mich für die immer sehr freundliche Zusammenarbeit, anregende Diskussionen und die zahlreichen Ideen.

Ich bedanke mich auch bei den wissenschaftlichen und technischen Mitarbeitern unseres Institutes Holger Franzen, Gitta Kohlmeyer-Yilmaz, Marion Höftmann, Dirk Meyer, Silke Rühl, Rolf Schmied, Andreas Wilms und Rüdiger Kargoll.

Mein besonderer Dank gilt Elwira Klima-Bartczak und Christine Haug, die immer ein offenes Ohr für mich hatten und mich bei meiner Arbeit sowohl wissenschaftlich als auch organisatorisch unterstützt haben. Ich freue mich euch kennengelernt zu haben!

Meine Arbeit wurde zudem tatkräftig von meinen Bachelorstudent(inn)en und F-Praktikantinnen Sven Ole Jaeschke, Franziska Reise, Marco Wilke, Maximiliane Landsmann, Mareike Schleupner und Carsten Wellm unterstützt. Es hat mir sehr viel Spaß gemacht mit Euch zusammenzuarbeiten. Danke!

Zudem Danke ich Dr. Katharina Kolbe und Claudia Fessele für die Hilfe und Einführung in das biologische Arbeiten im S1-Labor.

Die letzten Jahre wären ohne meine lieben Kollegen und Freunde im Arbeitskreis Lindhorst niemals so schön gewesen. Ich danke Euch für die tollen gemeinsamen Frühstücksrunden, lustige Kaffeepausen und gemeinsame Ausflüge. Auch den ehemaligen Mitarbeitern Dr. Lena Fernando und Dr. Vijayanand Chandrasekaran danke ich!

Ohne meine tollen Kollegen und Freunde aus Labor 109 Anna Ciuk, Dr. Femke Beiroth und Dr. Tobias-Elias Gloe wären die letzten Jahre niemals so schön gewesen. Ich danke Euch für eine angenehme und lustige Zeit in unserem Labor sowie für die vielen motivierenden und unterstützenden Gespräche! Ich habe die Zeit mit Euch sehr genossen.

Claudia Fessele, Dr. Katharina Kolbe und Franziska Reise danke ich ebenfalls für eure Unterstützung und Freundschaft während meiner gesamten Doktorarbeit. Nicht genug danken kann ich meiner „Herde“ und tollen Donnerstag-Treffen, die mich auch in stressigen Zeiten immer wieder aufbauten. Danke, dass ihr immer da seid!

Auch der Familie Heitmann danke ich, dass sie immer für mich da sind und ich jederzeit auf sie zählen kann.

Ein besonderer Dank gilt meinen Eltern für die Unterstützung in jeglicher Form. Ich bin froh, eine so tolle Familie zu haben, die immer an mich glaubt.

Schließlich danke ich den zwei wichtigsten Menschen in meinem Leben: meiner kleinen Schwester Luise und meinem Freund Gernot. Ihr seid immer für mich da und ohne eure Unterstützung und Liebe wäre diese Arbeit niemals zustande gekommen. Danke!

Abstract

Light as stimulus for molecular processes has been widely applied to modulate and control biological function. Light is especially well suited to trigger specific properties of biomolecules as it can be used as it is non-invasive, energy-efficient, does not leave unwanted chemical traces or side products and can be applied with high spatial and temporal resolution. In the glycosciences, light-responsive glycoconjugates represent a valuable class of biocompatible photoswitches for the control of carbohydrate-specific biological processes. They are readily accessible, can be easily modified towards a variety of functional derivatives and they and have remarkable photochromic properties.

Consequently, this thesis has focused on the synthesis and investigation of new glycoazobenzene derivatives for glycobiological studies such as the investigation of bacterial adhesion, and the control of peptide/protein structure and activity.

The first part describes the synthesis of homo- and hetero-bifunctional azobenzene derivatives to allow for site-selective cross-linking of proteins and peptides. First successful cross-linking of model peptides has demonstrated clearly that the new bifunctional azobenzene glycoconjugates favourably supplement the known photoresponsive cross-linkers for the control of protein function. They show improved water-solubility and possess suitable photochromic properties.

In the second part azobenzene glycosides were utilized for the investigation of carbohydrate-lectin interactions in the context of bacterial adhesion. In particular, the so far poorly understood influence of the configurational and conformational arrangement of ligand orientation of carbohydrate recognition was addressed in this project. For this purpose, glycoazobenzene derivatives were immobilized on quartz glass surfaces. The resulting photoresponsive glass slides, which are amenable to UV-vis spectroscopy, were investigated for their photochromic properties and tested as photoresponsive surfaces in bacterial adhesion studies. The adhesivity of these surface correlates with the orientation of the azobenzene-ligated carbohydrate ligand. Furthermore, azobenzene mannosides were applied to influence adhesion of *E. coli* bacteria to human cells. It was demonstrated that upon irradiation with light of an appropriate wavelength (UV or visible), the adhesivity of the cell surface could be switched between adhesive and less adhesive. Switching experiments were performed under static as well as under flow conditions. These are remarkable findings which raise new fundamental questions in this field of the glycosciences.

To facilitate the study of carbohydrate-lectin interactions a bead-based kit was developed. This is of interest as functionalization of magnetic PEG beads with azobenzene mannosides might allow for photoswitching the adhesivity of magnetic PEG-beads by reversible E/Z-isomerization. Photoswitchable magnetic beads can detect and eventually detach bound bacteria under the mild impact of light. They thus have the potential as diagnostic tool. However, when this chemistry was implemented, no significant difference in bacterial adhesion to glycosylated PEG beads depending on the configuration of the ligating azobenzene unit was observed. Carbohydrate-decorated PEG beads, on the other hand, could be employed to agglutinate bacteria allowing for an assay which is an alternative to the classical hemagglutination inhibition test.

To further elaborate photoswitching of carbohydrate recognition, orthogonally modified multivalent photoswitches are required. In the last part of this thesis, the first representative of a heteromultivalent glycophotoswitch was synthesised, based on a trifunctional glycoside core molecule. A detailed kinetic study has led to a comprehensive understanding of the photochromic properties of this unprecedented tool for “optoglycosciecnes”.

Kurzzusammenfassung

Licht als Stimulus für molekulare Prozesse wurde häufig verwendet, um biologische Funktionen gezielt zu beeinflussen und zu steuern, beispielsweise mittels des Schaltens bestimmter Eigenschaften von Biomolekülen. Licht ist nicht-invasiv, energieeffizient, besitzt eine hohe Zeit- sowie Ortsauflösung und hinterlässt keine unerwünschten chemischen Spuren oder Nebenprodukte. In den Glycowissenschaften stellen lichtresponsive Glycokonjugate eine nützliche Klasse biokompatibler Photoschalter für die Kontrolle Kohlenhydrat-spezifischer biologischer Prozesse dar, denn sie sind gut darstellbar, sie können leicht zu einer Vielzahl von funktionellen Derivaten modifiziert werden und besitzen äußerst vorteilhafte photochrome Eigenschaften.
Der Fokus dieser Arbeit liegt auf der Synthese und Untersuchung neuer Glycoazobenzole, welche zum Einen für glycobiologische Studien, wie beispielsweise die Untersuchung der bakteriellen Adhäsion und zum Anderen zur Steuerung der Aktivität und Struktur von Peptiden und Proteinen verwendet werden sollen.
Der erste Teil dieser Arbeit beschreibt die Synthese von homo- und heterobifunktionalen Azobenzolderivaten, welche die ortsspezifische Quervernetzung in biologisch aktiven Proteinen und Peptiden ermöglichen. Erste erfolgreiche Ligationsreaktionen mit Modellpeptiden unter wässrigen Bedingungen zeigen eindrucksvoll, dass diese neuartigen bifunktionalen Azobenzol-Glycokonjugate die Sammlung an bisher bekannten lichtresponsiven Crosslinkern zur Kontrolle der Funktion von Proteinen vorteilhaft ergänzen. Sie weisen des Weiteren verbesserte Wasserlöslichkeit und geeignete photochrome Eigenschaften auf.
Im zweiten Teil dieser Arbeit wurden Azobenzol-Glycoside für die Untersuchung von Kohlenhydrat-Lektin Wechselwirkungen im Kontext der bakteriellen Adhäsion verwendet. Der Fokus lag hierbei insbesondere auf dem bisher nur mäßig verstandenen Einfluss der konfigurativen und konformativen Ligand-Orientierung in Bezug auf die Kohlenhydrat-Erkennung. Hierfür wurden Glycoazobenzol-Derivate auf Quarzglas immobilisiert. Die somit erhaltenen photoresponsiven Glasoberflächen wurden mittels UV/Vis-Spektroskopie auf ihr Schaltverhalten untersucht und in bakteriellen Adhäsionsstudien als photoresponsive Oberflächen getestet. Es wurde gezeigt, dass die Adhäsivität der Oberfläche mit der Orientierung des immobilisierten Kohlenhydrat-Liganden korreliert. Des Weiteren wurden Azobenzol-Mannoside verwendet, um die Adhäsion von *E. coli* Bakterien an menschliche Zellen zu beeinflussen. Durch Bestrahlung mit Licht geeigneter Wellenlängen (UV- oder sichtbares Licht) war es möglich, die Adhäsivität der Zelloberfläche zwischen adhäsiv und weniger adhäsiv zu schalten. Die Schaltexperimente wurden sowohl unter statischen als auch unter Flussbedingungen durchgeführt. Diese bemerkenswerten Ergebnisse werfen neue fundamentale Fragestellungen in den Glycowissenschaften auf.
Um die Untersuchungen der Kohlenhydrat-Lektin-Wechselwirkungen zu vereinfachen wurde ein Bead-basiertes Kit entwickelt. Dies ist von Interesse, da durch die Funktionalisierung von magnetischen PEG Beads mit Azobenzol-Mannosiden die Photoschaltung der Adhesivität magnetischen Beads mittels reversibler E/Z-Isomerisierung ermöglicht werden könnte. Mittels photoschaltbaren magnetischen Beads könnten gebundene Bakterien detektiert und unter vergleichsweise milden Bedingungen durch Bestrahkung mit Licht wieder gelöst werden. Diese haben somit das Potenzial als diagnostisches Instrument eingesetzt werden zu können. Allerdings konnte keine signifikante photoinduzierte Änderung der bakteriellen Adhäsion an die glycosylierten PEG-Beads festgestellt werden. Kohlenhydrat funktionalisierte PEG Beads konnten allerdings verwendet werden, um Bakterien zu agglutinieren und somit einen Assay zu entwickeln, welcher eine Alternative zum klassischen Hämagglutinationshemmtest darstellt.
Um die Photoschaltung der Kohlenhydraterkennung weiterzuentwickeln werden orthogonal-modifizierte multivalente Photoschalter benötigt. Im letzten Teil dieser Arbeit, wurde basierend auf einem trifunktionalen Glycosid-Kern ein erster representativer heteromultivalenter Glyco-Photoschalter synthetisiert. Eine detaillierte kinetische Studie hat zu einem umfassenden Verständnis der photochromen Eigenschaften dieses neuartigen Instruments für die “Optoglycosciecnes” geführt.

Table of contents

A guide to this thesis

This thesis is comprised of eight chapters.
Chapter 1 gives a general introduction, providing fundamental information about the field of glycobiology, bacterial adhesion and azobenzene derivatives as photoswitches. This chapter is especially important for all readers who are not familiar with this research area in order to appreciate the research presented herein. While chapter 2 describes the objectives of the research embodied in this work, Chapter 3-6 comprise the results and discussion sections of the performed projects. Each of these chapters includes a specific introduction which is focused on the theoretial backround of the research presented in the respective chapter. These four chapters contain three published articles and three manuscripts (with the corresponding supporting information). In chapter 7 the obtained results are summarized and conlcusions are drawn. All experimental data as well as synthetic procedures are presented in the experimental section (Chapter 8).

1 General Introduction

1.1 Carbohydrates as essential components of life

Carbohydrates ubiquitously occur in nature and are the foundation of all life on Earth. In the human body for instance they have six different essential functions: they serve as i) energy source, ii) energy storage, iii) they build up macromolecules, iv) assist in lipid metabolism and v) they play an important role in biological recognition processes. One important function of carbohydrates in the human body is to provide energy to all cells for instance in form of glucose. If the glucose level in cells is high enough, the excess of glucose is stored in the form of the polysaccharide glycogen, which is mostly found in muscle and liver tissues. On the other hand, carbohydrates are fundamental constituents of every eukaryotic cell surface in the form of complex glycoconjugates. They play an essential role in cell-cell recognition, microbial adhesion and invasion and for pathogenicity (Figure 1.1). Thus, it is of great interest to gain deeper insight into the biology and function of naturally occurring glycoconjugates.

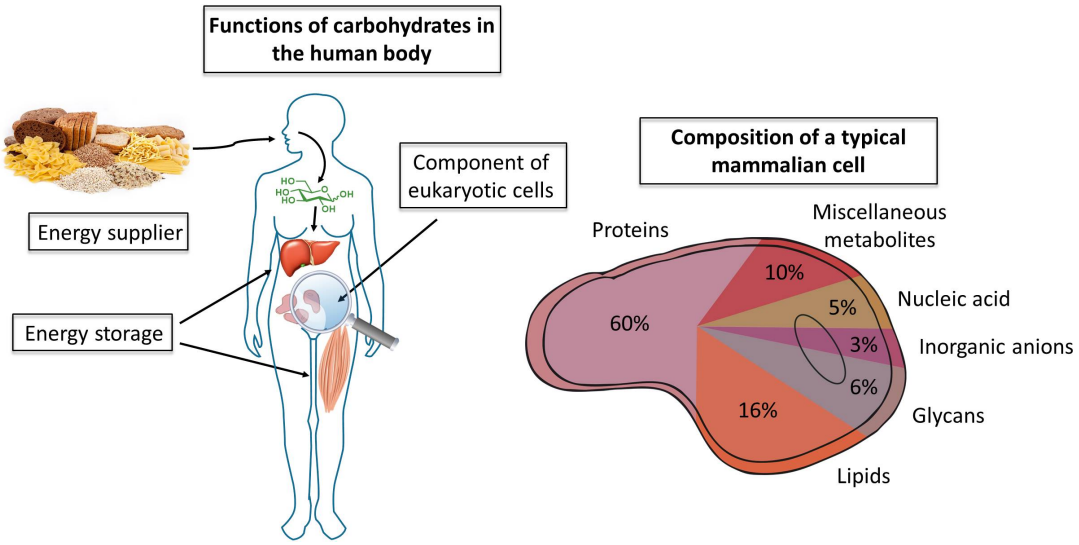

Figure 1.1. The occurence and functions of carbohydrates in the human body (left). The composition of a human cell (right).[1] Even though proteins comprise the largest component of a mammalian cell, it is excpected that more than half of them are glycosylated or modified with lipids as well as other metabolites.[2]

1.2 Glycobiolgy

The term Glycobiology was first coined in 1988 by W. Rademacher, R. B. Parekh and R. A. Dwek who recognized a profound connection of traditional areas of carbohydrate chemistry and biochemistry with the advanced understanding of the cellular and molecular biology of oligo- or polymeric glycoconjugates (glycans).[3] During the development of new methodologies to facilitate the analysis of complex glycans in the last 25 years a whole new area of scientific research has emerged. Hence, modern glycobiology is the study of structure, biosynthesis and biology of glycoconjugates which

occur in great variety in nature.[4] Especially the study of the biological relevance of extracellularly occurring carbohydrates (attached to proteins or lipids) is an interesting research area in glycobiology since carbohydrates play an important role in many biological processes such as the mediation of cell surface recognition and binding events.

1.2.1 Glycocalyx

The thick extracellular layer of complex, apparently unordered glycoconjugates surrounding every eukaryotic cell is referred to as the glycocalyx. The glycocalyx of various species differs significantly and serves diverse functions. Morphologically, a glycocalyx consists of an inhomogeneous highly complex mixture of glycoconjugates, comprising multiple oligosaccharide chains which are incorporated in the cell membrane either through proteins (proteoglycans) or as glycolipids or associated to the cell surface. Glycocalyces can expand to a width of 100 nm or more. Glycans which are embedded into proteins are divided into two major groups: *N*-linked and *O*-linked oligosaccharides (Figure 1.2).

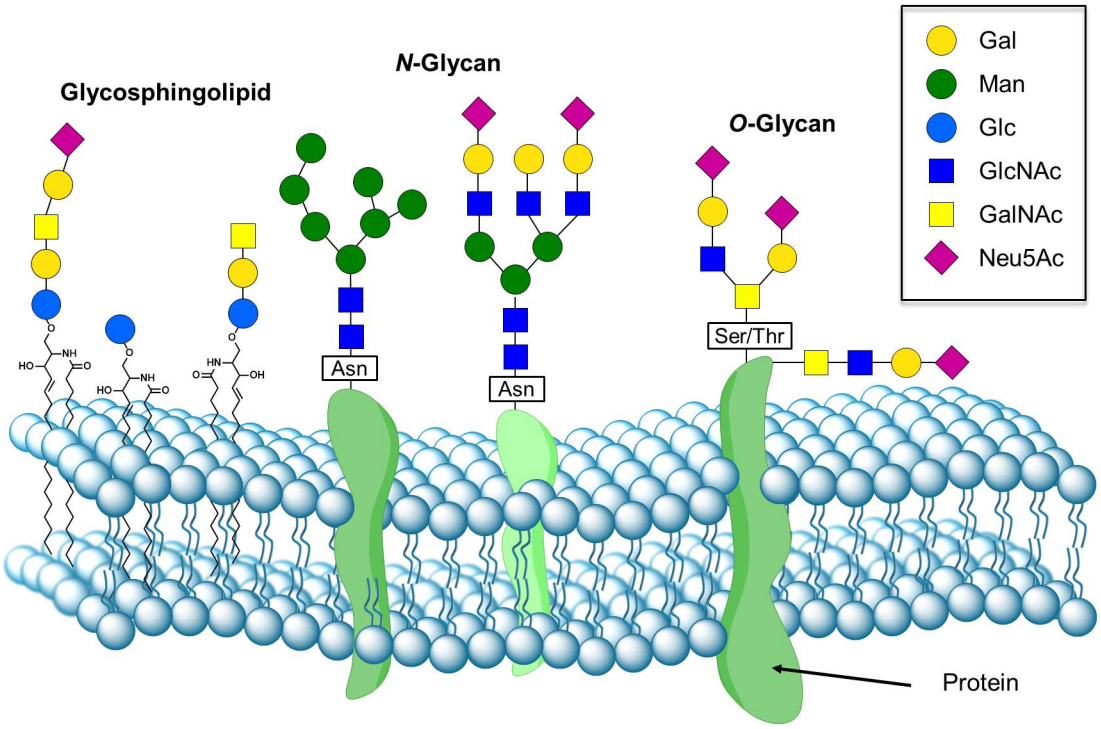

Figure 1.2. Schematic illustration of a cellular membrane with incorporated glycosylated proteins and lipids. The carbohydrates are represented according to the conventions suggested by the Consortium for Functional Glycomics (CFG)[5] by using following abbreviations: Asn (asparagine), Thr (threonine), Ser (serine), Gal (galactose), Man (mannose), Glc (glucose), GalNAc (*N*-acetylgalactosamine), GlcNAc (*N*-acetylglucosamine), Neu4Ac (*N*-acetylneuraminic acid).

N-linked glycans are β-glycosidically bound to the amide functional group in the side chain of asparagine (Asn). The Asn residue on the other hand is a constituent of the sequon (the sequence of consecutive amino acids) for *N*-glycosylation Asn-X-Ser or Asn-X-Thr while X representing any amino acid except proline.[4] All *N*-glycans exhibit the same core sequence consisting of Manα1-6(Manα1–3)Manβ1–4GlcNAcβ1–4GlcNAcβ1-Asn and depending on the their monosaccharide composition they are subdivided into three types, namely the high mannose, complex and hybrid type (Figure 1.3).[4]

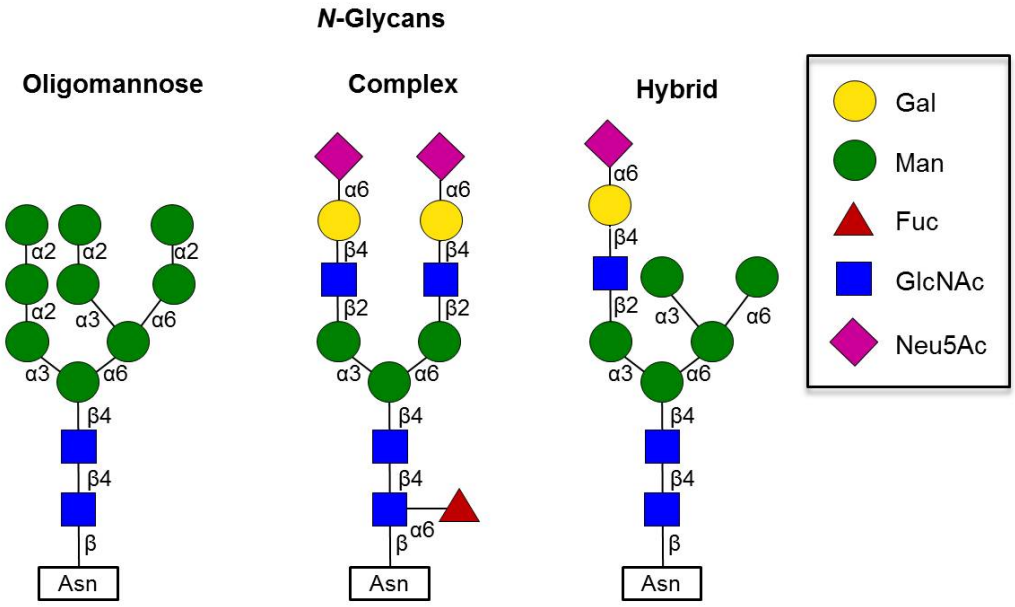

Figure 1.3. Schematic presentation of the three types of *N*-glycans: high-mannose, complex and hybrid. All glycans share the common core sequence $Man_3GlcNAc_2Asn$. The carbohydrates are represented according to the conventions suggested by the Consortium for Functional Glycomics (CFG)[5] by using following abbreviations: Asn (asparagine), Gal (galactose), Man (mannose), Fuc (fucose), GalNAc (*N*-acetylgalactosamine), Neu4Ac (*N*-acetylneuraminic acid).

Mucin-type *O*-linked glycoproteins consist of *O*-glycans which are usually covalently α-glycosidically bound via an an *N*-acetylgalactosamine (GalNAc) moiety to hydroxyl groups of serine (Ser) or threonine (Thr) residues. Whereas, GalNAc units on the other hand can be extended with other glycoconjugates such as *N*-acetylglucosamine (GlcNAc), galactose, fucose or sialic acid. In contrast to *N*-glycans, *O*-glycans possess less structural similarities.

However, the majority of cell surface glycoconjugates are part of glycolipids. Glycolipids comprise a nonpolar hydrophobic portion which is covalently linked by a glycosidic bond to mono- and oligosaccharides. The lipid part is usually incorporated within the cell membrane and thus the carbohydrate is located in the extracellular matrix. However, for instance glycolipids can also occur in the lumen of the endoplasmic reticulum (ER). The lipid part either consist of a 1,2-diacylglycerol residue or of the fatty acid amide from *N*-acylsphingosine.[6,7] While the carbohydrate moiety consist of galactose or glucose residues in case of cerebrosides and of complex oligosaccharide structures in the case of gangliosides. Prominent subfamilies of glycolipids are glycoglycerolipids, glycophosphoglycerolipids, glycosylated sterols as well as prenols, lipopolysaccharides and glycosphingolipids.

The composition of the glycocalyx is cell-specific and determined by the developmental and pathological status of the cell.[8] Due to the extracellular location of the glycocalyx the interaction with a broad spectrum of potential binding partners is feasible and thus different biological processes can be induced depending on the particular interaction. Many of these interactions have been extensively investigated and it has been shown that cell surface glycoconjugates mediate cellular processes, such as signalling,[9] molecular recognition[10] and cell adhesion.[11] For, example they can serve as attachment point for pathogenic organisms including bacteria and viruses, and for other cells. These cellular adhesion processes can be mediated by protein-protein interactions, carbohydrate-protein interactions and interestingly also by a number of glycan-glycan interactions.[12–15] The molecular mechanisms underlying the glycocalyx are not fully understood and thus the investigation of the biology and function of cell surface glycoconjugates is an important research area in glycobiology.

1.2.2 Carbohydrate-protein interactions

It has been revealed that cell surface glycans play an essential role in cell recognition processes. More precisely, these extracellular glycoconjugates may be recognized and bound by specific carbohydrate-binding proteins, the so called lectins.[16,17] Lectins neither have enzyme activity nor are they antibodies. They exist in most living organisms including viruses and bacteria as well as plants and animals.[18,19]

Lectins were first described by H. Stillmark in 1888 who discovered and isolated an extract from beans of the castor oil plant. He observed an agglutination of erythrocytes (red blood cells) by ricin (extracted active protein), however, this hemagglutination behaviour was not connected to carbohydrate specificity of proteins.[20] The first lectin which was isolated and identified to bind specifically carbohydrates was concanavalin A (Con A) from jack beans.[21] Further investigation revealed that the interaction between carbohydrates and proteins proceeds non-covalently, usually reversible and highly specific.[22,23] The part of the lectin which is responsible for the carbohydrate specificity is a conserved amino acid sequence forming the so-called carbohydrate recognition domain (CRD).[24,25] Since most lectins exhibit more than one CRD they are able to interlink several ligands which may lead to the formation of agglutinates. For example, they are involved in several biological processes such as in cell interactions in the immune system and in adhesion of infectious agents to host cells.[26–28]

1.2.3 Carbohydrate-specific bacterial adhesion

Many bacterial infections are caused by an initial adhesion step of the pathogen to a tissue cell. The bacterial adhesion process is often prerequisite for biofilm formation, invasion and colonization[29] and is commonly mediated by the interaction of bacterial proteins with cell surface glycoconjugates. Bacterial lectins which are responsible for binding are either located at the surface of bacteria or are part of their adhesive organelles, such as fimbriae.[30] One of the intensively investigated bacterial phatogenes are uropathogenic *Escherichia coli* (UPEC) which cause a number of infectious diseases including neonatal meningitis, urinary tract infections and gastroenteritis. *E. coli* bacteria adhere to urothelial cells via α-D-mannoside specific type 1 fimbriae (Figure 1.4).[31]

This special type of fimbriae is 1-2 µm long as well as 7 nm thick and consists of the main structural pilus subunit FimA which forms the pilus rod,[32] the subunits FimF, FimG and FimH. The α-D-mannose-specific adhesin FimH is located at the tip of the fimbriae and is further divided into two immunoglobulin-like domains, the C-terminal $FimH_P$ pilus domain and the *N*-terminal $FimH_L$ lectin domain.[33] The CRD which is capable to specifically bind α-configured D-mannosides is located at the tip of the $FimH_L$ pilus domain and is connected by a short linker to the C-terminal pilin domain, which anchors the adhesin to the pilus.

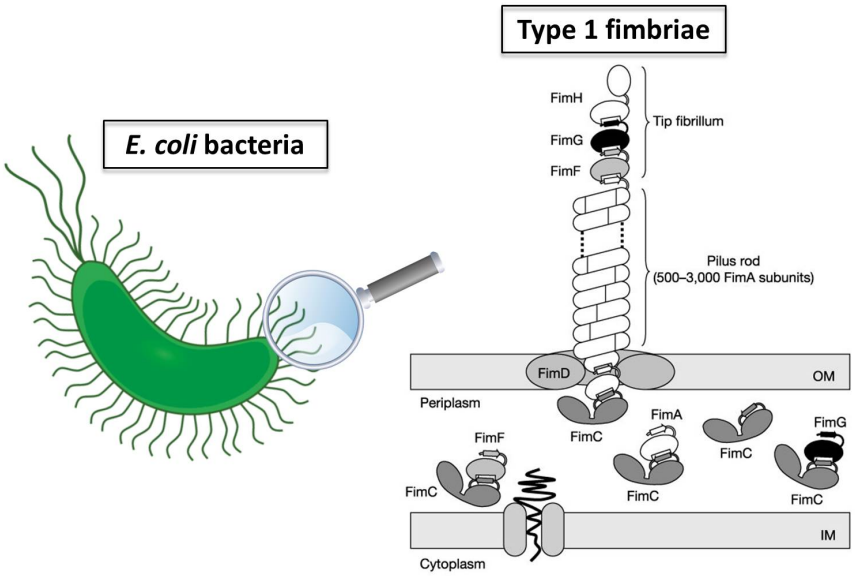

Figure 1.4. Schematic illustration of *E. coli* bacteria possessing fimbriae on the cell surface (left). Assembly of the type 1 fimbriae which proceeds by a chaperone-usher pathway inside the periplasm and is represented accordingly (right). IM: inner membrane; OM: outer membrane; FimH: fimbrial lectin; FimC: periplasmic chaperone; FimD: fimbrial usher protein; FimA, FimD, and FimG: other fimrial subunits. The schematic representation of the type 1 fimbriae was adapted by permission from Macmillan Publishers Ltd: *Nature* (M. Vetsch, C. Puorger, T. Spirig, U. Grauschopf, E. U. Weber-Ban, R. Glockshuber, *Nature* **2004**, *431*, 329-333), copyright © 2004.[34]

X-ray crystal structure analysis of FimH revealed that the hydroxyl groups of mannose form hydrogen bonds with the amino acids inside the CRD.[35,36] It has been shown that mannosides possessing a hydrophobic aromatic aglycone exhibit increased affinities for the CRD of FimH. The improved complexation within the CRD is caused by two distinct hydrophobic tyrosine residues Tyr48 and Tyr137 lining the entrance of the CRD. This so-called "tyrosine gate" is involved in π-π interactions with glycoconjugates containing an aromatic portion.[37] This increased affinity has for instance been considered in the design of mannose-based FimH antagonists, which can serve as antiadhesives in an anti-adhesion therapy to prevent bacterial infections.[38–43]

Even if many aspects of cell adhesion have been elucidated, the molecular and mechanistic details of cell-cell interactions are not fully understood.[44,45] A great variety of approaches and methods to facilitate the investigation of the biology and function of cell surface glycoconjugates have

emerged.[46] Hence, the concept of multivalency (Chapter 6), conformational as well as density[47] aspects and also the development of new tools such as glycoarrays (Chapter 4),[48] new adhesion assays and metabolic oligosaccharide engineering (MOE) (Chapter 5) may favourably contribute to reveal the underlying cellular mechanism of cell adhesion in greater depth.

1.3 Conformational and orientational control of biological processes

Conformational changes play an important role in many biological processes and are often induced by an alteration of the shape of a macromolecule. These structural changes are caused by environmental factors such as the pH value, temperature, voltage, ion concentration phosphorylation or the binding of a ligand. Initially a cell receives a chemical or physical external stimulus which is transmitted and triggers a reaction cascade leading to a specific biochemical reaction.[49] The conformational change is often the first step in this signaling cascade. The visual cascade is one of the prominent examples of a biological process which is controlled by a conformational change. The vision process is initiated through the absorption of a photon of light by rhodopsin (Figure 1.5). Rhodopsin is a light sensitive holoprotein consisting of seven transmembrane helices containing 11-*Z*-retinal which is covalently bound via a protonated Schiff base linkage to lysine-296 (opsin part of rhodopsin).[50,51] 11-*Z*-retinal represents an efficient *E*/*Z* chromophore which upon photoexcitation undergoes a *Z*→*E* isomerization leading to the 11-*E*-retinal.[52] The isomerization process of the chromophore is suggested to induce a conformational change in the transmembrane helices of rhodopsin and is known as the first step in the signal transduction process of the visual cascade.[53–56]

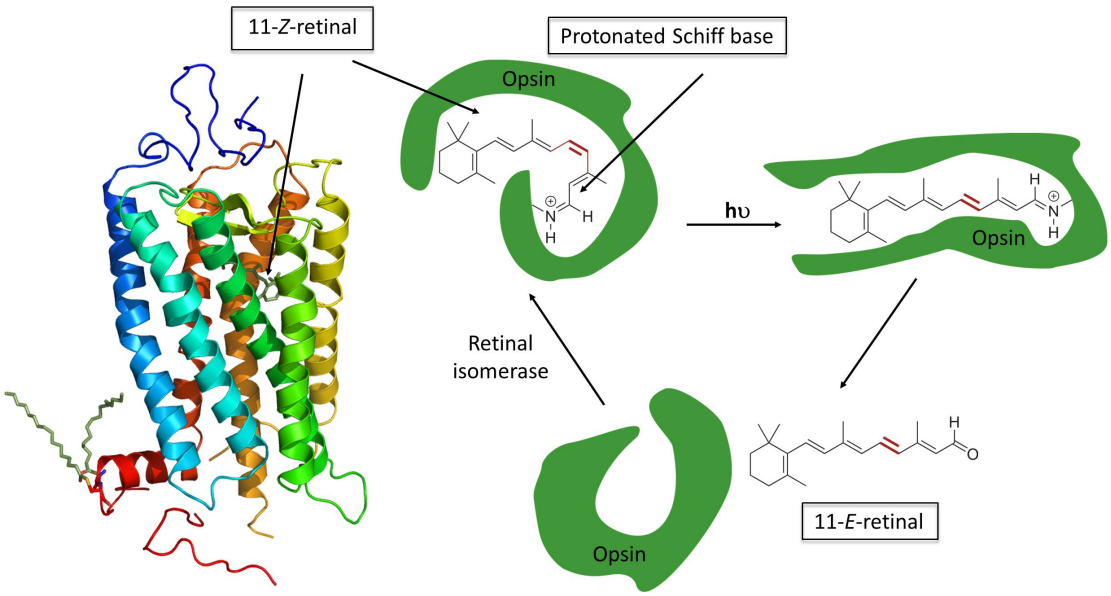

Figure 1.5. The three-dimensional structural model of the light sensitive holoprotein rhodopsin consisting of seven transmembrane helices. In the middle the 11-*Z*-retinal can be seen (left).[57] The 11-*Z*-retinal undergoes an efficient *E*→*Z* isomerization upon photoexcitation. This process is suggested to induce a conformational change within the protein and is known as the first step of the visual cascade (right).[53–56]

Besides the visual phototransduction there are many more examples of conformational control of biological function in nature.[49] For instance the binding of insulin to its receptor induces a conformational change within the protein.[58–61]
Even though molecular events occurring within the glycocalyx are not completely understood it is known that accessibility, density, and conformation of cell surface glycoconjugates play an important role in molecular recognition processes.[62] For instance galectin-mediated organization of cell surface carbohydrates is influencing glycoconjugate dynamics and important biological processes such as signalling.[63] It has been also shown that the orientation of saccharides of glycosphingolipids plays an essential role in their receptor function for bacterial adhesins. It was hypothesized that saccharide chain orientation might be a possible factor in signalling between cells during their normal or malignant development.[64–66] This sugestion is striking and need to be further investigated. A promising tool to examine the influence of conformational changes or orientation and their control of biological function is the modification of biologically relevant substances by the introduction of small molecular 'photoswitches'.[67–70] A molecular switch is defined as a system allowing performing mechanical movements when the system is exposed to an external stimulus such as light, resulting in a conformational alteration of the switch and therefore leading to environmental change. The most important prerequisite for a molecular switch is the existence of two different and stable isomeric forms which can be transmuted into one another.

1.4 Azobenzene

Of the various molecular photoswitches studied, azobenzene (**1**) is probably the oldest and one the most extensively investigated photoswitch. Its ability to undergo $E \rightarrow Z$ isomerization was first reported eight decades ago.[71] Azobenzene (**1**) is a favourable photoswitch as the conformation of this molecule can be altered between two defined states, the bent Z form and the planar E form with the E isomer representing the thermodynamically more stable form compared to the Z isomer.[72] Furthermore, upon isomerization the end-to-end distance of the *para* carbon atoms changes about 4 Å.[73–75] $E \rightarrow Z$ isomerization is achieved by excitation of the $\pi\pi^*$ band upon irradiation with UV light,[76] mechanical stress[77] or electrostatic stimulation.[78] $Z \rightarrow E$ isomerization on the other hand can be initiated by thermal relaxation with a half-life $\tau_{1/2}$,[79] by excitation of the $n\pi^*$ band with visible light or electrochemically.[80,81] The mechanism which underlies the isomerization process can proceed via four different proposed pathways, namely rotation, inversion, concerted inversion or inversion-assisted rotation (Scheme 1.1).[82–84]
In the rotation pathway the N=N π-bond is raptured allowing for free rotation about the N-N bond. Thus, upon rotation the C-N-N-C dihedral angle is changed, whereas the N-N-C angle remains fixed at ~120° (Scheme 1.1, A)).[82] The inversion mechanism on the other hand involves an increase of one N=N-C angle to 180° while the C-N=N-C dihedral angle remains fixed at 0 ° giving rise to a transition state with one sp-hybridized azo-nitrogen atom (Scheme 1.1, B)).[83,85,86] If the isomerization proceeds by a concerted inversion both N=N-C bond angles increase simultaneously to 180 ° which leads to a linear transition state (Scheme 1.1, C)).[87] The inversion-assisted rotation pathway involves a simultaneously occurring large change in the C-N=N-C dihedral angle and slight but significant alteration in the N=N-C angle (Scheme 1.1, D)).[84] Since all four transition

pathways are reversible photostationary states (PSS) consisting of both isomers are predicted. Which of the four proposed mechanism occurs has not been answered conclusively so far and is controversially discussed.[88–90] However it is known that the isomerization mechanism depends on the excitation mode (thermal or irradiation),[90,91] irradiation wavelength,[92–94] solvent properties,[92,95] substituents on the phenyl rings,[96,97] temperature[98–100] and pressure.[101]

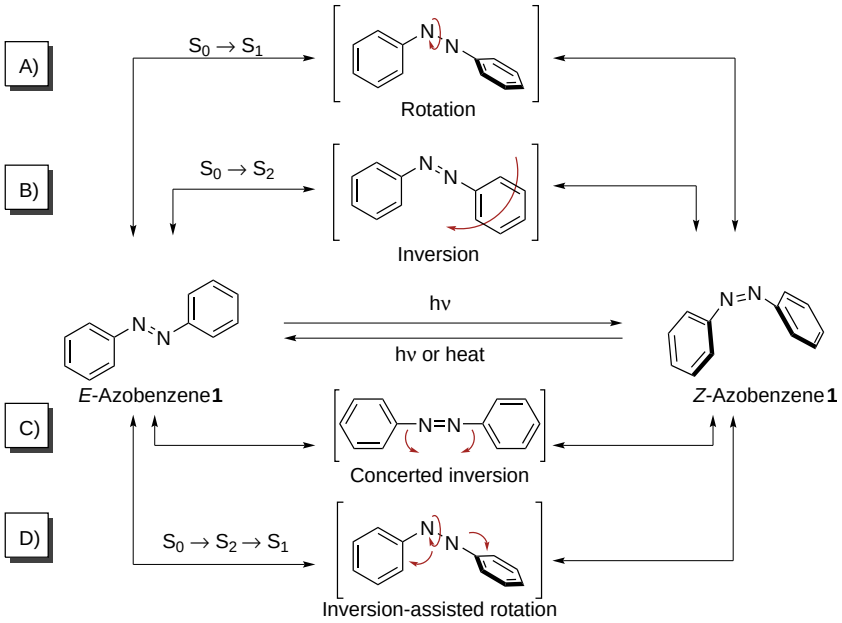

Scheme 1.1. Proposed mechanisms for the $E \rightarrow Z$ isomerization of azobenzene (**1**).

The photoinduced E/Z isomerization of azobenzene chromophores gives rise to a considerable change in the UV-vis absorption spectra, molecular geometry and polarity. Furthermore, azobenzene-derived photoswitches generally exhibit an excellent long-term photostability. Therefore, these systems have been widely utilized as a light-triggered switch for the photocontrol of biological processes.[102,103] However, the utilization of chromophores for biomolecular photocontrol requires several prerequisites such as: i) water solubility, ii) biocompatibility, iii) efficient isomerization with visible light and iv) a significant conformational change in order to induce a functional change in a biomolecule.[103] Considering the above described features, it becomes obvious that glycoazobenzene derivatives represent attractive photoswitchable tools to control biological function.

1.5 Glycoazobenzene derivatives

Surprisingly, relatively little work on glycoazobenzene derivatives has been reported in the literature[104] when Lindhorst and co-workers initiated a project about the synthesis of novel azobenzene glycoconjugates and the investigation of their photochromic properties and biological functions.[105–110] The synthesis of azobenzene glycosides can be achieved applying various synthetic strategies (Figure 1.6).

Mills coupling and glycosylation reactions were utilized for the synthesis of photoswitchable glycoconjugates with different anomeric configurations (α-D-mannosides, α- as well as β-D-glucosides).[110] To further derivatize *p*'-OH-substituted azobenzene glycosides the Mitsunobu reaction as well as Williamson ether synthesis were applied.

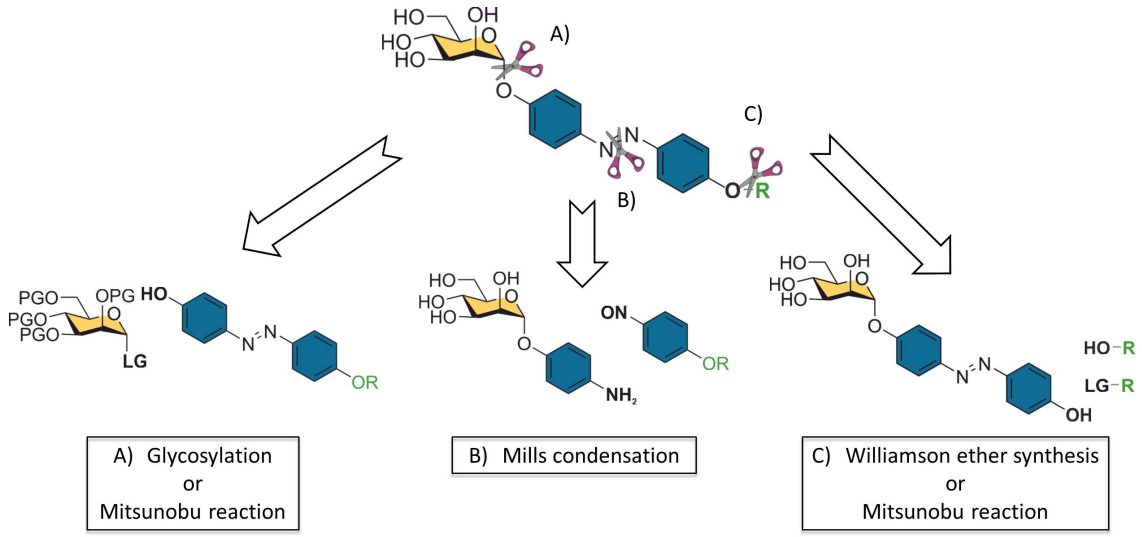

Figure 1.6. Retrosynthetic overview of applied methods to obtain photoswitchable azobenzene glycosides.

Additionally, Mitsunobu reaction was also used in the synthesis of hydroxyazobenzene with free D-mannose leading to a mixture of pyranosides and furanosides. Protected reducing mannose derivatives on the other hand furnished β-D-mannopyranosides, whereas alkyl α-D-mannosides were converted in respective 6-*O*-azobenzene modified glycosides.[109] With the utilization of copper(I) catalysed click chemistry[111,112] a variety of photoswitchable glycoclusters could be obtained (see Chapter 6.1.2).[106] Besides the synthesis of a variety of azobenzene monosaccharides, also a synthesis of a disaccharide derivative was accomplished.[105] The prepared disaccharide showed good water solubility and could be applied successfully in an adhesion-inhibition assay with green fluorescent protein (GFP) expressing *E. coli* bacteria.[113] It was demonstrated that azobenzene glycosides are potent ligands of FimH and therefore ideally suited to study type 1 fimbriae-mediated bacterial adhesion. However, no difference in binding to FimH was observed for *E*- or *Z*-configured azobenzene glycosides, respectively. The cytotoxicity of azobenzene mannosides is completely uncritical as was demonstrated by the investigation of bacterial adhesion and inhibition to mammalian cells.[114] The switching behaviour of the prepared photoswitchable glycoconjugates was determined and also the influence regarding carbohydrate configuration as well as azobenzene substitution on the photochromic properties were studied. Glycoazobenzene derivatives exhibit favourable photochromic properties. Upon irradiation of the *E* configured isomer almost quantitative isomerization to the *Z*-isomer was observed (PSS, >95%). They exhibit long thermal relaxation times (a half live time of several days) allowing for independent investigation of the *E*- and the *Z*-isomer of the respective azobenzene glycoside in biological adhesion assays. Azobenzene glycosides, which have been coined "sweet switches", are readily accessible, can be easily modified, are biocompatible and have remarkable photochromic properties. They represent a valuable tool for biomolecular photocontrol of macromolecules as well as for photo-biochemical investigations.[115–117]

2 Objectives

Carbohydrate recognition is fundamental for numerous essential biological processes. Typically, it involves a carbohydrate ligand and its protein receptor (a lectin). These interactions have been investigated widely and in great detail. However, carbohydrate-protein interactions typically take place in the supramolecular environment of a cell and involve multiple interaction partners. Therefore, multivalent glycoconjugates are needed as tools to investigate carbohydrate recognition. Furthermore, in order to manipulate and control carbohydrate recognition, many functional synthetic glycoconjugates have been invented. Only recently, photosensitive glycoconjugates have been introduced as tools in the glycosciences, allowing to interfere in carbohydrate recognition as well as interrogate carbohydrate-protein interactions with spatial and temporal resolution. This approach is derived from the field of "optogenetics" which has been considered as one of the "breakthroughs of the decade" in 2010.[118] In analogy to this, this approach might be called "optoglycomics" in the context of the glycosciences.
Photosensitive molecules allow to "switch" the situation of the molecule between two states, upon stimulation with light of the appropriate wavelength. Consequently, they allow to manipulate and control biological function, and most importantly, they bear the potential to observe functional control in a supramolecular environment such as the glycocalyx.

The projects described in this thesis are all dedicated to the synthesis and investigation of azobenzene glycoconjugates as photoswitchable tools to control protein and glycoconjugate function (Figure 2.1). Photoswitching of azobenzene glycoconjugates is based on the reversible E/Z isomerization of the N=N double bond of the azobenzene moiety. Various azobenzene glycoconjugates were prepared and their photochromic properties investigated.

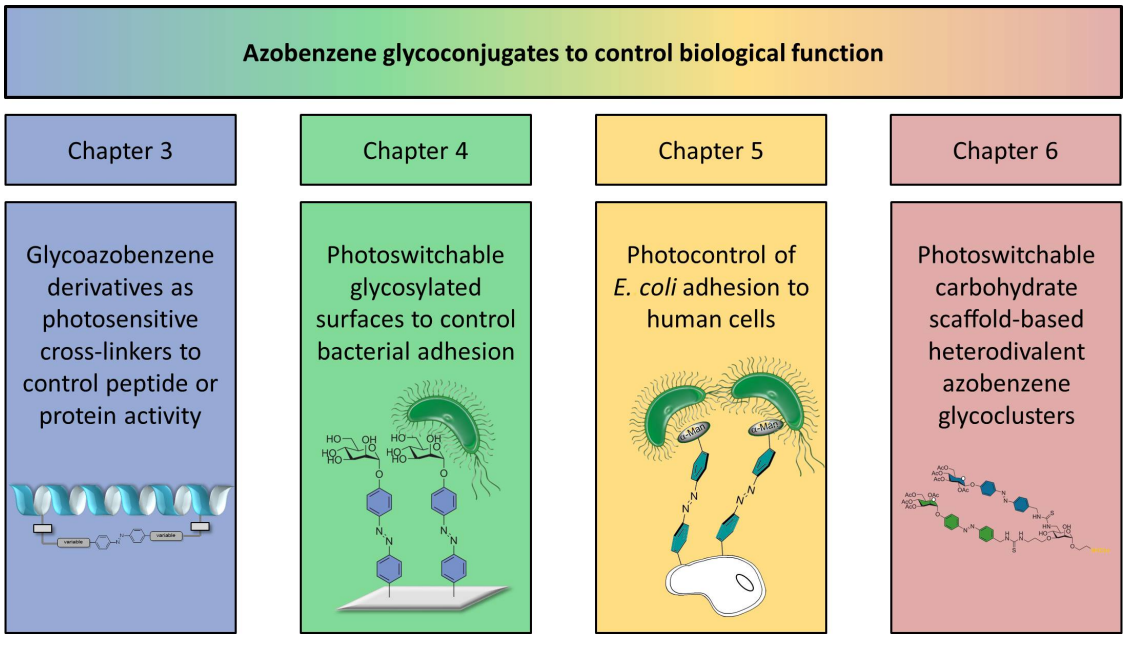

Figure 2.1. Overview about the topics which are discussed in the individual chapters.

Thus in the first project, described in Chapter 3 homo- and hetero-bifunctional glycoazobenzene-derivatives were synthesised to serve as cross-linkers for peptides and proteins aiming at the control of their conformation and , as a consequence, their function.

Chapters 4 and 5 are focused on the phenomenon of bacterial adhesion, which is carbohydrate-specific. In view of the increasing problem of antibiotic resistance, an antiadhesion approach to bacterial adhesion has been investigated for some time. Only recently, it has been shown in the Lindhorst group that the adhesivity of surfaces can be reversibly switched, employing azobenzene glycosides immobilized on a surface.[107,108] This approach has been extended and further elaborated here. Thus, photoswitchable glycosylated quartz glass surfaces were fabricated and the photochromic properties of the prepared solid support determined (Chapter 4.2). Quartz glass surfaces are benificial as UV-vis investigation is feasible and furthermore a variety of ligation methods can be applied to attach carbohydrates on the solid support. Additionally, an adhesion assay was performed to correlate azobenzene specific configuration of the immobilized azobenzene glycoside behavior with the adhesivity of the surface.

The development of new diagnostic tools and enhanced assay systems is an important step towards facilitating the study of bacterial adhesion. For this aim a bead-based kit for the investigation of carbohydrate-specific agglutination of *E. coli* bacteria was developed (Chapter 4.3). Furthermore, it was verified if bacterial adhesion to magnetic PEG-beads can be photocontrolled by reversible E/Z-isomerization of the immobilized azobenzene glycosides.

To expand the investigation of photocontrol of bacterial adhesion through re-orientation of the carbohydrate ligand to a more complex natural environment, glycoazobenzene derivatives were immobilized on the plasma membrane of human cells, by utilizing metabolic oligosaccharide engineering (MOE). Cell-cell adhesion studies were performed under static as well as under flow conditions (chapter 5).

In order to extend the field of "optoglycomics" towards a more complex manner novel photoresponsive azobenzene glycoconjugates are required. Thus, multivalent orthogonally modified azobenzene derivatives with increased complexity and more sophisticated photoswitching functions have to be synthesised. Orthogonality might be achieved in a dual approach. One approach is the introduction of diverse carbohydrates and the other one is the introduction of glycophotoswitches which can be addressed with different wavelengths. In chapter 6 a hetero-functionalisable approach is reported. Therein, an orthogonal trifunctional carbohydrate-based scaffold molecule was synthesised and utilized for the synthesis of a first representative of a heterodivalent glycophotoswitch. Furthermore, photochromic data as well as a detailed kinetic study of the switching behaviour of the prepared divalent azobenzene glycocluster was investigated.

3 Azobenzene glycoconjugates for photosensitive cross-linking of proteins or peptides

3.1 Introduction

3.1.1 Azobenzene as a molecular switch to control biological function

Azobenzene derivatives have been widely used as photoswitches to control biological function[69,102,103] since they have remarkable photochromic properties (see Chapter 1.3). They are fatigue-resistant, upon isomerization the distance between the two carbons at the *para* position of the phenyl rings changes by about 4 Å[73–75] and the isomerization process proceeds on a picosecond timescale, which is substantially faster than most biological events.[119,120] Switching between the two states is accomplished by irradiation with light of two different wavelengths. The control of the E/Z isomerization process with visible or even IR light is still a major challenge in biological applications thus, this is extensively studied.[121–128] Nevertheless, azobenzene derivatives have been successfully applied as photoswitches with applications in various fields ranging from material science, catalysis[129] to neurobiology.[102,103,130–133] Most of the biological applications rely on the site-selective conjugation of the azobenzene photochromic unit into the structure of biomolecules such as proteins, peptides, nucleic acids,[134–137] lipids or carbohydrates.[69,103] Through the conjugation of photosensitive azobenzene cross-linkers with the biomolecule switching of its function through irradiation can be affected. It is thus possible that biological function can be externally triggered and switched between an on and an off state, respectively, by selection of the appropriate wavelength for irradiation. This leads to the possibility to achieve temporal and spatial resolution of biomolecular activity.

Bioactive peptides and proteins have important functional roles in biology and are present in all living organisms. They serve as hormones as well as ligands for receptors in a host of systems. For instance organisms that live in subzero regions, e.g. fish, funghi, bacteria, plants, and insects, express antifreeze proteins (AFP) to protect themselves against death by freezing.[138–142] These proteins bind with high affinity and specificity on the surface of ice this allows for depressing the colligative freezing point of water, shaping the ice crystal form and inhibiting ice recrystallization. Their astonishing activity is of great interest for medical, food industrial and manufacturing applications.[143] Thus, it is of great interest to photocontrol their biological activity. The incorporation of a photoresponsive switch into a peptide or protein can be achieved via three different described methods (Figure 3.1).

One approach of crosslinking is the introduction of the molecular switch into the backbone of either cyclic or linear peptides and proteins (Figure 3.1 A).[144] Backbone incorporation of *p*-[(*p*'-aminomethyl)phenylazo]benzoic acid as a conformational switch within peptides was first achieved by J. Chmielewski and L. Ulysse. However, they did not follow this approach further.[145,146] In 1999 L. Moroder and colleagues introduced *p*-[(*p*'-amino)phenylazo]benzoic acid within cyclic peptides and their conformational properties were studied in detail. They could demonstrate that upon isomerization of the azobenzene unit remarkable conformational changes within the peptide were induced.[144,147,148] The backbone modification is therefore a favourable approach since large structural changes within peptide chains can be induced which is particularly useful to probe folding

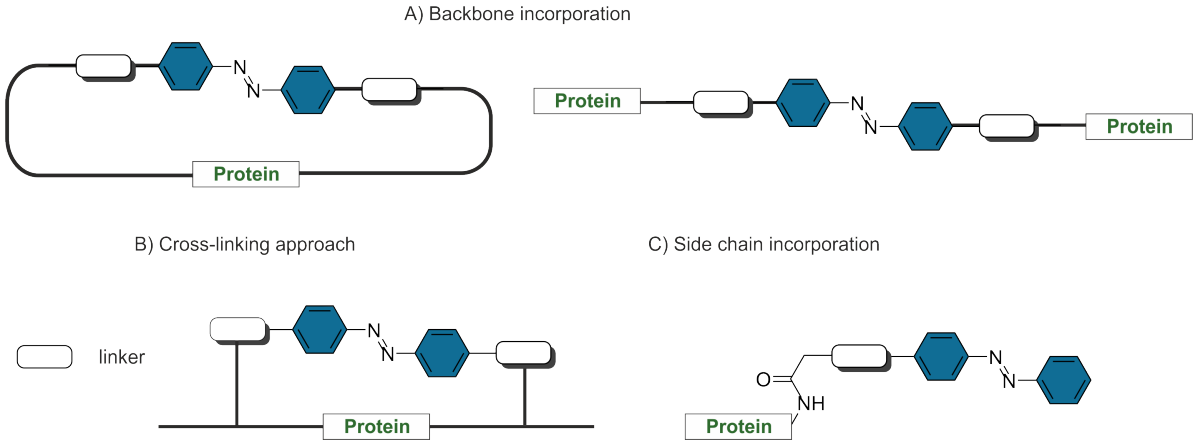

Figure 3.1. Schematic illustration of the possible methods used to incorporate photoresponsive azobenzene derivatives in peptides or proteins.

mechanisms and conformational dynamics.[119] For this purpose a variety of azobenzene amino acids were synthesised and incorporated in a peptide sequence by solid-phase peptide synthesis.[149] With the utilization of backbone modifications it was for example possible to photocontrol muscle fibers contraction[150]

Azobenzene photoswitches can be further cross-linked via peptide or protein side-chains rather than incorporated in their backbone (Figure 3.1 B). This has the advantage that the photoswitchable unit can be installed after peptide or protein synthesis. G. A. Woolley and co-workers reported on side-chain reactive molecular switches, namely *p*,*p*'-bis(iodooacetamido)azobenzene (**2**) and *m*,*m*'-bis(sulfonato)-*p*,*p*'-bis(chloroacetamido)azobenzene (**3**) which exhibit following characteristics: i) they possess two iodoacetamide or chloroacetamide groups, respectively *para* to the azo unit, incorporated to allow for a selective cross-coupling reaction with two cysteine (Cys) side-chains (Figure 3.2). Cysteine was chosen since it is rarely found in proteins and can be easily introduced within peptides or proteins by site-directed mutagenesis. Furthermore, ii) the azobenzene derivatives exhibit a minimum number of single bonds between the azo unit and the peptide backbone to facilitate that the conformational change affects the secondary structure of the peptide rather than dissipates. Additionally, iii) sulfonate groups in *meta* position to the azo unit were installed to improve water solubility.[151–154]

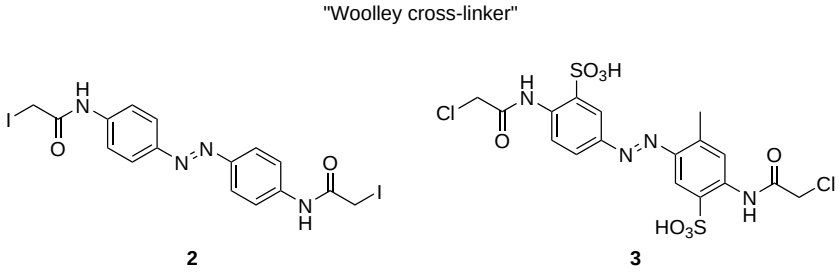

Figure 3.2. The depicted side-chain reactive molecular switches were prepared from G. A. Woolley and co-workers and were utilized to control peptide and protein activity.

The designed azobenzene cross-linkers were then coupled to α-helical peptides which were chosen due to the widespread occurrence of helices in proteins and the availability of biophysical data concerning helix stability and dynamics.[155] With the aid of molecular dynamic simulations the distance distribution between the two cysteine residues were computed in such a way that one spacing is for instance compatible with the *Z*-conformation and less compatible with the *E*-conformation of the linker.[156] Final cross-linking of azobenzene linker molecules with peptides possessing two Cys at positions i, i + 7 or i, i + 4, respectively revealed a substantial increase in helical content upon $E \rightarrow Z$ isomerization of the azobenzene derivatives in water.[152,156,157]

The reverse behaviour was observed with peptides where the cysteines are spaced i, i + 11 residues apart. Photoisomerization to the *Z*-isomer upon irradiation with UV light resulted now in destabilizing of the helical structure. The stable helix could be recovered via irradiation with visible light or relaxation from *Z* to *E* in the dark.[151,153,157] It is notable that the observed photo-control of helical content is not driven by high-affinity, noncovalent interactions between the photoswitchable unit and the peptide. Thus, this approach is generally suitable and might be used in larger protein systems.[158] R. K. Allemann and colleagues could extend the side-chain cross-linking approach to α-helical peptides derived from native proteins. They have targeted peptide segments from regions of anti-apoptotic proteins (blockers of cell death) and cross-linked them with azobenzene-based photoswitches to enable photocontrol of peptide binding affinity.[159] Furthermore, by installing azobenzene–derived cross-linkers into the DNA or RNA binding peptides, binding specifity could be reversibly controlled by irradiating with light.[160–162] Besides the photocontrol of peptides the site-selective approach could be also utilized to incorporate azobenzene-based cross-linkers within proteins and thus control protein structure and activity.[69,103,163] Protein-protein-interaction[164,165] as well as enzyme activity,[166] for instance, could be manipulated. Moreover this approach could be extended to photocontrol proteins *in vivo* and thus spatiotemporal regulation and even fluorescence imaging of protein activity in live cells is feasible.[167,168]

Most of the site-selective cross-linking approaches have been accomplished by connecting two cysteine residues with azobenzene derivatives bearing two thiol reactive anchoring groups. The drawback of this method is that undesired side products can be formed which is especially unfavourable for applications *in vivo* due to the presence of reactive thiols in cells. To overcome this limitation M. Beyermann and co-workers reported the preparation of photoswitchable click amino acids which allow for a specific and mild introduction of photo-switchable side chain-to-side chain bridges within peptides or proteins.[169–171] For this purpose, α-amino acid azobenzene derivatives containing an additional thiol reactive group are incorporated into the peptide and an intramolecular azobenzene bridge can be specifically formed by reacting with a nearby cysteine residue. With this approach it was possible to genetically incorporate photoswitchable click amino acids into *E. coli* and mammalian cells.[172]

The third possibility to photocontrol protein function is the introduction of photoswitchable ligands. This approach is based on the fact that proteins have known ligands such as inhibitors or activators which control their function. Usually these ligands bind to a defined active site of a protein. Trough a small change in the ligand structure protein activity can be affected. Conjugation of a ligand to an azobenzene unit may provide the possibility to modify the binding to the active site by light. A more precise photocontrol can be achieved by covalently tethering the photoswitchable ligand to the

protein. Photoswitchable ligands were utilized to control und investigate complex biological systems including folding of proteins and peptides, enzymatic reactions, or neuronal signalling.[69,103,173–179] D. Trauner and co-workers for instance utilized azobenzene-based photoswitches to control the opening and closing of pores in cellular membranes, which are essential for the transport of ions. Hence, it was possible to control ion channels and ionotropic glutamate receptor *in vitro* as well as *in vivo*.[173,180–184] Another remarkable example is the photocontrol of quorum sensing (QS), the complex communication system between bacteria. In a proof-of-principle study B. Feringa and co-workers applied photoswitchable signalling molecules and could specifically manipulate the QS mechanism.[185,186]

All these examples demonstrate the clear potential of azobenzene-based molecular switches to spatiotemporally control biological function and to study underlying molecular events in greater detail.

3.2 Glycoazobenzene derivatives as photosensitive cross-linkers to control peptide or protein activity

Proteins are the most abundant biomolecules in living organisms and play an important role in almost all biological processes in nature. For instance, some organisms that live in temperate or polar regions express antifreeze proteins (AFP) to adapt themselves to subzero temperatures. In order to investigate the structure-function relationship of peptides or proteins in more detail, different (glyco)azobenzene-based cross-linkers have been designed (Figure 3.3). A photoswitchable protein can be realized by the site-selective incorporation of the photoswitchable (glyco)conjugate to specific amino acids of the protein, thus enabling photocontrol of folding and consequently the ability to achieve time or spatial resolution of protein activity.

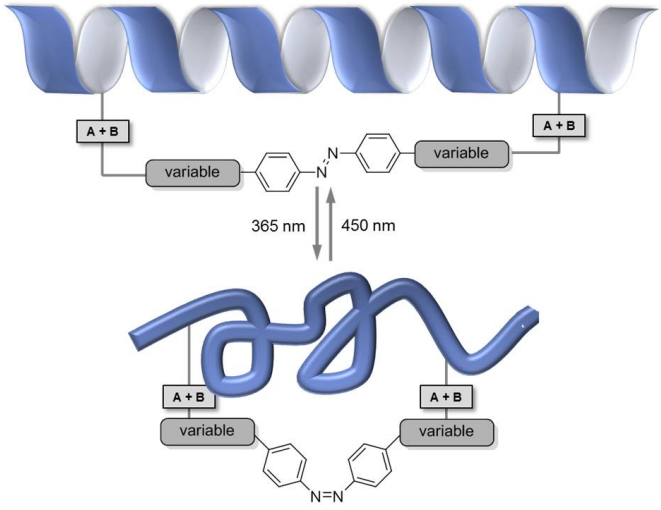

Figure 3.3. In this chapter the preparation of photosensitive cross-linkers to control peptide or protein activity is presented.

The following two articles describe the syntheses and photochromic properties of a variety of new homo- and hetero-bifunctional (glyco)azobenzene derivatives that vary in their functional groups and linker length. The obtained glycoazobenzene cross-linkers possessing two identical reactive thiol groups, for instance, exhibit improved water solubility. First ligation reactions of the prepared homo-bifunctional linker molecules with different sulfur containing residues were successful. Furthermore, the site selective conjugation of an azobenzene glycoside bearing two chloroacetamido anchoring groups with a helical model peptide was feasible. In the second article the synthesis of a new linker type comprising photoresponsive azobenzene conjugates with a hetero-bifunctionalization was achieved. These linkers allow for consecutive cross-linking with the respective peptide or protein. Azido-, alkine-, alkene- and thiol-functionalities were installed at the respective azobenzene (glyco)conjugate and thus, a variety of ligation methods for cross-linking of the photoswitchable unit into the peptide/protein are feasible. Furthermore, molecular dynamics simulations were performed to monitor the change in their end-to-end distances upon isomerization and to estimate the effect of the prepared azobenzene derivatives on the conformational properties of cross-linked peptides or proteins.

3.2.1 Bifunctional azobenzene glycoconjugates for cysteine-based photosensitive cross-linking of petides and proteins

"Synthesis of Bifunctional Azobenzene Glycoconjugates for Cysteine-Based Photosensitive Cross-Linking with Bioactive Peptides"

A. Müller, H. Kobarg, V. Chandrasekaran, J. Gronow, F. D. Sönnichsen, T. K. Lindhorst, *Chem. Eur. J.* **2015**, *21*, 13723–13731.

DOI: 10.1002/chem.201501571

Abstract: Azobenzene linker molecules can be utilized to control peptide/protein function when they are ligated to appropriately spaced amino acid side chains of the peptide. This is because the photochemical *E/Z* isomerization of the azobenzene N=N double bond allows to switch peptide conformation between folded and unfolded. In this context, we have introduced carbohydrate-functionalized azobenzene derivatives in order to advance the biocompatible properties of azobenzene peptide linkers. Chloroacetamide-functionalized and *O*-allylated carbohydrate derivatives were synthesised and conjugated with azobenzene to achieve new bifunctional cross-linkers, in order to allow ligation to cysteine side chains by nucleophilic substitution or thiol-ene reaction, respectively. The photochromic properties of the new linker glycoconjugates were determined and first ligation reactions performed.

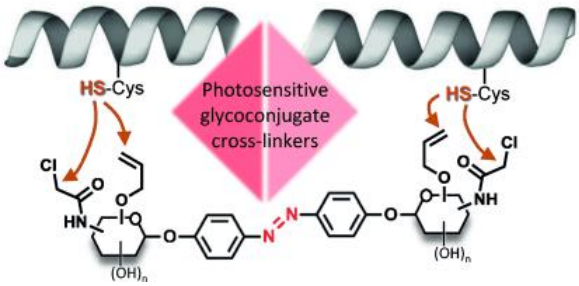

TOC Graphic 3.1. Photoisomerizable azobenzene glycoconjugates were synthesised as biocompatible, cross-linker molecules to control the conformation of peptides via ligation to Cys side chains (see scheme). Two types of ligation chemistries were enabled, thiol-ene addition to alkenes and nucleophilic substitution of chloro functional groups. This design provides high flexibility in adjusting spacing and reactivity for the cross-linking process.

Scientific contribution to this paper

In this project I carried out all synthetic and experimental work with the following support by the coauthors: H. Kobarg performed the ligation reaction with the helical nonadecapeptide, V. Chandrasekaran synthesised the chloroacetamido-functionalized cross-linker first, whereas its synthesis was optimized by me. J. Gronow performed the investigation of the photochromic properties and F. D. Sönnichsen performed the distance calculation and assisted in writing the article. T. K. Lindhorst and I coordinated the work and wrote the article together.

ChemPubSoc Europe

DOI: 10.1002/chem.201501571

CHEMISTRY A European Journal Full Paper

Glycoconjugates

Synthesis of Bifunctional Azobenzene Glycoconjugates for Cysteine-Based Photosensitive Cross-Linking with Bioactive Peptides

Anne Müller, Hauke Kobarg, Vijayanand Chandrasekaran, Joana Gronow, Frank D. Sönnichsen,* and Thisbe K. Lindhorst*[a]

Abstract: Azobenzene linker molecules can be utilized to control peptide/protein function when they are ligated to appropriately spaced amino acid side chains of the peptide. This is because the photochemical *E*/*Z* isomerization of the azobenzene N=N double bond allows to switch peptide conformation between folded and unfolded. In this context, we have introduced carbohydrate-functionalized azobenzene derivatives in order to advance the biocompatible properties of azobenzene peptide linkers. Chloroacetamide-functionalized and *O*-allylated carbohydrate derivatives were synthesized and conjugated with azobenzene to achieve new bifunctional cross-linkers, in order to allow ligation to cysteine side chains by nucleophilic substitution or thiol-ene reaction, respectively. The photochromic properties of the new linker glycoconjugates were determined and first ligation reactions performed.

Introduction

Switching the conformation of biomolecules, in particular peptides and proteins, is a means of controlling their function. Conformational switching of proteins can be effected through the conjugation of photosensitive cross-linkers that mediate structural changes after irradiation. In such a way, function can be controlled by light with temporal and spatial resolution. Hence, photochemical switches have become useful tools in biological chemistry and for applications in medical and material sciences.[1] A well-known and favorable photoswitch is azobenzene,[2] because photoisomerization of the azobenzene N=N double bond is reversible and provides the molecular basis for a pronounced structural change between the planar *E* form and the bent *Z* form, both isomers differing in length by about 4 Å. $E \rightarrow Z$ isomerization and $Z \rightarrow E$ back isomerization can be achieved with light of two different wavelengths $h\nu_1$ and $h\nu_2$. As the azobenzene *E* isomer is thermodynamically more stable, $Z \rightarrow E$ isomerization also occurs during thermal equilibration with a half-life $\tau_{1/2}$. As the thermodynamic stabilization of the azobenzene *E* isomer (10–12 kcal mol^{-1}) exceeds the folding free energy of most proteins, azobenzene derivatives have been employed as cross-linker molecules for photocontrol over protein folding and unfolding events.[3] However, simple azobenzene derivatives require UV light for at least one photoswitching direction. For applications in vivo it was important to develop substituted azobenzene photoswitches which can be isomerized even with red light (630–660 nm).[4] In addition to the photochemistry of azobenzene derivatives, their solubility is an important issue for many biological applications. Thus, in order to improve the water solubility and biocompatibility of azobenzene photoswitches it has become our goal to combine functional carbohydrate derivatives with the photosensitive azobenzene moiety. We have shown earlier that the preparation of azobenzene glycosides is rather facile.[5–7] Moreover, azobenzene glycosides offer various options for bifunctionalization. Besides the functionalization of the azobenzene moiety, regioselective modification of the primary 6-hydroxyl group of the sugar ring is easy. In addition, typical carbohydrate protecting group chemistry allows to install a second functional group for peptide ligation at any position of the sugar chair. Thus, adjustment of distances between the two cross-linking functionalities is facilitated in such a molecular architecture.

Based on Woolley's work, cysteine side chains are frequently used for intramolecular cross-linking of peptides and proteins.[3,8,9] Then, typically chloroacetylated cross-linkers are conjugated to Cys_2 peptides by nucleophilic substitution (Figure 1 A). Consequently, we targeted the dichloroacetamidoazobenzene glycoconjugate **1** as a sweet variation of Woolley's cross-linker.[8] In addition, we aimed at thiol-ene click chemistry between alkenes and thiols[10] to achieve cross-linking (Figure 1, B). For the latter approach, the diallyl-functionalized glycoconjugate cross-linkers **2** and **3** were designed. In this paper

[a] *A. Müller, H. Kobarg, Dr. V. Chandrasekaran, J. Gronow, Prof. F. D. Sönnichsen, Prof. T. K. Lindhorst*
Otto Diels Institute of Organic Chemistry
Christiana Albertina University of Kiel
Otto-Hahn-Platz 3/4, 24118 Kiel (Germany)
Fax: (+49) 431-8807410
E-mail: tklind@oc.uni-kiel.de

Supporting information for this article is available on the WWW under http://dx.doi.org/10.1002/chem.201501571.

ChemPubSoc Europe

CHEMISTRY A European Journal Full Paper

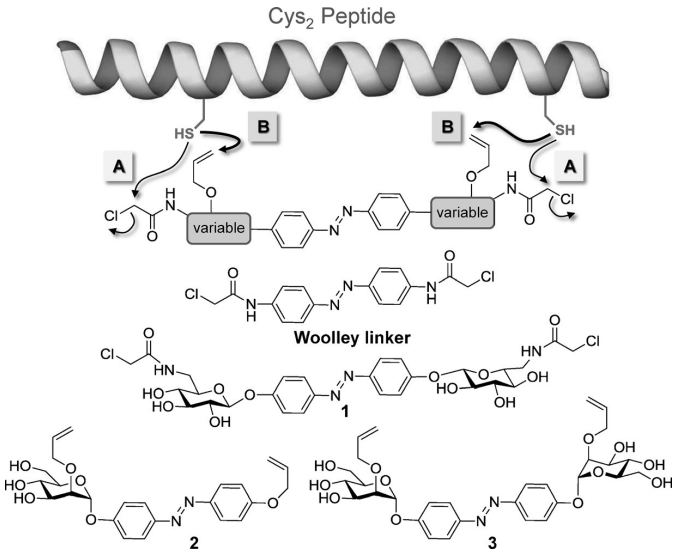

Figure 1. To control peptide/protein (un)folding, according to Woolley photoswitchable cross-linkers can be used and conjugated via cysteine side chains employing nucleophilic substitution (A) or the thiol-ene reaction (B). In order to test the benefit of carbohydrates in this approach, the azobenzene glycoconjugates **1**–**3** were targeted.

we describe the synthesis and photochromic properties of these novel azobenzene glycoconjugate cross-linkers and exemplify their ligation chemistries in first straightforward tests.

Results and Discussion

Synthesis of azobenzene glycoconjugates for protein cross-linking

The synthesis of the dichloroacetamido-functionalized glycoconjugate **1** started from the tosylated glucose derivative **4**, which was prepared according to literature (Scheme 1).[11] A nucleophilic substitution reaction using NaN_3 gave the 6-azido-functionalized glucose derivative **5** in good yield.[12] Then, treatment with hydrazinium acetate in dry DMF effected anomeric deprotection, resulting in the reducing sugar **6**.[13] Reaction of **6** with trichloroacetonitrile and DBU as the base yielded the glucosyl trichloroacetimidate **7**.[14] The glycosyl donor **7** was employed for glycosylation of *p,p'*-dihydroxy azobenzene (**8**), which was synthesized from *p*-nitrophenol in a single step according to literature.[15,16] The BF_3-etherate promoted reaction gave the symmetrical azobenzene glycoconjugate **9** in a yield of 32%. The monoglycosylated product was obtained as side product in a yield of 50%. To install the required chloroacetamido functional moieties, a Staudinger ligation[17] was performed. Chloroacetic acid in the presence of HATU and tributyl phosphine led to the symmetrical azobenzene glycoconjugate **10**. In this step, Staudinger ligation is clearly superior over the sequence of azide reduction and peptide coupling. Finally, the desired target compound **1** was obtained in high yield after deacetylation of **10** with potassium carbonate.

Next, diallylated cross-linkers were prepared. To obtain the simpler azobenzene glycoside **2**, a mono-allyloxy-functionalized azobenzene alcohol had to be prepared first. Thus, the commercially available Boc-protected aminophenol **11** was treated with allyl bromide under basic conditions to provide allyl ether **12** (Scheme 2). Then, the *N*-Boc-protecting group was removed with trifluoroacetic acid (TFA) to give the free

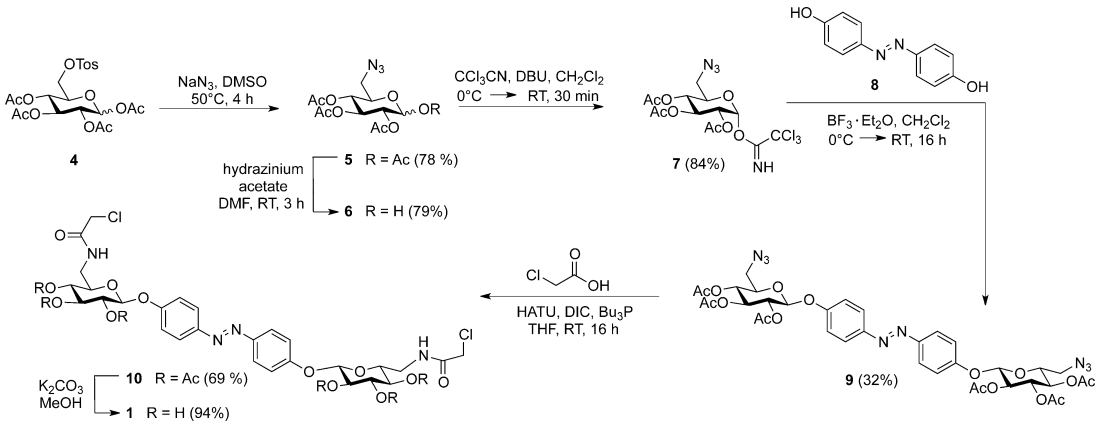

Scheme 1. Synthesis of dichloroacetamido-functionalized azobenzene glycoconjugate **1**.

ChemPubSoc Europe

CHEMISTRY A European Journal Full Paper

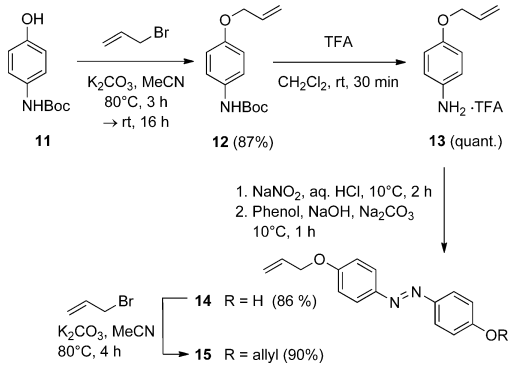

Scheme 2. Synthesis of the *O*-allyl-functionalized azobenzene derivatives **14** and **15**.

amine **13** and in the next step, classical azo coupling with phenol led to the mono-*O*-allylated azobenzene alcohol **14**. Another allylation step delivered the known diallyloxy-functionalized azobenzene **15**.[18]

For glycosylation of the azobenzene alcohol **14**, the well-known mannosyl donor **16**[19] was employed under Lewis acid catalysis leading to the α-D-glycoside **17** (Scheme 3). Deacetylation using potassium carbonate gave the unprotected azobenzene mannoside **18**. This served as starting material for the installation of the required 2-*O*-allyl function. Our first protecting group strategy comprised only four steps to achieve **2**. Butane-2,3-dione in methanol was intended to protect the 3- and 4-OH groups in **18** to yield **19**, followed by silylation and allylation. However, as mannoside **18** is poorly soluble in methanol, DMSO had to be added for the reaction with butane-2,3-dione and thus mannoside **19** was obtained only in poor yield even after four days reaction time. The crude product was subjected to silylation with TBDMS-chloride and subsequent allylation with sodium hydride and allyl bromide without intermediate purification. TFA was used for concomitant deprotection of the TBDMS group and the 3,4-acetal protecting group to yield the pure target molecule **2** after chromatography. This reaction sequence delivered **2** from **18** in only 5% overall yield. Our attempts to improve this reaction sequence failed.

An alternative synthetic sequence started with benzylidene protection of **18** using benzaldehyde dimethyl acetal (Scheme 3). This furnished the 4,6-protected mannoside **22** in 72% yield. To distinguish the 2- and 3-OH groups in the next step, dibutyl tin oxide was employed in refluxing methanol to provide an intermediate stannylene acetal. Then, the solvent was exchanged to DMF and a regioselective opening of the stannylene ring with *p*-methoxy benzylchloride (*p*MBnCl) in the presence of tetrabutyl ammonium iodide (TBAI) afforded the 2-OH-unprotected mannoside **23** in 60% over two steps. Next, reaction with allyl bromide and sodium hydride gave the desired 2-*O*-allylated azobenzene mannoside **24** quantitatively. Oxidative removal of the *p*MBn protecting group with DDQ and successive cleavage of the benzylidene acetal with TFA in

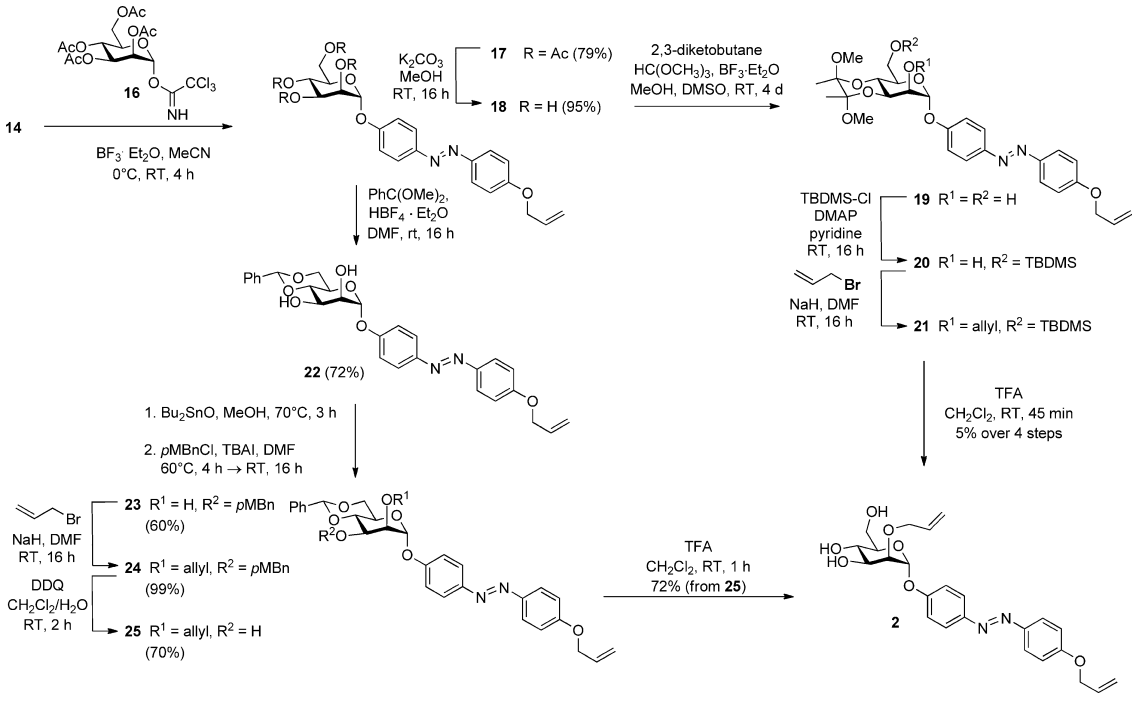

Scheme 3. Two synthetic pathways to achieve the synthesis of the di-*O*-allylated azobenzene glycoconjugate **2**.

ChemPubSoc Europe

CHEMISTRY A European Journal Full Paper

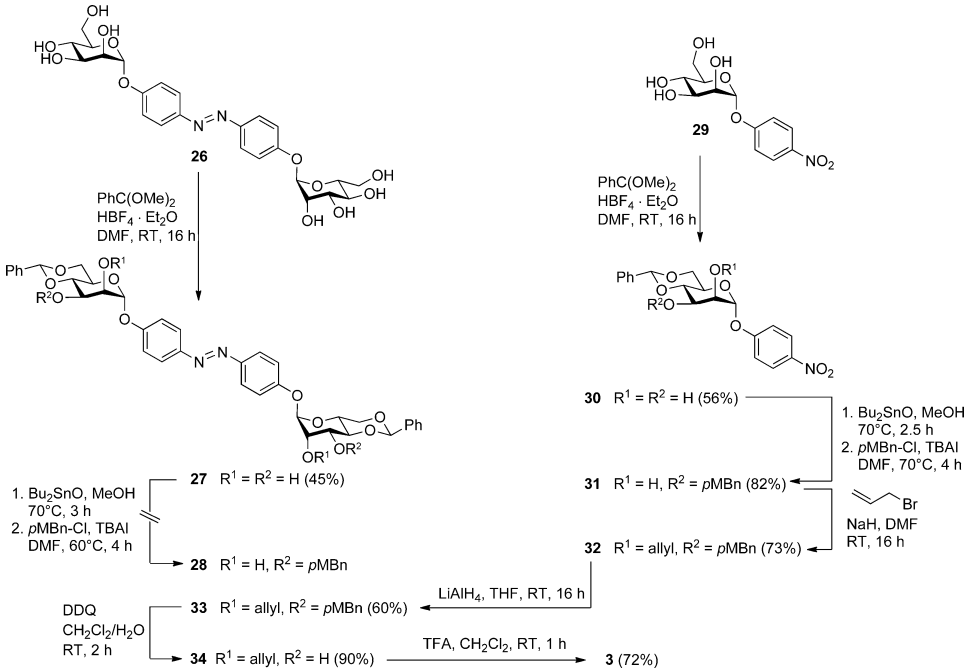

Scheme 4. Two synthetic pathways to achieve the synthesis of the di-*O*-allylated azobenzene glycoconjugate **3**.

dichloromethane led to the azobenzene glycoconjugate **2** in an overall yield of 22% over five steps.

Next, the synthesis of the second diallylated azobenzene glycoconjugate **3** was attempted according to the benzylidene route that had led to **2** (Scheme 4). Thus, the symmetrical azobenzene mannoside **26** was used as starting material and prepared according to literature.[6] Dibenzylidene protection to **27** occurred smoothly. However, the following tin-mediated regioselective protection of both sugar 3-OH groups failed, presumably due to the insolubility of the reaction partners in methanol. Only the starting material was recovered in this step. Unfortunately, a high-boiling co-solvent such as DMSO is not tolerated by the reaction. Therefore, again an alternative synthetic route was sought. To avoid solubility problems, we decided to establish the desired carbohydrate protecting group pattern first and form the azobenzene substructure at the end of the synthetic sequence. Thus, the reaction was started with *p*-nitrophenyl mannoside (**29**) that was benzylidene-protected according to the literature.[20] Then, tin-mediated regioselective 3-OH protection could be employed to deliver the 2-OH-unprotected mannoside **31**. After allylation with sodium hydride and allyl bromide the fully protected mannoside **32** was obtained. The next step was reductive azo coupling. However, the commonly used procedures using either $Zn/Ba(OH)_2$ or Mg/HCO_2HNEt_3[21] as reducing agents gave low coupling yields and led to azoxy side products. Finally, $LiAlH_4$[22] in THF turned out to effectively deliver the azobenzene glycoconjugate **33** in 60% yield. Oxidative deprotection of the *p*MBn protecting group with DDQ led to the 3-OH-free mannoside **34**, followed by acid-mediated deprotection of the benzylidene acetal to give the target diallyloxy-functionalized azobenzene bis-glycoside **3** in a yield of 90%.

First tests of the applicability of the envisaged ligation chemistries were performed with the cross-linkers **1**, **2**, **3** and **15** (Scheme 5). To test thiol-ene ligation, first the diallyloxy functionalized azobenzene derivative **15** was coupled with Boc-protected cysteamine (**35**) to yield **36** in 72% yield. With this promising result the more complex azobenzene glycoconjugates **2** and **3** were tested in a thiol-ene reaction as well, leading to **37** in 83% and to **38** in 91% yield, respectively. Then ligation of the glycoconjugate **1** with the protected cysteine derivative **39**[23] was attempted. This substitution reaction gave the corresponding azobenzene glycoamino acid conjugate **40** in 75%. Furthermore, the more complex tripeptide **41** (commercially available glutathione) was employed in a photoinduced addition to the diallyl-functionalized glycoconjugate **2** (Scheme 5). This thiol-ene reaction was carried out in a 1:2 $DMSO/H_2O$ mixture using 2,2-dimethoxy-2-phenylacetophenone (DPAP) as photoinitiator. The desired coupling product **42** was obtained in 70% isolated yield.

These results indicate that both ligation chemistries are suitable to conjugate azobenzene glycoconjugates to cysteine derivatives. Encouraged by this, we aimed at cross-linking a bifunctional peptide in the next step. Therefore the synthetic nonadecapeptide **43** (H-DTACDAEAAA-KLTACNAAR-NH_2, Scheme 6) was selected featuring two cysteine residues. Peptide **43** resembles a helical truncated sequence of a type I AFP (antifreeze protein). For cross-linking with the azobenzene gly-

ChemPubSoc Europe

CHEMISTRY A European Journal Full Paper

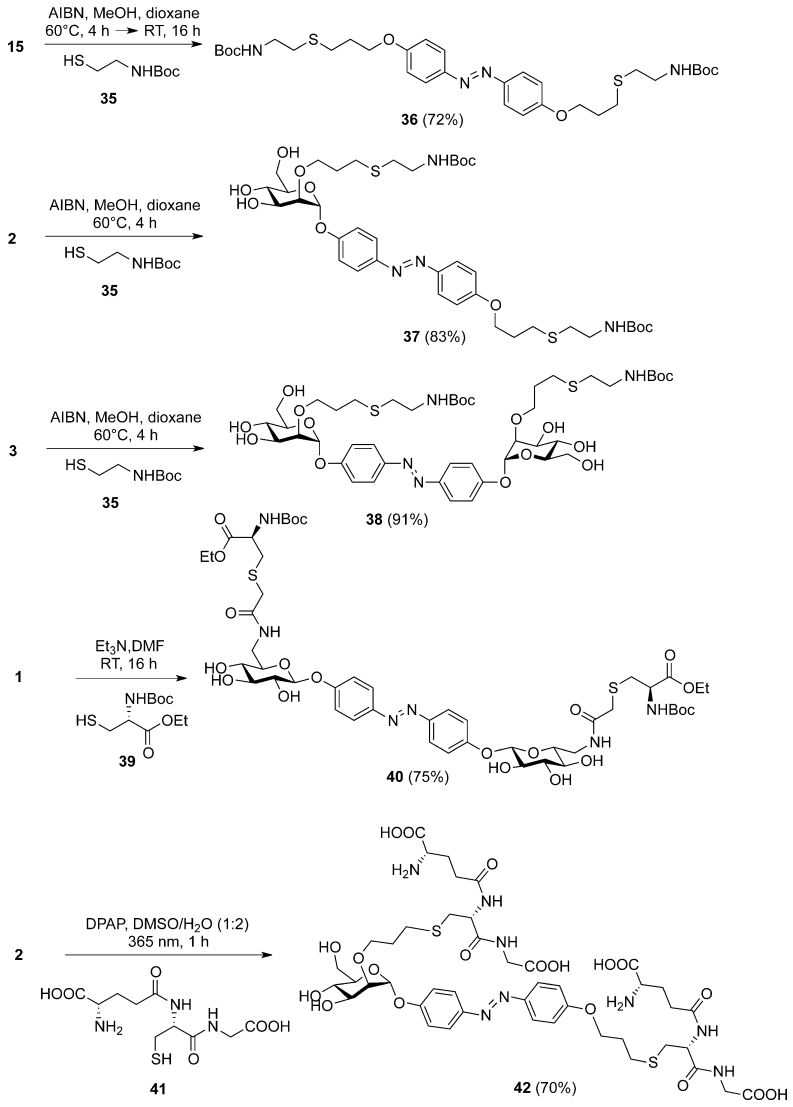

Scheme 5. First ligation tests: Thiol-ene reaction of **15**, **2**, and **3** with the *N*-Boc-protected derivative **35**; ligation of **1** in a nucleophilic substitution reaction with cysteine derivative **39**; and photoinduced ligation of **2** with the tripeptide glutathione (**41**) in aqueous solution.

coconjugate **1** it was first treated with tris(2-carboxyethyl)phosphine (TCEP) to ensure complete reduction of the sulfhydryl groups and was then combined with tetrabutylammonium iodide (TBAI) and **1** in a DMSO/buffer mixture. The course of the reaction was monitored by MALDI-TOF mass spectrometry, showing complete conversion of **43** after 24 h (Scheme 6). A more detailed product analysis by LC-MS revealed a number of side products that were co-eluted with the cross-linked peptide **44**. Apparently, the cross-linker **1** reacts with the reducing agent TCEP[24] (for details cf. Supporting Information, Figures S58 and S59). Hence, the cross-linking of peptides employing azobenzene glycoconjugates has to be advanced in future work.

Photochromic properties of difunctionalized azobenzene glycoconjugates

To effect $E \rightarrow Z$ isomerization, **1**, **2** and **3** were irradiated in deuterated DMSO employing a 365 nm light emitting diode (LED). All irradiation experiments were carried out at room temperature under exclusion of day light (Table 1). $E \rightarrow Z$ Isomerizations were monitored by ^{1}H NMR spectroscopy and UV/Vis spectroscopy. The photostationary states (PSS) were reached after 10 to 15 min. The photostationary states (PSS) were defined on the basis of the integration of the anomeric H-1 proton of the compounds in the ^{1}H NMR spectrum. The half-life times $\tau_{1/2}$ were determined by ^{1}H NMR spectroscopy by observing the thermal $Z \rightarrow E$ relaxation over time and fitting the intensity change of the H-1 protons to an exponential decay.

Fortunately, the azobenzene glycosides **1**, **2** and **3** exhibit favorable photochromic properties. Irradiation of the *E* isomers led to almost quantitative isomerization and showed that all *Z* isomers have lifetimes ranging from one to two days. Due to these extended lifetimes, separate investigation of both cross-linked peptide isomers is feasi-

Table 1. Characterization of the *E* and *Z* isomers of the azobenzene derivatives **1**, **2**, and **3**.[a]

Azobenzene glycoconjugate	H-1 of *E* and *Z* isomer [ppm]	*E*/*Z* (PSS)[b]	λ_{max} (*E* and *Z*) [nm]	Half-life, $\tau_{1/2}$ [h]
1	4.97	2:98	357.1	49.1
	4.80		447.1	
2	5.67	2:98	359.2	29.4
	5.52		440.7	
3	5.67	2:98	357.2	39.5
	5.52		445.9	

[a] For photochromic properties of **15** cf. Supporting Information. [b] According to the integration ratio of H-1 (*E*) and H-1 (*Z*) in the ^{1}H NMR spectra.

ChemPubSoc Europe

CHEMISTRY A European Journal Full Paper

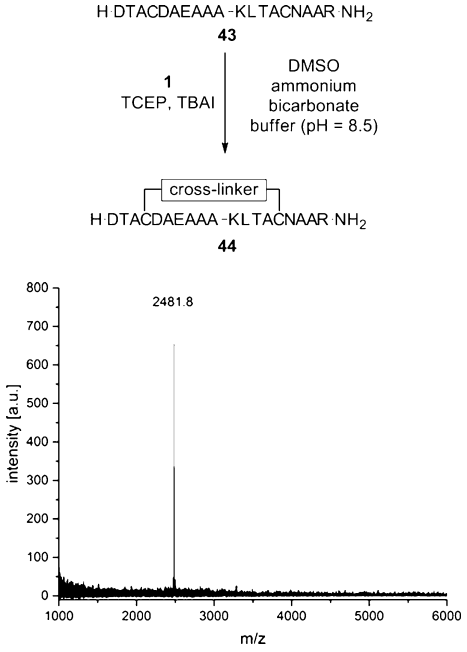

Scheme 6. Cross-linking of the nonadecapeptide **43** with the azobenzene glycoconjugate **1**. The MALDI-TOF MS spectrum after 24 h reaction time revealed the ligation product **44** as the only peak 2481.8 [M^+].

ble. Furthermore, reversible *E*/*Z* isomerization is stable over many switching cycles (Scheme 7).

Conclusion

Bifunctional azobenzene glycoconjugates have the potential to advance the existing collection of photosensitive protein cross-linkers as they show improved water solubility, for example (they are soluble in 10% DMSO in water). Furthermore, a wide variability in the distances between cross-linking functional groups is facilitated. A first computational analysis has been performed showing interesting structure-distance dependencies, which need further investigation in future work (cf. Supporting Information, Table S2). Here, we have shown the synthesis of three representatives of this new type of glycoazobenzene cross-linkers (**1**–**3**), combining a beneficial protecting group strategy with glycosylation of azobenzene alcohols. Ligation with cysteine thiol functional groups was demonstrated according to a thiol-ene reaction and via nucleophilic displacement. Moreover, first cross-linking of a helical peptide employing the azobenzene glycoconjugate **1** was shown. Thus, as the photochromic properties of the prepared azobenzene glycoconjugates are favorable they can now be employed with peptides such as antifreeze proteins (AFP) to switch their function.

Experimental Section

General methods

N-Boc-4-hydroxyaniline (**11**) was purchased from Sigma Aldrich, *p*-nitrophenyl mannoside (**29**) was purchased from Iris Biotech and 2-(Boc-amino)-ethanthiol (**35**) was purchased from Sigma Aldrich and used without further purification. Moisture-sensitive reactions were carried out in dry glassware and under a positive pressure of nitrogen. Analytical thin layer chromatography (TLC) was performed on silica-gel plates (GF 254, Merck). Visualization was achieved by UV light and/or with 10% sulfuric acid in ethanol followed by heat treatment at ~180 °C. Flash chromatography was performed on silica gel 60 (Merck, 230–400 mesh, particle size 0.040–0.063 mm) by using distilled solvents. Dichloromethane was dried over calcium hydride, THF was dried over sodium, acetonitrile was dried over calcium hydride, methanol was dried over magnesium and pyridine over potassium hydroxide all under a nitrogen atmosphere. Dry *N*,*N*-dimethylformamide, 1,4-dioxane and dimethyl sulfoxide over molecular sieves were purchased from Acros Organics and used without further purification. Melting points (m.p.) were determined on a Büchi 510 apparatus (Flawil, Switzerland). Optical rotations were measured with a PerkinElmer 241 polarimeter (sodium D-line: 589 nm, length of cell: 1 dm) in the solvents indicated. Proton (^{1}H) nuclear magnetic resonance spectra and carbon (^{13}C) nuclear magnetic resonance spectra were recorded on a Bruker DRX-500 and AV-600 spectrometer. Chemical shifts are referenced to internal tetramethylsilane or to the residual proton of the NMR solvent. Data are presented as follows: chemical shift, multiplicity (s = singlet, d = doublet, t = triplet, q = quartet, m = multiplet, and br = broad signal), coupling constant in Hertz (Hz), and integration. Full assignment of the peaks was achieved with the aid of 2D NMR techniques (^{1}H/^{1}H COSY and ^{1}H/^{13}C HSQC. For PSS determination, all ^{1}H NMR spectra were recorded in [D$_6$]DMSO (cf. Table 1). All NMR spectra of the *E* isomers of the azo-

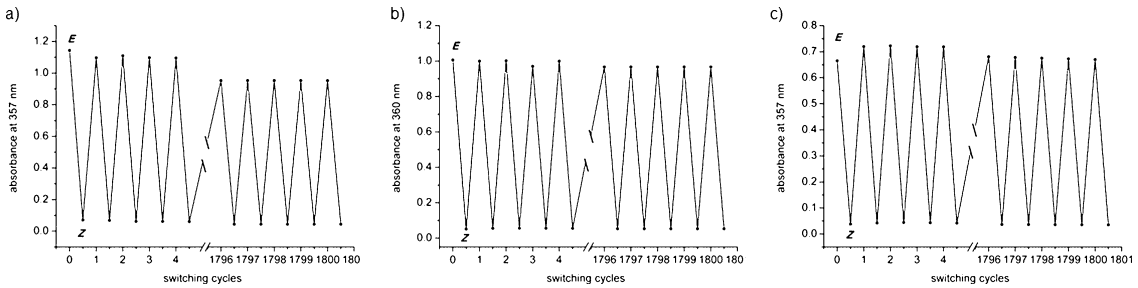

Scheme 7. Multiple *E*/*Z* isomerization (alternating irradiation with light of $\lambda = 365$ (30 s, $E \rightarrow Z$) and 435 nm (93 s, $Z \rightarrow E$), respectively) of a) **1**; b) **2**; and c) **3**; 60 μM solutions in DMSO. Only slight photobleaching is observed in case of the azobenzenze glycoconjugates **1** and **3** over ca. 1800 switching cycles.

ChemPubSoc Europe

CHEMISTRY A European Journal Full Paper

benzene derivatives were recorded after they were kept for 16 h in the dark at 40 °C. Infrared (IR) spectra were measured with a PerkinElmer FT-IR Paragon 1000 (ATR) spectrometer and are reported in cm^{-1}. ESI mass spectra were recorded on an Esquire-LC instrument from Bruker Daltonics. MALDI-TOF mass spectra were recorded on a Bruker Biflex III instrument with a 19 kV acceleration voltage, 2,5-dihydroxybenzoic acid (DHB) or α-cyano-4-hydroxycinnamic acid (CCA) were used as the matrix. Irradiation was performed using a LED (emitting 365 nm light) from Nichia Corporation (NC4U133 A) with a FWHW of 9 nm and optical power output (PO) ~1 W. UV/Vis absorption spectra were performed on PerkinElmer Lambda-241 at a temperature of 20 °C ±1 °C. Elemental analysis was performed using a Euro Vector CHNS-O-element analyzer (Euro EA 3000) at the Institute of Inorganic Chemistry, Christiana Albertina University of Kiel.

Procedures for the synthesis of **5**–**7**, **12**–**15**, **17**–**21** (leading to **2**), **27**, **36**, **37**, **38**, **40**, **42** and **44** as well as the photochromic properties of compound **15** are given in the Supporting Information.

Irradiation of *E*-configured azobenzene derivatives: The respective *E*-configured compound (5–10 mg) was dissolved in [D_6]DMSO (500 μL) in a NMR tube and irradiated for 15 min at 365 nm. Photostationary states (PSS) were reached after approximately 15 min. Then, the sample was kept in the dark, and ^{1}H NMR spectroscopy was performed immediately afterwards. For NMR data of *Z* isomers see the Supporting Information. In analogy, for UV/Vis spectroscopy, the *E*-configured azobenzene glycoside was dissolved in DMSO in a UV cuvette, irradiated for 15 min at 365 nm, and UV/Vis spectra were recorded immediately afterwards. Extinction coefficients (ε) were deduced from UV/Vis spectra measured at five different concentrations (10, 20, 40, 60, and 80 μm).

Half-life determination: Half-life $\tau_{1/2}$ determination of thermal *Z*→*E* back isomerization was determined using UV/Vis spectroscopy and ^{1}H NMR spectroscopy (for details see Supporting Information).

(*E*)-*p*,*p*′-Di-[6-(2-chloroacetylamido)-6-deoxy-β-D-glucopyranosyloxy]azobenzene (1): To a solution of **10** (42.8 mg, 51.0 μmol) in methanol (1 mL) potassium carbonate (2.80 mg, 20.4 μmol) was added. The reaction mixture was stirred for 16 h at room temperature and then the solvent was evaporated. The crude product was recrystallized from water and gave the target glycoconjugate **1** as a yellow solid (33.0 mg, 47.9 μmol, 94%). R_f = 0.10 (dichloromethane/methanol, 4:2); m.p. 236 °C$_{decomp}$; $[\alpha]_D^{23} = -23.9$ (c = 0.4 in DMSO); ^{1}H NMR (500 MHz, [D_6]DMSO, 300 K): δ = 8.22 (dd~t, ^3J(NH,H-6) = 6.0 Hz, ^3J(NH,H-6′) = 6.0 Hz, 2H, NH), 7.85–7.82 (m, 4H, Ar-H_{ortho}), 7.19–7.16 (m, 4H, Ar-H_{meta}), 5.42 (d, ^3J = 6.1 Hz, 2H, OH), 5.20 (d, ^3J = 5.3 Hz, 2H, 4-OH), 5.20 (d, ^3J = 4.6 Hz, 2H, OH), 4.97 (d, ^3J(H-1,H-2) = 7.5 Hz, 2H, H-1), 4.10 (s, 4H, CH_2Cl), 3.03 (ddd, ^3J(NH,H-6) = 6.0 Hz, ^3J(H-5,H-6) = 2.3 Hz, ^2J(H-6,H-6′) = 13.8 Hz, 2H, H-6), 3.55–3.51 (m, 2H, H-5), 3.32 (m, 4H, H-2, H-3), 3.15 (ddd, ^3J(NH,6′) = 6.0 Hz, ^3J(H-5,H-6′) = 7.9 Hz, ^2J(H-6,H-6′) = 13.8 Hz, 2H, H-6′), 3.03 ppm (ddd~dt, ^3J(H-4,H-5) = 9.0 Hz, ^3J(H-3,H-4) = 9.0 Hz, ^3J(H-4, 4-OH) = 5.3 Hz, 2H, H-4); ^{13}C NMR (125 MHz, [D_6]DMSO, 300 K): δ = 166.7 ($COCH_2$Cl), 159.9 (C-Ar_{para}), 147.4 (C-Ar_{ipso}), 124.5 (C-Ar_{ortho}), 117.1 (C-Ar_{meta}), 100.6 (C-1), 76.6 (C-3), 74.7 (C-5), 73.7 (C-2), 71.9 (C-4), 43.1 (CH_2Cl), 41.1 ppm (C-6); IR (ATR): $\tilde{\nu}$ = 3306, 1638, 1586, 1232, 1055, 1003, 846 cm^{-1}; UV/Vis (DMSO): λ_{max} (ε) = 358 nm (21 779 L mol^{-1} cm^{-1}); ESI-MS: *m*/*z* calcd for $C_{28}H_{34}N_4O_{12}$: 711.1 $[M+Na]^+$; found 711.2; elemental analysis calcd (%) $C_{27}H_{28}N_2O_7 \times 3.15\ H_2O$: C 45.07, H 5.44, N 7.51; found C 45.33, H 5.16, N 7.11.

***(E)*-*p*-(*p*′-Allyloxyphenylazo)phenyl 2-*O*-allyl-α-D-mannopyranoside (2)**: To a solution of the benzylidene-protected mannoside **25** (58.0 mg, 107 μmol) in dichloromethane (5 mL) trifluoroacetic acid (500 μL) was added. The reaction mixture was stirred for 1 h at room temperature and then the solvent was evaporated. Purification of the crude product by column chromatography (dichloromethane/methanol, 10:0.5) gave the target mannoside **2** as a yellow solid (35.0 mg, 76.6 μmol, 72%). R_f = 0.62 (dichloromethane/methanol, 10:1); m.p. 160 °C; $[\alpha]_D^{23} = +126.5$ (c = 0.2 in MeOH); ^{1}H NMR (500 MHz, [D_6]DMSO, 300 K): δ = 7.86–7.82 (m, 4H, Ar-H_{ortho}, Ar-$H_{ortho'}$), 7.29–7.26 (m, 2H, Ar-$H_{meta'}$), 7.15–7.12 (m, 2H, Ar-H_{meta}), 6.08 (ddt, ^3J(*CH*=CH_2,CH=*CH*) = 17.3 Hz, ^3J(*CH*=CH_2,CH=*CH*′) = 10.5 Hz, ^3J(OCH_2,*CH*=CH_2) = 5.2 Hz, 1H, *CH*=CH_2(Phenyl)), 5.93 (ddt, ^3J(*CH*=CH_2,CH=*CH*) = 17.3 Hz, ^3J(*CH*=CH_2,CH=*CH*′) = 10.6 Hz, ^3J(OCH_2,*CH*=CH_2) = 5.4 Hz, 1H, *CH*=CH_2(Man)), 5.67 (d, ^3J(H-1,H-2) = 1.7 Hz, 1H, H-1), 5.44 (ddt~qd, ^4J(OCH_2,CH=*CH*) = 1.7 Hz, ^3J(*CH*=CH_2,CH=*CH*) = 17.3 Hz, ^2J(CH=*CH*,CH=*CH*′) = 1.7 Hz 1H, CH=*CH*(Phenyl)), 5.35–5.29 (m, 2H, CH=*CH*(Man), CH=*CH*′(Phenyl)), 5.15 (ddt~ddd, ^4J(OCH_2,CH=*CH*′) = 1.4 Hz, ^3J(*CH*=CH_2,CH=*CH*′) = 10.6 Hz, ^2J(CH=*CH*,CH=*CH*′) = 3.4 Hz, 1H, CH=*CH*′(Man)), 4.90 (d, ^3J(OH,H-3) = 5.8 Hz, 1H, 3-OH), 4.88 (d, ^3J(OH,H-4) = 6.0 Hz, 1H, 4-OH), 4.69 (ddd~dt, ^4J(OCH_2,CH=*CH*′) = 1.7 Hz, ^4J(OCH_2,CH=*CH*) = 1.7 Hz, ^3J(OCH_2,*CH*=CH_2) = 5.2 Hz, 2H, OCH_2(Phenyl)), 4.48 (dd~t, ^3J(OH,H-6) = 6.0 Hz, ^3J(6-OH,H-6′) = 6.0 Hz, 1H, 6-OH), 4.25–4.17 (m, 2H, ManOCH_2), 3.80 (ddd, ^3J(H-2,H-3) = 3.4 Hz, ^3J(H-3,H-4) = 9.4 Hz, ^3J(OH,H-3) = 5.8 Hz, 1H, H-3), 3.71 (dd, ^3J(H-1,H-2) = 1.7 Hz, ^3J(H-2,H-3) = 3.4 Hz, 1H, H-2), 3.60 (ddd, ^3J(H-5,H-6) = 2.0 Hz, ^2J(H-6,H-6′) = 11.7 Hz, ^3J(OH,H-6) = 6.0 Hz, 1H, H-6), 3.54–3.45 (m, 2H, H-4, H-6′), 3.38 ppm (ddd, ^3J(H-4,H-5) = 9.6 Hz, ^3J(H-5,H-6) = 2.0 Hz, ^3J(H-5,H-6′) = 5.5 Hz, 1H, H-5); ^{13}C NMR (125 MHz, [D_6]DMSO, 300 K): δ = 161.0 (C-$Ar_{para'}$), 158.8 (C-Ar_{para}), 147.5 (C-Ar_{ipso}), 146.7 (C-$Ar_{ipso'}$), 136.1 (*CH*=CH_2(Man)), 133.8 (*CH*=CH_2(Phenyl)), 124.7 (C-Ar_{ortho}), 124.4 (C-$Ar_{ortho'}$), 118.3 (CH=CH_2(Phenyl)), 117.6 (C-$Ar_{meta'}$), 116.9 (CH=CH_2(Man)), 115.7 (C-Ar_{meta}), 96.8 (C-1), 78.0 (C-2), 75.7 (C-5), 72.1 (OCH_2(Man)), 70.9 (C-3), 69.0 (OCH_2(Phenyl)), 67.4 (C-4), 61.4 ppm (C-6); IR (ATR): $\tilde{\nu}$ = 3424, 3233, 2936, 1599, 1580, 1496, 1228, 1129, 983, 835 cm^{-1}; UV-Vis (DMSO): λ_{max} (ε) = 360 nm (24 765 L mol^{-1} cm^{-1}); MALDI-TOF-MS: *m*/*z* calcd for $C_{24}H_{28}N_2O_7$: 479.18 $[M+Na]^+$; found 479.28; elemental analysis calcd (%) $C_{27}H_{28}N_2O_7 \times 0.125$ MeOH: C 62.92, H 6.24, N 6.08; found C 63.17, H 6.26, N 6.06.

(*E*)-*p*,*p*′-Di-[(2-*O*-allyl-α-D-mannopyranosyloxy)]azobenzene (3): To a solution of the benzylidene-protected mannoside **34** (22.0 mg, 27.7 μmol) in dichloromethane (2 mL) trifluoroacetic acid (200 μL) was added. The reaction mixture was stirred for 1 h at room temperature and then the solvent was evaporated. Purification of the crude product by column chromatography (dichloromethane/methanol, 8:1) gave the title mannoside **3** as an orange solid (15.4 mg, 24.9 μmol, 72%). R_f = 0.29 (dichloromethane/methanol, 10:1); m.p. 108 °C; $[\alpha]_D^{23} = +79.5$ (c = 0.3 in MeOH); ^{1}H NMR (500 MHz, [D_6]DMSO, 300 K): δ = 7.86–7.82 (m, 4H, Ar-H_{ortho}), 7.29–7.26 (m, 4H, Ar-H_{meta}), 5.94 (ddt, ^3J(*CH*=CH_2,CH=*CH*) = 17.3 Hz, ^3J(*CH*=CH_2,CH=*CH*′) = 10.5 Hz, ^3J(OCH_2,*CH*=CH_2) = 5.4 Hz, 2H, *CH*=CH_2), 5.67 (d, ^3J(H-1,H-2) = 1.7 Hz, 2H, H-1), 5.32 (ddt, ^4J(OCH_2,CH=*CH*) = 2.0 Hz, ^3J(*CH*=CH_2,CH=*CH*) = 17.3 Hz, ^2J(CH=*CH*,CH=*CH*′) = 5.4 Hz 2H, CH=*CH*), 5.15 (ddt, ^4J(OCH_2,CH=*CH*′) = 4.8 Hz, ^3J(*CH*=CH_2,CH=*CH*′) = 10.5 Hz, ^2J(CH=*CH*,CH=*CH*′) = 2.0 Hz, 2H, CH=*CH*′), 4.90 (d, ^3J(H-4,4-OH) = 5.8 Hz, 2H, 4-OH), 4.88 (d, ^3J(H-3,3-OH) = 6.0 Hz, 2H, 3-OH), 4.48 (dd~t, ^3J(H-6,6-OH) = 5.8 Hz, ^3J(H-6′,6-OH) = 5.8 Hz, 2H, 6-OH), 4.24–4.17 (m, 4H, OCH_2), 3.8.81–3.78 (m, 2H, H-3), 3.71 (dd, ^3J(H-1,H-2) = 1.7 Hz, ^3J(H-2,H-3) = 3.3 Hz, 2H, H-2), 3.60 (ddd, ^3J(H-5,H-6) = 2.0 Hz, ^3J(H-6, 6-OH) = 5.8 Hz, ^2J(H-6,H-6′) = 11.7 Hz, 2H, H-6), 3.54–3.45 (m, 4H, H-4, H-6′), 3.37 ppm (ddd, ^3J(H-4,H-5) = 9.5 Hz, ^3J(H-5,H-6) = 2.0 Hz, ^3J(H-5, H-6′) = 5.9 Hz, 2H, H-5); ^{13}C NMR (125 MHz, [D_6]DMSO, 300 K): δ = 158.9 (C-Ar_{para}), 147.5 (C-Ar_{ipso}), 136.1 (CH=CH_2), 124.5 (C-Ar_{ortho}), 117.6 (CH=CH_2), 116.9 (C-Ar_{meta}), 96.8 (C-1), 78.1 (C-2), 75.7 (C-5), 72.1 (OCH_2), 70.9 (C-3), 67.4 (C-4), 61.4 ppm (C-6); IR (ATR): $\tilde{\nu}$ = 3424, 3325, 1675, 1597, 1496,

ChemPubSoc Europe

CHEMISTRY A European Journal Full Paper

1204, 1125, 992, 840 cm^{-1}; UV-Vis (DMSO): λ^{max} (ε) = 358 nm (15702 $L\,mol^{-1}\,cm^{-1}$); ESI-MS: *m/z* calcd for $C_{30}H_{38}N_2O_{12}$: 641.2 $[M+Na]^+$; found 641.4; elemental analysis calcd (%) $C_{30}H_{38}N_2O_{12}\times 0.7\ CH_2Cl_2$: C 54.38, H 5.86, N 4.13; found C 54.59, H 5.86, N 4.12.

(*E*)-*p*,*p*′-Di-(2,3,4-tri-*O*-acetyl-6-azido-6-deoxy-β-D-glucopyranosyloxy)azobenzene (9): The glucosyl donor **7** (244 mg, 514 μmol) and *p*,*p*′-dihydroxyazobenzene **8** (50.0 mg, 234 μmol) were dissolved in dry dichloromethane (5 mL) and $BF_3{\cdot}Et_2O$ (44.0 μL, 350 μmol) was added at 0 °C under N_2 atmosphere. The reaction mixture was stirred at room temperature overnight and then aq. $NaHCO_3$ (5 mL) was added to quench the reaction. It was diluted with ethyl acetate (100 mL), the phases were separated and the organic phase was washed with water (2×15 mL) and dried over Na_2SO_4. It was filtered and the filtrate concentrated under reduced pressure. Purification by flash column chromatography (cyclohexane/ethyl acetate, 8:2) gave the azobenzene glycoconjugate **9** as a pale yellow solid (62.1 mg, 73.8 μmol, 32%). R_f = 0.18 (cyclohexane/ethyl acetate, 2:1); m.p. 133 °C; $[\alpha]_D^{23} = -16.9$ (c = 0.3 in CH_2Cl_2); ^{1}H NMR (500 MHz, $CDCl_3$, 300 K,TMS): δ = 7.89 (m, 4H, Ar-H_{ortho}), 7.12 (m, 4H, Ar-H_{meta}), 5.34–5.28 (m, 4H, H-2, H-3), 5.20 (m, 2H, H-1), 5.01 (m, 2H, H-4), 3.83 (ddd, ^3J(H-4,H-5) = 9.9 Hz, ^3J(H-5,H-6) = 7.3 Hz, ^3J(H-5,H-6′) = 2.7 Hz, 2H, H-5), 3.45 (dd, ^2J(H-6,H-6′) = 13.4 Hz, ^3J(H-5,H-6) = 7.3 Hz, 2H, H-6), 3.35 (dd, ^2J(H-6,H-6′) = 13.4 Hz, ^3J(H-5,H-6′) = 2.7 Hz, 2H, H-6′), 2.08, 2.07, 2.05 ppm (each s, each 6H, 6 $COCH_3$); ^{13}C NMR (125 MHz, $CDCl_3$, 300 K, TMS): δ = 170.0, 169.5, 169.3 ($COCH_3$), 158.5 (C-Ar_{para}), 148.7 (C-Ar_{ipso}), 124.5 (C-Ar_{ortho}), 117.3 (C-Ar_{meta}), 98.8 (C-1), 73.7 (C-5), 72.5 (C-3), 71.2 (C-2), 69.4 (C-4), 51.3 (C-6), 20.6, 20.6, 20.6 ppm (6 $COCH_3$); IR (ATR): $\tilde{\nu}$ = 2993, 2100, 1745, 1587, 1215, 1040, 847 cm^{-1}; ESI-MS: *m/z* calcd for $C_{36}H_{40}N_8O_{16}$: 863.26 $[M+Na]^+$; found 863.25.

(*E*)-*p*,*p*′-Di-[2,3,4-tri-*O*-acetyl-6-(2-chloroacetylamido)-6-deoxy-β-D-glucopyranosyloxy]azobenzene (10): A mixture of **9** (50.0 mg, 59.5 μmol) and HATU (67.9 mg, 179 μmol) was dried under reduced pressure for about 30 min. Then, a solution of chloroacetic acid (16.9 mg, 179 μmol) in dry THF (7 mL) was added under inert atmosphere. The reaction mixture was cooled to 0 °C and DIC (27.9 μL, 179 μmol) was added followed by the addition of Bu_3P (36.0 mg, 179 μmol). The reaction mixture was stirred at room temperature for 16 h and then water (10 mL) was added. It was extracted with ethyl acetate (3×10 mL), and the combined organic phases were dried over Na_2SO_4. It was filtered and the filtrate concentrated under reduced pressure. Purification by flash column chromatography (dichloromethane/ethyl acetate, 6:4) provided **10** as a pale yellow solid (38.6 mg, 41.1 μmol, 69%). R_f = 0.18 (cyclohexane/ethyl acetate, 2:1); m.p. 124 °C; $[\alpha]_D^{23} = -22.7$ (c = 0.2 in MeOH); ^{1}H NMR (500 MHz, CD_3CN, 300 K): δ = 7.90–7.87 (m, 4H, Ar-H_{ortho}), 7.19–7.16 (m, 4H, Ar-H_{meta}), 7.06 (dd ~ t, ^3J(NH,H-6) = 5.9 Hz, ^3J(NH,H-6′) = 6.1 Hz, 2H, NH), 5.38–5.35 (m, 4H, H-1, H-3), 5.23 (dd, ^3J(H-1,H-2) = 7.9 Hz, ^3J(H-2,H-3) = 9.8 Hz, 2H, H-2), 5.02 (dd ~ t, ^3J(H-3,H-4) = 9.7 Hz, ^3J(H-4,H-5) = 9.7 Hz, 2H, H-4), 4.03 (m, 4H, CH_2Cl), 3.99 (ddd, ^3J(H-4,H-5) = 9.7 Hz, ^3J(H-5,H-6) = 7.0 Hz, ^3J(H-5,H-6′) = 2.8 Hz, 2H, H-5), 3.58 (ddd, ^3J(NH,H-6) = 5.9 Hz, ^3J(H-5,H-6) = 2.8 Hz, ^2J(H-6,H-6′) = 14.4 Hz, 2H, H-6′), 3.39–3.34 (m, 2H, H-6), 2.04, 2.03, 1.99 ppm (each s, each 6H, 6 $COCH_3$); ^{13}C NMR (125 MHz, CD_3CN, 300 K) δ = 170.8, 170.7, 170.3 ($COCH_3$), 167.2 ($COCH_2Cl$), 159.7 (C-Ar_{para}), 149.2 (C-Ar_{ipso}), 125.1 (C-Ar_{ortho}), 118.0 (C-Ar_{meta}), 98.9 (C-1), 73.3 (C-5), 73.0 (C-3), 71.7 (C-2), 70.2 (C-4), 43.5 (CH_2Cl), 40.5 (C-6), 20.9, 20.8, 20.7 ppm (6 $COCH_3$); IR (ATR): $\tilde{\nu}$ = 3306, 1749, 1672, 1371, 1219, 1055, 1036, 845 cm^{-1}; ESI-MS: *m/z* calcd for $C_{36}H_{40}N_8O_{16}$: 863.26 $(M+Na)^+$; found 863.25.

***(E)*-*p*-(*p*′-Allyloxyphenylazo)phenyl 2-*O*-allyl-4,6-*O*-benzylidene-α-D-mannopyranoside (25)**: To a solution of the mannoside **24** (110 mg, 165 μmol) in dichloromethane (2 mL) and water (100 μL) DDQ (75.0 mg, 331 μmol) was added. The reaction mixture was stirred for 2 h at room temperature and then saturated aq. $NaHCO_3$ solution (5 mL) was added. The mixture was extracted with dichloromethane (2×10 mL) and the combined organic phases were washed with sat. aq. $NaHCO_3$ solution (2×10 mL) and dried over $MgSO_4$. It was filtered and the filtrate concentrated under reduced pressure. Purification of the crude product by column chromatography (cyclohexane/ethyl acetate, 3:1→2:1) gave the mannoside **25** as a yellow solid (63.0 mg, 116 μmol, 70%). R_f = 0.49 (cyclohexane/ethyl acetate, 3:1); m.p. 156 °C; $[\alpha]_D^{23} = +173.8$ (c = 0.7 in CH_2Cl_2); ^{1}H NMR (500 MHz, [D_6]DMSO, 300 K): δ = 7.88–7.84 (m, 4H, Ar-H_{ortho}, Ar-$H_{ortho'}$), 7.46–7.44 (m, 2H, Ar-H_{Benz}), 7.38–7.36 (m, 3H, Ar-H_{Benz}), 7.31–7.28 (m, 2H, Ar-$H_{meta'}$), 7.15–7.12 (m, 2H, Ar-H_{meta}), 6.08 (ddt, ^3J(C*H*=CH_2,CH=C*H*) = 17.2 Hz, ^3J(C*H*=CH_2,CH=C*H*′) = 10.5 Hz, ^3J(OCH_2,C*H*=CH_2) = 5.2 Hz, 1H, C*H*=CH_2(Phenyl)), 5.97 (ddt, ^3J(C*H*=CH_2,CH=C*H*) = 17.3 Hz, ^3J(C*H*=CH_2,CH=C*H*′) = 10.8 Hz, ^3J(OCH_2,C*H*=CH_2) = 5.5 Hz, 1H, C*H*=CH_2(Man)), 5.82 (d, ^3J(H-1,H-2) = 1.5 Hz, 1H, H-1), 5.67 (s, 1H, CHPh), 5.44 (ddt ~ qd, ^4J(OCH_2,CH=C*H*) = 1.7 Hz, ^3J(C*H*=CH_2,CH=C*H*) = 17.2 Hz, ^2J(CH=C*H*,CH=C*H*′) = 1.7 Hz 1H, CH=C*H*(Phenyl)), 5.35 (ddt ~ ddd, ^4J(OCH_2,CH=C*H*) = 1.7 Hz, ^3J(C*H*=CH_2,CH=C*H*) = 17.3 Hz, ^2J(CH=C*H*,CH=C*H*′) = 3.5 Hz 1H, CH=C*H*(Man)), 4.68 (ddd ~ dt, ^4J(OCH_2,CH=C*H*′) = 1.7 Hz, ^4J(OCH_2,CH=C*H*) = 1.7 Hz, ^3J(OCH_2,C*H*=CH_2) = 5.2 Hz, 2H, OCH_2(Phenyl)), 5.28–5.27 (m, 1H, CH=C*H*′(Man)), 4.07 (ddd, ^3J(H-2,H-3) = 3.5 Hz, ^3J(H-3,H-4) = 9.8 Hz, ^3J(OH,H-3) = 6.2 Hz, 1H, H-3), 4.02 (dd, ^3J(H-5,H-6) = 4.7 Hz, ^2J(H-6,H-6′) = 10.1 Hz, 1H, H-6), 3.96 (dd ~ t, ^3J(H-3,H-4) = 9.8 Hz, ^3J(H-4,H-5) = 9.8 Hz, 1H, H-4), 3.83 (dd, ^3J(H-1,H-2) = 1.5 Hz, ^3J(H-2,H-3) = 3.5 Hz, 1H, H-2), 3.77 (dd ~ t, ^3J(H-5,H-6′) = 10.1 Hz, ^2J(H-6,H-6′) = 10.1 Hz, 1H, H-6′), 3.69–3.65 ppm (m, 1H, H-5); ^{13}C NMR (125 MHz, [D_6]DMSO, 300 K): δ = 161.1 (C-$Ar_{para'}$), 158.0 (C-Ar_{para}), 147.7 (C-Ar_{ipso}), 146.7 (C-$Ar_{ipso'}$), 138.2 (C-Ar_{Benz}), 135.9 (*C*H=CH_2(Man)), 133.8 (*C*H=CH_2(Phenyl)), 129.3 (C-Ar_{Benz}), 128.5 (C-Ar_{Benz}), 126.8 (C-Ar_{Benz}), 124.7 (C-Ar_{ortho}), 124.4 (C-$Ar_{ortho'}$), 118.3 (CH=*C*H_2(Phenyl)), 117.6 (C-Ar_{meta}), 117.3 (CH=*C*H_2(Man)), 115.7 (C-$Ar_{meta'}$), 101.6 (*C*HPh), 96.9 (C-1), 78.8 (C-2), 78.6 (C-4), 72.7 (OCH_2(Man)), 69.0 (OCH_2(Phenyl)), 68.1 (C-6), 67.9 (C-3), 65.5 ppm (C-5); IR (ATR): $\tilde{\nu}$ = 3392, 2920, 1596, 1497, 1457, 1247, 1093, 984, 839 cm^{-1}; ESI-MS: *m/z* calcd for $C_{31}H_{32}N_2O_7$: 545.225 $[M+H]^+$; found 545.228.

(*E*)-*p*,*p*′-Di-(2-*O*-allyl-4,6-*O*-benzylidene-α-D-mannopyranosyloxy)azobenzene (34): To a solution of the mannoside **33** (42.0 mg, 40.4 μmol) in dichloromethane (2 mL) and water (100 μL) DDQ (37.0 mg, 161 μmol) was added. The reaction mixture was stirred for 2 h at room temperature and then saturated aq. $NaHCO_3$ solution (5 mL) was added. The mixture was extracted with dichloromethane (2×10 mL) and the combined organic phases were washed with sat. aq. $NaHCO_3$ solution (2×10 mL). It was dried over $MgSO_4$, filtered and the filtrate was concentrated under reduced pressure. Purification of the crude product by column chromatography (cyclohexane/ethyl acetate, 3:1→2:1) gave the mannoside **34** as a yellow solid (29.0 mg, 36.5 μmol, 90%). R_f = 0.43 (cyclohexane/ethyl acetate, 2:1); m.p. 202 °C; $[\alpha]_D^{23} = +145.6$ (c = 0.1 in DMSO); ^{1}H NMR (600 MHz, [D_6]DMSO, 298 K): δ = 7.89–7.88 (m, 4H, Ar-H_{ortho}), 7.46–7.44 (m, 4H, Ar-H_{Benz}), 7.39–7.37 (m, 6H, Ar-H_{Benz}), 7.31–7.30 (m, 4H, Ar-H_{meta}), 6.01–5.94 (m, 2H, C*H*=CH_2), 5.74 (d ~ s, 2H, H-1), 5.68 (s, 2H, CHPh), 5.38–5.34 (m, 2H, CH=C*H*), 5.32 (d, ^3J(OH,H-3) = 6.0 Hz, 1H, 3-OH), 5.19–5.17 (m, 2H, CH=C*H*′), 4.28–4.27 (m, 4H, OCH_2), 4.07 (ddd, ^3J(H-4,H-5) = 9.6 Hz, ^3J(H-5,H-6) = 5.8 Hz, ^3J(H-5,H-6′) = 3.7 Hz, 2H, H-5), 4.02 (dd, ^3J(H-5,H-6) = 5.8 Hz, ^2J(H-6,H-6′) = 10.1 Hz, 2H, H-6), 3.96 (dd ~ t, ^3J(H-3,H-4) = 9.6 Hz, ^2J(H-4,H-5) = 9.6 Hz, 2H, H-4), 3.84–3.83 (m, 2H, H-2), 3.79–3.76 (m, 2H, H-6′), 3.69–3.65 ppm (m, 2H, H-3); ^{13}C NMR (150 MHz, [D_6]DMSO, 298 K): δ = 157.7 (C-Ar_{para}), 147.2 (C-Ar_{ipso}), 137.8 (C-Ar_{Benz}), 135.5 (CH=CH_2), 128.9 (C-Ar_{Benz}), 128.0 (C-Ar_{Benz}), 126.4 (C-

ChemPubSoc Europe

CHEMISTRY A European Journal Full Paper

Ar_{Benz}), 124.1 (C-Ar_{ortho}), 117.2 (CH=CH_2), 116.8 (C-Ar_{meta}), 101.1 (CHPh), 96.4 (C-1), 78.3 (C-4), 78.1 (C-2), 72.3 (OCH_2), 67.7 (C-6), 67.4 (C-5), 65.0 ppm (C-3); IR (ATR): $\tilde{\nu}$ = 3358, 2916, 1599, 1496, 1240, 1092, 976, 847 cm^{-1}; MALDI-TOF-MS: *m/z* calcd for $C_{44}H_{46}N_2O_{12}$: 817.29 $[M+Na]^+$; found 817.58.

Acknowledgements

We thank the Deutsche Forschungsgemeinschaft (DFG, collaborative network SFB 677) and Christiana Albertina University (Landesgraduiertenstipendium for J.G.) for financial support.

Keywords: azobenzene glycoconjugates · cysteine ligation · molecular switches · peptide cross-linking · photocontrol

[1] a) F. Bonardi, G. London, N. Nouwen, B. L. Feringa, A. J. M. Driessen, *Angew. Chem. Int. Ed.* **2010**, *49*, 7234 – 7238; *Angew. Chem.* **2010**, *122*, 7392 – 7396; b) A. Mourot, T. Fehrentz, D. Bautista, D. Trauner, R. Kramer, *Nat. Methods* **2012**, *9*, 396 – 402; c) R. S. Stoll, S. Hecht, *Angew. Chem. Int. Ed.* **2010**, *49*, 5054 – 5075; *Angew. Chem.* **2010**, *122*, 5176 – 5200; d) W. Szymanski, J. M. Beierle, H. A. V. Kistemaker, W. A. Velema, B. L. Feringa, *Chem. Rev.* **2013**, *113*, 6114 – 6178; e) A. Beharry, G. A. Woolley, *Chem. Soc. Rev.* **2011**, *40*, 4422 – 4437; f) B. Feringa, *Molecular Switches*, Wiley-VCH, Weinheim, **2001**.

[2] G. S. Hartley, *Nature* **1937**, *140*, 281 – 281.

[3] a) S. Samanta, A. Babalhavaeji, M. Dong, G. A. Woolley, *Angew. Chem. Int. Ed.* **2013**, *52*, 14127 – 14130; *Angew. Chem.* **2013**, *125*, 14377 – 14380; b) A. M. Ali, G. A. Woolley, *Org. Biomol. Chem.* **2013**, *11*, 5325 – 5331 and articles cited therein.

[4] S. Samanta, A. A. Beharry, O. Sadovski, T. M. McCormick, A. Babalhavaeji, V. Tropepe, G. A. Woolley, *J. Am. Chem. Soc.* **2013**, *135*, 9777 – 9784.

[5] V. Chandrasekaran, T. K. Lindhorst, *Chem. Commun.* **2012**, *48*, 7519 – 7521.

[6] V. Chandrasekaran, E. Johannes, H. Kobarg, F. D. Sönnichsen, T. K. Lindhorst, *Chem. Open* **2014**, *3*, 99 – 108.

[7] V. Chandrasekaran, K. Kolbe, F. Beiroth, T. K. Lindhorst, *Beilstein J. Org. Chem.* **2013**, *9*, 223 – 233.

[8] J. R. Kumita, O. S. Smart, G. A. Woolley, *Proc. Natl. Acad. Sci. USA* **2000**, *97*, 3803 – 3808.

[9] G. A. Woolley, *Acc. Chem. Res.* **2005**, *38*, 486 – 493.

[10] a) C. E. Hoyle, C. N. Bowman, *Angew. Chem. Int. Ed.* **2010**, *49*, 1540 – 1573; *Angew. Chem.* **2010**, *122*, 1584 – 1617; b) A. Dondoni, *Angew. Chem. Int. Ed.* **2008**, *47*, 8995 – 8997; *Angew. Chem.* **2008**, *120*, 9133 – 9135; c) M. van Dijk, D. T. S. Rijkers, R. M. J. Liskamp, C. F. van Nostrum, W. E. Hennink, *Bioconjugate Chem.* **2009**, *20*, 2001 – 2016; d) A. Dondoni, A. Massi, P. Nanni, A. Roda, *Chem. Eur. J.* **2009**, *15*, 11444 – 11449.

[11] E. Hardegger, R. M. Montavon, *Helv. Chim. Acta* **1946**, *29*, 1199 – 1203.

[12] V. Maunier, P. Boullanger, D. Lafont, D. Y. Chevalier, *Carbohydr. Res.* **1997**, *299*, 49 – 57.

[13] S. Mehta, M. Meldal, V. Ferro, J. Duus, K. Bock, *J. Chem. Soc. Perkin Trans. 1* **1997**, 1365 – 1374.

[14] C.-W. T. Chang, Y. Hui, B. Elchert, J. Wang, J. Li, R. Rai, *Org. Lett.* **2002**, *4*, 4603 – 4606.

[15] R. Willstätter, M. Benz, *Ber. Dtsch. Chem. Ges.* **1906**, *39*, 3492 – 3503.

[16] W.-h. Wei, T. Tomohiro, M. Kodaka, H. Okuno, *J. Org. Chem.* **2000**, *65*, 8979 – 8987.

[17] N. Röckendorf, T. K. Lindhorst, *J. Org. Chem.* **2004**, *69*, 4441 – 4445.

[18] a) A. Shukurov, S. D. Nasirdinov, A. G. Makhsumov, N. N. Edgarov, *J. Gen. Chem. USSR (Engl. Transl.)* **1986**, *56*, 2579 – 2582; b) A. Shukurov, S. D. Nasirdinov, A. G. Makhsumov, N. N. Edgarov, *J. Gen. Chem. USSR (Engl. Transl.)* **1986**, *56*, 2282–2284; c) S. Guo, W. Chaikittisilp, T. Okubo, A. Shimojima, *RSC Adv.* **2014**, *4*, 25319 – 25325.

[19] K. H. Jung, M. Hoch, R. R. Schmidt, *Liebigs Ann. Chem.* **1989**, 1099 – 1106.

[20] H.-G. Lerchen, K. von dem Bruch, U. Petersen, J. Baumgarten, N. Piel, H.-P. Antonicek, W. Weichel, M. Sperzel, K. D. Bremm, United States Patent, **2001**, US 6271342 B1.

[21] G. R. Srinivasa, K. Abiraj, D. C. Gowda, *Aust. J. Chem.* **2004**, *57*, 609 – 610.

[22] R. F. Nystrom, W. G. Brown, *J. Am. Chem. Soc.* **1948**, *70*, 3738 – 3740.

[23] J. C. Namyslo, C. Stanitzek, *Synthesis* **2006**, 3367 – 3369.

[24] D. E. Shafer, J. K. Inman, A. Lees, *Anal. Biochem.* **2000**, *282*, 161 – 164.

Received: April 29, 2015
Published online on August 6, 2015

3.2.2 Hetero-bifunctional azobenzene glycoconjugates for bioorthogonal photosensitive cross-linking of petides and proteins

"Synthesis of Hetero-bifunctional Azobenzene Glycoconjugates for Bioorthogonal Cross-Linking of Proteins"

A. Müller, T. K. Lindhorst, *Eur. J. Org. Chem.* **2016**, 1669–1672.

DOI: 10.1002/ejoc.201600136

Abstract: Modification of proteins with azobenzene derivatives allows their form and function to be controlled by photochemical *E/Z* isomerization of the azobenzene N=N bond. Because azobenzene glycoconjugates (ABGs) are particularly promising cross-linkers for the modification of peptides and proteins, we advanced the collection of so far known homo-bifunctional ABGs with the synthesis of hitherto unknown hetero-bifunctionalized ABGs. Alkyne and alkene, alkyne and sulfhydryl, and azido and alkene functions were combined in one molecule to serve as bioorthogonal reaction pairs. With this, access to a multitude of photosensitive proteins is provided.

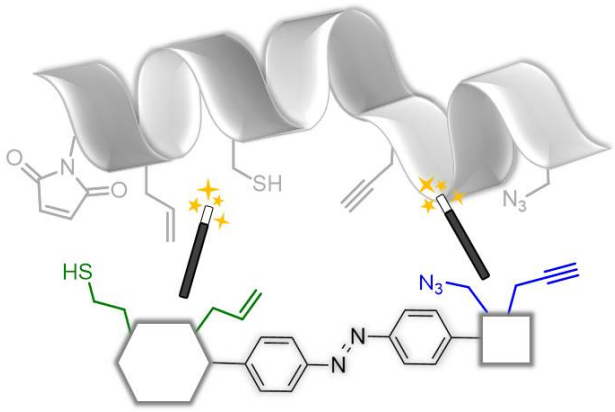

TOC Graphic 3.2. Cross-linking proteins with azobenzene derivatives allows their form and function to be controlled photochemically. For this, hetero-bifunctionalized glycoazobenzene cross-linker molecules are synthesised to enable bioorthogonal modification of proteins. Alkene, alkyne, azido, and sulfhydryl functional groups are combined accordingly.

Scientific contribution to this paper

I carried out all experimental work of this project. T. K. Lindhorst and I wrote the article together.

ChemPubSoc Europe

DOI: 10.1002/ejoc.201600136

EurJOC European Journal of Organic Chemistry

Communication

Bioorthogonal Cross-Linkers

Synthesis of Hetero-bifunctional Azobenzene Glycoconjugates for Bioorthogonal Cross-Linking of Proteins

Anne Müller[a] and Thisbe K. Lindhorst*[a]

Abstract: Modification of proteins with azobenzene derivatives allows their form and function to be controlled by photochemical *E*/*Z* isomerization of the azobenzene N=N bond. Because azobenzene glycoconjugates (ABGs) are particularly promising cross-linkers for the modification of peptides and proteins, we advanced the collection of so far known homo-bifunctional ABGs with the synthesis of hitherto unknown hetero-bifunctionalized ABGs. Alkyne and alkene, alkyne and sulfhydryl, and azido and alkene functions were combined in one molecule to serve as bioorthogonal reaction pairs. With this, access to a multitude of photosensitive proteins is provided.

Introduction

Currently there is tremendous interest in the development of functional molecules for the specific modification of peptides and proteins. Important fields of application are related to the labeling of proteins in biological environments, identification of peptides in complex mixtures, and changing and control of structure and function of proteins.[1]

Lately, azobenzene derivatives have been employed for intramolecular protein modification; this has resulted in photosensitive conjugates that can be reversibly manipulated by light. Hence, irradiation of azobenzene-modified proteins at appropriate wavelengths effects *E*/*Z* isomerization of the azobenzene unit, and concomitantly, the whole protein structure can be switched between two different states.[2] This approach allows modification of protein function with spatiotemporal resolution under minimally invasive conditions.

Ideally, the azobenzene derivatives used for protein modification should be water soluble and biocompatible to allow biological studies in a natural environment. Thus, we recently introduced bifunctional azobenzene glycoconjugates for cysteine-based cross-linking of peptides.[3] As azobenzene glycosides have favorable photochromic properties, glycoazobenzene cross-linkers are promising candidates for photoswitching of protein function. In addition, carbohydrates offer a number of advantages in protein modification. They are nontoxic, improve water solubility, and their derivatization can be easily adjusted to control distances between functional groups and their orientation. This was exemplified in our work by the synthesis of dichloroacetamido-functionalized and di-*O*-allylated azobenzene glycoconjugates.[3] However, the application of such homo-difunctionalized cross-linkers has limitations. Especially, the possibility of controlled consecutive cross-linking is excluded. Also, the orthogonal functionalization of peptides, modified with unnatural amino acids, cannot be fully addressed. Therefore, it has become our goal to advance the existing collection of homo-bifunctional glycoazobenzene cross-linkers by the synthesis of orthogonally bifunctionalized examples. On the basis of state-of-the-art approaches in the field of bioorthogonal ligations,[4] we focused on sulfhydryl, alkene, alkyne, and azido functional groups as complementary reaction pairs (Figure 1). Sulfhydryl groups can ligate with maleimides or alkene functionalities according to thiol–ene coupling.[5] The thiol–ene reaction is orthogonal to cross-linking between azido and alkyne functional groups, which can be ligated in a Cu^{I}-catalyzed[6] and copper-free click reaction,[7] respectively. Also, Staudinger–Bertozzi ligation[8] can be envisaged to achieve bioorthogonal peptide conjugation with, for example, an azido–alkene hetero-bifunctional cross-linker.

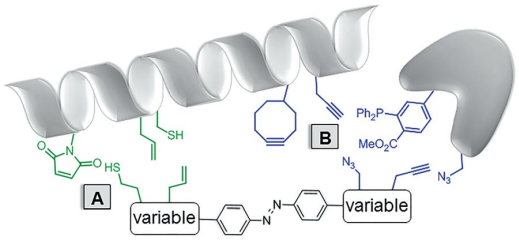

Figure 1. Hetero-bifunctional azobenzene derivatives enable the orthogonal inter- and intramolecular cross-linking of (modified) proteins. For cross-linking we aimed at thiol–ene coupling between thiols and alkenes or maleimides (a). This is compatible with a click reaction between azido and alkyne functional groups as well as Staudinger–Bertozzi ligation (b). As variable, carbohydrates were chosen and functionalized appropriately.

[a] *Otto Diels Institute of Organic Chemistry, Christiana Albertina University of Kiel,*
Otto-Hahn-Platz 3/4, 24118 Kiel, Germany
E-mail: tklind@oc.uni-kiel.de
www.otto-diels-institut.de/lind/index.html

Supporting information for this article is available on the WWW under http://dx.doi.org/10.1002/ejoc.201600136.

ChemPubSoc Europe

EurJOC European Journal of Organic Chemistry
Communication

Results and Discussion

We report on the synthesis of hetero-bifunctional (glyco)azobenzene derivatives for bioorthogonal cross-linking of proteins with unnatural amino acid residues.

Quite clearly, even azobenzene as such can be converted into many variations of bifunctional derivatives.[9,10] For example, *p,p'*-dihydroxyazobenzene has been used for the synthesis of symmetrical azobenzene glycosides;[3,10,11] however, it does not offer entry into hetero-bifunctional azobenzene derivatives. Thus, we employed propargyloxy-functionalized azobenzene alcohol **4** in our earlier work,[11] but here we thought of a more rational approach to *p,p'*-hetero-bifunctionalized azobenzene derivatives (Scheme 1). The synthesis started from commercially available *N*-*tert*-butoxycarbonyl (Boc)-aminophenol **1**. A synthetic sequence of propargylation to **2**,[12] removal of the Boc protecting group, and subsequent azo coupling of **3**[13] with phenol furnished azobenzene alcohol **4**[11] in 61 % overall yield. Then, allylation under classical Williamson etherification conditions gave hetero-bifunctionalized azobenzene **5**. Propargyl alcohol **4** could also be converted into thioacetate **6** with thioacetic acid *S*-(3-bromopropyl) ester under basic conditions to provide azobenzene derivative **7** after deacetylation with sodium methoxide in high yield. Azobenzene derivatives **5** and **7** allow bioorthogonal cross-linking according to click chemistry[6,7] on the one hand and to thiol–ene coupling[5] on the other hand. Cross-linker **7** also enables maleimide–sulfhydryl coupling, which has been widely used in protein conjugation and labeling.[4,14]

In the next step, we wished to include carbohydrate moieties in the azobenzene cross-linkers to improve their water solubility. In addition, if functional groups are installed at various positions of a sugar ring, the distance between two orthogonal functional groups can be adjusted. As we recently optimized access to 2-*O*-allylmannosyloxy azobenzene derivatives,[3] we utilized this synthetic pathway to access alkene–alkyne-bifunctional azobenzene glycoconjugate **14** (Scheme 2). Hence, known azobenzene mannoside **8**,[11] which can be obtained from D-mannose in four steps, was deprotected with potassium carbonate to afford OH-free azobenzene mannoside **9**[15] in 79 % yield. This was then subjected to benzylidenation under catalysis of tetrafluoroboric acid in the presence of benzaldehyde dimethyl acetal to provide 4,6-*O*-benzylidene acetal **10** in 76 % yield. To selectively protect the hydroxy group at C3 of diol **10**, dibutyltin oxide was employed in refluxing methanol to form a stannylidene acetal intermediate. After exchanging the solvent to dimethylformamide the stannylidene acetal was subsequently treated with *p*-methoxybenzyl chloride (PMBCl) and tetrabutylammonium iodide to afford exclusively 3-*O*-PMB-protected ether **11** in 84 % yield over two steps. Reaction with sodium hydride and propargyl bromide then gave fully protected azobenzene mannoside **12** in 86 % yield. Oxidative removal of the PMB group in **12** with 2,3-dichloro-5,6-dicyano-1,4-benzoquinone (DDQ) and subsequent cleavage of the benzylidene acetal with TFA in dichloromethane furnished desired 2-*O*-propargylated azobenzene glycoconjugate **14**.

Carbohydrate chemistry also provides facile access to hetero-bifunctional azobenzene glycosides that combine an azido functional group with an orthogonal alkene functionality. For this, 6-azido-6-deoxyglucosyl donor **18**[16] can be utilized, which is available in five steps from D-glucose.[17] Tosylate **15** was obtained after tosylation and acetylation in one pot and undergoes nucleophilic substitution to yield azide **16** and after anomeric modification functionalized glucosyl donor **18** (Scheme 3). Then, BF_3·OEt_2-catalyzed glycosylation of recently described allylated azobenzene derivative **19**[3] was performed in acetonitrile owing to the limited solubility of **19**. This glycosylation reaction led to bifunctional azobenzene glycoside **20** in moderate yield (Scheme 3). Final deprotection gave pure **21** in excellent yield. The azido group of azobenzene glycoside **21**

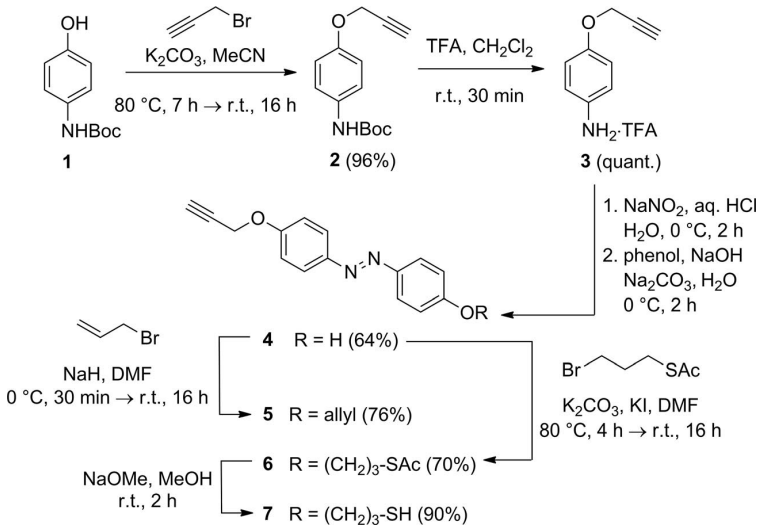

Scheme 1. Synthesis of hetero-bifunctional allyl–alkyne and alkyne–sulfhydryl azobenzene derivatives **5** and **7**, respectively (TFA = trifluoroacetic acid).

ChemPubSoc Europe

EurJOC European Journal of Organic Chemistry
Communication

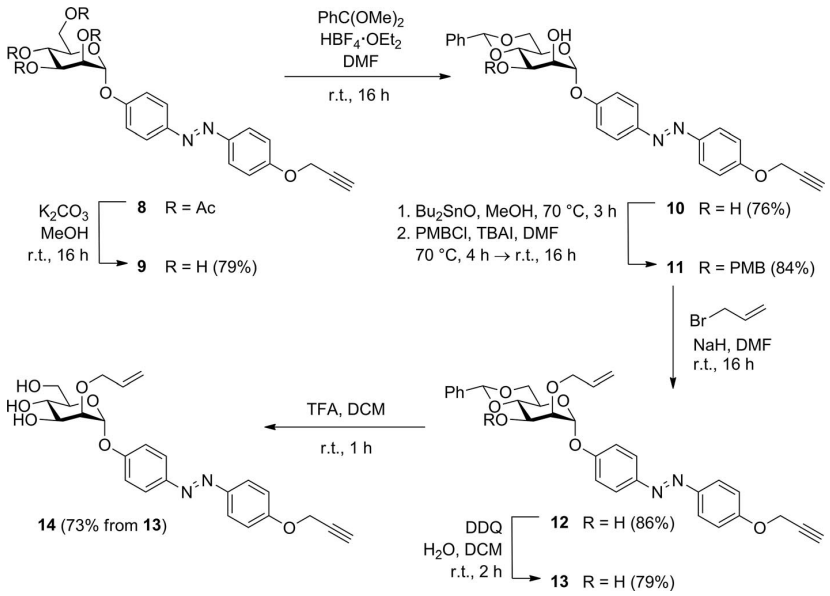

Scheme 2. Synthesis of hetero-bifunctional allyl–alkyne azobenzene glycoconjugate **14** (TBAI = tetrabutylammonium iodide).

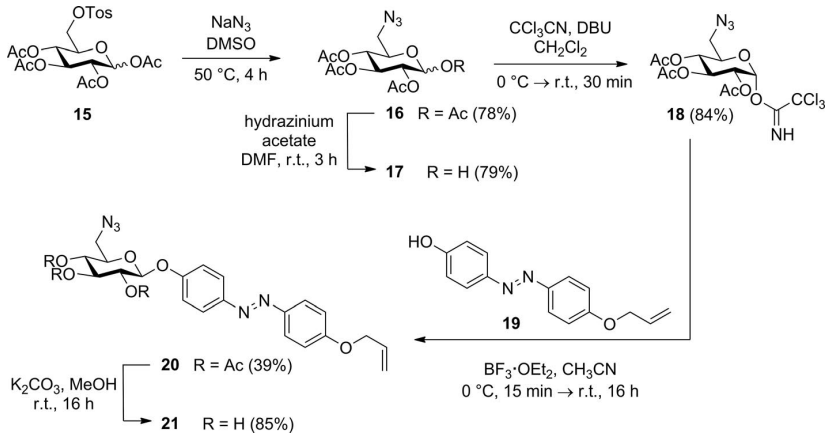

Scheme 3. Synthesis of hetero-bifunctional allyl–azido azobenzene glycoconjugate **21** (Tos = *para*-tolylsulfonyl, DBU = 1,8-diazabicyclo[5.4.0]undec-7-ene).

allows copper-catalyzed and strain-promoted alkyne–azide cycloaddition or Staudinger–Bertzozzi ligation. Consecutive cross-linking experiments with bifunctional peptides by employing allyl–azido-bifunctional azobenzene glycoside **21** are currently in progress.

For any photochemical application, the photochromic properties of hetero-bifunctional azobenzene derivative **5**, **7**, **14**, and **21** have to be known. Ideally, $E \rightarrow Z$ photoisomerization leads to photostationary states (PSSs), in which almost all *E* isomers have been converted. Photoirradiation was performed at room temperature in the dark, and the process was monitored by ^{1}H NMR and UV/Vis spectroscopy. The PSSs of the respective azobenzene derivatives in dimethyl sulfoxide were reached after approximately 10 min by employing a 365 nm light-emitting diode (LED). The resulting *E*/*Z* ratios were determined by integrating the ^{1}H NMR signals of the aromatic protons. The half-lives $\tau_{1/2}$ of the *Z* isomers were determined by ^{1}H NMR spectroscopy. The photochromic data obtained from respective azobenzene derivatives **5**, **7**, **14**, and **21** are collected in Table 1 (see also the Supporting Information).

Table 1. Characterization of the *E* and *Z* isomers of azobenzene derivatives **5**, **7**, **14**, and **21**.

Azobenzene derivative	λ_{max} [nm] *E* isomer	*Z* isomer	*E*/*Z* (PSS)[a]	$\tau_{1/2}$ [h]
5	360	312, 447	3:97	26.0
7	362	312, 448	2:98	24.5
14	362	309, 447	3:97	37.2
21	360	311, 447	3:97	49.9

[a] According to the integration ratio of the aromatic proton signals of the *E* and *Z* isomers in the ^{1}H NMR spectra.

Azobenzene derivatives **5**, **7**, **14**, and **21** showed favorable photochromic properties. Photoirradiation of the *E* isomers led to almost quantitative isomerization, and all of the *Z* isomers

ChemPubSoc Europe

EurJOC European Journal of Organic Chemistry
Communication

have half-lives ranging from 1 to 2 days. Thus, the independent investigation of both isomeric states of cross-linked peptides is feasible.

To estimate the effect of azobenzene derivatives **5**, **7**, **14**, and **21** on the conformational properties of cross-linked peptides or proteins, the change in their end-to-end distances upon isomerization were monitored by using molecular dynamics simulations (see the Supporting Information). The end-to-end distance distributions are collected in Table 2. The most probable end-to-end distances of the *E* isomers varies from about 15 to about 18 Å. The respective *Z* isomers show a more complex distribution with the most probable distances varying from around 8 to around 15 Å. The separation of the distance distributions between the *E* and *Z* states is characteristic for the individual cross-linkers.

Table 2. Distance calculations for azobenzene derivatives **5**, **7**, **14**, and **21**.

Azobenzene derivative	Config.	Most probable end-to-end end distance [Å][a]	Range of end-to-end distances [Å][a]
5	*E*	16.7	10.5–17.8
5	*Z*	8.4	3.1–14.6
7	*E*	17.4	10.1–19.5
7	*Z*	14.8	4.6–18.0
14	*E*	17.8	9.7–21.1
14	*Z*	15.5	5.1–19.8
21	*E*	15.1	7.7–19.8
21	*Z*	11.3	3.0–18.8

[a] The distances were calculated between the terminal allyl group carbon atom and the quaternary carbon atom of the propargyl group (for **5** and **14**), the terminal sulfhydryl group and the quaternary carbon atom of the propargyl group (for **7**), and the terminal allyl group carbon atom and the CH_2N group of the azido group (for **21**).

Conclusions

In conclusion, we synthesized bifunctionalized (glyco)azobenzene derivatives in which alkyne–alkene, alkyne–sulfhydryl, and alkene–azido reaction pairs were combined for bioorthogonal cross-linking of peptides and proteins. Hence, we combined variable ligation chemistries and varied the distances between the respective functional groups in both isomeric states (*E*/*Z*). All synthesized representatives of these hetero-bifunctional cross-linker molecules have favorable photochromic properties and should thus be tested in the photoswitching of the form and function of peptides and proteins. We hope to inspire corresponding studies with our work, as the introduced molecules can now be readily accessed and varied according to the synthetic pathways reported by us.

Acknowledgments

The authors thank the Deutsche Forschungsgemeinschaft (DFG), collaborative network SFB 677, for financial support and Prof. Dr. F. D. Sönnichsen for fruitful discussions.

Keywords: Glycoconjugates · Protein modifications · Bioorthogonality · Photochemistry

[1] a) F. Bonardi, G. London, N. Nouwen, B. L. Feringa, A. J. M. Driessen, *Angew. Chem. Int. Ed.* **2010**, *49*, 7234–7238; *Angew. Chem.* **2010**, *122*, 7392–7396; b) A. Beharry, G. A. Woolley, *Chem. Soc. Rev.* **2011**, *40*, 4422–4437; c) J. Rappsilber, *J. Struct. Biol.* **2011**, *173*, 530–540; d) A. Mourot, T. Fehrentz, D. Bautista, D. Trauner, R. Kramer, *Nat. Methods* **2012**, *9*, 396–402; e) S. A. Slavoff, A. Saghatelian, *Nat. Biotechnol.* **2012**, *30*, 959–961; f) C. S. McKay, M. G. Finn, *Chem. Biol.* **2014**, *21*, 1075–1101; g) C. Hoppmann, V. K. Lacey, G. V. Louie, J. Wei, J. P. Noel, L. Wang, *Angew. Chem. Int. Ed.* **2014**, *53*, 3932–3936; *Angew. Chem.* **2014**, *126*, 4013–4017; h) M. Díaz-Lobo, J. Garcia-Amorós, I. Fita, D. Velasco, J. J. Guinovarta, J. C. Ferrer, *Org. Biomol. Chem.* **2015**, *13*, 7282–7288; i) T. Podewin, M. S. Rampp, I. Turkanovic, K. L. Karaghiosoff, W. Zinth, A. Hoffmann-Röder, *Chem. Commun.* **2015**, *51*, 4001–4004.

[2] a) G. A. Woolley, *Acc. Chem. Res.* **2005**, *38*, 486–493; b) W. Szymanski, J. M. Beierle, H. A. V. Kistemaker, W. A. Velema, B. L. Feringa, *Chem. Rev.* **2013**, *113*, 6114–6178; c) S. Samanta, A. Babalhavaeji, M. Dong, G. A. Woolley, *Angew. Chem. Int. Ed.* **2013**, *52*, 14127–14130; *Angew. Chem.* **2013**, *125*, 14377–1480.

[3] A. Müller, H. Kobarg, V. Chandrasekaran, J. Gronow, F. D. Sönnichsen, T. K. Lindhorst, *Chem. Eur. J.* **2015**, *21*, 13723–13731.

[4] a) C. Hoppmann, P. Schmieder, N. Heinrich, M. Beyermann, *ChemBioChem* **2011**, *12*, 2555–2559; b) M. A. Kienzler, A. Reiner, E. Trautman, S. Yoo, D. Trauner, E. Y. Isacoff, *J. Am. Chem. Soc.* **2013**, *135*, 17683–17686; c) C. Hoppmann, I. Maslennikov, S. Choe, L. Wang, *J. Am. Chem. Soc.* **2015**, *137*, 11218–11221; d) M. Díaz-Lobo, J. Garcia-Amorós, I. Fita, D. Velasco, J. J. Guinovarta, J. C. Ferrer, *Org. Biomol. Chem.* **2015**, *13*, 7282–7288.

[5] a) C. R. Becer, R. Hoogenboom, U. S. Schubert, *Angew. Chem. Int. Ed.* **2009**, *48*, 4900–4908; *Angew. Chem.* **2009**, *121*, 4998–5006; b) A. Dondoni, A. Marra, *Chem. Soc. Rev.* **2012**, *41*, 573–586.

[6] a) V. V. Rostovtsev, L. G. Green, V. V. Fokin, K. B. Sharpless, *Angew. Chem. Int. Ed.* **2002**, *41*, 2596–2599; *Angew. Chem.* **2002**, *114*, 2708–2711; b) M. Meldal, C. W. Tornøe, *Chem. Rev.* **2008**, *108*, 2952–3015.

[7] J. C. Jewett, C. R. Bertozzi, *Chem. Soc. Rev.* **2010**, *39*, 1272–1279.

[8] a) E. Saxon, C. R. Bertozzi, *Science* **2000**, *287*, 2007–2010; b) S. S. van Berkel, M. B. van Eldijk, J. C. M. van Hest, *Angew. Chem. Int. Ed.* **2011**, *50*, 8806–8827; *Angew. Chem.* **2011**, *123*, 8968–8989.

[9] a) C. Hoppmann, R. Kühne, M. Beyermann, *Beilstein J. Org. Chem.* **2012**, *8*, 884–889; b) C. Hoppmann, V. K. Lacey, G. V. Louie, J. Wei, J. P. Noel, L. Wang, *Angew. Chem. Int. Ed.* **2014**, *53*, 3932–23936; *Angew. Chem.* **2014**, *126*, 4013–4017; c) C. Hoppmann, I. Maslennikov, S. Choe, L. Wang, *J. Am. Chem. Soc.* **2015**, *137*, 11218–11221; d) P. Gorostiza, M. Volgraf, R. Numano, S. Szobota, D. Trauner, E. Y. Isacoff, *Proc. Natl. Acad. Sci. USA* **2007**, *104*, 10865–10870.

[10] V. Chandrasekaran, E. Johannes, H. Kobarg, F. D. Sönnichsen, T. K. Lindhorst, *ChemistryOpen* **2014**, *3*, 99–108.

[11] V. Chandrasekaran, Th. K. Lindhorst, *Chem. Commun.* **2012**, *48*, 7519–7521.

[12] J. Mo, D. Eom, E. Lee, P. H. Lee, *Org. Lett.* **2012**, *14*, 3684–3687.

[13] M. Becker, F. Lin, WO2015048728 (A1), **2015**.

[14] a) S. S. Ghosh, P. M. Kao, A. W. McCue, H. L. Chappelle, *Bioconjugate Chem.* **1990**, *1*, 71–76; b) S. Ravi, V. R. Krishnamurthy, J. M. Caves, C. A. Haller, E. L. Chaikof, *Acta BioMater.* **2012**, *8*, 627–635.

[15] L. Möckl, A. Müller, C. Bräuchle, T. K. Lindhorst, *Chem. Commun.* **2016**, *52*, 1254–1257.

[16] C.-W. T. Chang, Y. Hui, B. Elchert, J. Wang, J. Li, R. Rai, *Org. Lett.* **2002**, *4*, 4603–4606.

[17] E. Hardegger, R. M. Montavon, *Helv. Chim. Acta* **1946**, *29*, 1199–1203.

Received: February 8, 2016
Published Online: March 4, 2016

4 Fabrication of photoswitchable glycosylated surfaces

4.1 Introduction

The glycosciences are still lagging behind the fields of nucleic acid or protein research due to the fact that not enough methodology is available yet to handle the enormous structural and functional diversity of cell surface glycoconjugates. As glycan biosynthesis is not directly encoded by genes such as in protein biosynthesis, but build up by specific glycosyltransferases and various other enzymes, microhetereogeniety of cell surface glcoslation occurs to a large extent. Furthermore the composition of cell surface glycans is significantly altered by the type and state of cells. Thus, the investigation of glycan function and structure is rather complicated. Tools which are available in proteomics and genomics including polymerase chain reaction (PCR), automated sequencing, automated synthesis, high-throughput microarray screening as well as detailed structure elucidation (X-ray analysis) are less developed in the field of glycobiology. The two main goals in the glycosciences are firstly, the full characterisation of the carbohydrate structure present on a cell surface or organism and secondly, the investigation of carbohydrate-lectin interactions to unravel the biological significance of the complexity of cell surface glycans. Methods which are suited to advance the glycosciences are carbohydrate sequencing as well as the synthesis and the isolation from natural sources of various defined oligosaccharides and other glycoconjugates.[46,187–193] Besides that, the structural analysis, identification and quantification of carbohydrates and lectins as well carbohydrate-lectin complexes by various analytical methods such as nuclear magnetic resonance spectroscopy (NMR)[194–196] and mass spectrometry (MS)[197–199] have contributed to delineate the details of the complex recognition process.[200] Especially glycoarrays (arrays displaying carbohydrates) (chapter 4.1.1) represent an advanced approach for the glycosciences to further investigate carbohydrate-lectin interactions.[201–203]

Classical methods to investigate carbohydrate-lectin interactions are the hemagglutination inhibition assay (HI or HAI),[204–206] the enzyme-linked lectin assay (ELLA),[207–209] isothermal titration calorimetry (ITC),[210,211] and surface plasmon resonance spectroscopy (SPR).[212,213] With a hemagglutination inhibition assay it is possible to obtain semi-quantitative data of the carbohydrate-binding specificity of lectins as well as to determine the potency of inhibitor molecules of lectin-mediated agglutination. The HAI is based on the ability of lectins to agglutinate erythrocytes by recognizing cell surface glycoconjugates and forming a cross-linked network in suspension (Figure 4.1).
Adding soluble glycoconjugates inhibits this hemagglutination process as a consequence of competitive binding of the carbohydrate ligand to the active side of a lectin. As a result it is possible to determine the lowest concentration of the carbohydrate solution, at which the hemagglutination process is still completely inhibited. However, this classical approach suffers from a lack of reproducibility owing to many unspecific factors related to the nature of erythrocytes. Besides that, artificial glycosylation patterns as well as specific parameters such as the influence of carbohydrate orientation cannot be addressed.

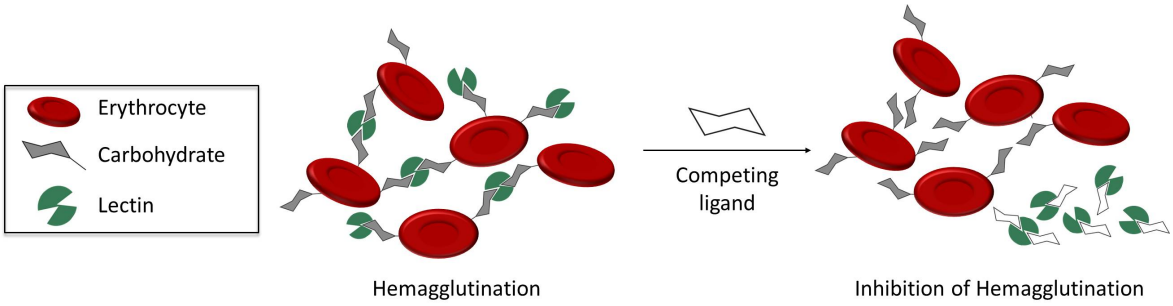

Figure 4.1. Schematic representation of the hemagglutination inhibition assay. Lectins have the ability to agglutinate erythrocytes by recognizing carbohydrates on the cell surface. By adding competing ligands, the hemagglutination process can be inhibited.

Another method to investigate carbohydrate-lectin interactions is the enzyme-linked lectin assay which offers the possibility to evaluate lectin binding properties of natural or synthetic carbohydrates quantitatively in solution.[207–209] In this assay, lectin-enzyme conjugates as well as soluble ligands were added to microtiter plates, coated with a reference ligand such as (neo)glycoproteins or polysaccharides (Figure 4.2).

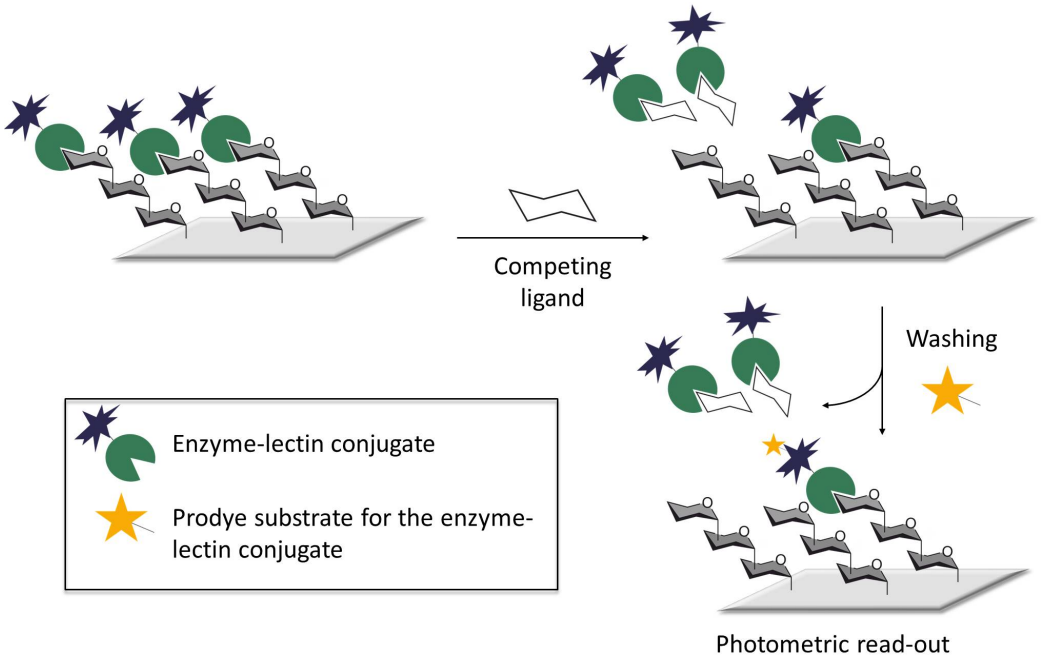

Figure 4.2. Schematic representation of the enzyme-linked lectin assay. Oligosaccharides or glycoproteins, respectively are immobilized on a microtiter plate and incubated with a lectin-enzyme conjugate and a carbohydrate ligand. After a washing step, a prodye substrate for the lectin is added and the results are spectrophotochemically evaluated.

After an incubation period, plates are subsequently washed and a prodye substrate for the enzyme conjugate is added. Thereon, plates are spectrophotochemically evaluated and the amount of colour formed is proportional to the concentration of immobilized lectin-enzyme conjugates which is consequently inversely proportional to the affinity of added glycoconjugates. Hence, IC_{50} values of

inhibitor carbohydrates can be deduced. The IC_{50} value of an inhibitor represents the concentration at which 50% of the binding of lectin-enzyme conjugate to the immobilized reference ligand is prevented. Relative inhibitory potencies of carbohydrate conjugates determined with ELLA are usually similar to those determined with a HAI-assay. However, large differences in IC_{50} values are often observed. The advantage of this method compared to solid-phase binding assays such as SPR spectroscopy is that lectin and the ligand to be tested are both in solution.
To determine thermodynamic and kinetic parameters of carbohydrate-lectin binding, methods including ITC[210,211] and SPR[212,213] can be applied. These methods provide data about the stoichiometry of binding, the binding constant and the enthalpy of binding. However, the drawbacks of these described methods are that they are time-consuming, labour-intensive and often a great amount of the carbohydrate to be examined is needed. This is particularly disadvantageous for glycoconjugates isolated from natural sources and oligosaccharides produced in a complex synthetically pathway as they are both usually available only in small quantities.
Therefore, several advanced methods have been developed to further investigate carbohydrate-lectin interactions such as carbohydrate microarrays, atomic force microscopy (AFM)[214] or the use of glycosylated particles. Especially glycoarrays (arrays displaying carbohydrates) represent an advanced approach for the glycosciences as they provide an alternative to the classical methods and their problems discussed above.[201–203]

4.1.1 Glycoarrays

Glycoarrays have been developed in the twenty first century, facilitating an approach to examine and analyse carbohydrate-lectin interactions in greater depth.[215–220] Carbohydrate arrays have the advantage that the time for biochemical measurement is shortened Less precious carbohydrate material can be used due to the option of miniaturisation which is not possible in studies in solution. In recent years a variety of sophisticated array platforms have been developed which enable the qualitative and quantitative analysis of carbohydrate binding to surfaces with the aid of fluorescence spectroscopy, mass spectrometry[221,222] and SPR spectroscopy.[223,224] Thus, the investigation, systematic identification and characterisation of carbohydrate binding proteins as well as a variety of other applications are feasible (Figure 4.3).[201,225,226]

To construct glycoarrays, various immobilisation strategies have been utilized. Carbohydrates can be either immobilized by a covalent attachment or by physical adsorption (Figure 4.3).[48,202] The suitable method for the immobilization of glycoconjugates on surfaces depends strongly on the nature of the carbohydrate (synthetically produced or isolated from natural sources). However, in most cases specific covalent attachment methods are applied (Figure 4.4). Thus, highly stable arrays are produced and a loss of substance through washing procedures is diminished. Whereas synthetically obtained carbohydrates can be easily functionalized and immobilized on surfaces, the functionalization of oligosaccharides isolated from natural sources is challenging.

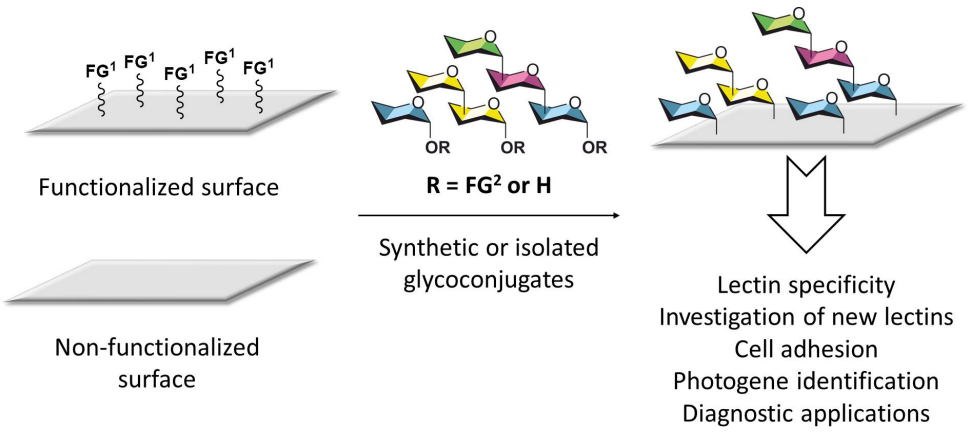

Figure 4.3. Glycoarrays can be produced from synthetic or isolated glycoconjugates which can be immobilized on a functionalized or non-functionalized surface (e.g. glass, polystyrene or gold). A multitude of applications have emerged as a result.

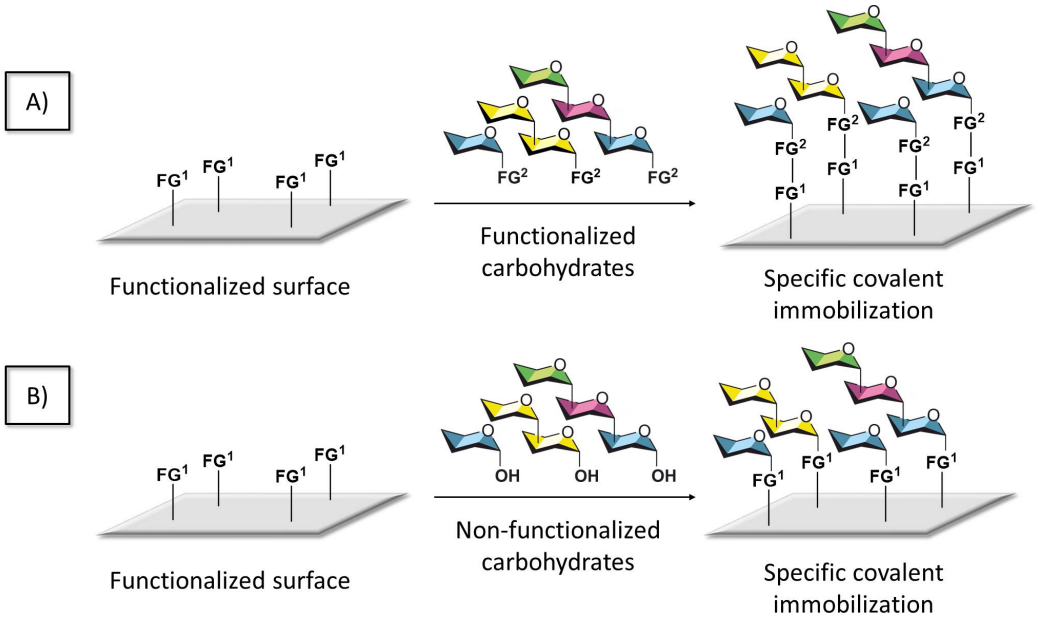

Figure 4.4. Schematic illustration of the specific covalent immobilization of A) functionalized and B) non-functionalized carbohydrates on activated surfaces (e.g. glass, polystyrene or gold).

Many strategies have been developed to facilitate the covalent immobilization of carbohydrates on surfaces. An overview of selected examples is given in Table 4.1; a detailed overview can be found in several current reviews.[201,202,225–227]

Table 4.1. Covalent attachment methods to immobilize carbohydrates on surfaces, R = carbohydrate.

Entry	Functional group on the surface	Functional group on the carbohydrate	Resulting linkage	Ref.
1	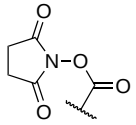			[228–232]
2			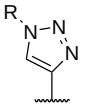	[233–236]
3	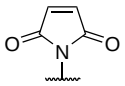		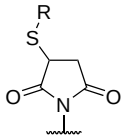	[237–240]
4		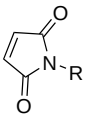	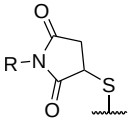	[217,241]
5			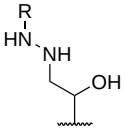	[242,243]
6	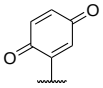	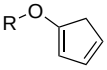	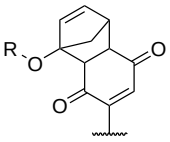	[216]
7			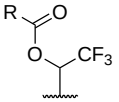	[244]

The among most commonly used techniques are: amide coupling between amino-functionalized carbohydrates and an activated ester-derivatized surface (entry 1),[228–232] 1,3-dipolar cycloaddition between an azide and an alkyne (entry 2)[233–236] and the chemoselective thiol-maleimide ligation, whereas the thiol function is either located on the carbohydrate or on the surface (entry 3 and 4).[217,237–241] On epoxide derivatized surfaces hydrazine-functionalized carbohydrates can be attached (entry 5).[242,243] Another immobilization approach is based on cycloaddition reactions. Thus, in a classical Diels-Alder reaction carbohydrate-cyclopentadiene conjugates are immobilized on benzoquinone coated surfaces (entry 6).[216] Diels–Alder reactions with inverse electron demand can similarly employed to build up glycoarrays.[245,246] Photochemical methods can also be utilized to attach carbohydrate probes on the solid support. For this purpose, diazirine-functionalized surfaces are irradiated with UV-light under the formation of a reactive carbene, which then further reacts with an acid function on the carbohydrate moiety (entry 7).[244] The need of chemical modification of

the carbohydrate to introduce a functional group, allowing for reaction with the solid support is the main limitation of these described methods. Usually, a complex multistep protection-glycosylation-deprotection sequence is required. This is particularly disadvantageous for oligosaccharides extracted and purified from natural sources. Therefore, a covalent immobilization strategy using unmodified glycoconjugates is sometimes preferable. In order to facilitate this, photoactivatable surfaces derivatized with photolabile groups such as aryl(trifluoromethyl)diazirine are utilized.[247] Upon irradiation, singlet carbenes are formed which can rapidly react with unmodified carbohydrate structures. Another possibility to immobilize unmodified glycoconjugates on surfaces is a condensation reaction between the reducing-end aldehyde and a hydrazide function on a surface.[248,249]
Non-covalent functionalization is achieved through ionic interactions,[250] hydrogen bonding and hydrophobic interactions.[220,251,252] Thus, for instance, trityl-terminated glycosides could be directly adsorbed onto black polystyrene surfaces[238,253] and also amphiphilic glycoconjugates[254,255] could be successfully immobilized to polystyrene, forming stable glycoarrays.
Besides the choice of the immobilization strategy the selection of the solid support is at least equally important. There are two aspects to be considered. On the one hand if derivatization of the carbohydrate is necessary and on the other hand which type of ligation chemistry is required for immobilization of glycoconjugates onto the solid support. Several different supports such as functionalized glass slides,[222,256–258] prefunctionalized polystyrene microtiter plates,[209,220,222,251] nitrocellulose-coated[218] slides and gold slides[238,259] have been utilized to build up various glycoarrays. Certainly, all these surfaces have different properties and can therefore be employed in different applications. Moreover, with the choice of the surface, the detection method to investigate the respective functionalized solid support in more detail is determined. As the detection method strongly depends on the properties of the surface. For instance, gold-based substrates are compatible for fluorescence measurements applying a microarray scanner, and besides that it is also possible to use them as a platform for Matrix-assisted laser desorption ionization mass spectroscopy (MALDI-MS),[216,222,260–262] infrared reflection-absorption spectroscopy (IRRAS) or SPR spectroscopy.[216,224,263,264] While the formation of glycoarrays on gold relies on the use of sulfur-functionalized carbohydrate ligands (usually thiols),[233,265] a variety of immobilization methods are feasible to covalently attach glycoconjugates on glass. Besides that, carbohydrate-coated glass can be easily investigated with UV-vis absorption spectroscopy. The most commonly used techniques for the investigation of glycoarrays is fluorescence detection, which is based on the direct or indirect binding of fluorescence tagged proteins to the carbohydrate structures present on the surface.[202,203,225]
In addition to glycosylated microtiter plates and various functionalized slides (gold, glass, nitrocellulose), also glycosylated particles have been utilized to investigate carbohydrate-lectin interactions.[266–274] Examples are collected in Table 4.2.

With the rapid development of glycoarrays and glycosylated particles the screening of molecular interactions as well as the functional investigation of whole organisms such as eukaryotic cells, bacteria and viruses are possible.[201–203,229,230,280,281] Many aspects concerning the extent of bacterial binding to glycoconjugates can be addressed. These include the carbohydrate specificity of lectins, the influence of the molecular structure of employed carbohydrates with regard to the chemical

Table 4.2. Examples of glycosylated particles and corresponding applications in the glycosciences.

Carbohydrates attached to	Use	Ref.
Nanodiamonds	Detection and isolation of bacteria	[267,268]
Quantum dots	Detection of bacteria and lectins	[275,276]
Gold beads	Visualization of carbohydrate-protein and carbohydrate-cell interactions	[277]
Magnetic beads	Detection, isolation and purification of carbohydrate-proteins	[278]
Fluorescent polymers	Detection of bacteria	[275,279]

nature of its aglycon as well as its valency.[215,225,266] However, also spatial distribution and relative orientation of the carbohydrate ligands on the cell surface are crucial for specific carbohydrate-lectin interactions. Hence, glycoarrays have been also utilized to investigate the arrangement of carbohydrates and the associated influence on bacterial adhesion in greater detail.

4.1.2 Photoswitchable glycoarrays

To address the influence of carbohydrate orientation or conformation in the glycosciences, several approaches have been developed in our group (Figure 4.5).

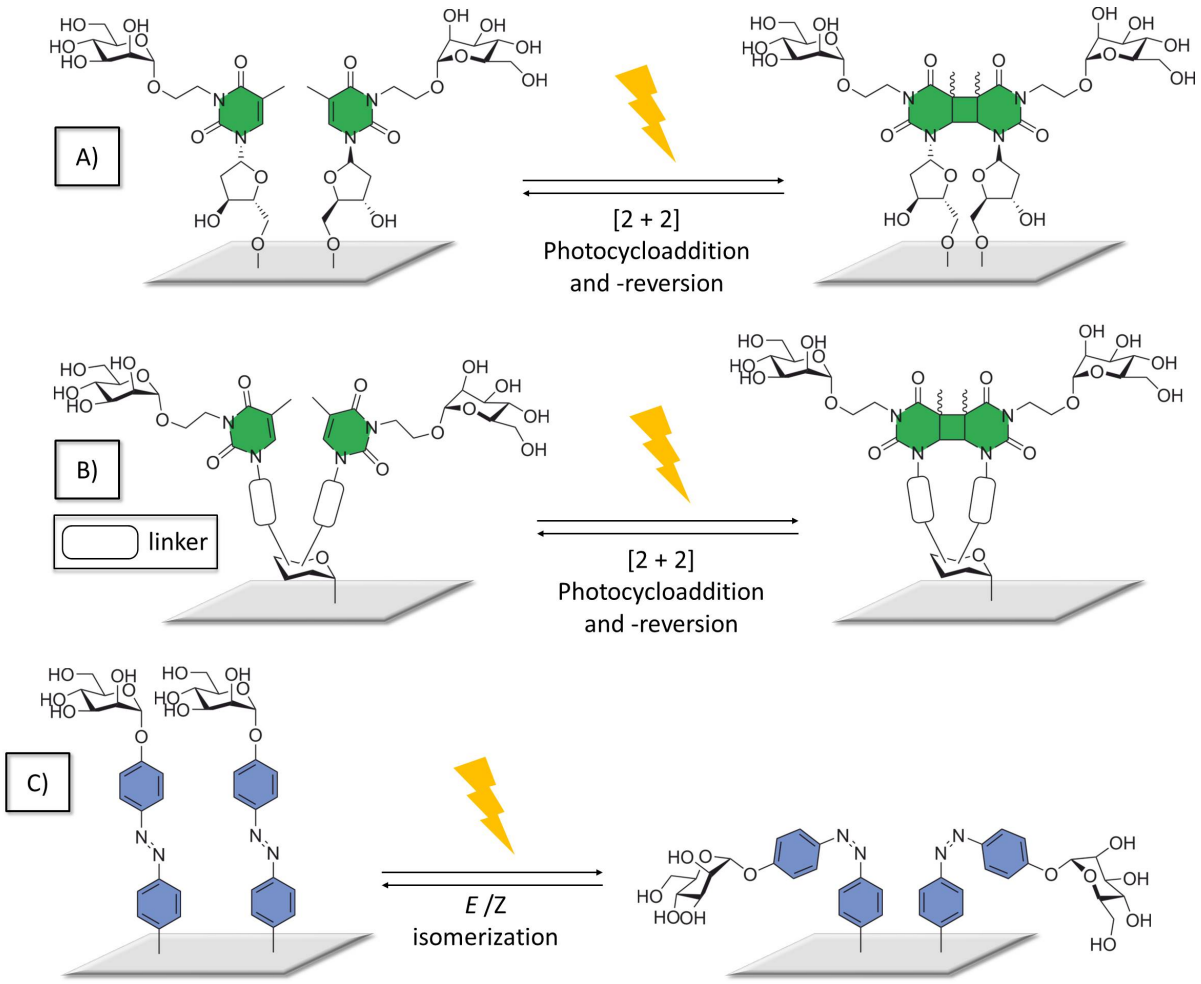

Figure 4.5. Schematic illustration of photoswitchable glycoarrays to conrol bacterial adhesion to surfaces immobilized with; A) glycotyhmidine derivatives, B) glycothymine derivatives and C) glycoazobenzene derivatives.

Therefore, biologically relevant substances were modified by introducing small molecular photoswitches.[67] Upon irradiation it is then possible to switch between two different conformations. The photochemical switch thymidine has been chosen because of its ability to undergo [2+2]-cycloaddition and -cycloreversion at different wavelengths (Figure 4.5 A).[282] Thus, glycothymidine derivatives were immobilized onto surfaces (PS, gold or glass) and irradiated with light of $\lambda = 295$ nm. Upon irradiation two immobilized thymidine derivatives can dimerize which induces a conformational change within the glycosylated surface and can then be tested in bacterial adhesion studies.[283,284] It has been shown there is a small influence on bacterial adhesion to surfaces derivatized with

glyothymidine conjugates after irradiation but these results could not yet be clearly proven. Also carbohydrate-centered glycothymine derivatives have been synthesised which also give the opportunity to determine the influence of conformational changes, induced by a conformational switching process ([2+2]-cycloaddition), in carbohydrate-protein interactions (Figure 4.5 B).[285]

Besides the described methods above, the effect through orientation of the carbohydrate moiety can be also addressed with the aid of photoswitchable azobenzene-functionalized glycoarrays (Figure 4.5 C).

Table 4.3. Selected examples of azobenzene derivatized photoswitchable surfaces and their applications.

Material of the surface	Immobilized azobenzene derivative	application	Ref.
Poly methyl methacrylate (PMMA)	Cyclic arginylglycylaspartic acid (RGD) peptides	Photochemical control of cell adhesion	[286]
Gold	RGD peptide	Azobenzene-embedded SAMs to photochemically control cell adhesion	[287]
Quartz glass	α-Cylodextrine (CD) terminal alkanesilane assembled with an azo-GRGDS via host-guest interaction	Photochemical control of cell adhesion	[288]
Glass coated with a PEG layer	c(RGDfK)-peptide	Photoswitching of integrin-mediated cell adhesion	[289]
Gold, glass	β-CD assembled with glycoazobenzene conjugates via host-guest interactions	Photoresponsive immobilization of ConA and *E. coli*	[290]
Quartz glass	Lipase from *Candida rugosa*	Photo-controlled deactivation of the immobilized lipase	[291]
Quartz glass	Fluorinated azobenzene molecules	Photoswitching of wettability (superhydrophobic and superhydrophilic)	[292]

While azobenzene has long been known as efficient photoswitch and has been applied for switching of the properties of designer surfaces (an overview about a few selected examples is given in Table 4.3),[102,131,293–303] the immobilization of glycoazobenzenes onto a solid support to investigate the effect of bacterial adhesion through re-orientation upon E/Z isomerization is still underrepresented. The first contribution which demonstrated photoswitching of glycoazobenzene self-assembled monolayers (SAMs) was made by Chandrasekaran *et al.* in 2014.[108] Therein, an *O*-acetyl protected azobenzene mannoside thioacetate was utilized for SAM preparation under slightly basic conditions. Thus in situ deprotection of the sulfhydryl function was achieved and the formation of disulfides is avoided. It has been shown if only the azobenzene mannoside was immobilized onto the gold slide, the

photoisomerization on surface was not effective. However, with employing an appropriate "diluter" molecule (undecyl thioacetate) $E \rightarrow Z \rightarrow E$ photoisomerization was achieved. The photoisomerization process was monitored via IRRAS, which indicated a small decrease of the band at 1250 cm^{-1} which corresponds to the C_{aryl}-O(mannosyl) stretching vibrations of the azobenzene derivative. Since the change of the band is reversible, it can be reasonably concluded that the effect is caused by the E/Z isomerization of the azobenzene moiety. After the successful demonstration of photoswitching of azobenzene glyco-SAMs on Au(111), Weber *et al.* showed that E/Z isomerization of immobilized azobenzene mannosides on gold surfaces and thus the resulting change of spatial orientation of the carbohydrate moiety, affects type 1 fimbriae-mediated bacterial adhesion (Figure 4.6). [107]

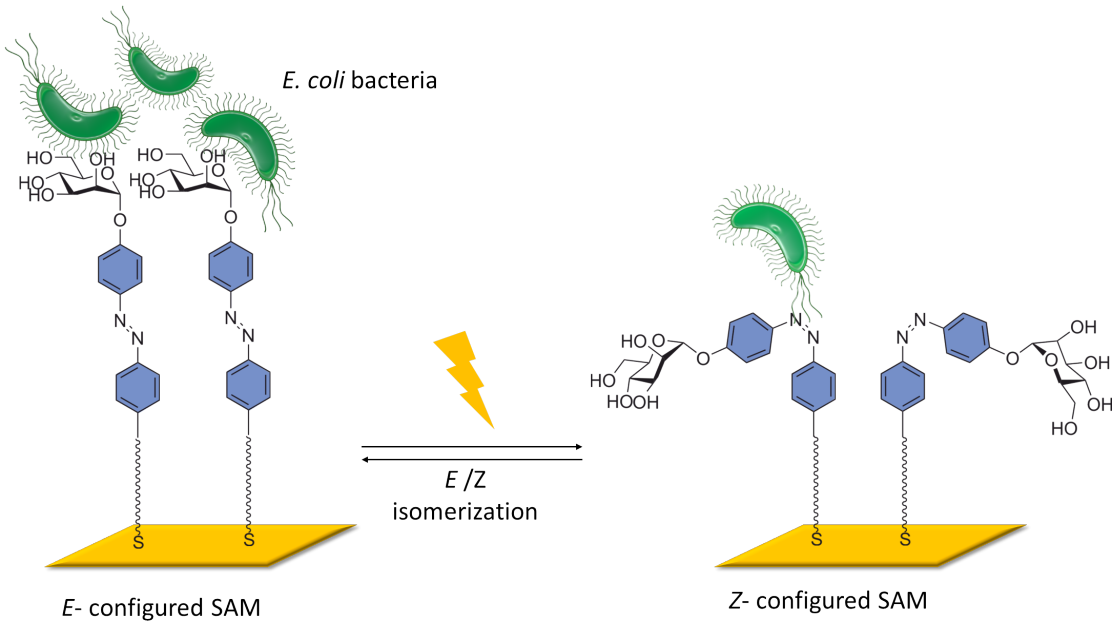

Figure 4.6. Schematic illustration of a photoswitchable glyco-SAM. Irradiation of the SAM by applying the respective wavelengths (365 and 450 nm) resulted in switching of bacterial adhesion.

Therefore, an unprotected sulfhydryl functionalized azobenzene mannoside, additionally equipped with an oligoethylene glycol (OEG) spacer to ensure biorepulsive properties (i.e. prevent unspecific adhesion of bacteria to the solid support), was attached onto a non-physiological surface (Au(111)). The E/Z isomerization process was again monitored via IRRAS and it was found that if just the azobenzene mannoside without employing any "diluter" molecules was immobilized on the gold wafer, an effective switching could be determined. The prepared azobenzene glycoarrays were then studied in a bacterial adhesion assay with type 1 fimbriated *E. coli* bacteria. Upon photoisomerization and thus the change in ligand orientation bacterial adhesion to the surface was diminished by ~80% compared to the *E*-configured glyco-SAM. Indeed the adhesivity of the solid support correlates with the configuration of the glyco-SAM. This was the first time that such an effect through re-orientation of the carbohydrate ligand exposed on the surface was seen in carbohydrate-specific cellular adhesion

studies. The obtained results are highly encouraging for follow-up studies to investigate selective switching of the adhesivity of glycosylated surfaces in more detail and thus to establish new potential applications. The ability to reversibly control surface properties by an external stimulus may facilitate the implementation of switchable glycosylated surfaces in diagnostics.

4.2 Fabrication of photoswitchable quartz glass surfaces

In the following manuscript the work of the Lindhorst group on the preparation of photoswitchable glycosylated surfaces to control cellular adhesion is extended (Figure 4.7). In the course of the study on the effect of orientation in carbohydrate recognition, sulfur containing azobenzene mannosides have been successfully immobilized on gold surfaces and applied in a bacterial adhesion assay with type I fimbriated *E. coli* bacteria. The E/Z isomerization process on the surfaces was monitored with IRRAS spectroscopy. However, no quantitative data of switching efficiencies or thermal relaxation times could be determined.

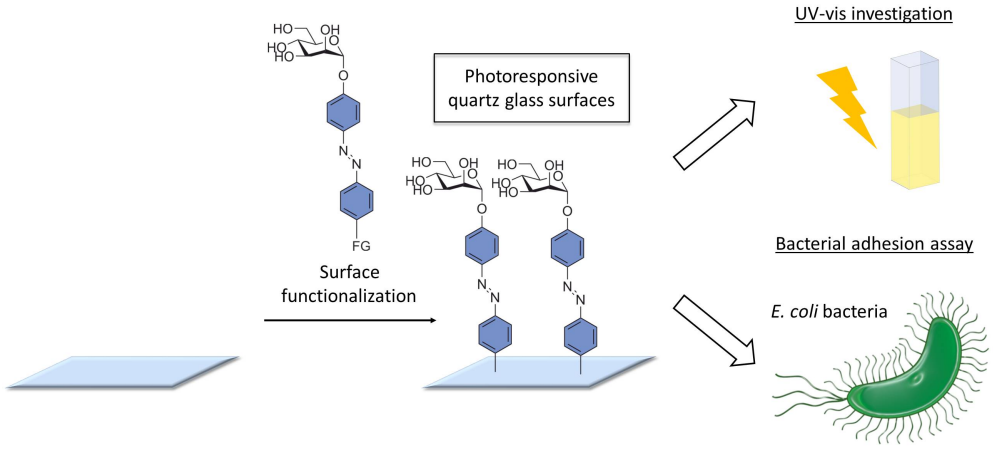

Figure 4.7. In this chapter the preparation of azobenzene mannoside functionalized quartz glass surfaces is reported. The prepared photoresponsive quartz glass surfaces were investigated with UV-vis spectroscopy and a bacterial adhesion assay was performed.

Hence, gold surfaces were substituted with quartz glass slides which have the advantage that they are translucent. Thus, the E/Z isomerization process can be easily monitored via UV-vis spectroscopy. Furthermore, a great variety of immobilization methods are feasible to covalently attach glycoazobenzene derivatives on glass and electronic effects of metal surfaces which might influence the switching behavior of the immobilized azobenzene glycoconjugates are diminished. Photoswitchable quartz glass surfaces were obtained by the preparation of an isothiocyanato-functionalized azobenzene mannosides in a straightforward synthesis pathway and consecutively its immobilization on the solid support. UV-vis absorption spectroscopy as well as contact angle measurements provided evidence of successful surface functionalization. With the aid of UV-vis absorption spectroscopy it was further possible to determine thermal relaxation times and a highly efficient E/Z isomerization of the immobilized azobenzene mannoside could be monitored. As a further step the obtained photoswitchable adhesive slides were employed in a bacterial adhesion study with type 1 fimbriated *E. coli* bacteria. Irradiation of the quartz slides with two different wavelengths (365 and 440 nm) resulted in switching of bacterial adhesion. Thus, the azobenzene configuration of the immobilized azobenzene mannoside correlates with the adhesivity of the surface.

4.2.1 Manuscript on the fabrication of photoswitchable quartz glass surfaces to reversibly control and investigate photoswitchable cell adhesion

"Azobenzene glycosides on glass: A tool to investigate photoswitchable cell adhesion"

This chapter was written in manuscript form with the view of a timeley publication of these results.

A. Müller, C. Fessele, K. Kolbe, L. Daumlechner, T. K. Lindhorst.

Abstract: We report about the fabrication of photoswitchable quartz glass surfaces to further investigate previous obtained results on photoswitching of bacterial adhesion on glyco-SAMs. The prepared slides are amenable to UV-vis apsorption spectroscopy and thus switching behaviour of immobilized azobenzene glycosides could be determined. It was found that the photoresponsive glass surfaces fulfill all the requirements needed for a bacterial adhesion studies such a fast and effective E/Z isomerization process with a relatively thermally-stable Z form and almost no fatigue of the azobenzene switch after several switching cycles. Consequently, the prepared slides were utilized in bacterial adhesion studies and indeed irradiating of the surface resulted in switching of bacterial adhesion.

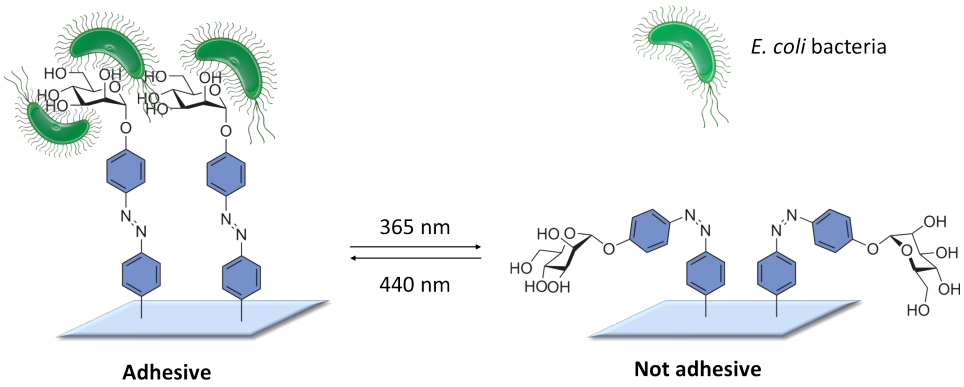

TOC Graphic 4.1. The influence of bacterial adhesion to glycoazobenzene functionalized quartz glass surfaces uppon E/Z isomerisation was shown.

Scientific contribution to this paper

In this project I carried out the synthesis of all synthetic compounds, prepared the quartz glass surfaces and determined the photochromic data of the surface. C. Fessele and myself performed bacterial adhesion studies together. C. Fessele, T. K. Lindhorst, and I wrote the manuscript together.

4.2.1.1 Introduction

Carbohydrate-lectin interactions are essential for health and disease of living organisms. Lectins are ubiquitous in all kind of organisms.[1] In bacterial adhesion they play crucial roles in host infections and biofilm formation.[2] Especially, uropathogenic *Escherichia coli* (UPEC) bacteria cause severe infections during first contact between lectins and the glycocalyx on the cell surface.[3] Among the best investigated lectin of UPEC is the α-D-mannoside specific FimH, which is located on the tip of type 1 fimbriae. These fimbriae are widely spread on the surface of *E. coli* bacteria.[4] Still, due to the complexity and the disordered structure of the glycocalyx the molecular interactions between the lectin FimH and carbohydrates are not yet fully understood.[5] Thus, it is of great interest to get deeper insight into the biology and function of cell surface glycoconjugates and their interactions. It has been shown that not only the carbohydrate structure is crucial for specific carbohydrate-protein interactions but also spatial distribution and relative orientation of the carbohydrate ligands on the cell surface.[6] To probe carbohydrate-protein interactions and the specificity of carbohydrate ligands and their receptors (lectins), adhesive glycoarrays have become an important tool in the glycosciences.[7] Glycoarrays various surfaces coated or functionalized with carbohydrates. To further investigate the influence of spatial distribution and relative orientation of the carbohydrate ligand on the cell surface, we have recently reported on the preparation of photoswitchable azobenzene glyco-SAMs on Au(111).[8] It was shown that bacterial adhesion to such surfaces was diminished by ~80% in the *Z*-state of the SAM compared to the *E*-configured SAM. Thus, the adhesivity of the fabricated surfaces indeed correlate with the configuration of the immobilized azobenzene glycoconjugate. While various azobenzene derivatives have been utilized as photoresponsive units to control numerous properties of designer surfaces,[9] our studies of switching carbohydrate-specific bacterial adhesion by reversible *E*/*Z*-isomerization of immobilized azobenzene glycosides on non-physiological surfaces or cell surface[10], respectively is still unprecedented.
In order to investigate selective switching of the bacterial adhesivity in more detail, we describe herein the fabrication of glycosylated quartz glass surfaces (Figure 4.8).

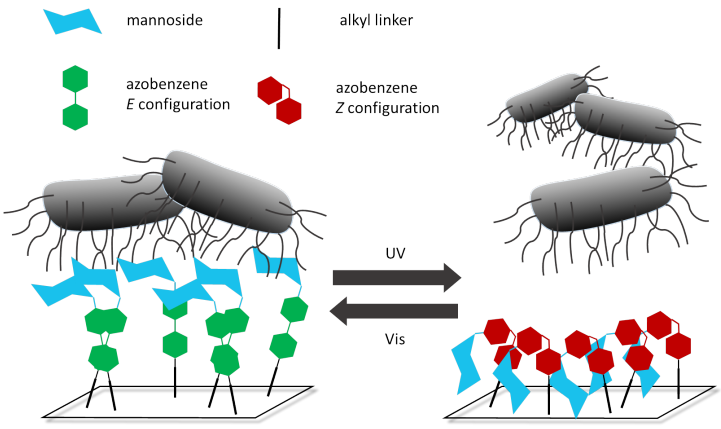

Figure 4.8. Switching of the immobillized azobenzene mannosides on the quartz glass surface determines bacterial adhesion.

These have the advantage that the E/Z isomerization process of immobilized azobenzene derivatives can be easily monitored via UV-vis absorption spectroscopy. Besides that, fabricated quartz glass surfaces were tested in biological adhesion studies and adhesive properties of UPEC were determined upon E/Z isomerization. Our experimental approach is depicted in Figure 4.8. Initially a silane functionalized azobenzene mannoside was immobilized on a quartz glass surface and in a subsequent step photochemical E/Z isomerization of the installed azobenzene moieties was achieved by irradiation with UV (365 nm) or blue light (440 nm), respectively. In a final step, bacterial adhesion was measured by read out of fluorescence intensity and additionally verified by fluorescence microscopy. For adhesion studies GFP expressing type 1-fimbriated *E. coli* bacteria (PKL1162)[11] were used.

4.2.1.2 Preparation of photoswitchable glycosylated quartz glass surfaces

For the preparation of photoswitchable glycosylated quartz glass surfaces, a photoswitchable azobenzene derivative **6** was required (Scheme 4.1).

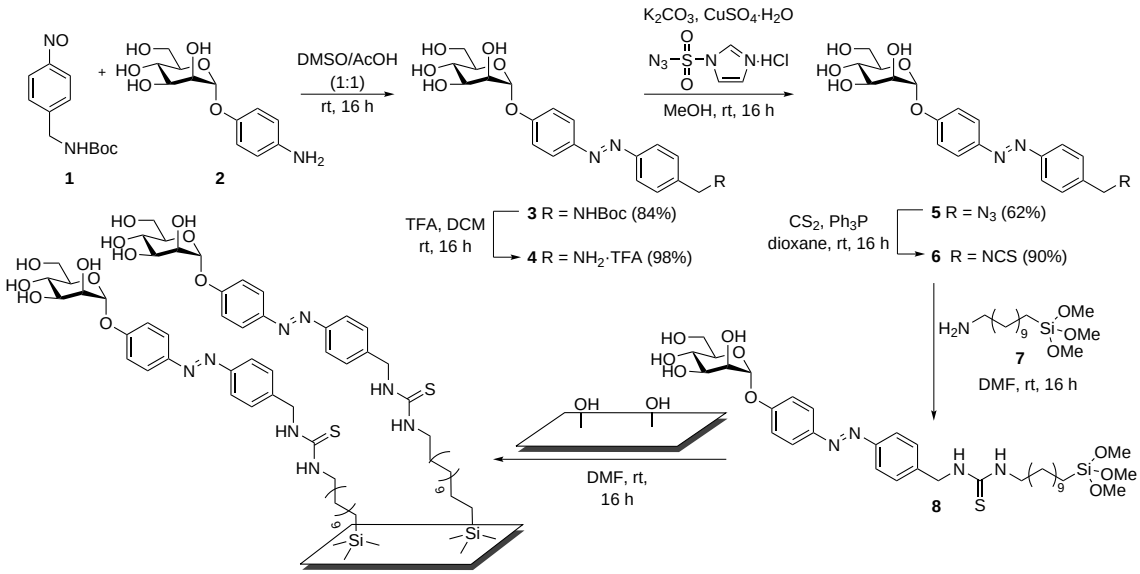

Scheme 4.1. Synthesis of the isothiocyanato functionalized azobenzene mannoside **7** and preparation of the photoswitchable quartz glass surface.

It incorporates in its structure an isothiocyanato group, which allows for isothiocyanate-amine coupling with an amine functionalized silane **7** and a α-D-mannoside head group to effect type 1 fimbriae-mediated bacterial adhesion. Isothiocyanato azobenzene mannoside **6** was synthesised from the known *p*-aminophenyl mannoside **2**[11], which was initially subjected to a Mills condensation with the crude nitrososarene **1**[12], readily obtained from 4-(*N*-Boc-aminoethyl)aniline by reported methods,[12] in a dimethyl sulfoxide acetic acid mixture (1:1). The unsymmetrical azobenzene mannoside **3** was obtained in 84% yield. Subsequent cleavage of the Boc-protecting group with trifluoroacetic acid (TFA) furnished the ammonium salt **4** in nearly quantitative yield. Next, in a copper catalyzed diazotransfer reaction with the diazo donor imidazole-1-sulfonyl azide in methanol[13] the free amine **4** was converted in the corresponding azide **5** in 62% yield. The isothiocyanato functionalized mannoside **6** was obtained in high yield in an aza-Wittig reaction

with carbon disulfide and triphenylphosphine. In a next step, mannoside **6** was utilized in an isothiocyanate-amine coupling reaction with silane **7** and led to the silane functionalized azobenzene derivative **8**. Silane **8** was then immediately immobilized on quartz slides, which were initially cleaned and activated with piranha solution.

Surface modification was monitored by UV-vis absorption spectroscopy. For quartz glass surfaces functionalized with silane **8**, the characteristic azobenzene absorption at 350 nm was observed and provides an evidence of successful surface functionalization. By applying sequential irradiations with UV (365 nm) and visible light (440 nm), $E \rightarrow Z$ isomerization of the immobilized mannoside **8** was achieved (Figure 4.2).

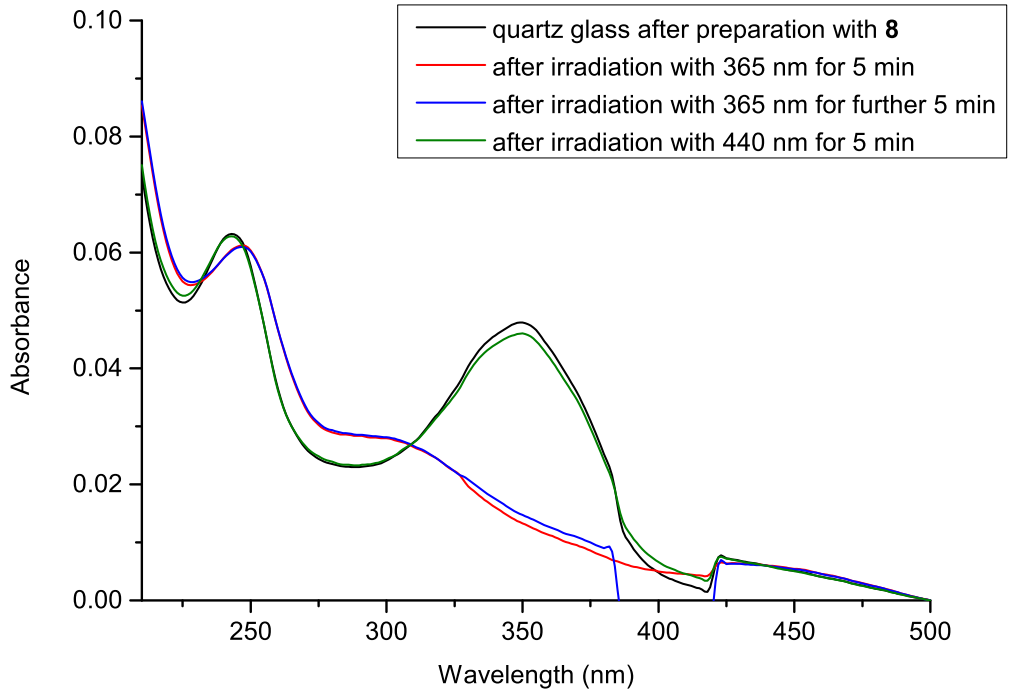

Scheme 4.2. UV-vis spectra for monitoring the changes of absorption during the alternating irradiation at 365 nm and at 440 nm of the immobilized silane **8**.

The E/Z isomerization process was reversible over at least 3.5 switching cycles and almost no photobleaching was observed (Figure 4.3). The half-life for the Z isomer to revert to the E isomer of the immobilized azobenzene derivative **8** on the glass surface was found to be around 6 h. Furthermore, contact angle measurements were performed to provide an additional evidence of successful immobilization of azobenzene mannoside **8** on the quartz glass surface. The contact angle of the cleaned quartz surface was 27°, whereas upon functionalization with **8** the contact angle increased to 86°. Immobilized azobenzene mannoside **8** fulfills all the requirements needed for a bacterial adhesion studies, i.e. a fast and effective E/Z isomerization process with relatively thermally-stable Z form and almost no fatigue of the azobenzene switch after several switching cycles.

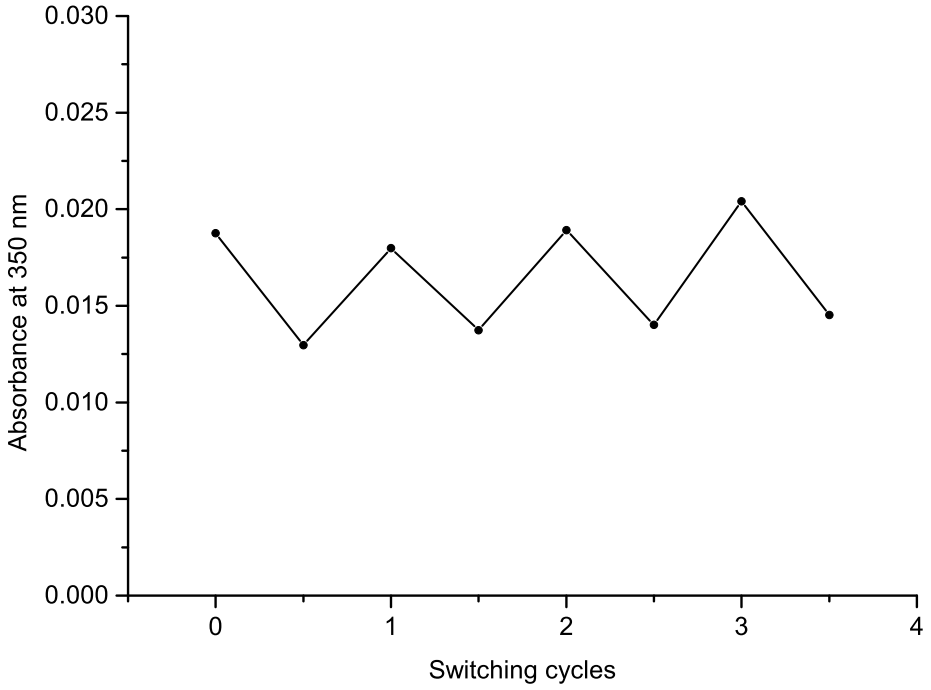

Scheme 4.3. Multiple E/Z isomerization (alternating irradiation with light of $\lambda = 365$ (60 s, $E \rightarrow Z$) and 435 nm (60 s, $Z \rightarrow E$), respectively of immobilized mannoside **8**.

4.2.1.3 Adhesion assay with GFP expressing *E. coli* bacteria

Consequently, the functionalized glass slides were employed in bacterial adhesion studies with type 1 fimbriated *E. coli* bacteria (Figure 4.4).

We used a 96-well microarray format to obtain triplicate results of each slide. We exposed all glass slides in two switching cycles with 365 nm and 440 nm to receive Z and E configured mannosides on the glass surface. Afterwards, all glass slides were incubated with type 1 fimbriated GFP-expressing *E. coli* bacteria. With our microarray system we were able to quantitate the adhered bacteria. Our results show that bacterial adhesion to the glycosylated glass slides was diminished by switching from E to Z configuration significantly about 75 %, which is in accordance with earlier results.[8,10]

With switching the azobenzene mannosides back to E configuration, we again obtained the start adhesion value P with stands for a glass slide, which was not exposed to a bacteria suspension. Additionally, fluorescence microscopy was performed. We prepared pictures of all configurations showed in Figure 8.12 Supporting information. Here, previous results were confirmed. Bacteria adhered in P state and E configuration of the azobenzene mannosides whereas almost no adhesion in Z configuration is observed.

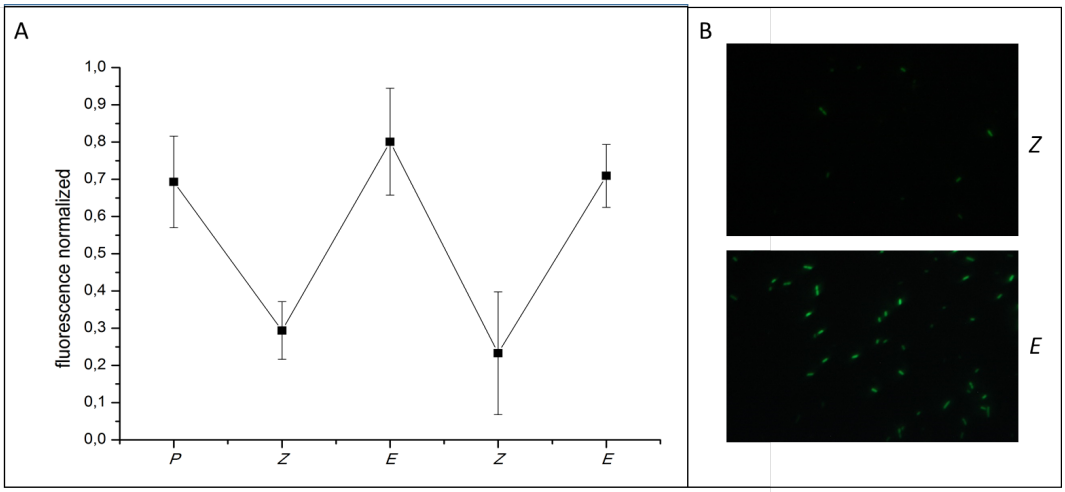

Scheme 4.4. (A) Bacterial adhesion to *Z* and *E*-configured **8** on glass slides during two switching cycles between *E* and *Z* configuration of **8**. *P* depicts a glass slide which was not exposed to bacteria suspension. Error bars result from triplicate values. (B) Fluorescence microscopy of the adhered bacteria.

4.2.1.4 Conclusion

Conclusively, we were able to fabricate photoswitchable glycosylated quartz glass surfaces which were tested as adhesive surfaces for type 1 fimbriated UPEC. A straightforward synthesis lead to the NCS-functionalized azobenzene mannoside **8**, which was successfully immobilized on a quartz glass surface. Direct UV-vis absorption spectroscopy as well as contact angle measurement demonstrated successful surface functionalization. Besides that, photochromic properties of functionalized glass surfaces were determined. Due to effective *E*/*Z* isomerization and half-life times around 6 h the prepared surfaces were used in bacterial adhesion studies. Irradiation of the quartz slides with two different wavelength (365 and 440 nm) resulted in switching of bacterial adhesion. The obtained findings are in accordance with earlier results, showing that the azobenzene configuration of the immobilized azobenzene mannoside **8** correlates with the adhesivity of the surface.

4.2.2 References

[1] N. Sharon, *Biochem. Soc. Trans.* **2008**, *36*, 1457-1460.

[2] a) J. L Reyman, M. Bergmann, T. Darbre, *Chem. Soc. Rev.* **2013**, *42*, 4814-4822; b) A. Persat, C. D. Nadell, M. K. Kim, F. Ingremeau, A. Sirvaporn, K. Drescher, N. S. Wingreen, B. L. Bassler, Z. Gitai, H. A. Stone, *Cell* **2015**, *161*, 988-997.

[3] P. D. Olson, D. A. Hunstad, *Pathogens.* **2016**, *5*, 2-10.

[4] a) J. Lillington, S. Geibel, G. Waksman, *Biochim. Biophys. Acta.* **2014**, *1840*, 2783-2793; b) M. Hartmann, T. K. Lindhorst, *Eur. J. Org. Chem.* **2011**, 3583-3609.

[5] a) J. M. Rini, *Annu. Rev. Biophys. Biomol. Struct.* **1995**, *24*, 551-577; b) N. Sharon, H. Lis, *Glycobiology* **2004**, *14*, 53R-62R.

[6] a) H.-J. Gabius, S. André, J. Jimènez-Barbero, A. Romero, D. Solís, *Trend Biochem. Sci.* **2011**, *36*, 298-313; b) M. A. Wolfert, G.-J. Boons, *Nature Chem. Biol.* **2013**, *9*, 776–784; c) C. R. Bertozzi, L. L. Kiessling, *Science* **2001**, *291*, 2357-2364.

[7] a) Y. Liu, A. S. Palma, T. Feizi, *Biol. Chem.* **2009**, *390*, 647–656; b) N. Laurent, J. Voglmeir, S. L. Flitsch, *Chem. Commun.* **2008**, 4400-4412; c) T. Horlacher, P. H. Seeberger, *Chem. Soc. Rev.* **2008**, *37*, 1414–1422; d) J. E. Turnbull, R. A. Field, *Nat. Chem. Biol.* **2007**, *3*, 74-77; e) M. Kleinert, T. Winkler, A. Terfort, T. K. Lindhorst, *Org. Biomol. Chem.* **2008**, *6*, 2118-2132.

[8] a) V. Chandrasekaran, H. Jacob, F. Petersen, K. Kathirvel, F. Tuczek, T. K. Lindhorst, *Chem. Eur. J.* **2014**, *20*, 8744-8752; b) T. Weber, V. Chandrasekaran, I. Stamer, M. B. Thygesen, A. Terfort, T. K. Lindhorst, *Angew. Chem.* **2014**, *126*, 14812-14815; *Angew. Chem. Int. Ed.* **2014**, *53*, 14583-14586.

[9] a) J. Auernheimer, C. Dahmen, U. Hersel, A. Bausch and H. Kessler, *J. Am. Chem. Soc.* **2005**, *127*, 16107-16110; b) P. M. Mendes, *Chem. Soc. Rev.* **2008**, *37*, 2512-2529; c) W. R. Browne, B. L. Feringa, *Annu. Rev. Phys. Chem.* **2009**, *60*, 407-428; d) M.-M. Russew, S. Hecht, *Adv. Mater.* **2010**, *22*, 3348-3360; e) C. Poloni, W. Szymanski, B. L. Feringa, *Chem. Commun.* **2014**, *50*, 12645-12648; f) Y. Huang, H. Kang, G. Li, C. Wang, Y. Huang, R. Liu, *RSC Advances* **2013**, *3*, 15909-15916; g) E. Vaselli, C. Fedele, S. Cavalli, P. A. Netti, *ChemPlusChem* **2015**, *80*, 1547-1555.

[10] L. Möckl, A. Müller, C. Bräuchle, T. K. Lindhorst, *Chem. Commun.* **2016**, *52*, 1254-1257.

[11] M. Hartmann, A. K. Horst, P. Klemm and T. K. Lindhorst, *Chem. Commun.* **2010**, *46*, 330-332.

[12] B. Priewisch, K. Rück-Braun, *J. Org. Chem.* **2005**, *70*, 2350-2352.

[13] E. D. Goddard-Borger, R. V. Stick, *Org. Lett.* **2007**, *9*, 3797-3800.

4.3 Fabrication of photoswitchable glycosylated beads

The development of new diagnostic tools as well as enhanced assay system to facilitate the investigation of carbohydrate-lectin interactions is a fundamental task in the glycosciences. In this chapter the utilization of carbohydrate-coated beads to develop a bead-based kit for the investigation of carbohydrate-specific agglutination of *E. coli* bacteria as an alternative to the classical hemagglutination assay is presented.

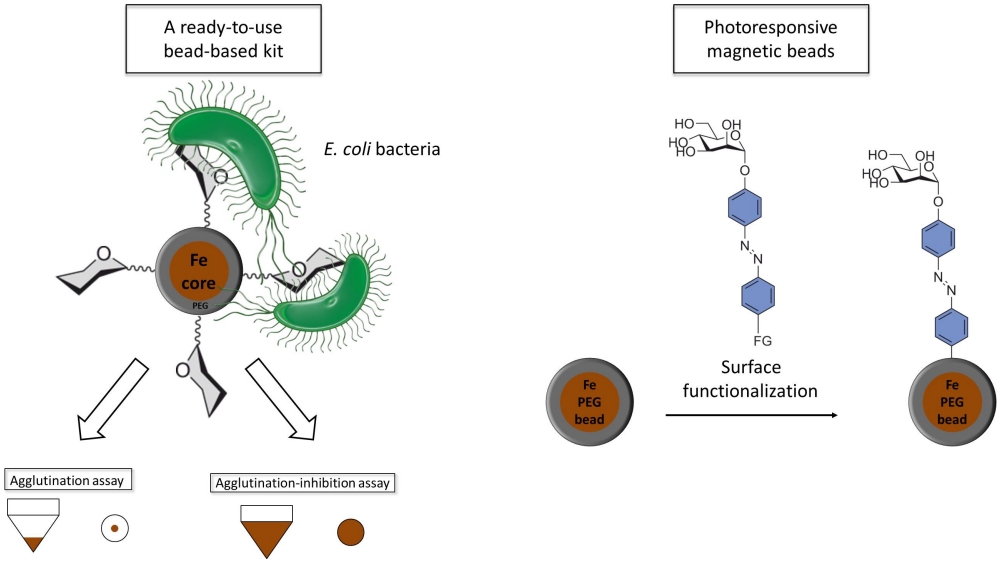

Figure 4.9. In this chapter the development of a bead-based kit and the preaparation of azobenzene mannoside functionalized magnetic PEG beads is reported.

Initially, *manno*-, *gluco*- as well as *arabino*-configured azido-functionalized glycosides possessing either an aromatic or aliphatic aglycone were synthesised and coupled to a trifunctional linker molecule in a cooper- catalyzed click reaction. In a three step synthesis comprising a deprotection step, activation of carboxylic acid beads and amide coupling, immobilization on the solid support (magnetic bead) was enabled. Subsequently, the prepared carbohydrate-coated beads could be successfully utilized in a carbohydrate specific agglutination and agglutination-inhibition assay with type 1 fimbriated *E. coli* bacteria. Since, the prepared beads have the advantage that they can be stored for several months until use, the developed assay provides a ready-to-use bead-based kit (Figure 4.9), which may facilitate the investigation of wild-type bacterial lectins as well as the inhibitory potency of new anti-adhesive compounds.
In order to make the bead-based kit photoswitchable additionally, a glycoazobenzene derivate was immobilized on the surface of magnetic beads and tested in bacterial adhesion studies. However, no significant difference in bacterial adhesion upon isomerization of the immobilized mannoside was observed. Nevertheless, this approach is especially advantageous as bound bacteria could be detached from beads under relatively mild conditions (hν) which offers the possibility to develop new detection methods of bacteria, also for diagnostic applications..

4.3.1 Manuscript on the preparation of glycosylated magnetic PEG-beads to study carbohydrate-dependent adhesion of *E. coli* bacteria

"Sweet and magnetic: A bead-based kit to study carbohydrate-specific adhesion of *E. coli* bacteria"

This chapter was written in manuscript form with the view of a timeley publication of these results.

A. Müller, K. Kolbe, D. Pussack, L. Hartmann, T. K. Lindhorst.

Abstract: Carbohydrate-lectin binding assay - easier than ever: Many bacterial adhesins and toxins are of lectin origin and strongly contribute to the virulence characteristics of the pathogen. New magnetic glycosylated beads enable to precisely study carbohydrate-lectin interactions of non-labeled bacteria and simultaneously isolate the agglutinates. An approach that might facilitate the development of new diagnostic tools in future.

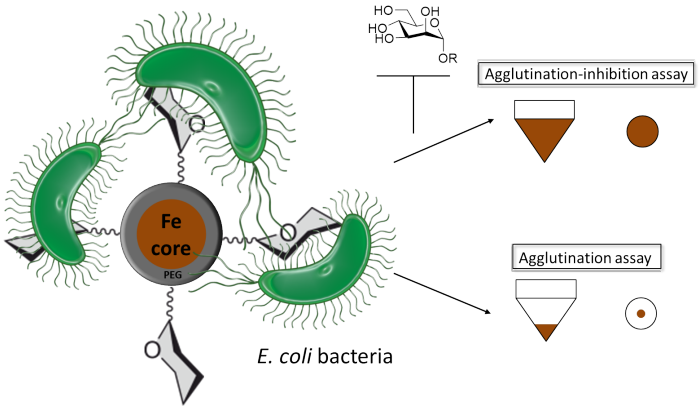

TOC Graphic 4.2. A bead-based kit to study carbohydrate-specific adhesion of *E. coli* bacteria. An agglutination and agglutination-inhibition assay was reported.

Scientific contribution to this paper

In this project I carried out all experimental work with the support of K. Kolbe who performed the synthesis of arabinofuranoside derivatives. K. Kolbe and I performed all bacterial adhesion studies together. K. Kolbe, T. K. Lindhorst, and I wrote the manuscript together.

4.3.1.1 Introduction

The classical method for the investigation of carbohydrate binding of bacteria is the hemagglutination inhibition assay (HAI) developed in the 1940s.[1] It is based on the ability of lectins to agglutinate cells such as erythrocytes (Figure 4.10). HAI is useful to screen the carbohydrate specificity of microbes and to quantify the potency of inhibitor molecules of lectin-mediated agglutination. Other than microtiter plate based-testing of bacterial adhesion employing glycoarrays for example, testing of hemagglutination also reflects the picture of the 3D effects of carbohydrate-protein interactions. Formerly, we used HAI to evaluate synthetic inhibitors of lectin-mediated carbohydrate binding of uropathogenic *Escherichia coli* (UPEC) bacteria using guinea pig erythrocytes.[2] However, this assay is dependent on many unspecific factors related to the nature of the erythrocytes. Also, it falls short to test artificial glycosylation patterns and specific parameters of carbohydrate recognition such as sugar orientation.

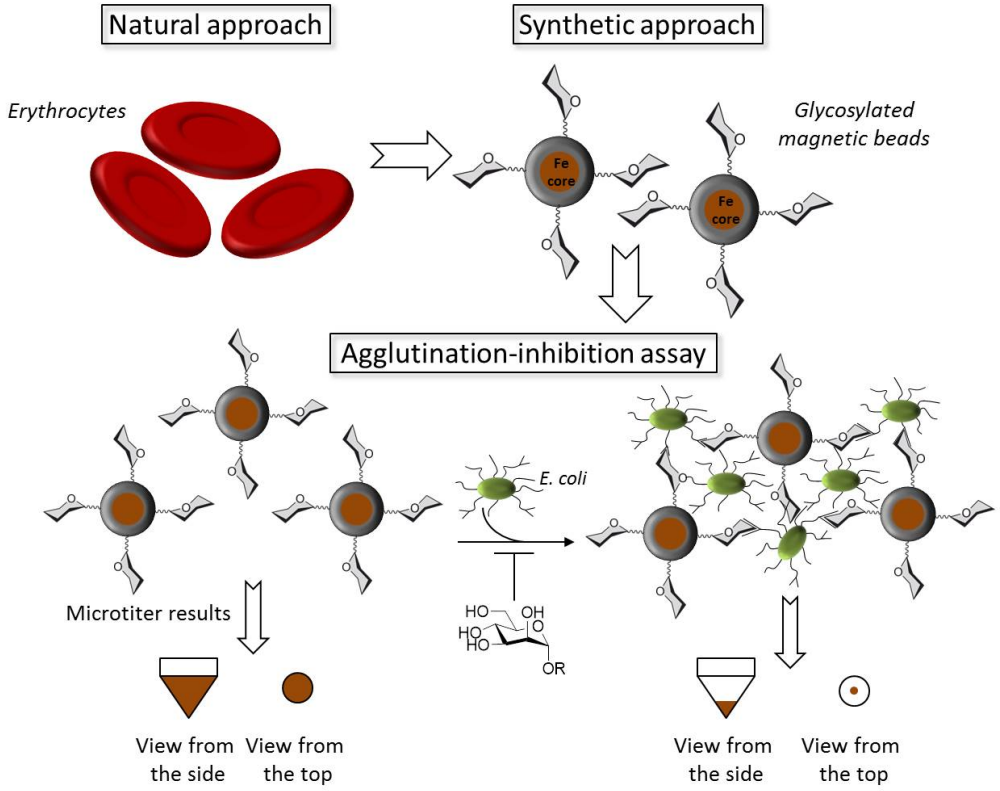

Figure 4.10. Schematic representation of the bead based kit to study carbohydrate-specific adhesion of *E. coli* bacteria. In contrast to the classical HAI, erythrocytes are substituted by tailor-made glycomagnetic beads.

Therefore, it is worthwhile to substitute erythrocytes by synthetic glycosylated beads. Mannoside-functionalized fluorescent polymers[3] or carbohydrate-functionalized nanodiamonds[4] were employed before to isolate *E. coli* bacteria. In particular, magnetic beads coated with antibodies[5], lectins[6] or carbohydrates[7,8] were used to capture *E. coli* bacteria from complex media including stagnant water or food, respectively. Magnetic particles offer many unique characteristics. The separation of bound bacteria from complex mixtures is possible by using a simple magnet. Due to the high

surface-to-volume ratios of magnetic beads, a high contact surface area is offered to capture photogenes. In addition, magnetic beads can be decorated with a variety of different functional groups. The conjugation of inexpensive carbohydrates is possible and thus a multivalent presentation of glycoconjugates on the surface is provided. Carbohydrate-coated beads can surpass the capturing capacity of antibody-coated beads.[8] Carbohydrate-coated beads were utilized in several adhesion-based diagnostic applications to isolate pathogens such as *E. coli* and *Streptococcus suis*.[7-9]Inspired by the classical HAI on the one hand and the advantages of magnetic beads on the other hand, it became our goal to apply glycosylated magnetic beads in a new agglutination-inhibition assay. In this approach erythrocytes are substituted by tailor-made glycomagnetic beads, ideally allowing to directly screen specific requirements of carbohydrate recognition of bacteria and their inhibition (Figure 4.10). In contrast to known microtiter plate based adhesion assays, wild-type bacteria can be analyzed without prior fluorescent labelling or biotin-tagging.[10] Additionally, adhered bacteria to glycosylated beads can be further investigated with a variety of analytical methods, including microscopic analysis, flow cytometry and cultivation. This can be particularly useful for the evaluation of antagonists of bacterial lectins, which may serve as antiadhesives in an anti-adhesion therapy against bacterial infections.[11] Antiadhesives could become an alternative therapy against bacterial infections such as by UPEC,[12] as antibiotics are losing their power due to rising antibiotic resistances.
Following our earlier work[10,13,14], we focused on UPEC and designed building blocks for a bead-based agglutination assay accordingly. Adhesion of UPEC to the urinary bladder is mediated by the type 1 fimbrial lectin FimH recognizing α-D-mannoside residues displayed on urothelial epithelial cells. Consequently, we have used α-D-mannosides for our assay, a multifunctional linker and commercially available magnetic polyethylene glycol (PEG) beads to develop a bead-based kit for the investigation of carbohydrate-specific agglutination of *E. coli* bacteria (Figure 4.10). We report a successful proof of concept study suggesting a variety of further applications.

4.3.1.2 Results and discussion

Our synthetic approach towards carbohydrate-functionalized magnetic beads is based on the synthesis of glycosides, functionalized with an azido function in the aglycone moiety, their ligation with a functional linker molecule via click chemistry and final amide coupling to carboxylic acid magnetic PEG beads. To allow for testing with UPEC, α-D-mannosides were synthesised and *gluco*- and *arabino*-configured glycosides were prepared as control compounds.

4.3.1.2.1 Synthesis of azido-functionalized glycoconjugates

To access the azido-functionalized glycosides **5**, **8** and **15**, the phenol derivative **2**[15] had to be prepared first (Scheme 4.5). Thus, in a diazotransfer reaction with imidazole-1-sulfonyl azide as a diazo donor,[16] commercial readily available tyramine **1** was converted into the corresponding azide **2**[15] under copper catalysis in 73% yield. The azide **2** was then utilized as glycosyl acceptor

in a Lewis acid-promoted mannosylation with the glycosyl donor **3**[17], to yield the fully protected mannoside **4**[18]. Whereas glucoside was obtained directly from the pentaacetate **6**[19] in 69%. Subsequent deacetylation of **4** and **7** under Zemplén conditions[20] led to the desired glycosides **5** and **8**.

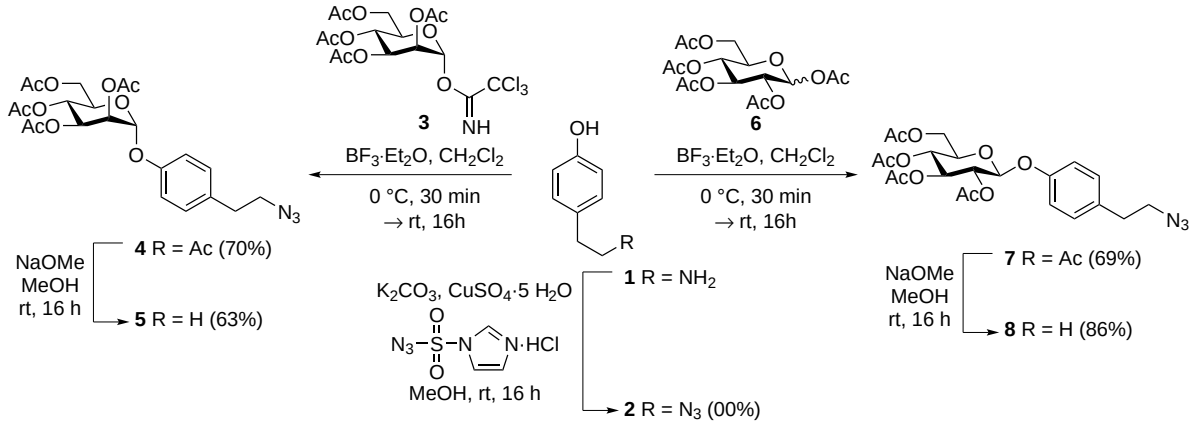

Scheme 4.5. Synthesis of azido-functionalized glycosides **5** and **8**.

The synthesis of the appropriate azido-functionalized arabinofuranosides **15** and **18**[21] was commenced from D-arabinose (Scheme 4.6).

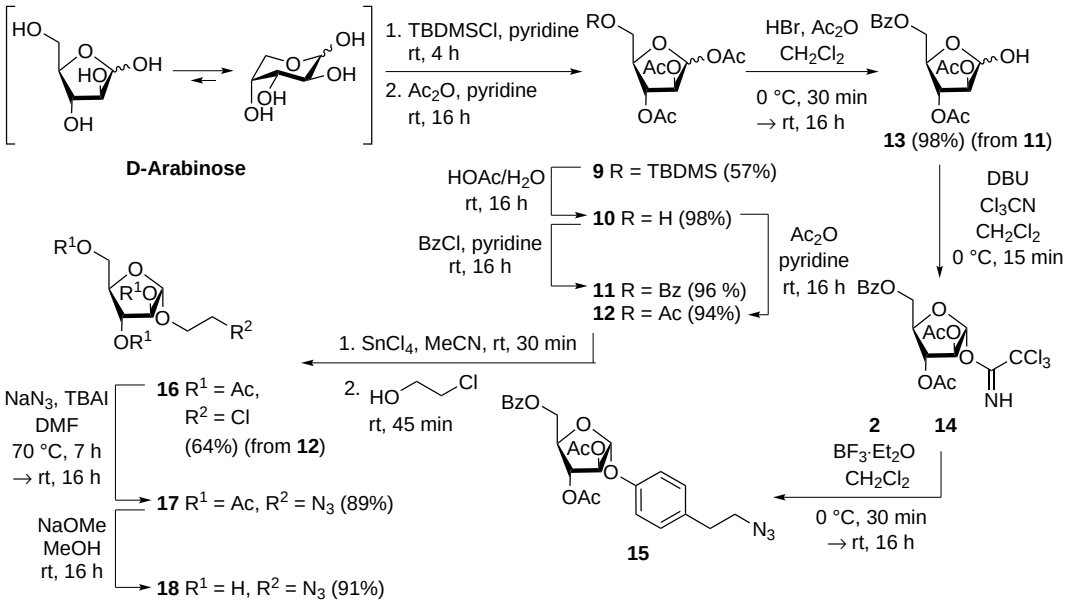

Scheme 4.6. Synthesis of azido functionalized arabinofuranosides **15** and **18**.

Initially, the 5-position of D-arabinose was regioselectively protected with *tert*-butyldimethylsilyl chloride (TBDMS-Cl) in pyridine, subsequent acetylation of the remaining free OH groups was accomplished with acetic anhydride in pyridine and furnished **9**[22] in 57% over two steps. Following deprotection of the TBDMS group using a mixture of acetic acid and water gave **10**[23] possessing free 5-OH group in 98% isolated yield. The 5-hydroxyl group was subsequently protected with benzoylchloride in pyridine to yield **11** in 96%. Desired glycosyl donor **14** was then prepared from **11** in a two-step sequence: deprotection of the anomeric position under acidic conditions

followed by base-catalysed formation of the trichloracetimidate **14**. The synthesis of the desired azido-functionalized arabinofuranoside **15** was carried out by coupling the acceptor azide **2** with crude glycosyl donor **14** in presence of the promoter boron trifluoride to produce **15** in a moderate isolated yield of 28% over two steps.

Aliphatic arabinofuranoside **18** was prepared next starting from **10**[23] which was treated with acetic anhydride in pyridine to yield the fully protected arabinose derivative **12**[24] in 94%. In a tin tetrachloride promoted glycosylation of **12**[24] with 2-chlorethanol, **16**[21] was obtained as the pure α-isomer in a good yield of 64%. A nucleophilic substitution reaction with sodium azide in dimethylformamide gave **17**[21] in 89% yield. In a final step, the removal of the acetyl groups under Zemplén conditions[20] proceeded smoothly and the desired target arabinofuranoside **18** was isolated in high yield.

The azido-functionalized glycosides **5**, **8**, **15**, and **18** possessing either an aromatic or aliphatic aglycon, can be utilized for the fabrication of glycosylated PEG beads of different kind via copper catalysed click reaction.[25]

4.3.1.2.2 Fabrication of glycosylated magnetic PEG beads

In order to couple the prepared glycosides to magnetic beads the orthogonal trifunctional linker molecule **19**[26] was synthesised, bearing two orthogonally protected amino groups and a triple bond, which enables azide-alkyne 1,3-dipolar cycloaddition.[25] As depicted in Scheme 4.7 treatment of the respective azido-functionalized glycoside with the linker molecule **19** using Cu(I)-catalyzed click reaction provided the corresponding conjugated glycosides in yields ranging from 67% to 89% (q.v. Scheme 4.7 and Figure 4.11).

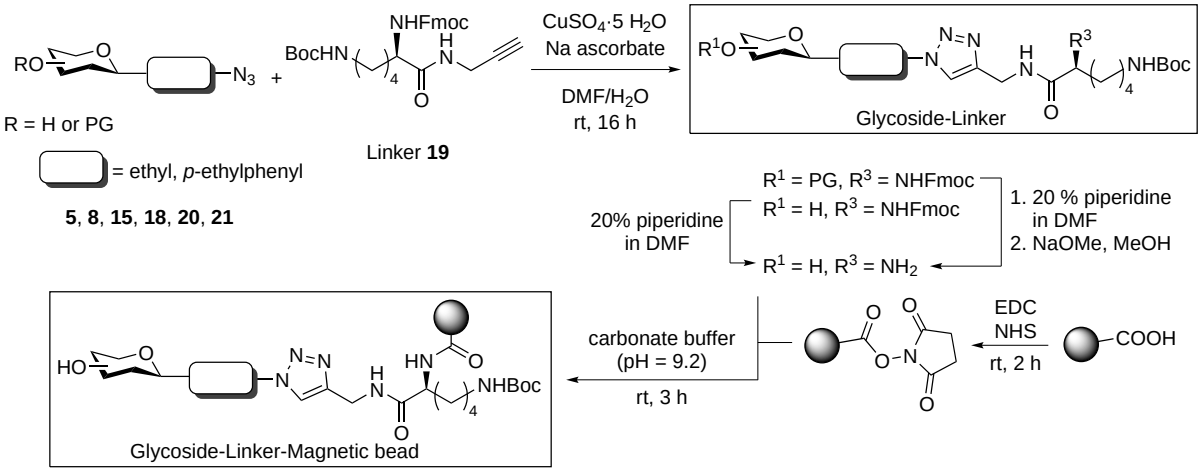

Scheme 4.7. General reaction scheme for the preparation of amino-functionalized glycosides and coupling to the solid support (magnetic bead), PG = protecting group. Azidoethyl mannoside **20**[27] and glucoside **21**[28] were prepared according to literature.

Subsequent cleavage of the Fmoc-protecting group with 20% piperidine in dimethylformamide gave the free amines **28**, **29** and **31**-**33**. However, in case of arabinofuranoside **24**, after cleavage of the Fmoc-protecting group, remaining acetyl or benzoyl groups, respectively, were removed with sodium methoxide in methanol to yield the free amine **30**. In a two-step synthesis comprising carbodiimide-

activation of the surface carboxyl groups with 1-ethyl-3-(3-dimethylaminopropyl)carbodiimide (EDC) and *N*-hydroxysuccinimide (NHS) in 2-(*N*-morpholino)ethanesulfonic acid (MES)-buffer and subsequent coupling of the respective free amines (Figure 4.11) **28-33** to the solid support, glycosylated magnetic PEG beads were obtained. The prepared beads suspension in phosphate-buffered saline (PBS) could be stored for several months at 4 °C until use. Successful functionalization of magnetic beads was detected by a Concanavalin A (Con A) assay (for details cf. Supporting Information).

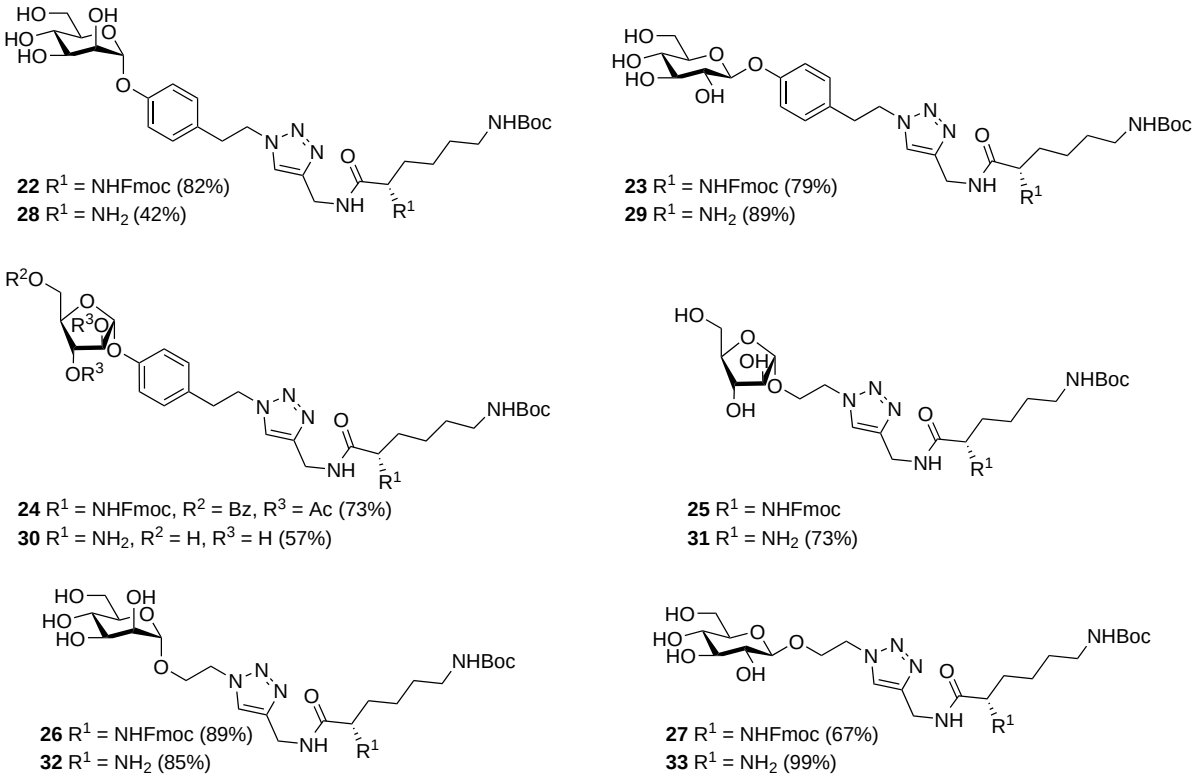

Figure 4.11. Results of 1,3-dipolar cycloaddition and following deprotection reaction of the respective glycoside as shown in Scheme 4.7.

4.3.1.2.3 Adhesion-inhibition assay with GFP expressing *E. coli* bacteria

Initially, all prepared amino glycosides (**28-33**), which have been used for the functionalization of the magnetic PEG beads, were examined as soluble inhibitors of type 1 fimbriae-mediated bacterial adhesion in a well established microtiter plate-based assay.[10] This assay was performed as a reference for the following new bead-based assays giving indications of the binding efficiencies of the putative FimH ligands. Serial dilutions of the respective glycosides **28-33** in buffer were used to interfere with bacterial adhesion of green fluorescent protein (GFP) expressing *E. coli* bacteria (strain pPKL1162[10]) to mannan-coated microtiter plates. On each individual plate methyl α-D-mannopyranoside (MeMan) was tested in parallel to provide a universal reference inhibitor of type 1 fimbriae-mediated bacterial adhesion. For each tested glycoside sigmoidal inhibition curves were determined, from which IC_{50} values of the respective inhibitors were deduced (for details cf.

Supporting Information). The IC_{50} value of an inhibitor represents the concentration at which 50% of bacterial adhesion is prevented. Furthermore relative inhibitory potencies (RIP values) were specified for the glycosides **28**-**33** with regard to the IC_{50} value obtained for MeMan, which was defined as reference inhibitor (Table 4.4).

Table 4.4. Inhibition of type 1 fimbriae-mediated *E. coli* bacteria adhesion to a mannan-coated surface. Only for **28**, **29** and **32** IC_{50} values could be determined. IC_{50} and RIP values are averaged from mean values from at least two independent tests.

Glycoside	IC_{50}[mM] (SD)[a]	RIP (MeMan)[b] (SD)[a]
28	0.03 (0.01)	174.75 (21.44)
29	13.70 (2.45)	0.09 (0.01)
32	1.96 (0.03)	1.40 (0.12)

[a] SD: standard deviation;
[b] RIP: relative inhibitory potency referenced to MeMan (MeMan was tested simultaneously on the same microtiter plate.)

As expected the mannosides **28** and **32** showed the best IC_{50} values and were identified as potent molecules for interaction with FimH. As well glycoside **29** showed a certain inhibitory potency even though it was smaller than that of MeMan (Figure 8.21, 8.22 and 8.23 cf. Supporting information). As opposed to that the glucopyranoside **33** possessing an aliphatic aglycon as well as arabinofuranosides **30** and **31** did not inhibit bacterial adhesion in the analyzed concentration value. Those results comply with earlier findings and are in accordance with literature.[13,11d]

4.3.1.2.4 Agglutination assay with *E. coli* bacteria

In the next step of our study we tested the prepared glycosylated magnetic beads for their ability to agglutinate the same *E. coli* bacteria strain as used in the known microtiter plate-based assay. Hence, in a serial dilution respective glycosylated beads of corresponding glycosides **28**-**33** in buffer were transferred to 96-well V-bottom plates, a constant amount of type 1-fimbriated *E. coli* bacteria were added and the plated incubated while intensely shaking (600 rpm). To exclude non-specific binding of bacteria to beads, carboxylic acid PEG beads blocked with ethanolamine and beads decorated with the Fmoc-deprotected linker molecule were tested as controls, in parallel on each individual plate. Results were optical evaluated (Figure 4.12, and 8.24 and 8.25 cf. Supporting information).

Beads functionalized with the mannosides **28** or **32** resulted in a prominent agglutination (Figure 4.12), while no agglutination was determined for *gluco*- and *arabino*-configured glycosylated beads (Figure 8.24 and 8.25 cf. supporting information). Furthermore, in case of beads functionalized with mannoside **28** even at a concentration of $11.3 \cdot 10^6$ beads per milliliter agglutination was observed. However, beads decorated with **32** showed a less pronounced effect as at a concentration of $4.5 \cdot 10^7$ beads/mL no further settling of beads suspension was detected.

Figure 4.12. Agglutination of magnetic PEG beads in a serial dilution decorated with mannosides **28** or **32**; using type 1-fimbriated *E. coli* bacteria. The depicted figures are representative examples from at least three independent experiments. Carboxylic acid beads blocked with ethanolamine and beads decorated with the Fmoc-deprotected linker molecule were tested simultaneously on each plate.

To validate the results determined by optical evaluation beads were subsequently isolated using a magnetic separation rack and adhered bacteria were detected by read out of fluorescence intensity (Figure 4.13).

The obtained results confirm clearly the effective adhesion of bacteria to beads decorated with mannosides **28** or **32**. Beside that the adhesion of bacteria is much higher to mannoside-functionalized beads possessing an aromatic aglycon whereas the adhesivity of bacteria is decreased of about 69% for *manno*-configured beads possessing an aliphatic aglycon. Glycosylated beads prepared from glucosides **29** and **33** or arabinofuranosides **30** and **31**, respectively, were not suited to mediate type 1 fimbriae-mediated bacterial adhesion. Also, no unspecific binding to blocked carboxylic acid beads as well as to beads treated with the linker molecule was observed. These findings are in accordance with the output of the microtiter plate-based assays made before and demonstrate that glycosylated beads can be perfectly used to study adhesion of *E. coli* bacteria, avoiding the necessity to label the bacteria prior investigation. In order to examine the amount of bacteria needed for successful agglutination, type 1-fimbriated *E. coli* bacteria were added in serial dilution to a constant number of the respective glycosylated beads of corresponding glycosides **28**-**33** in buffer. Optical evaluation of the obtained results showed that at a concentration of $5 \cdot 10^6$ bacteria/mL an unambiguous settling of agglutinated beads could still be observed (Figure 8.26 and 8.27 cf. supporting information). However, for undisputed read out the bacteria concentration was subsequently standardized to a concentration of $2 \cdot 10^7$ bac/mL.

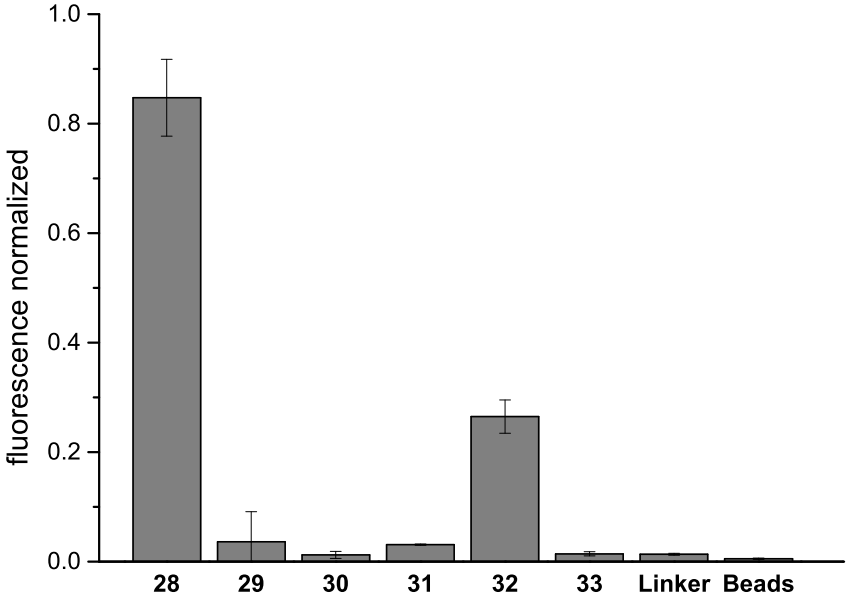

Figure 4.13. Bacterial binding to respective magnetic glycosylated PEG-beads of corresponding glycosides **28**-**33** as well as blocked carboxylic acid PEG-beads and beads decorated with the Fmoc-deprotected linker molecule. Error bars are standard deviation (SD) of triplicates of at least two independent experiments.

4.3.1.2.5 Agglutination-inhibition assay with *E. coli* bacteria

In the next step of our study, we wanted to verify whether inhibition of agglutination could be achieved by adding appropriate competing carbohydrates (Figure 4.14).
Manno-configured PEG-beads prepared from **28** were utilized since these showed the best results for an effective agglutination with *E. coli* bacteria. *p*-Aminophenyl mannoside (*p*APMan) and MeMan were applied as inhibitors. While *p*APMan is known as strong inhibitor, MeMan only weakly inhibits type 1 fimbriae-mediated bacterial adhesion.[13] Hence, a solution of the respective inhibitor in PBS-buffer was employed in different concentrations (*p*APMan: 10 mM, 1 mM, 0.1 mM, 0.01 mM and 0.001 mM; MeMan: 100 mM, 10 mM, 1 mM, 0.1 mM and 0.01 mM) to beads decorated with **28**. A constant number of *E. coli* bacteria were added to each sample. Beads decorated with **28** were tested as a positive control without the addition of an inhibitor, simultaneously on each individual plate. Results were then optical analysed (Figure 4.14).
At a concentration of 1 mM in the presence of *p*APMan agglutination of type 1 fimbriae-mediated bacterial adhesion was clearly inhibited, while concentrations lower than this (0.1 mM) resulted in settling of beads decorated with **28**. However, in the presence of MeMan inhibition of bacterial adhesion to the beads was still observed at a concentration of 10 mM inhibitor solution. The obtained results demonstrate that *p*APMan has an approximately tenfold higher inhibitory potency than MeMan and showed the agglutination is FimH specific. These findings are again in accordance with earlier results.[13] Conclusively, glycosylated beads can be easily utilized in an agglutination-

inhibition assay and appropriate competing sugars can be added in relatively low concentrations, which is particularly important if they are not available in huge amounts. Thus, this method provides a fast and easy reliable testing system to investigate the inhibitory potency of various ligands for FimH.

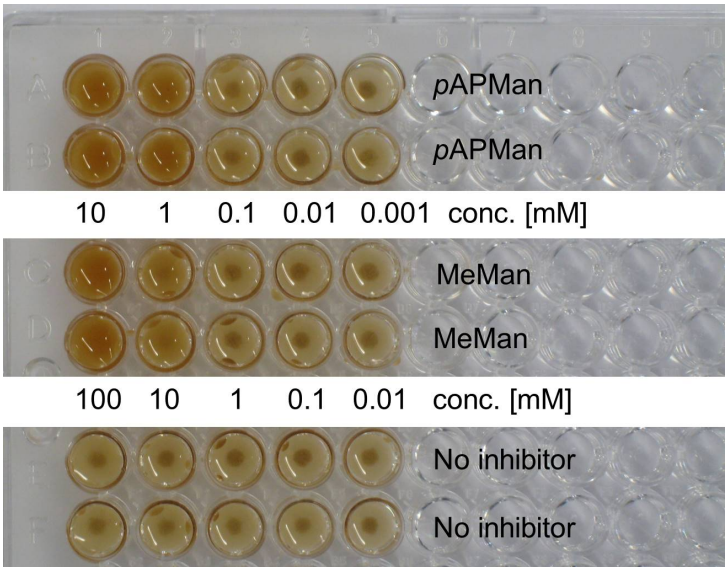

Figure 4.14. Inhibition of type 1 fimbriae-mediated bacterial adhesion to magnetic glycosylated with a) *p*APMan applied in concentrations of 10 mM, 1 mM, 0.1 mM, 0.01 mM and 0.001 mM and b) MeMan applied in concentrations of 100 mM, 10 mM, 1 mM, 0.1 mM and 0.01 mM as inhibitors. As positive control PEG beads prepared from **28** were tested simultaneously on each plate without the addition of an inhibitor (c)). A constant number of *E. coli* bacteria were used in the inhibition experiment. The depicted pictures are representative examples from at least three independent experiments.

4.3.1.3 Conclusion

A successful carbohydrate specific agglutination and agglutination-inhibition assay involving glycosylated magnetic beads was established and the obtained results are in total accordance with the literature. Due to the unique characteristics of magnetic PEG particles, in a straightforward approach carbohydrate-coated beads could be easily prepared, stored for several months until use and be directly applied to study carbohydrate-lectin interactions of non-labeled bacteria. This ready-to-use bead-based kit can therefore facilitate the investigation of wild-type bacterial lectins as well as the inhibitory potency of new anti-adhesive compounds. Using a bead-based assay is additionally favoured due to the broad analytical scope.

4.3.1.4 References

[1] G. K. Hirst, *J. Exp. Med.* **1942**, *75*, 49-64.

[2] T. K. Lindhorst, C. Kieburg, U. Krallmann-Wenzel, *Glycoconj. J.* **1998**, *15*, 605-613.

[3] M. D. Disney, J. Zheng, T. M. Swager, P. H. Seeberger, *J. Am. Chem. Soc.* **2004**, *126*, 13343-13346.

[4] a) M. Hartmann, P. Betz, Y. Sun, S. N. Gorb, T. K. Lindhorst, A. Krueger, *Chem. Eur. J.* **2012**, *18*, 6485-6492; C. Fessele, S. Wachtler, V. Chandrasekaran, C. Stiller, T. K. Lindhorst, A. Krueger, *Eur. J. Org. Chem.* **2015**, 5519-5525.

[5] a) P. M. Fratamico, F. J. Schultz, R. L. Buchanan, *Food Microbiol.* **1992**, *9*, 105-113; b) A. Lund, A. L. Hellemann, F. Vartdal, *J. Clin. Microbiol.* **1988**, *26*, 2572-2575.

[6] J. Porter, J. Robinson, R. Pickup, C. Edwards, *J. Appl. Microbiol.* **1998**, *84*, 722-732.

[7] a) K. El-Boubbou, C. Gruden, X. Huang, *J. Am. Chem. Soc.* **2007**, *129*, 13392-13393; b) M. Behra, N. Azzouz, S. Schmidt, D. V. Volodkin, S. Mosca, M. Chanana, P. H. Seeberger, L. Hartmann, *Biomacromolecules* **2013**, *14*, 1927-1935.

[8] a) D. M. Hatch, A. A. Weiss, R. R. Kale, S. S. Iyer, *ChemBioChem* **2008**, *9*, 2433–2442; b) H. O. Yosief, A. A. Weiss, S. S. Iyer, *ChemBioChem* **2013**, *14*, 251-259.

[9] N. Parera Pera, A. Kouki, S. Haataja, H. M. Branderhorst, R. M. J. Liskamp, G. M. Visser, J. Finne, R. J. Pieters, *Org. Biomol. Chem.* **2010**, *8*, 2425-2429.

[10] M. Hartmann, A. K. Horst, P. Klemm, T. K. Lindhorst, *Chem. Commun.* **2010**, *46*, 330-332.

[11] a) S. Sattin, A. Bernardi, *Trends Biotechnol.* **2016**, *34*, 483-495; b) N. Sharon, I. Ofek, *Glycoconj. J.* **2000**, *17*, 659-664; c) K.-A. Karlsson, *Mol. Microbiol.* **1998**, *29*, 1-11; d) M. Hartmann, T. K. Lindhorst, *Eur. J. Org. Chem.* **2011**, 3583-3609.

[12] a) C. K. Cusumano, J. S. Pinkner, Z. Han, S. E. Greene, B. A. Ford, J. R. Crowley, J. P. Henderson, J. W. Janetka, S. J. Hultgren *Sci. Transl. Med.* **2011**, *3*, 109-115; b) A. Barras, F. A. Martin, O. Bande, J.-S. Baumann, J.-M. Ghigo, R. Boukherroub, C. Beloin, A. Siriwardena, S. Szunerits, *Nanoscale* **2013**, *5*, 2307-2316; c) S. Altarac, D. Papeš, *BJU Int.* **2014**, *113*, 9-10; d) X. Jiang, D. Abgottspon, S. Kleeb, S. Rabbani, M. Scharenberg, M. Wittwer, M. Haug, O. Schwardt, Beat Ernst, *J. Med. Chem.* **2012**, *55*, 4700-4713.

[13] C. Fessele, T. K. Lindhorst, *Biology* **2013**, *2*, 1135-1149.

[14] C. Grabosch, M. Hartmann, J. Schmidt-Lassen, T. K. Lindhorst, *ChemBioChem* **2011**, *12*, 1066-1074.

[15] C. Sibbersen, L. Lykke, N. Gregersen, K. A. Jørgensena, M. Johannsen, *Chem. Commun.* **2014**, *50*, 12098-12100.

[16] E. D. Goddard-Borger, R. V. Stick, *Org. Lett.* **2007**, *9*, 3797-3800.

[17] K. H. Jung, M. Hoch, R. R. Schmidt, *Liebigs Ann. Chem.* **1989**, 1099-1106.

[18] M. Touaibia, T. C. Shiao, A. Papadopoulos, J. Vaucher, Q. Wang, K. Benhamioud, R. Roy, *Chem. Commun.* **2007**, 380-382.

[19] M. L. Wolfrom, A. Thompson, Meth. *Carbohydr. Chem.* **1963**, *2*, 211-215.

[20] G. Zemplén, E. Pascu, *Ber. Dtsch. Chem. Ges. B*, **1929**, *62*, 1613-1614.

[21] A. K. Pathak, V. Pathak, N. Bansal, J. A. Maddry, R. C. Reynolds, *Tetrahedron Lett.* **2001**, *42*, 979-982.

[22] T. K. Lindhorst *Essentials of Carbohydrate Chemistry and Biochemistry.* Edn 3, Wiley-VCH, Weinheim, **2007**.

[23] G. Legler, A. E. Stütz, H. Immich, H., *Carbohydr. Res.* **1995**, *272*, 17-30.

[24] B. L. Kam, J. L. Barascut, J. L. Imbach, J. L., *Carbohydr. Res.* **1979**, *69*, 135-142.

[25] a) V. V. Rostovtsev, L. G. Green, V. V. Fokin, K. B. Sharpless, *Angew. Chem.* **2002**, *114*, 2708–2711; *Angew. Chem. Int. Ed.* **2002**, *41*, 2596-2599; b) C. W. Tornøe, C. Christensen, M. Meldal, *J. Org. Chem.* **2002**, *67*, 3057-3064.

[26] S. Deshayes, V. Maurizot, M.-C. Clochard, C. Baudin, T. Berthelot, S. Esnouf, D. Lairez, M. Moenner G. Déléris, *Pharm. Res.* **2011**, *28*, 1631-1642.

[27] T. K. Lindhorst, S. Kötter, U. Krallmann-Wenzel, S. Ehlers, *J. Chem. Soc., Perkin Trans. 1* **2001**, 823-831.

[28] T. M. Tagmose, M. BoIs, *Chem. Eur. J.* **1997**, *3*, 453-462.

4.4 Photoswitchable glycosylated beads to control adhesion of *E. coli* bacteria

We also wanted to investigate whether bacterial adhesion to magnetic PEG-beads can be photocontrolled by reversible E/Z-isomerization of the immobilized azobenzene mannoside **11**.
Therefore, azobenzene mannoside **8** carrying an azido functional group was required (Scheme 4.8). Synthesis started from the known *p*-aminophenyl mannoside **5**,[113] obtained by catalytical reduction of the commercially available *p*-nitrophenyl mannoside. **5** was then subjected to Mills condensation in a dimethyl sulfoxide acetic acid mixture (1:1) with crude nitrososarene **4**, readily obtained from 4-(*N*-Boc-aminoethyl)aniline by reported methods,[304] to yield the unsymmetrical azobenzene mannoside **6** in 84% (Scheme 4.8). Subsequent cleavage of the Boc-protecting group with trifluoroacetic acid (TFA) furnished the ammonium salt **7** in nearly quantitative yield. In a following diazotransfer reaction with the diazo donor imidazole-1-sulfonyl azide[305] in methanol under copper catalysis the free amine **7** was converted in the corresponding azide which was immediately submitted to *O*-acetylation, using acetic anhydride in pyridine to yield the fully protected azobenzene mannoside **8** in 70% yield over two steps. Subsequently, the prepared **8** was coupled to the linker molecule **9** in a copper-(I)-ctalyzed azide alkyne cycloaddition. Next, the Fmoc protecting group was removed under basic conditions together with the acetyl protecting groups to yield azobenzene mannoside **11**.

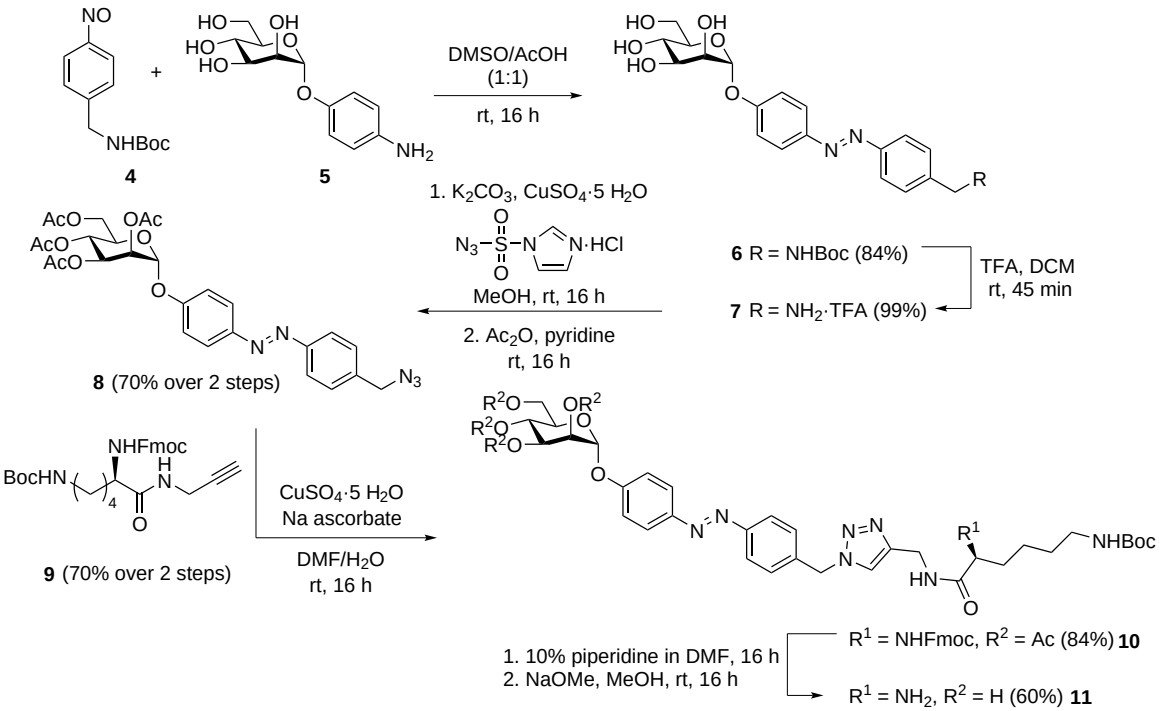

Scheme 4.8. Synthesis of azido functionalized azobenzene mannoside **8** and subsequent coupling to the linker molecule **9**.

The obtained azobenzene derivative **11** was then coupled to the magnetic PEG beads as described in Chapter 4.3.1. To investigate if E/Z-isomerization has an influence on bacterial adhesion to glycoazobenzene functionalized magnetic PEG beads, beads functionalized with **11** were divided into two portions. One set was irradiated with UV light (365 nm) for 15 min to effect E/Z-isomerization of the conjugated azobenzene moiety. The other portion of beads remained untreated. Then, both set

of beads were incubated with GFP-fluorescent *E. coli* for 30 min, subsequently washed with PBS buffer. The number of adhered bacteria was measured by readout of fluorescence intensity (Figure 4.15). As a control, blocked CO_2H-functionalized PEG-beads were tested analogously to exclude unspecific effects arising from changes of the beads due to irradiation.

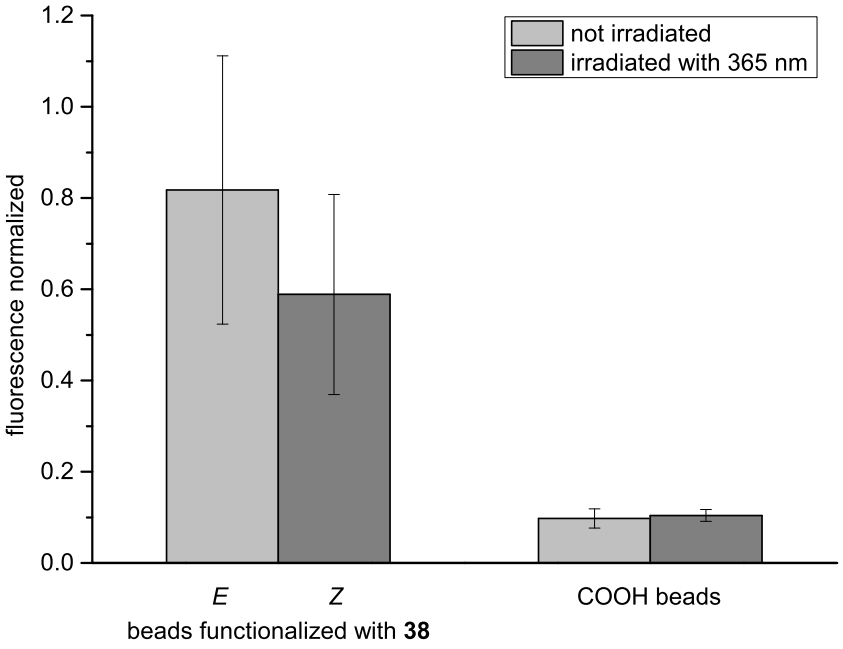

Figure 4.15. Magnetic beads prepared from **11** (left side) and blocked carboxylic acid PEG-beads (right side), respectively were split into two portions, whereas one set was irradiated with UV light (365 nm) and the other set remained untreated. After incubation with fluorescent *E. coli* bacteria, bacterial binding was detected by readout of fluorescence intensity. Error bars are standard deviation (SD) of duplicates of at least three independent experiments.

The switching experiment resulted in no significant difference in bacterial adhesion to glycosylated PEG-beads upon E/Z-isomerization of the immobilized azobenzene mannoside **11** (Figure 4.15). Bacterial adhesion to blocked CO_2H-functionalized beads was very low as expected but was not affected by irradiation. In spite of the fact that photoswitchability of bacterial adhesion to PEG beads could not be shown at this stage, functionalized PEG beads can be regarded as an interesting tool for glycobiological investigatons such as bacterial adhesion studies. They also have potential in the development of new detection methods gor bacteria and also for diagnostic applications.

5 Photocontrol of *E. coli* adhesion to human cells

5.1 Inroduction

As descripted in chapter 3.1 many methods have been developed to facilitate the investigation of cell surface glycoconjugates and their interaction with other biomolecules or even whole organisms. Another important approach to glycobiological studies is metabolic oligosaccharide engineering (MOE).[306,307] With the aid of MOE glycan biosynthesis can be interrupted, cells can be chemically modified, the metabolic flux inside cells can be probed and also specific glycoprotein subtypes from the proteome can be identified.[306]

5.1.1 Metabolic oligosaccharide engineering (MOE)

MOE allows for introduction of specific subtle modifications into monosaccharide residues within cellular glycoconjugates. Therefore, chemically modified substrates are incorporated into the cell envelop of live cells (*e.g.* eukaryotic cells or bacteria), through their cell surface machinery (Figure 5.1).

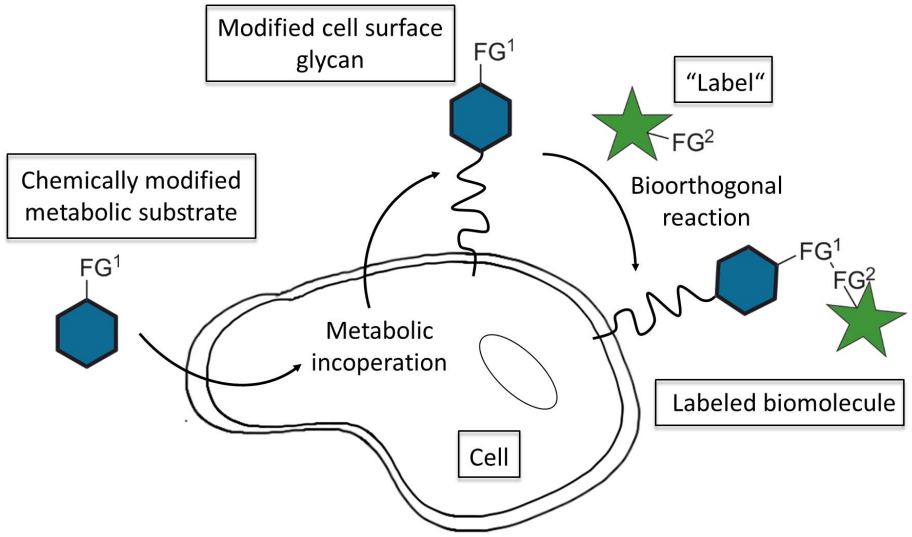

Figure 5.1. Schematic illustration of a two-step bioorthogonal chemistry strategy comprising a first metabolic labelling step and a following bioorthogonal ligation reaction. Therefore, unnatural substrates are transported to the cytoplasm, metabolized and introduced into structures within cellular glycans and respective biomolecules can then be selctively modified with a label (*e.g.* diagnostic or therapeutic probe).

The pioneering scientific work in the field of MOE to study and target eukaryotic glycans was initiated by W. Reutter,[308,309] and elaborated into a standard tool for glycn labeling by C. R. Bertozzi[310,311] and co-workers. In 1992 Reutter *et al.* reported on the discovery that synthetic *N*-acyl-modified D-mannosamines can be incorporated by cells and are tolerated by the entire sialic acid biosynthetic pathway.[312] *N*-Acetylmannosamine (ManNAc) or modified ManNAc derivatives, respectively, serve as the first committed intermediate in the metabolic pathway of sialic acid. Chemically modified ManNAc analogues once taken up by the cell have to compete with physiological

intracellular ManNAcs which are either biosynthesised inside the cell from uridine diphosphate-*N*-acetylglucosamine (UDP-GlcNAc) or also taken up from the cell's milieu, to enter the sialic acid biosynthetic pathway. In five consecutive enzymatic transformation reactions and a transport step into the Golgi apparatus, ManNAc derivatives are converted to sialosides which are mainly introduced at the terminal part of oligosaccharide chains of glycoproteins and glycolipids. Despite the complexity of the sialic acid metabolism, a great variety of *N*-acyl modified mannosamines could be taken up by mammalian cells and efficiently metabolized to the respective unnatural *N*-acyl sialic acid derivatives *in vitro* and *in vivo* (Figure 5.2).[308]

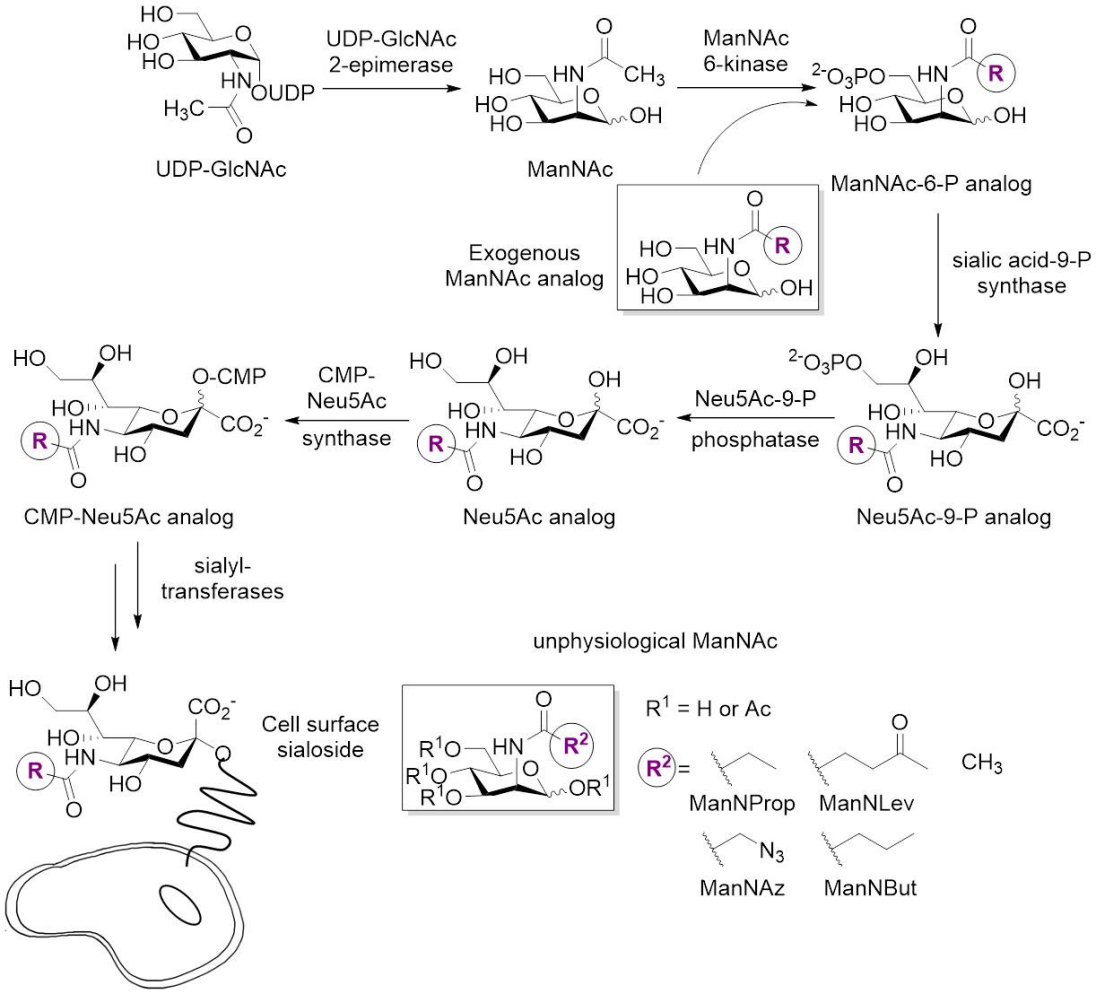

Figure 5.2. Illustration of the biosynthetic sialic acid pathway involving enzymatic conversion of UDP-GlcNAc into ManNAc which is subsequently phosphorylated to yield ManNAc-6-phosphate (ManNAc-6-P). Following condensation with phosphoenolpyruvate results in *N*-acetylneuraminic acid-9-phosphate (Neu5Ac-9-P). In a subsequent dephosphorylation step Neu5Ac is obtained which is converted into the nucleotide carbohydrate donor cytidine-5'-monophospho-Neu5Ac (CMP-Neu5Ac) in the nucleus. CMP-sialic acid is then transported into the Golgi apparatus, utilized by the sialyltransferases and finally, the resulting sialylated glycan structures are delivered to the cell surface.

Additionally to the sialic acid pathway, also the *N*-acetylgalactosamine (GalNAc) and GlcNAc pathway are permissive to unnatural carbohydrate derivatives bearing bioorthogonal functionalities. Thus, keto[313] and azido[314] GalNAc analogues such as *N*-azidoacetylgalactosamine (GalNAz) can be metabolically introduced into mucin-type *O*-linked glycoproteins. Similarly, azido functionalized GlcNAc analogues (GlcNAz) are incorporated into cytosolic and nuclear glycoproteins.[315]
The ability to incorporate structurally altered sialic acids with modified *N*-acyl side chains as well as GalNAc and GlcNAc analogues into cell surface glycoconjugates provides a new tool which allows to study cellular function in more detail.[306] But not only the direct perturbation of glycan function, also the ability to incorporate functional groups into structures of the cell envelope led to new applications of MOE. It is possible to deliver various functional groups through glycan biosynthetic pathways into cell surface glycoconjugates. These small functional groups allow for further modification with exogenous reagents on the cell surface by a selective reaction. However, substrates used for MOE can also directly carry exogenous reagents such as a diagnostic or therapeutic probes, but the incorporation into the cell surface envelop of substrates carrying large functional groups is limited owing to the substrate specificity of metabolic enzymes. Hence, MOE is often used in combination with bioorthogonal chemistry since small modifications are usually tolerated (Figure 5.1). A bioorthogonal chemoselective ligation is a reaction between two functional groups which are selective for each other. Moreover, the ligation occurs in a richly functionalized biological milieu such as at the cell surface or even within living organisms without interfering with natural occuring biochemical processes.[316–318] To be utilized in a bioorthogonal reaction, the respective substrates possess following properties: i) they should be water soluble and stable in water, exhibit functional groups that ii) are compatible with naturally occurring functional groups, iii) undergo a fast and clean (without formation of side products) selective covalent reaction with the desired ligation partner under physiological conditions. A great variety of bioorthogonal ligation methods have been developed for this purpose.[319–323] Bertozzi and co-workers initially utilized ketone-hydrazide chemistry for selective labelling of cells. This method is based on the ability of ketones to specifically react with hydrazide probes to form hydrazine products.[310] In following studies ManNAc derivatives containing an azido group, which are totally absent on the cell surface, were incorporated into cell surface glycans and selectively labelled in a Staudinger ligation reaction with triarylphosphines to yield the respective amides.[311] Triarylphosphines, however, have slow reaction kinetics and can be easily inactivated through oxidation which is especially disadvantageous for targeting cells *in vivo*.[318] Another possibility is the utilization of the regioselective copper(I) catalyzed cycloaddition between an alkyne and an azide forming triazoles.[111,112] However, applications of this method *in vivo* are limited due to the toxicity of copper(II).[324,325] To overcome this problem, the strain promoted azide-alkyne cycloaddition (SPAAC), first discovered by G. Wittig and A. Krebs in 1961,[326] was utilized just recently in biological applications.[327,328] The SPAAC between a strained cyclooctyne derivative and an azide proceeds without the need of elevated temperature or any catalysis. This is based on the ring-strain of the applied alkyne which lowers the activation energy of the cycloaddition reaction. Besides the utilization of ketone-hydrazide and azide-based chemistry[329] many other bioorthogonal ligation methods for metabolic labelling have been developed such as inverse electron demand Diels-Alder[330–333] and transition metal-catalyzed bioorthogonal reactions.[334–336] Nevertheless, SPAAC is still the most commonly used ligation method, owing to fast reaction rates and great

substrate stability *in vivo*.

With the development of MOE in combination with bioorthogonal ligation chemistry, very precise chemical modifications of biomolecules *in vivo* and *in vitro* are possible.[337] MOE allows for non-invasive real-time visualization of molecules and processes within cells or living organism. In combination with fluorescence microscopy for instance, it is possible to monitor spatiotemporal dynamics of labelled biomolecules. Modification with an affinity tag on the other hand enables postlabeling purification. The metabolic approach could be further enhanced by applying improved labelling reagents and detection strategies.[338] Finally, MOE could be also applied to bacterial cell envelop structures.[339–342] Moreover, specific glycan labelling has been extended from studies in cell culture to living organisms such as zebrafish[343,344] and even mice[345,346]. All these diverse biological applications demonstrate clearly the potential of MOE to facilitate investigation of complex cellular processes such as glycan expression as well as dynamics, and might hopefully contribute to further understanding of the importance of glycans for human diseases like cancer or infectious diseases, ehich is the basis for carbohydrate-dependent therapy.

5.2 Switching first contact: photocontrol of *E. coli* adhesion to human cells

Based on the remarkable results which were achieved on photocontrol of bacterial adhesion through re-orientation of carbohydrate presentation on artificial surfaces we extended our investigation to a more complex biological environment (Figure 5.3).

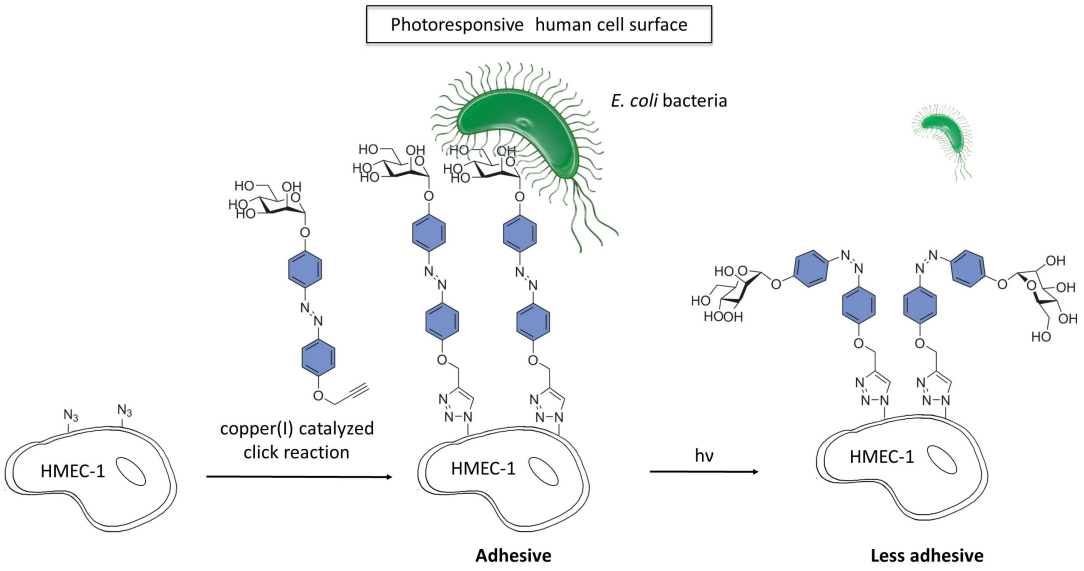

Figure 5.3. In this chapter the photocontrol of *E. coli* bacteria adhesion to human cells is reported.

Therefore, the surface of human cells was modified with glycoazobenzene derivatives, turing the cell surface into a photoswitchable designer surface. To install azobenzene glycosides on the cell surface, azido groups were incorporated into the cell surface envelop according to metabolic oligosaccharide engineering (MOE). The utilization of regioselective copper(I) catalyzed cycloaddition of an alkyne-functionalized azobenzene derivative with the azidefunctionalized cell surface allowed for conjugation with a photoresponsive α-D-mannoside and a β-D-glucoside. Finally, photoisomerization of the installed azobenzene moieties was triggered by irradiation with UV or visible light, respectively and bacterial adhesion was subsequently quantified via high-resolution live-cell fluorescence microscopy. Indeed, switching of the installed azobenzene mannoside configuration allowed for controlling the adhesivity of cells. The bacterial adhesion to cells was increased by ~50% after irradiation with visible light compared to the cell which were *Z*-configured. Owing to these striking results switching of cellular adhesion was further investigated in a real-time, flow-based experiment. In accordance with the experiments under static conditions, also the results observed in the flow assay indicate that the orientation of the immobilized azobenzene mannoside on the surface of human cells has a strong influence on bacterial adhesion. Different control experiments were performed to investigate the obtained results in more detail. Thus, it was shown, that the presented mannose ligand must be located at the terminus of cell surface glycans to guarantee that the difference in bacterial adhesion is not small upon irradiation.

It was demonstrated that the adhesion of bacteria to azobenzene glycoside-modified cell surface is higher after irradiation with visible light than after irradiation with UV light and furthermore it was shown that the effect could be specifically modulated.

"Switching first contact: photocontrol of *E. coli* adhesion to human cells"

Reproduced from L. Möckl, A. Müller, C. Bräuchle, T. K. Lindhorst, *Chem. Commun.* **2016**, *52,* 1254-1257 with permission from the Royal Society of Chemistry.

DOI: 10.1039/c5cc08884d

Abstract: We have shown previously that carbohydrate-specific bacterial adhesion to a non-physiological surface can be photocontrolled by reversible *E/Z* isomerisation using azobenzene-functionalized sugars. Here, this approach is applied to the surface of human cells. We show not only that bacterial adhesion to the azobenzene glycoside-modified cell surface is higher in the *E* than in the *Z* state, but add data about the specific modulation of the effect.

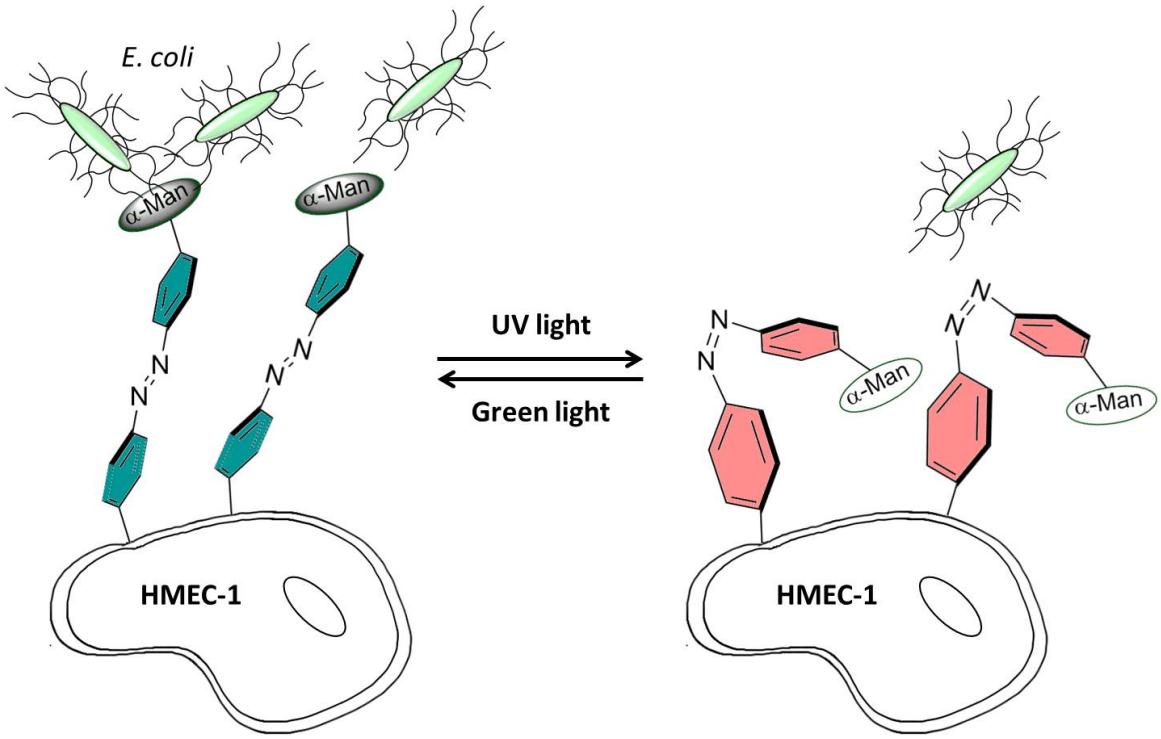

TOC Graphic 5.1. The influence of bacterial adhesion to human cells uppon *E/Z* isomerisation of azobenzene functionalized carbohydrates, was shown.

Scientific contribution to this paper

In this project I carried out all synthesis and the chemical characterisation of the alkyne- functionalized azobenzene derivatives, as well as the investigation of the photochromic propertise of the synthetic compounds. L. Möckl carried out all the bacterial adhesion erxperiments under static as well as under flow conditions and the biophysical analysis. L. Möckl, T. K. Lindhorst, C. Bräuchle and I wrote the article together.

ChemComm

COMMUNICATION

View Article Online
View Journal | View Issue

Cite this: *Chem. Commun.*, 2016, 52, 1254

Received 28th October 2015,
Accepted 18th November 2015

DOI: 10.1039/c5cc08884d

www.rsc.org/chemcomm

Switching first contact: photocontrol of *E. coli* adhesion to human cells†

L. Möckl,‡[a] A. Müller,‡[b] C. Bräuchle*[a] and T. K. Lindhorst*[b]

We have shown previously that carbohydrate-specific bacterial adhesion to a non-physiological surface can be photocontrolled by reversible *E*/*Z* isomerisation using azobenzene-functionalised sugars. Here, this approach is applied to the surface of human cells. We show not only that bacterial adhesion to the azobenzene glycoside-modified cell surface is higher in the *E* than in the *Z* state, but add data about the specific modulation of the effect.

Cell adhesion is a fundamental principle of biology. Many of its aspects have been elucidated,[1,2] but the molecular details of cell interactions are not fully understood. As the first contact of cells is mediated through their glycosylated surfaces, our research on cell adhesion is focused on carbohydrate recognition.

All organisms can recognise and distinguish between carbohydrates with the help of specialised proteins, the lectins.[3] Lectin function has been described in the context of, *i.e.*, signalling, trafficking, and quality control, thus involving indispensable processes of life.[4,5] Also bacterial cells utilise their own lectins to mediate adhesion to glycosylated surfaces such as the membrane of the target cells.[6,7] Furthermore, bacterial adhesion enables bacterial colonization, biofilm formation, biofouling, or it precedes infection of cells.[8,9] Hence, investigation and control of bacterial adhesion is important, especially in a medical context, given the high incidence rates of infectious diseases worldwide.[10]

In recent years we have studied the α-D-mannoside-specific adhesion of *Escherichia coli* bacteria,[11,12] which is mediated by the bacterial lectin FimH. FimH is located at the tips of adhesive organelles, called type 1 fimbriae,[13] which are projecting from the bacterial cell surface. Previously we have shown that type 1 fimbriae-mediated bacterial adhesion to a non-physiological surface can be photochemically controlled. In this specific case azobenzene-functionalised α-D-mannoside derivatives were assembled on a gold surface in the form of a glyco-SAM (self-assembled monolayer).[14,15] Photochemical isomerisation of the azobenzene moiety between its *E* and *Z* form then allowed to reversibly switch the orientation of the attached carbohydrate ligands. In parallel with this *E*/*Z* isomerisation, the adhesiveness of the surface was altered leading to reduction of bacterial adhesion in the *Z* state of the SAM by ~80% in comparison to the *E* state.

While the azobenzene photoswitch is long known[16] and has been used before for switching of the properties of designer surfaces,[17–20] our work on the control of bacterial adhesion through re-orientation of carbohydrate presentation is unprecedented. Here it has been our goal to challenge our system in the context of cell–cell adhesion, thus changing the artificial glyco-SAM surface against the plasma membrane of human cells. For this, we had to incorporate azobenzene mannosides in the cell surface of live cells, effect their *E*/*Z* isomerisation to switch the orientation of the attached mannoside moieties, and to finally test the influence of this isomerisation on *E. coli* adhesion.

Our experimental approach is explained in Fig. 1: metabolic oligosaccharide engineering (MOE)[21,22] was employed to install bioorthogonal azido groups on the cell surface. This allows their subsequent modification with alkyne-functionalised azobenzene glycosides by well-known click chemistry.[23–26] In a final step, photochemical *E*/*Z* isomerisation of the installed azobenzene moieties was effected by irradiation with light of the appropriate wavelength, and subsequently bacterial adhesion was measured *via* high-resolution live-cell fluorescence microscopy. For these experiments, human microvascular endothelial cells, variant 1 (HMEC-1) and GFP-fluorescent type 1 fimbriated *E. coli* PKL1162[27] were used.

To install the required bioorthogonal azido functional groups on the cell surface, HMEC-1 were incubated with 50 μM tetra-acetylated *N*-azidoacetyl-D-mannosamine (Ac_4ManNAz, Fig. 1). Ac_4ManNAz is taken up by the cells and proceeded to result in azido labelling of terminal sialic acid units of membrane glycoproteins. When Ac_4GalNAz is employed on the other hand, the

[a] *Department of Physical Chemistry, Ludwig Maximilian University of Munich, Butenandtstr. 11, D-81377 Munich, Germany*
[b] *Otto Diels Institute of Organic Chemistry, Christiana Albertina University of Kiel, Otto-Hahn-Platz 3/4, D-24118 Kiel, Germany. E-mail: tklind@oc.uni-kiel.de; Fax: +49 431-8807410*

† Electronic supplementary information (ESI) available: Synthetic procedures and analytical data of synthesised compounds, their photochromic properties, and fluorescence images. See DOI: 10.1039/c5cc08884d

‡ These authors contributed equally to the paper.

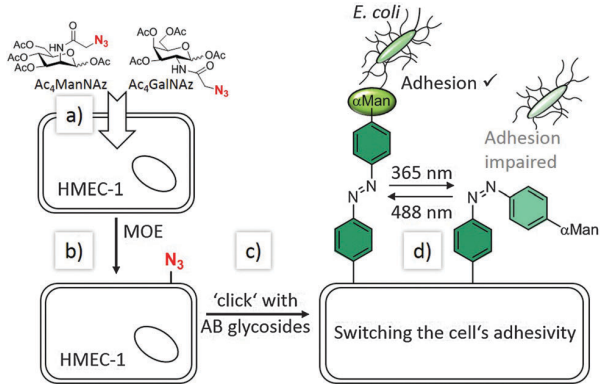

Fig. 1 Our approach of switching the adhesivity of cells. Azido groups can be incorporated into cell surface glycoconjugates according to metabolic oligosaccharide engineering (MOE): (a) synthetic carbohydrates (Ac_4ManNAz or Ac_4GalNAz) are taken up by the cells (HMEC-1) and processed by their biosynthetic machinery (b). Bioorthogonal click chemistry (c) then allows conjugation with azobenzene (AB) glycosides (such as AB α-D-mannosides, αMan) at the cell surface. Reversible *E*/*Z* isomerisation (d) employing UV or visible light, respectively, allows to change the orientation of the azobenzene-conjugated sugar and to manipulate sugar-specific bacterial adhesion in parallel.

azido label is incorporated into mucin-type glycoproteins.[28] For the chemical functionalisation of the azido-modified cells, the azobenzene derivatives **5–7**, carrying an alkyne functional group were required (Scheme 1). Synthesis started with the known *p*-aminophenyl glycosides **1**[27] and **2**,[29] which were subjected to a classical azo coupling with phenol to furnish the respective hydroxyazobenzene derivatives **3** and **4**.[30] Then, Williamson etherification with propargyl bromide led to the desired alkyne-functionalised azobenzene glycosides **5** and **6**. The azobenzene alkyne **7** was needed as control and was directly obtained from hydroxyazobenzene.[31]

At first, the azobenzene α-D-mannoside **5** was conjugated to azido-functionalised HMEC-1 after Ac_4ManNAz labelling. For this reaction, 200 μM azobenzene α-D-mannoside, 50 μM $CuSO_4$, 250 μM tris(3-hydroxypropyltriazolylmethyl)amine, 1 mM aminoguanidine, and 2.5 mM sodium ascorbate in buffered saline solution were employed at 4 °C for 5 minutes.[32] A 200 μM solution of **5** was sufficient to ensure complete labelling of all azido groups on the cell surface (*cf.* ESI,† Fig. S13). Copper(I), which is produced during the reaction, is known to exhibit toxic side effects after some time, however, we applied conditions that were shown earlier not to be harmful for cells.

Labelled cells were split into two portions and both sets were irradiated with UV light (365 nm), to effect $E \rightarrow Z$ isomerisation of the conjugated azobenzene moiety. Then, cells were incubated with GFP-fluorescent *E. coli* (*cf.* ESI,† Fig. S14–S18) and the number of adhered bacteria was counted employing high-resolution live-cell fluorescence microscopy. For both sets of HMEC-1 the number of adhered bacteria is similarly low at this stage, as it is expected (Fig. 2).

In a subsequent step, only one of both cell sets was irradiated again; this time with green light (488 nm) to reverse the initial isomerisation and thus effect $Z \rightarrow E$ isomerisation of the azobenzene configuration. Then, a second incubation with fluorescent *E. coli* was performed, and adhesion again quantified. Whereas the adhesivity of the cells without a second irradiation treatment remained the same, a significant increase of bacterial adhesion was measured for the cells that were irradiated at 488 nm (about 50%). We attribute this observation to the mode of mannose orientation, which is changed with the isomerisation of the azobenzene hinge. In accordance with the observation made with photoswitchable glyco-SAMs,[15] the adhesivity of the azobenzene mannoside-modified cell surface is higher in the *E* than in the *Z* state.

In order to investigate photoswitching of cell adhesion in real-time, flow-based experiments[33] were performed next. Thus, HMEC-1 were cultivated in flow chambers, again incubated with Ac_4ManNAz and labelled with azobenzene mannoside **5** in analogy to our experiments under static conditions. Then, a bacterial suspension (1 : 50 dilution of a suspension with OD_{600} = 0.1) was employed at continuous flow with a shear rate of 1.5 dyn cm^{-2} (a typical shear rate for microvascules). The flow was not interrupted during irradiation (300 seconds). Adhering bacteria were monitored by fluorescence microscopy while switching the configuration of HMEC-conjugated azobenzene mannosides multiple times between

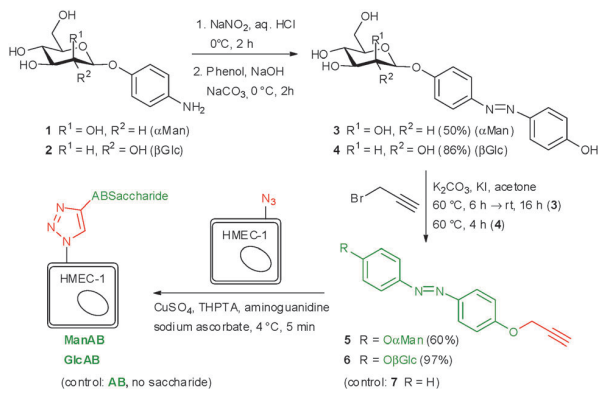

Scheme 1 Synthesis of alkyne-functionalised azobenzene glycosides and labelling of engineered human cells (HMEC-1). The α-D-mannopyranoside **5** was used as specific ligand for bacterial adhesion and the β-D-glucopyranoside **6** and **7** were needed as control compounds.

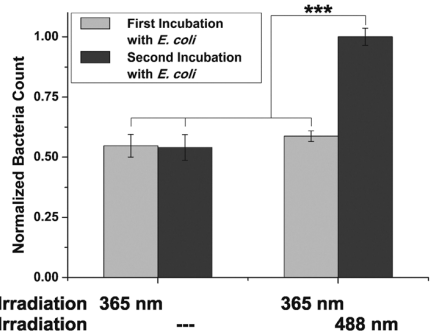

Fig. 2 Switching of **ManAB** configuration allows to control adhesion of *E. coli*. After incubation of two sets of Ac_4ManNAz-engineered HMEC-1, conjugated with **5** in *Z*-configuration, bacterial adhesion is similar for both sets. Switching of **ManAB** configuration to *E* (365 nm) increases bacterial adhesion (second incubation). Error bars are standard error of the mean (SEM) of experiments with four independent sets of cells/condition. ***$p < 0.001$ (*cf.* ESI,† Fig. S14).

E and *Z* (Fig. 3). The development of the recorded bacterial GFP-fluorescence is then a direct measure for the adhesion of *E. coli*. The obtained curves clearly show that alternating irradiation using light of 365 nm and 488 nm has a strong effect on bacterial adhesion (Fig. 3a). After irradiation of the flow chamber with 488 nm light, the slopes of the bacterial GFP signal are significantly higher than after irradiation with 365 nm. This is also clearly seen after fitting of the curves, assuming a linear development of fluorescence (Fig. 3b).

Only after several switching events (starting at 1500 s), the measured slopes are no longer correlated with azobenzene configuration. This can be attributed to increasing coverage of HMEC-1 with bacterial cells (see also microscopic images, ESI,† Fig. S19). When more and more bacteria adhere to bacterial cells and not to HMEC-1, the adhesion is naturally not sensitive to *E*/*Z* isomerisation.

As under static conditions, the results obtained in the flow experiments indicate that the orientation of mannoside **5** conjugated to the surface of HMEC-1 has a strong influence on the adhesion of bacteria, suggesting that the bent *Z* form is less accessible for bacteria than the *E* form. Thus, adhesion is reduced after $E \rightarrow Z$ isomerisation. Next, two important control experiments were performed in order to understand the observed effects in greater detail. First, the question of carbohydrate specificity of the observed effects was addressed by employing the azobenzene derivative **7** (**AB** in Fig. 4) devoid of a carbohydrate, and the β-D-glucoside **6** (**GlcAB** in Fig. 4) for HMEC-1 labelling. The glucoside **6** exhibits a similar structure and polarity as **5** but is no ligand for the bacterial lectin FimH. Labelling of HMEC-1 was done as before and bacterial adhesion measured after irradiation. All experiments were compared to azido-labelled HMEC-1, which had not been reacted with either of the azobenzene derivatives (Control in Fig. 4).

These experiments show that adhesion of *E. coli* to cells reacted with either **6** or **7**, is significantly decreased compared to untreated cells. This observation suggests a shielding effect for both derivatives, prohibiting bacterial adhesion to the surface of HMEC-1 to some extent. On the other hand, this effect is not significantly sensitive to *E*/*Z* isomerisation. This finding indicates that the adhesion of bacteria to cells treated with **5** is indeed carbohydrate-specific. Control cells showed a slight response to irradiation with 365 nm light, but the effects caused by **6** or **7** are more significant.

How can the orientation of a rather small molecule (such as an azobenzene glycoside) within the complex environment of a cell's surface exert such a pronounced effect on cell adhesion? To answer this question, the azobenzene mannoside ligand was positioned differently on the surface of HMEC-1. This is possible by labelling HMEC-1 with Ac_4GalNAz instead of Ac_4ManNAz. Whereas Ac_4ManNAz leads to labelling of sialic acids, which are almost exclusively found at the terminal positions of cell surface glycans, Ac_4GalNAz labels mucin-type glycoproteins. These are characterised by LacNAc moieties, which are localised deeper within the glycosylated cell surface.[28]

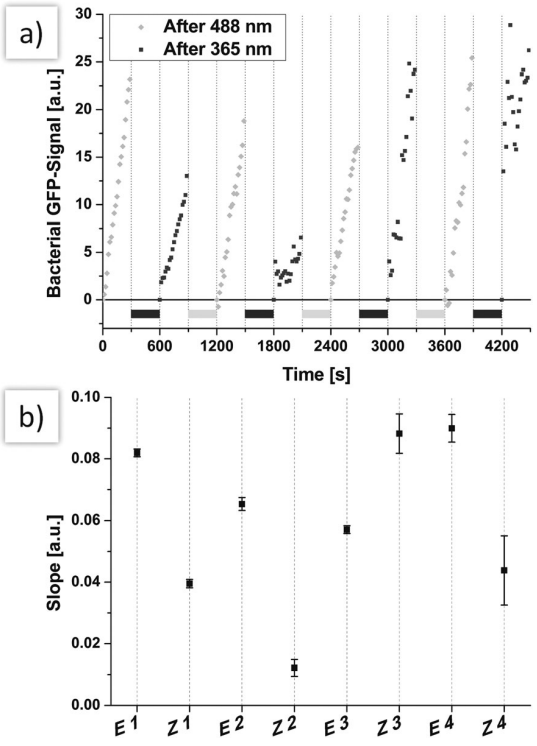

Fig. 3 (a) The azobenzene mannoside **5** was switched several times between *Z* and *E* while flowing a continuous stream of bacterial solution over the cells. The adhesion of bacteria was lower if **5** was in *Z*-configuration. Only after several switching cycles this tendency was no longer observed, caused by increasing coverage of the cells with bacteria. During irradiation with 365 nm (light grey bars) or 488 nm (dark grey bars), the flow was not stopped. (b) The slopes of linear curves that were fitted to the data of the middle panel clearly resembles the effect of reversible switching. Error bars are given as SEM of the fitting. For easier comparison, the slopes are set to start at a common origin by subtraction of the fluorescence intensity of the first frame from the subsequent frames.

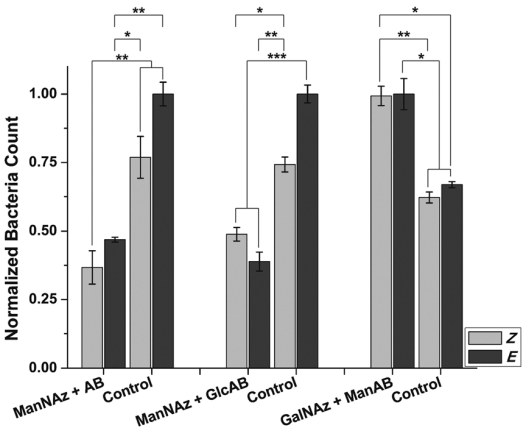

Fig. 4 Control experiments. Left & middle: Ac_4ManNAz labelling and conjugation with **AB** (no sugar residue) or **GlcAB** (β-Glc instead of α-Man) leads to reduced adhesion in comparison to control cells independent of **AB** configuration. Right: Ac_4GalNAz labelling and conjugation with **ManAB** leads to increased adhesion independent of AB configuration. Errors are given as SEM. Four independent sets of cells were tested for each condition. $*p < 0.1$, $**p < 0.01$, $***p < 0.001$.

Indeed, bacterial adhesion to HMEC-1, labelled with Ac_4GalNAz and modified with mannoside **5** is increased in comparison to control cells (Fig. 4). This observation can be rationalised by the increased concentration of mannosides present on the cell surface after modification. However, the observed increased adhesion is not photosensitive in this case. As LacNAc groups are typically not exposed at the cell surface, conjugated **ManAB** moieties might be buried under a layer of other glycoconjugates so that an orientational change of mannoside ligands is not effective. On the other hand, we cannot measure the extent of azobenzene isomerisation, which might be different in both investigated cases (Ac_4ManNAz or Ac_4GalNAz labelling).

Taken together, we show that the azobenzene mannoside **5** can be employed to influence adhesion of *E. coli* to HMEC-1. We postulate the following mechanism that underlies this photocontrol: (i) bacterial FimH binds to mannose, which serves as ligand for specific interaction between the bacterium and the modified cell surface (*cf.* Ac_4ManNAz + **5** *vs.* Ac_4ManNAz + **6**). (ii) If no mannose ligand is present or if it adopts a disadvantageous orientation (*Z*-configuration), the azobenzene groups shield the cell, leading to reduced binding of *E. coli* (*cf.* Ac_4ManNAz + **5** *vs.* Ac_4ManNAz + **AB**). (iii) The FimH ligand mannose must be localised at the terminus of glycans to ensure that the change in configuration upon a *Z*/*E* transition is not small (Ac_4ManNAz + **5** *vs.* Ac_4GalNAz + **5**).

It is surprising that this orientation effect can be found not only on an artificial, ordered glyco-SAM as we described before,[15] but even in the complex, in comparison rather chaotic setting of the cell surface. Of course, this finding bears implications for the way how cells interact with their environment and offers options for prevention of bacterial adhesion with temporal and spatial resolution.

Financial support by SFB 677 is gratefully acknowledged. We also thank the excellence clusters Nano Systems Initiative Munich (NIM), the Centre for Integrated Protein Science Munich (CIPSM), and the Centre for Nanoscience Munich (CeNS).

Notes and references

1 A. A. Khalili and M. R. Ahmad, *Int. J. Mol. Sci.*, 2015, **16**, 18149–18184.
2 M. E. Taylor and K. Drickamer, *Curr. Opin. Cell Biol.*, 2007, **19**, 572–5772.
3 N. Sharon and H. Lis, *Glycobiology*, 2004, **14**, 53R–62R.
4 C. R. Bertozzi and L. L. Kiessling, *Science*, 2001, **291**, 2357–2364.
5 F.-T. Liu and G. A. Rabinovich, *Nat. Rev.*, 2005, **5**, 29–41.
6 I. Ofek, D. Mirelman and N. Sharon, *Nature*, 1977, **265**, 623–625.
7 K. Ohlsen, T. A. Oelschlaeger, J. Hacker and A. S. Khan, *Top. Curr. Chem.*, 2009, **288**, 17–65.
8 L. Hall-Stoodley, J. W. Costerton and P. Stoodley, *Nat. Rev. Microbiol.*, 2004, **2**, 95–108.
9 D. Ribet and P. Cossart, *Microbes Infect.*, 2015, **17**, 173–183.
10 K. E. Jones, N. G. Patel, M. A. Levy, A. Storeygard, D. Balk, J. L. Gittleman and P. Daszak, *Nature*, 2008, **451**, 990–993.
11 M. Hartmann and T. K. Lindhorst, *Eur. J. Org. Chem.*, 2011, 3583–3609.
12 A. Bernardi, *et al.*, *Chem. Soc. Rev.*, 2013, **42**, 4709–4727.
13 J. Lillington, S. Geibel and G. Waksman, *Biochim. Biophys. Acta*, 2014, **1840**, 2783–2793.
14 V. Chandrasekaran, H. Jacob, F. Petersen, K. Kathirvel, F. Tuczek and T. K. Lindhorst, *Chem. – Eur. J.*, 2014, **20**, 8744–8752.
15 T. Weber, V. Chandrasekaran, I. Stamer, M. B. Thygesen, A. Terfort and T. K. Lindhorst, *Angew. Chem.*, 2014, **126**, 14812–14815 (*Angew. Chem., Int. Ed.*, 2014, **53**, 14583–14586).
16 G. S. Hartley, *Nature*, 1937, **140**, 281.
17 J. Auernheimer, C. Dahmen, U. Hersel, A. Bausch and H. Kessler, *J. Am. Chem. Soc.*, 2005, **127**, 16107–16110.
18 P. M. Mendes, *Chem. Soc. Rev.*, 2008, **37**, 2512–2529.
19 W. R. Browne and B. L. Feringa, *Annu. Rev. Phys. Chem.*, 2009, **60**, 407–428.
20 M.-M. Russew and S. Hecht, *Adv. Mater.*, 2010, **22**, 3348–3360.
21 E. M. Sletten and C. R. Bertozzi, *Acc. Chem. Res.*, 2011, **44**, 666–676.
22 M. S. Siegrist, B. M. Swarts, D. M. Fox, S. A. Lim and C. R. Bertozzi, *FEMS Microbiol. Rev.*, 2015, **39**, 184–202.
23 V. V. Rostovtsev, L. G. Green, V. V. Fokin and K. B. Sharpless, *Angew. Chem.*, 2002, **114**, 2708–2711 (*Angew. Chem., Int. Ed.*, 2002, **41**, 2596–2599).
24 M. Meldal and C. W. Tornøe, *Chem. Rev.*, 2008, **108**, 2952–3015.
25 M. Kleinert, T. Winkler, A. Terfort and T. K. Lindhorst, *Org. Biomol. Chem.*, 2008, **6**, 2118–2132.
26 C. Grabosch, M. Kind, Y. Gies, F. Schweighöfer, A. Terfort and T. K. Lindhorst, *Org. Biomol. Chem.*, 2013, **11**, 4006–4015.
27 M. Hartmann, A. K. Horst, P. Klemm and T. K. Lindhorst, *Chem. Commun.*, 2010, **46**, 330–332.
28 J. M. Baskin, J. A. Prescher, S. T. Laughlin, N. J. Agard, P. V. Chang, I. A. Miller, A. Lo, J. A. Codelli and C. R. Bertozzi, *Proc. Natl. Acad. Sci. U. S. A.*, 2007, **104**, 16793–16797.
29 G. R. Gustafson, C. M. Baldino, M.-M. E. O'Donnell, A. Sheldon, R. J. Tarsa, C. J. Verni and D. L. Coffen, *Tetrahedron*, 1998, **54**, 4051–4065.
30 V. Chandrasekaran, E. Johannes, H. Kobarg, F. D. Sönnichsen and T. K. Lindhorst, *ChemistryOpen*, 2014, **3**, 99–108.
31 G. Mantovani, V. Ladmiral, L. Tao and D. M. Haddleton, *Chem. Commun.*, 2005, 2089–2091.
32 V. Hong, N. F. Steinmetz, M. Manchester and M. G. Finn, *Bioconjugate Chem.*, 2010, **21**, 1912–1916.
33 E. V. Sokurenko, V. Vogel and W. E. Thomas, *Cell Host Microbe*, 2008, **4**, 314–323.

6 Photoswitchable carbohydrate scaffold-based glycoclusters

6.1 Introduction

One of the noteworthy characteristics of the glycocalyx is the occurrence of multivalent cell surface glycoconjugates which are typically highly branched and tend to be oligomeric. Compared to the rather weak interactions between a single carbohydrate ligand and its receptor (lectin), multiple carbohydrate-lectin binding events acting in concert lead to considerably increased avidities, often referred to as multivalency effect.[347–350] It has been shown that there is not only one multivalent principle which influences carbohydrate recognition, however many different multivalency effects are operating and cooperating in carbohydrate-lectin binding events.[351] To understand the role of multivalent carbohydrate recognition in more detail, a variety of diverse scaffolds have been utilized. Theses scaffolds include rather low-molecular weight glycoclusters, dendrimers and polymers.

6.1.1 Carbohydrate scaffold-based glycoclusters

A great variety of molecules have been utilized as scaffolds for the construction of complex glycodendrimers and glycoclusters.[271,352–359] A scaffold molecule represents a multifunctional compound, which allows for orthogonal attachment of various moieties with different spatial orientation. Furthermore, with the choice of the core molecule the valency of cluster glycosides can be easily varied (Figure 6.1). Aromatic core molecules such as 1,3,5-tris(bromomethyl)benzene (**12**) can be utilized as planar scaffolds.[353,360] However, due to the planarity of the aryl core, the spatial variation of attached carbohydrates is restricted. In contrast, the utilization of pentaerythritol (**13**) as a core molecule allows for functionalization in a tetrahedral manner and also the preparation of heteroglycoclusters can be achieved.[361–363] To directly obtain trivalent glycoclusters, tris(hydroxymethyl)aminomethane (**14**, TRIS) can be employed.[364] Moreover, with the orthogonal functional group at the focal point, glycoclusters derived from TRIS can be attached to further multivalent moieties or immobilized on a surface. Also heteroglycoclusters were obtained from TRIS through attaching a second type of carbohydrate ligand to the core.[365]

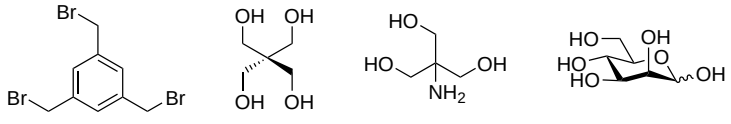

12 **13** **14** **15**

Figure 6.1. Examples of frequently used scaffold molecules to construct glycoclusters.

Another group of promising synthons for organizing multivalency are carbohydrate-based scaffolds.[366] They are perfectly suited to build up glycoclusters as a wide range of different carbohydrates are readily available. They are inexpensive, have a molecular rigidity and a fixed stereochemistry. Due to their multifunctionality and the distinct reactivity of the individual positions at the sugar ring, glycoclusters of different architecture can be obtained (Figure 6.2). The anomeric position for instance can be independently addressed in a glycosylation reaction and thus a great variety of functional groups can be introduced in the aglycon. Besides the anomeric position also the primary

hydroxyl group at the C-6 position of the hexapyranose ring can be discriminated from the other secondary alcohol functions. The difference in reactivity is most likely to steric control. Finally, the chemical reactivity of the secondary hydroxyl groups is also controlled by stereoelectronic factors of the respective monosaccharide (e.g. equatorial or axial configuration). With regard to the different reactivities of the individual hydroxyl groups in combination with an appropriate protecting group strategy it is possible to orthogonally introduce a variety of functional groups at the sugar ring.

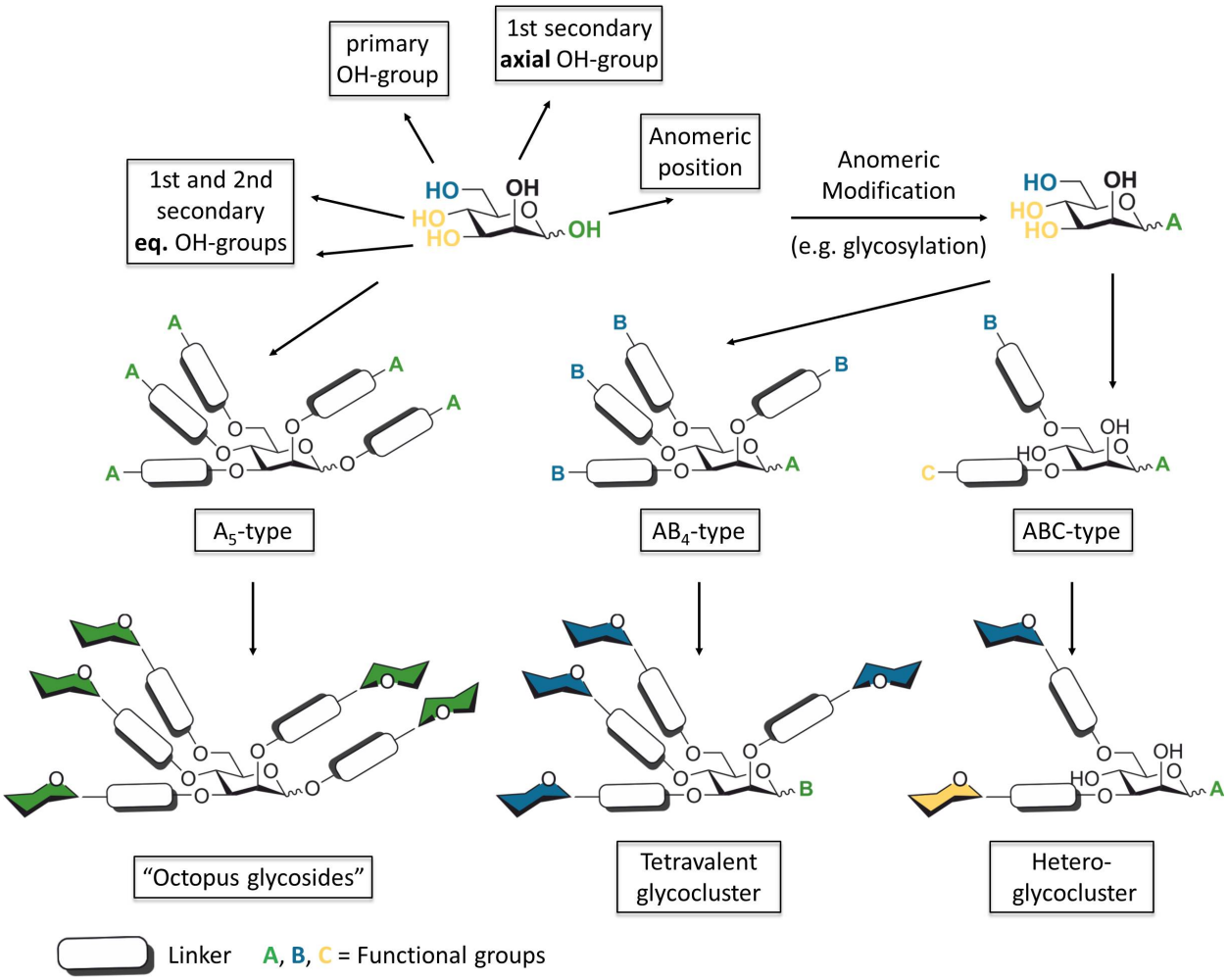

Figure 6.2. Special features of carbohydrates and different types of scaffold molecules which can be obtained from a carbohydrate core.

The pioneering scientific work on carbohydrate scaffold-based glycoclusters was done by T. K. Lindhorst and co-workers, who introduced in a straightforward approach five equal functional groups (allyl groups) at the sugar ring, which were used to create pentavalent mannosylclusters.[367–370] Similarly, also trehalose-, melibiose- and raffinose-based glycoclusters were prepared and coined as "octopus glycosides".[371–374] With further branching of the installed allyl groups it was even possible to obtain highly branched glycodendrimers.[354,372,375] As described above, the anomeric position is specific and readily accessible and can be easily modified with an "A" functional group in the aglycon. Whereas the remaining hydroxyl groups can be subsequently altered with a functional group "B" and thus the facile access to AB_4-type scaffolds is feasible.[352,354,376–380] In this way a

great variety of tetravalent glycoclusters were prepared.[352,371,375,381–383] Just recently T.-E. Gloe *et al.* reported about the synthesis of a $N_3(NHBoc)_4$-functionalized mannoside-based scaffold **16** which was utilized for the synthesis of a tetravalent mannosylcluster **19** (Figure 6.1).[384] These AB_4-type carbohydrate-based scaffolds have the potential to be further derivatized in an orthogonal manner or immobilized on a surface. Gloe *et al.* could demonstrate the potential of the prepared compound **17** by introducing an azobenzene moiety **20** at the aglycone leading to the photoresponsive scaffold molecule **21**. This compound represents a favourable starting point for the synthesis of multivalent photoresponsive glycoclusters which can be used to further investigate photoswitchable cell adhesion in a multivalent manner.

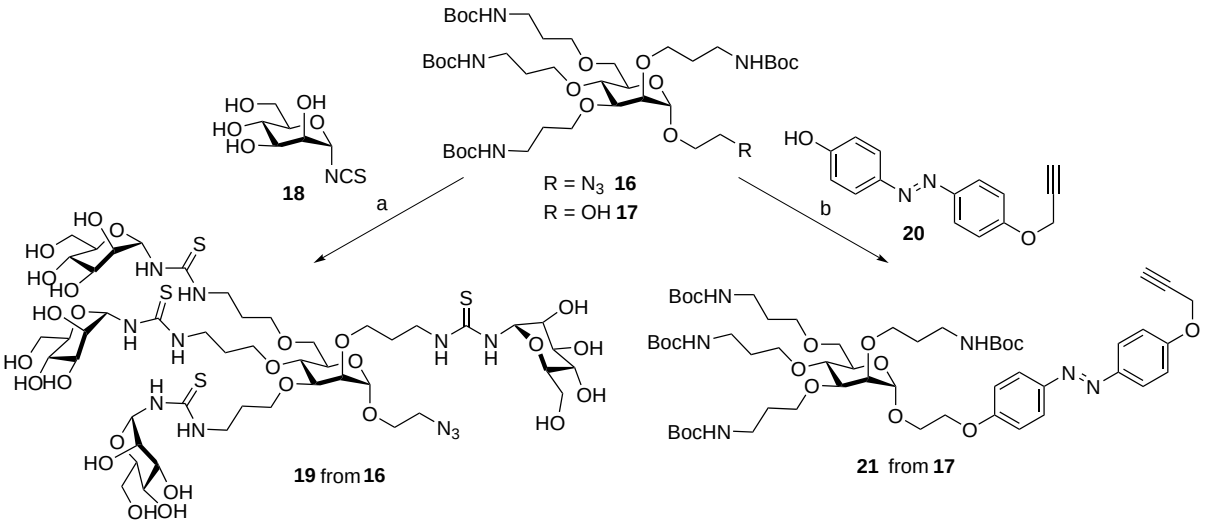

Scheme 6.1. The depicted $N_3(NHBoc)_4$-functionalized mannoside-based scaffold was previously reported by T.-E. Gloe *et al.* and was utilized for the synthesis of glycoclusters as well as for the preparation of a photoresponsive scaffold molecule.[384]

Besides the utilization of carbohydrates to prepare A_5- or AB_4-type scaffold molecules, also the preparation of versatile AB_2- or ABC-type building blocks to obtain glycoclusters or even heteroglycoclusters is feasible and was extensively studied in the Lindhorst group (Scheme 6.2).[285,385–389]

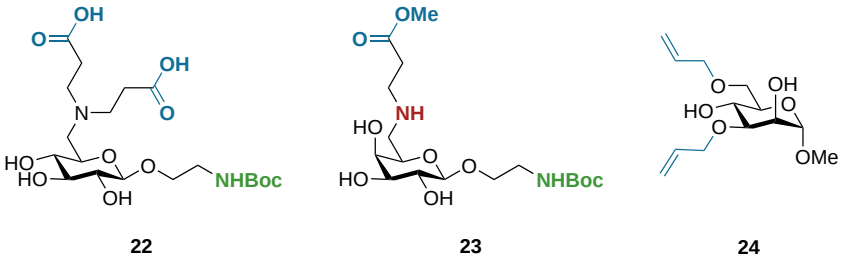

Scheme 6.2. Examples of AB_2 and ABC-type building blocks prepared in the Lindhorst group.

Hence, amino diacid derivative **22** was utilized for the synthesis of hyperbranched glycopeptide dendrons, while the oligofunctional ABC-type scaffold **23** was readily applied to obtain a heteroglycocluster containing a mannosyl, lactosyl and fucosyl moiety. 3,6-Diallylated mannoside **24**, prepared in a regioselective one-pot bis(tributyltin)oxide-mediated reaction,[390–392] represents another valuable carbohydrate-based scaffold which was utilized for the synthesis of dendritic chiral polyols.[393] A

further example which exhibits the potential of monosaccharide units as attractive scaffold molecules is the introduction of five different functionalities at the sugar ring.[394–397] These orthogonally protected carbohydrate-based scaffolds were utilized in combinatorial chemistry. Consequently, due to their stereodiversity, occurrence in a wide range of natural states, conformations as well as anomeric configurations carbohydrates are valuable building blocks for the synthesis of a variety of versatile glycoclusters, glycodendrimers and even heteroglycoclusters.

6.1.2 Photoswitchable multivalent glycoclusters

As described in the previous chapters the interaction of carbohydrate ligands with other biomolecules such as lectins is dependent on the correct configuration and the orientation of the respective glycoconjugate. To understand glycocalyx function in means of carbohydrate orientation in more detail stimuli-responsive glycoconjugates which are able to undergo reversible dynamic conformational changes have been emerged. To combine multivalency and the crucial influence of conformational changes Jayaraman *et al.* reported about the first photoresponsive azobenzene-based glycocluster (Scheme 6.3).[398,399]

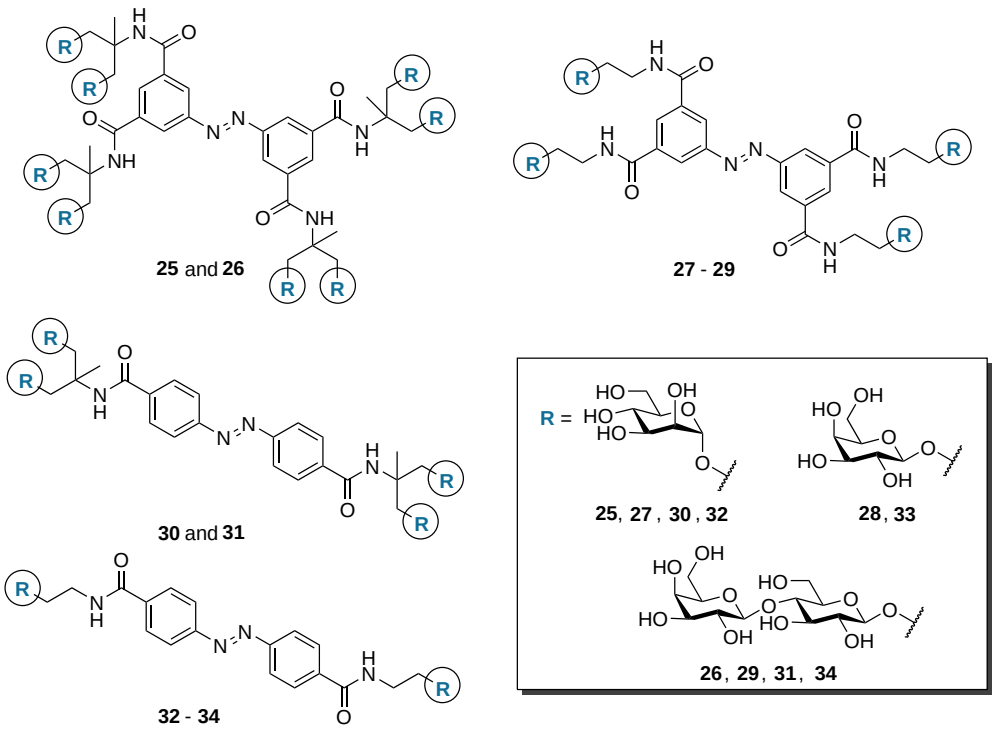

Scheme 6.3. First synthesised azobenzene-based glycoclusters.

Towards this aim, lacto-, manno- and galactopyranoside azobenzene derivatives **25-34** with various valences were prepared and their reversible photoisomerization properties investigated. Photoisomerization studies in aqueous media revealed a rather slow $Z \rightarrow E$ thermal relaxation processes and the formation of ~55-70% Z isomer at the photostationary state (PSS) of the respective azobenzene glycosides. Additionally, lectin binding studies by employing ITC to study the interaction of the prepared photoisomerisable glycoside derivatives with *Peanut lectin* (PNA) or *Concanavalin A* (ConA), respectively were performed. Results indicated that multivalent glycoclusters exhibit an improved

binding affinity compared to the monovalent ligands. Besides that, the *Z* stereoisomer-enriched PSS mixtures showed a better binding with the relevant lectins in comparison to the corresponding *E*-isomers. Even though the effect observed for the *Z*-configured glycocluster was not well elucidated it can be assumed that valency, spatial orientation as well as geometry of the employed carbohydrate ligand are prerequisites for the cooperative binding behavior to occur.

To further investigate the understanding of conformational aspects related to multivalency in carbohydrate lectin recognition processes Chandrasekaran *et al.* prepared a variety of azobenzene glycoclusters (Scheme 6.4).[106]

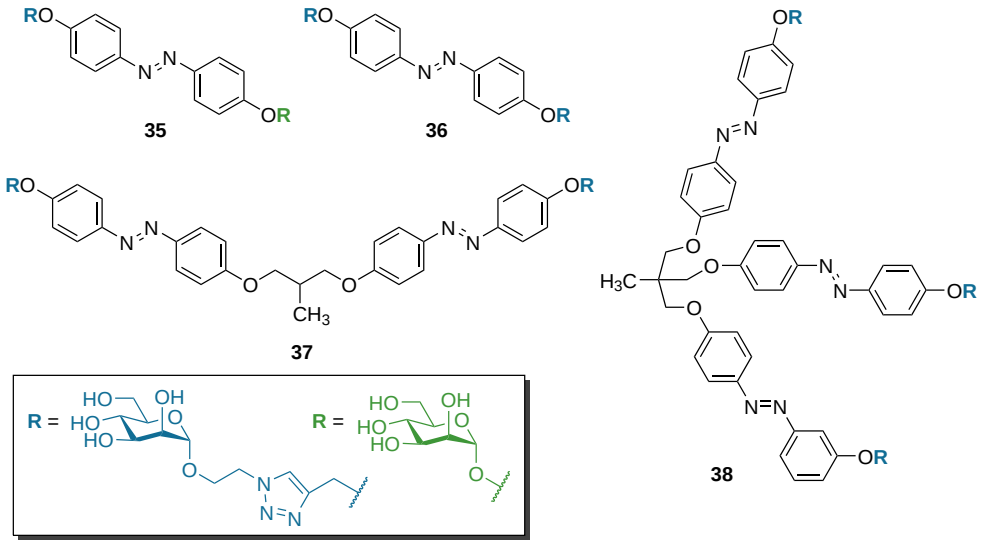

Scheme 6.4. Azobenzene glycoclusters prepared in the Lindhorst group which were coined as 'sweet switches'.

For this purpose they utilized copper(I) catalysed click chemistry[111,112] to achieve symmetrical divalent azobenzene mannoside **36**. While the unsymmetrical homologue **35** was obtained in a three-step sequence comprising lewis acid-promoted mannosylation, click chemistry and subsequent acetyl deprotection. In order to prepare clustered glycoazobenzene derivatives **37** as well as **38**, AB_2 and AB_3 branching units containing either two or three propargyl functions were employed. Investigation of the photochromic properties in DMSO of the prepared compounds showed that an almost quantitative *E*/*Z* ratio in the PSS was obtained for divalent azobenzene mannosides **35** and **36**, whereas the *E*→*Z* isomerization process seemed to be less efficient for the clustered derivatives (*E* : *Z* ratios of 33 : 67 and 63 : 37). The obtained ratios are averaged values of an equilibrium mixture of *EE*, *EZ* and *ZZ* isomers for **37** comprising two azobenzene branches and a mixture of *EEE*, *EEZ*, *EZZ* and *ZZZ* isomers for **38** comprising three azobenzene branches. The observed results are most likely influenced by electronic effects such as intramolecular quenching processes (*e.g.* excitonic coupling). This might be due to the stacking of the azobenzene moiety leading to a decay of the excited state before the isomerization process takes place. A detailed kinetic study was not accomplished so far.

6.2 Synthesis of an orthogonal trifunctional carbohydrate scaffold for the preparation of azobenzene heteroglycoclusters

The synthesis of multivalent glycomimetics is the aim of synthetic chemists since the discovery of the multivalent nature of carbohydrate-mediated interactions. Carbohydrates are excellent scaffold molecules for the construction of multivalent glycoclusters as they exhibit molecular rigidity, defined stereochemistry, are readily available and mostly inexpensive. Due to their multifunctionality and the distinct reactivity of the individual hydroxyl groups at the sugar ring, carbohydrate-based scaffold molecules have been widely applied to prepare various multivalent glycomimetics. By utilizing the different reactivities of specific hydroxyl groups in combination with an appropriate protecting group strategy it is possible to introduce orthogonal functionalization at the sugar ring and thus, for instance ABC-type scaffolds can be obtained. The potential for orthogonal functionalization of glycosides, allows for the synthesis of heteroglycoclusters inlcudig the option of their immobilization to a solid support or surface, respectively.
In the following manuscript, the preparation of a trifunctional mannoside-based scaffold molecule is reported, which is equipped with three orthogonally protected/masked amino functional groups. Installation of a threefold orthogonality was straightforward and did not require a complex protecting group strategy. The resulting ABC-type scaffold glycoside was utilized to prepare a heterodivalent azobenzene glycoconjugate, in which each azobenzene glycoside "branch" was introduced independently from the other and could have different characteristics (Figure 6.3). This approach allows the synthesis of azobenzene glycoconjugates with increased complexity and more sophisticated photoswitching functions, as carbohydrates of different types can be installed onto the carbohydrate scaffold and even azobenzene derivatives can be utilized which can be switched between their *E*- and *Z*-state using different wavelengths.

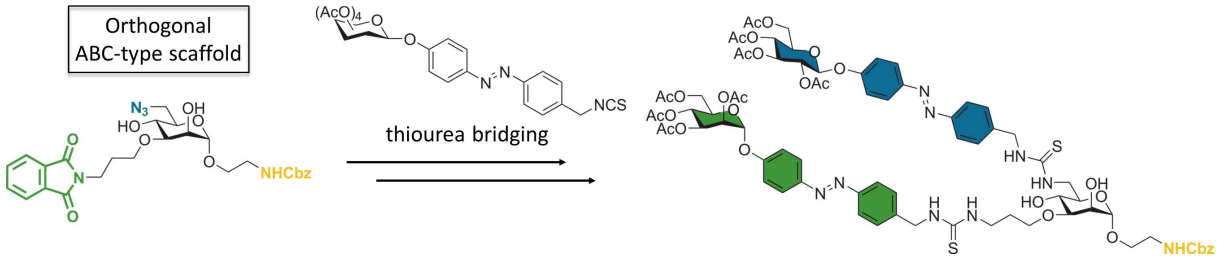

Figure 6.3. A heterodivalent azobenzene glycocluster was prepared by thiourea bridging based on an orthogonal trifunctional mannoside-based scaffold.

Here, as a first example, α-D-*manno*-, α- as well as β-D- *gluco*-configured isothiocyanato-functionalized azobenzene derivatives were prepared and installed onto the designed orthogonally functionalized carbohydrate scaffold molecule by thiourea bridging (Figure 6.3). Beyond that, also the determination of the photochromic data as well as a detailed kinetic study of the switching behavior of the obtained divalent glycocluster was accomplished.

6.2.1 Manuscript on the synthesis of an orthogonal trifunctional carbohydrate scaffold for the preparation of azobenzene heteroglycoclusters

"Synthesis of an orthogonal trifunctional carbohydrate scaffold for the preparation of azobenzene glycoclusters "

This chapter was written in manuscript form with the view of a timeley publication of these results.

A. Müller, T. K. Lindhorst.

Abstract: The preparation of a heterodivalent azobenzene glycoside derivative is reported, which is derived from a trifunctional carbohydrate scaffold molecule with orthogonal functionalization in a straightforward synthesis. A detailed kinetic study revealed that the installed azobenzene units are electronically decoupled and show photoswitching independently from each other. Furthermore, this molecule can be immobilized at the aglyconic functionality and utilized in cell adhesion studies of the influence of carbohydrate orientation. The newly introduced architecture allows for higher complexity and variability of photoswitchable glycoconjugates.

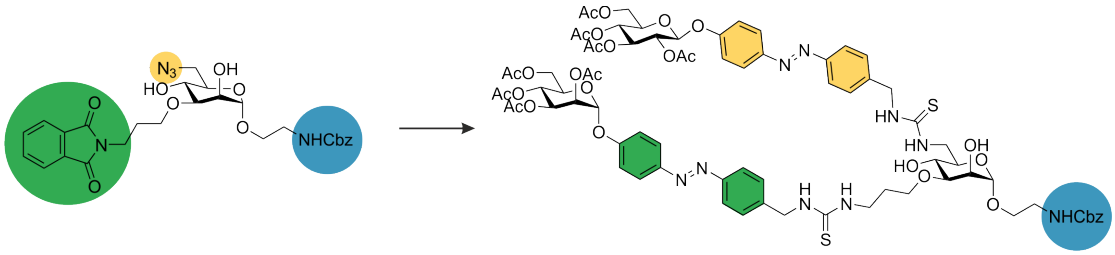

TOC Graphic 6.1. An orthogonal trifunctional carbohydrate scaffold was prepared to achieve a heterodivalent azobenzene glycocluster by thiourea bridging. The scaffold bears a Cbz-protected amino function, a phthalimido-protected amino function and an azide functionality which can be utilized for further derivatization or for the immobilization on surfaces.

Scientific contribution to this paper

In this project I carried out the synthesis and characterization of all compounds as well as the analysis of their photochromic properties. I wrote the current manuscript.

6.2.1.1 Introduction

Carbohydrates can be utilized as polyfunctional molecular scaffolds and thus represent a valuable tool for the synthesis of carbohydrate-centered multivalent glycomimetics. The resulting glycoclusters can be specifically designed and employed to elucidate carbohydrate recognition events and multivalency effects in glycobiology.[1] Carbohydrates are perfectly suited as multifunctional scaffold molecules as they are readily available, mostly inexpensive and exhibit a molecular rigidity as well as a defined stereochemistry. Owing to the different reactivites of hydroxyl groups at the sugar ring, tailor-made heteromultivalent glycoconjugates can be obtained. When all five OH-groups of a monosaccharide (or more in case of di- and oligosaccharides) are hydroxypropylated, the preparation of carbohydrate-centered octopus glycosides is feasible by glycosylation.[2] Another interesting class of carbohydrate-based scaffolds are those bearing an AB_4-type functionalization.[3] Facile access to AB_4-type scaffolds is mostly achieved by the early introduction of an "A" functional group in the aglycone, using the fact that the anomeric position of carbohydrates is readily accessible and can be easily modified, for instance, by a glycosylation reaction. The remaining hydroxyl groups on the other hand can then be subsequently altered with a functional group "B" and thus highly versatile scaffolds with an orthogonal functionality become available. Just recently Gloe *et al.* reported about the synthesis of a $N_3(NHBoc)_4$-functioalized mannoside-based scaffold which was successfully utilized in the synthesis of a tetravalent mannosylcluster.[4] Besides the preparation of A_5- or AB_4-type carbohydrate-based scaffolds also versatile AB_2- or ABC-type building blocks can be obtained.[5,6] The orthogonality of this type of scaffold may be accomplished be utilizing the different reactivities of the individual hydroxyl groups of the sugar ring in combination with an appropriate protecting group strategy. Various AB_2- or ABC-type carbohydrate scaffolds have been described and were readily applied for the synthesis of glycoclusters or heteroglycoclusters. By further branching of the installed functional groups it was even possible to obtain highly branched glycodendrimers.[5] Based on earlier work, we report here on the preparation of the trifunctional mannoside **1** carrying three orthogonally protected/masked amino functional groups (Figure 6.4).[7]

The prepared scaffold molecule allows for the orthogonal deprotection of the amino groups and the reduction of the azido function. The amino functions are amenable for instance to isothiocyanate-amine coupling which was applied in earlier studies to construct various glycoclusters.[8,6] Through conjugation of the trifunctional scaffold with different carbohydrate epitopes, heteroglycoclusters[9] are accessible. Additionally, the anomeric functionality can be employed for immobilization of the glycocluster, for example on a surface such as polystyrene (PS) or glass and thus be utilized in surface-based cell adhesion assays.[10] Recently, we have reported on photoswitchable glycoarrays employing azobenzene glycosides to study the effect of orientation in carbohydrate recognition.[11] Here, the carbohydrate scaffold **1** is utilized for the synthesis of a first representative example of a heterodivalent glycophotoswitch, extending the collection of "sweet switches"[12] and to further investigate their photochromic properties.

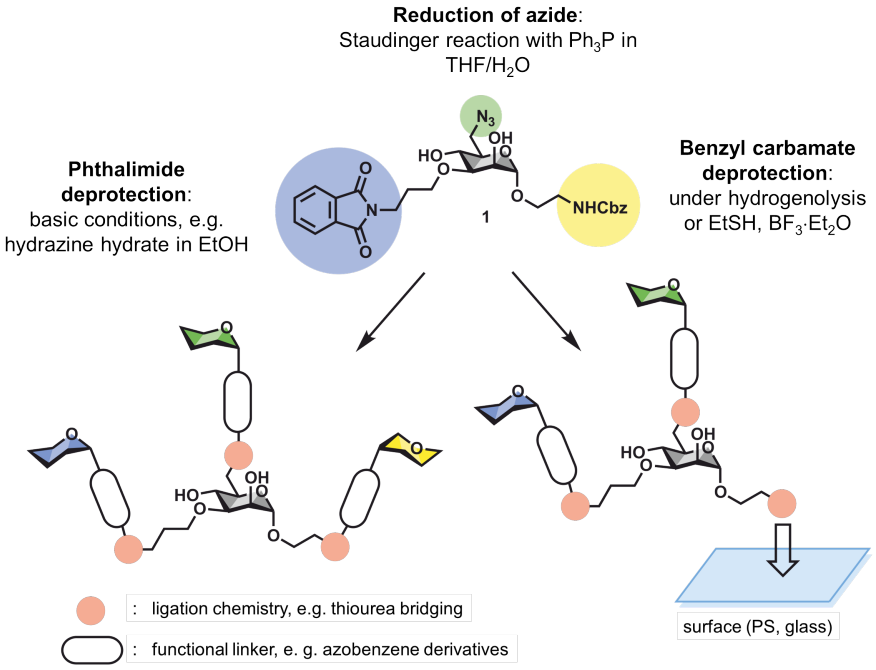

Figure 6.4. Illustration of the trivalent orthogonal mannoside scaffold **1** with the respective deprotection conditions of the protected amino functions as well as the reduction of the azide. At the bottom part of the figure the schematic illustration of hetero azobenzene glycoclusters is shown.

6.2.1.2 Results and discussion

Synthesis of an orthogonal trifunctional carbohydrate scaffold and the preparation of azobenzene glycocluster

The synthesis of the trifunctional carbohydrate scaffold molecule **1** started from the well-known mannosyl donor **2**[13], which was prepared in three steps from D-mannose. **2** was then employed for glycosylation with commercially available *N*-Cbz-ethanolamine leading to the α-D-mannoside **3**[14] (Scheme 6.5).

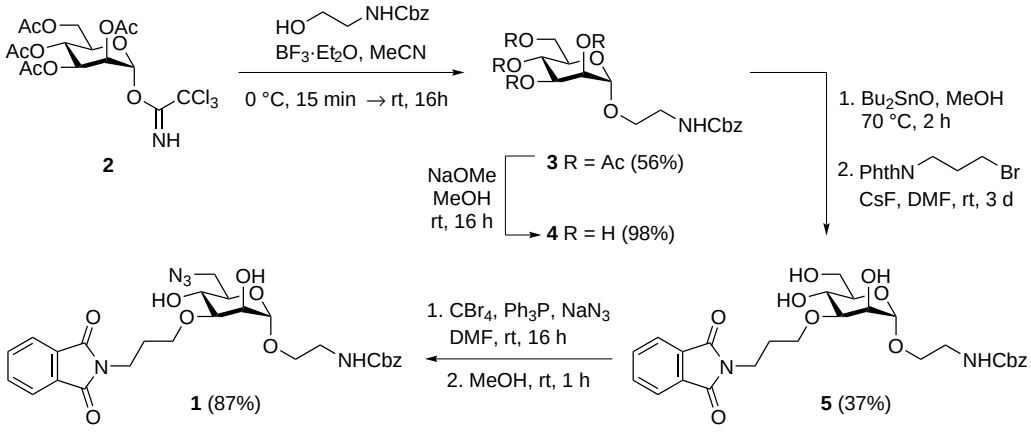

Scheme 6.5. Synthesis of the orthogonal trivalent scaffold molecule **1**.

After deacetylation of **3**,[15] the second protected amino functionality was introduced in a previously described regioselective *O*-phthalimidopropylation reaction.[7] This was achieved in a one-pot procedure by employing bisdibutyltin oxide in refluxing methanol to form a stannyliden acetal intermediate. After exchanging the solvent to dimethylformamide, ring opening of the stannylidene acetal with *N*-(3-bromopropyl)phthalimide under caesiumflouride catalysis furnished the 1,3-amino functionalized mannoside **5** in a moderate yield of 37% over two steps.[16] Notwithstanding the low yield, the reaction is feasible due to the fact that non-reacted starting material can be recovered unaltered and used again. Direct azidation of the primary hydroxyl group at the sugar ring was accomplished in an APPEL reaction with a carbon tetrabromide-triphenylphosphine-sodium azide reagent system.[17] Therefore, formation of the phosphonium salt species was performed first and then the carbohydrate derivative **5** was added. Quenching the reaction mixture with an excess of methanol furnished the desired 6-azido-6-deoxymannopyranoside **1** in a yield of 87%. It is notable, that the three orthogonal functionalities could be introduced without the requirement of a complex protecting group strategy.

To build up azobenzene heteroglycoclusters thiourea bridging was envisaged. Thus, NCS-functionalized α-D-mannoside **21**, β-D-glucoside **22** and α-D-glucoside **23** derivatives were prepared next (Scheme 6.6).

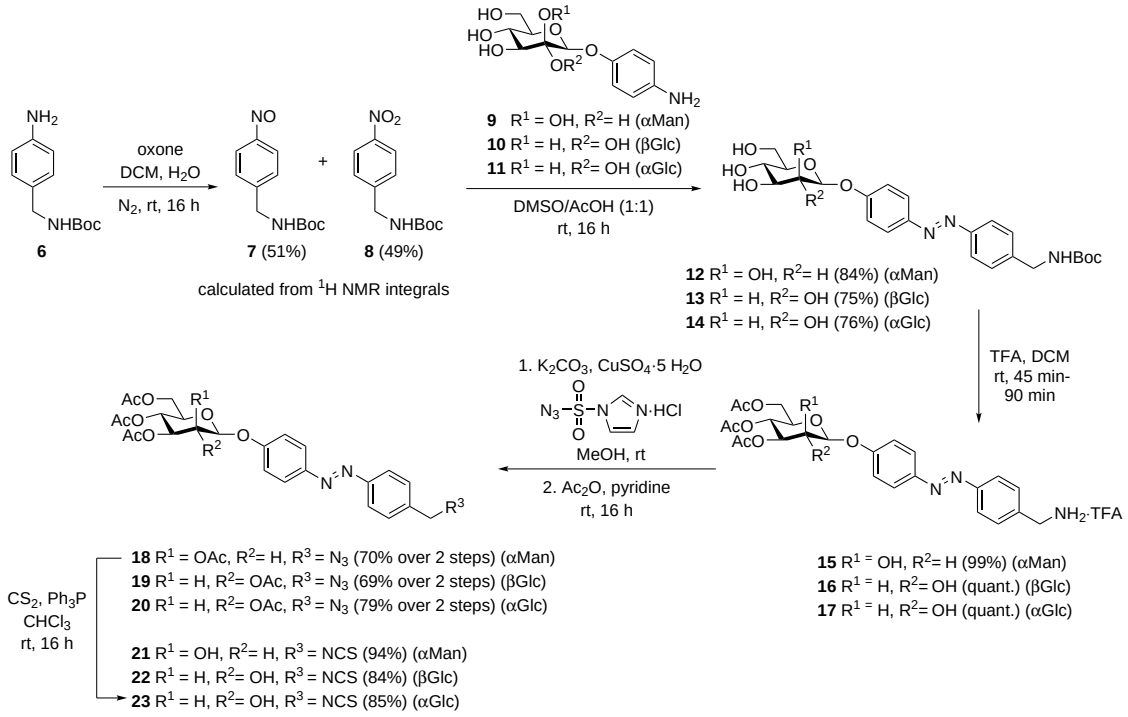

Scheme 6.6. Synthesis of NCS-functionalized glycoazobenzene derivatives **21**, **22** and **23**.

As an earlier studies[18] Mills condensation[19] was utilized to prepare glycoazobenzene derivatives **12**, **13** and **14**. The reaction comprises an acid-promoted condensation of nitrosoarenes and aniline derivatives. Initially, oxidation of aniline derivative **6**[20] with oxone in a water/dichloromethane biphasic system was performed.[21] After aqueous work-up a mixture of nitrosoarene **7**[21] and nitro side product **8** were isolated. The crude mixture was not further purified. Hence, purification of less stable nitroso compound led to partial decomposition and impurities of nitro compounds do

not interfere with the azobenzene condensation reaction. The synthesis of the unsymmetrically substituted glycoazobenze derivatives **12**, **13** and **14** was achieved in a DMSO acetic acid mixture (1:1) while treating the crude nitrosoarene **7** with the known *p*-aminophenyl glycosides **9**[22], **10**[23] and **11**[24] which were obtained by catalytical reduction of the respective commercially available *p*-nitrophenyl glycoside. Subsequent cleavage of the Boc-protecting group with trifluoroacetic acid (TFA) furnished the tetraammonium salts **15**, **16** and **17** in quantitative yield. In a diazotransfer reaction with imidazole-1-sulfonyl azide as a diazo donor,[25] amines **15**, **16** and **17** were converted into the corresponding azides under copper catalysis and were immediately submitted to *O*-acetylation, using acetic anhydride in pyridine to yield the fully protected azobenzene glycosides **18**, **19** and **20** in a yield ranging from 69% to 79% over two steps. Under aza-Wittig reaction conditions with carbon disulfide as nucleophile the desired NCS-functionalized derivatives **21**, **22** and **23** were obtained in high yields. The orthogonal trifunctional carbohydrate scaffold **1** and NCS-functionalized derivatives can be utilized for the synthesis of azobenzene heteroglycoclusters of different kind via thiourea bridging.

Consequently, in order to achieve the envisaged heterodivalent azobenzene glycocluster **27**, we employed the *O*-(3-aminopropyl)-mannoside **26** obtained in nearly quantitative yield by hydrazinolysis of the 3-*O*-(3-phthalimidopropyl)-modified mannoside **5** in ethanol (Scheme 6.7).[16]

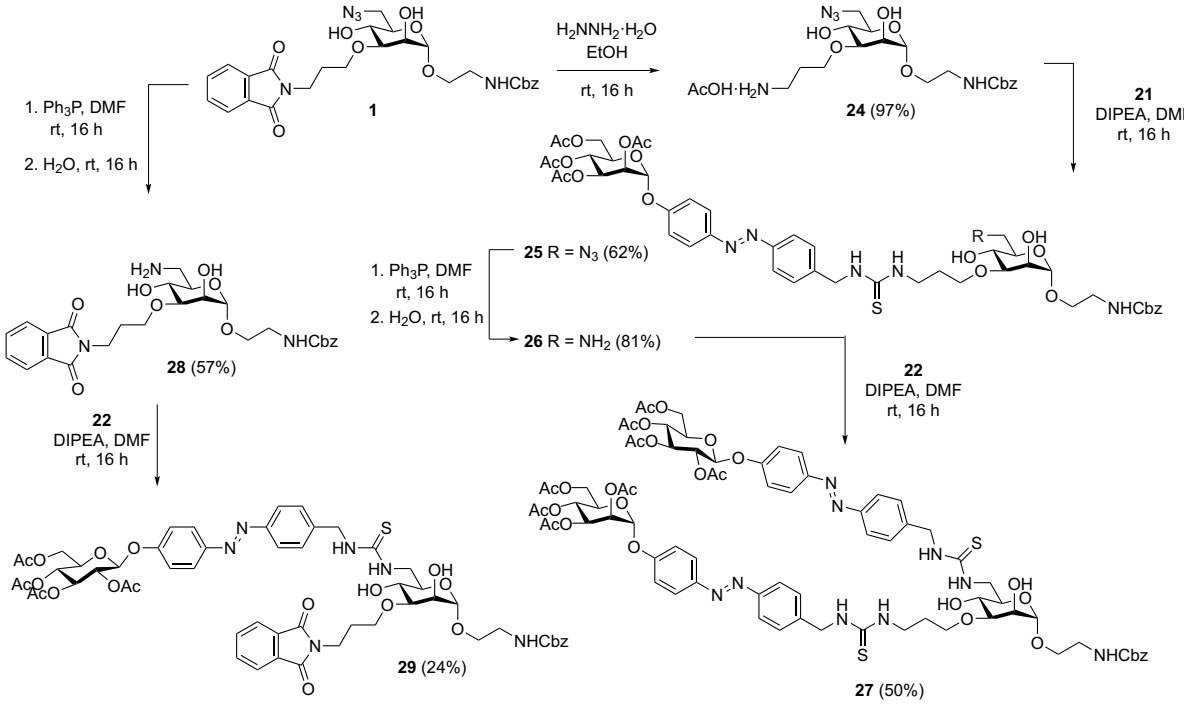

Scheme 6.7. Synthesis of the heterodivalent azobenzene glycocluster **28**.

In a subsequent thiourea bridging reaction of the azobenzene mannoside **21** and the trifunctional scaffold **24** in dimethylformamide and diisopropylethylamine (DIPEA), the monovalent azobenzene mannoside **25** could be isolated in a yield of 62%. Staudinger reduction of the azido function in **25** was accomplished with triphenylphosphin and water and led to the amine **26** in 81%. Its subsequent reaction with isothiocyanate functionalized β-D-glucoside **19** provided the desired divalent glycocluster **27**. In order to compare the switching behaviour of the glycoclustes **27** with

monovalent derivatives **25** and **29**, theβ-D-gluco configured azobenzene glycoside **30** was prepared next (Scheme 6.7). Thus, Staudinger reduction was employed to deliver free amine **2**8, which was utilized for the synthesis of **29** in 24% yield via azobenzene glucoside **22** in a thiourea bridging reaction. With the monovalent derivatives **25** and **29** and the divalent azobenzene glycoclusters **27** in hand photochromic properties of these were investigated.

Photochromic properties of monovalent and divalent glycozobenzene derivatives

To induce $E \rightarrow Z$ or $Z \rightarrow E$ isomerization of **25**, **27** and **29** a 365 nm (UV light) light emitting diode (LED) and a 460 nm (green light) LED, respectively, was employed. Irradiation experiments were performed at room temperature under exclusion of day light. The isomer-specific photoisomerization to the photostationary states (PSS) and the thermal $Z \rightarrow E$ back isomerization ($\tau_{1/2}$) as a function of time of the azobenzene glycosides **25**, **27** and **29** were determined in deuterated methanol by ^{1}H NMR spectroscopy. $E \rightarrow Z$ isomerization was monitored by UV-vis spectroscopy (for details cf. Supporting Information). Photostationary states were reached after irradiation with UV light for approx. 15 min. E/Z ratios of the isomeric mixtures were quantified on the basis of integration of the H-1 anomeric proton of the coupled mannoside **21** and the H-2 proton of the coupled glucoside **22**, respectively. The photochromic data obtained from glycoazobenzene derivatives **25**, **27** and **29** are collected in Table 6.1.

Table 6.1. Comparison of photochromic properties of synthesised azobenzene (AB) glycosides.

Azobenzene glycoconjugate	E/Z (PSS) AB_{Man}	E/Z (PSS) AB_{Glc}	Half-life AB_{Man} $\tau_{1/2}$ [h]	Half-life AB_{Glc} $\tau_{1/2}$ [h]
25	5/95	-	10	-
27	4/96	7/93	17	29
29	-	8/92	-	16

Figure 6.5 displays the spectra of the divalent azobenzene glycocluster in methanol after excitation to the photostationary state PSS_{365} as a function of time. It can be clearly seen that four doublets of the H-1 proton resonance of the coupled mannoside **21** of the four different isomers ($E_{Man}E_{Glc}$, $E_{Man}Z_{Glc}$, $Z_{Man}E_{Glc}$, $Z_{Man}Z_{Glc}$) co-exist in the PSS_{365}. On the basis of their chemical shift and with the aid of 2D NMR spectra (^{1}H/^{13}C HSQC) the four doublets could be readily assigned to the respective isomer (Figure 6.6).

The isomer composition in the PSS_{365} was found to be: 1% $E_{Man}E_{Glc}$, 6% $Z_{Man}E_{Glc}$, 3% $E_{Man}Z_{Glc}$, and 90% $Z_{Man}Z_{Glc}$. Isomer-specific thermal lifetimes could be determined by a kinetic analysis of the respective intergrated doublet signals of the H-1 signals of the coupled mannoside **21**. The following kinetic model for the thermalt back iosmerization was assumed for the respective isomers:

$$Z_{Man}Z_{Glc} \rightarrow E_{Man}Z_{Glc} \rightarrow E_{Man}E_{Glc}$$

$$Z_{Man}Z_{Glc} \rightarrow Z_{Man}E_{Glc} \rightarrow E_{Man}E_{Glc}$$

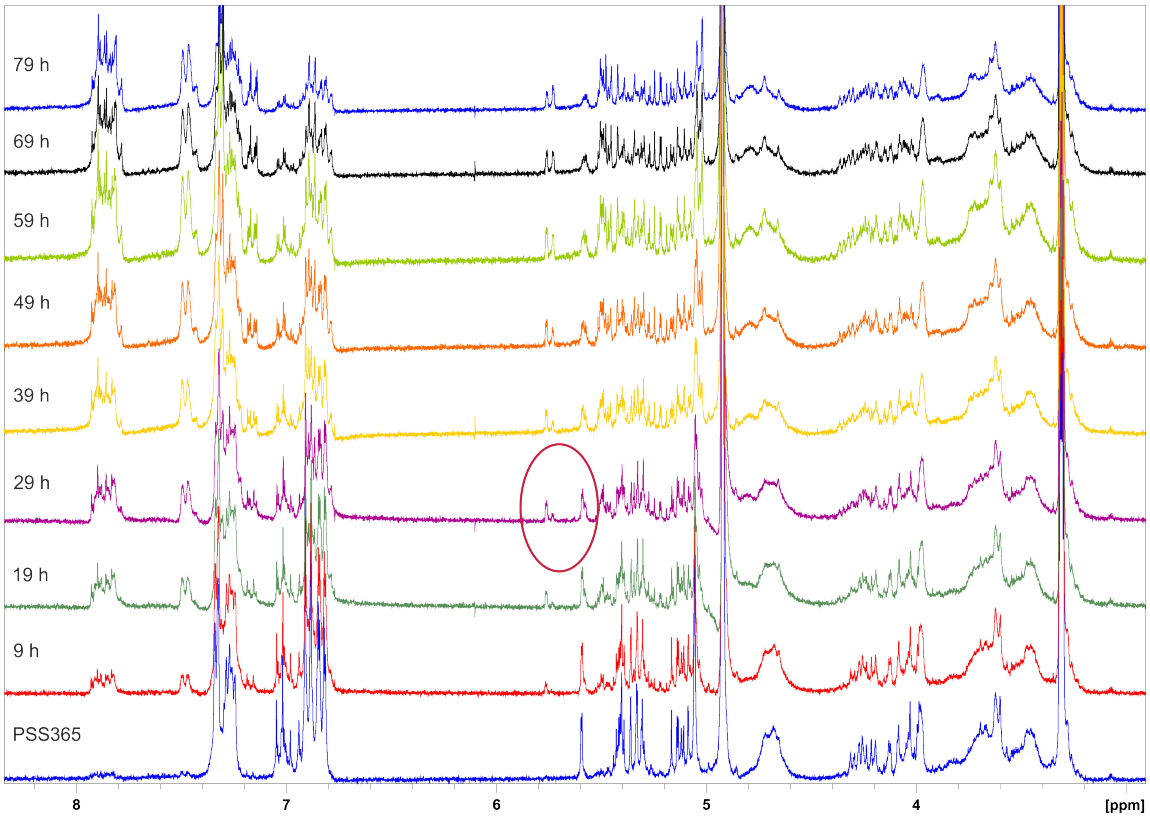

Figure 6.5. ^{1}H NMR spectra of **27** in methanol as a function of time after excitation to the photostationary state at $t = 0$. The circle in the middle highlights the H-1 proton signals of the coupled mannoside **21** of the four diffrent isomers.

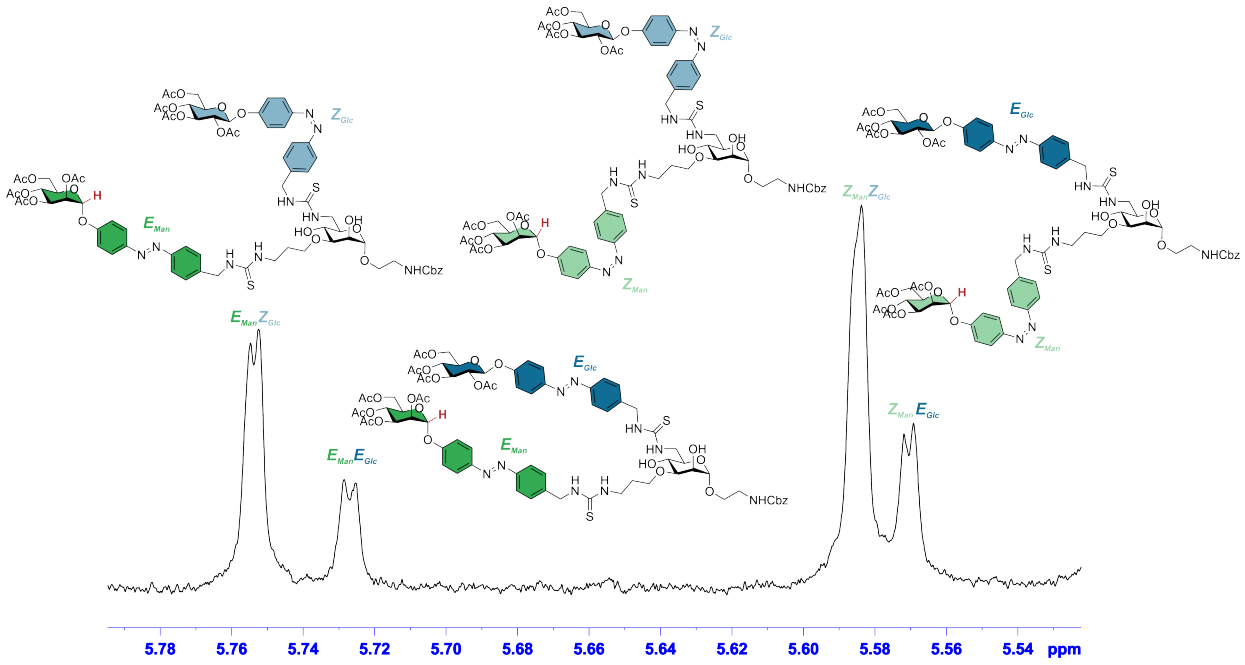

Figure 6.6. ^{1}H NMR spectra of **27** in methanol after 16 h 29 min after excitation to the photostationary state. The assignment of the four different isomers ($E_{Man}E_{Glc}$, $E_{Man}Z_{Glc}$, $Z_{Man}E_{Glc}$, $Z_{Man}Z_{Glc}$) were made on the basis of the respective chemical shift with the aid of 2D NMR spectra.

The resulting isomer specific lifetimes are $\tau_{Z_{Man}Z_{Glc} \rightarrow E_{Man}Z_{Glc}} = 18$ h, $\tau_{E_{Man}Z_{Glc} \rightarrow E_{Man}E_{Glc}} = 27$ h, $\tau_{Z_{Man}Z_{Glc} \rightarrow Z_{Man}E_{Glc}} = 30$ h, and $\tau_{Z_{Man}E_{Glc} \rightarrow E_{Man}E_{Glc}} = 17$ h.

The monovalent as well as the divalent azobenzene glycosides **25**, **27** and **29** are efficient photoswitches. Remarkably, even the divalent glycocluster consists of 90% all-*Z* isomer in the PSS_{365}. Furthermore, it was revealed that all four conceivable photoisomers exist after irradiation. The thermal half life time for each isomer could be determined. The thermal back isomerization from the $Z_{Man}Z_{Glc}$ isomer to the $E_{Man}Z_{Glc}$ isomer is faster compared to the isomerization process from the $E_{Man}Z_{Glc}$ to the $E_{Man}E_{Glc}$ isomer. Thermal isomerization from the all- *Z*-isomer to the $Z_{Man}E_{Glc}$ is faster than the isomerzation process from $Z_{Man}E_{Glc}$ to $E_{Man}E_{Glc}$. The thermal relaxation times of the isomerization processes $Z_{Man}Z_{Glc} \rightarrow E_{Man}Z_{Glc}$ and $Z_{Man}E_{Glc} \rightarrow E_{Man}E_{Glc}$ as well as $Z_{Man}Z_{Glc} \rightarrow Z_{Man}E_{Glc}$ and $E_{Man}Z_{Glc} \rightarrow E_{Man}E_{Glc}$ are of comparable length. The isomerzation process $Z_{Man} \rightarrow E_{Man}$ and the isomerization process $Z_{Glc} \rightarrow E_{Glc}$ are independet from each other. Thus, in contrast to previously reported multivalent azobenzene systems the azobenzene units of the divalent azobenzene glycocluster may be electonically decoupled.[26]

6.2.1.3 Conclusion

We have successfully synthesised the orthogonal trifunctional mannoside scaffold **1** which was realized in a straightforward synthetic pathway. The NCS-functionalized azobenzene derivatives **21**-**23** were prepared as applied to build up a divalent atobenzene glycocluster **27** in a isothiocyanate-amine coupling reaction. Additionally, the determination of the photochromic data as well as a detailed kinetic study of the switching behavior of the hetero-divalent azobenzeneglycocluster **27** was accomplished. The findings revealed that the installed azobenzene units are electronically decoupled and can be switched independently. Thus, the trifunctional mannoside **1** is an excellent scaffold molecule to prepare multivalent azobenzene glycoclusters which might facilitate the investigation of photoswitchable cell adhesion in a heteromultivalent manner. Furthermore, it would be interesting to incorporate azobenzene glycosides that can be isomerized with different wavelength.

6.2.1.4 References

[1] a) C. Müller, G. Despras, T. K. Lindhorst, *Chem. Soc. Rev.* **2016**, *45*, 3275-3302; b) R. Roy, T. C. Shiao, *Chem. Soc. Rev.* **2015**, *44*, 3924-3941; c) M. Mammen, S.-K. Choi, G. M. Whitesides, *Angew. Chem.* **1998**, *110*, 2908-2953; *Angew. Chem. Int. Ed.* **1998**, *37*, 2754-2794; d) C. Fasting, C. A. Schalley, M. Weber, O. Seitz, S. Hecht, B. Koksch, J. Dernedde, C. Graf, E.-W. Knapp, R. Haag, *Angew. Chem.* **2012**, *124*, 10622-10650; *Angew. Chem. Int. Ed.* **2012** , *51*, 10472-10498; e) L. L. Kiessling, J. E. Gestwicki; L. E Strong, *Angew. Chem.* **2006**, *118*, 2408-2429; *Angew. Chem. Int. Ed.* **2006**, *45*, 2348-2368; f) W. Meutermans, G. T. Le, B. Becker, *ChemMedChem.* **2006**, *1*, 1164-1194.

[2] a) C. Papin, G. Doisneau, J.-M. Beau, *Chem. Eur. J.* **2009**, *15*, 53-57; b) B. Gerland, A. Goudot, G. Pourceau, A. Meyer, V. Dugas, S. Cecioni, S. Vidal, E. Souteyrand, J.-J. Vasseur, Y. Chevolot, F. Morvan Gerland B, Goudot, *Bioconjugate Chem.* **2012**, *23*, 1534-1547; c) T. K. Lindhorst, M. Dubber, *Carbohydr. Res.* **2015** , *403*, 90-97.

[3] a) M. Dubber, T. K. Lindhorst, *J. Org. Chem.* **2000**, *65*, 5275-5281; b) J. Ni, H. Song, Y. Wang, N. M. Stamatos, L.-X. Wang, *Bioconjugate Chem.* **2006**, *17*, 493-500; c) R. P. McGeary, I. Jablonkai, I. Toth, *Tetrahedron* **2001**, *57*, 8733-8742; d) O. Sperling, M. Dubber, T. K. Lindhorst, *Carbohydr. Res.* **2007**, *342*, 696-703; e) W. Zhong, M. Skwarczynski, P. Simerska, M. F. Good, I. Toth, *Tetrahedron* **2009**, *65*, 3459-3464; f) V. Fagan, I. Toth, P. Simerska, *Beilstein J. Org. Chem.* **2014**, *10*, 1741-1748; g) T. C. Shiao, R. Rej, M. Rose, G. M. Pavan, R. Roy, *Molecules* **2016**, *21*, 448-464.

[4] T.-E. Gloe, A. Müller, A. Ciuk, T. M. Wrodnigg, T. K. Lindhorst, *Carbohydr. Res.* **2016**, *425*, 1-9.

[5] a) C. Kieburg, K. Sadalapure, T. Lindhorst, *Eur. J. Org. Chem.* **2000**, *2000*, 2035–2040; b) K. Sadalapure, T. K. Lindhorst, *Angew. Chem.* **2000**, *112*, 2066–2069; *Angew. Chem. Int. Ed.* **2000**, *41*, 2596-2599; c) A. Patel, T. K. Lindhorst, *J. Org. Chem.* **2001**, *66*, 2674–2680; d) M. Dubber, O. Sperling, T. K. Lindhorst, *Org. Biomol. Chem.* **2006**, *4*, 3901–3912; A. Patel, e) T. Lindhorst, *Eur. J. Org. Chem.* **2002**, *2002*, 79–86; f) A. K. Ciuk, T. K. Lindhorst, *Beilstein J. Org. Chem.* **2015**, *11*, 668–674 .

[6] J. L. Jiménez Blanco, P. Bootello, C. Ortiz Mellet, J. M. García Fernández, *Eur. J. Org. Chem.* **2006**, 183-196.

[7] C. D. Heidecke, T. K. Lindhorst, *Synthesis* **2006**, *1*, 161-165.

[8] a) M. Gingras, Y. M. Chabre, M. Roya, R. Roy, *Chem. Soc. Rev.* **2013**, *42*, 4823-4841; b) T.K. Lindhorst, C. Kieburg, *Angew. Chem.* **1996**, *118*, 2083-2086; *Angew. Chem. Int. Ed. Engl.* **1996**, *35*, 1953-1956; c) C. Ortiz Mellet, J. Defaye, J.M. Garcia Fernandez, *Chem. Eur. J.* **2002**, *8*, 1982-1990; d) M. Köhn, J. M. Benito, C. Ortiz Mellet, T. K. Lindhorst, J. M. García Fernández, *Chem- BioChem* **2004**, *5*, 771-777.

[9] a) B. Thomas, M. Fiore, I. Bossu, P. Dumy, O. Renaudet, *Beilstein J. Org. Chem.* **2012**, *8*, 421-427; b) J. L. Jiménez Blanco,C. Ortiz Melleta, J. M. García Fernández, *Chem. Soc. Rev.* **2013**, *42*, 4518-4531; c) B. Thomas, M. Fiore, G. C. Daskhan, N. Spinelli, O. Renaudet, *Chem.Commun.* **2015**, *51* ,5436-5439.

[10] M. Hartmann, A. K. Horst, P. Klemm, T. K. Lindhorst, *Chem. Commun.* **2010**, *46*, 330-332.

[11] a) T. Weber, V. Chandrasekaran, I. Stamer, M. B. Thygesen, A. Terfort, T. K. Lindhorst, *Angew. Chem.* **2014**, *126*, 14812-14815; *Angew. Chem. Int. Ed.* **2014**, *53*, 14583-14586; b) V. Chandrasekaran, H. Jacob, F. Petersen, K. Kathirvel, F. Tuczek, T. K. Lindhorst, *Chem. Eur. J.* **2014**, *20*, 8744-8752.

[12] V. Chandrasekaran, T. K. Lindhorst, *Chem. Commun.* **2012**, *48*, 7519-7521.

[13] K. H. Jung, M. Hoch, R. R. Schmidt, *Liebigs Ann. Chem.* **1989**, 1099-1106.

[14] G. T. Noble, S. L. Flitsch, K. Ping Liema, S. J. Webb, *Org. Biomol. Chem.* **2009**, *7*, 5245-5254.

[15] N. Jayaraman, J. F. Stoddart, *Tetrahedron Letters* **1997**, *38*, 6767-6770.

[16] C. Hojnik, A. Müller, T.-E. Gloe, T. K. Lindhorst, T. M. Wrodnigg, *Eur. J. Org. Chem.* **2016**, *2016*, 4328-4337.

[17] J. L. Jiménez Blanco, J. M. García Fernández, A. Gadelle, J. Defaye, *Carbohydr. Res.* **1997**, *303*, 367-372.

[18] V. Chandrasekaran, E. Johannes, H. Kobarg, F. D. Sönnichsen, T. K. Lindhorst, *Chemistry-Open* **2014**, *3*, 99-108.

[19] a) E. Merino, *Chem. Soc. Rev.* **2011**, *40*, 3835-3853; b) F. Hamona, F. Djedaini-Pilardb, F. Barbota, C. Len, *Tetrahedron* **2009**, *65*, 10105-10123.

[20] E. B. Park, K.-S. Jeong, *Chem.Commun.* **2015**, *51*, 9197-9200.

[21] B. Priewisch, K. Rück-Braun, *J. Org. Chem.* **2005**, *70*, 2350-2352.

[22] M. Hartmann, A. K. Horst, P. Klemm and T. K. Lindhorst, *Chem. Commun.* **2010**, *46*, 330-332.

[23] G. R. Gustafson, C. M. Baldino, M.-M. E. O'Donnell, A. Sheldon, R. J. Tarsa, C. J. Verni and D. L. Coffen, *Tetrahedron* **1998**, *54*, 4051-4065.

[24] C. Grabosch, M. Hartmann, J. Schmidt-Lassen, T. K. Lindhorst, *ChemBioChem* **2011**, *12*, 1066-1074.

[25] E. D. Goddard-Borger, R. V. Stick, *Org. Lett.* **2007**, *9*, 3797-3800.

[26] J. Bahrenburg, C. M. Sievers, J. B. Schönborn, B. Hartke, F. Renth, F. Temps, C. Näther, F. D. Sönnichsen, *Photochem. Photobiol. Sci.* **2013**, *12*, 511-518.

7 Conclusion

The aim of this thesis was the synthesis and investigation of azobenzene glycoconjugates as photoswitchable tools to control protein and glycoconjugate function. The first section of this thesis is focused on the synthesis of homo- and hetero-bifunctional (glyco)azobenzene derivatives for the photosensitive cross-linking of peptides and proteins aiming at the control of their conformation and, as a consequence, their function. In the second part, azobenzene glycoconjugates were utilized to further study the phenomenon of carbohydrate-specific bacterial adhesion.

Azobenzene glycoconjugates for photosensitive cross-linking of proteins or peptides

Since bioactive peptides and proteins are the main component of every mammalian cell and perform a vast array of fundamental functions within all living organism it is of great interest to get a deeper insight into the underlying molecular events. Consequently, azobenzene-based cross-linkers have been widely utilized to spatiotemporal control form and function of bioactive peptides or proteins. These applications rely on the site-selective conjugation of the azobenzene photochromic unit into the structure of the biomolecule. Through the conjugation of photosensitive azobenzene cross-linkers that mediate structural changes after irradiation, conformational switching of proteins and peptides can be affected. Thus it is possible to control function by light with temporal and spatial resolution. This project aims at advancing the collection of known photosensitive cross-linkers by introducing bifunctional azobenzene glycoconjugates and non-carbohydrate derivatives (Figure 7.1) Additionally, the obtained photoswitches were supposed to serve as cross-linkers for antifreeze proteins.

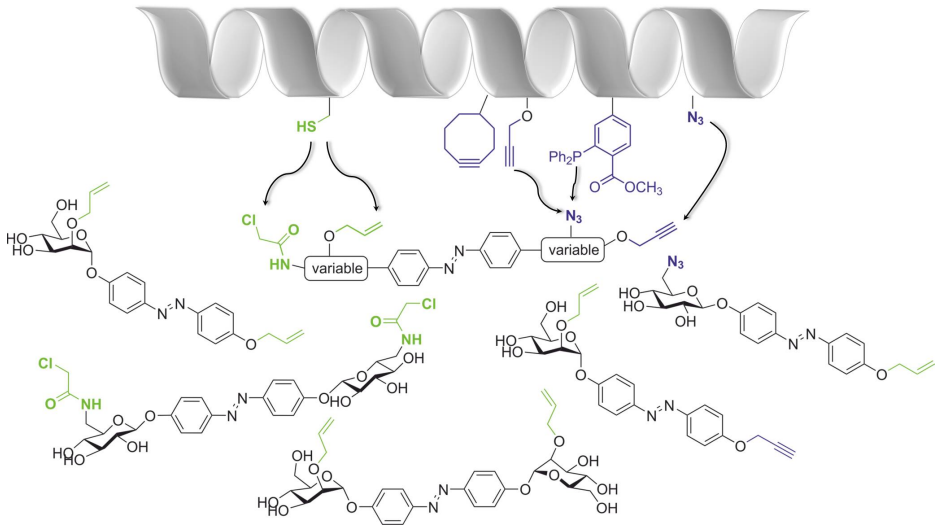

Figure 7.1. Illustration of the designed linker molecules with the "variable"region represented by a pyranose ring in most cases. The synthesised homo- and hetero-bifunctional glycoazobenzene derivatives varied in their length and functional groups which were combined accordingly allowing for site-selective cross-linking of proteins and peptides using different ligation methods.

Two different types of (glyco)azobenzene derivatives were prepared, one type comprising cross-linker possessing two equal thiol anchoring groups which allow for conjugation to the protein in a concerted fashion. The other type comprises photoresponsive azobenzene conjugates that carry a bioorthogonal hetero-functionalization allowing for consecutive cross-linking of the respective peptide or protein. The designed linker molecules varied in their length and their functional groups. Variation of the linker length was achieved by utilizing the possibility of bifunctionalization of azobenzene glycosides. Apart from the functionalization of the azobenzene moiety, the primary 6-hydroxyl group of the sugar was addressed regioselectively. Moreover, a second functional group for peptide cross-linking was installed at the 2-OH-position of the sugar moiety. Therefore, a beneficial protecting group strategy was established which allows to for faciliating the adjustment of various distances between the two cross-linking functionalities. Besides that various functional groups, namely alkene, alkyne, azido and chloroacetamido groups were combined accordingly allowing for site-selective cross-linking of proteins and peptides using different ligation methods. The prepared cross-linkers exhibit favourable photochromic properties and improved water solubility. First ligation reactions of chloroacetamido- as well as alkene-functionalized homo-bifunctional glycoazobenzene derivatives with model peptides (tripeptide and a nonadecapeptide) in a thiol-ene reaction and via a nucleophilic displacement reaction in aqueous media demonstrated impressively that the new bifunctional azobenzene glycoconjugates favourably supplement the known photoresponsive cross-linkers for the control of protein function. To estimate the effect of azobenzene glycoconjugates on the conformational properties of cross-linked peptides or proteins molecular dynamics simulations were performed. The change of their end-to-end distances upon isomerization was monitored and revealed that the separation of the distance distributions between the E and Z states is characteristic for the individual cross-linkers. However, the distance distribution of the respective isomers is rather broad and they are overlapping each other, thus the effect upon isomerization of the glycoazobenzene derivatives might not strongly affect the conformational properties of the cross-linked peptides or proteins. Cross-linking with antifreeze proteins was not accomplished so far as their preparation by Fmoc solid phase peptide synthesis was unexpectedly complicated. The yields were rather low, resulting in complicated purification needs. Additionally, the ligation of cross-linkers to the cysteine side-chain of proteins might not be suitable as several tested linker molecules including the chloracetamido functionalized homo-bifunctional glycoazobenzene derivative yielded unexpected complications. The yields were generally low, multiple products were obtained and foremost, reproducibility was lacking. Nevertheless, the applicability of homo- and hetero-bifunctional glycoazobenzene cross-linkers should further be tested in the photoswitching of the form and function of peptides and proteins in future as they provide a multitude of photosensitive proteins.

Azobenzene glycoconjugates to control bacterial adhesion

In the second part of this thesis azobenzene glycoconjugates were synthesised to control bacterial adhesion. In Chapter 4 the work on photoswitchable surfaces was extended. Herein, previously utilized glyco-SAMs were changed to a quartz glass surface to make photoswitchable glycosylated amenable for UV-vis absorption spectroscopy (Figure 7.2).

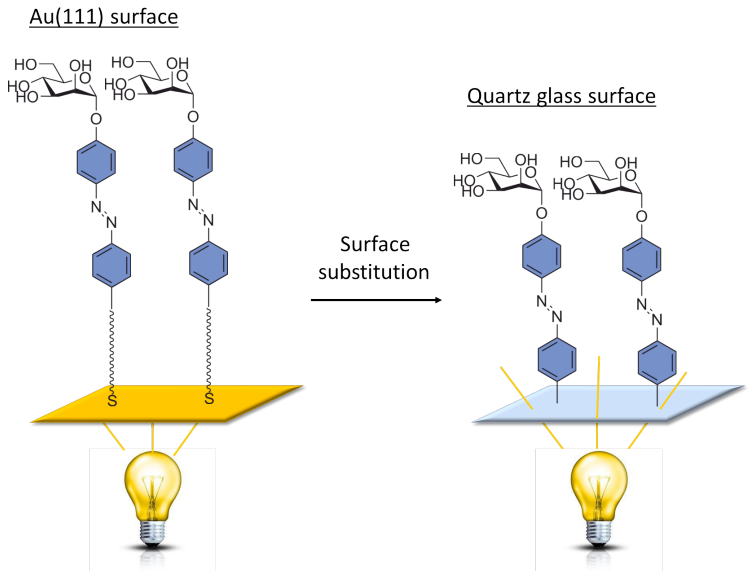

Figure 7.2. Previously utilized glyco-SAMs were substituted by quartz glass surface which have the advantage that they are translucent and thus amenable to UV-vis absorption spectroscopy.

For this purpose azobenzene glycosides were covalently immobilized on quartz glass surfaces. Therefore, an isothiocyanato-functionalized azobenzene mannoside was prepared which was initially coupled with the commercially available 11-aminoundecyltrimethoxysilane and subsequently assembled on the quartz slides. Successful surface modification was verified by UV-vis absorption spectroscopy and contact angle measurements. As the characteristic azobenzene absorption at 350 nm was observed successful surface functionalization was verified. By applying sequential irradiation with λ = 365 nm and visible light (λ = 440 nm), $E \rightarrow Z$ isomerization of the immobilized mannoside was achieved. It could be demonstrated that the E/Z isomerization process was reversible over at least 3.5 switching cycles and almost no fatigue of the azobenzene switch was observed. Furthermore, the immobilized azobenzene mannoside exhibits a thermal half life time of around 6 h. Thus, the assembled azobenzene switch fulfils all requirements to be applied as adhesive surfaces in bacterial adhesion studies. Consequently, the prepared quartz slides were employed in bacterial adhesion studies with type 1 fimbriated *E. coli*. The results revealed that upon irradiation with two different wavelength (365 and 440 nm) the adhesivity of the surface resulted in switching between adhesive and less adhesive as by switching from E to Z configuration bacterial adhesion was diminished about 75%. These findings are in accordance with earlier results.[107] Thus, the studies encourage the assumption that the configuration of the azobenzene N=N double bond determines the orientation of the carbohydrate moiety presented on the surface. The E-configured azobenzene glycosides should be projecting from the surface and able to interact with bacterial lectins (FimH), while in the case of the Z-configured surface the carbohydrate head groups should be re-oriented and thus be less accessible for complexation with bacterial lectins.

Photoresponsive glycoazobenzene functionalized glass slides represent a valuable tool to further investigate the influence of configurational and conformational arrangement of ligand orientation

of carbohydrate recognition. They are therefore perfectly suited as they are amenable for UV-vis investigation. Furthermore, a vast variety of ligation methods can be applied to attach various azobenzene glycoconjugates on the solid support. Glycosylated glass slides can be also easily utilized under flow.

The development of new diagnostic tools and enhanced assay systems is an important step to facilitate the study of bacterial adhesion. In the second part of Chapter 4 we wanted to examine if photoresponsive surfaces can be used as new diagnostic tools. For this purpose the solid support was changed to UV-stable magnetic PEG beads.
Initially a bead based kit for the investigation of carbohydrate-specific agglutination of *E. coli* bacteria as an alternative to the classical hemagglutination assay was established. Therefore, various *manno*-, *gluco*- and *arabino*-configured azido-functionalized glycosides were synthesised, coupled to a trifunctional linker molecule via copper (I) catalysed azide-alkyne click reaction and subsequently immobilized on the surface of commercially available magnetic beads. The obtained carbohydrate-coated beads were then successfully applied in a carbohydrate specific agglutination and agglutination-inhibition assay with type 1 fimbriated *E. coli*. The prepared beads have the advantage that they can be stored for several months until use and be directly applied to study carbohydrate-lectin interactions of non-labeled bacteria. It was possible to establish a ready-to-use bead-based kit which may facilitate the investigation of wild-type bacterial lectins as well as the inhibitory potency of new anti-adhesive compounds.
Encouraged by the previous results of preparing photoresponsive surfaces to control bacterial adhesion we wanted to examine whether the adhesivity of magnetic PEG-beads can be photocontrolled by reversible E/Z-isomerization of an immobilized azobenzene mannoside. For this purpose an azido-functionalized azobenzene derivative was synthesised, coupled to a linker molecule and immobilized on the surface of magnetic-PEG beads. The azobenzene-coated beads were subsequently employed in bacterial adhesion studies. Switching of the azobenzene configuration resulted in no significant difference in bacterial adhesion to glycosylated PEG-beads. Further optimization of the switching behaviour needs to be performed in future.
To achieve photoswitching of the adhesivity of magnetic PEG-beads, a coorperation project with T.-E. Gloe and O. Jaeschke was initiated which is based on the capability of cyclodextrines (CD) to encapsulate appropriate hydrophobic molecules such as E-configured azobenzene derivatives.[400,401] Z-configured azobenzene molecules are not encapsulated within CDs. In this project azobenzene derivatives were immobilized on magnetic beads and different CD derivatives were utilized for inclusion on the photoresponsive surface. It was found that upon irradiation the bacterial adhesion to beads could indeed be diminished but so far switching of bacterial adhesion is not optimal and need to be further optimized. Nevertheless, these results further underline the potency of using functionalized magnetic beads to study bacterial adhesion. Especially, photoswitchable magnetic beads are of great interest as bacteria might be detached from beads under relatively mild conditions (hν) offering great potential in the development of new detection methods of bacteria, also for diagnostic applications.

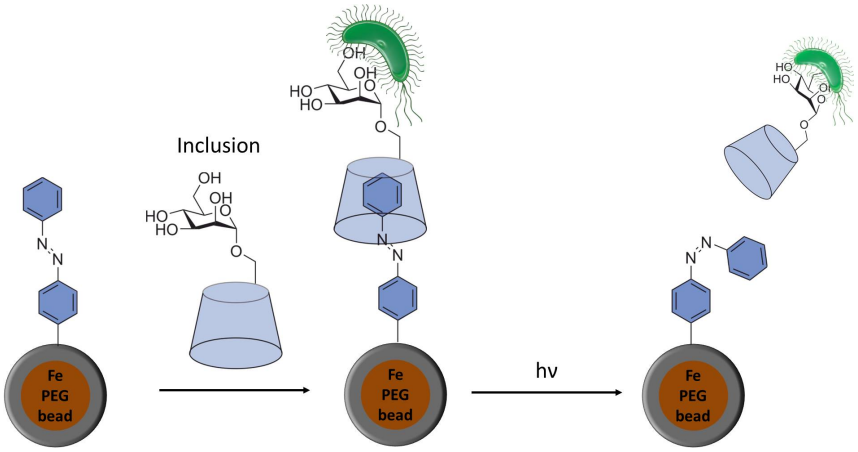

Figure 7.3. Magnetic PEG beads functionalized with azobenzene derivatives were treated with cyclodextrine conjugates. Switching of bacterial adhesion was achieved by E/Z isomerization of the azobenzene unit.

Since the photocontrol of bacterial adhesion on glass surfaces was successfully demonstrated we wanted to challenge our system in a more complex natural environment. In chapter 5 artificial designer surfaces were substituted by the membrane of human cells (Figure 7.4).

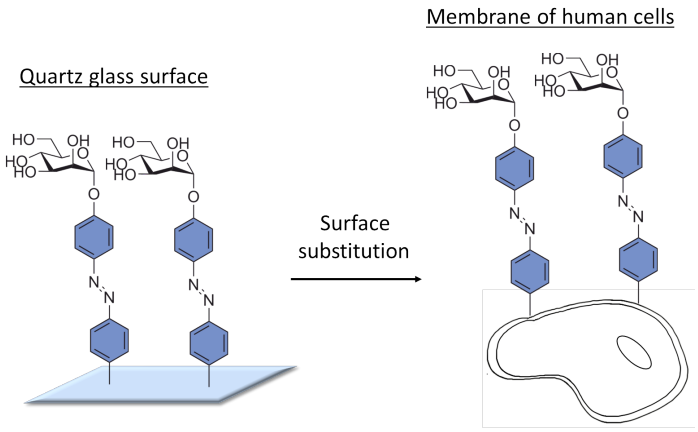

Figure 7.4. Artificial photoresponsive glass slides were substituted by the membrane of human cells.

By utilizing metabolic oligosaccharide engineering, azide functional groups could be incorporated within cell surface glycans of human microvascular endothelial cells variant 1 (HMEC-1), which were subsequently modified with alkyne-functionalized azobenzene derivatives in a bioorthogonal click reaction. Bacterial adhesion studies with type I fimbriated *E. coli* bacteria were performed. For this purpose, azobenzene-modified cells were divided into two portions and irradiated with UV light, then, cells were incubated with GFP-fluorescent *E. coli* bacteria. The number of adhered bacteria was quantified via high-resolution live-cell fluorescence microscopy. As expected the number of adhered bacteria to both sets of HMEC-1 was similarly low at this stage. However, irradiating of just on set of cell with visible light and subsequent incubation with *E. coli* bacteria resulted in increased bacterial adhesion (50%). The study suggested that the mode of mannoside orientation which is altered upon isomerization of the azobenzene hinge is responsible for the observed results.

The obtained results are in total accordance with results observed with photoswitchable surfaces. Next, switching of cellular adhesion was investigated in a real-time, flow-based experiment. The results obtained in the flow assay are in agreement with the experiments under static conditions as it was indicated that the orientation of the immobilized azobenzene mannoside on the surface of human cells has a strong influence on bacterial adhesion even under flow. To further investigate the observed results in more detail a number of control experiments were performed.
In conclusion, it was demonstrated that azobenzene mannosides can be applied to influence adhesion of *E. coli* bacteria to human cells. We have postulated following mechanism: i) the bacterial lectin FimH binds specifically to mannosides presented on the cell surface, thus a specific interaction between the bacterium and the cell surface takes place; ii) unless there is a glucose or a non-carbohydrate azobenzene ligand (no mannose) present or if the mannose adopts an unfavourable orientation, the azobenzene hinge shields the cell surface which results in a reduced adhesion of *E. coli* bacteria; iii) the present mannose ligand must be located at the terminus of cell surface glycans to guarantee a difference in bacterial adhesion upon irradiation.
These astonishing results are highly encouraging for further studies since the effect through orientation of the carbohydrate ligand can be observed not only on artificial designer surfaces but even in a complex rather chaotic natural environment like the surface of human cells. These results are raising new fundamental questions in the glycosciences, and offer implications how cells interact with their environment and might facilitate the prevention of bacterial adhesion with temporal and spatial resolution.

To extend the field of "optoglycomics", multivalent, orthogonally modified photoresponsive azobenzene glycoconjugates with increased complexity and more sophisticated photoswitching functions are required. To facilitate orthogonality a dual approach can be utilized. One approach involves the introduction of diverse carbohydrates, whereas the other one involves the introduction of glycophotoswitches which can be addressed with different wavelengths. Consequently, the last chapter was focused on an orthogonal hetero-functionalization approach.
For this purpose a trifunctional mannoside-based scaffold molecule containing three orthogonally protected/masked amino functional groups was prepared. The introduction of the three orthogonal functionalities was achieved in a straightforward synthesis pathway without the requirement of a complex protecting group strategy. This trifunctional, carbohydrate-based scaffold molecule was further utilized for the synthesis of a novel type of a heterodivalent glycophotoswitch. The introduction of the two azobenzene units was achieved independently from the each other. Photochromic and kinetic properties of the switching behaviour of the heterodivalent glycocluster was investigated. The heterodivalent azobenzene glycocluster is a potent candidate to study photoswitchable cell adhesion, as the cluster exhibits favourable photochromic properties such as efficient switching of the two installed azobenzene units and long thermal relaxation times. Moreover, the kinetic studies revealed that the installed azobenzene units are electronically decoupled and switch independently. The prepared orthogonal trifunctional mannoside-based scaffold represents an excellent candidate to prepare orthogonal heteromultivalent azobenzene glycoclusters. It is possible to install up to three different glycoazobenzene "branches" with different characteristics in order to obtain orthogonal heteromultivalent azobenzene glycoclusters which can be addressed with different wavelengths.

Furthermore, divalent azobenzene heteroglycocluster can be immobilized at the aglyconic functionality on surfaces (cell, PS or glass) and utilized in cell adhesion studies about the influence of carbohydrate orientation. This remarkable newly introduced architecture allows for increased complexity and sophisticated photoswitching functions of photoswitchable glycoconjugates.

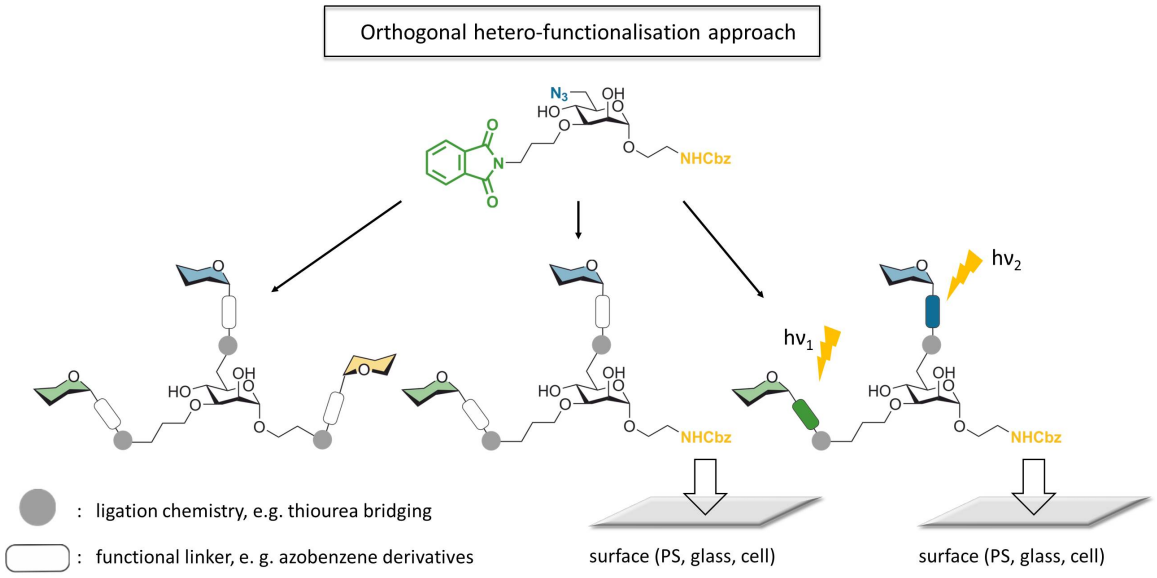

Figure 7.5. Illustration of the trifunctional mannoside-based scaffold molecule which allows for different functionalisation possibilities. The trifunctional scaffold molecule can be utilized to install up to three different azobenzene "branches"with different characteristics. Thus, orthogonal heteromultivalent azobenzene glycoclusters with sophisticated photoswitching functions can be obtained. Furthermore, heterodivalent azobenzene glycoclusters can be immobilized at the aglyconic functionality on various surfaces.

The results presented in this thesis have tremendously promoted the field of “optoglycomics”. New homo- and hetero-bifunctional glycoazobenzene derivatives have been prepared and first successful cross-linking of model peptides, improved water-solubility as well as suitable photochromic properties demonstrate clearly that these new bifunctional azobenzene glycoconjugates favourably supplement the known photoresponsive cross-linkers for the control of protein function. Photoresponsive glass surfaces were fabricated which significantly improve the investigation of photoswitchable cell adhesion on surfaces as the can be easily prepared and analysed with UV-vis spectroscopy. Furthermore, azobenzene mannosides were utilized to influence the adhesivity of *E. coli* bacteria to human cells. Upon irradiation with light, the adhesivity of the cell surface could be switched between adhesive and less adhesive. These astonishing results are now raising new interesting questions in the glycosciences. First steps towards the application of photoswitchable diagnostic tools have been made with the development of a bead-based kit to study bacterial adhesion of *E. coli* bacteria. To further elaborate photoswitching of carbohydrate recognition a hetero-functionalization approach based on a trifunctional glycoside core was established allowing for the synthesis of orthogonal heteromultivalent azobenzene glycoclusters which might be addresses with different wavelengths. The remarkable findings of this thesis may contribute to the development of novel targets as well

as new diagnostic tools for the investigation of bacterial adhesion. Furthermore, the results on the effect of carbohydrate orientation on artificial or even biological surfaces might implement new approaches for the investigation of complex carbohydrate-lectin interactions and will be topic of future research in the Lindhorst group.

8 Experimental section

8.1 Supporting Information on Chapter 3

8.1.1 Supporting information for the publication *Synthesis of Bifunctional Azobenzene Glycoconjugates for Cysteine-Based Photosensitive Cross-Linking with Bioactive Peptides*

Supporting Information

for

Synthesis of Bifunctional Azobenzene Glycoconjugates for Cysteine-Based Photosensitive Cross-Linking with Bioactive Peptides

A. Müller, H. Kobarg, V. Chandrasekaran, J. Gronow, F. D. Sönnichsen, T. K. Lindhorst

CHEMISTRY
A European Journal

Supporting Information

Synthesis of Bifunctional Azobenzene Glycoconjugates for Cysteine-Based Photosensitive Cross-Linking with Bioactive Peptides

Anne Müller, Hauke Kobarg, Vijayanand Chandrasekaran, Joana Gronow, Frank D. Sönnichsen,* and Thisbe K. Lindhorst*[a]

chem_201501571_sm_miscellaneous_information.pdf

List of contents

1. Synthesis of glycoconjugates

1,2,3,4-Tetra-*O*-acetyl-6-azido-6-deoxy-α,β-D-glucopyranose (5):[1] The glucose derivative **4** (13.1 g, 26.1 mmol) and sodium azide (3.60 g, 55.4 mmol) were dissolved in dry DMSO (110 mL) and heated to 50 °C for 4 h followed by stirring at room temperature overnight. Ice water (10 mL) was added followed by addition of ethyl acetate (100 mL). The phases were separated and the organic phase was washed with water (20 mL) and dried over Na_2SO_4. It was filtered and the filtrate was evaporated to dryness. Purification of the crude product by flash chromatography (ethyl acetate/cyclohexane, 1:1) gave the title compound **5** as a 3:1 α/β-mixture (according to ^{1}H NMR) as a colorless solid (7.12 g, 19.1 mmol, 78%). R_f = 0.27 (cyclohexane/ethyl acetate, 2:1); ^{1}H NMR of the α-anomer (500 MHz, $CDCl_3$, 300 K, TMS): δ = 6.36 (d, $^3J_{1,2}$ = 3.7 Hz, 1H, H-1), 5.47 (dd~t, $^3J_{3,4}$ = 10.0 Hz, $^3J_{4,5}$ = 10.0 Hz, 1H, H-4), 5.15-5.05 (m, 2H, H-2, H-3), 4.08 (ddd, $^3J_{5,6}$ = 3.0 Hz, $^3J_{5,6'}$ = 5.3 Hz, $^3J_{4,5}$ = 10.2 Hz, 1H, H-5), 3.34-3.14 (m, 2H, H-6, H-6'), 2.19, 2.06, 2.03, 2.02 (each s, each 3H, 4 $COCH_3$) ppm; ^{13}C NMR (125 MHz, $CDCl_3$ 300 K): δ = 170.1, 169.4, 169.2, 168.9 (4 *C*OCH_3), 88.7 (C-1), 70.9 (C-5), 70.1 (C-4), 69.2 (C-3), 69.0 (C-2), 50.7 (C-6), 20.7, 20.6 (4 CO*C*H_3) ppm.

2,3,4-Tri-*O*-acetyl-6-azido-6-deoxy-α,β-D-glucopyranose (6):[2] The azide **5** (433 mg, 1.16 mmol) and hydrazinium acetate (160 mg, 1.74 mmol) were dissolved in dry dimethylformamide (10 mL) and stirred at room temperature for 4 h. The reaction was quenched by addition of ethyl acetate (15 mL) and then dichloromethane (15 mL) was added. It was stirred at room temperature for 5 min. The organic phase was washed with aq. NaCl solution (5%, 15 mL) and dried over $MgSO_4$. It was filtered and the filtrate was evaporated to dryness. Purification of the crude product by flash chromatography (ethyl acetate/cyclohexane, 1:2→1:1) gave the title compound **6** as a 3:1 α/β-mixture (according to ^{1}H NMR) as a colorless oil (303 mg, 914 µmol, 79%). R_f = 0.23 (cyclohexane/ethyl acetate, 1:1); ^{1}H NMR of α-anomer (500 MHz, $CDCl_3$, 300 K, TMS): δ = 5.06-5.00 (m, 1H, H-3), 5.49 (d, $^3J_{1,2}$ = 3.6 Hz, 1H, H-1), 5.47 (dd~t, $^3J_{3,4}$ = 9.2 Hz, $^3J_{4,5}$ = 9.2 Hz, 1H, H-4), 4.91-4.87 (m, 1H, H-2), 4.24 (ddd, $^3J_{5,6}$ = 2.8 Hz, $^3J_{5,6'}$ = 5.6 Hz, $^3J_{4,5}$ = 9.2 Hz, 1H, H-5), 3.40-3.31 (m, 2H, H-6, H-6'), 2.09, 2.05, 2.02 (each s, each 3H, 3 $COCH_3$) ppm; ^{13}C NMR (125 MHz, $CDCl_3$ 300 K): δ = 170.2, 170.1, 168.7 (3 *C*OCH_3), 90.4 (C-1), 71.0 (C-2), 69.6 (C-3), 69.5 (C-4), 68.4 (C-5), 51.0 (C-6), 20.7, 20.6 (3 CO*C*H_3) ppm.

***O*-(2,3,4-Tri-*O*-acetyl-6-azido-6-deoxy-α-D-glucopyranosyl)-trichloroacetimidate (7):**[3] The glucose derivative **6** (250 mg, 755 µmol) was dissolved in dry dichloromethane (5 mL) and trichloroacetonitrile (908 µL, 9.06 mmol) and DBU (33.0 µL, 230 µmol) were added at 0 °C under N_2 atmosphere. The reaction mixture was stirred at room temperature for ~30 min, evaporated and the immediately subjected to flash column chromatography (cyclohexane/ethyl acetate, 7:3) to yield the mannosyl donor **7** as a colorless solid (293 mg, 618 µmol, 84%). R_f = 0.31 (cyclohexane/ethyl acetate, 4:1); ^{1}H NMR (500 MHz, $CDCl_3$, 300 K, TMS): δ = 8.70 (s, 1H, C(N*H*)CCl_3), 6.59 (d, $^3J_{1,2}$ = 3.7 Hz, 1H, H-1), 5.56 (m_c, H-3), 5.14-5.11 (m, 2H, H-2, H-4), 4.19 (ddd, $^3J_{4,5}$ = 10.2 Hz, $^3J_{5,6}$ = 5.5 Hz, $^3J_{5,6}$ = 2.7 Hz, 1H, H-5), 3.39 (dd, $^2J_{6,6'}$ = 13.5 Hz, $^3J_{5,6}$ = 2.7 Hz, 1H, H-6), 3.34 (dd, $^2J_{6,6'}$ = 13.6 Hz, $^3J_{5,6'}$ = 5.5 Hz, 1H, H-6'), 2.06, 2.04, 2.02 (each s, each 3H, 3$COCH_3$) ppm; ^{13}C NMR (125 MHz, $CDCl_3$) δ = 170.0, 169.8, 169.5 (3 *C*OCH_3), 160.7 (*C*(NH)CCl_3), 92.7 (C-1), 71.2 (C-5), 70.6 (C-3), 69.7 (C-2), 68.9 (C-4), 50.6 (C-6), 20.7, 20.6, 20.4 (3 CO*C*H_3) ppm; ESI-MS: *m/z* calcd for $C_{14}H_{17}Cl_3N_4O_8$: 497.02 $[M+Na]^+$; found 497.00.

***N*-Boc-amino-4-(allyloxy)benzene (12):** To a suspension of *N*-Boc-4-hydroxyaniline (**11**, 8.01 g, 28.3 mmol) and potassium carbonate (5.29 g, 38.3 mmol) in acetonitrile (350 mL) allyl bromide (3.30 mL, 38.3 mmol) was added. The reaction mixture was stirred for 3 h at 80 °C and for 16 h at room temperature. Ethyl acetate (350 mL) and water (300 mL) were added, the phases were separated and the organic phase was washed consecutively with water (2 × 350 mL) and saturated aq. NaCl solution (2 × 350 mL) and dried over $MgSO_4$. It was filtered and the filtrate concentrated under reduced pressure. Purification of the crude product by column chromatography (cyclohexane/ethyl acetate, 4:1) gave **12** as a colorless solid (8.28 g, 33.3 mmol, 87%). R_f = 0.64 (cyclohexane/ethyl acetate, 4:1); m.p. 76°C; ^{1}H NMR (600 MHz, $CDCl_3$, 298 K, TMS): δ = 7.26-7.24 (m, 2H, Ar-H_{meta}), 6.86-6.84 (m, 2H, Ar-H_{ortho}), 6.34 (s, 1H, NH), 6.04 (ddt, $^3J_{(CH=CH2,CH=CH')}$ = 17.2 Hz, $^3J_{(CH=CH2,CH=CH')}$ = 10.6 Hz, $^3J_{(OCH2,CH=CH2)}$ = 5.3 Hz, 1H, C*H*=CH_2), 5.44 (ddt~ddd, $^4J_{(OCH2,CH=CH)}$ = 1.4 Hz, $^3J_{(CH=CH2,CH=CH)}$ = 17.2 Hz, $^2J_{(CH=CH,CH=CH')}$ = 3.0 Hz 1H, CH=C*H*), 5.27 (ddt~ddd, $^4J_{(OCH2,CH=CH')}$ = 1.4 Hz, $^3J_{(CH=CH2,CH=CH')}$ = 10.6 Hz, $^2J_{(CH=CH,CH=CH')}$ = 3.0 Hz, 1H, CH=C*H'*), 4.50 (ddd~dt, $^4J_{(OCH2,CH=CH')}$ = 1.4 Hz, $^4J_{(OCH2,CH=CH)}$ = 1.4 Hz, $^3J_{(OCH2,CH=CH2)}$ = 5.3 Hz, 2H, OCH_2), 1.51 (s, 9H, $C(CH_3)_3$) ppm; ^{13}C NMR (150

MHz, $CDCl_3$, 298 K, TMS): δ=154.7 (C-Ar_{para}), 153.1 (C-=O), 133.4 (*C*H=CH_2), 131.6 (C-Ar_{ipso}), 120.5 (C-Ar_{meta}), 117.6 (CH=*C*H_2), 115.2 (C-Ar_{ortho}), 80.3 (*C*$(CH_3)_3$), 69.2 (O*C*H_2), 28.4 (C(*C*$H_3)_3$) ppm; IR (ATR): $\tilde{\nu}$ =3355, 2979, 1696, 1519, 1232, 1158, 998, 915, 822, 812 cm^{-1}; ESI-MS *m/z* calcd for $C_{14}H_{19}NO_3$: 248.1 $[M-H]^-$; found 248.1.

4-(Allyloxy)aniline·TFA (13): To a solution of **12** (3.74 g, 15.0 mmol) in dichloromethane (150 mL) trifluoroacetic acid (25 mL) was added. The reaction mixture was stirred for 30 min at room temperature and then the solvent was evaporated and the residue co-evaporated with toluene (10 mL) and dichloromethane (10 mL) to give **13** as a colorless solid (3.94 g, quant.). The TFA salt was used in the next step without further purification. R_f = 0.21 (dichloromethane/methanol, 10:1); m.p. 80°C; ^{1}H NMR (500 MHz, CD_3OD, 300 K): δ = 7.32-7.30 (m, 2H, Ar-H_{meta}), 7.11-7.97 (m, 2H, Ar-H_{ortho}), 6.08 (ddt, $^3J_{(CH=CH2,CH=CH)}$ = 17.3 Hz, $^3J_{(CH=CH2,CH=CH')}$ = 10.5 Hz, $^3J_{(OCH2,CH=CH2)}$ = 5.2 Hz, 1H, C*H*=CH_2), 5.43 (ddt~ddd, $^4J_{(OCH2,CH=CH)}$ = 1.6 Hz, $^3J_{(CH=CH2,CH=CH)}$ = 17.3 Hz, $^2J_{(CH=CH,CH=CH')}$ = 3.2 Hz 1H, CH=C*H*), 5.30 (ddt~ddd, $^4J_{(OCH2,CH=CH')}$ = 1.6 Hz, $^3J_{(CH=CH2,CH=CH')}$ = 10.5 Hz, $^2J_{(CH=CH,CH=CH')}$ = 3.2 Hz, 1H, CH=C*H'*), 4.62 (ddd~dt, $^4J_{(OCH2,CH=CH')}$ = 1.6 Hz, $^4J_{(OCH2,CH=CH)}$ = 1.6 Hz, $^3J_{(OCH2,CH=CH2)}$ = 5.2 Hz, 2H, OCH_2) ppm; ^{13}C NMR (150 MHz, $CDCl_3$, 298 K, TMS): δ = 160.1 (C-Ar_{para}), 134.4 (*C*H=CH_2), 125.1 (C-Ar_{ipso}), 124.9 (C-Ar_{meta}), 117.8 (CH=*C*H_2), 117.1 (C-Ar_{ortho}), 70.1 (O*C*H_2) ppm; IR (ATR): $\tilde{\nu}$ =3363, 3284, 2981, 1691, 1518, 1234, 1157, 1022, 811 cm^{-1}.

***(E)-p-*(*p'*-Allyloxy-phenylazo)phenol (14):** To a solution of 4-(allyloxy)aniline (**13**, 870 mg, 3.30 mmol) in water (10 mL) 37% hydrochloric acid (260 µL, 3.30 mmol) was added and the reaction mixture was cooled to 0 °C. Then an ice-cold solution of sodium nitrite (228 mg, 3.30 mmol) in water (10 mL) was added dropwise at 0 °C and the reaction mixture stirred for 2 h at 10 °C. This solution was added dropwise to a solution of phenol (311 mg, 3.30 mmol), sodium hydroxide (132 mg, 3.30 mmol) and sodium carbonate (368 mg, 3.30 mmol) in water (10 mL) at 10 °C. The reaction mixture was stirred for 1 h at 10 °C. The precipitated product was filtered and washed with water. Purification of the crude product by column chromatography (cyclohexane/ethyl acetate, 6:1→4:1) gave the azobenzene derivative **14** as an orange solid (664 mg, 2.61 mmol, 86%). R_f = 0.32 (cyclohexane/ethyl acetate, 4:1); m.p. 107 °C; ^{1}H NMR (600 MHz, $CDCl_3$, 298 K, TMS): δ = 7.88-7.82 (m, 4H, Ar-H_{ortho}, Ar-$H_{ortho'}$), 7.03-7.00 (m, 2H, Ar-$H_{meta'}$), 6.94-6.91 (m, 2H, Ar-H_{meta}), 6.08 (ddt, $^3J_{(CH=CH2,CH=CH)}$ = 17.1 Hz, $^3J_{(CH=CH2,CH=CH')}$ = 10.6 Hz, $^3J_{(OCH2,CH=CH2)}$ = 5.3 Hz, 1H, C*H*=CH_2), 5.51 (s, 1H, OH), 5.46-5.43 (m, 1H, CH=C*H*), 5.34-5.32 (m, 1H, CH=C*H'*), 4.62-4.61 (m, 2H, OCH_2) ppm; ^{13}C NMR (150 MHz, $CDCl_3$, 298 K, TMS): δ = 160.6 (C-$Ar_{para'}$), 157.9 (C-Ar_{para}), 147.2 (C-Ar_{ipso}), 147.0 (C-$Ar_{ipso'}$), 132.8 (*C*H=CH_2), 124.6 (C-Ar_{ortho}), 124.3 (C-$Ar_{ortho'}$), 118.1 (CH=*C*H_2), 118.1 (C-$Ar_{meta'}$), 115.0 (C-Ar_{meta}), 69.0 (OCH_2) ppm; IR (ATR): $\tilde{\nu}$ =3112, 1597, 1581, 1494, 1234, 1148, 995, 932, 840, 823 cm^{-1}; ESI-MS: *m/z* calcd for $C_{15}H_{14}N_2O_2$: 255.112 $[M+H]^+$; found 255.113.

(*E*)-*p,p'*-Di-(allyloxy)azobenzene (15):[4] To a solution of **14** (104 mg, 409 µmol) in acetonitrile (15 mL) potassium carbonate (57.0 mg, 409 µmol) and allyl bromide (40.0 µL, 409 µmol) were added. The reaction mixture was stirred for 3 h at 80 °C and 16 h at room temperature. Then ethyl acetate (15 mL) and water (7 mL) were added and the phases separated. The organic phase was washed with water (2 × 15 mL) and saturated aq. NaCl solution (2 × 15 mL). It was dried over $MgSO_4$, filtered and the filtrate was concentrated under reduced pressure. The crude product was recrystallized from acetonitrile to give **15** as a yellow solid (108 mg, 368 µmol, 90%). R_f = 0.64 (cyclohexane/ethyl acetate, 7:1); m.p. 152 °C; ^{1}H NMR (600 MHz, $CDCl_3$, 298 K, TMS): δ = 7.91-7.88 (m, 4H, Ar-H_{ortho}), 7.05-7.02 (m, 4H, Ar-H_{meta}), 6.14-6.07 (m, 2H, C*H*=CH_2), 5.49-5.46 (m, 2H, CH=C*H*), 5.36-5.34 (m, 2H, CH=C*H'*), 4.64-4.63 (m, 4H, OCH_2) ppm; ^{13}C NMR (150 MHz, $CDCl_3$, 298 K, TMS): δ =160.6 (C-Ar_{para}), 147.1 (C-Ar_{ipso}), 132.8 (*C*H=CH_2), 124.3 (C-Ar_{ortho}), 118.0 (CH=*C*H_2), 114.9 (C-Ar_{meta}), 69.0 (OCH_2) ppm; IR (ATR): $\tilde{\nu}$ =2919, 1594, 1579, 1494, 1229, 992, 940, 839 cm^{-1}; EI-MS: *m/z* (%): calcd for $C_{18}H_{18}N_2O_2$: 294.137 $[M]^+$; found 294.130 (100), 295.130 (19.5), 296.140 (1.8); elemental analysis calcd (%) $C_{18}H_{18}N_2O_2$ × 0.1 MeCN: C 73.43, H 6.17, N 9.55; found C 73.55, H 6.17, N 9.58.

***(E)-p-*(*p'*-Allyloxy-phenylazo)phenyl 2,3,4,6-tetra-*O*-acetyl-α-D-mannopyranoside (17):** To a solution of the mannosyl donor **16** (1.62 g, 3.28 mmol) and *p*-(*p'*-allyloxy-phenylazo)phenol (**14**, 834 mg, 3.28 mmol) in dry acetonitrile (34 mL) BF_3·Et_2O (600 µL, 4.92 mmol) was added under N_2 atmosphere at 0 °C. The reaction mixture was stirred at 0 °C for 30 min and for 16 h at room temperature. Then it was diluted with dichloromethane (70 mL) and washed with a saturated aq. $NaHCO_3$ solution (3 × 70 mL). The organic phase was dried over $MgSO_4$, it was filtered and the filtrate concentrated under reduced pressure. Purification of the crude product by column chromatography

(cyclohexane/ethyl acetate, 3:1 → 2:1) gave mannoside **17** as an orange solid (1.52 g, 2.60 mmol, 79%). R_f=0.38 (cyclohexane/ethyl acetate, 2:1); m.p. 52 °C; $[\alpha]_D^{23}$ = +72.3 (*c*=0.3 in CH_2Cl_2); ^{1}H NMR (500 MHz, $CDCl_3$, 300 K, TMS): δ = 7.90-7.86 (m, 4H, Ar-H_{ortho}, Ar-$H_{ortho'}$), 7.22-7.19 (m, 2H, Ar-$H_{meta'}$), 7.04-7.01 (m, 2H, Ar-H_{meta}), 6.08 (ddt, $^3J_{(CH=CH2,CH=CH)}$ = 17.3 Hz, $^3J_{(CH=CH2,CH=CH')}$ = 10.6 Hz, $^3J_{(OCH2,CH=CH2)}$ = 5.3 Hz, 1H, C*H*=CH$_2$), 5.61 (d, $^3J_{1,2}$ = 1.8 Hz, 1H, H-1), 5.58 (dd, $^3J_{3,4}$ = 10.0 Hz, $^3J_{2,3}$ = 3.5 Hz, 1H, H-3), 5.48 (dd, $^3J_{1,2}$ = 1.8 Hz, $^3J_{2,3}$ = 3.5 Hz, 1H, H-2) 5.45 (ddt~ddd, $^4J_{(OCH2,CH=CH)}$ = 1.5 Hz, $^3J_{(CH=CH2,CH=CH)}$ = 17.3 Hz, $^2J_{(CH=CH,CH=CH')}$ = 3.1 Hz, 1H, CH=C*H*), 5.38 (dd, $^3J_{3,4}$ = 10.0 Hz, $^3J_{4,5}$ = 10.1 Hz, 1H, H-4), 5.33 (ddt~qd, $^4J_{(OCH2,CH=CH')}$ = 1.5 Hz, $^3J_{(CH=CH2,CH=CH')}$ = 10.6 Hz, $^2J_{(CH=CH,CH=CH')}$ = 1.4 Hz, 1H, CH=C*H'*), 4.62 (ddd~dt, $^4J_{(OCH2,CH=CH')}$ = 1.5 Hz, $^4J_{(OCH2,CH=CH)}$ = 1.5 Hz, $^3J_{(OCH2,CH=CH2)}$ = 5.3 Hz, 2H, OCH$_2$), 4.30 (dd, $^3J_{5,6}$ = 5.5 Hz, $^2J_{6,6'}$ = 12.3 Hz, 1H, H-6), 4.12-4.07 (m, 2H, H-5, H-6'), 2.21, 2.06, 2.05, 2.03 (each s, each 3H, 4 COC*H*$_3$) ppm; ^{13}C NMR (125 MHz, $CDCl_3$, 300 K, TMS): δ = 170.5, 169.9, 169.9, 169.7 (*C*OCH$_3$), 160.9 (C-Ar$_{para'}$), 157.2 (C-Ar$_{para}$), 148.5 (C-Ar$_{ipso}$), 147.0 (C-Ar$_{ipso'}$), 132.8 (*C*H=CH$_2$), 124.6 (C-Ar$_{ortho}$), 124.2 (C-Ar$_{ortho'}$), 118.0 (CH=*C*H$_2$), 116.7 (C-Ar$_{meta'}$), 115.0 (C-Ar$_{meta}$), 95.7 (C-1), 69.4 (C-2), 69.3 (C-3), 69.0 (O*C*H$_2$), 68.8 (C-5), 62.1 (C-4), 62.1 (C-6), 20.9, 20.7 (4 CO*C*H$_3$) ppm; IR (ATR): $\tilde{\nu}$ = 2930, 1743, 1597, 1497, 1368, 1211, 1030, 983, 841 cm^{-1}; MALDI-TOF-MS: *m/z* calcd for $C_{29}H_{32}N_2O_{11}$: 585.21 [M+H]$^+$; found 585.42.

***(E)-p*-(*p'*-Allyloxy-phenylazo)phenyl α-D-mannopyranoside (18):** To a solution of the acetyl-protected mannoside **17** (1.50 g, 2.57 mmol) in methanol (50 mL) potassium carbonate (71.0 mg, 515 µmol) was added. The reaction mixture was stirred for 16 h at room temperature. The solvent was evaporated und the crude product was purified by flash column chromatography (dichloromethane/methanol, 10:1→9:1) to give mannoside **18** as an orange solid (1.02 g, 2.45 mmol, 95%). R_f=0.24 (dichloromethane/methanol, 10:1); m.p. 212 °C; $[\alpha]_D^{23}$ = +134.0 (*c*=0.2 in DMSO); ^{1}H NMR (500 MHz, DMSO-d_6, 300 K): δ = 7.85-7.81 (m, 4H, Ar-H_{ortho}, Ar-$H_{ortho'}$), 7.26-7.24 (m, 2H, Ar-$H_{meta'}$), 7.15-7.12 (m, 2H, Ar-H_{meta}), 6.08 (ddt, $^3J_{(CH=CH2,CH=CH)}$ = 17.3 Hz, $^3J_{(CH=CH2,CH=CH')}$ = 10.5 Hz, $^3J_{(OCH2,CH=CH2)}$ = 5.2 Hz, 1H, C*H*=CH$_2$), 5.61 (d, $^3J_{1,2}$ = 1.8 Hz, 1H, H-1), 5.44 (ddt~qd, $^4J_{(OCH2,CH=CH)}$ = 1.5 Hz, $^3J_{(CH=CH2,CH=CH)}$ = 17.3 Hz, $^2J_{(CH=CH,CH=CH')}$ = 1.7 Hz, 1H, CH=C*H*), 5.30 (ddt~ddd, $^4J_{(OCH2,CH=CH')}$ = 1.5 Hz, $^3J_{(CH=CH2,CH=CH')}$ = 10.5 Hz, $^2J_{(CH=CH,CH=CH')}$ = 1.7 Hz, 1H, CH=C*H'*), 5.09 (d, $^3J_{2,OH}$ = 2.4 Hz, 1H, 2-OH), 4.86 (d, $^3J_{3,OH}$ = 5.7 Hz, 1H, 3-OH), 4.78 (d, ^3J = 5.9 Hz, 1H, OH), 4.68 (ddd~dt, $^4J_{(OCH2,CH=CH')}$ = 1.5 Hz, $^4J_{(OCH2,CH=CH)}$ = 1.5 Hz, $^3J_{(OCH2,CH=CH2)}$ = 5.2 Hz, 2H, OCH$_2$), 4.53 (t, ^3J = 3.0 Hz, 1H, OH), 3.87 (br s~ddd, 1H, H-2), 3.71 (ddd, $^3J_{3,4}$ = 9.0 Hz, $^3J_{3,OH}$ = 5.5 Hz, $^3J_{2,3}$ = 3.5 Hz, 1H, H-3), 3.62 (m, 1H, H-6), 3.55-3.46 (m, 2H, H-4, H-6'), 3.42-3.39 (m, 1H, H-5) ppm; ^{13}C NMR (125 MHz, DMSO-d_6, 300 K): δ = 161.0 (C-Ar$_{para'}$), 158.9 (C-Ar$_{para}$), 147.4 (C-Ar$_{ipso}$), 146.7 (C-Ar$_{ipso'}$), 133.7 (*C*H=CH$_2$), 124.7 (C-Ar$_{ortho}$), 124.4 (C-Ar$_{ortho'}$), 118.3 (CH=*C*H$_2$), 117.6 (C-Ar$_{meta'}$), 115.7 (C-Ar$_{meta}$), 99.2 (C-1), 69.4 (C-2), 69.3 (C-3), 69.0 (O*C*H$_2$), 68.8 (C-5), 62.1 (C-4), 61.5 (C-6) ppm; IR (ATR): $\tilde{\nu}$ =3410, 3290, 2925, 1597, 1582, 1494, 1224, 1148, 1008, 972, 837 cm^{-1}; ESI-MS: *m/z* calcd for $C_{21}H_{24}N_2O_7$: 417.164 [M+H]$^+$; found 417.166 [M+H]$^+$.

***(E)-p*-(*p'*-Allyloxy-phenylazo)phenyl 3,4-*O*-(2',3'-dimethoxybutane-2',3'-diyle)-α-D-mannopyranoside (19):** To a solution of the mannoside **18** (388 mg, 932 µmol) in a mixture of dry DMSO and dry MeOH (1:1, 10 mL), 2,3-diketobutane (100 µL, 1.02 mmol) and trimethyl orthoformate (600µL, 5.59 mmol) were added. Then two drops of $BF_3 \cdot Et_2O$ were added under ice cooling. The reaction mixture was stirred for 4 d at room temperature. Then the solvent was evaporated and the residual filtered over a layer of silica gel (cyclohexane/ethyl acetate, 2:1 → 1:1). This procedure led to the protected title mannoside **19** (99.0 mg) in the form of an orange oil, that was carried on in the next step without further purification.

***(E)-p*-(*p'*-Allyloxy-phenylazo)phenyl 3,4-*O*-(2',3'-dimethoxybutane-2',3'-diyle)-6-*O*-*tert*-butyldimethylsilyl-α-D-mannopyranoside (20):** Mannoside **19** (99.0 mg) was dissolved in dry pyridine (5 mL) and a spatula tip of DMAP and TBDMS-Cl (34.0 mg, 224 µmol) were added under ice cooling. The reaction mixture was stirred for 15 min at 0 °C and for 16 h at room temperature. Then saturated aq. $NaHCO_3$ solution (10 mL) was added. The aqueous phase was extracted with dichloromethane (3 × 10 mL). The organic phases were combined and dried over $MgSO_4$. It was filtered and the filtrate concentrated under reduced pressure. The residual was filtered over a layer of silica gel (cyclohexane/ethyl acetate, 4:1) to give the title mannoside **20** (82.0 mg) as an orange oil crude that was used without further purification.

***(E)-p*-(*p'*-Allyloxy-phenylazo)phenyl 2-*O*-allyl-3,4-*O*-(2',3'-dimethoxybutane-2',3'-diyle)-6-*O*-*tert*-butyldimethylsilyl-α-D-mannopyranoside (21):** To a solution of **20** (72.0 mg) in dry DMF (5 mL) NaH

(60% dispersion in mineral oil, 5.00 mg, 123 µmol) was added under ice cooling. The reaction mixture was stirred for 30 min at 0 °C and then allyl bromide (30.0 µL, 336 µmol) was added. It was stirred for 16 h at room temperature, then ice water (20 mL) was added. The aqueous phase was extracted with dichloromethane (3 × 10 mL), the organic phases were combined and dried over $MgSO_4$. It was filtered and the filtrate concentrated under reduced pressure. The residual was filtered over a layer of silica gel (cyclohexane/ethyl acetate, 6:1) to give the title mannoside **21** (49.0 mg) as an orange oil crude that was used without further purification.

***(E)-p-(p'-*Allyloxy-phenylazo)phenyl 2-*O*-allyl-α-D-mannopyranoside (2) from 21:** To a solution of the mannoside **21** (45.0 mg) in dichloromethane (6 mL) trifluoroacetic acid (800 µL) was added. The reaction mixture was stirred for 45 min at room temperature and then the solvent was evaporated. Purification of the crude product by column chromatography (dichloromethane/methanol, 10:0.25 → 10:0.5) gave the target mannoside **2** as a yellow solid (20.0 mg, 44.8 µmol, ~5% over 4 steps from **18**); R_f = 0.62 (dichloromethane/methanol, 10:1). For analytical data see main manuscript.

***(E)-p-(p'-*Allyloxy-phenylazo)phenyl 4,6-*O*-benzylidene-α-D-mannopyranoside (22):** To a solution of the unprotected mannoside **18** (344 mg, 826 µmol) in dry dimethylformamide (15 mL) benzaldehyde dimethyl acetal (150 µL, 884 µmol) and $HBF_4 \cdot Et_2O$ (110 µL, 826 mmol) were added. The reaction mixture was stirred for 16 h at room temperature and then was quenched with triethylamine (120 µL, 826 µmol). The solvent was evaporated and purification of the crude product by column chromatography (cyclohexane/ethyl acetate, 2:1→1:1) gave the title mannoside **22** as a pale yellow solid (300 mg, 595 µmol, 72%). R_f = 0.15 (cyclohexane/ethyl acetate, 2:1); m.p. 203 °C; $[\alpha]_D^{23}$ = +226.7 (*c* = 0.4 in acetone); ^{1}H NMR (500 MHz, DMSO-d_6, 300 K): δ = 7.87-7.83 (m, 4H, Ar-H$_{ortho}$, Ar-H$_{ortho'}$), 7.46-7.44 (m, 2H, Ar-H$_{Benz}$), 7.38-7.36 (m, 3H, Ar-H$_{Benz}$), 7.28-7.25 (m, 2H, Ar-H$_{meta'}$), 7.15-7.12 (m, 2H, Ar-H$_{meta}$), 6.08 (ddt, $^3J_{(CH=CH2,CH=CH)}$ = 17.3 Hz, $^3J_{(CH=CH2,CH=CH')}$ = 10.5 Hz, $^3J_{(OCH2,CH=CH2)}$ = 5.2 Hz, 1H, C*H*=CH$_2$), 5.66 (d, $^3J_{1,2}$ = 1.1 Hz, 1H, H-1), 5.64 (s, 1H, CHPh), 5.48 (d, $^3J_{2,OH}$ = 4.3 Hz, 1H, 2-OH), 5.44 (ddt~ddd, $^4J_{(OCH2,CH)}$=C*H*=1.7 Hz, $^3J_{(CH=CH2,CH=CH)}$ = 17.3 Hz, $^2J_{(CH=CH,CH=CH')}$ = 3.4 Hz 1H, CH=C*H*), 5.30 (ddt~ddd, $^4J_{(OCH2,CH=CH')}$ = 1.7 Hz, $^3J_{(CH=CH2,CH=CH')}$ = 10.5 Hz, $^2J_{(CH=CH,CH=CH')}$ = 3.4 Hz, 1H, CH=C*H'*), 5.21 (d, $^3J_{3,OH}$ = 5.6 Hz, 1H, 3-OH), 4.69 (ddd~dt, $^4J_{(OCH2,CH=CH')}$ = 1.7 Hz, $^4J_{(OCH2,CH=CH)}$ = 1.7 Hz, $^3J_{(OCH2,CH=CH2)}$ = 5.2 Hz, 2H, OCH$_2$), 4.03 (dd, $^3J_{5,6}$ = 4.6 Hz, $^2J_{6,6'}$ = 9.9 Hz, 1H, H-6), 3.99-3.96 (m, 3H, H-2, H-3, H-4), 3.78-3.73 (m, 1H, H-6'), 3.71-3.66 (m, 1H, H-5) ppm; ^{13}C NMR (125 MHz, DMSO-d_6, 300 K): δ = 161.0 (C-Ar$_{para'}$), 158.1 (C-Ar$_{para}$), 147.7 (C-Ar$_{ipso}$), 146.7 (C-Ar$_{ipso'}$), 138.3 (C-Ar$_{Benz}$), 133.8 (*C*H=CH$_2$), 129.3 (C-Ar$_{Benz}$), 128.5 (C-Ar$_{Benz}$), 126.8 (C-Ar$_{Benz}$), 124.7 (C-Ar$_{ortho}$), 124.5 (C-Ar$_{ortho'}$), 118.3 (CH=*C*H$_2$), 117.5 (C- Ar$_{meta'}$), 115.7 (C-Ar$_{meta}$), 101.7 (*C*HPh), 99.3 (C-1), 78.6 (C-2), 70.9 (C-3), 69.0 (O*C*H$_2$), 68.2 (C-6), 67.8 (C-4), 65.5 (C-5) ppm; IR (ATR): $\tilde{\nu}$ = 3453, 2936, 1599, 1582, 1497, 1456, 1383, 1234, 1100, 1007, 986, 842 cm^{-1}; ESI-MS: *m/z* calcd for $C_{28}H_{28}N_2O_7$: 505.19 $[M+H]^+$; found 505.19.

***(E)-p-(p'-*Allyloxy-phenylazo)phenyl 4,6-*O*-benzylidene-3-*O*-(*p*-methoxybenzyl)-α-D-mannopyranoside (23):** A suspension of **22** (272 mg, 539 µmol) and dibutyltin oxide (174 mg, 70.1 µmol) in dry methanol (24 mL) was refluxed for 3 h. Then the solvent was evaporated and the crude product was dissolved in dry dimethylformamide (24 mL). TBAI (100 mg, 2.70 µmol) and *p*-methoxy benzylchloride (90.0 µL, 64.7 µmol) were added and the reaction mixture was stirred for 4 h at 60 °C and then for 16 h at room temperature. The reaction was quenched by addition of ethyl acetate (60 mL) and saturated aq. NH_4Cl solution (35 mL). The phases were separated and the organic phase was consecutively washed with saturated aq. NH_4Cl solution (2 × 35 mL) and saturated aq. NaCl solution (35 mL). It was dried over $MgSO_4$, filtered and the solvent was evaporated. Purification of the crude product by column chromatography (cyclohexane/ethyl acetate, 4:1→3:1) gave the title mannoside **23** as an orange solid (200 mg, 320 µmol, 60%). R_f = 0.44 (cyclohexane/ethyl acetate, 3:1); m.p. 105 °C; $[\alpha]_D^{23}$ = +184.2 (*c* = 0.7 in acetone); ^{1}H NMR (500 MHz, CD_3CN, 300 K): δ = 7.88-7.85 (m, 4H, Ar-H$_{ortho}$, Ar-H$_{ortho'}$), 7.48-7.46 (m, 2H, Ar-H$_{Benz}$), 7.41-7.38 (m, 3H, Ar-H$_{Benz}$), 7.35-7.33 (m, 2H, Ar-H$_{PMB}$), 7.24-7.22 (m, 2H, Ar-H$_{meta'}$), 7.10-7.07 (m, 2H, Ar-H$_{meta}$), 6.91-6.89 (m, 2H, Ar-H$_{PMB}$), 6.10 (ddt, $^3J_{(CH=CH2,CH=CH)}$ = 17.3 Hz, $^3J_{(CH=CH2,CH=CH')}$ = 10.7 Hz, $^3J_{(OCH2,CH=CH2)}$ = 5.3 Hz, 1H, C*H*=CH$_2$), 5.69 (d, $^3J_{1,2}$ = 1.5 Hz, 1H, H-1), 5.66 (s, 1H, CHPh), 5.45 (ddt, $^4J_{(OCH2,CH=CH)}$ = 1.7 Hz, $^3J_{(CH=CH2,CH=CH)}$ = 17.3 Hz, $^2J_{(CH=CH,CH=CH')}$ = 5.1 Hz 1H, CH=C*H*), 5.30 (ddt~qd, $^4J_{(OCH2,CH=CH')}$ = 1.7 Hz, $^3J_{(CH=CH2,CH=CH')}$ = 10.7 Hz, $^2J_{(CH=CH,CH=CH')}$ = 5.1 Hz, 1H, CH=C*H'*), 4.27-4.64 (m, 4H, OCH$_2$, CH$_2$Ph), 4.29-4.26 (m, 1H, H-2), 4.13 (dd~t, $^3J_{3,4}$ = 9.6 Hz, $^3J_{4,5}$ = 9.6 Hz, 1H, H-4), 4.08 (dd, $^3J_{5,6}$ = 4.5 Hz, $^2J_{6,6}$ = 9.9 Hz, 1H, H-6), 4.04 (dd, $^3J_{2,3}$ = 3.3 Hz, $^3J_{3,4}$ = 9.6 Hz, 1H, H-3), 3.85 (ddd~dt, $^3J_{4,5}$ = 9.6 Hz, $^3J_{5,6}$ = 4.5 Hz, $^3J_{5,6'}$ =

9.3 Hz, 1H, H-5); 3.81-3.77 (m, 1H, H-6'), 3.78 (s, 3H, OCH_3) ppm; ^{13}C NMR (150 MHz, CD_3CN, 298 K): δ = 161.9 (C-$Ar_{para'}$), 160.2 (C-Ar_{PMB}), 158.8 (C-Ar_{para}), 148.8 (C-Ar_{ipso}), 147.7 (C-$Ar_{ipso'}$), 138.9 (C-Ar_{Benz}), 134.1 (*C*H=CH_2), 131.5 (C-Ar_{PMB}), 130.3 (C-Ar_{PMB}), 129.8 (C-Ar_{Benz}), 129.0 (C-Ar_{Benz}), 127.0 (C-Ar_{Benz}), 125.2 (C-Ar_{ortho}), 124.9 (C-$Ar_{ortho'}$), 118.2 (CH=*C*H_2), 116.0 (C- $Ar_{meta'}$), 114.5 (C-Ar_{meta}), 102.3 (*C*HPh), 99.7 (C-1), 78.8 (C-4), 76.1 (C-3), 72.2 (*C*H_2Ph), 69.7 (O*C*H_2), 69.5 (C-2), 69.1 (C-6), 65.6 (C-5), 55.8 (O*C*H_3) ppm; IR (ATR): $\tilde{\nu}$ =3416, 2921, 1597, 1581, 1497, 1456, 1232, 1095, 997, 839 cm^{-1}; ESI-MS: *m/z* calcd for $C_{36}H_{36}N_2O_8$: 625.256 $[M+H]^+$; found 625.254.

***(E)-p-(p'*-Allyloxy-phenylazo)phenyl 2-*O*-allyl-4,6-*O*-benzylidene-3-*O*-(*p*-methoxybenzyl)-α-D-mannopyranoside (24):** To a solution of **23** (114 mg, 182 µmol) in dry dimethylformamide (8 mL) NaH (60% dispersion in mineral oil, 8.00 mg, 201 µmol) was added under ice cooling. The reaction mixture was stirred for 30 min at 0 °C and then allyl bromide (50.0 µL, 546 µmol) was added. It was stirred for 16 h at room temperature and then the solvent was evaporated. Purification of the crude product by column chromatography (cyclohexane/ethyl acetate, 4:1) gave the mannoside **24** as an orange solid (120 mg, 180 µmol, 99%). R_f = 0.67 (cyclohexane/ethyl acetate, 4:1); m.p.112 °C; $[\alpha]_D^{23}$ = +178.0 (*c* = 0.6 in CH_2Cl_2); ^1H NMR (500 MHz, CD_3CN, 300 K): δ = 7.89-7.86 (m, 4H, Ar-H_{ortho}, Ar-$H_{ortho'}$), 7.48-7.45 (m, 2H, Ar-H_{Benz}), 7.42-7.38 (m, 3H, Ar-H_{Benz}), 7.34-7.31 (m, 2H, Ar-H_{PMB}), 7.25-7.31 (m, 2H, Ar-$H_{meta'}$), 7.11-7.08 (m, 2H, Ar-H_{meta}), 6.92-6.89 (m, 2H, Ar-H_{PMB}), 6.11 (ddt, $^3J_{(CH=CH2,CH=CH)}$ = 17.3 Hz, $^3J_{(CH=CH2,CH=CH')}$ = 10.6 Hz, $^3J_{(OCH2,CH=CH2)}$ = 5.3 Hz, 1H, C*H*=CH_2(Phenyl)), 5.98 (ddt, $^3J_{(CH=CH2,CH=CH)}$ = 17.3 Hz, $^3J_{(CH=CH2,CH=CH')}$ = 10.5 Hz, $^3J_{(OCH2,CH=CH2)}$ = 5.6 Hz, 1H, C*H*=CH_2*Man*), 5.74 (d, $^3J_{1,2}$ = 1.8 Hz, 1H, H-1), 5.67 (s, 1H, CHPh), 5.45 (ddt~ddd, $^4J_{(OCH2,CH=CH)}$ = 1.7 Hz, $^3J_{(CH=CH2,CH=CH)}$ = 17.3 Hz, $^2J_{(CH=CH,CH=CH')}$ = 5.2 Hz 1H, CH=C*H*(Phenyl)), 5.36 (ddt~ddd, $^4J_{(OCH2,CH=CH)}$ = 1.9 Hz, $^3J_{(CH=CH2,CH=CH)}$ = 17.2 Hz, $^2J_{(CH=CH,CH=CH')}$ = 5.2 Hz 1H, CH=C*H*(Man)), 5.31 (ddt~ddd, $^4J_{(OCH2,CH=CH')}$ = 1.7 Hz, $^3J_{(CH=CH2,CH=CH')}$ = 10.6 Hz, $^2J_{(CH=CH,CH=CH')}$=5.2 Hz 1H, CH=C*H'*(Phenyl)), 5.22-5.19 (m, 1H, CH=C*H'*(Man)), 4.68 (s, 2H, CH_2Ph), 4.66 (ddd~dt, $^4J_{(OCH2,CH=CH')}$ = 1.7 Hz, $^4J_{(OCH2,CH=CH)}$ = 1.7 Hz, $^3J_{(OCH2,CH=CH2)}$=5.3 Hz, 2H, OCH_2(Phenyl)), 4.26-4.24 (m, 2H, OCH_2(Man)), 4.17-4.07 (m, 3H, H-3, H-5, H-6), 4.03 (dd, $^3J_{1,2}$ = 1.8 Hz, $^3J_{2,3}$ = 2.9 Hz, 1H, H-2), 3.86-3.76 (m, 2H, H-4, H-6'), 3.79 (s, 3H, OCH_3) ppm; ^{13}C NMR (125 MHz, CD_3CN, 300 K): δ =161.9 (C-$Ar_{para'}$), 160.2 (C-Ar_{para}), 158.8 (C-Ar_{PMB}), 148.9 (C-Ar_{ipso}), 147.8 (C-$Ar_{ipso'}$), 139.0 (C-Ar_{Benz}), 136.1 (*C*H=CH_2(Man)), 134.2 (CH=CH_2(Phenyl)), 131.7 (C-Ar_{PMB}), 130.3 (C-Ar_{PMB}), 129.8 (C-Ar_{Benz}), 129.1 (C-Ar_{Benz}), 127.1 (C-Ar_{Benz}), 125.2 (C-Ar_{ortho}), 124.9 (C-$Ar_{ortho'}$), 118.2 (CH=*C*H_2(Phenyl), CH=*C*H_2(Man)), 117.5 (C- $Ar_{meta'}$), 116.0 (C-Ar_{meta}), 114.5 (C-Ar_{PMB}), 102.3 (*C*HPh), 98.2 (C-1), 79.2 (C-3), 77.0 (C-2), 76.4 (C-5), 73.4 (O*C*H_2(Man)), 72.7 (*C*H_2Ph), 69.8 (O*C*H_2(Phenyl)), 69.1 (C-6), 66.0 (C-4), 55.8 (O*C*H_3) ppm; IR (ATR): $\tilde{\nu}$ =2917, 1597, 1581, 1496, 1456, 1232, 1095, 994, 840 cm^{-1}; MALDI-TOF-MS: *m/z* calcd for $C_{39}H_{40}N_2O_8$: 687.26 $[M+Na]^+$; found 687.40.

(*E*)-*p,p'*-Di-(4,6-*O*-benzylidene-α-D-mannopyranosyloxy)azobenzene (27): To a solution of the unprotected mannoside **26** (110 mg, 204 µmol) in dry dimethylformamide (4 mL) benzaldehyde dimethyl acetal (70.0 µL, 437 µmol) and $HBF_4 \cdot Et_2O$ (60.0 µL, 409 µmol) were added. The reaction mixture was stirred for 16 h at room temperature and then was quenched with triethylamine (60.0 µL, 409 µmol). The solvent was evaporated and purification of the crude product by column chromatography (dichloromethane/methanol, 10:0.5→10:1) gave the title mannoside **27** as a pale yellow solid (65.0 mg, 91.0 µmol, 45%). R_f = 0.20 (dichloromethane/methanol, 10:0.5); m.p. 252 °C; $[\alpha]_D^{23}$=+263.4 (*c*=0.4 in DMSO); ^1H NMR (500 MHz, DMSO-d_6, 300 K): δ = 7.89-7.86 (m, 4H, Ar-H_{ortho}), 7.46-7.44 (m, 4H, Ar-H_{Benz}), 7.38-7.35 (m, 6H, Ar-H_{Benz}), 7.29-7.26 (m, 4H, Ar-H_{meta}), 5.66 (d, $^3J_{1,2}$ = 1.6 Hz, 2H, H-1), 5.64 (s, 2H, CHPh), 5.49 (d, $^3J_{OH,H-2}$ = 4.2 Hz, 2H, 2-OH), 5.22-5.21 (m, 2H, 3-OH), 4.03 (dd, $^3J_{5,6}$ = 4.6 Hz, $^2J_{6,6'}$ = 9.8 Hz, 2H, H-6), 4.00-3.95 (m, 6H, H-2, H-3, H-4), 3.78-3.74 (m, 2H, H-6'), 3.71-3.66 (m, 2H, H-5) ppm; ^{13}C NMR (125 MHz, DMSO-d_6, 300 K): δ = 158.3 (C-Ar_{para}), 147.6 (C-Ar_{ipso}), 138.3 (C-Ar_{Benz}), 129.3 (C-Ar_{Benz}), 128.5 (C-Ar_{Benz}), 126.8 (C-Ar_{Benz}), 124.6 (C-Ar_{ortho}), 117.6 (C-Ar_{meta}), 101.7 (*C*HPh), 99.3 (C-1), 78.6 (C-2), 71.0 (C-3), 68.2 (C-6), 67.8 (C-4), 65.5 (C-5) ppm; IR (ATR): $\tilde{\nu}$ =3361, 1597, 1496, 1377, 1236, 1094, 990, 846 cm^{-1}; MALDI-TOF-MS: *m/z* calcd for $C_{38}H_{38}N_2O_{12}$: 737.23 $[M+Na]^+$; found 737.48.

***p*-Nitrophenyl 4,6-*O*-benzylidene-3-*O*-(*p*-methoxybenzyl)-α-D-mannopyranoside (31):** A suspension of **30** (994 mg, 2.55 mmol) and dibutyltin oxide (826 mg, 3.32 mmol) in dry methanol (48 mL) was refluxed for 2.5 h. Then the solvent was evaporated and the crude product was resolved in dry dimethylformamide (48 mL). TBAI (470 mg, 1.28 mmol) and *p*-methoxy benzylchloride (410 µL, 3.06, mmol) were added and the reaction mixture was stirred for 4 h at 70 °C and then for 16 h at

room temperature. The reaction was quenched by addition of ethyl acetate (150 mL) and saturated aq. NH_4Cl solution (150 mL). The organic phase was washed with saturated aq. NH_4Cl solution (2 × 100 mL) and saturated aq. NaCl solution (100 mL). It was dried over $MgSO_4$, filtered and the solvent was evaporated. Purification of the crude product by column chromatography (cyclohexane/ethyl acetate, 3:1→2:1) gave the mannoside **31** as a white solid (1.06 g, 2.09 mmol, 82%). R_f = 0.13 (cyclohexane/ethyl acetate, 3:1); m.p. 72 °C; $[\alpha]_D^{23}$ = +154.8 (*c*=0.2 in CH_2Cl_2); ^{1}H NMR (500 MHz, MeOH-d_4, 300 K): δ = 8.28-8.25 (m, 2H, Ar-H$_{meta}$), 7.51-7.49 (m, 2H, Ar-H$_{Benz}$), 7.41-7.35 (m, 5H, Ar-H$_{Benz}$, Ar-H$_{PMB}$), 7.29-7.25 (m, 2H, Ar-H$_{ortho}$), 6.92-6.89 (m, 2H, Ar-H$_{PMB}$), 5.74 (d, $^3J_{1,2}$ = 1.7 Hz, 1H, H-1), 5.68 (s, 1H, CHPh), 4.76 (s, 2H, CH_2Ph), 4.27 (dd, $^3J_{1,2}$ = 1.7 Hz, $^3J_{2,3}$ = 3.3 Hz, 1H, H-2), 4.27-4.23 (m, 1H, H-4), 4.11 (dd, $^3J_{5,6}$ = 4.6 Hz, $^2J_{6,6'}$=10.0 Hz, 1H, H-6), 4.06 (dd, $^3J_{2,3}$ = 3.3 Hz, $^3J_{3,4}$ = 9.9 Hz, 1H, H-3), 3.89-3.85 (m, 1H, H-6'), 3.81 (s, 3H, OCH_3), 3.81-3.77 (m, 2H, H-5, 2-OH); ^{13}C NMR (125 MHz, MeOH-d_4, 300 K): δ = 162.2 (C-Ar$_{ipso}$), 160.9 (C-Ar$_{PMB}$), 144.1 (C-Ar$_{para}$), 139.2 (C-Ar$_{Benz}$), 131.7 (C-Ar$_{PMB}$) 130.7 (C-Ar$_{PMB}$), 129.9 (C-Ar$_{Benz}$), 129.1 (C-Ar$_{Benz}$), 127.4 (C-Ar$_{Benz}$), 126.8 (C-Ar$_{meta}$), 117.7 (C-Ar$_{ortho}$), 114.7 (C-Ar$_{PMB}$), 103.1 (*C*HPh), 100.5 (C-1), 79.5 (C-4), 76.1 (C-3), 73.1 (*C*H_2Ph), 70.1 (C-2), 69.5 (C-6), 66.6 (C-5), 55.7 (O*C*H_3) ppm; IR (ATR): $\tilde{\nu}$ = 2921, 1611, 1593, 1513, 1342, 1245, 1096, 992, 751 cm^{-1}; ESI-MS: *m/z* calcd for $C_{27}H_{27}NO_9$: 532.156 [M+Na]$^+$; found 532.158.

***p*-Nitrophenyl 2-*O*-allyl-4,6-*O*-benzylidene-3-*O*-(*p*-methoxybenzyl)-α-D-mannopyranoside (32):** To a solution of **31** (249 mg, 489 µmol) in dry dimethylformamide (21 mL) NaH (60% dispersion in mineral oil, 21.0 mg, 538 µmol) was added under ice cooling. The reaction mixture was stirred for 30 min at 0 °C and then allyl bromide (130 µL, 538 µmol) was added. It was stirred for 16 h at room temperature then the solvent was evaporated. Purification of the crude product by column chromatography (cyclohexane/ethyl acetate, 4:1) gave mannoside **32** as a white hygroscopic foam (196 mg, 357 µmol, 73%). R_f = 0.41 (cyclohexane/ethyl acetate, 4:1); $[\alpha]_D^{20}$ = 133.2 (*c* = 0.6 in CH_2Cl_2); ^{1}H NMR (500 MHz, CD_3CN, 300 K): δ = 8.27-8.22 (m, 2H, Ar-H$_{meta}$), 7.50-7.47 (m, 2H, Ar-H$_{Benz}$), 7.44-7.40 (m, 3H, Ar-H$_{Benz}$,), 7.36-7.33 (m, 2H, Ar-H$_{PMB}$), 7.27-7.24 (m, 2H, Ar-H$_{ortho}$), 6.94-6.91 (m, 2H, Ar-H$_{PMB}$), 6.00 (ddt, $^3J_{(CH=CH2,CH=CH)}$=17.3 Hz, $^3J_{(CH=CH2,CH=CH')}$ = 10.5 Hz, $^3J_{(OCH2,CH=CH2)}$=5.6 Hz, 1H, C*H*=CH_2), 5.81 (d, $^3J_{1,2}$=1.8 Hz, 1H, H-1), 5.69 (s, 1H, CHPh), 5.37 (ddt~ddd, $^4J_{(OCH2,CH=CH)}$= 1.7 Hz, $^3J_{(CH=CH2,CH=CH)}$ = 17.3 Hz, $^2J_{(CH=CH,CH=CH')}$ = 3.5 Hz 1H, CH=C*H*), 5.24-5.21(m, 1H, CH=C*H'*) 4.70 (s, 2H, CH_2Ph), 4.30-4.23 (m, 2H, OCH_2), 4.19-4.07 (m, 3H, H-3, H-4, H-6), 4.04 (dd, $^3J_{1,2}$ = 1.8 Hz, $^3J_{2,3}$=3.1 Hz, 1H, H-2), 3.83-3.76 (m, 5H, H-5, H-6', OCH_3) ppm; ^{13}C NMR (125 MHz, CD_3CN, 300 K): δ = 161.8 (C-Ar$_{ipso}$), 160.2 (C-Ar$_{PMB}$), 143.6 (C-Ar$_{para}$), 138.9 (C-Ar$_{Benz}$), 131.6 (C-Ar$_{PMB}$) 130.3 (C-Ar$_{PMB}$), 129.8 (C-Ar$_{Benz}$), 129.1 (C-Ar$_{Benz}$), 127.1 (C-Ar$_{Benz}$), 126.6 (C-Ar$_{meta}$), 117.7 (C-Ar$_{ortho}$), 114.5 (C-Ar$_{PMB}$), 102.3 (*C*HPh), 98.1 (C-1), 79.0 (C-4), 76.7 (C-2), 76.2 (C-3), 73.5 (O*C*H_2), 72.7 (*C*H_2PH), 69.0 (C-6), 66.2 (C-5), 55.8 (O*C*H_3) ppm; IR (ATR): $\tilde{\nu}$ =2918, 1611, 1592, 1512, 1342, 1242, 1096, 984, 750 cm^{-1}; ESI-MS *m/z* Calcd for $C_{30}H_{31}NO_9$: 572.191 [M+Na]$^+$; found 572.189.

(*E*)-*p,p'*-Di-[2-*O*-allyl-4,6-*O*-benzylidene-3-*O*-(*p*-methoxybenzyl)-α-D-mannopyranosyloxy]azobenzene (33): To a suspension of $LiAlH_4$ (10.0 mg, 195 µmol) in dry THF (1 mL) a solution of mannoside **32** (107 mg, 195 µmol) in dry THF (2 mL) was added dropwise. The reaction mixture was stirred for 16 h at room temperature and then water was added under ice cooling. The solution was extracted with dichloromethane (2 × 5 mL) and the combined organic phases were washed with saturated aq. NaCl solution (5 mL) and dried over $MgSO_4$. It was filtered and the solvent evaporated. Purification of the crude product by column chromatography (cyclohexane/ethyl acetate, 4:1) gave the title mannoside **33** as an orange solid (61.0 mg, 58.9 µmol, 60%). R_f = 0.47 (cyclohexane/ethyl acetate, 4:1); m.p. 82 °C; $[\alpha]_D^{23}$ = +189.4 (*c* = 0.2 in CH_2Cl_2); ^{1}H NMR (600 MHz, CD_3CN, 298 K): δ = 7.90-7.88 (m, 4H, Ar-H$_{ortho}$), 7.48-7.47 (m, 4H, Ar-H$_{Benz}$), 7.42-7.38 (m, 6H, Ar-H$_{Benz}$), 7.34-7.32 (m, 4H, Ar-H$_{PMB}$), 7.26-7.23 (m, 4H, Ar-H$_{meta}$), 6.92-7.89 (m, 4H, Ar-H$_{PMB}$), 6.02-5.95 (m, 2H, C*H*=CH_2), 5.75 (d, $^3J_{1,2}$ = 1.7 Hz, 2H, H-1), 5.67 (s, 2H, CHPh), 5.36 (ddt~ddd, $^4J_{(OCH2CH,CH=CH)}$ = 1.6 Hz, $^3J_{(CH=CH2,CH=CH)}$ = 17.3 Hz, $^2J_{(CH=CH,CH=CH')}$ = 3.4 Hz 2H, CH=C*H*), 5.22-5.20 (m, 2H, CH=C*H'*), 4.68 (s, 4H, CH_2Ph), 4.28-4.22 (m, 4H, OCH_2CH), 4.17-4.06 (m, 6H, H-3, H-5, H-6), 4.03 (dd, $^3J_{1,2}$=1.7 Hz, $^3J_{2,3}$ = 2.9 Hz, 2H, H-2), 3.85-3.79 (m, 4H, H-4, H-6'), 3.79 (s, 6H, OCH_3) ppm; ^{13}C NMR (125 MHz, CD_3CN, 298 K): δ = 160.2 (C-Ar$_{para}$), 159.0 (C-Ar$_{PMB}$), 148.8 (C-Ar$_{ipso}$), 138.9 (C-Ar$_{Benz}$), 136.0 (*C*H=CH_2), 131.6 (C-Ar$_{PMB}$) 130.3 (C-Ar$_{PMB}$), 129.8 (C-Ar$_{Benz}$), 129.1 (C-Ar$_{Benz}$), 127.1 (C-Ar$_{Benz}$), 125.0 (C-Ar$_{ortho}$), 117.5 (CH=*C*H_2), 118.2 (C-Ar$_{meta}$), 114.5 (C-Ar$_{PMB}$), 102.3 (*C*HPh), 98.1 (C-1), 79.2 (C-3), 76.9 (C-2), 76.3 (C-5), 73.4 (O*C*H_2CH), 72.7 (*C*H_2Ph), 69.1 (C-6), 66.0 (C-4), 55.8 (OCH_3) ppm; IR (ATR): $\tilde{\nu}$ = 2921, 1597, 1513, 1372, 1237, 1095, 993, 817 cm^{-1}; MALDI-TOF-MS: *m/z* calcd for $C_{60}H_{62}N_2O_{14}$: 1057.41 [M+Na]$^+$; found 1057.69.

(*E*)-*p,p'*-Di-(*N*-tert-butoxycarbonyl-6-amino-4-thiahexyloxy)azobenzene (36): A solution of **15** (22.0 mg, 74.7 µmol) and **35** (106 mg, 598 µmol) in a 1:1-mixture of dry methanol and dry dioxane (2 mL) was heated to 60 °C and then a spatula tip of AIBN was added. The reaction mixture was stirred at 60 °C for 4 h and then at room temperature for 16 h. The solvent was evaporated and the residual purified by column chromatography (toluene/ethyl acetate, 3:1) to give the title mannoside **36** as an orange solid (35.0 mg, 53.9 µmol, 72%). R_f = 0.19 (cyclohexane/ethyl acetate, 3:1); m.p. 122 °C; ^{1}H NMR (500 MHz, $CDCl_3$, 300 K, TMS): δ = 7.88-7.85 (m, 4H, Ar-H_{ortho}), 7.01-6.98 (m, 4H, Ar-H_{meta}), 4.90 (br s, 2H, NH), 4.14 (t, $^3J_{(OCH2,OCH2CH2)}$ = 6.4 Hz, 4H, OCH_2), 3.37-3.31 (m, 4H, CH_2NH), 2.75 (t, $^3J_{(OCH2CH2CH2,OCH2CH2)}$ = 6.4 Hz, 4H, $OCH_2CH_2CH_2$), 2.68 (t, $^3J_{(CH2NH, SCH2CH2NH)}$ = 6.5 Hz, 4H, SCH_2 CH_2NH), 2.10 (quint, $^3J_{(OCH2CH2CH2,OCH2CH2)}$ = 6.4 Hz, $^3J_{(OCH2,OCH2CH2)}$ = 6.4 Hz, 4H, OCH_2CH_2) 1.45 (s, 18H, $C(CH_3)_3$) ppm; ^{13}C NMR (125 MHz, $CDCl_3$, 300 K, TMS): δ = 160.8 (C-Ar_{para}), 155.8 (C=O), 147.1 (C-Ar_{ipso},), 124.4 (C-Ar_{ortho}), 114.7 (C-Ar_{meta}), 79.5 ($C(CH_3)_3$), 66.4 (OCH_2), 39.7 (CH_2NH), 32.4 (SCH_2CH_2NH), 29.2 (OCH_2CH_2), 28.4 ($C(CH_3)_3$), 28.2 ($OCH_2CH_2CH_2$) ppm; IR (ATR): $\tilde{\nu}$ =3324, 1699, 1653, 1498, 1160, 1054 cm^{-1}; IR (ATR): $\tilde{\nu}$ =3367, 2922, 1678, 1594, 1505, 1463, 125, 954, 843, cm^{-1}; HRMS (EI, 70 eV): *m/z* calcd for $C_{32}H_{48}N_4O_6S_2$: 648.3015 [M]$^+$; found 648.3015.

(*E*)-*p*-[*p'*-(*N*-tert-butoxycarbonyl-6-amino-4-thiahexyloxy)-phenylazo)phenyl] 2-*O*-(*N*-*tert*-butoxycarbonyl-6-amino-4-thiahexyl)-α-D-mannopyranoside (37): A solution of **2** (19.0 mg, 41.6 µmol) and **35** (59.0 mg, 333 µmol) in a 1:1-mixture of dry methanol and dry dioxane (2 mL) was heated to 60 °C and then a spatula tip of AIBN was added. The reaction mixture was stirred at 60 °C for 4 h. Then the solvent was evaporated and the residual purified by column chromatography (dichloromethane/methanol, 10:0.5) to give the title mannoside **37** as an orange oil (28.0 mg, 34.6 µmol, 83%). R_f = 0.33 (dichloromethane/methanol, 10:1); $[\alpha]_D^{23}$=+52.6 (*c*=0.6 in MeOH), ^{1}H NMR (500 MHz, CD_3OD, 300 K): δ = 7.88-7.83 (m, 4H, Ar-H_{ortho}), 7.29-7.26 (m, 2H, Ar-H_{meta}), 7.08-7.05 (m, 2H, Ar-$H_{meta'}$), 5.73 (d, $^3J_{1,2}$ = 1.5 Hz, 1H, H-1), 4.18 (t, $^3J_{(ArOCH2,ArOCH2CH2)}$ = 6.1 Hz, 2H, $ArOCH_2$), 3.97 (dd, $^3J_{2,3}$ = 3.5 Hz, $^3J_{3,4}$ = 9.5 Hz, 1H, H-3), 3.83-3.66 (m, 6H, ManOCH, ManOCH', H-2, H-4, H-6, H-6'), 3.57 (ddd, $^3J_{4,5}$ = 8.0 Hz, ^3J5,6 = 2.5 Hz, $^3J_{5,6'}$ = 5.6 Hz, 1H, H-5), 3.23 (t, $^3J_{(CH2NH,SCH2CH2NH)}$ = 7.0 Hz, 4H, CH_2NH), 2.76 (t, $^3J_{(ArOCH2CH2CH2,ArOCH2CH2)}$ = 7.2 Hz, 2H, $ArOCH_2CH_2CH_2$), 2.71 (t, $^3J_{(ManOCH2CH2CH2,ManOCH2CH2)}$ = 7.2 Hz, 2H, $ManOCH_2CH_2CH_2$), 2.66-2.60 (m, 4H, CH_2CH_2NH), 2.11-2.06 (m, 2H, $ArOCH_2CH_2$), 1.98-1.82 (m, 2H, $ManOCH_2CH'$, $ManOCH_2CH$), 1.43 (s, 18H, $C(CH_3)_3$) ppm; ^{13}C NMR (125 MHz, CD_3OD, 300 K): δ = 162.0 (C-$Ar_{para'}$), 159.9 (C-Ar_{para}), 149.3 (C-Ar_{ipso}), 148.3 (C-$Ar_{ipso'}$), 158.4 (C=O), 125.5 (C-Ar_{ortho}), 125.1 (C-$Ar_{ortho'}$), 118.1 (C- $Ar_{meta'}$), 115.9 (C-Ar_{meta}), 97.6 (C-1), 80.2 (C-2), 75.7 (C-5), 72.3 (C-3), 70.9 ($ManOCH_2$), 68.7 (C-4), 67.8 ($ArOCH_2$), 62.7 (C-6), 41.4 (CH_2NH), 32.7, 32.6 (SCH_2CH_2NH), 31.0 ($ManOCH_2CH_2$), 30.4 ($ArOCH_2CH_2$), 29.2 ($ManOCH_2CH_2CH_2$), 29.1 ($ArOCH_2CH_2CH_2$), 28.8 ($C(CH_3)_3$) ppm; IR (ATR): $\tilde{\nu}$ =3356, 2975, 1686, 1499, 1365, 1235, 1163, 999, 843 cm^{-1}; ESI-MS: *m/z* calcd for $C_{38}H_{58}N_4O_{11}S_2$: 833.3 [M+Na]$^+$; found 833.4.

(*E*)-*p,p'*-Di-[2-*O*-(*N*-*tert*-butoxycarbonyl-6-amino-4-thiahexyl)-α-D-mannopyranosyloxy]azobenzene (38): A solution of **3** (7.00 mg, 11.3 µmol) and **35** (16.0 mg, 90.5 µmol) in a 1:1-mixture of dry methanol and dry dioxane (2 mL) was heated to 60 °C and then a spatula tip of AIBN was added. The reaction mixture was stirred at 60 °C for 4 h. Then the solvent was evaporated and the residual purified by column chromatography (dichloromethane/methanol, 10:1) to give the title mannoside **38** as yellow solid (10.0 mg, 10.3 µmol, 91%). R_f = 0.38 (dichloromethane/methanol, 10:1); m.p. 252 °C; $[\alpha]_D^{23}$=+72.8 (*c*=0.5 in MeOH), ^{1}H NMR (600 MHz, CD_3OD, 300 K): δ = 7.88-7.84 (m, 4H, Ar-H_{ortho}), 7.30-7.26 (m, 4H, Ar-H_{meta}), 5.73 (d~s, 2H, H-1), 3.97 (dd, $^3J_{2,3}$ = 3.4 Hz, $^3J_{3,4}$ = 9.5 Hz, 2H, H-3), 3.83-3.68 (m, 12H, ManOCH, ManOCH', H-2, H-4, H-6, H-6'), 3.58-3.55 (m, 2H, H-5), 3.23 (t, $^3J_{(CH2NH,SCH2CH2NH)}$ = 7.0 Hz, 4H, CH_2NH), 2.71 (t, $^3J_{(ManOCH2CH2CH2,ManOCH2CH2)}$ = 7.1 Hz, 4H, $ManOCH_2CH_2CH_2$), 2.62 (t, $^3J_{(CH2NH,SCH2CH2NH)}$ = 7.0 Hz, 4H, CH_2CH_2NH), 1.97-1.83 (m, 4H, $ManOCH_2CH'$, $ManOCH_2CH$), 1.43 (s, 18H, $C(CH_3)_3$) ppm; ^{13}C NMR (151 MHz, CD_3OD, 300 K): δ = 160.1 (C-Ar_{para}), 158.4 (C=O), 149.3 (C-Ar_{ipso}), 125.3 (C-Ar_{ortho}), 118.1 (C- Ar_{meta}), 97.6 (C-1), 80.2 (C-2), 75.8 (C-5), 72.3 (C-3), 70.9 ($ManOCH_2$), 68.7 (C-4), 62.7 (C-6), 41.4 (CH_2NH), 32.6 (SCH_2CH_2NH), 31.0 ($ManOCH_2CH_2$), 29.2 ($ManOCH_2CH_2CH_2$), 28.8 ($C(CH_3)_3$) ppm; IR (ATR): $\tilde{\nu}$ =3361, 2925, 1688, 1597, 1496, 1366, 1233, 1107, 997, 844 cm^{-1}; ESI-MS: *m/z* calcd for $C_{44}H_{68}N_4O_{16}S_2$: 995.4 [M+Na]$^+$; found 995.2.

(*E*)-*p,p'*-Di-{6-[2-(*N*-Boc-cysteinyl ethyl ester)acetylamido]-6-deoxy-β-D-glucopyranosyloxy}azobenzene (40): To a solution of **1** (6.00 mg, 8.70 µmol) and the cysteine

derivative **39** (4.50 mg, 17.4 µmol) in dry dimethylformamide (1 mL) one drop of triethylamine was added. The reaction mixture was stirred for 16 h at room temperature and then the solvent was evaporated. Purification of the crude product by column chromatography (dichloromethane/methanol, 7:1) gave **40** as a pale yellow solid (7.50 mg, 6.55 µmol, 75%). R_f = 0.25 (dichloromethane/methanol, 7:1); m.p. 125 °C; $[\alpha]_D^{23}$=-67.5 (*c*=0.2 in MeOH); ^{1}H NMR (500 MHz, CD_3OD, 300 K): δ = 7.90-7.87 (m, 4H, Ar-H_{ortho}), 7.23-7.20 (m, 4H, Ar-H_{meta}), 5.06-5.01 (m, 2H, H-1), 4.34 (dd, $^3J_{(CH\text{NHBoc,SCH})}$ = 5.1 Hz, $^3J_{(CH\text{NHBoc,SCH'})}$ = 8.0 Hz, 2H, C*H*NHBoc), 4.15 (q, $^3J_{(CH_2\text{CH3,CH2C}H_3)}$ = 7.1 Hz, 4H, CH_2CH$_3$), 3.76 (dd, $^3J_{5,6}$ = 2.7 Hz, $^2J_{6,6'}$ = 14.1 Hz, 2H, H-6), 3.60 (ddd, $^3J_{4,5}$ = 9.9 Hz, $^3J_{5,6}$ = 2.7 Hz, $^3J_{5,6'}$ = 7.2 Hz, 2H, H-5), 3.53-3.48 (m, 4H, H-2, H-3), 3.43 (dd, $^3J_{5,6'}$ = 7.2 Hz, $^2J_{6,6'}$ = 14.1 Hz, 2H, H-6'), 3.39-3.23 (m, 6H, H-4, CH_2S), 3.06 (dd, $^3J_{(CH\text{NHBoc,SCH})}$ = 5.1 Hz, $^2J_{(\text{SCH,SCH'})}$ = 13.8 Hz, 2H, SCH), 2.91 (dd, $^3J_{(CH\text{NHBoc,SCH'})}$ = 8.0 Hz, $^2J_{(\text{SCH,SCH'})}$ = 13.8 Hz, 2H, SCH'), 1.41 (s, 18H, C(CH_3)$_3$), 1.23 (t, $^3J_{(CH_2\text{CH3,CH2C}H_3)}$ = 7.1 Hz, 6H, CH_2CH_3) ppm; ^{13}C NMR (125 MHz, MeOH-d_4, 300 K): δ = 172.6 (*C*OCH$_2$S,*C*OOEt), 161.0 (C-Ar$_{para}$), 157.8 (*C*=O$_{Boc}$), 149.3 (C-Ar$_{ipso}$,), 125.3 (C-Ar$_{ortho}$), 118.0 (C-Ar$_{meta}$), 101.8 (C-1), 80.8 (*C*(CH_3)$_3$), 77.4 (C-5), 76.0 (C-3), 74.9 (C-2), 73.0 (C-4), 62.6 (*C*H$_2$CH$_3$), 55.1 (*C*HNHBoc), 41.9 (C-6), 36.4 (*C*H$_2$S), 35.4 (S*C*H$_2$), 28.7 (C(*C*H$_3$)$_3$), 14.5 (CH$_2$*C*H$_3$) ppm; IR (ATR): $\tilde{\nu}$ =3324, 1699, 1653, 1498, 1160, 1054 cm^{-1}; MALDI-TOF-MS: *m/z* calcd for $C_{48}H_{70}N_6O_{20}S_2$: 1137.40 [M+Na]$^+$; found 1137.77.

Glutathione glycoconjugate (42): To a solution of glutathione (**41**, 44.0 mg, 145 µmol) in water (2 mL), **2** (11.0 mg, 42.1 µmol) and 2,2-dimethoxy-2-phenyl-acetophenone (3.70 mg, 14.5 µmol), dissolved in dimethylsulfoxide (1 mL), were added. The reaction mixture was degassed under vacuum and saturated with nitrogen. The mixture was irradiated at 365 nm at room temperature for 1 h and then concentrated. Purification of the crude product by C18 reverse phase column chromatography (water/acetonitrile, 4:1) gave **42** as a pale yellow solid (18.1 mg, 16.9 µmol, 70%). R_f = 0.35 (water/acetonitrile, 4:1); m.p. 230-245 °C$_{decomp}$; $[\alpha]_D^{23}$=-1.33 (*c*=0.6 in H_2O); ^{1}H NMR (500 MHz, D_2O, 300 K): δ = 7.66-7.63 (m, 4H, Ar-H_{ortho}), 7.16-7.14 (m, 2H, Ar-H_{meta}), 6.94-6.92 (m, 2H, Ar-$H_{meta'}$), 5.67 (d~s, 1H, H-1), 4.54-4.50 (m, 2H, SCH$_2$C*H*NH), 4.03-4.01 (m, 3H, H-3, ArOCH$_2$), 3.80-3.58 (m, 16H, H-2, H-4, H-5, H-6, H-6', NH$_2$C*H*COOH, NHCH_2COOH, ManOCH', ManOCH), 3.05-2.99 (m, 2H, SC*H*'CHNH), 2.84-2.78 (m, 2H, SC*H*CHNH), 2.66-2.58 (m, 4H, ArOCH$_2$CH$_2$CH_2, ManOCH$_2$CH$_2$CH_2), 2.49-2.45 (m, 4H, NHCOCH_2), 2.12-2.07 (m, 4H, NHCOCH$_2$CH_2), 1.97-1.94 (m, 2H, ArOCH$_2$CH_2), 1.87-1.80 (m, 2H, ManOCH$_2$CH_2) ppm; ^{13}C NMR (150 MHz, D_2O, 300 K): δ = 176.0, 174.8 (COOH), 173.9, 171.9 (C=O), 160.9 (C-Ar$_{para'}$), 159.7 (C-Ar$_{para}$), 147.4 (C-Ar$_{ipso}$), 146.3 (C-Ar$_{ipso'}$), 124.4 (C-Ar$_{ortho}$), 124.0 (C-Ar$_{ortho'}$), 117.2 (C- Ar$_{meta'}$), 115.2 (C-Ar$_{meta}$), 95.6 (C-1), 78.2 (C-2), 73.5 (C-5), 70.3 (C-3), 70.2 (ManOCH$_2$), 66.9 (ArOCH$_2$), 66.8 (C-4), 60.6 (C-6), 54.1 (NH$_2$*C*HCOOH) 53.1 (SCH$_2$*C*HNH), 43.3 (NH*C*H$_2$COOH), 32.9 (S*C*H$_2$CHNH), 31.4 (NHCO*C*H$_2$), 28.8 (ManOCH$_2$*C*H$_2$), 28.3 (ArOCH$_2$CH_2), 28.1 (ManOCH$_2$CH$_2$*C*H$_2$) 28.0 (ArOCH$_2$CH$_2$*C*H$_2$), 26.2 (NHCOCH$_2$*C*H$_2$) ppm; IR (ATR): $\tilde{\nu}$ =3276, 2931, 1638, 1595, 1581, 1498, 1392, 1234, 1106, 999, 838 cm^{-1}; MALDI-TOF-MS: *m/z* calcd for $C_{44}H_{62}N_8O_{19}S_2$: 1093.3 [M+Na]$^+$; found 1093.5.

Synthesis of cross-linked peptide 44: To a solution of the peptide **43** (750 µg, 0.400 µmol) in 0.1 mM NH_4HCO_3 buffer (pH = 8.5, 500 µL) TCEP was added and stirred for 1 h at room temperature to ensure a complete reduction of the sulfhydryl groups. Then **1** (1.00 mg, 1.45 µmol), dissolved in a dimethylsulfoxide/water mixture (1:1 v/v, 500 µL), was added to the peptide solution. To the reaction mixture a catalytic amount of tetrabutylammonium iodide was added and it was stirred for 24 h at room temperature in the dark. The crude reaction mixture was then analyzed by mass spectrometry (cf. Figs S58 and S59).

2. ^{1}H and ^{13}C NMR spectra of synthetic compounds

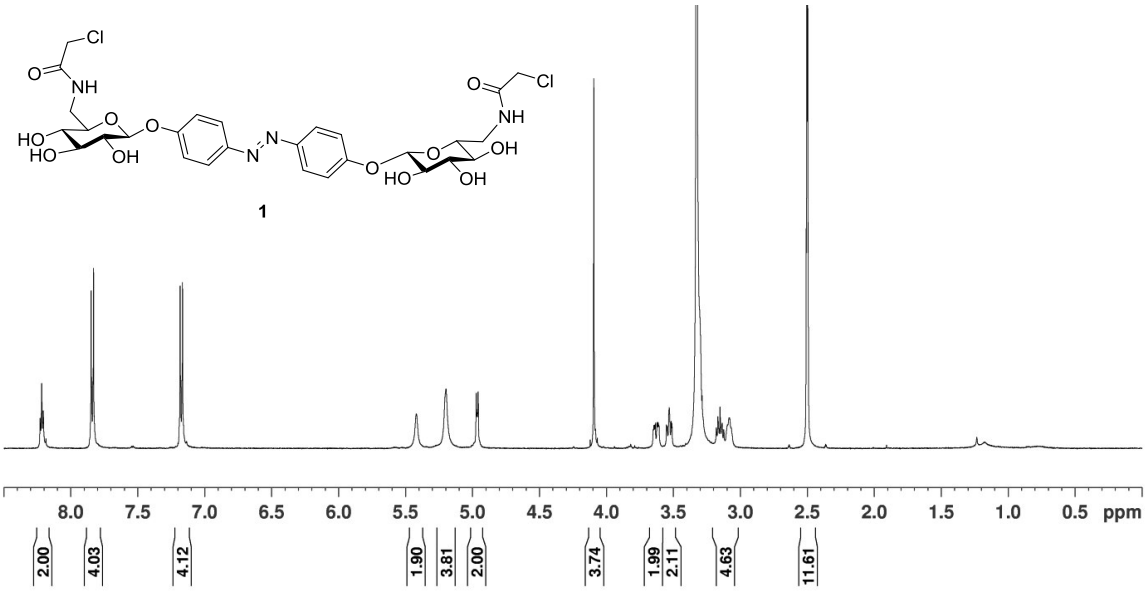

Figure S1. ^{1}H NMR spectrum of **1** (500 MHz, DMSO-d_6, 299.9 K).

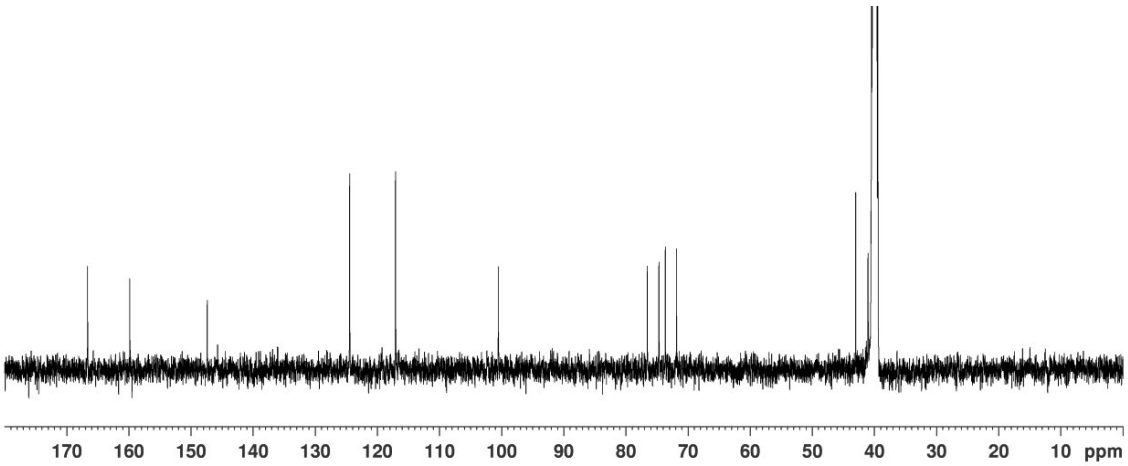

Figure S2. ^{13}C NMR spectrum of **1** (125 MHz, DMSO-d_6, 300.1 K).

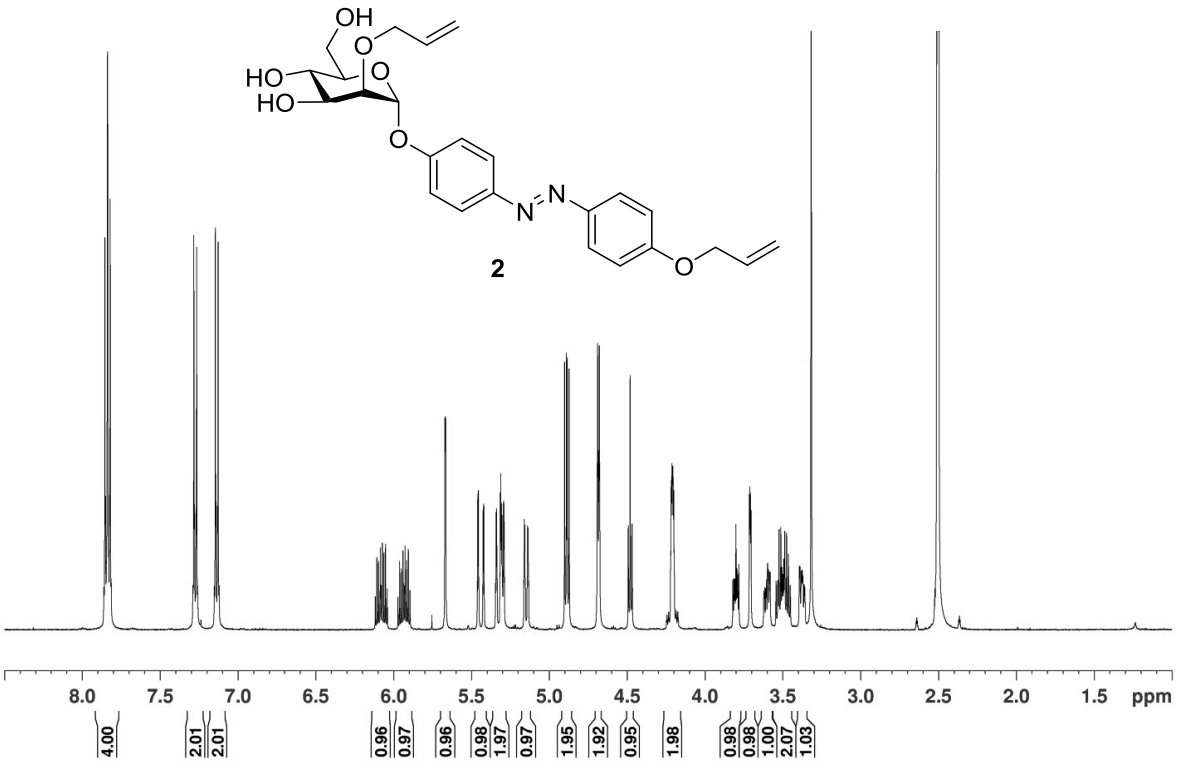

Figure S3. ^{1}H NMR spectrum of **2** (500 MHz, DMSO-d_6, 300.2 K).

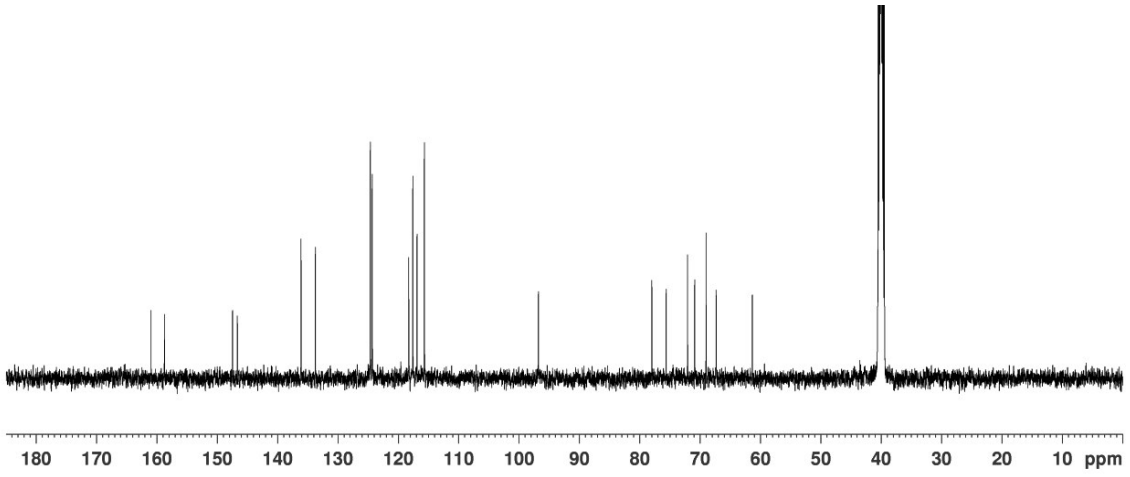

Figure S4. ^{13}C NMR spectrum of **2** (125 MHz, DMSO-d_6, 299.7 K).

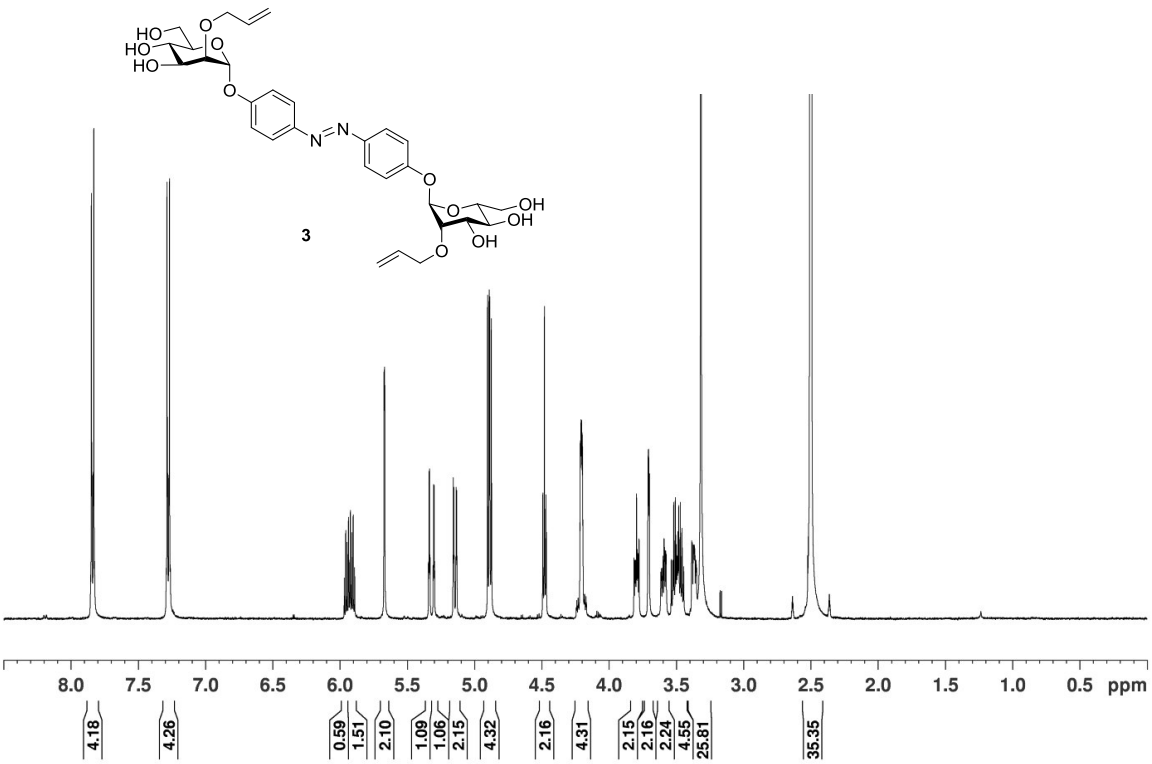

Figure S5. ^{1}H NMR spectrum of **3** (500 MHz, DMSO-d_6, 299.9 K).

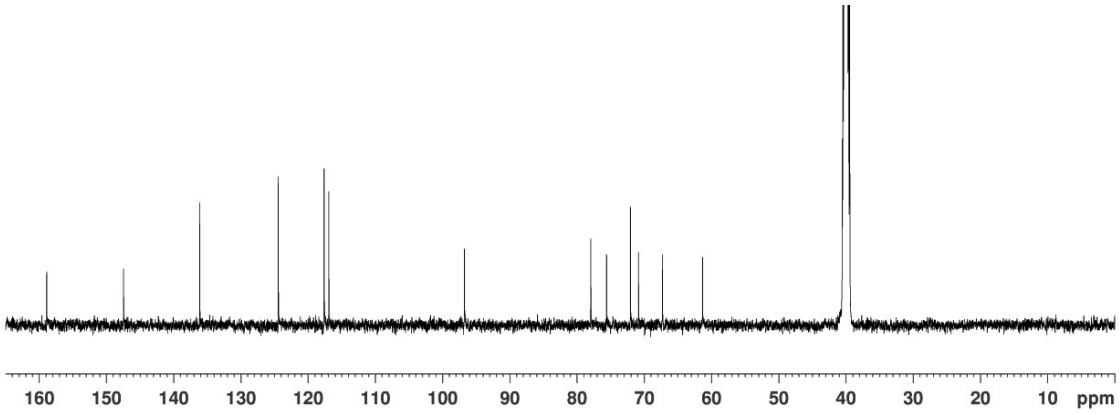

Figure S6. ^{13}C NMR spectrum of **3** (125 MHz, DMSO-d_6, 300.1 K).

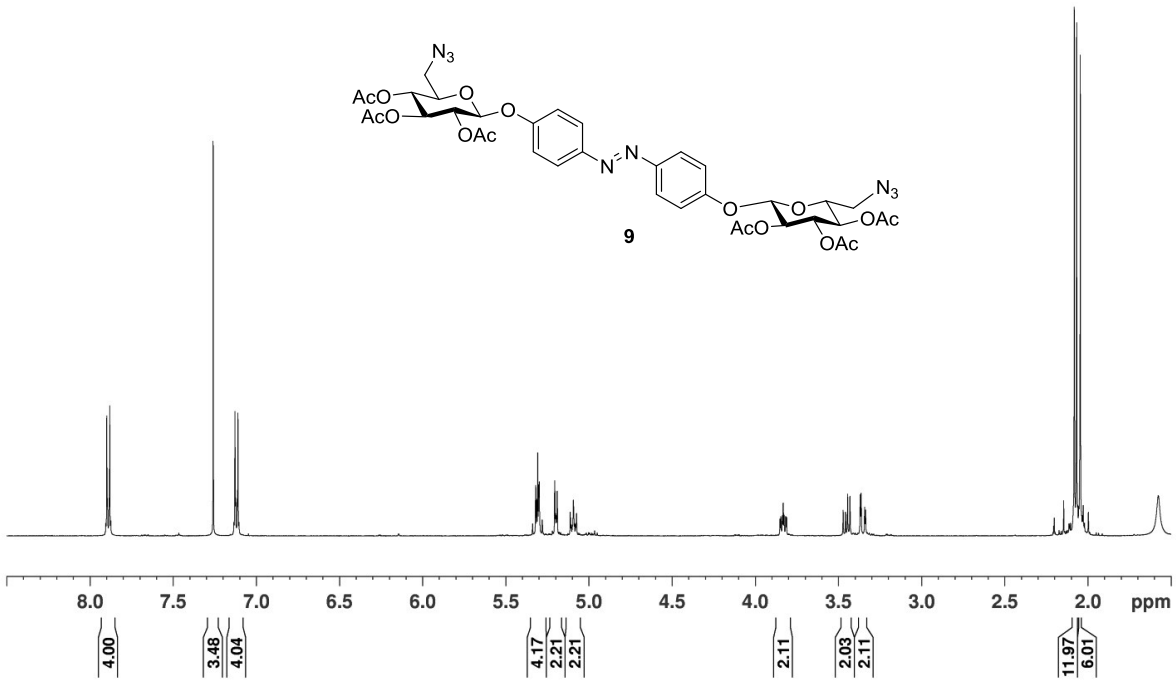

Figure S7. ^{1}H NMR spectrum of **9** (500 MHz, $CDCl_3$, 299.9 K).

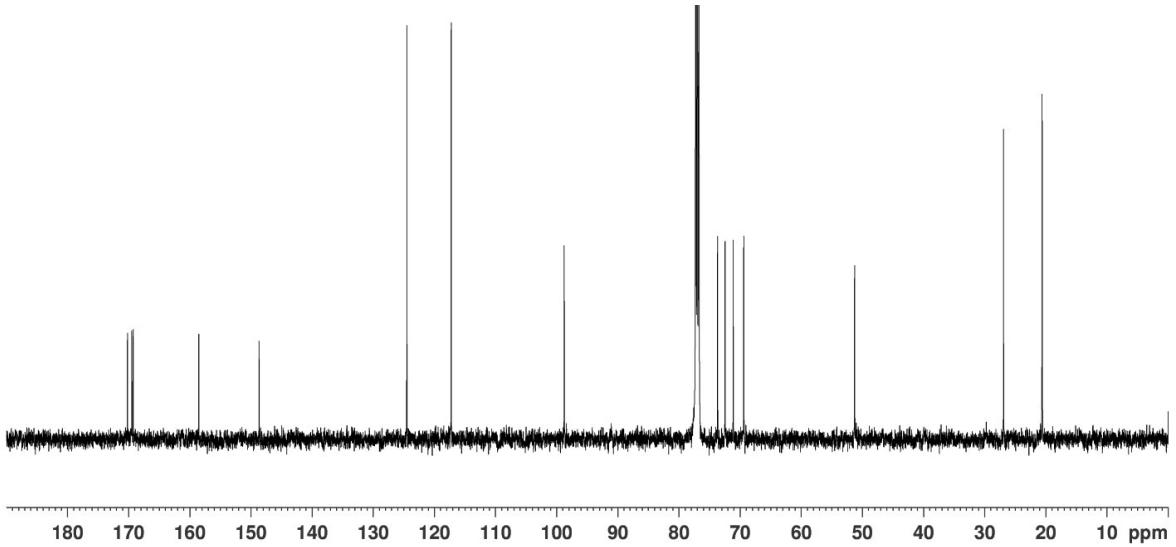

Figure S8. ^{13}C NMR spectrum of **9** (125 MHz, $CDCl_3$, 300.1 K).

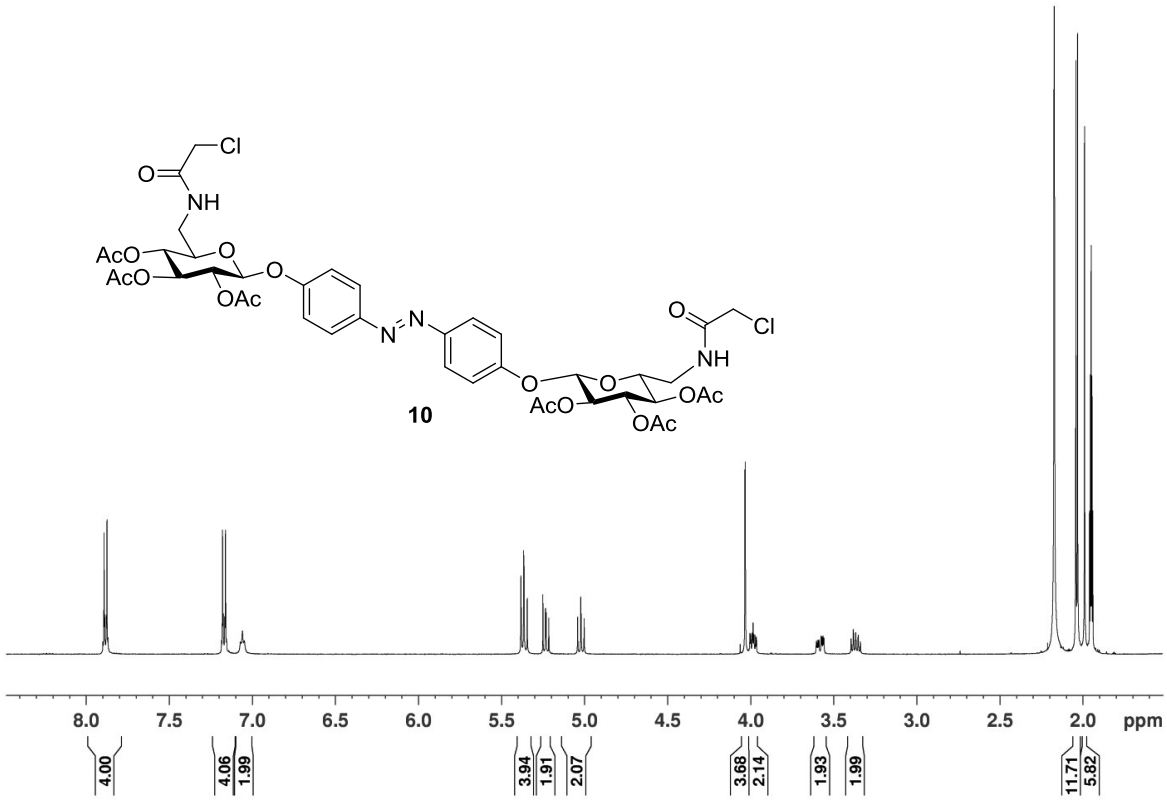

Figure S9. ^{1}H NMR spectrum of **10** (500 MHz, CD_3CN, 299.9 K).

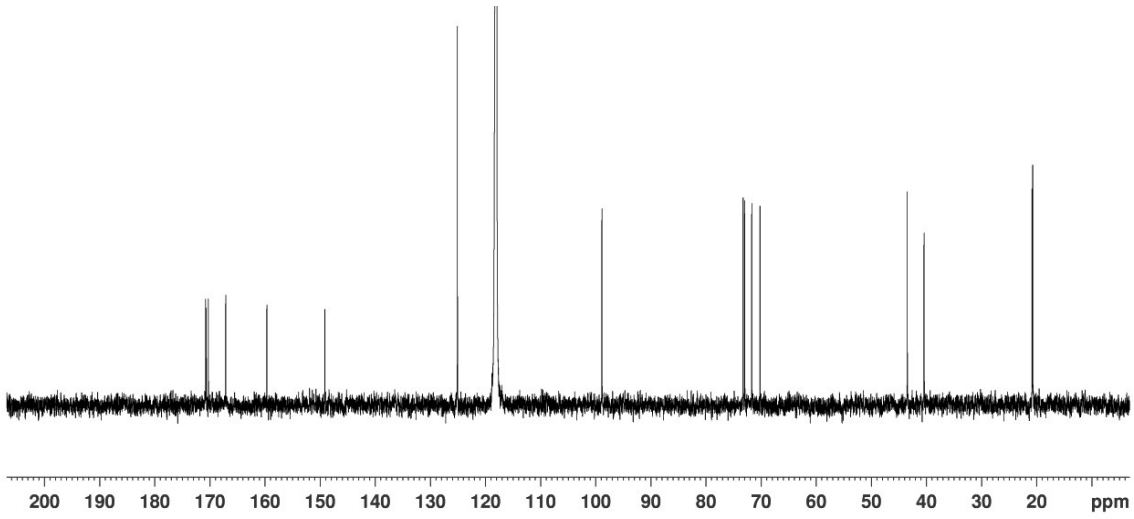

Figure S10. ^{13}C NMR spectrum of **10** (125 MHz, CD_3CN, 300.1 K).

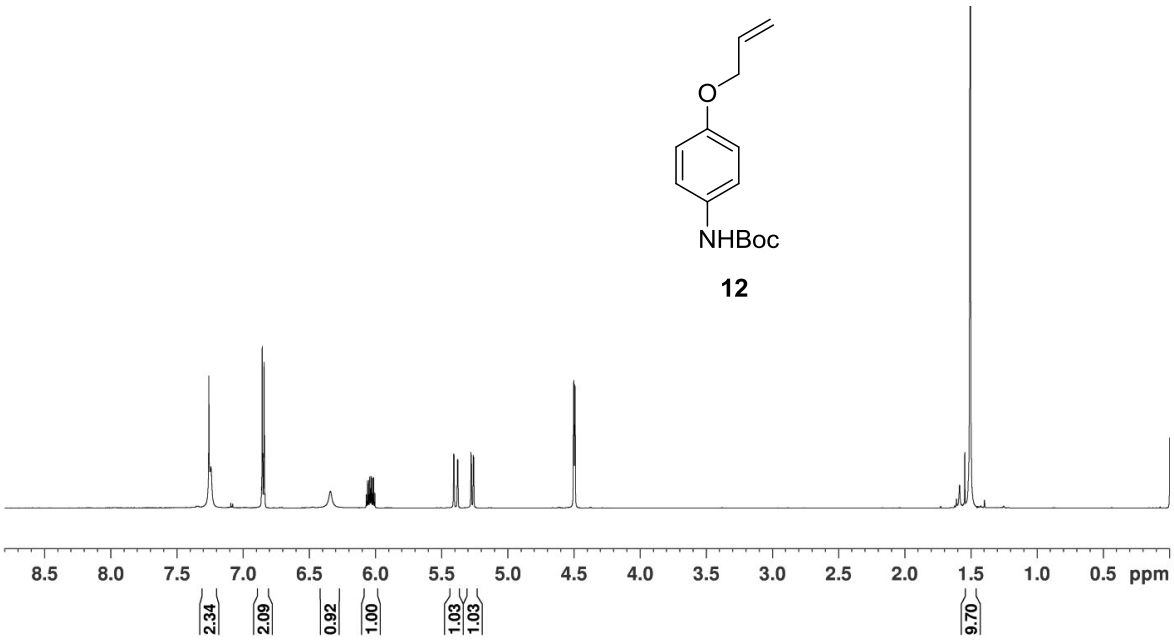

Figure S11. ^{1}H NMR spectrum of **12** (600 MHz, $CDCl_3$, 298.0 K).

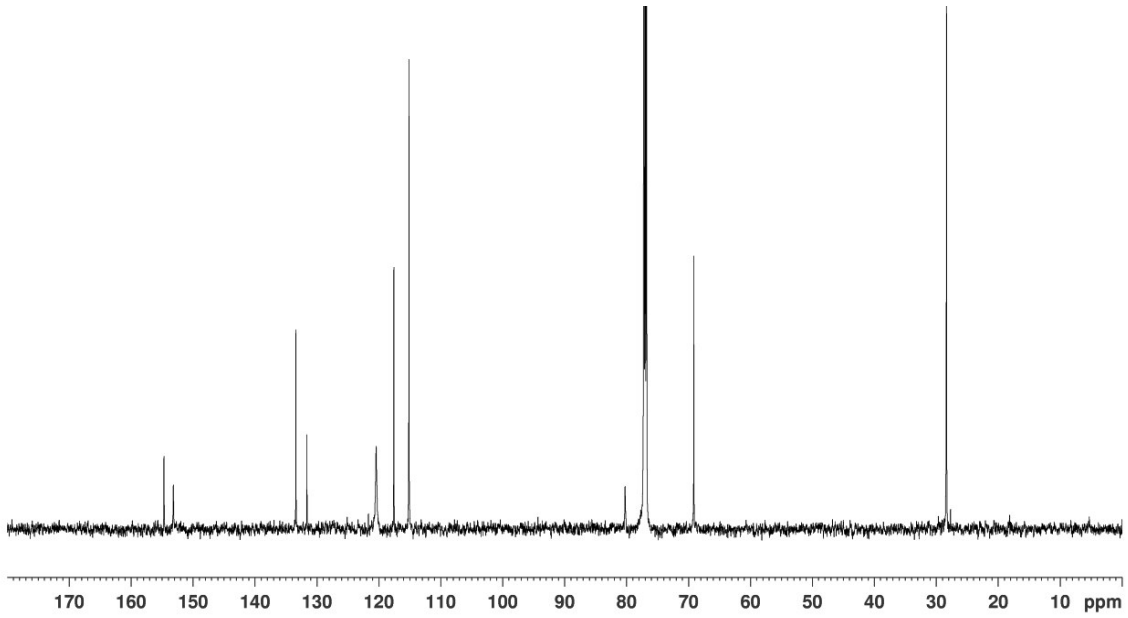

Figure S12. ^{13}C NMR spectrum of **12** (150 MHz, $CDCl_3$, 298.0 K).

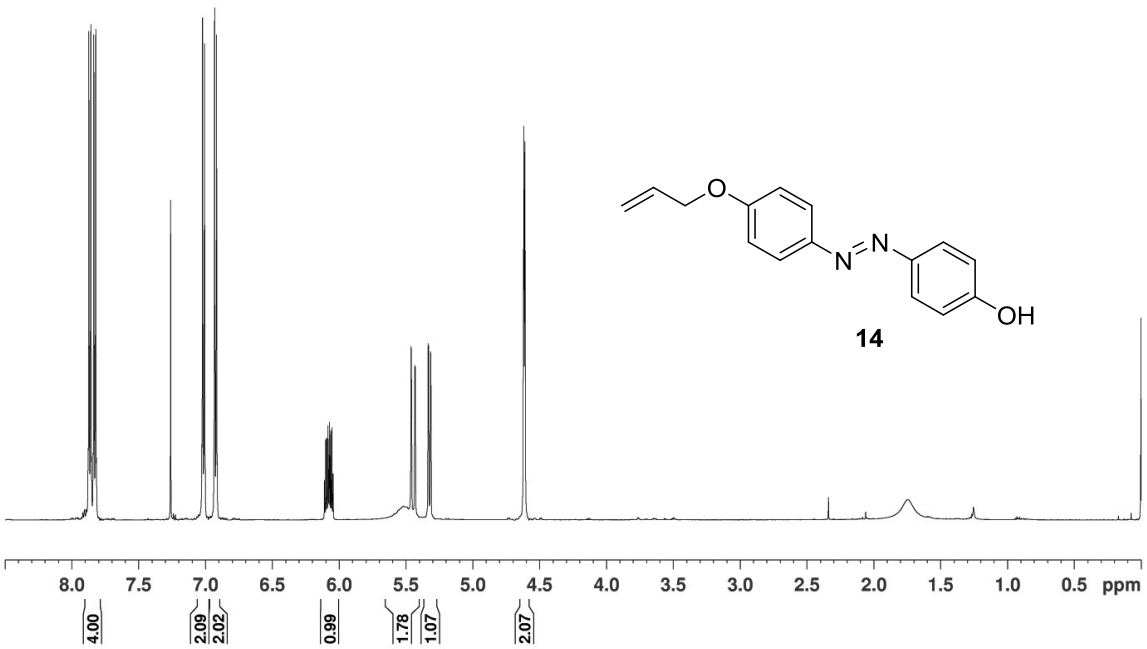

Figure S13. ^{1}H NMR spectrum of **14** (600 MHz, $CDCl_3$, 298.0 K).

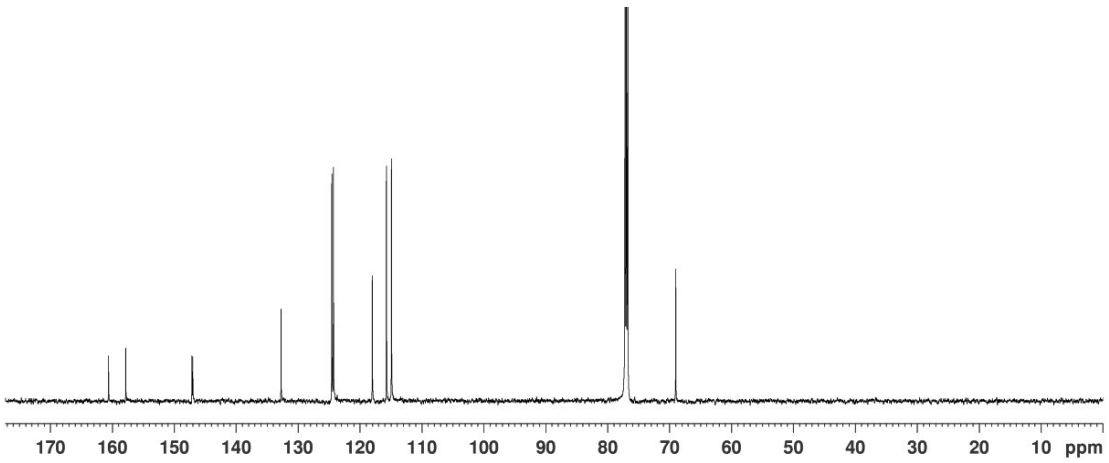

Figure S14. ^{13}C NMR spectrum of **14** (150 MHz, $CDCl_3$, 298.0 K).

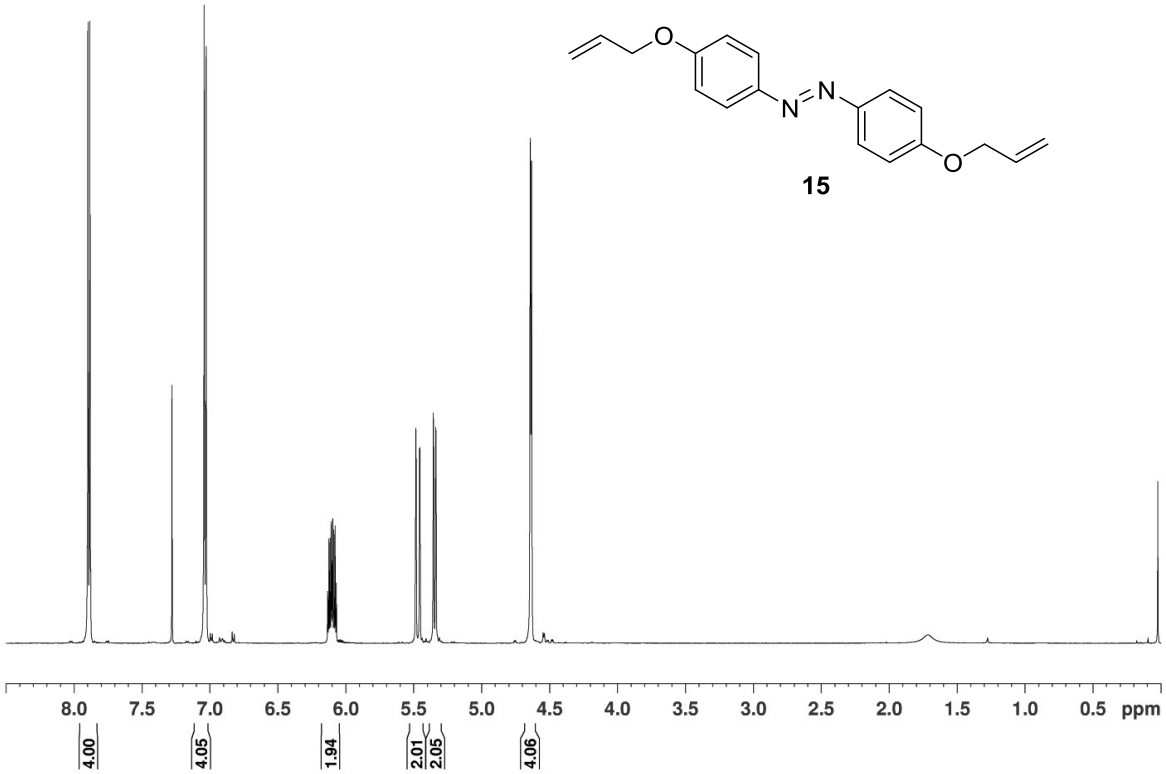

Figure S15. ^{1}H NMR spectrum of **15** (600 MHz, $CDCl_3$, 298.0 K).

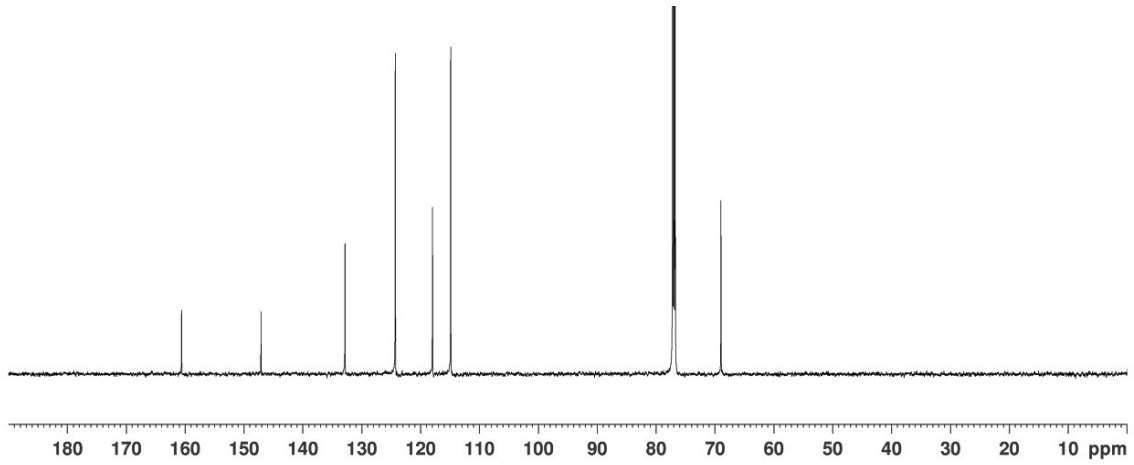

Figure S16. ^{13}C NMR spectrum of **15** (150 MHz, $CDCl_3$, 298.0 K).

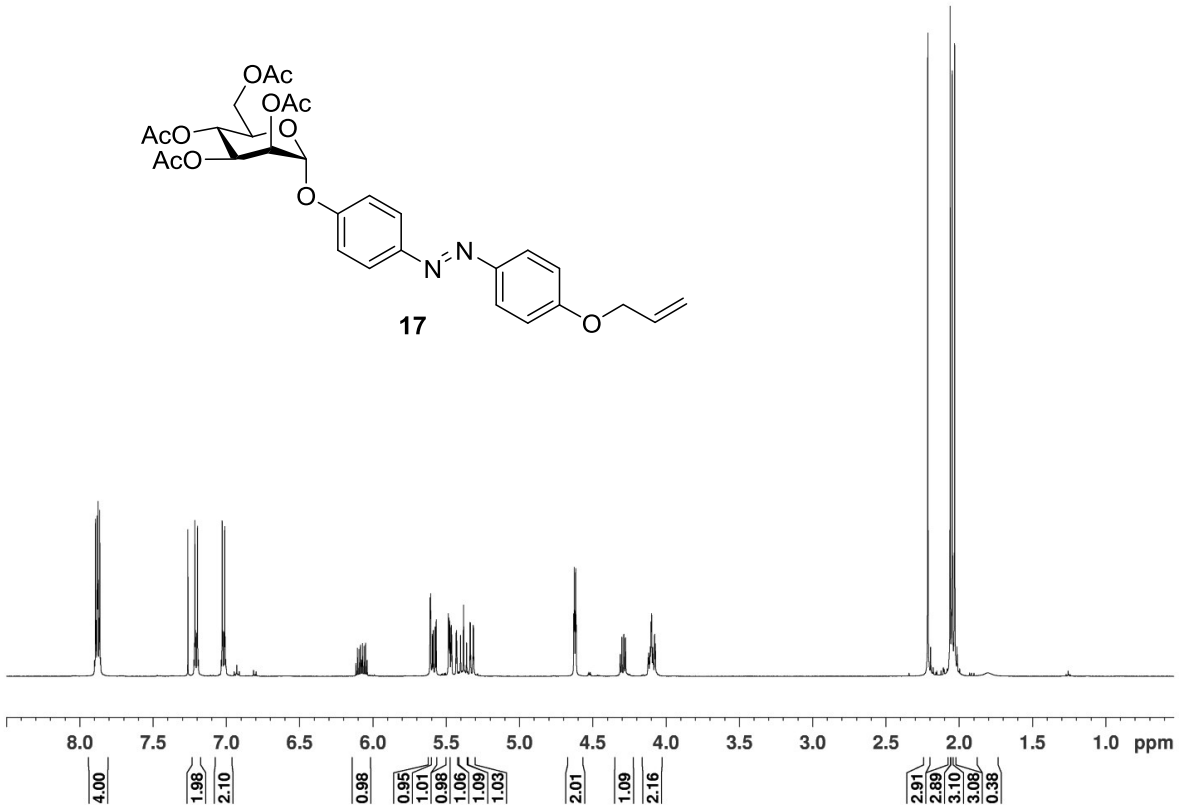

Figure S17. ^{1}H NMR spectrum of **17**(500 MHz, $CDCl_3$, 300.1 K).

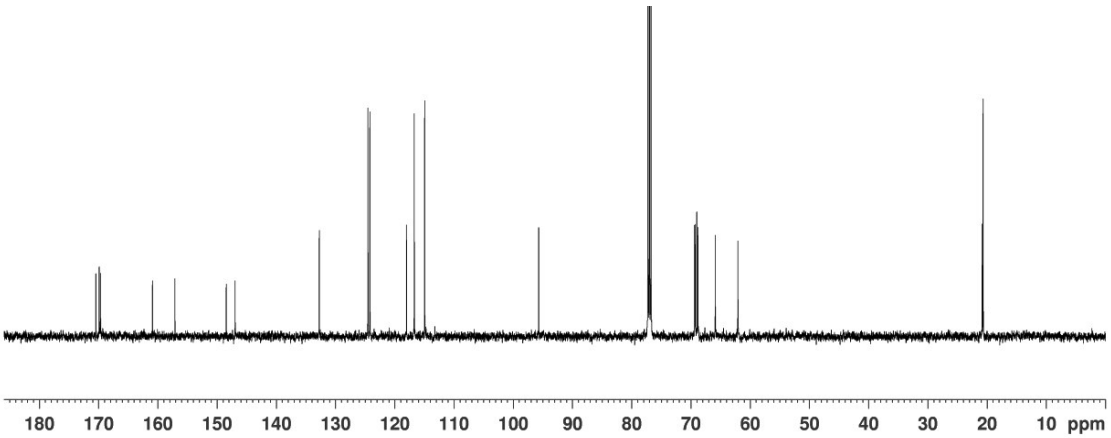

Figure S18. ^{13}C NMR spectrum of **17** (125 MHz, $CDCl_3$, 299.8 K).

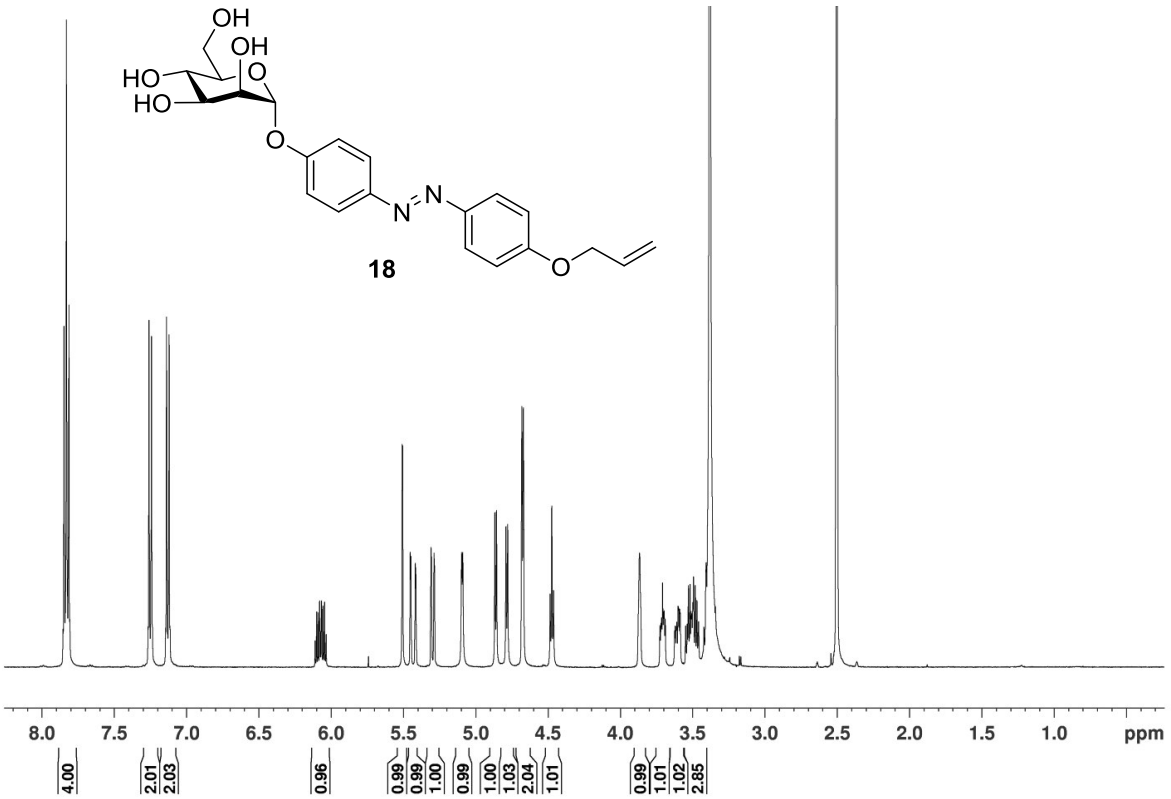

Figure S19. ^{1}H NMR spectrum of **18** (500 MHz, DMSO-d_6, 300.2 K).

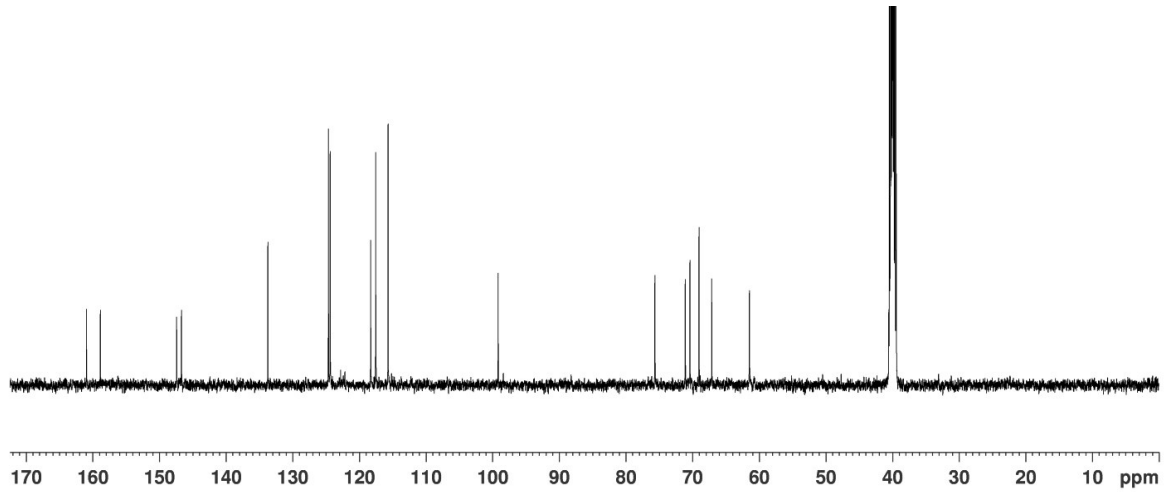

Figure S20. ^{13}C NMR spectrum of **18** (125 MHz, DMSO-d_6, 299.7 K).

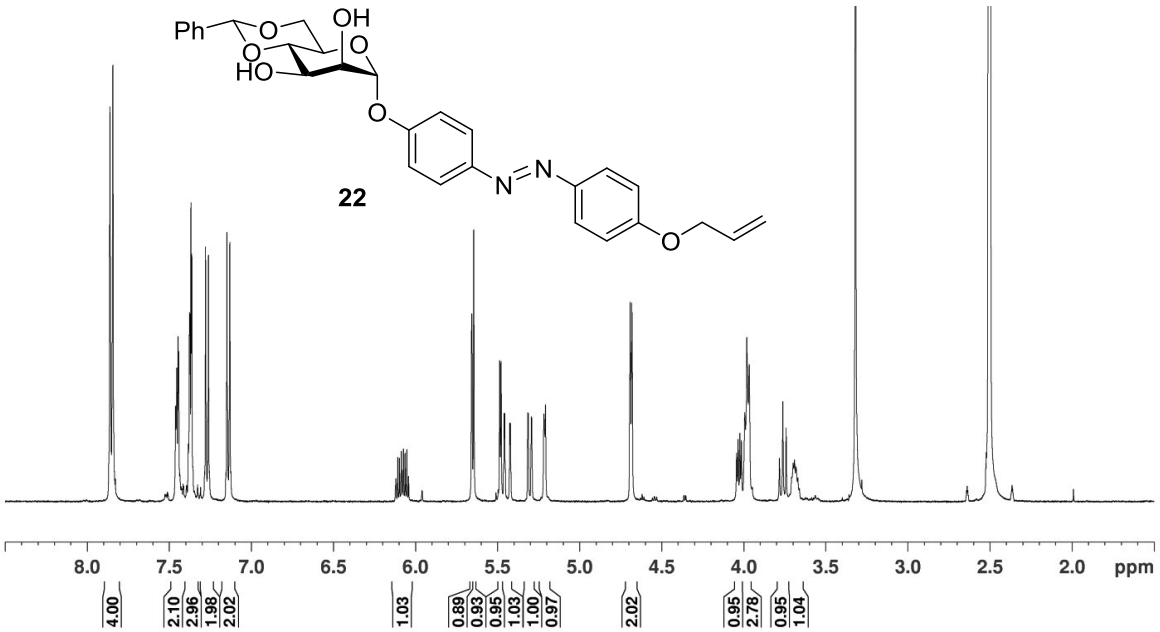

Figure S21. ^{1}H NMR spectrum of **22** (500 MHz, DMSO-d_6, 299.9 K).

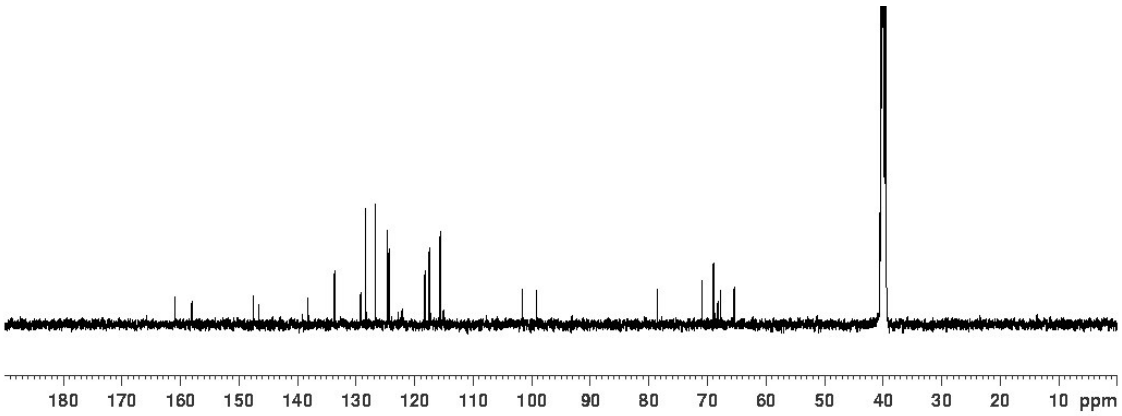

Figure S22. ^{13}C NMR spectrum of **22** (125 MHz, DMSO-d_6, 299.9 K).

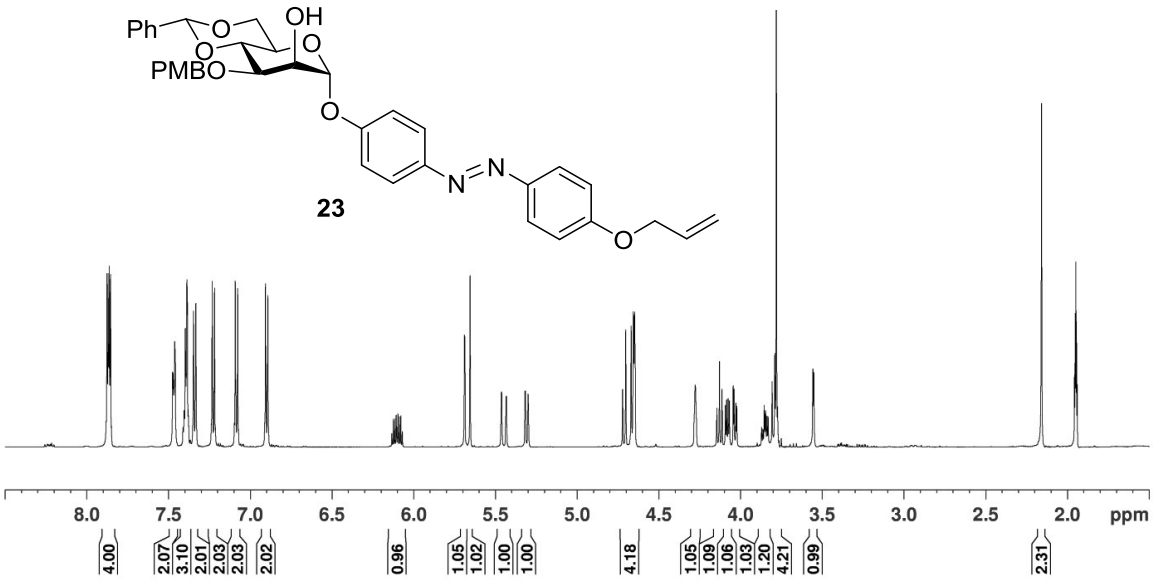

Figure S23. ^{1}H NMR spectrum of **23** (600 MHz, CD_3CN, 298.0 K).

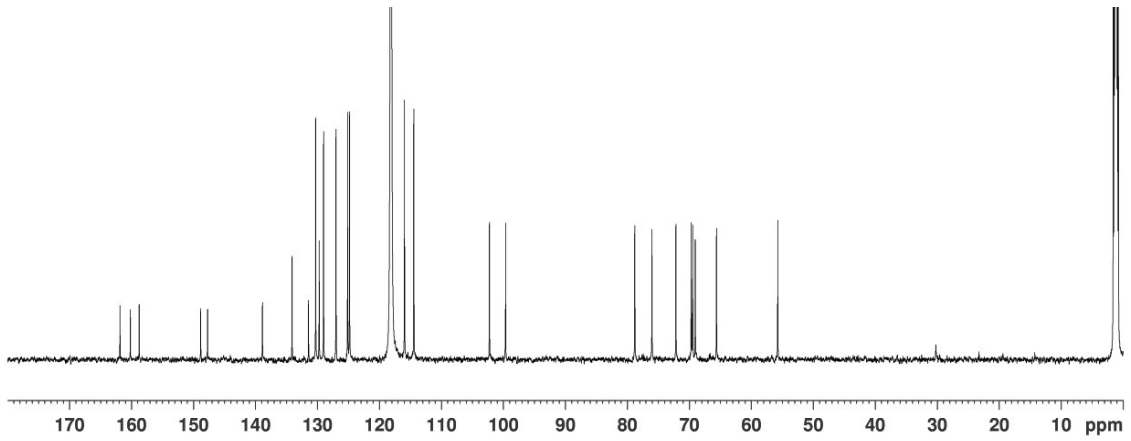

Figure S24. ^{13}C NMR spectrum of **23** (150 MHz, CD_3CN, 298.0 K).

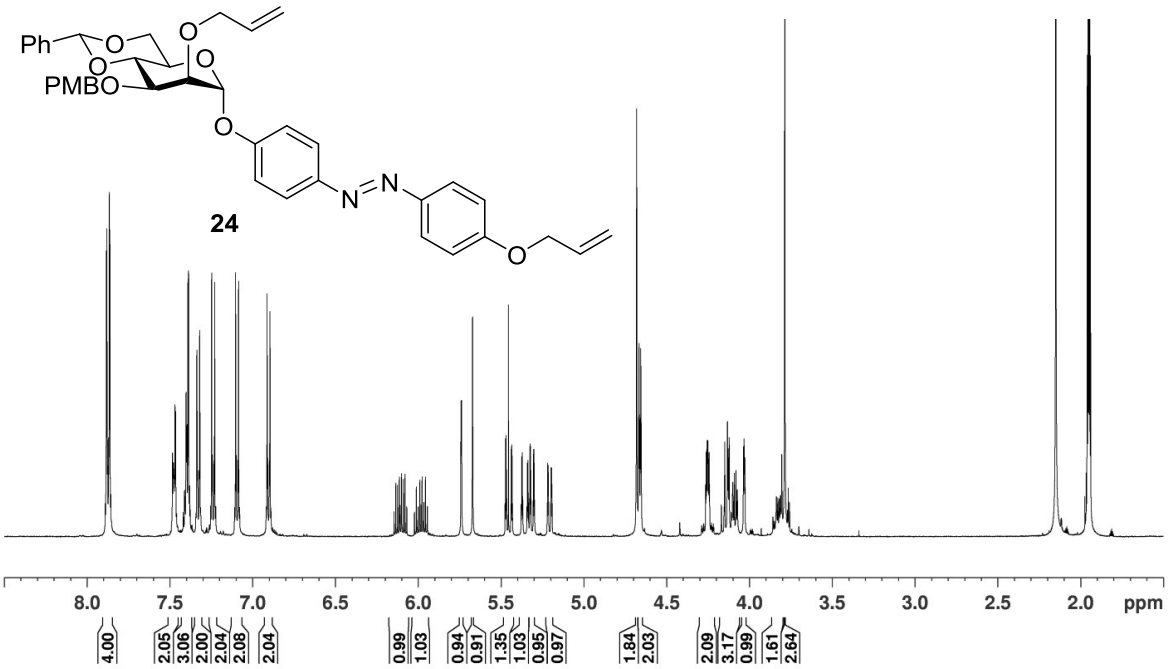

Figure S25. ^{1}H NMR spectrum of **24** (500 MHz, CD_3CN, 299.9 K).

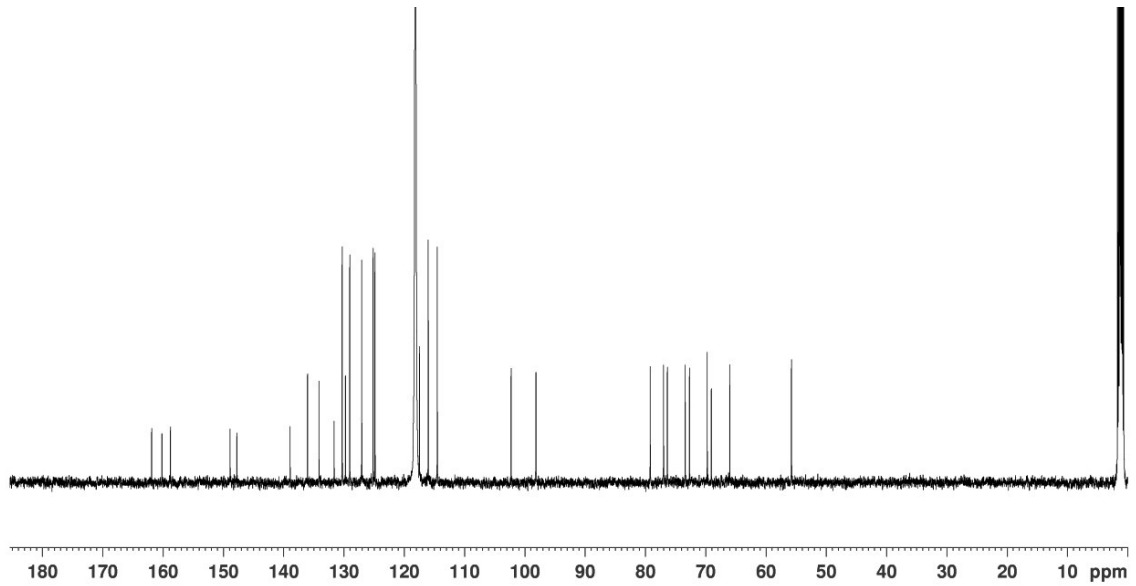

Figure S26. ^{13}C NMR spectrum of **24** (125 MHz, CD_3CN, 300.1 K).

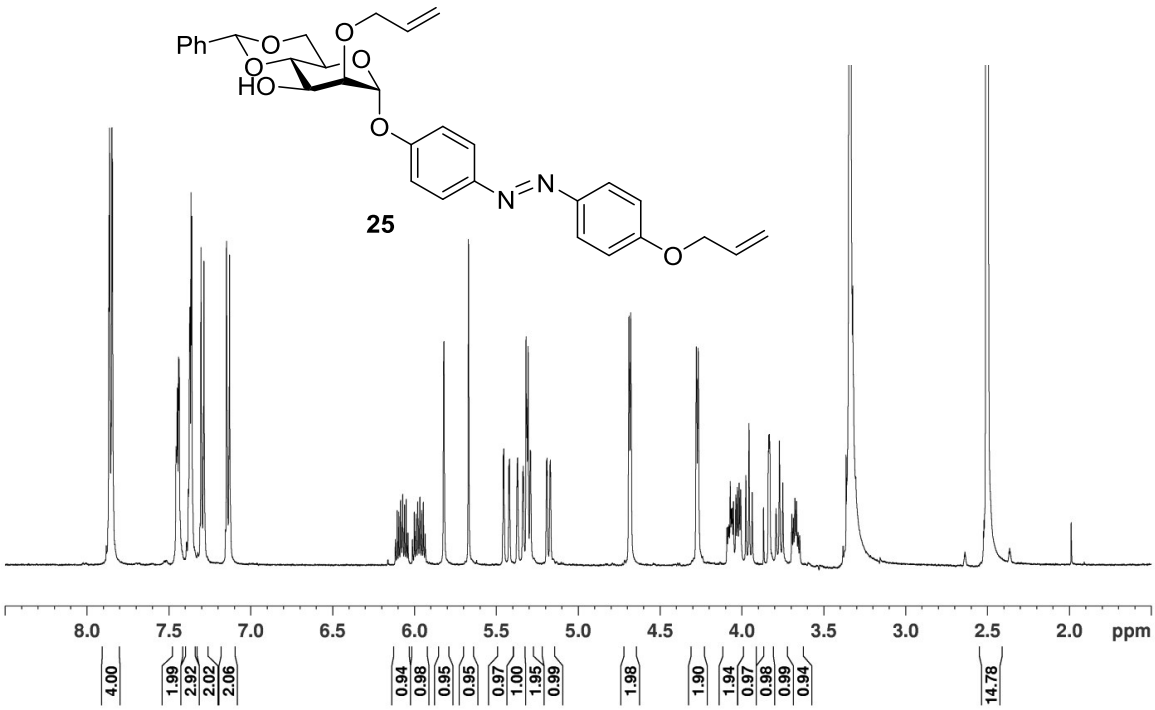

Figure S27. ^{1}H NMR spectrum of **25** (500 MHz, DMSO-d_6, 300.2 K).

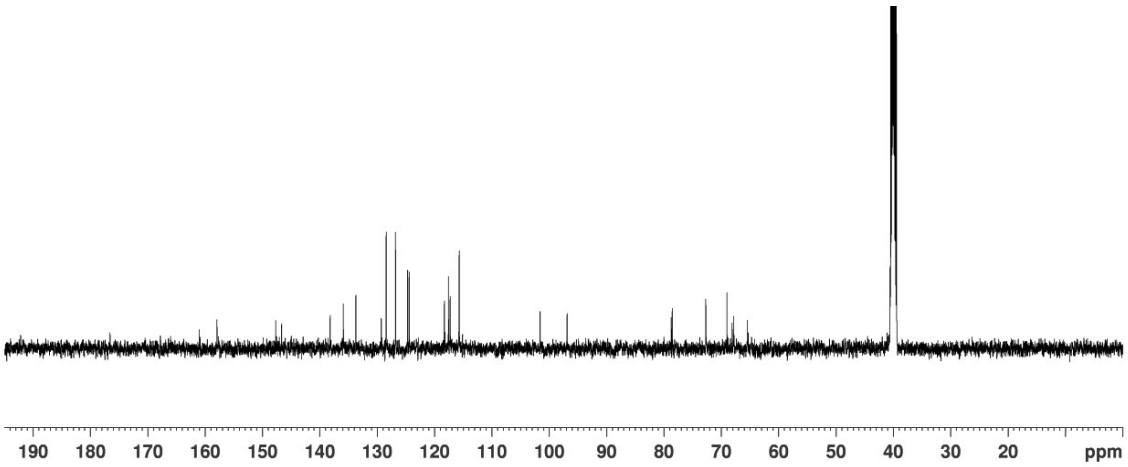

Figure S28. ^{13}C NMR spectrum of **25** (125 MHz, DMSO-d_6, 299.9 K).

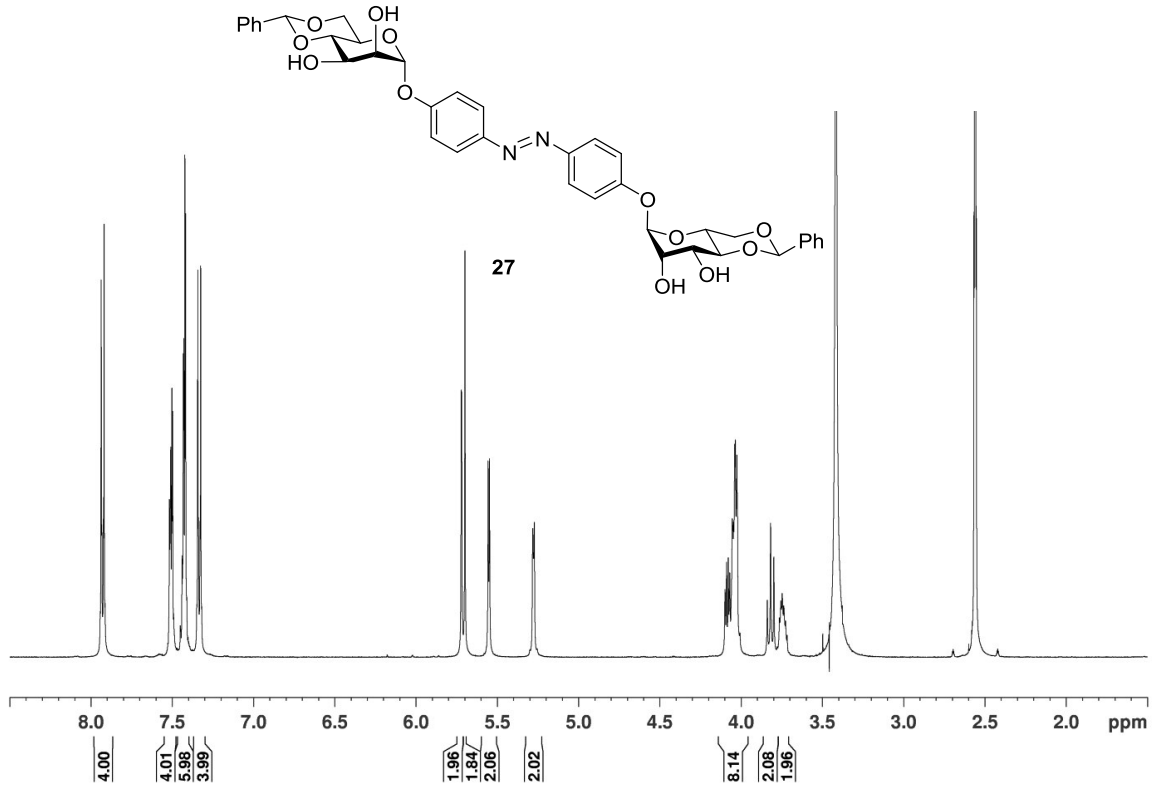

Figure S29. ^{1}H NMR spectrum of **27** (500 MHz, DMSO-d_6, 300.1 K).

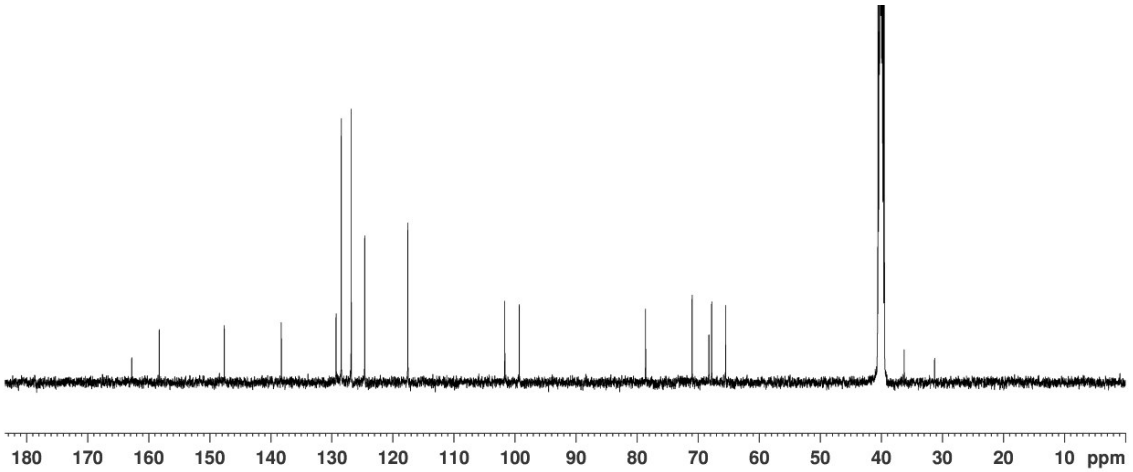

Figure S30. ^{13}C NMR spectrum of **27** (125 MHz, DMSO-d_6, 300.1 K).

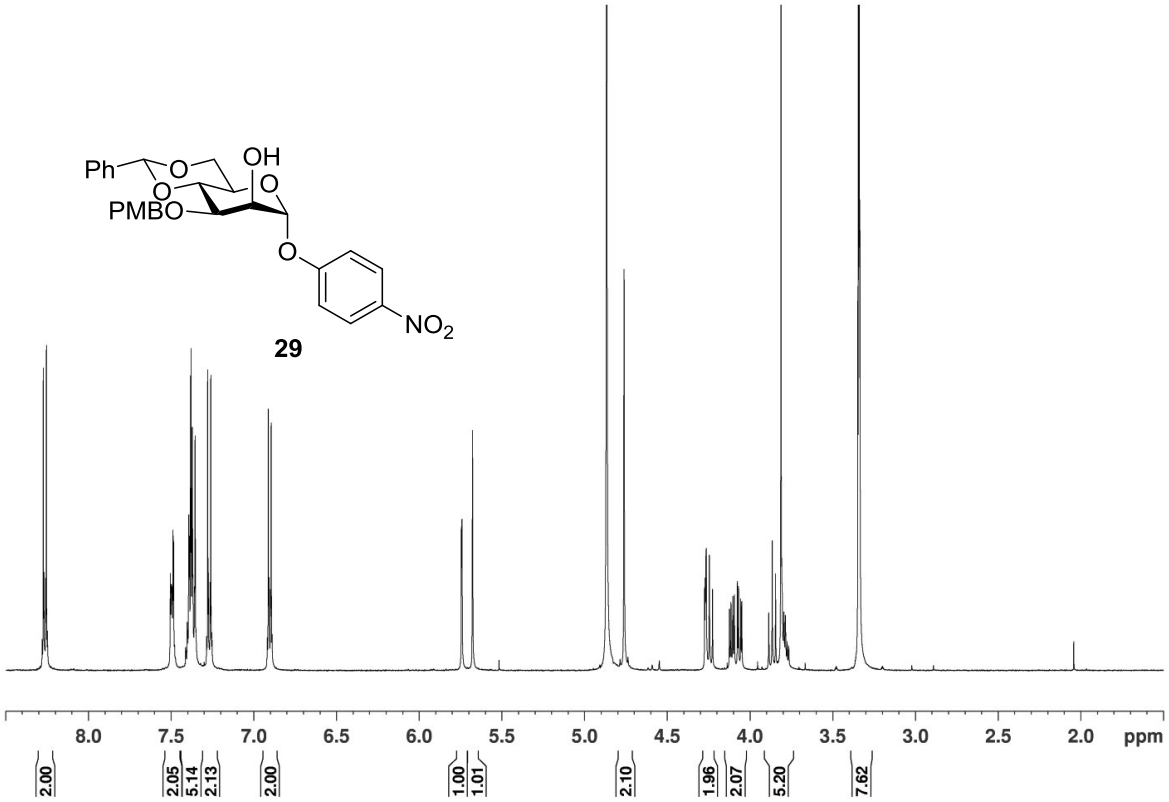

Figure S31. ^{1}H NMR spectrum of **29** (500 MHz, MeOH-d_4, 300.1 K).

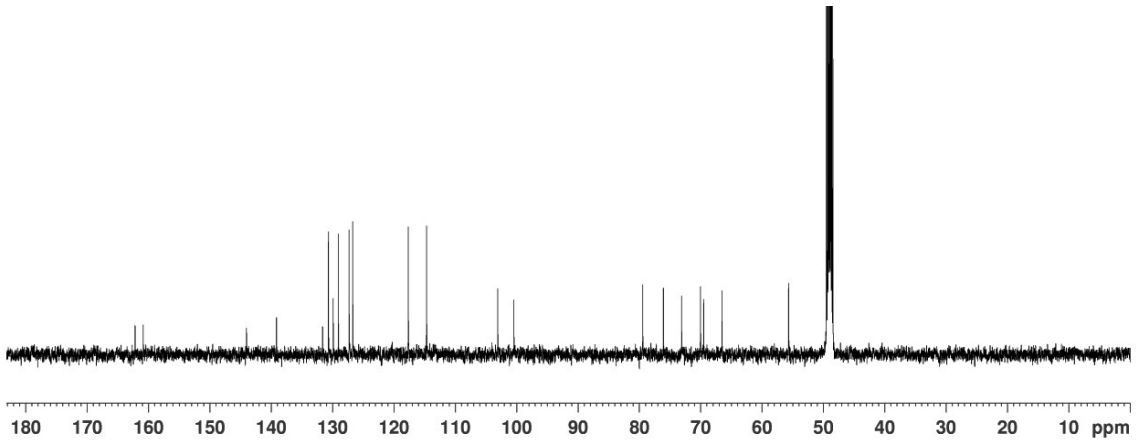

Figure S32. ^{13}C NMR spectrum of **29** (125 MHz, MeOH-d_4, 299.9 K).

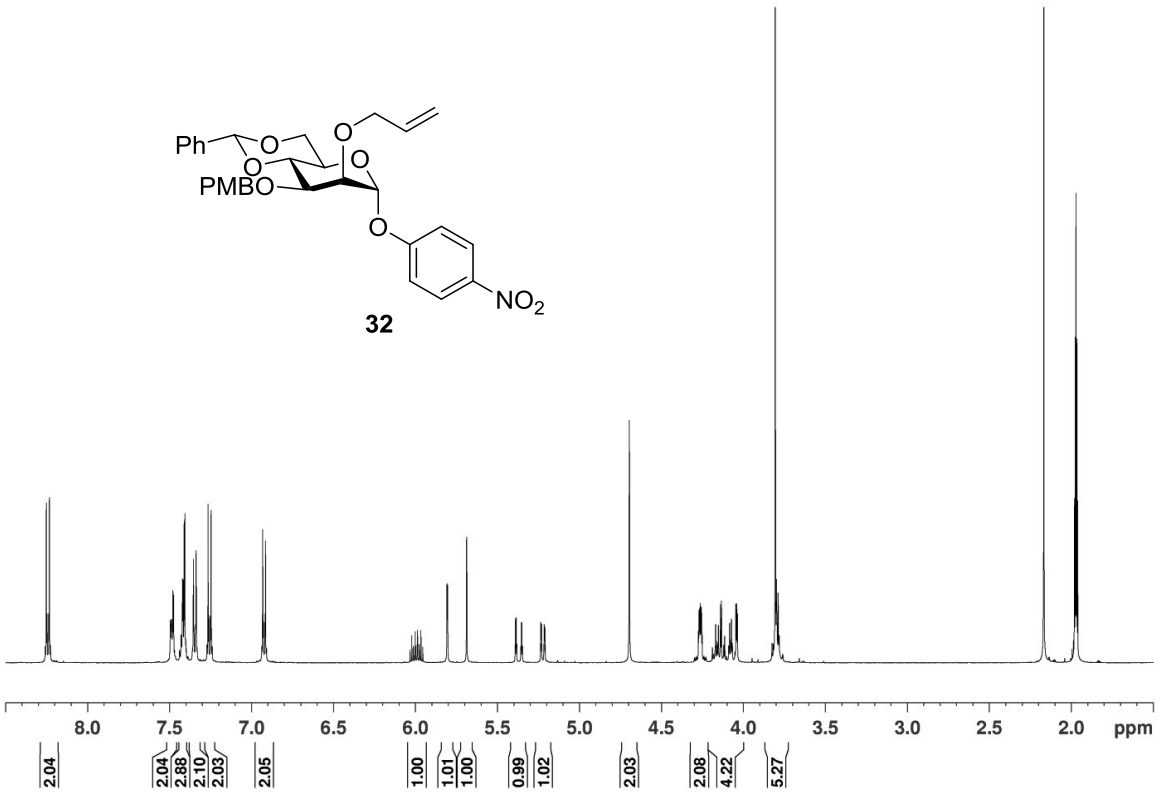

Figure S33. ^{1}H NMR spectrum of **32** (500 MHz, CD_3CN, 299.9 K).

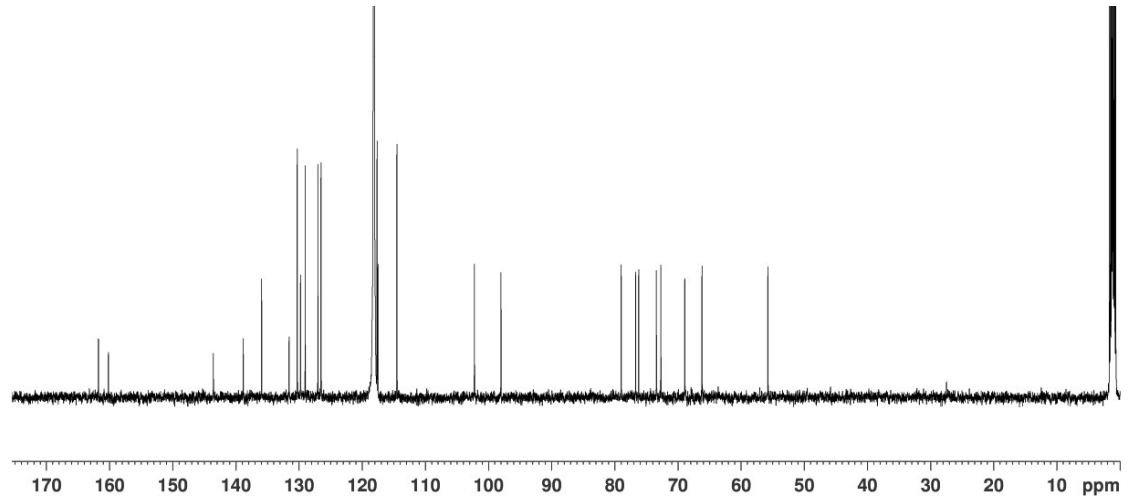

Figure S34. ^{13}C NMR spectrum of **32** (125 MHz, CD_3CN, 299.9 K).

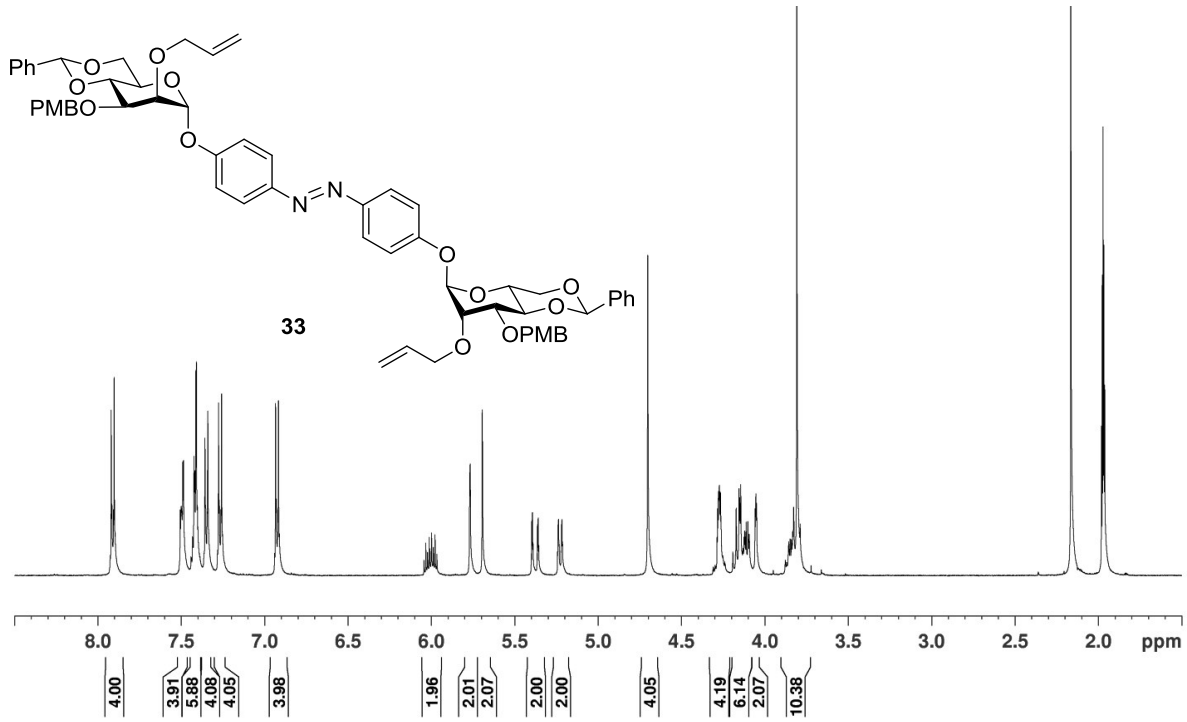

Figure S35. ^{1}H NMR spectrum of **33** (500 MHz, CD_3CN, 299.9 K).

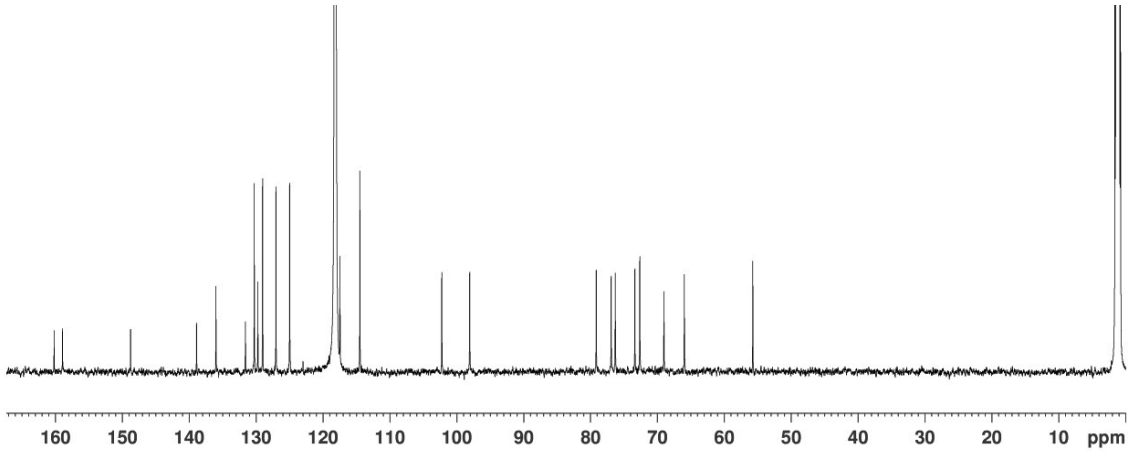

Figure S36. ^{13}C NMR spectrum of **33** (150 MHz, CD_3CN, 298.0 K).

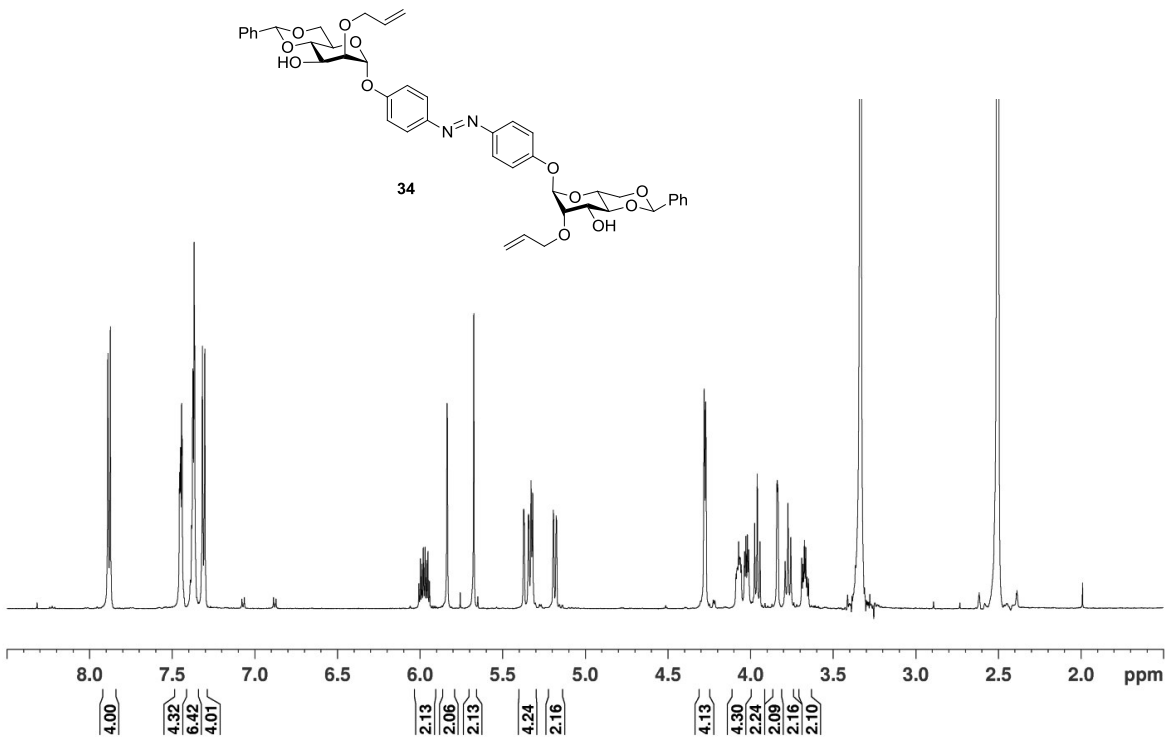

Figure S37. ^{1}H NMR spectrum of **34** (600 MHz DMSO-d_6, 298.0 K).

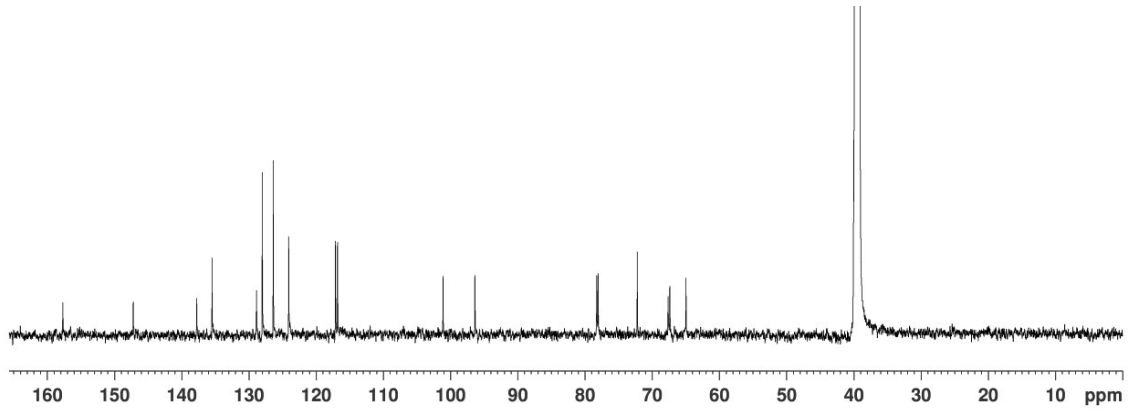

Figure S38. ^{13}C NMR spectrum of **34** (150 MHz, DMSO-d_6, 298.0 K).

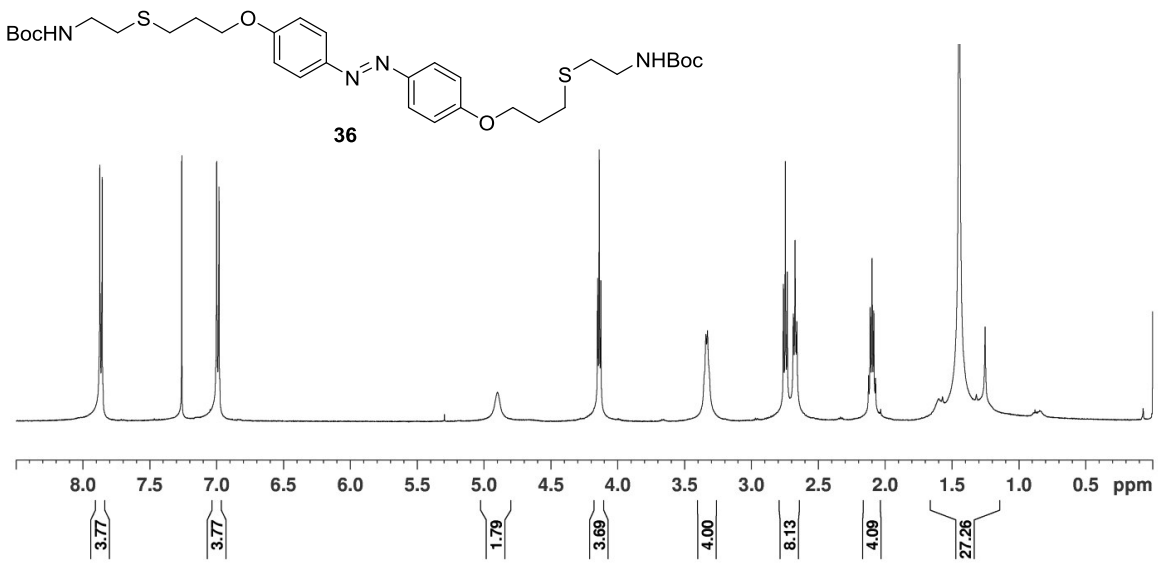

Figure S39. ^{1}H NMR spectrum of **36** (500 MHz, CD_3CN, 299.9 K).

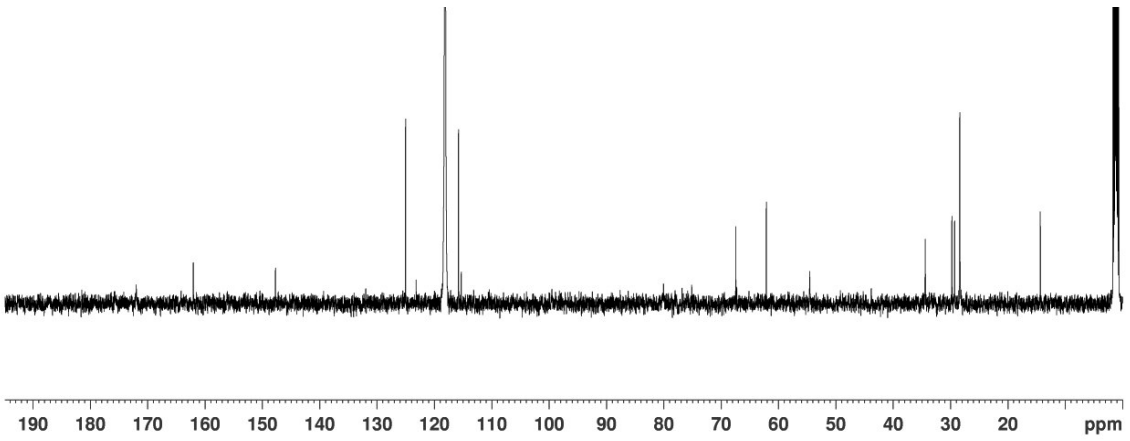

Figure S40. ^{13}C NMR spectrum of **36** (125 MHz, CD_3CN, 299.9 K).

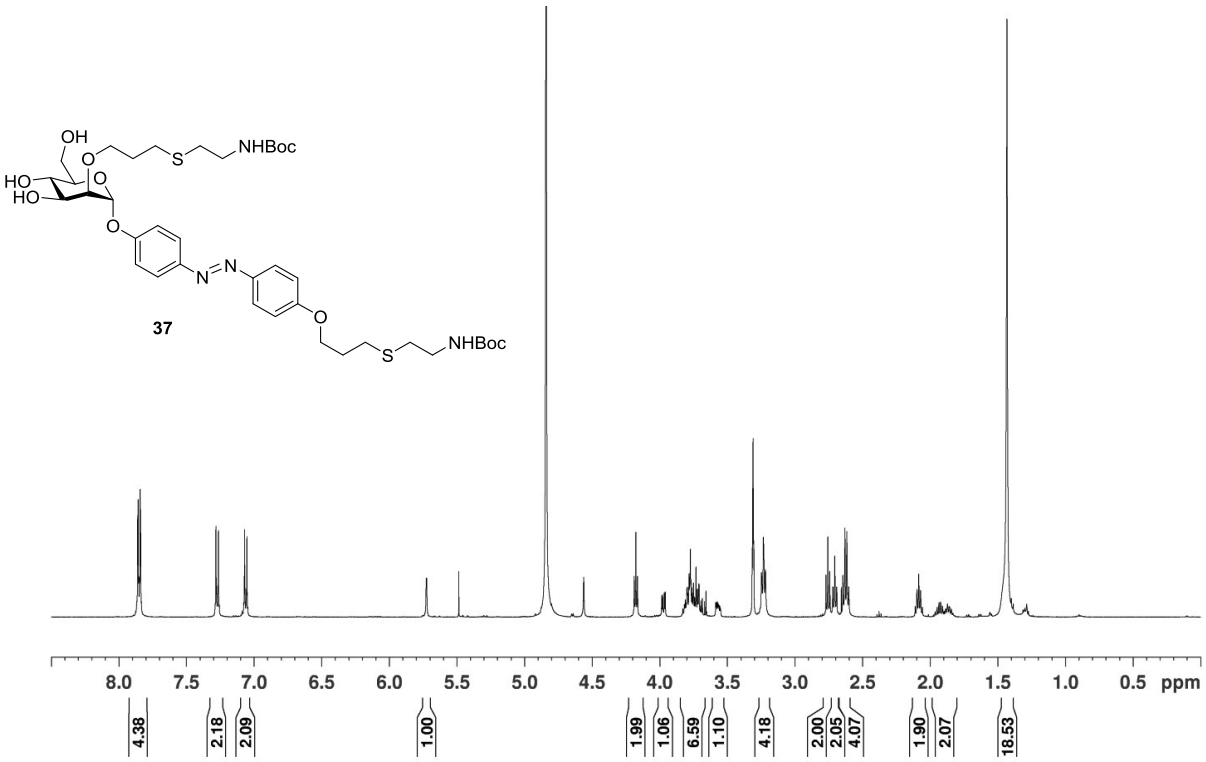

Figure S41. ^{1}H NMR spectrum of **37** (500 MHz, MeOH-d_4, 299.9 K).

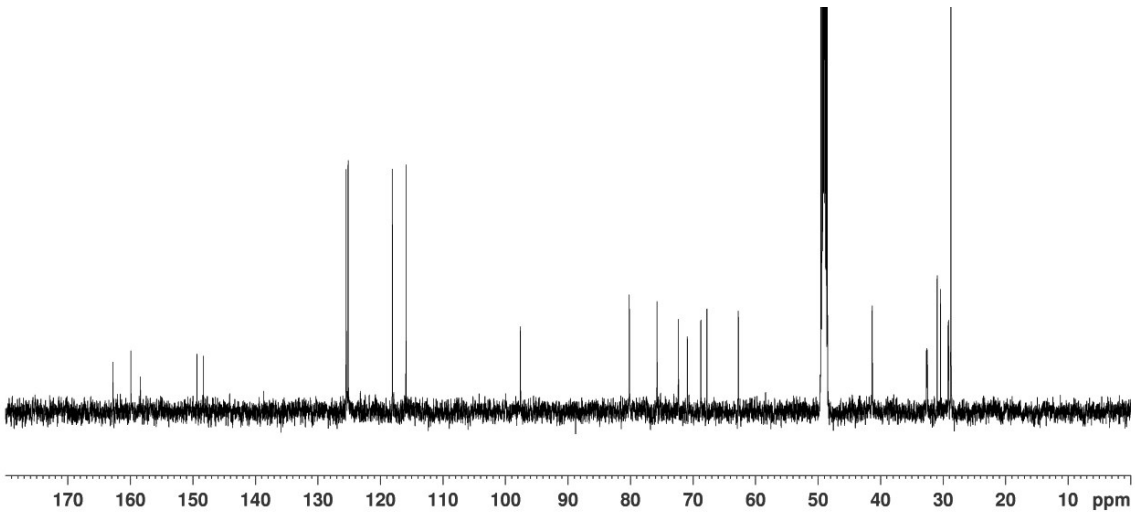

Figure S42. ^{13}C NMR spectrum of **37** (125 MHz, MeOH-d_4, 300.1 K).

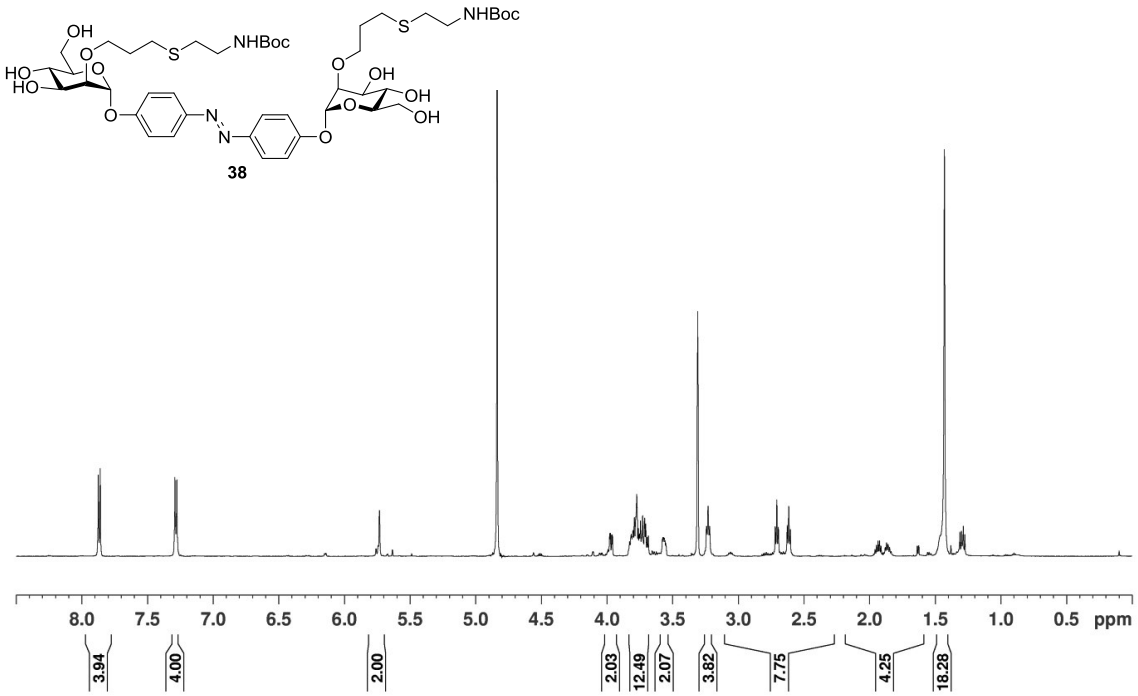

Figure S43. ^{1}H NMR spectrum of **38** (600 MHz, MeOH-d_4, 300.0 K).

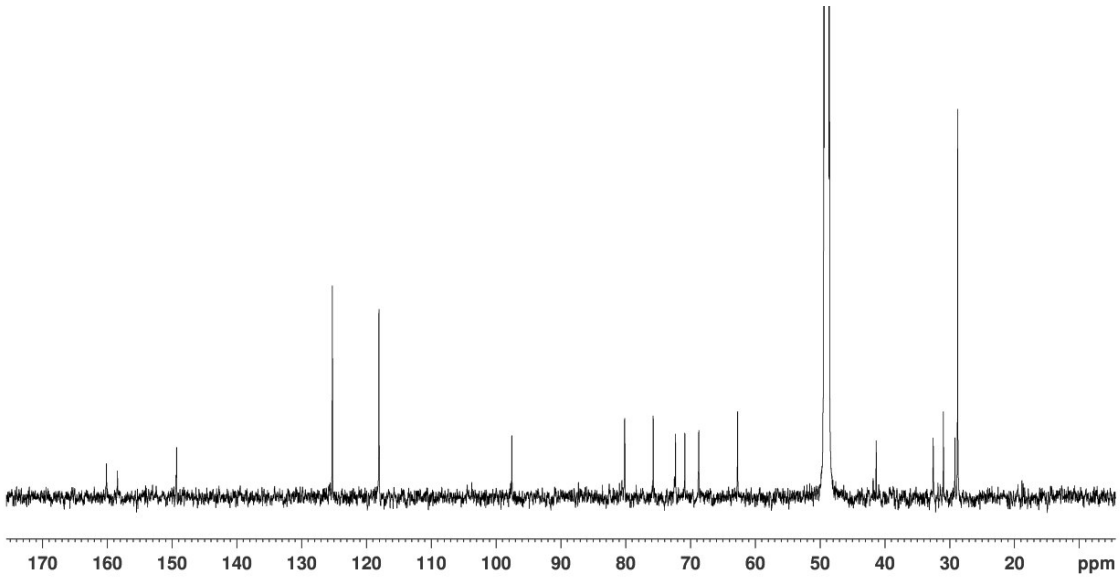

Figure S44. ^{13}C NMR spectrum of **38** (151 MHz, MeOH-d_4, 300.0 K).

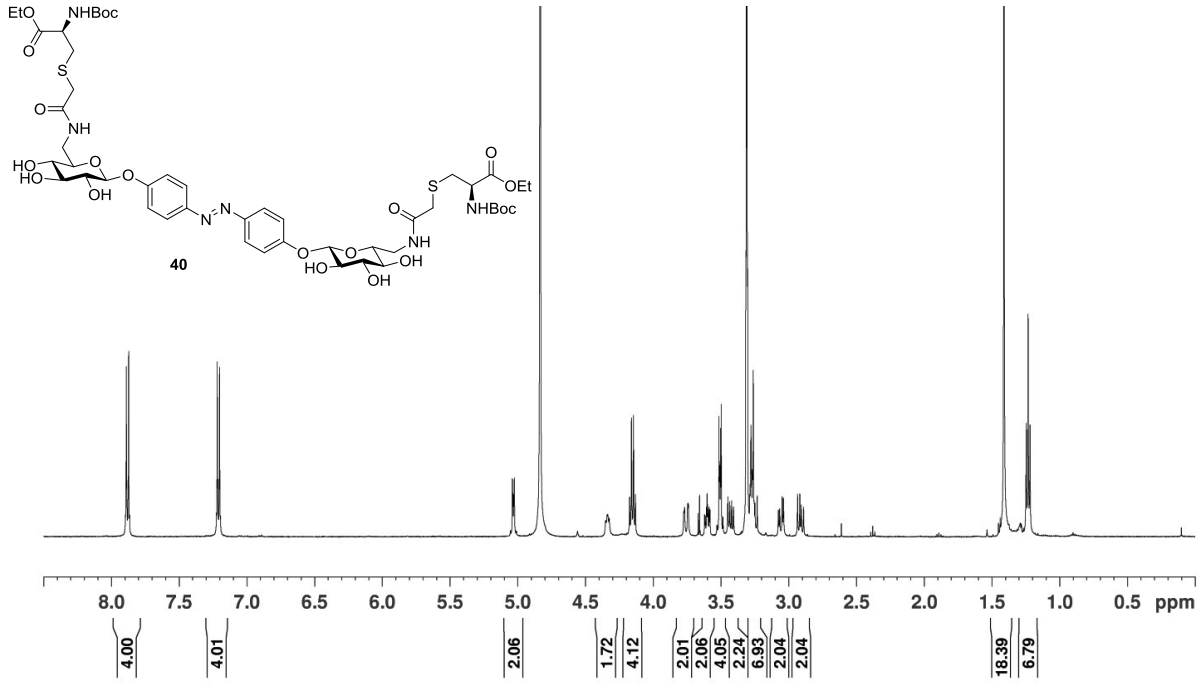

Figure S45. ^{1}H NMR spectrum of **40** (500 MHz, MeOH-d_4, 299.9 K).

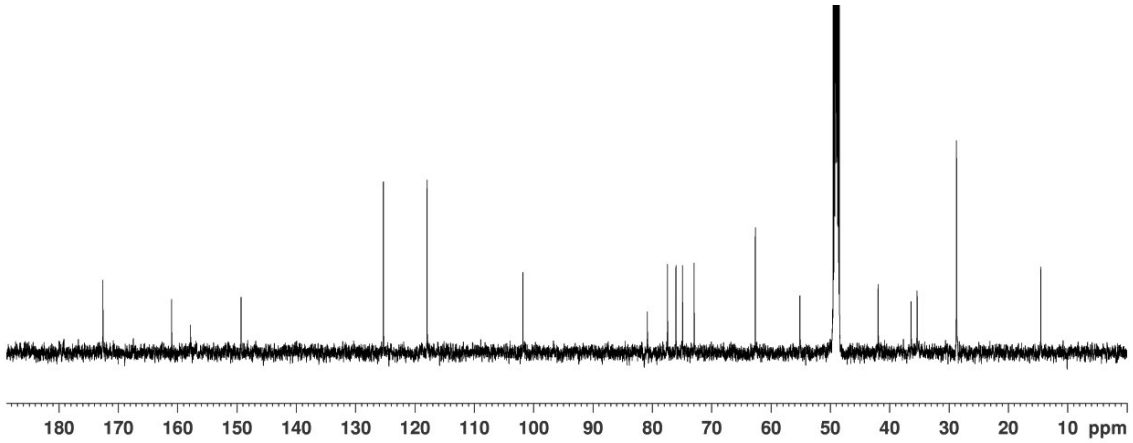

Figure S46. ^{13}C NMR spectrum of **40** (125 MHz, MeOH-d_4, 300.1 K).

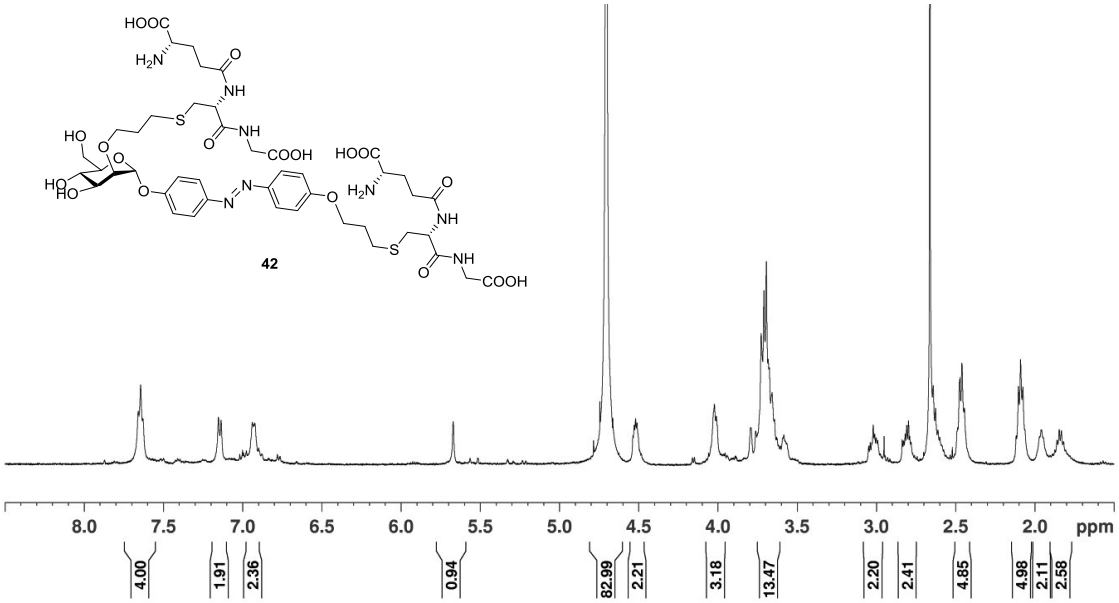

Figure S47. ^{1}H NMR spectrum of **42** (500 MHz, D_2O, 299.9 K).

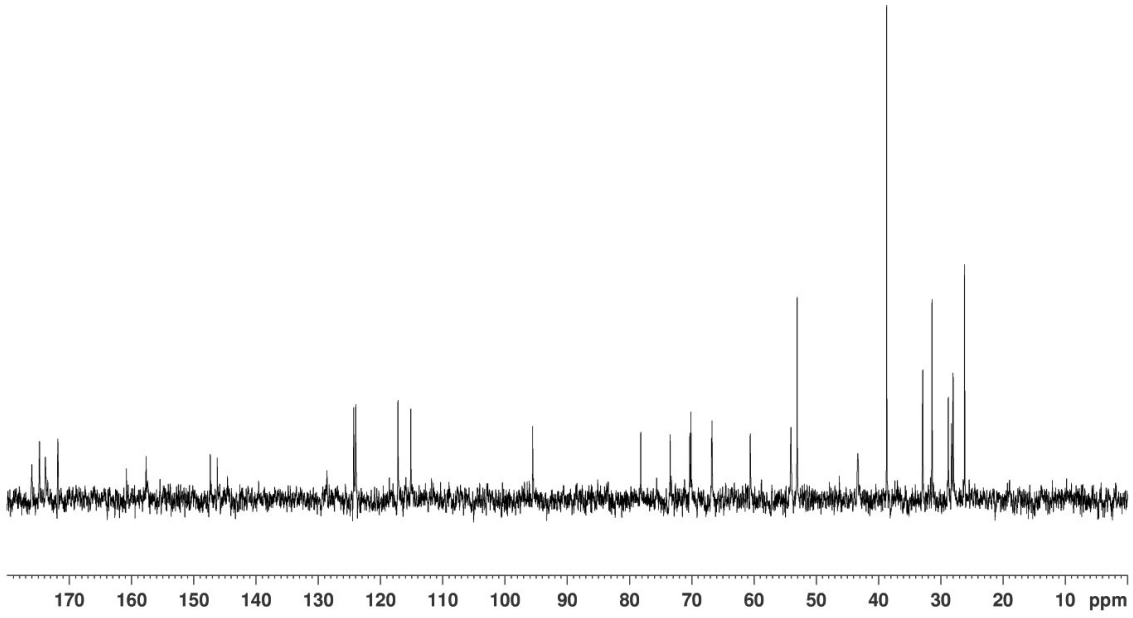

Figure S48. ^{13}C NMR spectrum of **42** (150 MHz, D_2O, 300.0 K).

3. Irradiation experiments

Irradiation was performed using a LED (emitting 365 nm light) from the Nichia Corporation (NC4U133A) with a FWHW of 9 nm and optical power output (P_O) ~1 W. *E*/*Z* ratios were calculated by irradiating the sample in the NMR tube followed by ^{1}H NMR spectroscopy. The distance between the LED and sample in the NMR tube was about ~5 cm. The photostationary state (PSS) was determined by integration of the anomeric H-1 protons of the prepared compounds (or by integration of aryl signals on case of **15**).

For UV-Vis spectroscopy, samples were irradiated in a UV cuvette with a distance between LED and cuvette of ~5 cm. Upon irradiation of azobenzene glycosides at 365 nm, the absorption spectra showed an increase of the absorbance in the n-π* transition and simultaneous decrease in the π-π* transition, indicating the formation of the respective *Z* isomer.

The kinetics of thermal $Z \rightarrow E$ relaxation processes were determined by NMR spectroscopy in the dark. The half-life $\tau_{1/2}$ was determined as $\tau_{1/2} = \ln 2/k$. After irradiation, the ^{1}H NMR spectra of the samples were recorded in regular intervals over a period of 10 to 17 days. For the determination of the half-life the *Z* and *E* signals of the respective azobenzene moiety were integrated. A signal that was not influenced by irradiation was set as reference. The decay of the integral of the *Z* and the increase of the integral of the *E* species were plotted and an exponential decay of first order fitted to the data.

NMR spectra of *Z*-configured compounds and UV-Vis spectroscopy

(*Z*)-*p*,*p'*-Di-[6-(2-chloroacetylamido)-6-deoxy-β-D-glucopyranosyloxy]azobenzene (1):

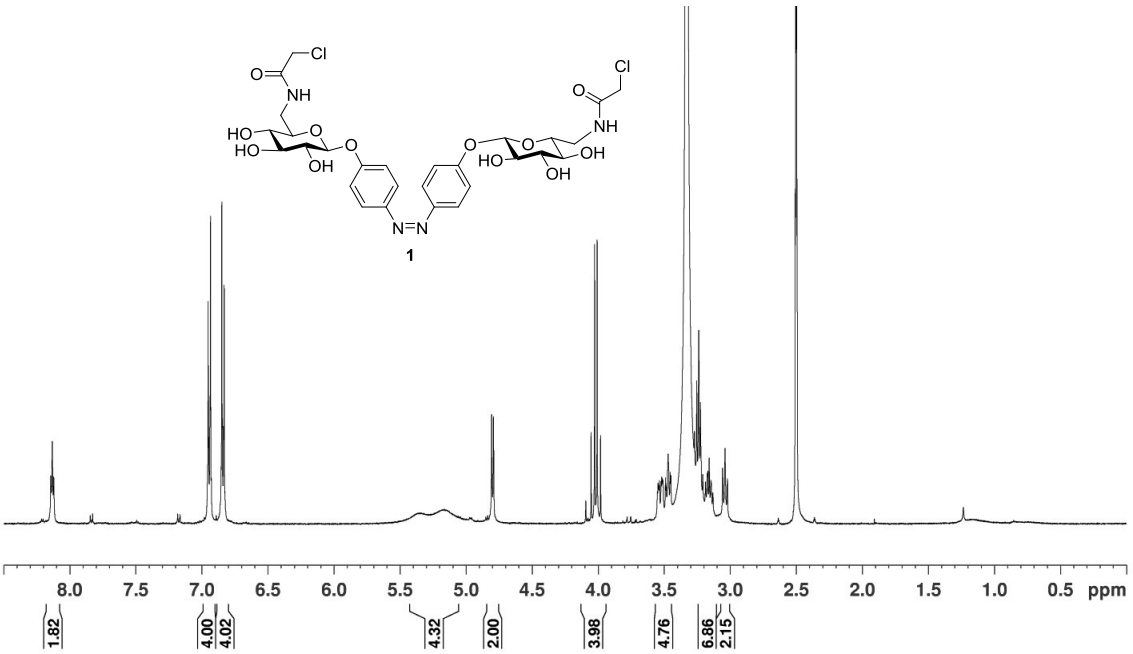

Figure S49. ^{1}H NMR spectrum of (*Z*)-**1** (500 MHz, DMSO-d_6, 300.0 K).

^{1}H NMR (500 MHz, DMSO-d_6, 300 K): δ = 8.14 (dd~t, $^{3}J_{NH,H-6}$ = 5.6 Hz, $^{3}J_{NH,H-6'}$ = 5.0 Hz, 2H, NH), 6.96-6.93 (m, 4H, Ar-H$_{ortho}$), 6.86-6.83 (m, 4H, Ar-H$_{meta}$), 5.36 (d, ^{3}J = 4.9 Hz, 2H, OH), 5.17-5.15 (m, 4H, OH), 4.80 (d, $^{3}J_{1,2}$ = 7.4 Hz, 2H, H-1), 4.04 (d, $^{2}J_{CHCl,CH'Cl}$ = 13.2 Hz, 2H, CHCl), 4.00 (d, $^{2}J_{CHCl,CH'Cl}$ = 13.2 Hz, 2H, CH'Cl), 3.53 (ddd, $^{3}J_{NH,H-6}$ = 5.0 Hz, $^{3}J_{5,6}$ = 2.6 Hz, $^{2}J_{6,6'}$ = 13.7 Hz, 2H, H-6), 3.49-3.45 (m, 2H, H-5), 3.28-3.14 (m, 6H, H-2, H-3, H-6), 3.04 (ddd~dt, $^{3}J_{4,5}$ = 8.8 Hz, $^{3}J_{3,4}$ = 8.7 Hz, $^{3}J_{OH,4}$ = 5.3 Hz, 2H, H-4) ppm.

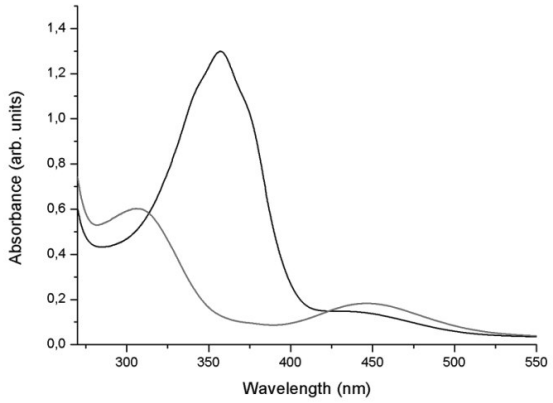

Figure S50. UV-Vis spectra of **1**: *E* isomer in black, *Z* isomer in red; irradiation with 365 nm and 440 nm, respectively, in DMSO-d_6 at 293 K.

(*Z*)-*p*-(*p'*-Allyloxy-phenylazo)phenyl 2-*O*-allyl-α-D-mannopyranoside (**2**):

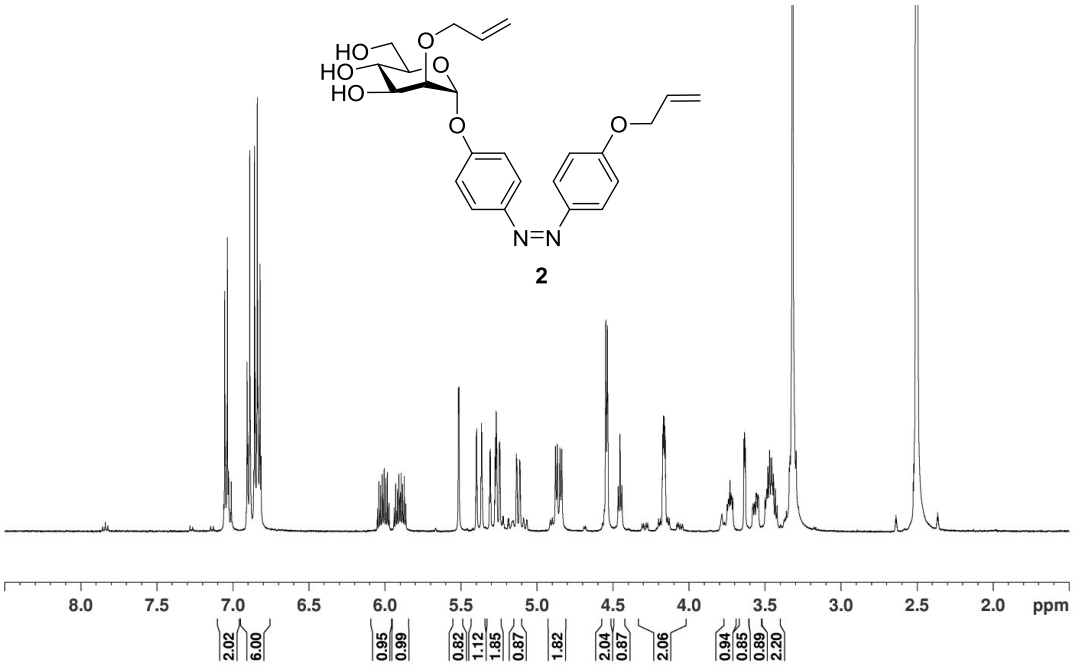

Figure S51. ^{1}H NMR spectrum of (*Z*)-**2** (500 MHz, DMSO-d_6, 300.0 K).

^{1}H NMR (500 MHz, DMSO-d_6, 300 K): δ = 7.06-7.03 (m, 2H, Ar-H$_{ortho}$), 6.91-6.82 (m, 6H, Ar-H$_{ortho'}$, Ar-H$_{meta'}$, Ar-H$_{meta}$), 6.01 (ddt, $^{3}J_{CH=CH2,CH=CH}$ = 17.3 Hz, $^{3}J_{CH=CH2,CH=CH'}$ = 10.6 Hz, $^{3}J_{OCH2,CH=CH2}$ = 5.3 Hz, 1H, C*H*=CH$_2$(Phenyl)), 5.90 (ddt, $^{3}J_{CH=CH2,CH=CH}$ = 17.2 Hz, $^{3}J_{CH=CH2,CH=CH'}$ = 10.6 Hz, $^{3}J_{OCH2,CH=CH2}$ = 5.4 Hz, 1H, C*H*=CH$_2$(Man)), 5.52 (d, $^{3}J_{1,2}$ = 1.7 Hz, 1H, H-1), 5.38 (ddt~qd, $^{4}J_{OCH2,CH=CH}$ = 1.6 Hz, $^{3}J_{CH=CH2,CH=CH}$ = 17.3 Hz, $^{2}J_{CH=CH,CH=CH'}$ = 1.6 Hz 1H, CH=C*H*(Phenyl)), 5.32-5.24 (m, 2H, CH=C*H*(Man), CH=C*H'*(Phenyl)), 5.12 (ddt~ddd, $^{4}J_{OCH2,CH=CH'}$ = 1.6 Hz, $^{3}J_{CH=CH2,CH=CH'}$ = 10.6 Hz, $^{2}J_{CH=CH,CH=CH'}$ = 3.4 Hz, 1H, CH=C*H'*(Man)), 4.87 (d, $^{3}J_{OH,H-3}$ = 5.7 Hz, 1H, 3-OH), 4.84 (d, $^{3}J_{OH,H-4}$ = 5.9 Hz, 1H, 4-OH), 4.54 (ddd~dt, $^{4}J_{OCH2,CH=CH'}$ = 1.4 Hz, $^{4}J_{OCH2,CH=CH}$ = 1.4 Hz, $^{3}J_{OCH2,CH=CH2}$ = 5.3 Hz, 2H, OCH$_2$(Phenyl)), 4.46 (dd~t, $^{3}J_{OH,H-6}$ = 6.0 Hz, $^{3}J_{OH,H-6'}$ = 6.0 Hz, 1H, 6-OH), 4.20-4.13 (m, 2H, OCH$_2$(Man)), 3.73 (ddd, $^{3}J_{2,3}$ = 3.4 Hz, $^{3}J_{3,4}$ = 9.1 Hz, $^{3}J_{OH,H-3}$ = 5.7 Hz, 1H, H-3), 3.64 (dd, $^{3}J_{1,2}$ = 1.7 Hz, $^{3}J_{2,3}$ = 3.3 Hz, 1H, H-2), 3.56 (ddd, $^{3}J_{5,6}$ = 2.0 Hz, $^{2}J_{6,6'}$ = 11.7 Hz, $^{3}J_{OH,H-6}$ = 5.8 Hz, 1H, H-6), 3.50-3.42 (m, 2H, H-4, H-6'), 3.34-3.30 (m,1H, H-5) ppm.

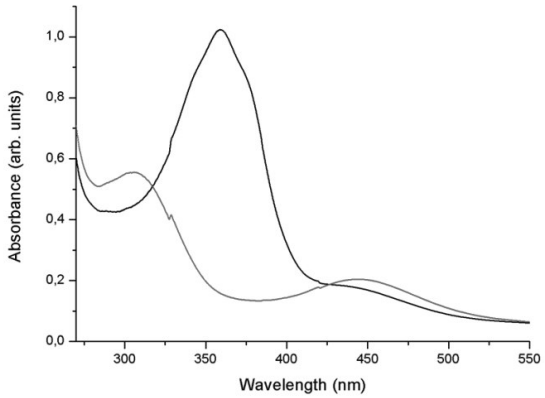

Figure S52. UV-Vis spectra of **2**: *E* isomer in black, *Z* isomer in red; irradiation with 365 nm and 440 nm, respectively, in DMSO-d_6 at 293 K. (Dents in graphs are caused by change of lamp).

(*Z*)-*p*,*p'*-Di-[(2-*O*-allyl-α-D-mannopyranosyloxy)]azobenzene (3):

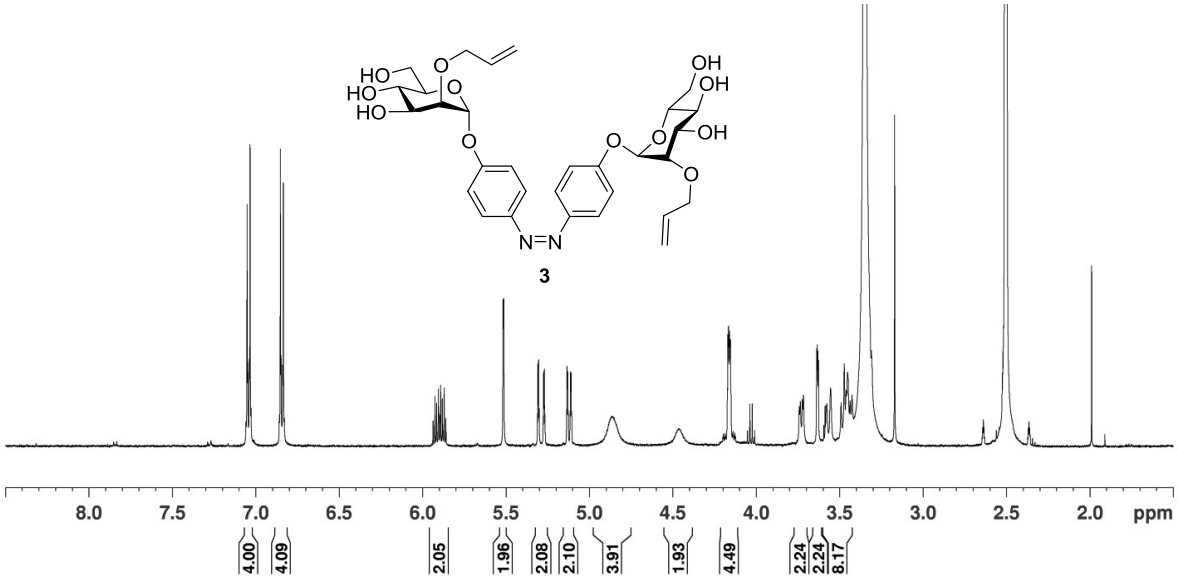

Figure S53. ^{1}H NMR spectrum of (*Z*)-**3** (500 MHz, DMSO-d_6, 300.0 K).

^{1}H NMR (500 MHz, DMSO-d_6, 300 K): δ=7.06-7.03 (m, 4H, Ar-H$_{ortho}$), 6.86-6.83 (m, 4H, Ar-H$_{meta}$), 5.90 (ddt, $^{3}J_{CH=CH2,CH=CH}$ = 17.3 Hz, $^{3}J_{CH=CH2,CH=CH'}$ = 10.7 Hz, $^{3}J_{OCH2,CH=CH2}$ = 5.4 Hz, 1H, C*H*=CH$_2$), 5.52 (d, $^{3}J_{1,2}$ = 1.7 Hz, 1H, H-1), 5.29 (ddt, $^{4}J_{OCH2,CH=CH}$ = 1.7 Hz, $^{3}J_{CH=CH2,CH=CH}$ = 17.3 Hz, $^{2}J_{CH=CH,CH=CH'}$ = 3.7 Hz 1H, CH=C*H*), 5.12 (ddd, $^{4}J_{OCH2,CH=CH'}$ = 3.7 Hz, $^{3}J_{CH=CH2,CH=CH'}$ = 10.7 Hz, $^{2}J_{CH=CH,CH=CH'}$ = 1.7 Hz, 1H, CH=C*H'*), 4.87 (br s, 4H, 4-OH, 3-OH), 4.46 (br s, 2H, 6-OH), 4.20-4.13 (m, 4H, OCH$_2$), 3.73 (dd, $^{3}J_{2,3}$ = 3.2 Hz, $^{3}J_{3,4}$ = 9.4 Hz, 2H, H-3), 3.63 (dd, $^{3}J_{1,2}$ = 1.7 Hz, $^{3}J_{2,3}$ = 3.2 Hz, 2H, H-2), 3.60-3.43 (m, 8H, H-4, H-5, H-6, H-6') ppm.

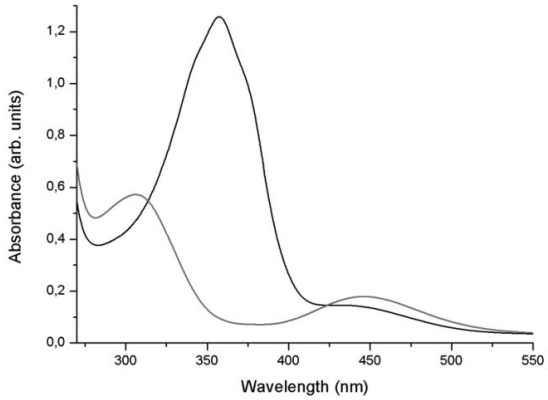

Figure S54. UV-Vis spectra of **3**: *E* isomer in black, *Z* isomer in red; irradiation with 365 nm and 440 nm, respectively, in DMSO-d_6 at 293 K.

(*Z*)-*p*,*p'*-Di-(allyloxy)azobenzene (15):[

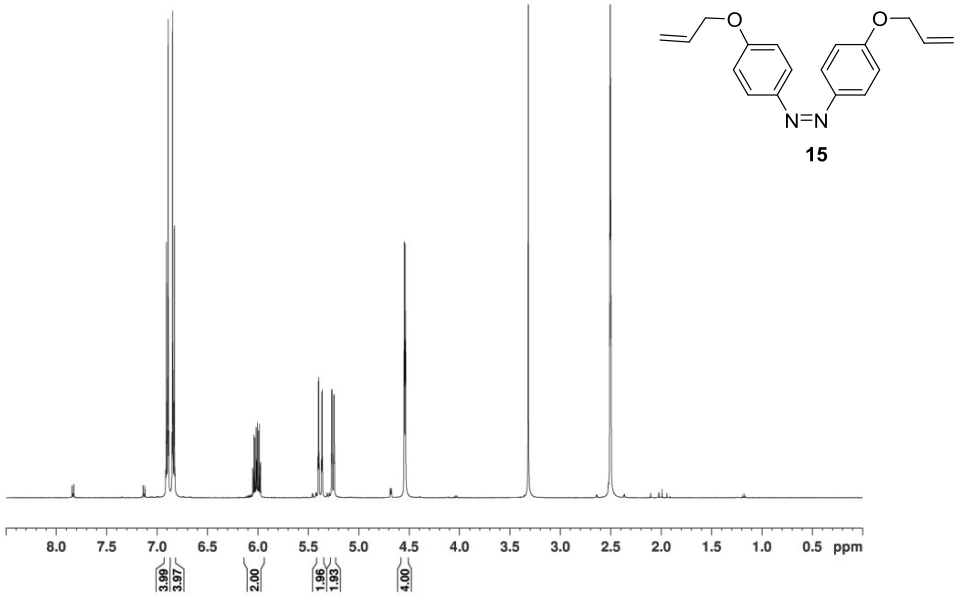

Figure S55. ^{1}H NMR spectrum of (*Z*)-**15** (500 MHz, DMSO-d_6, 300.1 K).

^{1}H NMR (500 MHz, DMSO-d_6, 300 K): δ=6.91-7.89 (m, 4H, Ar-H$_{ortho}$), 6.85-6.82 (m, 4H, Ar-H$_{meta}$), 6.01 (ddt, $^{3}J_{CH=CH2,CH=CH}$ = 17.3 Hz, $^{3}J_{CH=CH2,CH=CH'}$ = 10.6 Hz, $^{3}J_{OCH2,CH=CH2}$ = 5.3 Hz, 1H, C*H*=CH$_2$), 5.38 (ddt, $^{4}J_{OCH2,CH=CH}$ = 1.6 Hz, $^{3}J_{CH=CH2,CH=CH}$ = 17.3 Hz, $^{2}J_{CH=CH,CH=CH'}$ = 1.6 Hz 1H, CH=C*H*), 5.26 (ddd, $^{4}J_{OCH2,CH=CH'}$=1.6 Hz, $^{3}J_{CH=CH2,CH=CH'}$ = 10.6 Hz, $^{2}J_{CH=CH,CH=CH'}$ = 1.6 Hz, 1H, CH=C*H'*), 4.54 (dt, $^{3}J_{OCH2,CH=CH2}$ = 5.3 Hz, $^{4}J_{OCH2,CH=CH'}$ = 1.6 Hz, $^{4}J_{OCH2,CH=CH}$ = 1.6 Hz, 4H, OCH$_2$) ppm.

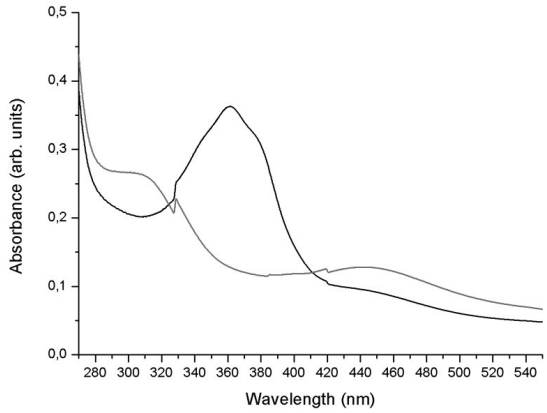

Figure S56. UV-Vis spectra of **15**: *E* isomer in black, *Z* isomer in red; irradiation with 365 nm and 440 nm, respectively, in DMSO-d_6 at 293 K. (Dents in graphs are caused by change of lamp).

Table S1. Characterization of the *E* and *Z* isomer of the azobenzene derivative **15**.

***E*/*Z* (PSS)[a]**	**λ_{max} (*E* and *Z*) [nm]**	**half-life, $\tau_{1/2}$ [h]**
3:97	361.5 447.7	25.8

[a] According to the integration ratio of aromatic protons in the ^{1}H NMR spectra.

4.

MALDI-TOF and LC-MS spectra of the cross-linked peptide 44

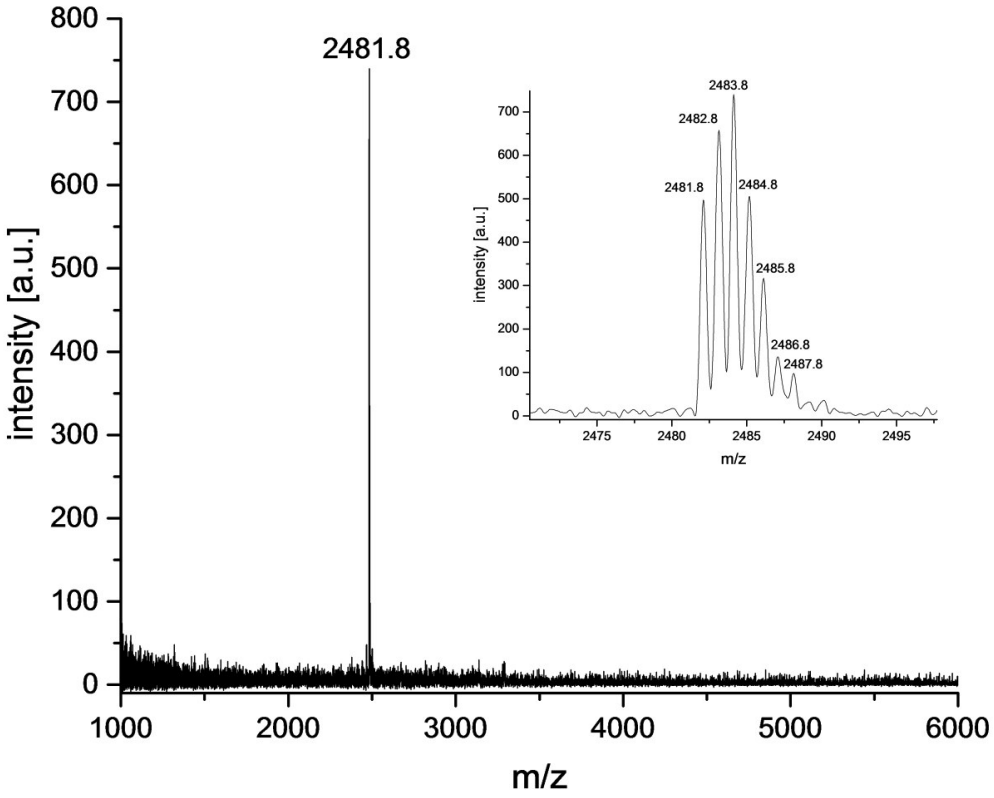

Figure S57. MALDI-TOF MS spectra of the peptide **44** (M^+ = 2481.8).

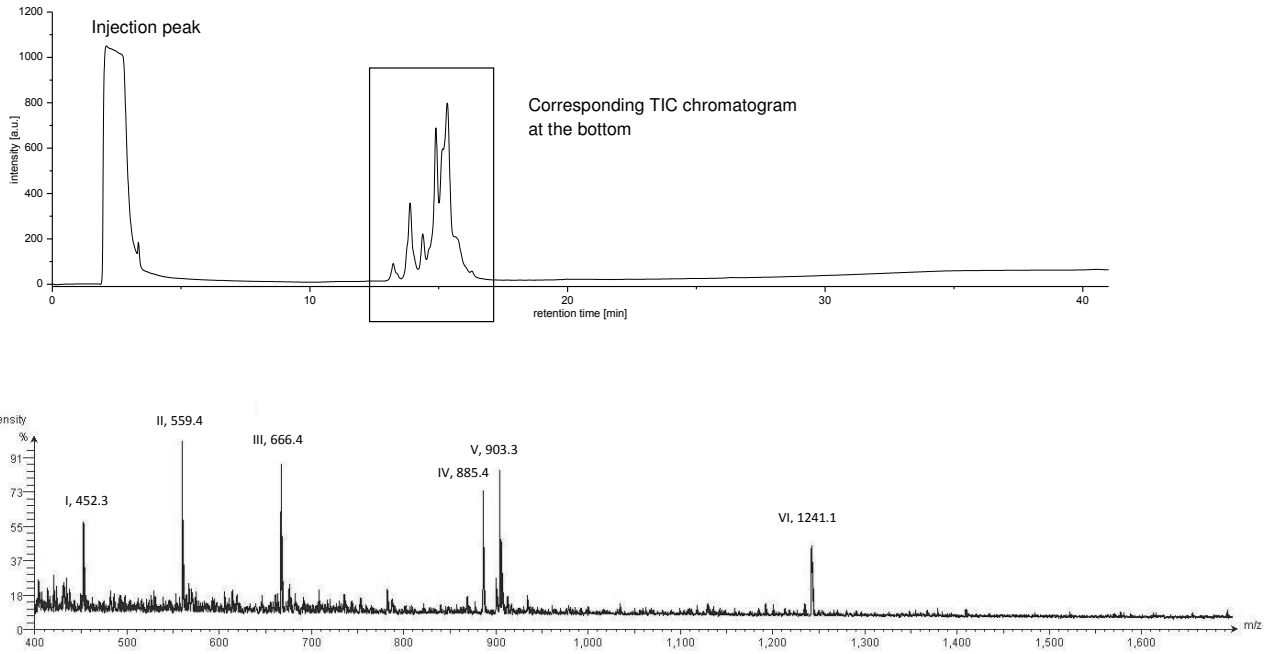

Figure S58. UV chromatogram (top) and corresponding TIC (total ion current) chromatogram of crude peptide **44** (bottom; elution time 12-18 min).

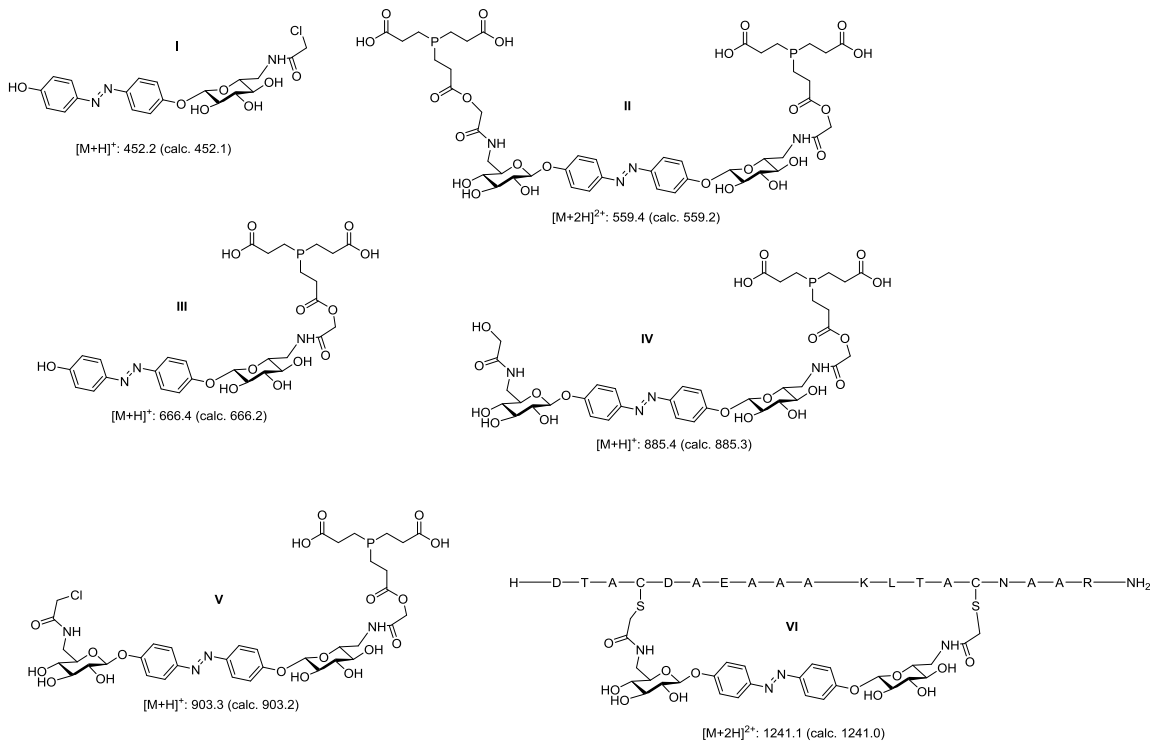

Figure S59. Structures of side products of the cross-linking reaction of **1** and **43** as deduced from the TIC of the crude cross-linked product **44** (cf. Figure S58).

5. Distance measurements of 1, 2, and 3

For all molecules, the end groups can come into direct VDW contact (minimal distance) owing to the conformational freedom. Maximal distances were estimated for extended rotamer conformations, drawn in ChemDraw and optimized by energy minimization with MM2 in Chem3DPro. The distances were measured between the α-carbon atoms of the chloroacetamide groups (**1**) or the terminal allyl group carbons (**2** and **3**) (Table S2).

Table S2. Distance measurements for the azobenzene glycoconjugates **1**, **2**, and **3**.

Azobenzene glycoconjugate	**Configuration**	**Approx. maximum distance (Å)**
1	*E* *Z*	23.3 22.3
2	*E* *Z*	20.4 17.6
3	*E* *Z*	22.3 18.6

6. References

[1] V. Maunier, P. Boullanger, D. Lafont, D. Y. Chevalier, *Carbohydr. Res.***1997**, *299*, 49-57.

[2] S. Mehta, M. Meldal, V. Ferro, J. Duus, K. Bock, J. *Chem. Soc., Perkin Trans. 1* **1997**, 1365-1374.

[3] C.-W. T. Chang, Y. Hui, B. Elchert, J. Wang, J. Li, R. Rai, *Org. Lett*. **2002**, *4*, 4603-4606.

[4] a) A. Shukurov, S. D. Nasirdinov, A. G. Makhsumov, N. N. Edgarov, *J. Gen. Chem. USSR (Engl. Transl.)* **1986**, *56*, 2579-2582; b) *ibid*. 2282-2284; c) S. Guo, W. Chaikittisilp, T. Okubo, A. Shimojima, *RSC Adv*. **2014**, *4*, 25319-25325.

8.1.2 Supporting information for the publication *Synthesis of heterobifunctional azobenzene glycoconjugates for bioorthogonal cross- linking of proteins*

Supporting Information

for

Synthesis of heterobifunctional azobenzene glycoconjugates for bioorthogonal cross- linking of proteins

A. Müller, T. K. Lindhorst

Electronic Supporting Information

Synthesis of heterobifunctional azobenzene glycoconjugates for bioorthogonal cross-linking of proteins

Anne Müller, Thisbe K. Lindhorst*

List of contents

1. Materials and methods

General methods

N-Boc-4-hydroxyaniline (**1**) was purchased from Sigma Aldrich and used without further purification. Moisture sensitive reactions were carried out in dry glassware and under a positive pressure of nitrogen. Analytical thin layer chromatography (TLC) was performed on silica-gel plates (GF 254, Merck). Visualization was achieved by UV light and/or with 10% sulfuric acid in ethanol followed by heat treatment at ~180 °C. Flash chromatography was performed on silica gel 60 (Merck, 230-400 mesh, particle size 0.040-0.063 mm) by using distilled solvents. Acetonitrile was dried over calcium hydride and methanol was dried over magnesium under a nitrogen atmosphere. Dry *N*,*N*-dimethylformamide over molecular sieves were purchased from Acros Organics and used without further purification. Melting points (mp) were determined on a Büchi M-56 apparatus. Optical rotations were measured with a Perkin-Elmer 241 polarimeter (sodium D-line: 589 nm, length of cell: 1 dm) in the solvents indicated. Proton (^{1}H) nuclear magnetic resonance spectra and carbon (^{13}C) nuclear magnetic resonance spectra were recorded on a Bruker DRX-500 and AV-600 spectrometer. Chemical shifts are referenced to internal tetramethylsilane or to the residual proton of the NMR solvent. Data are presented as follows: chemical shift, multiplicity (s=singlet, d=doublet, t=triplet, q=quartet, m=multiplet, and br=broad signal), coupling constant in hertz (Hz) and, integration. Full assignment of the peaks was achieved with the aid of 2D NMR techniques (^{1}H/^{1}H COSY and ^{1}H/^{13}C HSQC. For photostationary state (PSS) determination, all ^{1}H NMR spectra were recorded in DMSO-d_6 (cf. Table 1). All NMR spectra of the *E*-isomers of the azobenzene derivatives were recorded after they were kept for 16 h in the dark at 40 °C. Infrared (IR) spectra were measured with a Perkin Elmer FT-IR Paragon 1000 (ATR) spectrometer and were reported in cm^{-1}. ESI mass spectra were recorded on a LCQ Classic from Thermo Finnigan and HRMS ESI spectra on an Agilent 6224 ESI-TOF. Photoirradiation was performed using LED (emitting 365 nm light). From the Nichia Corporation (NC4U133A) with a FWHW of 9 nm and optical power output (PO) ~1 W. UV-Vis absorption spectra were performed on Perkin-Elmer Lambda-241 at a temperature of 20 °C ± 1 °C. Extinction coefficients (ε) were deduced from UV-Vis spectra measured at six different concentrations (10 µm, 20 µm, 40 µm, 60 µm, 80 µm and 90 µm).

2. Synthesis of azobenzene derivatives

***N*-Boc-amino-4-(propargyloxy)benzene (2):**[1] To a suspension of *N*-Boc-4-hydroxyaniline (**1**, 3.83 g, 18.3 mmmol) and potassium carbonate (2.53 g, 18.3 mmol) in acetonitrile (105 mL) propargyl bromide (80% in toluene, 2.00 mL, 18.3 mmol) was added. The reaction mixture was stirred for 7 h at 80 °C and for 16 h at room temperature. Then ethyl acetate (100 mL) and water (100 mL) were added, the phases separated and the organic phase was washed with water (3 × 70 mL) and saturated aq. NaCl solution (3 × 70 mL). It was dried over $MgSO_4$, filtered and the filtrate was concentrated under reduced pressure. Purification of the crude product by column chromatography (cyclohexane/ethyl acetate, 4:1) gave **2** as a colorless solid (4.06 g, 17.6 mmol, 96%). R_f=0.33 (cyclohexane/ethyl acetate, 4:1); m.p. 78°C; ^{1}H NMR (600 MHz, $CDCl_3$, 300 K, TMS): δ=7.30-7.26 (m, 2H, Ar-H$_{meta}$), 6.93-6.89 (m, 2H, Ar-H$_{ortho}$), 6.37 (br s, 1H, NH), 4.65 (d, $^4J_{OCH2,C≡CH}$=2.4 Hz, 2H, OCH_2), 2.50 (t, $^4J_{OCH2,C≡CH}$=2.4 Hz, 1H, C≡CH), 1.51 (s, 9H, $C(CH_3)_3$) ppm; ^{13}C NMR (150 MHz, $CDCl_3$, 300 K, TMS): δ=153.6 (C-Ar$_{para}$), 153.1 (C=O), 132.4 (C-Ar$_{ipso}$), 120.4 (C-Ar$_{meta}$), 115.5 (C-Ar$_{ortho}$), 80.4 (*C*$(CH_3)_3$), 78.7 (*C*≡CH), 75.4 (C≡*C*H), 56.3 (OCH_2), 28.4 (C(*C*$H_3)_3$) ppm; IR (ATR): $\tilde{\nu}$ =3362, 3283, 2983, 1690, 1513, 1229, 1155, 1022, 919, 823, 811 cm^{-1}; HRMS (EI, 70 eV): *m/z* calcd for $C_{14}H_{17}NO_3$: 247.1208 [M]; found 247.1205.

4-(Propargyloxy)aniline-TFA salt (3):[2] Trifluoroacetic acid (8 mL) was added to a solution of **2** (1.36 g, 5.86 mmol) in dichloromethane (80 mL). The reaction mixture was stirred for 30 min at room temperature. Afterwards the solvent was evaporated and **3** was obtained as a colorless solid (1.52 g, quant) and could be used without further purification. R_f=0.21 (dichloromethane/methanol, 10:1); m.p. 137°C; ^{1}H NMR (500 MHz, MeOH-*d*$_4$, 300 K): δ=7.39-7.35 (m, 2H, Ar-H$_{meta}$), 7.18-7.15 (m, 2H, Ar-H$_{ortho}$), 4.82 (d, $^4J_{OCH2,C≡CH}$=2.5 Hz, 2H, OCH_2), 3.01 (t, $^4J_{OCH2,C≡CH}$=2.5 Hz, 1H, C≡CH) ppm; ^{13}C NMR (126 MHz, MeOH-*d*$_4$, 300 K): δ=159.3 (C-Ar$_{para}$), 125.2 (C-Ar$_{ipso}$), 125.1 (C-Ar$_{meta}$), 117.4 (C-Ar$_{ortho}$), 79.2 (*C*≡CH), 77.3 (C≡*C*H), 57.0 (OCH_2) ppm; IR (ATR): $\tilde{\nu}$ =3309, 2909, 2632, 1674, 1639, 1589, 1121, 1022, 1024, 836 cm^{-1}; EI-MS (70 eV): *m/z* (%): 147.08 (30) $[M]^+$, 108.05 (100) $[C_6H_6NO]^+$.

(*E*)-*p*-[*p*′-(Propargyloxy)phenylazo]phenol (4)[3] was obtained by employing a new procedure: To an ice-cold solution of 4-(propargyloxy)aniline·TFA (**3**, 3.21 g, 13.1 mmol) and hydrochloric acid (37%, 1.02 mL, 13.1 mmol) in water (38 ml) was added dropwise an ice-cold solution of sodium nitrite (903 mg, 13.1 mmol) in water (38 mL). The reaction mixture was then stirred for 2 h at 0 °C. Afterwards the above mixture was added dropwise to a cold solution of phenol (1.23 g, 13.1 mmol), sodium hydroxide (523 mg, 13.1 mmol) and sodium carbonate (1.46 g, 13.7 mmol) in water (38 mL). The reaction mixture was stirred for 2 h at 0 °C. Then the reaction was acidified by adding hydrochloric acid and the precipitated solid was filtered off and washed with water. The crude product was recrystallized from a mixture of methanol and water (1:1). The azobenzene derivative **4** was obtained as an orange solid (2.12 g, 8.42 mmol, 64%). R_f=0.32 (cyclohexane/ethyl acetate, 4:1); m.p. 139 °C; ^{1}H NMR (500 MHz, MeOH-*d*$_4$, 300 K): δ=7.84-7.76 (m, 4H, Ar-H$_{ortho}$, Ar-H$_{ortho'}$), 7.12-7.09 (m, 2H, Ar-H$_{meta'}$), 6.91-6.88 (m, 2H, Ar-H$_{meta}$), 4.81 (d, $^4J_{OCH2,C≡CH}$=2.4 Hz, 2H, OCH_2), 2.98 (t, $^4J_{OCH2,C≡CH}$=2.4 Hz, 1H, C≡CH) ppm; ^{13}C NMR (126 MHz, MeOH-*d*$_4$, 300 K): δ=161.6 (C-Ar$_{para'}$), 161.0 (C-Ar$_{para}$), 148.8 (C-Ar$_{ipso}$), 147.5 (C-Ar$_{ipso'}$), 125.6 (C-Ar$_{ortho}$), 125.0 (C-Ar$_{ortho'}$), 116.7 (C-Ar$_{meta'}$), 116.3 (C-Ar$_{meta}$), 79.5 (*C*≡CH), 77.1 (C≡*C*H), 56.9 (OCH_2) ppm; IR (ATR): $\tilde{\nu}$ =3264, 3140, 1588, 1503, 1220, 1157, 1029, 826 cm^{-1}; HRMS (EI, 70 eV): *m/z* calcd for $C_{15}H_{12}N_2O_2$: 252.0900 [M]; found 252.0900.

(*E*)-[*p*-(Allyloxy)-*p*′-(propargyloxy)]azobenzene (5): To an ice-cold solution of **4** (467 mg, 1.85 mmol) in dry dimethylformamide (15 mL) sodium hydride (60% dispersion in mineral oil, 78.0 mg, 2.04 mmol) was added slowly and stirred for 30 min at 0 °C. Then allyl bromide (500 µL, 5.55 mmol) was added and the reaction mixture was stirred for 16 h at room temperature. Afterwards ice water (20 mL) was added, the phases separated and the aqueous phase extracted with ethyl acetate (2 × 20 mL). It was dried over $MgSO_4$, filtered and the filtrate was concentrated under reduced pressure. The crude product was recrystallized from a mixture of acetonitrile and methanol (1:1) and gave **5** as an orange solid (412 mg, 1.41 mmol, 76%). R_f=0.64 (cyclohexane/ethyl acetate, 7:1); m.p. 169 °C; ^{1}H NMR (600 MHz, $CDCl_3$, 300 K, TMS): δ=7.89-7.86 (m, 4H, Ar-H$_{ortho}$, Ar-H$_{ortho'}$), 7.10-7.07 (m, 2H, Ar-H$_{meta'}$), 7.03-7.01 (m, 2H, Ar-H$_{meta}$), 6.08 (ddt, $^3J_{CH=CH2,CH=CH}$=15.9 Hz, $^3J_{CH=CH2,CH=CH'}$=10.6 Hz, $^3J_{OCH2Allyl,CH=CH2}$=5.3 Hz, 1H, C*H*=CH_2), 5.47-543 (m, 1H, CH=C*H*), 5.34-5.31 (m, 1H, CH=C*H*′), 4.77 (d, $^4J_{OCH2,C≡CH}$=2.4 Hz, 2H, $OCH_{2Propragyl}$), 4.63-4.61 (m, 2H, OCH_{2Allyl}), 2.56 (t, $^4J_{OCH2,C≡CH}$=2.4 Hz, 1H, C≡CH) ppm; ^{13}C NMR (151 MHz, $CDCl_3$, 300 K, TMS): δ=161.6 (C-Ar$_{para}$), 159.3 (C-Ar$_{para'}$), 147.6 (C-Ar$_{ipso}$), 147.1 (C-Ar$_{ipso'}$), 132.8 (*C*H=CH_2), 124.4 (C-Ar$_{ortho}$), 124.3 (C-Ar$_{ortho'}$), 118.0 (CH=*C*H_2), 115.1 (C-Ar$_{meta'}$), 114.9 (C-Ar$_{meta}$),

69.0 (OCH_{2Allyl}), 56.0 ($OCH_{2Propargyl}$) ppm; IR (ATR): $\tilde{\nu}$ =3273, 2916, 1594, 1579, 1495, 1231, 946, 841 cm^{-1}; UV-Vis (DMSO): λ^{max} (ε)=360 nm (20484 L mol^{-1} cm^{-1}); HRMS (EI, 70 eV): *m/z* calcd for $C_{18}H_{16}N_2O_2$: 292.1212 [M]; found 292.1215.

(*E*)-[*p*-(3-(Acetylthio)propoxy)-*p'*-(propargyloxy)]azobenzene (6): To a solution of **4** (111 mg, 440 µmol) and *S*-3-bromopropyl ethanethioate in dimethylformamide (5 mL) potassium iodide (7.00 mg, 44.0 µmol) as well as potassium carbonate (243 mg, 1.76 mmol) were added. The reaction mixture was stirred for 4 h at 80 °C and 16 h at room temperature. Then the solvent was removed under reduced pressure and the crude product was dissolved in dichloromethane (30 mL). The organic phase was washed with water (3 × 20 mL). It was dried over $MgSO_4$, filtered and the filtrate was concentrated under reduced pressure. Purification of the crude product by column chromatography (toluene) gave **6** as a yellow solid (114 mg, 309 µmol, 70%). R_f=0.64 (cyclohexane/ethyl acetate, 7:1); m.p. 107 °C; ^{1}H NMR (500 MHz, $CDCl_3$, 300 K, TMS): δ=7.90-7.85 (m, 4H, Ar-H_{ortho}, Ar-$H_{ortho'}$), 7.09-7.06 (m, 2H, Ar-$H_{meta'}$), 7.00-6.97 (m, 2H, Ar-H_{meta}), 4.76 (d, $^4J_{OCH2,C\equiv CH}$=2.3 Hz, 2H, $OCH_{2Propragyl}$), 4.09 (t, $^3J_{OCH2CH2,OCH2CH2}$=6.1 Hz, 2H, OCH_2CH_2), 3.08 (t, $^3J_{CH2SAc,OCH2CH2}$=7.1 Hz, 2H, CH_2SAc), 2.56 (t, $^4J_{OCH2,C\equiv CH}$=2.4 Hz, 1H, C≡CH), 2.25 (s, 3H, CH_3), 2.13-2.08 (m, 2H, OCH_2CH_2) ppm; ^{13}C NMR (126 MHz, $CDCl_3$, 300 K, TMS): δ=195.7 (C=O), 160.9 (C-Ar_{para}), 159.4 (C-$Ar_{para'}$), 147.6 (C-Ar_{ipso}), 147.1 (C-$Ar_{ipso'}$), 124.4 (C-Ar_{ortho}), 124.3 (C-$Ar_{ortho'}$), 115.1 (C-$Ar_{meta'}$), 114.7 (C-Ar_{meta}), 78.1 (*C*≡CH), 75.9 (C≡*C*H), 66.5 (OCH_2CH_2), 56.0 ($OCH_{2Propargyl}$), 30.6 (CH_3), 29.3 (OCH_2CH_2), 25.8 (CH_2SAc) ppm; IR (ATR): $\tilde{\nu}$ =3279, 2927, 1688, 1580, 1496, 1235, 1146, 1015, 842 cm^{-1}; HRMS (EI, 70 eV): *m/z* calcd for $C_{20}H_{20}N_2O_3S$: 368.1195 [M]; found 368.1193.

(*E*)-[*p*-(3-Mercaptopropoxy)-*p'*-(propargyloxy)]azobenzene (7): To a solution of **6** (114 mg, 309 µmol) in dry methanol (4 mL) a solution of sodium methylate in methanol (1 M, 460 µL) was added and the reaction mixture was stirred for 2 h at room temperature. After neutralization with Amberlite IR120®, the solvent was removed under reduced pressure. Purification of the crude product by column chromatography (toluene) gave **7** as a yellow solid (91.0 mg, 278 µmol, 90%). R_f=0.64 (cyclohexane/ethyl acetate, 7:1); m.p. 131 °C; ^{1}H NMR (500 MHz, $CDCl_3$, 300 K, TMS): δ=7.90-7.86 (m, 4H, Ar-H_{ortho}, Ar-$H_{ortho'}$), 7.10-7.06 (m, 2H, Ar-$H_{meta'}$), 7.01-6.97 (m, 2H, Ar-H_{meta}), 4.77 (d, $^4J_{OCH2,C\equiv CH}$=2.4 Hz, 2H, $OCH_{2Propragyl}$), 4.16 (t, $^3J_{OCH2CH2,OCH2CH2}$=6.0 Hz, 2H, OCH_2CH_2), 2.78-2.74 (m, 2H, CH_2SH), 2.56 (t, $^4J_{OCH2,C\equiv CH}$=2.4 Hz, 1H, C≡CH), 2.14-2.09 (m, 2H, OCH_2CH_2), 1.41 (t, $^3J_{CH2SH,SH}$=8.1 Hz, 1H, SH) ppm; ^{13}C NMR (126 MHz, $CDCl_3$, 300 K, TMS): δ=160.9 (C-Ar_{para}), 159.4 (C-$Ar_{para'}$), 147.6 (C-Ar_{ipso}), 147.1 (C-$Ar_{ipso'}$), 124.4 (C-Ar_{ortho}), 124.3 (C-$Ar_{ortho'}$), 115.1 (C-$Ar_{meta'}$), 114.7 (C-Ar_{meta}), 78.1 (*C*≡CH), 76.0 (C≡*C*H), 65.9 (OCH_2CH_2), 56.0 ($OCH_{2Propargyl}$), 33.3 (OCH_2CH_2), 21.2 (CH_2SH) ppm; IR (ATR): $\tilde{\nu}$ =3278, 2930, 1595, 1497, 1235, 1146, 1015, 844 cm^{-1}; UV-Vis (DMSO): λ^{max} (ε)=362 nm (19872 L mol^{-1} cm^{-1}); HRMS (EI, 70 eV): *m/z* calcd for $C_{18}H_{18}N_2O_2S$: 326.1089 [M]; found 326.1081.

(*E*)-*p*-[*p'*-(Propargyloxy)]phenylazophenyl α-D-mannopyranoside (9)[3] was obtained by employing a new procedure: The acetyl-protected mannoside **8**[4] (850 mg, 1.46 mmol) was dissolved in methanol (15 mL) and potassium carbonate (40.0 mg, 292 µmol) was added. The reaction mixture was stirred for 16 h at room temperature. Then the solvent was evaporated and the crude product was recrystallized from a mixture of methanol and water (1:1). The mannoside **9** was obtained as an orange solid (476 mg, 1.15 mmol, 79%). R_f=0.30 (ethyl acetate/methanol, 8:1); m.p. 227 °C; $[\alpha]_D^{23}$=+25.7 (*c*=0.5 in methanol); ^{1}H NMR (600 MHz, DMSO-d_6, 298 K): δ=7.87-7.82 (m, 4H, Ar-H_{ortho}, Ar-$H_{ortho'}$), 7.27-7.25 (m, 2H, Ar-$H_{meta'}$), 7.19-7.16 (m, 2H, Ar-H_{meta}), 5.51 (d, $^3J_{1,2}$=1.5 Hz, 1H, H-1), 5.09 (d, $^3J_{2,OH}$=4.4 Hz, 1H, OH_{C-2}), 4.92 (d, $^4J_{OCH2,C\equiv CH}$=2.3 Hz, 2H, $OCH_{2Propragyl}$), 4.86 (d, $^3J_{3,OH}$=5.9 Hz, 1H, OH_{C-3}), 4.80 (d, $^3J_{4,OH}$=6.0 Hz, 1H, OH_{C-4}), 4.47 (t~dd, $^3J_{6,OH}$=6.0 Hz, $^3J_{6',OH}$=6.0 Hz, 1H, OH_{C-6}), 3.87-3.86 (m, 1H, H-2), 3.71 (ddd, $^3J_{3,4}$=9.3 Hz, $^3J_{3,OH}$=5.9 Hz, $^3J_{2,3}$=3.4 Hz, 1H, H-3), 3.64 (t, $^4J_{OCH2,C\equiv CH}$=2.3 Hz, 1H, C≡CH), 3.60 (ddd, $^2J_{6,6'}$=11.8 Hz, $^3J_{6,OH}$=6.0 Hz, $^3J_{5,5}$=2.0 Hz, 1H, H-6), 3.54-3.46 (m, 2H, H-4, H-6'), 3.40-3.37 (m, 1H, H-5) ppm; ^{13}C NMR (150 MHz, DMSO-d_6, 298 K): δ=159.4 (C-$Ar_{para'}$), 158.5 (C-Ar_{para}), 146.9 (C-Ar_{ipso}), 146.6 (C-$Ar_{ipso'}$), 124.1 (C-Ar_{ortho}), 124.0 (C-$Ar_{ortho'}$), 117.1 (C-$Ar_{meta'}$), 115.5 (C-Ar_{meta}), 98.7 (C-1), 78.9 (*C*≡CH), 78.7 (C≡*C*H), 75.2 (C-5), 70.6 (C-3), 69.9 (C-2), 66.6 (C-4), 61.0 (C-6), 55.8 ($OCH_{2Propargyl}$) ppm; IR (ATR): $\tilde{\nu}$ =3400, 3291, 2939, 1580, 1493, 1227, 1123, 1008, 985, 840 cm^{-1}; ESI-MS: *m/z* calcd for $C_{21}H_{22}N_2O_7$: 437.1 $[M+Na]^+$; found 437.4.

(*E*)-*p*-[*p'*-(Propargyloxy)]phenylazophenyl 4,6-*O*-benzylidene-α-D-mannopyranoside (10): Benzaldehyde dimethyl acetal (180 µL, 1.22 mmol) and $HBF_4{\cdot}Et_2O$ (160 µL, 1.14 mmol) were added to a solution of the unprotected mannoside **9** (471 mg, 114 mmol) in dry dimethylformamide (15 mL). After the reaction mixture was stirred for 16 h at room temperature the reaction was quenched by adding triethylamine (160 µL,

1.14 mmol) and the solvent was evaporated. Purification of the crude product by column chromatography (cyclohexane/ethyl acetate, 3:1→2:1→1:1) gave **10** as an orange solid (437 mg, 870 µmol, 76%). R_f=0.33 (cyclohexane/ethyl acetate, 1:1); m.p. 193 °C; $[\alpha]_D^{23}$=+236.2 (*c*=0.5 in acetone); ^{1}H NMR (500 MHz, DMSO-*d*$_6$, 300 K): δ=7.88-7.83 (m, 4H, Ar-H$_{ortho}$, Ar-H$_{ortho'}$), 7.46-7.43 (m, 2H, Ar-H$_{Benz}$) , 7.38-7.35 (m, 3H, Ar-H$_{Benz}$), 7.28-7.25 (m, 2H, Ar-H$_{meta'}$), 7.19-7.16 (m, 2H, Ar-H$_{meta}$), 5.66 (d, $^3J_{1,2}$=1.1 Hz, 1H, H-1), 5.64 (s, 1H, CHPh), 5.51 (d, $^3J_{OH,2}$=4.4 Hz, 1H, OH$_{C-2}$), 5.23-5.22 (m, 1H, OH$_{C-3}$), 4.91 (d, $^4J_{OCH2,C\equiv CH}$=2.4 Hz, 2H, OCH$_{2Propragyl}$), 4.04-3.95 (m, 4H, H-2, H-3, H-4, H-6), 3.78-3.64 (m, 2H, H-5, H-6'), 3.61 (t, $^4J_{OCH2,C\equiv CH}$=2.4 Hz, 1H, C≡CH) ppm; ^{13}C NMR (125 MHz, DMSO-*d*$_6$, 300 K): δ=159.9 (C-Ar$_{para'}$), 158.2 (C-Ar$_{para}$), 147.6 (C-Ar$_{ipso}$), 147.1 (C-Ar$_{ipso'}$), 138.2 (C-Ar$_{Benz}$), 129.3 (C-Ar$_{Benz}$), 128.5 (C-Ar$_{Benz}$), 126.8 (C-Ar$_{Benz}$), 124.7 (C-Ar$_{ortho}$), 124.6 (C-Ar$_{ortho'}$), 117.5 (C- Ar$_{meta'}$), 115.9 (C-Ar$_{meta}$), 101.7 (*C*HPh), 99.3 (C-1), 79.3 (*C*≡CH), 79.1 (C-2), 78.6 (C≡*C*H), 71.0 (C-3), 68.2 (C-6), 67.8 (C-4), 65.5 (C-5), 56.3 (OCH$_{2Propargyl}$) ppm; IR (ATR): $\tilde{\nu}$ =3243, 2908, 1597, 1495, 1375, 1215, 1092, 992, 920, 841 cm^{-1}; ESI-MS: *m/z* calcd for $C_{28}H_{26}N_2O_7$: 525.2 $[M+Na]^+$; found 525.4.

(*E*)-*p*-[*p'*-(Propargyloxy)]phenylazophenyl 4,6-*O*-benzylidene-3-*O*-*p*-methoxybenzyl-α-D-mannopyranoside (11): To a solution of **10** (386 mg, 768 µmol) in dry methanol (35 mL) dibutyl tin oxide (249 mg, 999 µmol)) was added and reaction mixture was refluxed for 3 h at 70 °C. Afterwards the solvent was evaporated and the crude product was dissolved in dry dimethylformamide (35 mL). Then TBAI (142 mg, 384 µmol) and *p*-methoxy benzylchloride (120 µL, 922 µmol) were added. After the reaction mixture was stirred for 4 h at 70 °C and for 16 h at room temperature, the solvent was evaporated. Purification of the crude product by column chromatography (cyclohexane/ethyl acetate, 3:1) gave **11** as an orange solid (400 mg, 642 µmol, 84%). R_f=0.21 (cyclohexane/ethyl acetate, 3:1); m.p. 67 °C; $[\alpha]_D^{23}$=+193.7 (*c*=0.3 in acetone); ^{1}H NMR (600 MHz, CD_3CN, 298 K): δ=7.91-7.86 (m, 4H, Ar-H$_{ortho}$, Ar-H$_{ortho'}$), 7.48-7.46 (m, 2H, Ar-H$_{Benz}$), 7.42-7.38 (m, 3H, Ar-H$_{Benz}$), 7.35-7.34 (m, 2H, Ar-H$_{PMB}$), 7.25-7.23 (m, 2H, Ar-H$_{meta'}$), 7.16-7.13 (m, 2H, Ar-H$_{meta}$), 6.92-6.89 (m, 2H, Ar-H$_{PMB}$), 5.70 (d, $^3J_{1,2}$=1.5 Hz, 1H, H-1), 5.66 (s, 1H, CHPh), 4.84 (d, $^4J_{OCH2,C\equiv CH}$=2.4 Hz, 2H, OCH$_{2Propragyl}$), 4.72 (d, $^2J_{CHPhOMe,CH'PhOMe}$=11.5 Hz, 1H, CHPhOMe), 4.67 (d, $^2J_{CHPhOMe,CH'PhOMe}$=11.5 Hz, 1H, CH'PhOMe), 4.29-4.28 (m, 1H, H-2), 4.13 (dd~t, $^3J_{3,4}$=9.5 Hz, $^3J_{4,5}$=9.5 Hz, 1H, H-4), 4.09 (dd, $^2J_{6,6'}$=9.8 Hz, $^3J_{5,6}$=4.4 Hz, 1H, H-6), 4.04 (dd, $^3J_{2,3}$=3.3 Hz, $^3J_{3,4}$=9.5 Hz, 1H, H-3), 3.85 (ddd, $^3J_{4,5}$=9.5 Hz, $^3J_{5,6}$=4.4 Hz, $^3J_{5,6'}$=13.9 Hz, 1H, H-5); 3.81-3.78 (m, 4H, H-6', OCH$_3$), 3.58 (d, $^3J_{2,OH}$=3.5 Hz, 1H, OH$_{C-2}$), 2.87 (t, $^4J_{OCH2,C\equiv CH}$=2.4 Hz, 1H, C≡CH) ppm; ^{13}C NMR (151 MHz, CD_3CN, 298 K): δ=160.7 (C-Ar$_{para'}$), 160.2 (C-Ar$_{PMB}$), 158.9 (C-Ar$_{para}$), 148.8 (C-Ar$_{ipso}$), 148.2 (C-Ar$_{ipso'}$), 138.9 (C-Ar$_{Benz}$), 131.5 (C-Ar$_{PMB}$), 130.3 (C-Ar$_{PMB}$), 129.8 (C-Ar$_{Benz}$), 129.1 (C-Ar$_{Benz}$), 127.1 (C-Ar$_{Benz}$), 125.1 (C-Ar$_{ortho}$), 124.9 (C-Ar$_{ortho'}$), 118.2 (C- Ar$_{meta'}$), 116.2 (C-Ar$_{meta}$), 114.5 (C-Ar$_{PMB}$), 102.3 (*C*HPh), 99.7 (C-1), 79.2 (*C*≡CH), 78.8 (C-4), 77.1 (C≡*C*H), 76.1 (C-3), 72.2 (*C*H$_2$Ph), 69.5 (C-2), 69.1 (C-6), 65.7 (C-5), 56.8 (OCH$_{2Propargyl}$), 55.8 (O*C*H$_3$) ppm, IR (ATR): ν̃ =3286, 2914, 1597, 1497, 1215, 1095, 999, 840 cm^{-1}; ESI-MS: *m/z* calcd for $C_{36}H_{34}N_2O_8$: 645.2 $[M+H]^+$; found 645.2.

(*E*)-*p*-[*p'*-(Propargyloxy)]phenylazophenyl 2-*O*-allyl-4,6-*O*-benzylidene-3-*O*-*p*-methoxybenzyl-α-D-mannopyranoside (12): To an ice-cold solution of **11** (363 mg, 583 µmmol) in dry dimethylformamide (35 mL) was added NaH (60% dispersion in mineral oil, 29.2 mg, 758 µmol) and the reaction mixture was stirred for 30 min at 0 °C. Then allyl bromide (150 µL, 1.75 mmol) was added and it was stirred for 16 h at room temperature. Afterwards the solvent was evaporated and purification of the crude product by column chromatography (cyclohexane/ethyl acetate, 4:1) gave the mannoside **12** as an orange oil (332 mg, 501 µmol, 86%). R_f=0.67 (cyclohexane/ethyl acetate, 4:1); $[\alpha]_D^{23}$=+189.1 (*c*=0.4 in CH_2Cl_2), ^{1}H NMR (500 MHz, CD_3CN, 300 K): δ=7.89-7.87 (m, 4H, Ar-H$_{ortho}$, Ar-H$_{ortho'}$), 7.48-7.47 (m, 2H, Ar-H$_{Benz}$), 7.42-7.38 (m, 3H, Ar-H$_{Benz}$), 7.33-7.32 (m, 2H, Ar-H$_{PMB}$), 7.26-7.23 (m, 2H, Ar-H$_{meta'}$), 7.15-7.12 (m, 2H, Ar-H$_{meta}$), 6.92-6.89 (m, 2H, Ar-H$_{PMB}$), 5.74 (d, $^3J_{1,2}$=1.7 Hz, 1H, H-1), 5.67 (s, 1H, CHPh), 5.36 (ddt, $^4J_{OCH2,CH=CH}$=3.5 Hz $^3J_{CH=CH2,CH=CH}$=17.3 Hz, $^2J_{CH=CH,CH=CH'}$=5.2 Hz 1H, CH=C*H*), 5.22-5.19 (m,, 1H, CH=C*H'*), 4.84 (d, $^4J_{OCH2,C\equiv CH}$=2.4 Hz, 2H, OCH$_{2Propragyl}$), 4.68 (s, 2H, CH$_2$Ph), 4.29-4.21 (m, 2H, OCH$_{2Allyl}$), 4.17-4.07 (m, 3H, H-3, H-5, H-6), 4.03 (dd, $^3J_{1,2}$= 1.7 Hz, , $^3J_{2,3}$=2.9 Hz, 1H, H-2), 3.86-3.77 (m, 5H, OCH$_3$, H-4, H-6'), 2.87 (t, $^4J_{OCH2,C\equiv CH}$=2.4 Hz, 1H, C≡CH) ppm; ^{13}C NMR (126 MHz, CD_3CN, 300 K): δ=160.7 (C-Ar$_{para'}$), 160.2 (C-Ar$_{PMB}$), 158.9 (C-Ar$_{para}$), 148.8 (C-Ar$_{ipso}$), 148.2 (C-Ar$_{ipso'}$), 138.9 (C-Ar$_{Benz}$), 136.0 (*C*H=CH$_2$), 131.6 (C-Ar$_{PMB}$), 130.3 (C-Ar$_{PMB}$), 129.8 (C-Ar$_{Benz}$), 129.1 (C-Ar$_{Benz}$), 127.1 (C-Ar$_{Benz}$), 125.1 (C-Ar$_{ortho}$), 124.9 (C-Ar$_{ortho'}$), 118.2 (CH=*C*H$_2$), 117.5 (C- Ar$_{meta'}$), 116.2 (C-Ar$_{meta}$), 114.5 (C-Ar$_{PMB}$), 102.3 (*C*HPh), 99.1 (C-1), 79.2 (C-5), 77.1 (*C*≡CH), 77.0 (C≡*C*H, C-2), 76.4 (C-3), 73.4 (O*C*H$_{2Allyl}$), 72.7 (*C*H$_2$Ph), 69.1 (C-6), 66.0 (C-4), 56.8 (OCH$_{2Propargyl}$), 55.8 (O*C*H$_3$) ppm, IR (ATR): $\tilde{\nu}$ =3286, 2910, 1597, 1583, 1513, 1496, 1216, 1095, 995, 840 cm^{-1}; ESI-MS: *m/z* calcd for $C_{39}H_{38}N_2O_8$: 663.3 $[M+H]^+$; found 663.3.

(*E*)-*p*-[*p'*-(Propargyloxy)]phenylazophenyl 2-*O*-allyl-4,6-*O*-benzylidene-α-D-mannopyranoside (13): DDQ (203 mg, 893 µmol) was added to a solution of the mannoside **12** (296 mg, 447 µmol) in dichloromethane (5 ml) and water (300 µL). After the reaction mixture was stirred for 2 h at room temperature, a saturated aq. $NaHCO_3$ solution (15 mL) was added. The aqueous phase was extracted with dichloromethane (2 × 25 mL) and the combined organic phases were washed with a saturated aq. $NaHCO_3$ solution (20 mL). It was dried over $MgSO_4$, filtered and the filtrate concentrated under reduced pressure. Purification of the crude product by column chromatography (cyclohexane/ethyl acetate, 3:1) gave the mannoside **13** as an orange solid (191 mg, 352 µmol, 79%). R_f=0.25 (cyclohexane/ethyl acetate, 3:1); m.p. 164 °C; $[\alpha]_D^{23}$=+203.1 (*c*=0.3 in CH_2Cl_2); ^{1}H NMR (600 MHz, acetone-d_6, 300 K): δ=7.93-7.89 (m, 4H, Ar-H$_{ortho}$, Ar-H$_{ortho'}$), 7.50-7.49 (m, 2H, Ar-H$_{Benz}$), 7.38-7.35 (m, 3H, Ar-H$_{Benz}$), 7.31-7.29 (m, 2H, Ar-H$_{meta'}$), 7.20-7.17 (m, 2H, Ar-H$_{meta}$), 6.03 (ddt, $^3J_{CH=CH2,CH=CH}$=17.3 Hz, $^3J_{CH=CH2,CH=CH'}$=10.7 Hz, $^3J_{OCH2,CH=CH2}$=5.5 Hz, 1H, C*H*=CH$_2$), 5.83 (d, $^3J_{1,2}$=1.4 Hz, 1H, H-1), 5.66 (s, 1H, CHPh), 5.34-5.36 (m, 1H, CH=C*H*), 5.20-5.17 (m, 1H, CH=C*H'*), 4.92 (d, $^4J_{OCH2,C\equiv CH}$=2.4 Hz, 2H, OCH$_{2Propragyl}$), 4.41-4.31 (m, 3H, OH$_{C-3}$, OCH$_{2Allyl}$), 4.22 (ddd, $^3J_{2,3}$=3.5 Hz, $^3J_{3,4}$=10.3 Hz, $^3J_{OH,3}$=7.1 Hz, 1H, H-3), 4.12-4.08 (m, 1H, H-6), 4.06-4.02 (m, 1H, H-4), 3.99 (dd, $^3J_{1,2}$=1.4 Hz, $^3J_{2,3}$=3.5 Hz, 1H, H-2), 3.83-3.78 (m, 2H, H-5, H-6'), 3.14 (t, $^4J_{OCH2,C\equiv CH}$=2.4 Hz, 1H, C≡CH) ppm; ^{13}C NMR (151 MHz, acetone-d_6, 300 K): δ=160.9 (C-Ar$_{para'}$), 159.1 (C-Ar$_{para}$), 148.8 (C-Ar$_{ipso}$), 148.2 (C-Ar$_{ipso'}$), 139.2 (C-Ar$_{Benz}$), 136.4 (*C*H=CH$_2$), 129.5 (C-Ar$_{Benz}$), 128.8 (C-Ar$_{Benz}$), 127.3 (C-Ar$_{Benz}$), 125.1 (C-Ar$_{ortho}$), 125.0 (C-Ar$_{ortho'}$), 117.9 (C-Ar$_{meta'}$), 117.1 (CH=*C*H$_2$), 116.2 (C-Ar$_{meta}$), 102.6 (*C*HPh), 98.0 (C-1), 80.1 (C-4), 79.4 (C-2), 79.3 (*C*≡CH), 77.4 (C≡*C*H), 73.7 (OCH$_{2Allyl}$), 69.4 (C-3), 69.3 (C-6), 65.9 (C-5), 56,7 (OCH$_{2Propargyl}$) ppm; IR (ATR): $\tilde{\nu}$ =3307, 1596, 1502, 1248, 1149, 1101, 987, 973, 839 cm^{-1}; ESI-MS: *m/z* calcd for $C_{31}H_{30}N_2O_7$: 543.2 $[M+H]^+$; found 543.2.

(*E*)-*p*-[*p'*-(Propargyloxy)]phenylazophenyl 2-*O*-allyl-α-D-mannopyranoside (14): Trifluoroacetic acid (1 mL) was added to a solution of the benzylidene protected mannoside **13** (107 mg, 197 µmol) in dichloromethane (10 mL) and the reaction mixture was stirred for 1 h at room temperature. Then the solvent was evaporated and the crude product was purified by column chromatography (dichloromethane/methanol, 10:0.5). The target mannoside **14** was obtained as a yellow solid (65.0 mg, 143 µmol, 73%). R_f=0.22 (dichloromethane/methanol, 10:0.5); m.p. 133 °C; $[\alpha]_D^{23}$=+77.8 (*c*=0.4 in methanol); ^{1}H NMR (500 MHz, DMSO-d_6, 300 K): δ=7.87-7.82 (m, 4H, Ar-H$_{ortho}$, Ar-H$_{ortho'}$), 7.29-7.26 (m, 2H, Ar-H$_{meta'}$), 7.18-7.15 (m, 2H, Ar-H$_{meta}$), 5.92 (ddt, $^3J_{CH=CH2,CH=CH}$=17.3 Hz, $^3J_{CH=CH2,CH=CH'}$=10.6 Hz, $^3J_{OCH2,CH=CH2}$=5.5 Hz, 1H, C*H*=CH$_2$), 5.66 (d, $^3J_{1,2}$=1.8 Hz, 1H, H-1), 5.31 (ddt, $^4J_{OCH2,CH=CH}$=1.7 Hz, $^3J_{CH=CH2,CH=CH}$=17.3 Hz, $^2J_{CH=CH,CH=CH'}$=3.7 Hz 1H, CH=C*H*), 5.16-5.13 (m, 1H, CH=C*H'*), 4.93 (d, $^3J_{OH,3}$=5.8 Hz, 1H, OH$_{C-3}$), 4.91-4.90 (m, 3H, OH$_{C-4}$, OCH$_{2Propragyl}$), 4.52 (dd~t, $^3J_{OH,6}$)=6.0 Hz, $^3J_{OH,6}$=6.0 Hz, 1H, OH$_{C-6}$), 4.23-4.16 (m, 2H, OCH$_{2Allyl}$), 3.79 (ddd, $^3J_{2,3}$=3.5 Hz, $^3J_{3,4}$=9.4 Hz, $^3J_{OH,3}$=6.0 Hz, 1H, H-3), 3.70 (dd, $^3J_{1,2}$=1.8 Hz, $^3J_{2,3}$=3.5 Hz, 1H, H-2), 3.60 (t, $^4J_{OCH2,C\equiv CH}$=2.4 Hz, 1H, C≡CH), 3.60-3.57 (m, 1H, H-6), 3.53-3.49 (m, 2H, H-4, H-6'), 3.38-3.35 (m, 1H, H-5) ppm; ^{13}C NMR (126 MHz, DMSO-d_6, 300 K): 159.9 (C-Ar$_{para'}$), 158.8 (C-Ar$_{para}$), 147.5 (C-Ar$_{ipso}$), 147.1 (C-Ar$_{ipso'}$), 136.1 (*C*H=CH$_2$), 124.6 (C-Ar$_{ortho}$), 124.4 (C-Ar$_{ortho'}$), 117.6 (C- Ar$_{meta'}$), 117.0 (CH=*C*H$_2$), 115.9 (C-Ar$_{meta}$), 96.8 (C-1), 79.3 (*C*≡CH), 79.1 (C≡*C*H), 78.0 (C-2), 75.6 (C-5), 72.1 (O*C*H$_{2Allyl}$), 70.9 (C-3), 67.3 (C-4), 61.4 (C-6), 56.3 (OCH$_{2Propargyl}$) ppm; IR (ATR): $\tilde{\nu}$=3399, 3239, 2911, 1599, 1581, 1496, 1228, 1122, 1006, 847 cm^{-1}; UV-Vis (DMSO): λ^{max} (ε)=362 nm (20348 L mol^{-1} cm^{-1}); HRMS (ESI): *m/z* calcd for $C_{24}H_{26}N_2O_7$: 455.1818 $[M+H]^+$; found 455.1823.

(*E*)-*p*-[*p'*-(Propargyloxy)]phenylazophenyl 2,3,4-tri-*O*-acetyl-6-azido-6-deoxy-β-D-glucopyranoside (20): To a solution of the mannosyl donor[5] **18** (634 mg, 1.33 mmol) and (*E*)-*p*-(*p'*-allyloxy-phenylazo)phenol[6] (**19**, 407 mg, 1.60 mmol) in dry acetonitrile (14 mL) was added molecular sieve 3 Å and the solution was stirred for 30 min at room temperature. Then the reaction mixture was cooled to 0 °C and $BF_3{\cdot}Et_2O$ (250 µL, 2.00 mmol) was added slowly. After stirring for 15 min at 0 °C, the reaction mixture was stirred for 16 h at room temperature. Then dichloromethane (25 mL) was added and the organic phase was washed with a saturated aq. $NaHCO_3$ solution (3 × 10 mL). It was dried over $MgSO_4$, filtered and the filtrate concentrated under reduced pressure. Purification of the crude product by column chromatography (cyclohexane/ethyl acetate, 2:1) gave the glucoside **20** as a yellow solid (295 mg, 520 µmol, 39%). R_f=0.25 (cyclohexane/ethyl acetate, 2:1); m.p. 135 °C; $[\alpha]_D^{23}$=-21.2 (*c*=0.5 in CH_2Cl_2); ^{1}H NMR (600 MHz, $CDCl_3$, 298 K,TMS): δ=7.89-7.86 (m, 4H, Ar-H$_{ortho}$, Ar-H$_{ortho}$), 7.13-7.10 (m, 2H, Ar-H$_{meta}$), 7.03-7.01 (m, 2H, Ar-H$_{meta'}$), 6.08 (ddd $^3J_{CH=CH2,CH=CH}$=17.3 Hz, $^3J_{CH=CH2,CH=CH'}$=10.6 Hz, $^3J_{OCH2,CH=CH2}$=5.3 Hz, 1H, C*H*=CH$_2$), 5.45 (ddt, $^4J_{OCH2,CH=CH}$=1.6 Hz, $^3J_{CH=CH2,CH=CH}$=17.3 Hz, $^2J_{CH=CH,CH=CH'}$=3.0 Hz 1H, CH=C*H*), 5.34-5.29 (m, 3H, H-2, H-3, CH=C*H'*), 5.21-5.17 (m, 1H, H-1), 5.12-5.07 (m, 1H, H-4), 4.62 (ddd~dt, $^4J_{OCH2,CH=CH'}$=2.8 Hz, $^4J_{OCH2,CH=CH}$=1.6 Hz, $^3J_{OCH2,CH=CH2}$=5.3 Hz, 2H, OCH$_2$), 3.83 (ddd, $^3J_{4,5}$=9.9 Hz, $^3J_{5,6}$=7.3 Hz, $^3J_{5,6'}$=2.6 Hz, 1H, H-5), 3.45 (dd, $^2J_{6,6'}$=13.4 Hz, $^3J_{5,6}$=7.3 Hz, 1H, H-6), 3.36 (dd, $^2J_{6,6'}$=13.4 Hz, $^3J_{5,6'}$=2.6 Hz, 1H, H-

6'), 2.08, 2.07, 2.05 (s, 9H, $COCH_3$) ppm; ^{13}C NMR (151 MHz, $CDCl_3$, 298 K, TMS): δ=170.2, 169.5, 169.3 ($COCH_3$), 160.9 (C-$Ar_{para'}$), 158.2 (C-Ar_{para}), 148.8 (C-Ar_{ipso}), 147.0 (C-$Ar_{ipso'}$), 132.8 ($CH=CH_2$), 124.6 (C-Ar_{ortho}), 124.3 (C-$Ar_{ortho'}$), 118.1 ($CH=CH_2$), 117.3 (C-$Ar_{meta'}$), 115.0 (C-Ar_{meta}), 98.8 (C-1), 73.6 (C-5), 72.5 (C-3), 71.1 (C-2), 69.4 (C-4), 69.0 (OCH_2), 51.3 (C-6), 20.6, 20.6, 20.6 ($COCH_3$) ppm; IR (ATR): $\tilde{\nu}$ =2926, 2101, 1744, 1582, 1365, 1216, 1048, 1032, 843 cm^{-1}; ESI-MS: *m/z* calcd for $C_{27}H_{30}N_5O_9$: 568.2 $[M+H]^+$; found 568.0.

(*E*)-*p*-[*p'*-(Propargyloxy)]phenylazophenyl 6-azido-6-deoxy-β-D-glucopyranoside (21): The glucoside **20** (295 mg, 520 µmol) was dissolved in methanol (10 mL) and potassium carbonate (14.0 mg, 104 µmol) was added. The reaction mixture was stirred for 16 h at room temperature. Then the solvent was evaporated and the crude product was purified by column chromatography (dichloromethane/methanol, 10:0.5). The glucoside **21** was obtained as an orange solid (194 mg, 439 µmol, 85%). R_f=0.27 (dichloromethane/methanol, 10:1); m.p. 175 °C; $[\alpha]_D^{23}$=-94.3 (*c*=0.6 in methanol); ^1H NMR (500 MHz, DMSO-d_6, 300 K): δ=7.86-7.82 (m, 4H, Ar-H_{ortho}, Ar-H_{ortho}), 7.23-7.20 (m, 2H, Ar-H_{meta}), 7.15-7.13 (m, 2H, Ar-$H_{meta'}$), 6.08 (ddd $^3J_{CH=CH2,CH=CH}$=17.3 Hz, $^3J_{CH=CH2,CH=CH'}$=10.6 Hz, $^3J_{OCH2,CH=CH2}$=5.3 Hz, 1H, $CH=CH_2$), 5.48 (d, ^3J=5.0 Hz, 1H, OH), 5.44 (ddt, $^4J_{OCH2,CH=CH}$=1.7 Hz, $^3J_{CH=CH2,CH=CH}$=17.3 Hz, $^2J_{CH=CH,CH=CH'}$=3.4 Hz 1H, CH=CH), 5.33 (d, $^3J_{OH,4}$=5.4 Hz, 1H, OH_{C-4}), 5.44 (ddt, $^4J_{OCH2,CH=CH'}$=1.5 Hz, $^3J_{CH=CH2,CH=CH'}$=10.6 Hz, $^2J_{CH=CH,CH=CH'}$=3.4 Hz 1H, CH=CH'), 5.22 (d, ^3J=4.9 Hz, 1H, OH), 5.12 (d, $^3J_{1,2}$=7.5 Hz, 1H, H-1), 4.68 (ddd~dt, $^4J_{OCH2,CH=CH'}$=1.5 Hz, $^4J_{OCH2,CH=CH}$=1.7 Hz, $^3J_{OCH2,CH=CH2}$=5.3 Hz, 2H, OCH_2), 3.68 (ddd, $^3J_{4,5}$=9.5 Hz, $^3J_{5,6}$=6.9 Hz, $^3J_{5,6'}$=2.5 Hz, 1H, H-5), 3.50 (dd, $^3J_{5,6}$=2.5 Hz, $^2J_{6,6'}$=13.2 Hz, 1H, H-6), 3.45 (dd, $^3J_{5,6'}$=6.9 Hz, $^2J_{6,6'}$=13.2 Hz, , 1H, H-6'), 3.36-3.30 (m, 2H, H-3, H-2), 3.20-.3.12 (m, 1H, H-4) ppm; ^{13}C NMR (126 MHz, , DMSO-d_6, 300 K): δ=161.0 (C-$Ar_{para'}$), 159.6 (C-Ar_{para}), 147.5 (C-Ar_{ipso}), 146.7 (C-$Ar_{ipso'}$), 133.7 ($CH=CH_2$), 124.7 (C-Ar_{ortho}), 124.3 (C-$Ar_{ortho'}$), 118.3 ($CH=CH_2$), 117.1 (C-$Ar_{meta'}$), 115.7 (C-Ar_{meta}), 100.2 (C-1), 76.5 (C-3), 75.7 (C-5), 73.6 (C-2), 71.1 (C-4), 69.0 (OCH_2), 51.8 (C-6) ppm; IR (ATR): $\tilde{\nu}$ =3298, 2921, 2087, 1582, 1498, 1221, 1062, 835 cm^{-1}; UV-Vis (DMSO): λ^{max} (ε)=360 nm (16029 L mol^{-1} cm^{-1}); HRMS (ESI): *m/z* calcd for $C_{21}H_{23}N_5O_6$: 442.1727 $[M+H]^+$; found 442.1723.

3. ^{1}H and ^{13}C NMR spectra of synthetic compounds

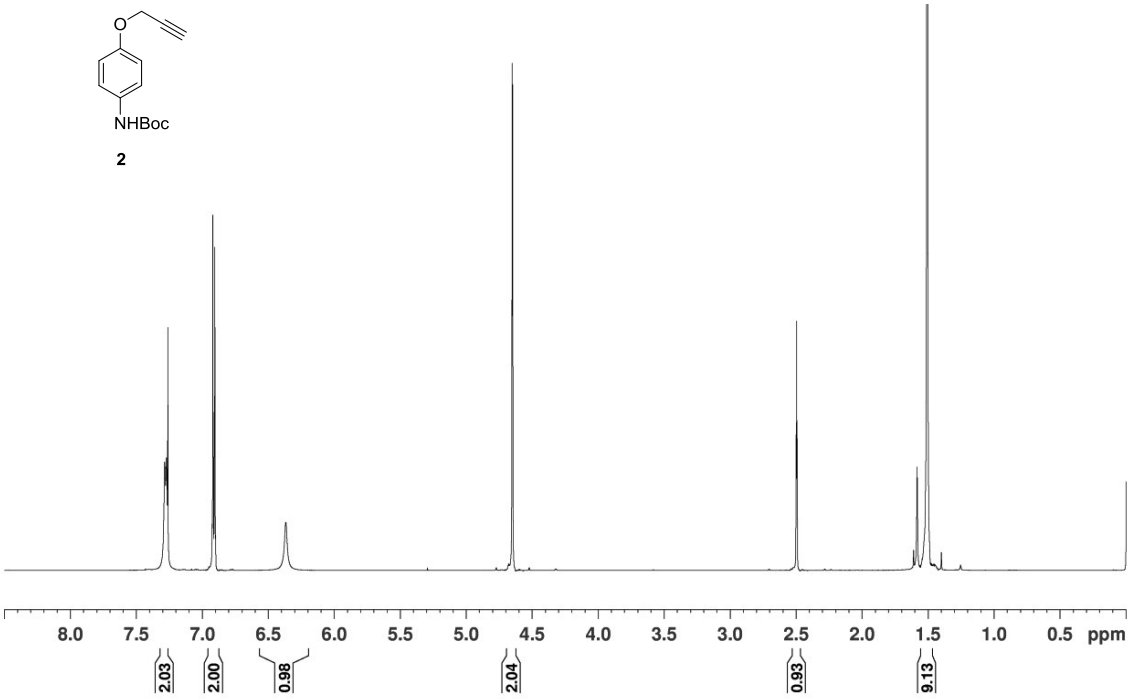

Figure S1. ^{1}H NMR spectrum of **2** (600 MHz, $CDCl_3$, 300 K, TMS).

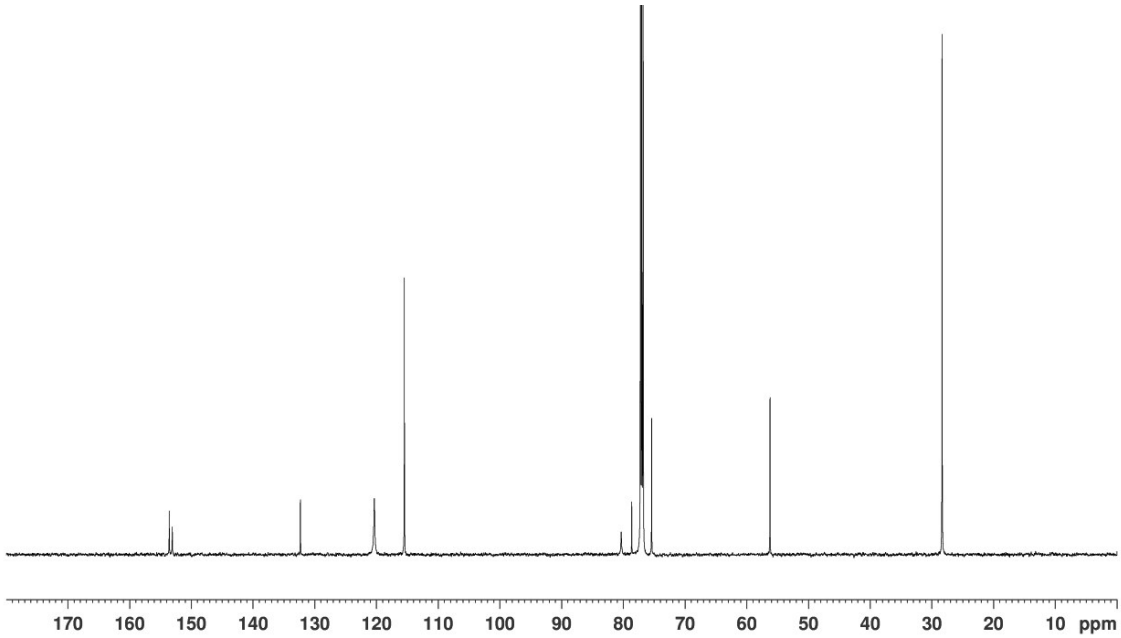

Figure S2. ^{13}C NMR spectrum of **2** (150 MHz, $CDCl_3$, 300 K, TMS).

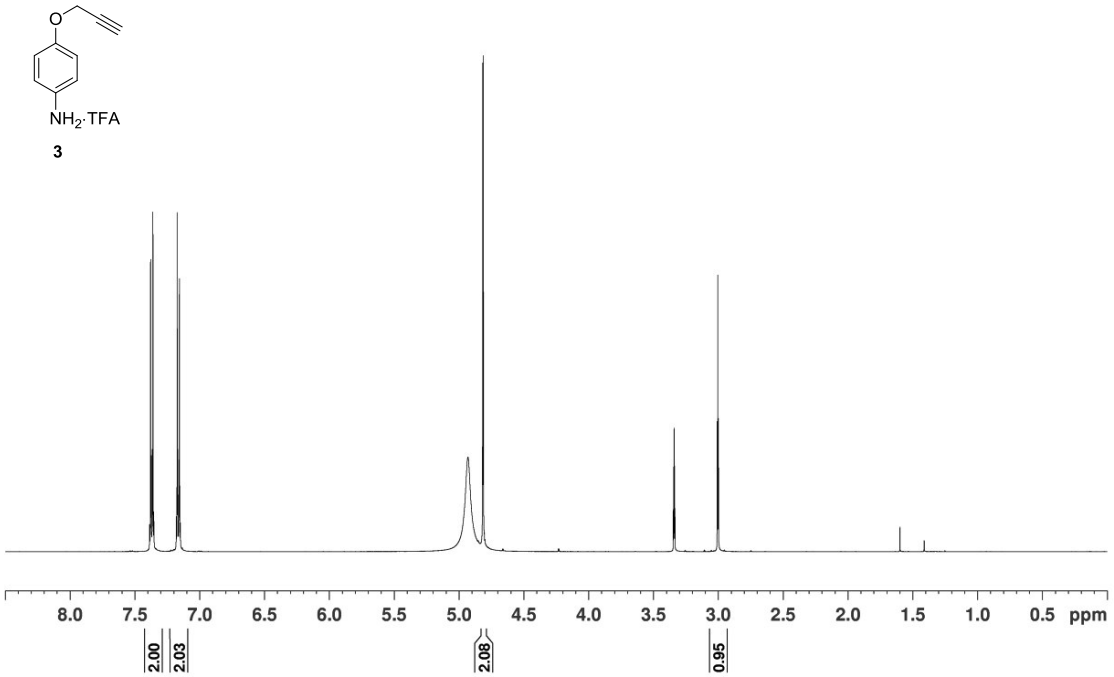

Figure S3. ^{1}H NMR spectrum of **3** (500 MHz, MeOH-d_4, 300 K).

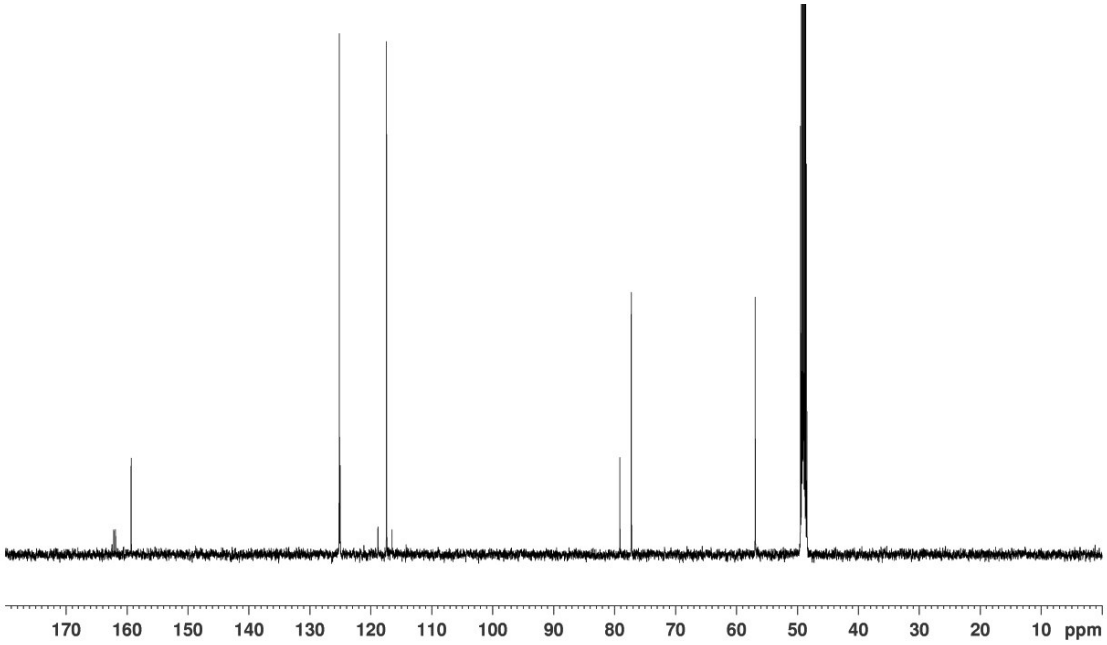

Figure S4. ^{13}C NMR spectrum of **3** (126 MHz, MeOH-d_4, 300 K).

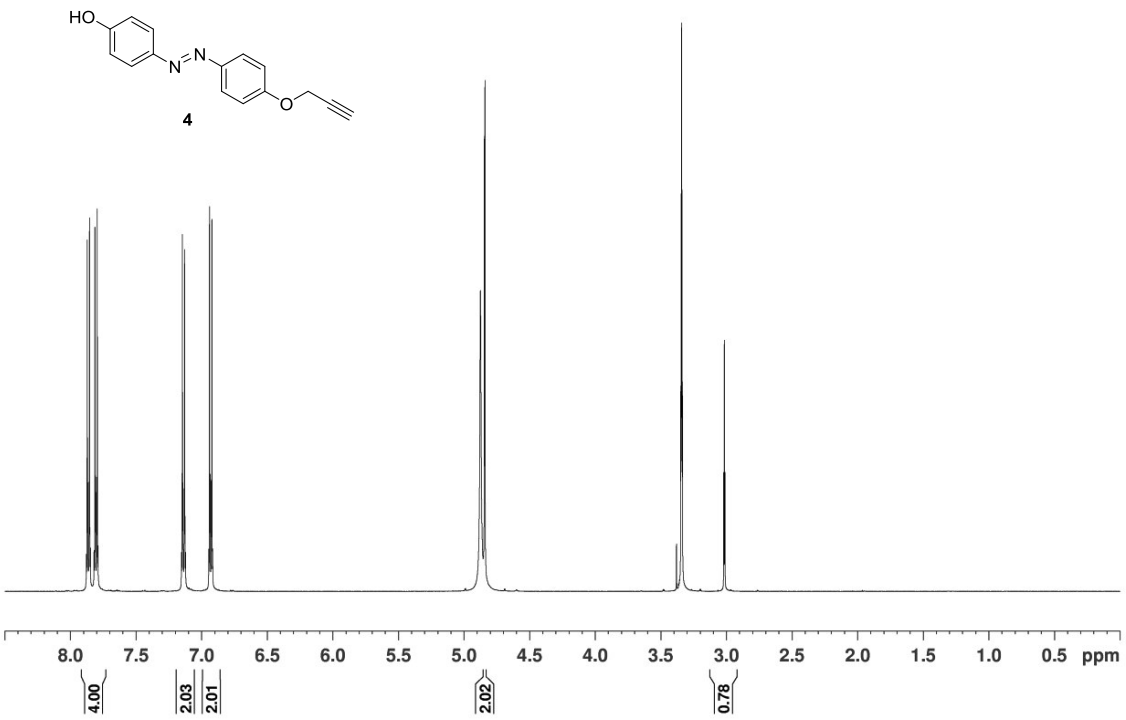

Figure S5. ^{1}H NMR spectrum of **4** (500 MHz, MeOH-d_4, 300 K).

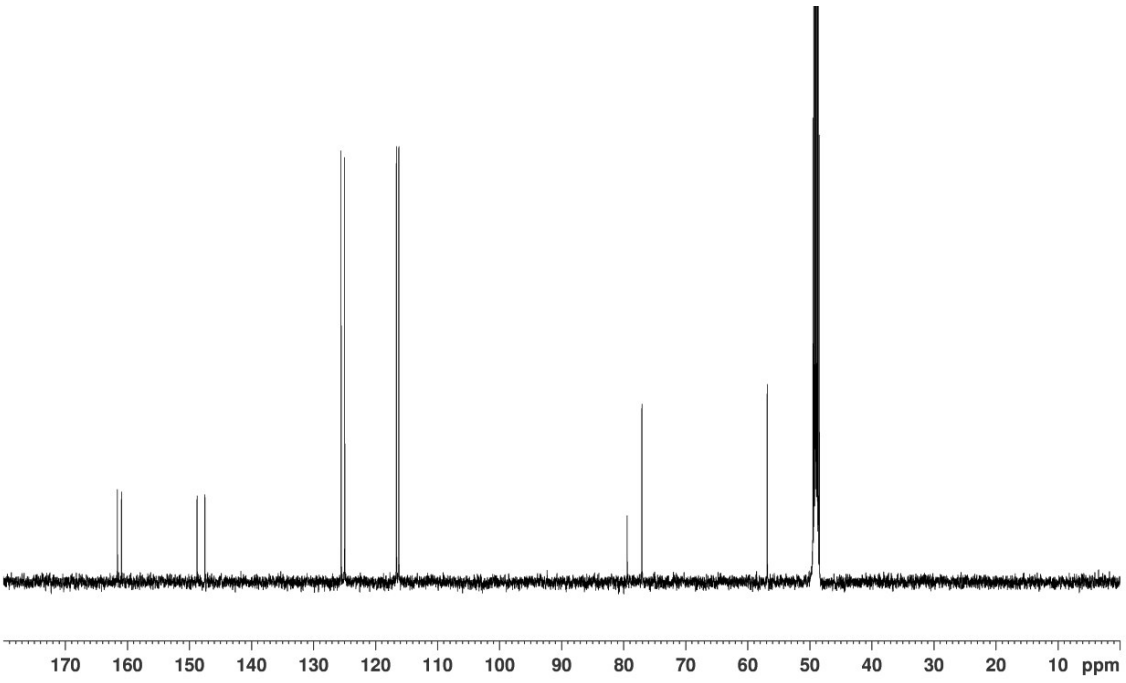

Figure S6. ^{13}C NMR spectrum of **4** (126 MHz, MeOH-d_4, 300 K).

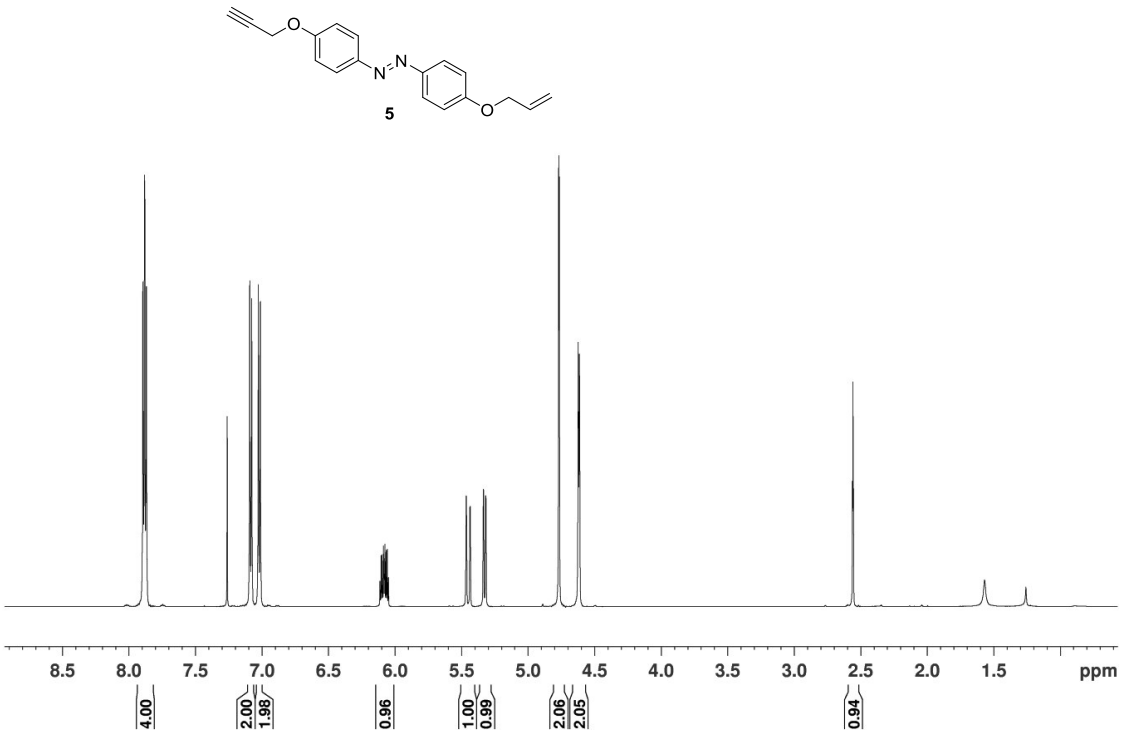

Figure S7. ^{1}H NMR spectrum of **5** (600 MHz, $CDCl_3$, 300 K, TMS).

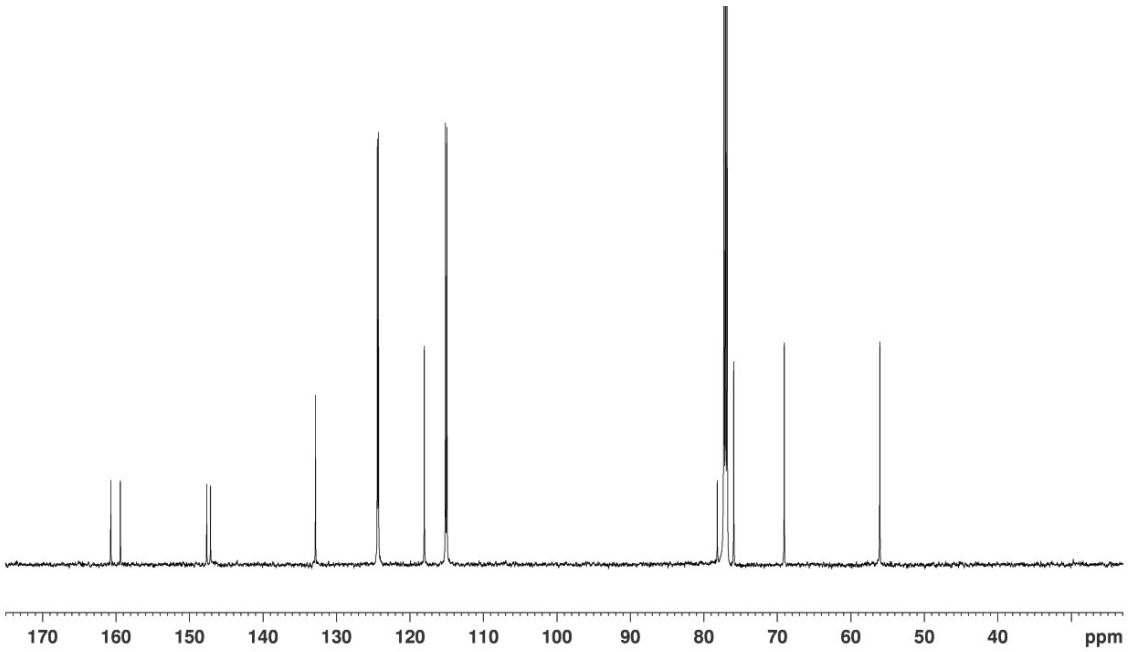

Figure S8. ^{13}H NMR spectrum of **5** (151 MHz, $CDCl_3$, 300 K, TMS).

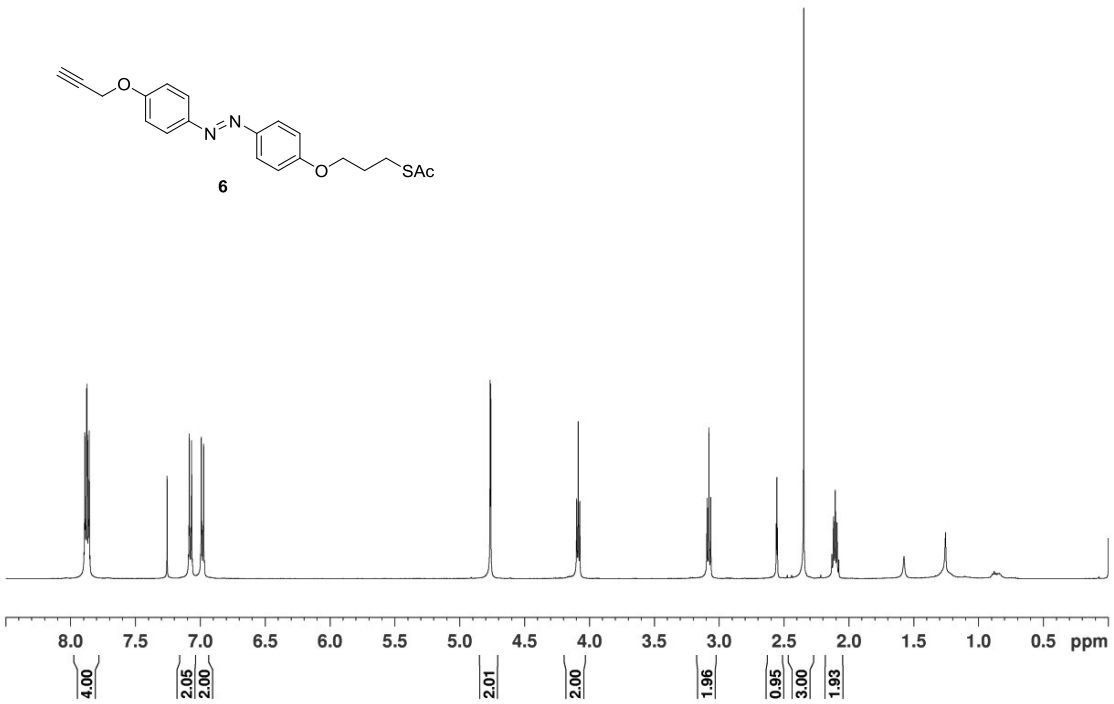

Figure S9. ^{1}H NMR spectrum of **6** (500 MHz, $CDCl_3$, 300 K, TMS).

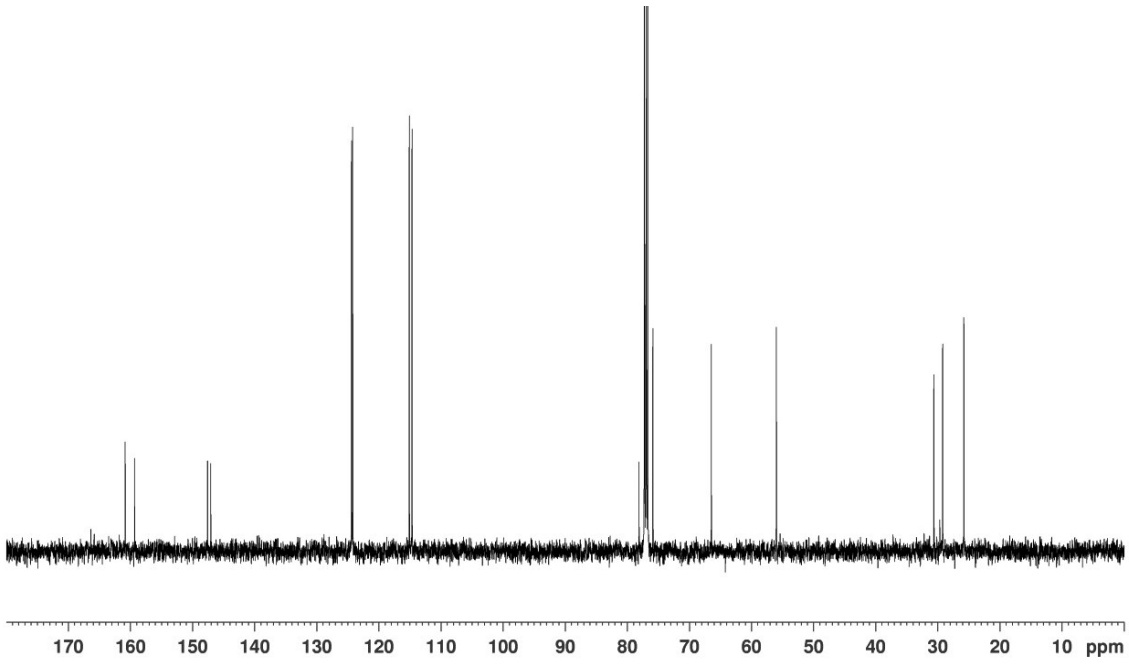

Figure S10. ^{13}C NMR spectrum of **6** (126 MHz, $CDCl_3$, 300 K, TMS).

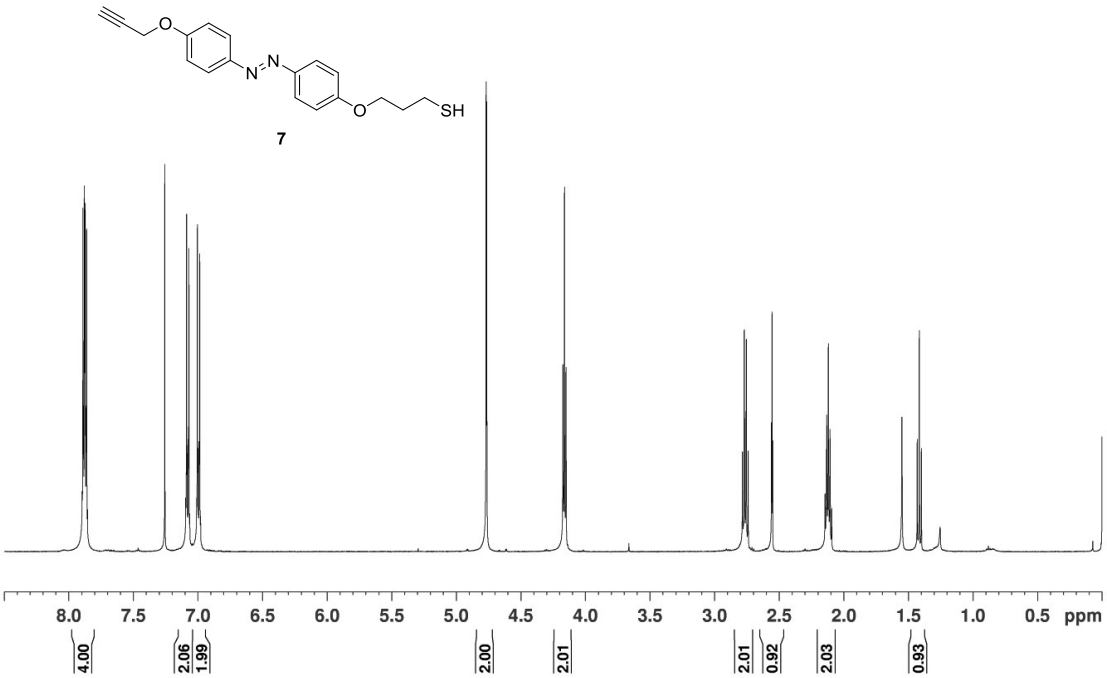

Figure S11. ^{1}H NMR spectrum of **7** (500 MHz, $CDCl_3$, 300 K, TMS).

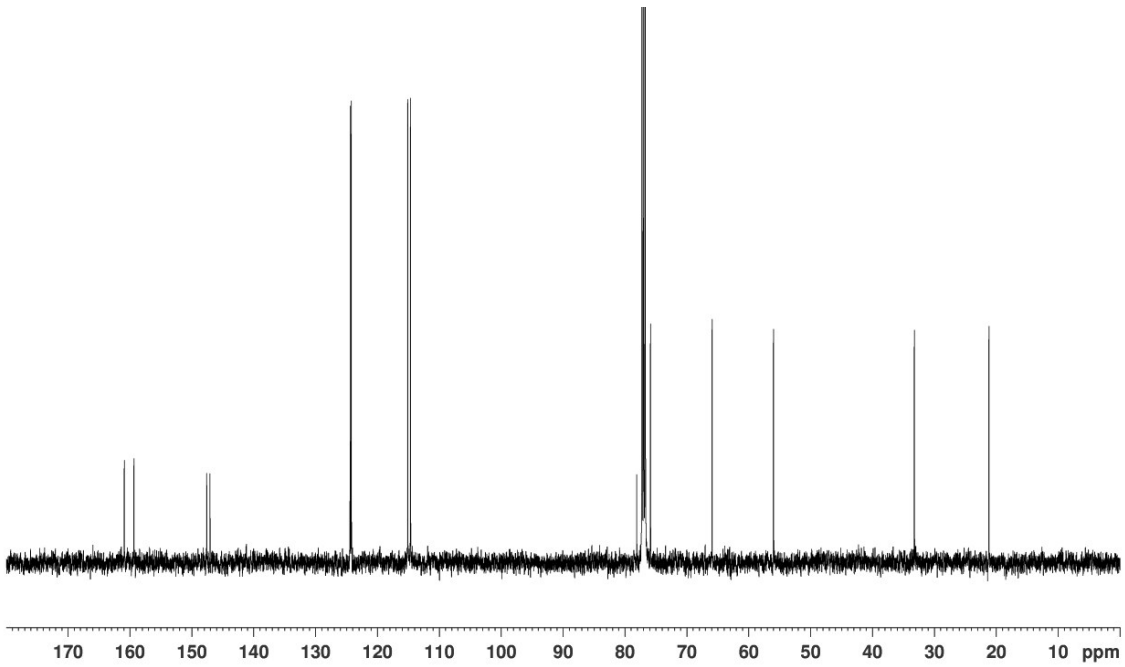

Figure S12. ^{13}C NMR spectrum of **7** (126 MHz, $CDCl_3$, 300 K, TMS).

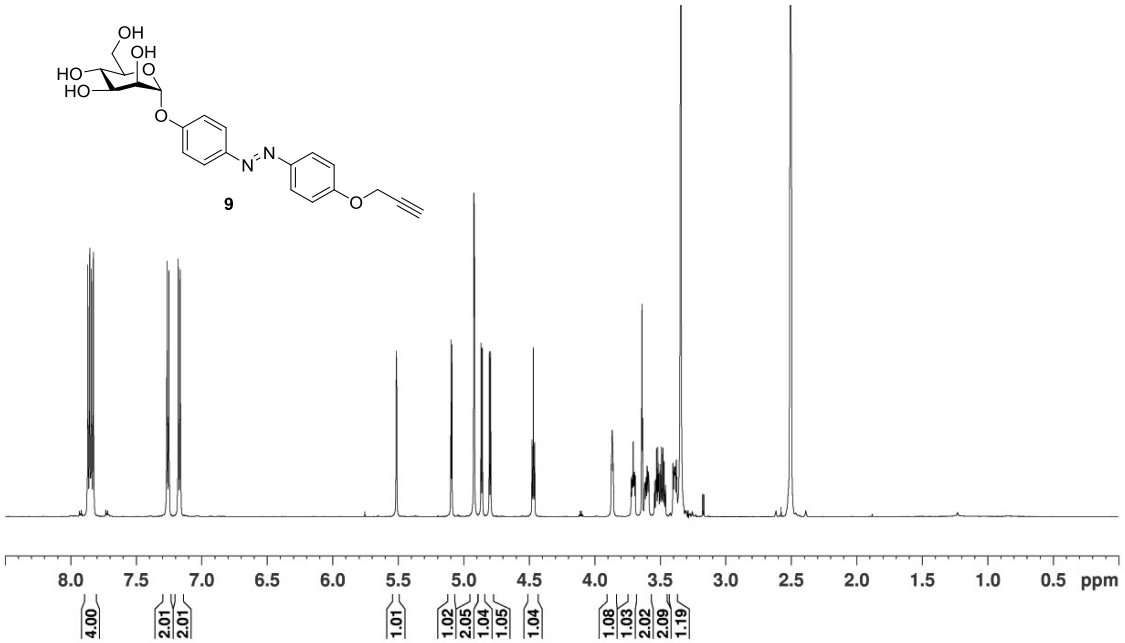

Figure S13. ^{1}H NMR spectrum of **9** (600 MHz, DMSO-d_6, 298 K).

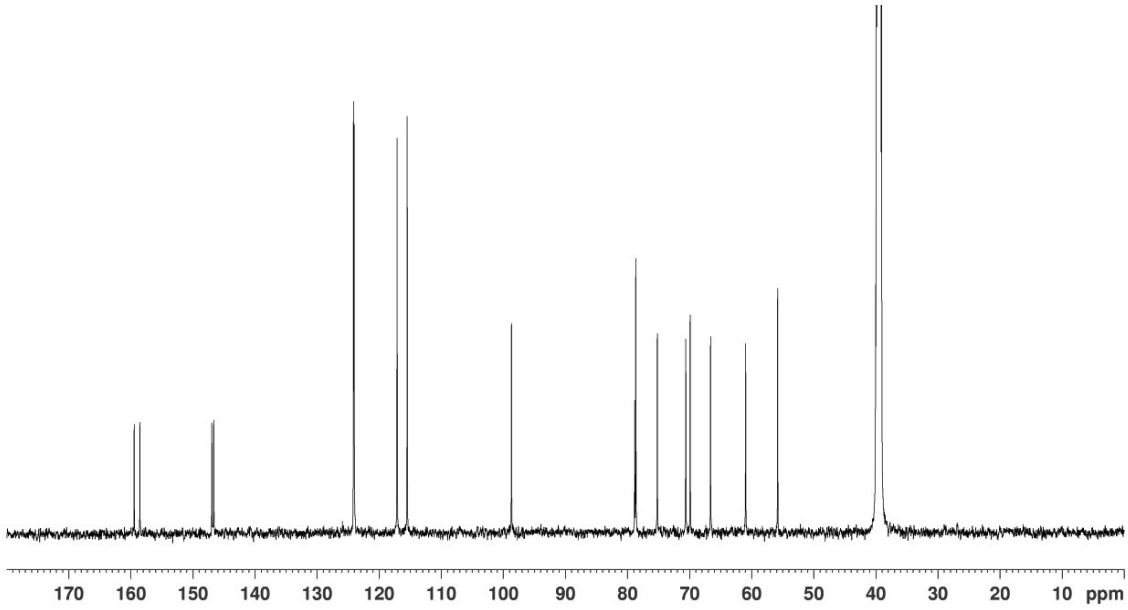

Figure S14. ^{13}C NMR spectrum of **9** (150 MHz, DMSO-d_6, 298 K).

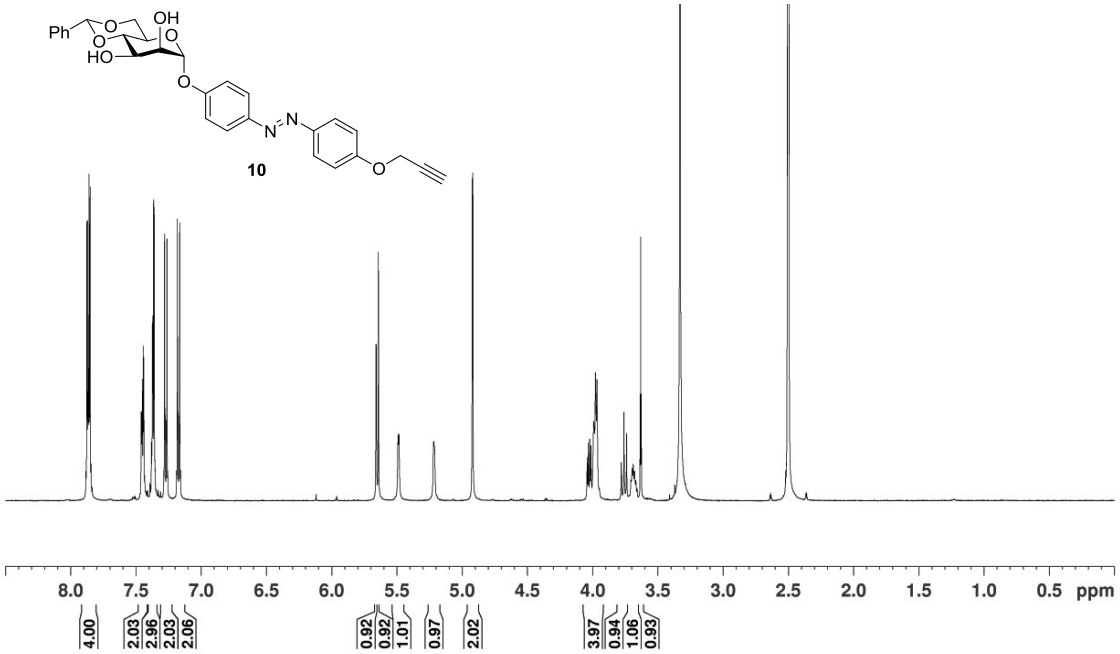

Figure S15. ^{1}H NMR spectrum of **10** (500 MHz, DMSO-d_6, 300 K).

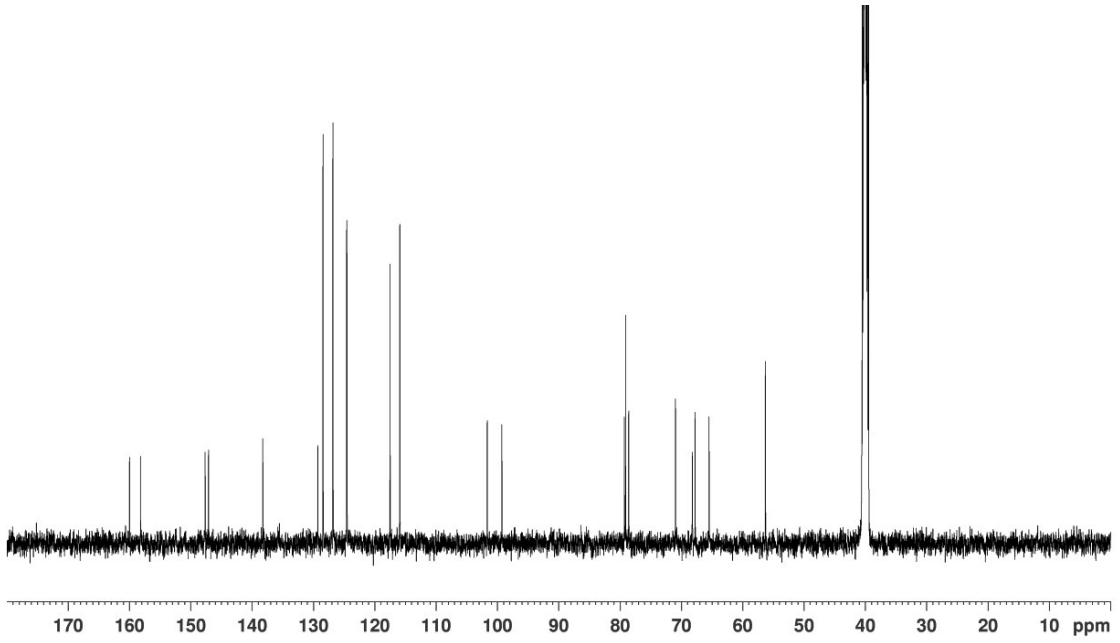

Figure S16. ^{13}C NMR spectrum of **10** (125 MHz, DMSO-d_6, 300 K).

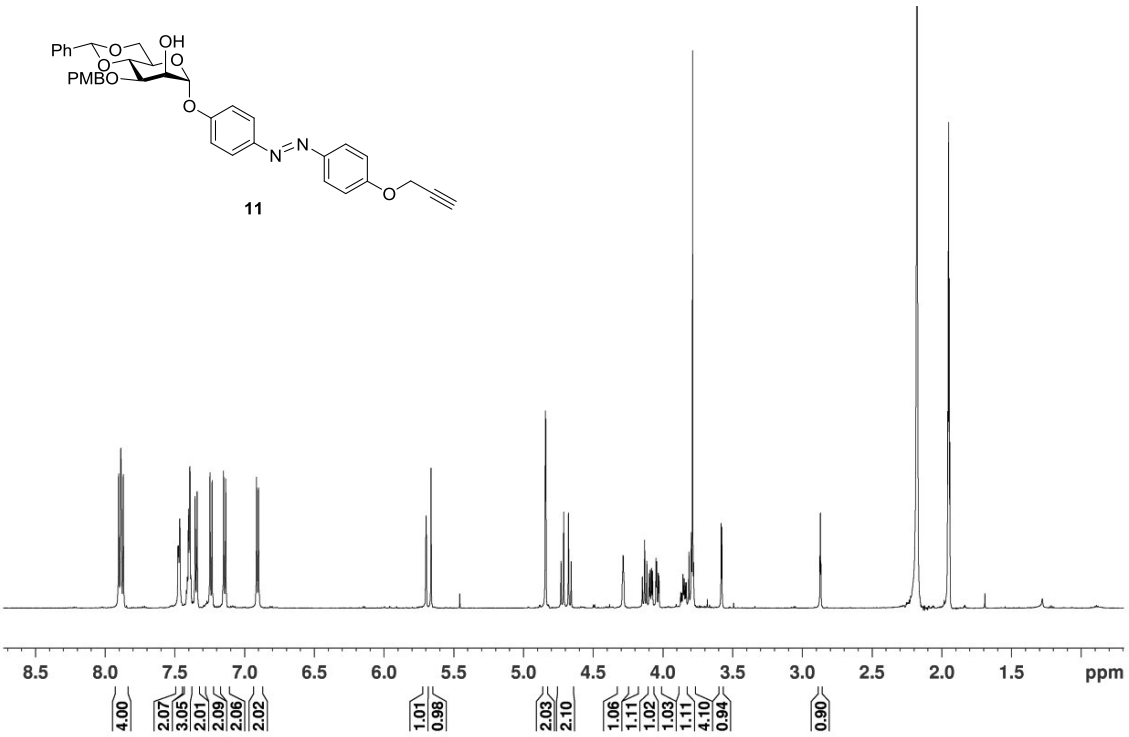

Figure S17. ^{1}H NMR spectrum of **11** (600 MHz, CD_3CN, 298 K).

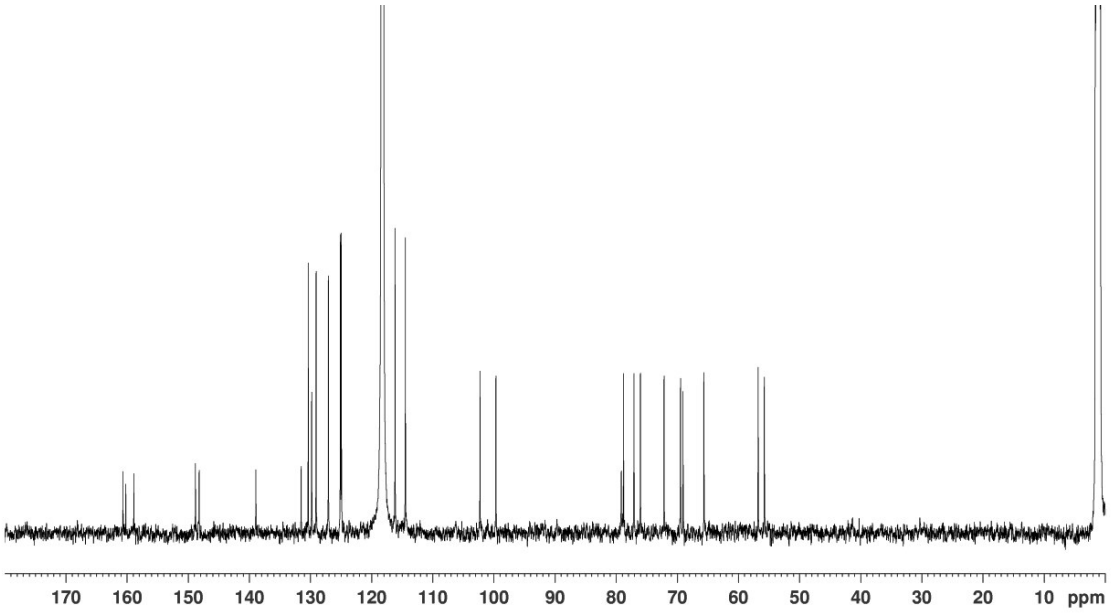

Figure S18. ^{13}C NMR spectrum of **11** (151 MHz, CD_3CN, 298 K).

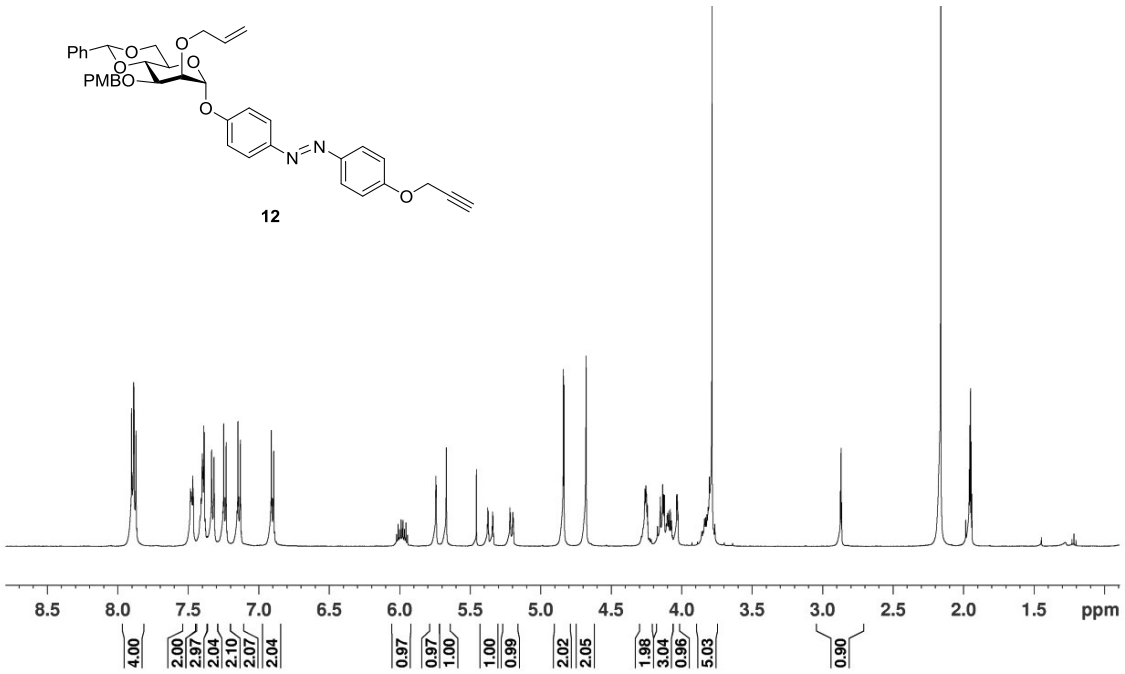

Figure S19. ^{1}H NMR spectrum of **12** (500 MHz, CD_3CN, 300 K).

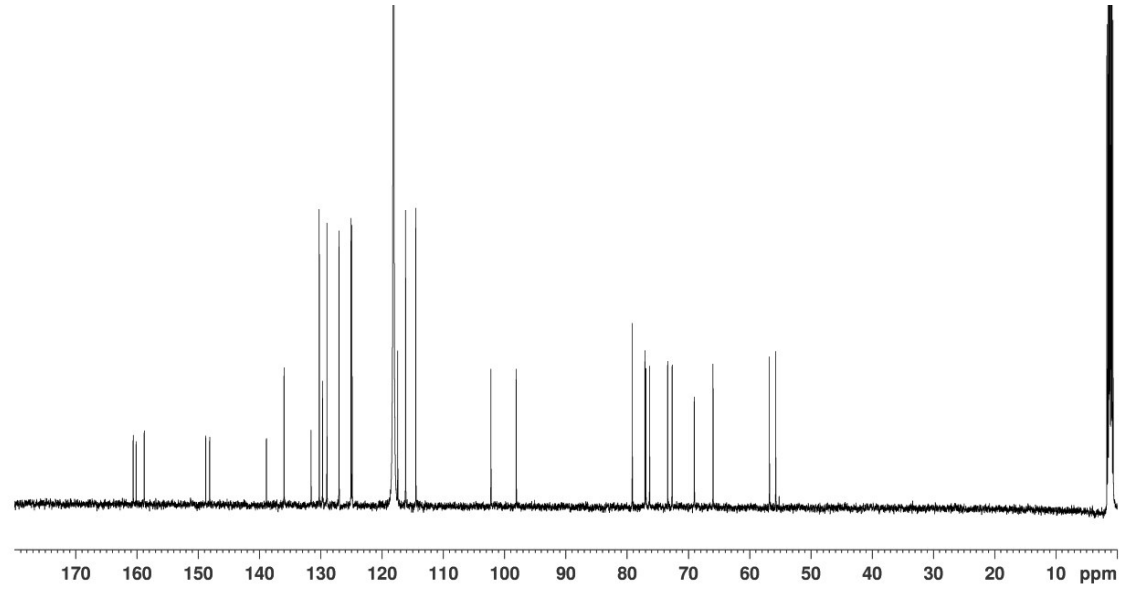

Figure S20. ^{13}C NMR spectrum of **12** (126 MHz, CD_3CN, 300 K).

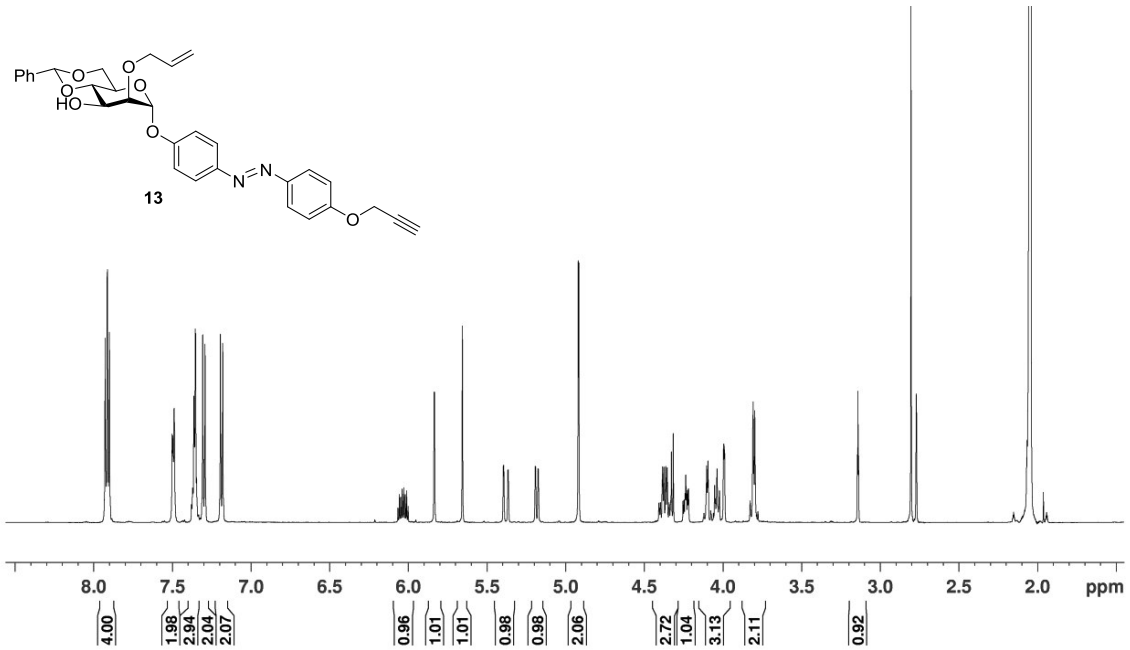

Figure S21. ^{1}H NMR spectrum of **13** (600 MHz, acetone-d_6, 300 K).

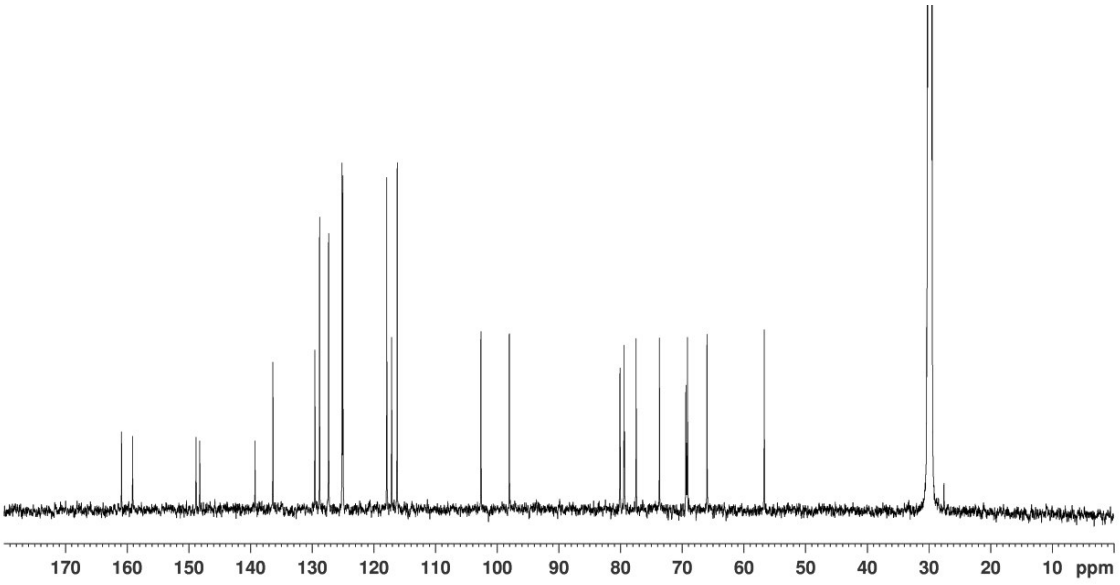

Figure S22. ^{13}C NMR spectrum of **13** (151 MHz, acetone-d_6, 300 K).

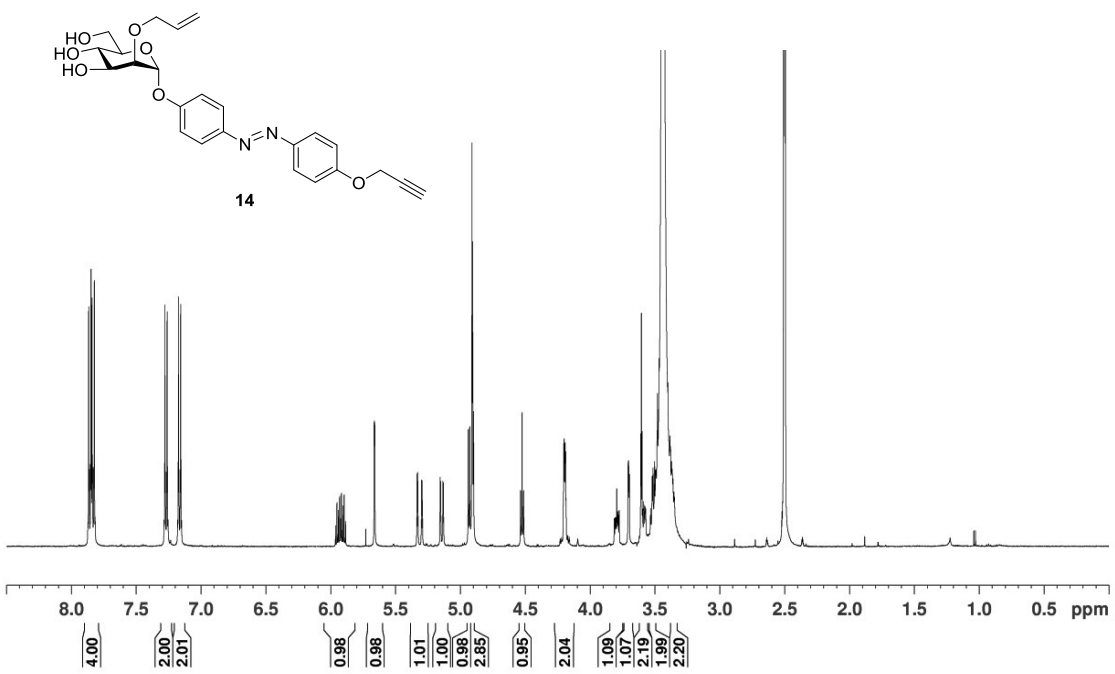

Figure S23. ^{1}H NMR spectrum of **14** (500 MHz, DMSO-d_6, 300 K).

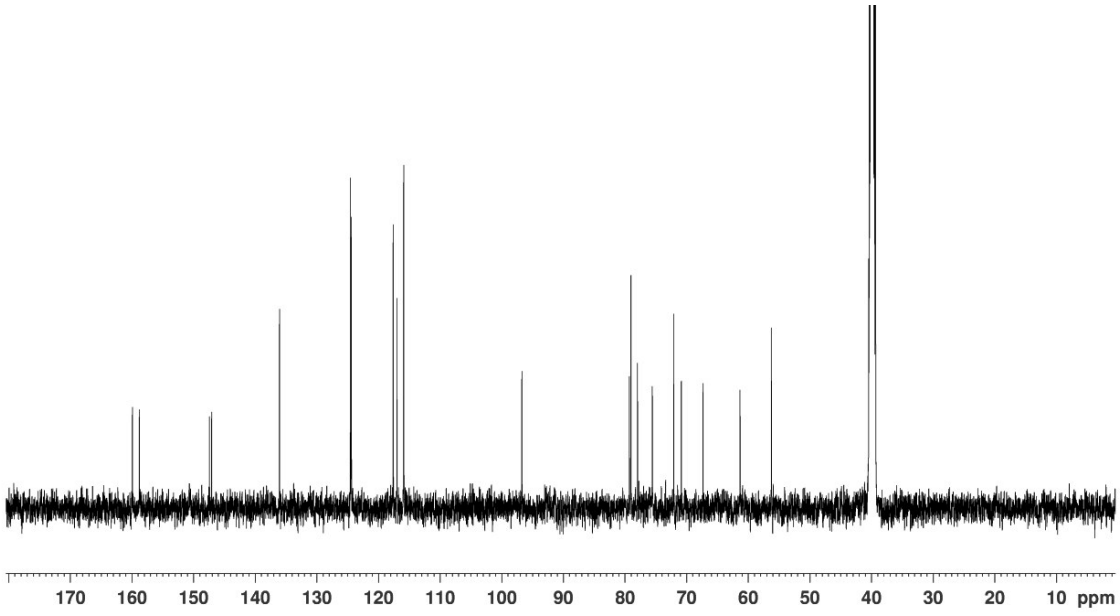

Figure S24. ^{13}C NMR spectrum of **14** (126 MHz, DMSO-d_6, 300 K).

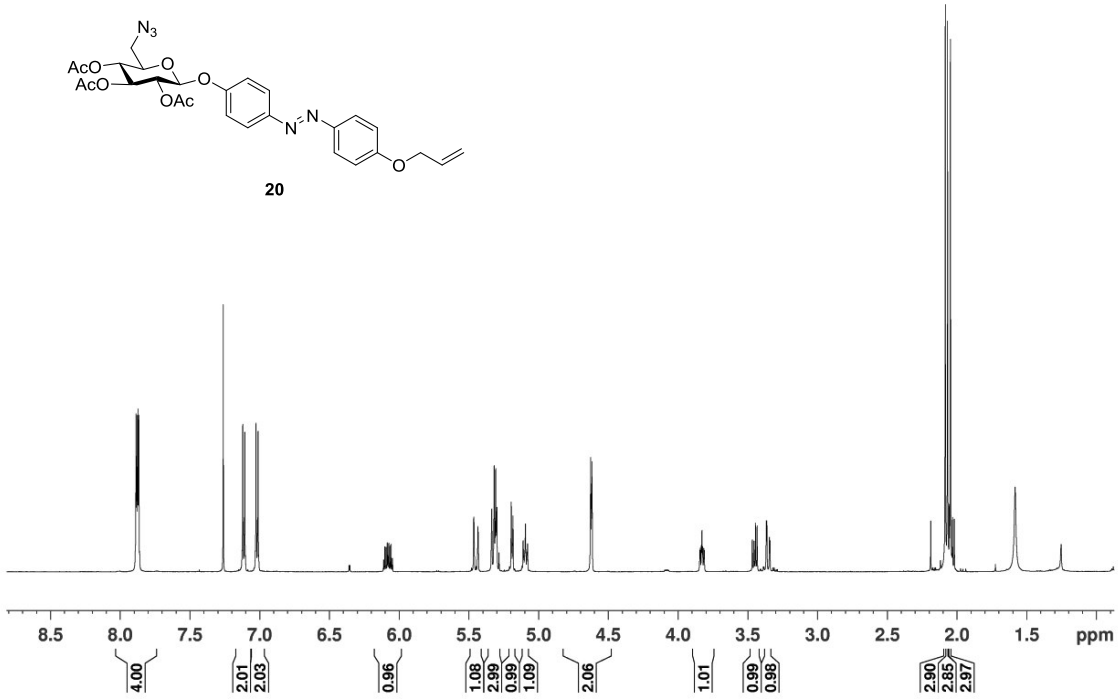

Figure S25. ^{1}H NMR spectrum of **20** (600 MHz, $CDCl_3$, 298 K,TMS).

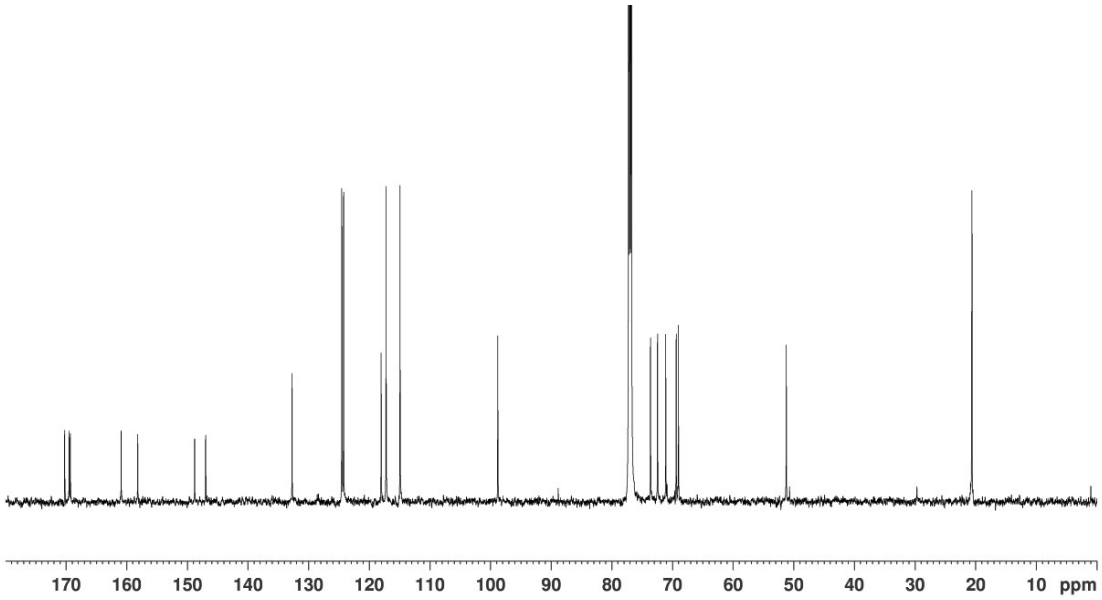

Figure S26. ^{13}C NMR spectrum of **20** (151 MHz, $CDCl_3$, 298 K, TMS).

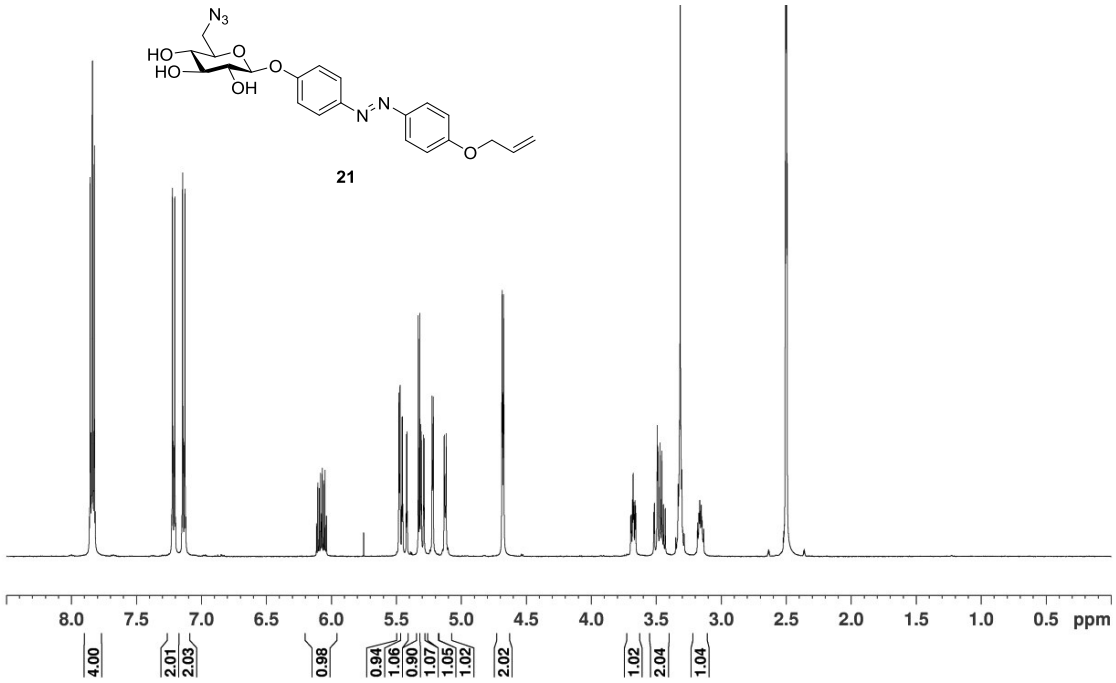

Figure S27. ^{1}H NMR spectrum of **21** (500 MHz, DMSO-d_6, 300 K).

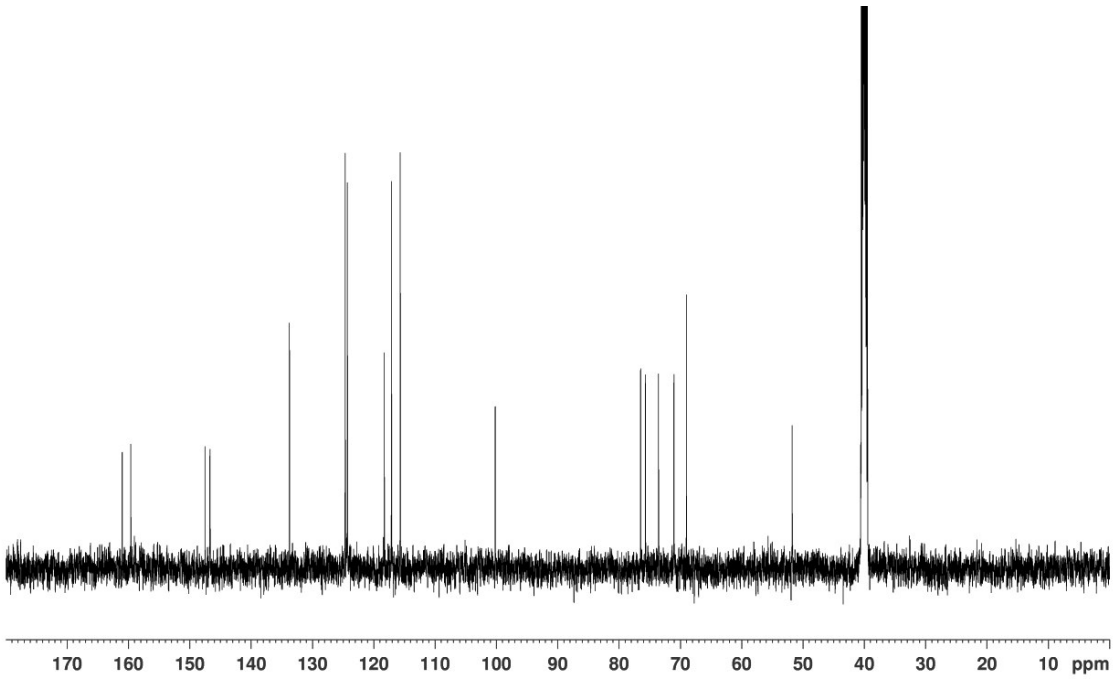

Figure S28. ^{13}C NMR spectrum of **21** (126 MHz , DMSO-d_6, 300 K).

4. Photoirradiation experiments

Photoirradiation was performed using a LED (emitting 365 nm light) from the Nichia Corporation (NC4U133A) with a FWHW of 9 nm and optical power output (P_O) ~1 W. The respective *E*-configured azobenzene (5-10 mg) was dissolved in DMSO-d_6 (500 µL) in a NMR tube and irradiated for 15 min at 365 nm. The distance between the LED and sample in the NMR tube was about ~5 cm. Photostationary states (PSS) were reached after approx. 15 min and the *E*/*Z* ratios were calculated by ^{1}H NMR spectroscopy. The photostationary state (PSS) was determined by integration of the anomeric H-1 protons of the prepared compounds (or by integration of aryl signals on case of **5** and**7**).

In analogy, for UV-Vis spectroscopy, the *E*-configured azobenzene derivatives was dissolved in DMSO (80 µm) in a UV cuvette, irradiated for 15 min at 365 nm with a distance between LED and cuvette of ~5 cm, and UV-Vis spectra were recorded immediately afterwards. The absorption spectra showed an increase of the absorbance in the n-π* transition and simultaneous decrease in the π-π* transition, indicating the formation of the respective *Z* isomer.

The kinetics of thermal *Z*→*E* relaxation process was determined by NMR spectroscopy in the dark. The half-life $\tau_{1/2}$ was determined as $\tau_{1/2} = \ln 2/k$. After irradiation, the ^{1}H NMR spectra of the samples were recorded in regular intervals over a period of 4 to 6 days. For the determination of the half-life the *Z* and *E* signals of the respective azobenzene moiety were integrated. A signal that was not influenced by irradiation was set as reference. The decay of the integral of the *Z* and the increase of the integral of the *E* species were plotted and an exponential decay of first order fitted to the data.

NMR spectra of *Z*-configured compounds and UV-Vis spectroscopy

(*Z*)-[*p*-(Allyloxy)-*p'*-(propargyloxy)]azobenzene (5):

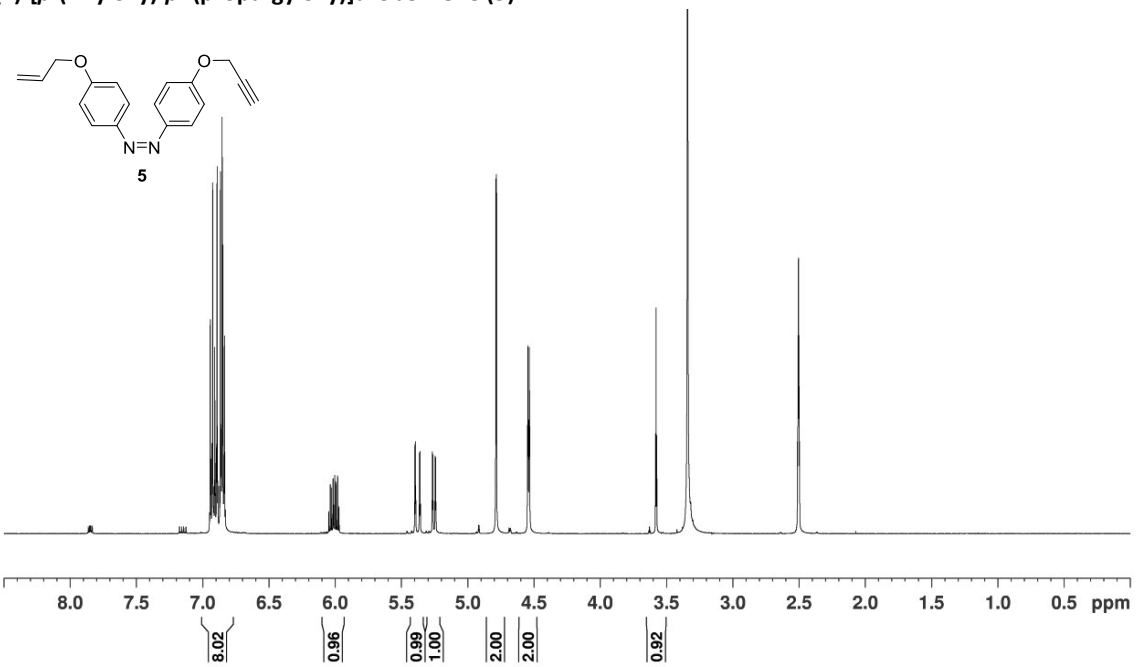

Figure S29. ^{1}H NMR spectrum of (*Z*)-**5** (500 MHz, DMSO-d_6, 300 K).

^{1}H NMR (500 MHz, DMSO-d_6, 300 K): δ=6.94-6.84 (m, 8H, Ar-H$_{ortho}$, Ar-H$_{ortho'}$, Ar-H$_{meta'}$, Ar-H$_{meta}$), 6.01 (ddt, $^{3}J_{CH=CH2,CH=CH}$=17.2 Hz, $^{3}J_{CH=CH2,CH=CH'}$=10.5 Hz, $^{3}J_{OCH2Allyl,CH=CH2}$=5.3 Hz, 1H, C*H*=CH$_2$), 5.38 (ddt, $^{4}J_{OCH2,CH=CH}$=1.5 Hz, $^{3}J_{CH=CH2,CH=CH}$=17.3 Hz, $^{2}J_{CH=CH,CH=CH'}$=3.2 Hz 1H, CH=C*H*), 5.25 (ddt, $^{4}J_{OCH2,CH=CH'}$=1.5 Hz, $^{3}J_{CH=CH2,CH=CH'}$=10.5 Hz, $^{2}J_{CH=CH,CH=CH'}$=3.2 Hz, 1H, CH=C*H'*), 4.79 (d, $^{4}J_{OCH2,C≡CH}$=2.4 Hz, 2H, OCH$_{2Propragyl}$), 4.54 (ddd~dt, $^{4}J_{OCH2,CH=CH'}$=3.0 Hz, $^{4}J_{OCH2,CH=CH}$=1.5 Hz, $^{3}J_{OCH2,CH=CH2}$=5.3 Hz, 2H, OCH$_{2Allyl}$), 3.58 (t, $^{4}J_{OCH2,C≡CH}$=2.4 Hz, 1H, C≡CH) ppm.

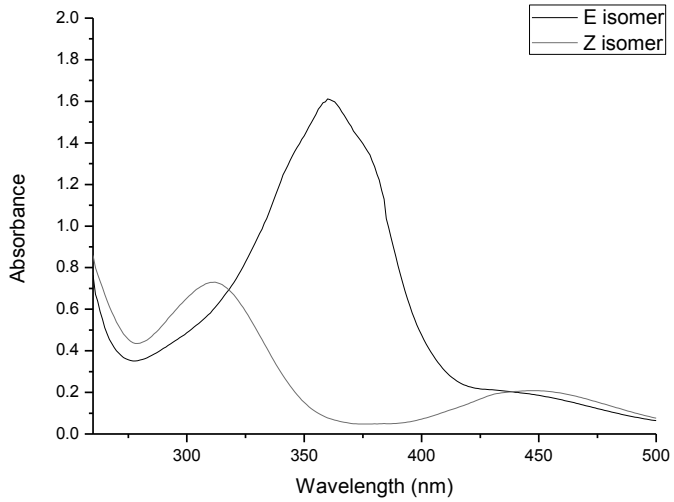

Figure S30. UV-Vis spectra of **5**: *E* isomer in black, *Z* isomer in red; irradiation with 365 nm and 440 nm, respectively, in DMSO at 293 K.

(*Z*)-[*p*-(3-Mercaptopropoxy)-*p'*-(propargyloxy)]azobenzene (7):

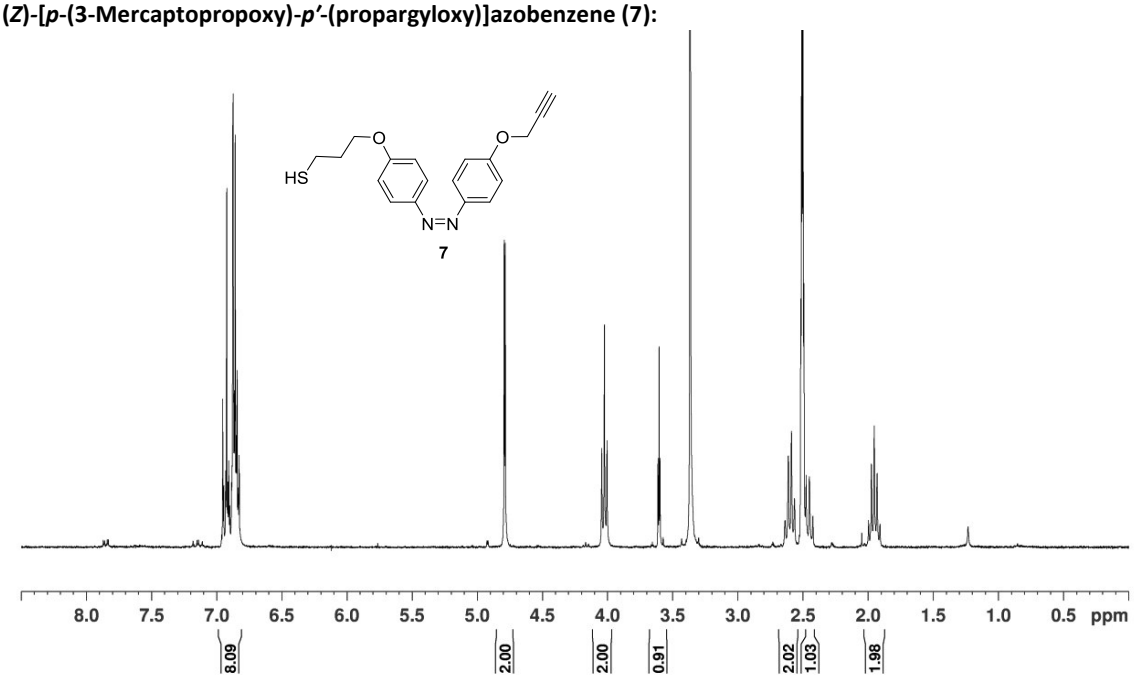

Figure S31. ^{1}H NMR spectrum of (*Z*)-**7** (300 MHz, DMSO-d_6, 300.0 K).

^{1}H NMR (300 MHz, , DMSO-d_6, 300 K): δ=6.95-6.83 (m, 8H, Ar-H$_{ortho}$, Ar-H$_{ortho'}$, Ar-H$_{meta'}$, Ar-H$_{meta}$), 4.79 (d, $^{4}J_{OCH2,C\equiv CH}$=2.4 Hz, 2H, OCH$_2$$_{Propragyl}$), 4.02 (t, $^{3}J_{OCH2CH2,OCH2CH2}$=6.2 Hz, 2H, OC*H*$_2$CH$_2$), 3.60 (t, $^{4}J_{OCH2,C\equiv CH}$=2.4 Hz, 1H, C≡CH), 2.64-2.56 (m, 2H, C*H*$_2$SH), 2.50-2.42 (m, 2H, SH), 2.00-1.91 (m, 2H, OCH$_2$*CH*$_2$) ppm.

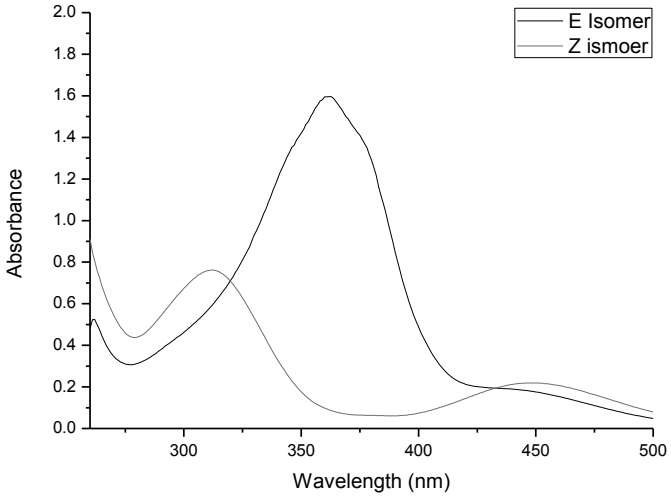

Figure S32. UV-Vis spectra of **7**: *E* isomer in black, *Z* isomer in red; irradiation with 365 nm and 440 nm, respectively, in DMSO.

(*Z*)-*p*-[*p'*-(Propargyloxy)]phenylazophenyl 2-*O*-allyl-α-D-mannopyranoside (14):

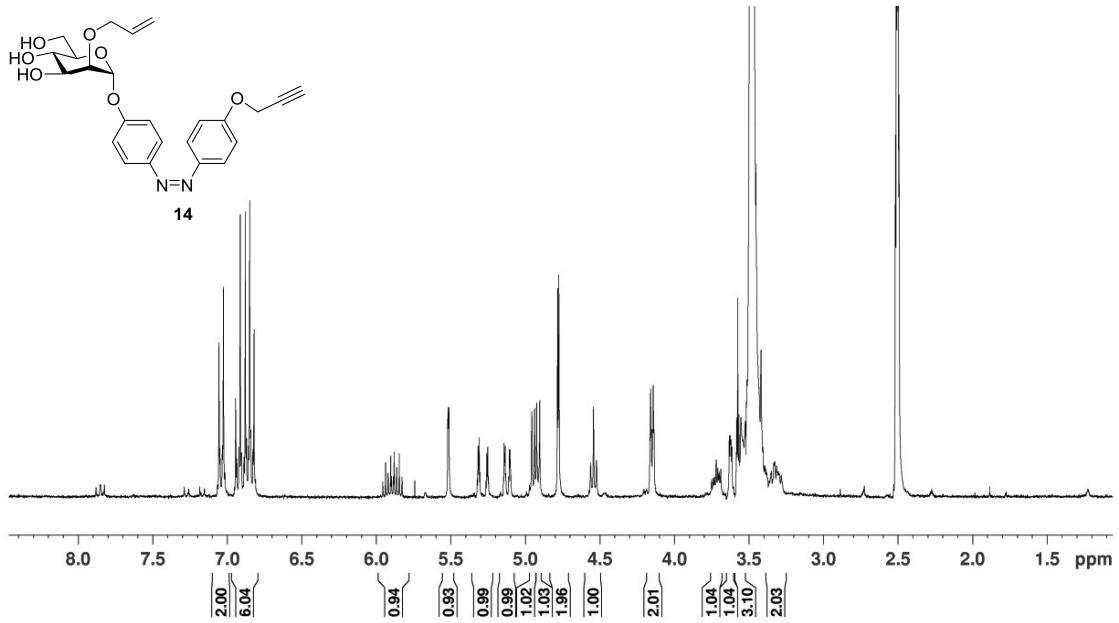

Figure S33. ^{1}H NMR spectrum of (*Z*)-**14** (300 MHz, DMSO-d_6, 300 K).

^{1}H NMR (300 MHz, DMSO-d_6, 300 K): δ=7.07-7.02 (m, 2H, Ar-H$_{ortho}$), 6.95-6.81 (m, 6H, Ar-H$_{ortho'}$, Ar-H$_{meta'}$, Ar-H$_{meta}$), 5.89 (ddt, $^{3}J_{CH=CH2,CH=CH}$=17.3 Hz, $^{3}J_{CH=CH2,CH=CH'}$=10.6 Hz, $^{3}J_{OCH2,CH=CH2}$=5.9 Hz, 1H, C*H*=CH$_2$), 5.52 (d, $^{3}J_{1,2}$=1.7 Hz, 1H, H-1), 5.31 (ddt, $^{4}J_{OCH2,CH=CH}$=1.6 Hz, $^{3}J_{CH=CH2,CH=CH}$=17.3 Hz, $^{2}J_{CH=CH,CH=CH'}$=3.8 Hz 1H, CH=C*H*), 5.15-5.10 (m, 1H, CH=C*H'*), 4.95 (d, $^{3}J_{OH,3}$=5.8 Hz, 1H, OH$_{C-3}$), 4.91 (d, $^{3}J_{OH,4}$=6.0 Hz, 1H, OH$_{C-4}$), 4.78 (d, $^{4}J_{OCH2,C≡CH}$=2.2 Hz, 2H, OCH$_{2Propragyl}$), 4.54 (dd~t, $^{3}J_{OH,6}$=5.9 Hz, $^{3}J_{OH,6'}$=5.9 Hz, 1H, OH$_{C-6}$), 4.15 (ddd~dt, $^{4}J_{OCH2,CH=CH'}$=2.9 Hz, $^{4}J_{OCH2,CH=CH}$=1.5 Hz, $^{3}J_{OCH2,CH=CH2}$=5.2 Hz, 2H, OCH$_{2Allyl}$), 3.75-3.69 (m, 1H, H-3), 3.62 (dd, $^{3}J_{1,2}$=1.7 Hz, $^{3}J_{2,3}$=3.2 Hz, 1H, H-2), 3.57 (t, $^{4}J_{OCH2,C≡CH}$=2.5 Hz, 1H, C≡CH), 3.56-3.52 (m, 2H, H-6, H-6'), 3.39-3.28 (m, 2H, H-4, H-5) ppm.

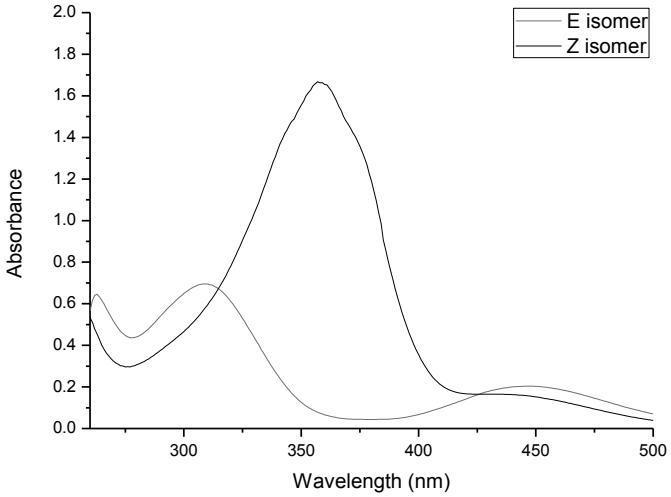

Figure S34. UV-Vis spectra of **14**: *E* isomer in black, *Z* isomer in red; irradiation with 365 nm and 440 nm, respectively, in DMSO at 293 K.

(*Z*)-*p*-[*p'*-(Propargyloxy)]phenylazophenyl 6-azido-6-deoxy-β-D-glucopyranoside (21):

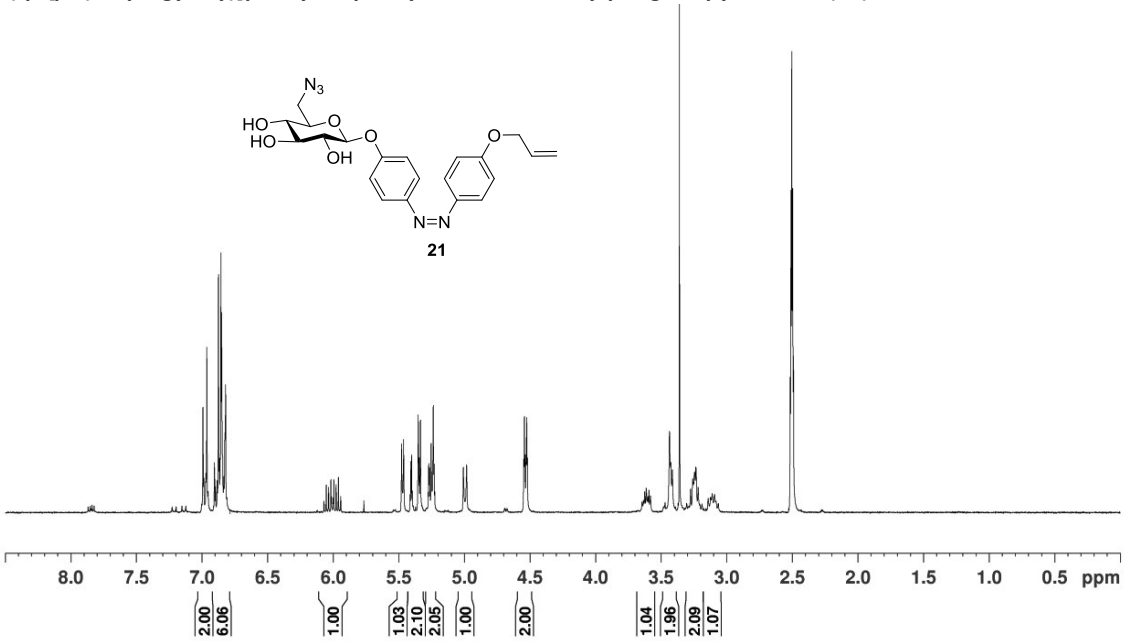

Figure S35. ^{1}H NMR spectrum of (*Z*)-**21** (300 MHz, DMSO-d_6, 300 K)

^{1}H NMR (300 MHz, DMSO-d_6, 300 K): δ=6.99-6.96 (m, 2H, Ar-H$_{ortho}$), 6.87-6.82 (m, 6H, Ar-H$_{ortho'}$, Ar-H$_{meta}$, Ar-H$_{meta'}$), 6.01 (ddd $^{3}J_{CH=CH2,CH=CH}$=17.2 Hz, $^{3}J_{CH=CH2,CH=CH'}$=10.5 Hz, $^{3}J_{OCH2,CH=CH2}$=5.2 Hz, 1H, C*H*=CH$_2$), 5.47 (d, ^{3}J=4.8 Hz, 1H, OH), 5.41-5.34 (m, 2H, CH=C*H*, OH$_{C-4}$), 5.28-5.23 (m, 1H, CH=C*H'*, OH), 5.00 (d, $^{3}J_{1,2}$=7.3 Hz, 1H, H-1), 4.53 (ddd~dt, $^{4}J_{OCH2,CH=CH'}$=1.5 Hz, $^{4}J_{OCH2,CH=CH}$=2.9 Hz, $^{3}J_{OCH2,CH=CH2}$=5.3 Hz, 2H, OCH$_2$), 3.65-3.58 (m, 1H, H-5), 3.47-3.42 (m, 2H, H-6', H-6), 3.31-3.18 (m, 2H, H-3, H-2), 3.16-.3.06 (m, 1H, H-4) ppm.

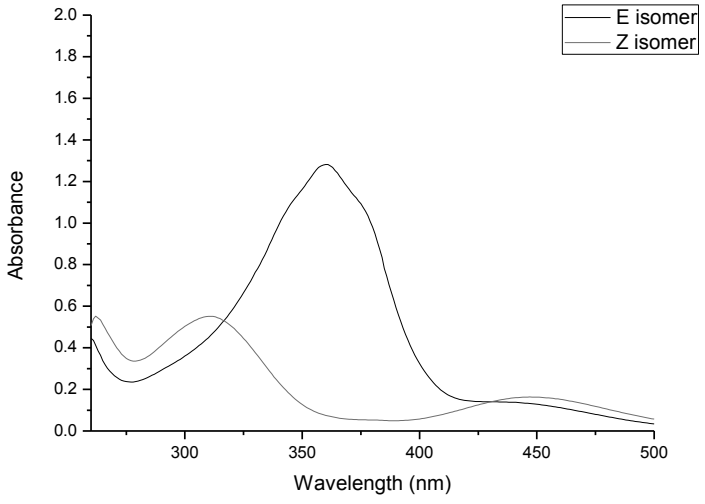

Figure S36. UV-Vis spectra of **21**: *E* isomer in black, *Z* isomer in red; irradiation with 365 nm and 440 nm, respectively, in DMSO at 293 K.

5. Molecular Modeling

Models of the *E* and *Z* isomers of the respective azobenzene derivatives **5**, **7**, **14** and **21** were built using Schrödinger Maestro 10.4[7] and minimized using MacroModel[8] (OPLS_2005 force field). The distances were measured between the terminal allyl group carbon and the quaternary carbon of the propargyl group (**5** and **14**), the terminal sulfhydryl group and the quaternary carbon of the propargyl group (**7**) and the terminal allyl group carbon and the CH_2N of the azido group (**21**). Restraints were added to the azo bond for the *Z* isomer (force constant 100). For the *E* and the *Z* isomer a molecular dynamics run of 10 ns was performed using the OPLS_2005 force field. Constant energy molecular dynamic was performed in water with a step size of 1 fs and 300 K as the simulation temperature. All points histograms were then produced for the respective azobenzene derivatives (Figures S37-S40).

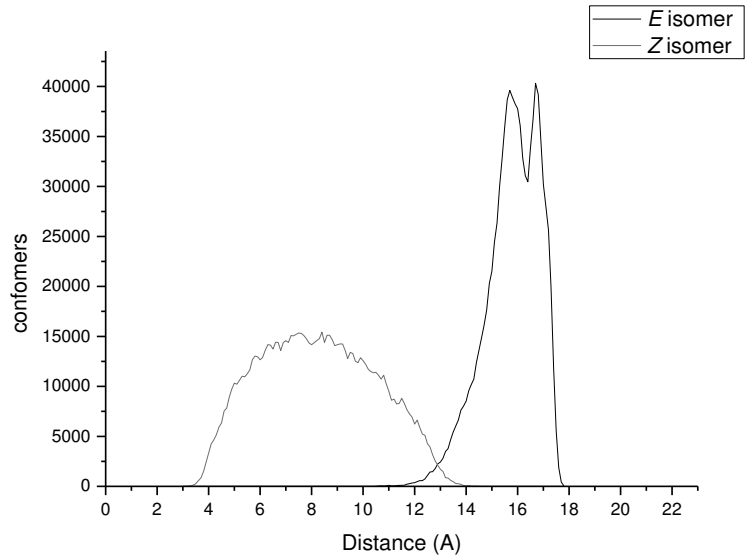

Figure S37. Calculated change in the end-to-end distance of **5**: *E* isomer in black, *Z* isomer in red.

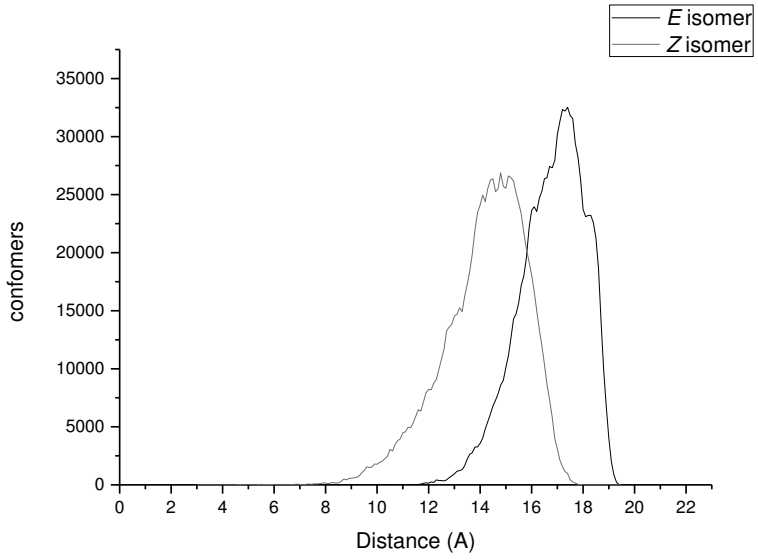

Figure S38. Calculated change in the end-to-end distance of **7**: *E* isomer in black, *Z* isomer in red.

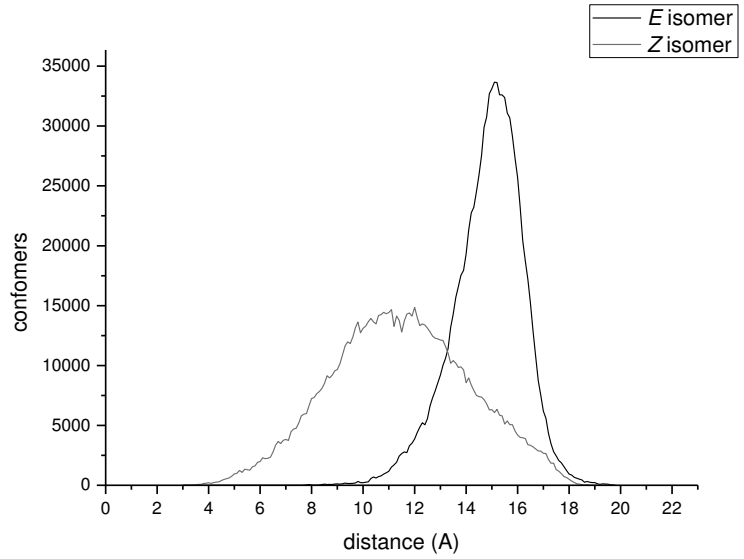

Figure S39. Calculated change in the end-to-end distance of **14**: *E* isomer in black, *Z* isomer in red.

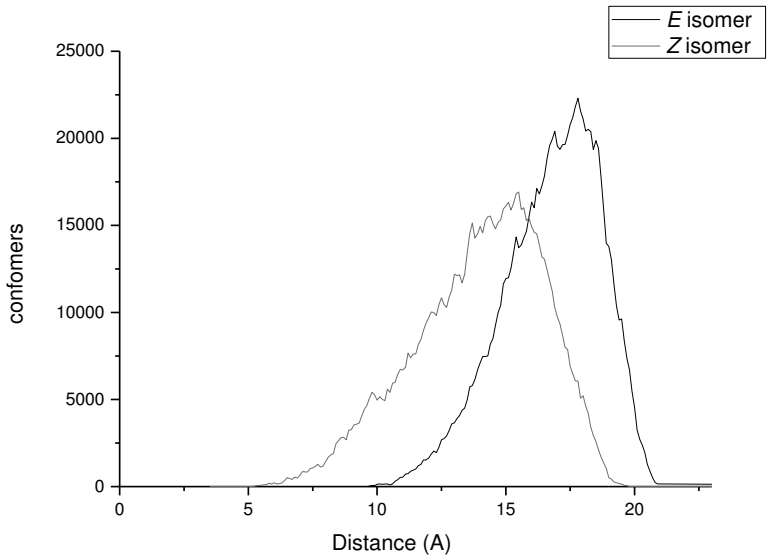

Figure S40. Calculated change in the end-to-end distance of **21**: *E* isomer in black, *Z* isomer in red.

6. References

[1] J. Mo, D. Eom, E. Lee, P. H. Lee, *Org.Lett.* **2012**, *14*, 3684-3687.

[2] M. Becker, F. Lin, patent, WO2015048728 (A1) — 2015-04-02.

[3] L. Möckl, A. Müller, C. Bräuchle, T. K. Lindhorst *Chem. Commun.* **2016**, *52*, 1254-1257.

[4] V. Chandrasekaran, h. K. Lindhorst, *Chem. Commun.* **2012**, *48*, 7519-7521.

[5] C.-W. T. Chang, Y. Hui, B. Elchert, J. Wang, J. Li, R. Rai, *Org. Lett.* **2002**, *4*, 4603-4606.

[6] A. Müller, H. Kobarg, V. Chandrasekaran, J. Gronow, F. D. Sönnichsen, T. K. Lindhorst, *Chem. Eur. J.* **2015**, *21*, 13723-13731.

[7] Schrödinger Release 2015-4**:** Maestro, version 10.4, Schrödinger, LLC, New York, NY, 2015.

[8] Schrödinger Release 2015-4**:** MacroModel, version 11.0, Schrödinger, LLC, New York, NY, 2015.

8.2 Supporting Information on Chapter 4

8.2.1 Supporting information for the manuscript *Azobenzene glycosides on glass: A tool to investigate photoswitchable cell adhesion*

Supporting Information

for

Azobenzene glycosides on glass: A tool to investigate photoswitchable cell adhesion

A. Müller, Claudia Fessele, T. K. Lindhorst

Methods and materials

11-Aminoundecyltrimethoxysilane (**7**) was purchased from AlfaAesar and used without further purification. Quartz slides were purchased from Plano, GPE Scientific Limited and Chemglass Life Science. Quartz slides have been cut to a size of 2.5 × 1 cm and functionalized in Falcon™ 15mL Conical centrifuge tubes. Moisture-sensitive reactions were carried out in dry glassware and under a positive pressure of nitrogen. Analytical thin layer chromatography (TLC) was performed on silica gel plates (GF 254, Merck). Visualization was achieved by UV light and/or with 10% sulfuric acid in ethanol followed by heat treatment at ~180 °C. Flash chromatography was performed on silica gel 60 (Merck, 230-400 mesh, particle size 0.040-0.063 mm) by using distilled solvents. Dry 1,4-dioxane and *N*,*N*-dimethylformamide over molecular sieves was purchased from Acros Organics and used without further purification. Melting points (mp) were determined on a Büchi M-56 apparatus. Optical rotations were measured with a Perkin-Elmer 241 polarimeter (sodium D-line: 589 nm, length of cell: 1 dm) in the solvents indicated. Proton (^{1}H) nuclear magnetic resonance spectra and carbon (^{13}C) nuclear magnetic resonance spectra were recorded on a Bruker DRX-500 and AV-600 spectrometer. Chemical shifts are referenced to the residual proton of the NMR solvent. Data are presented as follows: chemical shift, multiplicity (s=singlet, d=doublet, t=triplet, q=quartet, m=multiplet, and br=broad signal), coupling constant in hertz (Hz) and, integration. Full assignment of the peaks was achieved with the aid of 2D NMR techniques (^{1}H/^{1}H COSY and ^{1}H/^{13}C HSQC. All NMR spectra of the *E*-isomers of the azobenzene derivatives were recorded after they were kept for 16 h in the dark at 40 °C. Infrared (IR) spectra were measured with a Perkin Elmer FT-IR Paragon 1000 (ATR) spectrometer and were reported in cm^{-1}. ESI mass spectra were recorded on a LCQ Classic from Thermo Finnigan. UV-vis absorption spectra were performed on Perkin-Elmer Lambda-241 at a temperature of 20 °C ± 1 °C. For irradiation experiments with 365 nm an apparatus with 10 LEDs (Nichia NCSU276A U365) with a total power of 7500 W was used with 50 % (3750 W). For irradiation with 440 nm a similar apparatus with 10 LEDs (10 x Roithner VL440) with total power of 4500 W was used with 50 % (2250 W). Both apparatus were built from Sahlmann Photochemical Solutions. Fluorescence read out was accomplished with an Infinite® 200 PRO multimode reader from Tecan.

Synthesis of glycoconjugates

(*E*)-*p*-[*p*'-(*N*-*tert*-Butoxycarbonyl-aminomethyl)phenylazo]phenyl α-D-mannopyranoside (3): Crude **1**[1] (541 mg, 1.55 mmol, calculated via ^{1}H NMR spetroscopy) and *p*-aminophenyl α-D-mannopyranoside[2] (**2**, 420 mg, 1.55 mmol) were dissolved in a mixture of dimethyl sulfoxide and acetic acid (1:1, 14 mL). The reaction mixture was stirred for 16 h at room temperature. The product was precipitated by addition of water, filtered off and washed with water. Purification of the crude product by column chromatography (dichloromethane/methanol, 9:1→8:1) gave **3** as an orange solid (640 mg, 1.31 mmol, 84%). R_f = 0.38 (ethyl acetate/methanol, 10:1); m.p. 137 °C; $[\alpha]_D^{23}$ = +114.6 (c = 0.4 in methanol); ^{1}H NMR (600 MHz, MeOH-d_4, 300 K): δ = 7.90-7.83 (m, 4H, Ar-H$_{ortho}$, Ar-H$_{ortho'}$), 7.44-7.42 (m, 2H, Ar-H$_{meta'}$), 7.30-7.27 (m, 2H, Ar-H$_{meta}$), 5.60 (d, $^3J_{1,2}$ = 1.8 Hz, 1H, H-1), 4.31 (s, 2H, CH_2NHBoc), 4.04 (dd, $^3J_{1,2}$ = 1.8 Hz, $^3J_{2,3}$ = 3.3 Hz, 1H, H-2), 3.93 (dd, $^3J_{2,3}$ = 3.4 Hz, $^3J_{3,4}$ = 9.5 Hz, 1H, H-3), 3.80-3.71 (m, 3H, H-4, H-6, H-6'), 3.59 (ddd, $^3J_{4,5}$ = 9.7 Hz, $^3J_{5,6}$ = 5.4 Hz, $^3J_{5,6'}$ = 2.5 Hz, 1H, H-5), 1.47 (s, 9H, C(CH$_3$)$_3$) ppm; ^{13}C NMR (126 MHz, MeOH-d_4, 300 K): δ = 160.3 (C-Ar$_{para}$), 158.6 (C=O$_{Boc}$), 153.1 (C-Ar$_{ipso'}$), 149.2 (C-Ar$_{ipso}$), 144.0 (C-Ar$_{para'}$), 128.8 (C-Ar$_{meta'}$), 125.5 (C-Ar$_{ortho}$), 123.7 (C-Ar$_{ortho'}$), 118.0 (C-Ar$_{meta}$), 100.1 (C-1), 80.3 (*C*(CH$_3$)$_3$), 75.7 (C-5), 72.4 (C-3), 71.9 (C-2), 68.3 (C-4), 62.7 (C-6), 44.8 (*C*H$_2$NHBoc), 28.8 (C(*C*H$_3$)$_3$) ppm; IR (ATR): $\tilde{\nu}$ = 3281, 2922, 1683 1600, 1581, 1470, 1363, 1339, 1228, 1098, 1017, 846 cm^{-1}; ESI-MS: m/z calcd for $C_{24}H_{31}N_3O_8$: 512.2 $[M+Na]^+$; found 512.2.

(*E*)-*p*-[*p*'-(Aminomethyl)phenylazo]phenyl α-D-mannopyranoside · TFA (4): To a suspension of the mannoside **3** (832 mg, 1.70 mmol) in dichloromethane (20 mL), trifluoroacetic acid (2 mL) was added. The reaction mixture was stirred for 1.5 h at room temperature. Then the solvent was evaporated and **4** was obtained as an orange solid (850 mg, 1.68 mmol, 99%). The TFA salt was used in the next step without further purification. R_f = 0.15 (ethyl acetate/methanol, 5:1); m.p. 119 °C; $[\alpha]_D^{23}$ = -4.50 (c=0.6 in methanol); ^{1}H NMR (500 MHz, MeOH-d_4, 300 K): δ = 7.95-7.91 (m, 4H, Ar-H$_{ortho}$, Ar-H$_{ortho'}$), 7.64-7.61 (m, 2H, Ar-H$_{meta'}$), 7.30-7.27 (m, 2H, Ar-H$_{meta}$), 5.61 (d, $^3J_{1,2}$ = 1.8 Hz, 1H, H-1), 4.21 (s, 2H, CH_2NH$_2$), 4.05 (dd, $^3J_{1,2}$ = 1.8 Hz, $^3J_{2,3}$ = 3.5 Hz, 1H, H-2), 3.92 (dd, $^3J_{2,3}$ = 3.5 Hz, $^3J_{3,4}$ = 9.5 Hz, 1H, H-3), 3.80-3.71 (m, 3H, H-4, H-6, H-6'), 3.59 (ddd, $^3J_{4,5}$ = 9.7 Hz, $^3J_{5,6}$ = 5.3 Hz, $^3J_{5,6'}$ = 2.6 Hz, 1H, H-5) ppm; ^{13}C NMR (126 MHz, MeOH-d_4, 300 K): δ = 160.7 (C-Ar$_{para}$), 154.3 (C-Ar$_{ipso'}$), 149.1 (C-Ar$_{ipso}$), 136.8 (C-Ar$_{para'}$), 130.9 (C-Ar$_{meta'}$), 125.8 (C-Ar$_{ortho}$), 124.2 (C-Ar$_{ortho}$'), 118.1 (C-Ar$_{meta}$), 100.1 (C-1), 75.7 (C-5), 72.4 (C-2), 71.8 (C-3), 68.3 (C-4), 62.6 (C-6), 44.0 (CH$_2$NH$_2$) ppm; IR (ATR): $\tilde{\nu}$ = 2929, 1663, 1494, 1233, 1188, 1000, 845 cm^{-1}; ESI-MS: m/z calcd for $C_{19}H_{23}N_3O_6$: 412.2 $[M+Na]^+$; found 412.2.

(*E*)-*p*-[*p*'-(Azidomethyl)phenylazo]phenyl α-D-mannopyranoside (5): To a suspension of the amine **4** (394 mg, 758 µmol), potassium carbonate (210 mg, 1.52 mmol) and $CuSO_4 \cdot 5\ H_2O$ (2.00 mg, 7.58 µmol) in methanol (4 mL), imidazole-1-sulfonyl azide hydrochloride[3] (254 mg, 1.21 mmol) was added. The reaction mixture was stirred for 16 h at room temperature. Then the solvent was evaporated and afterwards ethyl acetate (10 mL) and water (10 mL) were added. The phases were separated and the aqueous phase extracted with ethyl acetate (4 × 10 mL). The combined organic phases were dried over $MgSO_4$, it was filtered and the filtrate concentrated under reduced pressure. The crude product was recrystallized from a mixture of methanol and water (1:7) and the azobenzene derivative **5** was obtained as an orange solid (195 mg, 469 µmol, 62%). R_f =

0.50 (ethyl acetate/methanol, 10:1); m.p. 198 °C; $[\alpha]_D^{23}$ = +135.6 (c = 0.4 in dimethylsulfoxide); ^{1}H NMR (600 MHz, DMSO-d_6, 300 K): δ = 7.90-7.87 (m, 4H, Ar-H$_{ortho}$, Ar H$_{ortho'}$), 7.58-7.57 (m, 2H, Ar-H$_{meta'}$), 7.29-7.28 (m, 2H, Ar H$_{meta}$), 5.53 (d, $^3J_{1,2}$ = 1.4 Hz, 1H, H-1), 5.10 (d, $^3J_{2,OH}$ = 4.4 Hz, 1H, OH$_{C\text{-}2}$), 4.86 (d, $^3J_{4,OH}$ = 5.8 Hz, 1H, OH$_{C\text{-}4}$), 4.79 (d, $^3J_{3,OH}$ = 5.9 Hz, 1H, OH$_{C\text{-}3}$), 4.58 (s, 2H, CH_2N_3), 4.46 (t, $^3J_{6,OH}$ = 5.9 Hz, $^3J_{6',OH}$ = 5.9 Hz, 1H, OH$_{C\text{-}6}$), 3.88-3.86 (m, 1H, H-2), 3.72-3.69 (m, 1H, H-3), 3.61 (ddd, $^2J_{6,6'}$ = 11.7 Hz, $^3J_{5,6}$ = 1.9 Hz, $^3J_{6,OH}$ = 5.9 Hz, 1H, H-6), 3.54-3.46 (m, 2H, H-4, H-6'), 3.41-3.38 (m, 1H, H-5) ppm; ^{13}C NMR (151 MHz, DMSO-d_6, 300 K): δ = 159.1 (C-Ar$_{para}$), 151.6 (C-Ar$_{ipso'}$), 146.9 (C-Ar$_{ipso}$), 138.5 (C-Ar$_{para'}$), 129.4 (C-Ar$_{meta'}$), 124.4 (C-Ar$_{ortho}$), 122.6 (C-Ar$_{ortho'}$), 117.1 (C-Ar$_{meta}$), 98.7 (C-1), 75.3 (C-5), 70.6 (C-3), 69.9 (C-2), 66.6 (C-4), 61.0 (C-6), 53.1 (CH_2N_3) ppm; IR (ATR): $\tilde{\nu}$ = 3249, 2889, 2165, 2104, 1578, 1493, 1347, 1234, 1119, 1073, 1009, 973, 853 cm^{-1};cm-1; ESI-MS: m/z calcd for $C_{19}H_{21}N_5O_6$: 438.1 $[M+Na]^+$; found 438.3.

(*E*)-*p*-[*p*'-(Isothiocyanatomethyl)phenylazo]phenyl α-D-mannopyranoside (6): To a solution of the azide **5** (36.0 mg, 86.7 µmol) in dry dioxane (6.5 mL), first carbon disulfide (100 µL, 1.73 mmol) and then triphenylphosphin (25.0 mg, 95.4 µmol) were added. The reaction mixture was stirred for 16 h at room temperature. Then the solvent was evaporated and purification of the crude product by column chromatography (dichloromethane/methanol, 10:1) gave **6** as an orange solid (33.6 mg, 78.0 µmol, 90%). R_f = 0.29 (dichloromethane/methanol, 9:1); m.p. 191 °C; $[\alpha]_D^{23}$ = +131.0 (c = 0.6 in methanol); ^{1}H NMR (500 MHz, DMSO-d_6, 300 K): δ = 7.91-7.89 (m, 4H, Ar-H$_{ortho}$, Ar H$_{ortho'}$), 7.59-7.57 (m, 2H, Ar-H$_{meta'}$), 7.29-7.27 (m, 2H, Ar H$_{meta}$), 5.54 (d, $^3J_{1,2}$ = 1.6 Hz, 1H, H-1), 5.09 (d, $^3J_{2,OH}$ = 4.5 Hz, 1H, OH$_{C\text{-}2}$), 5.07 (s, 2H, *C*H$_2$NCS), 4.85 (d, $^3J_{4,OH}$ = 5.8 Hz, 1H, OH$_{C\text{-}4}$), 4.79 (d, $^3J_{3,OH}$ = 6.0 Hz, 1H, OH$_{C\text{-}3}$), 4.46 (t, $^3J_{6,OH}$ = 5.9 Hz, $^3J_{6',OH}$ = 5.9 Hz, 1H, OH$_{C\text{-}6}$), 3.88-3.86 (m, 1H, H-2), 3.73-3.69 (m, 1H, H-3), 3.63-3.59 (m, 1H, H-6), 3.55-3.46 (m, 2H, H-4, H-6'), 3.40-3.37 (m, 1H, H-5) ppm; ^{13}C NMR (126 MHz, DMSO-d_6, 300 K): δ = 159.1 (C-Ar$_{para}$), 151.7 (C-Ar$_{ipso'}$), 146.8 (C-Ar$_{ipso}$), 137.4 (C-Ar$_{para'}$), 128.2 (C-Ar$_{meta'}$), 124.4 (C-Ar$_{ortho}$), 122.8 (C-Ar$_{ortho'}$), 117.1 (C-Ar$_{meta}$), 98.7 (C-1), 75.3 (C-5), 70.6 (C-3), 69.9 (C-2), 66.6 (C-4), 61.0 (C-6), 47.7 (*C*H$_2$NCS) ppm; IR (ATR): $\tilde{\nu}$ =2972, 2069, 1743, 1597 1496, 1365, 1213, 1126, 1026, 976, 851 cm^{-1}; UV-vis (MeOH): λmax (ε) = 341 nm (12992 L mol^{-1} cm^{-1}); ESI-MS: m/z calcd for $C_{20}H_{21}N_3O_6S$: 454.1 $[M+Na]^+$; found 454.3.

^{1}H and ^{13}C NMR spectra of synthetic compounds

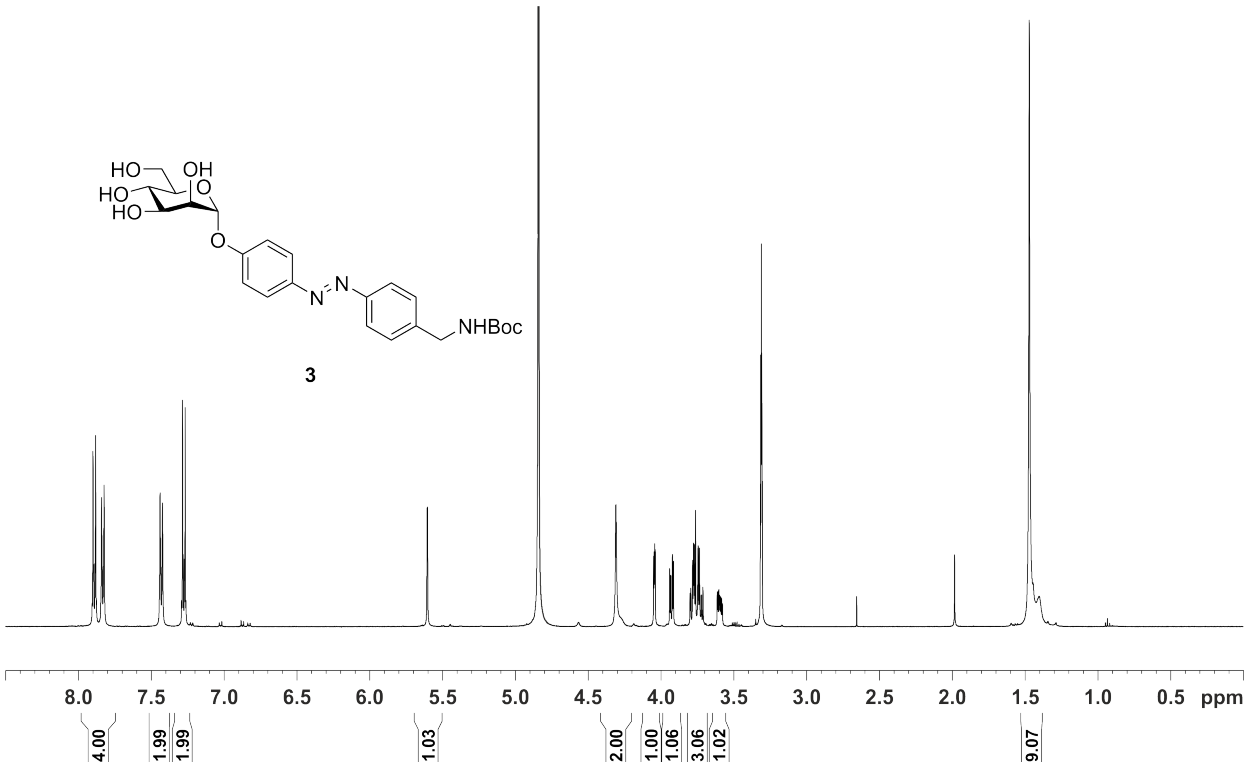

Figure 8.1. ^{1}H NMR spectrum of **3** (500 MHz, MeOH-d_4, 300 K).

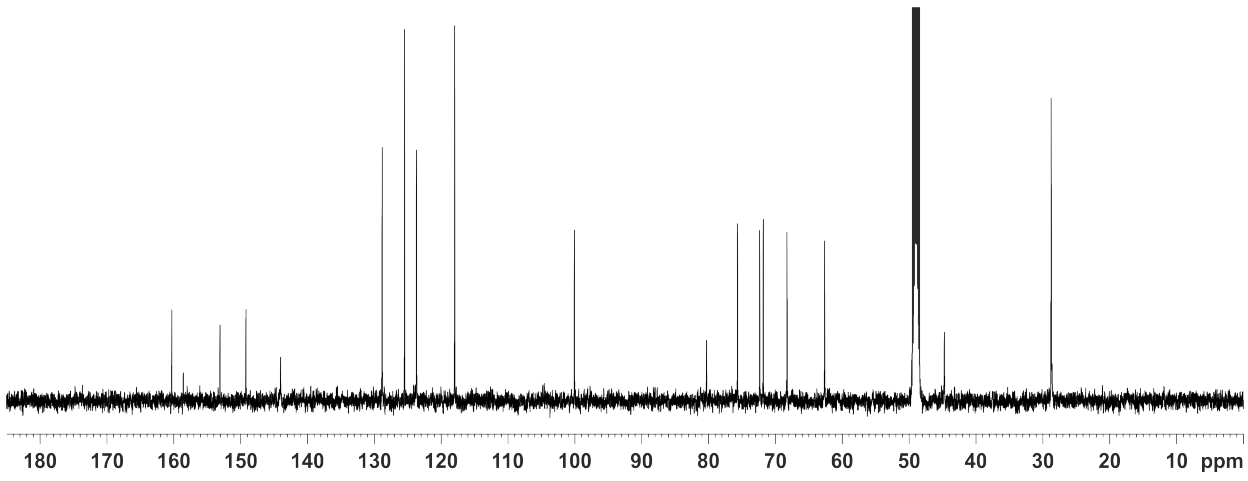

Figure 8.2. ^{13}C NMR spectrum of **3** (126 MHz, MeOH-d_4, 300 K).

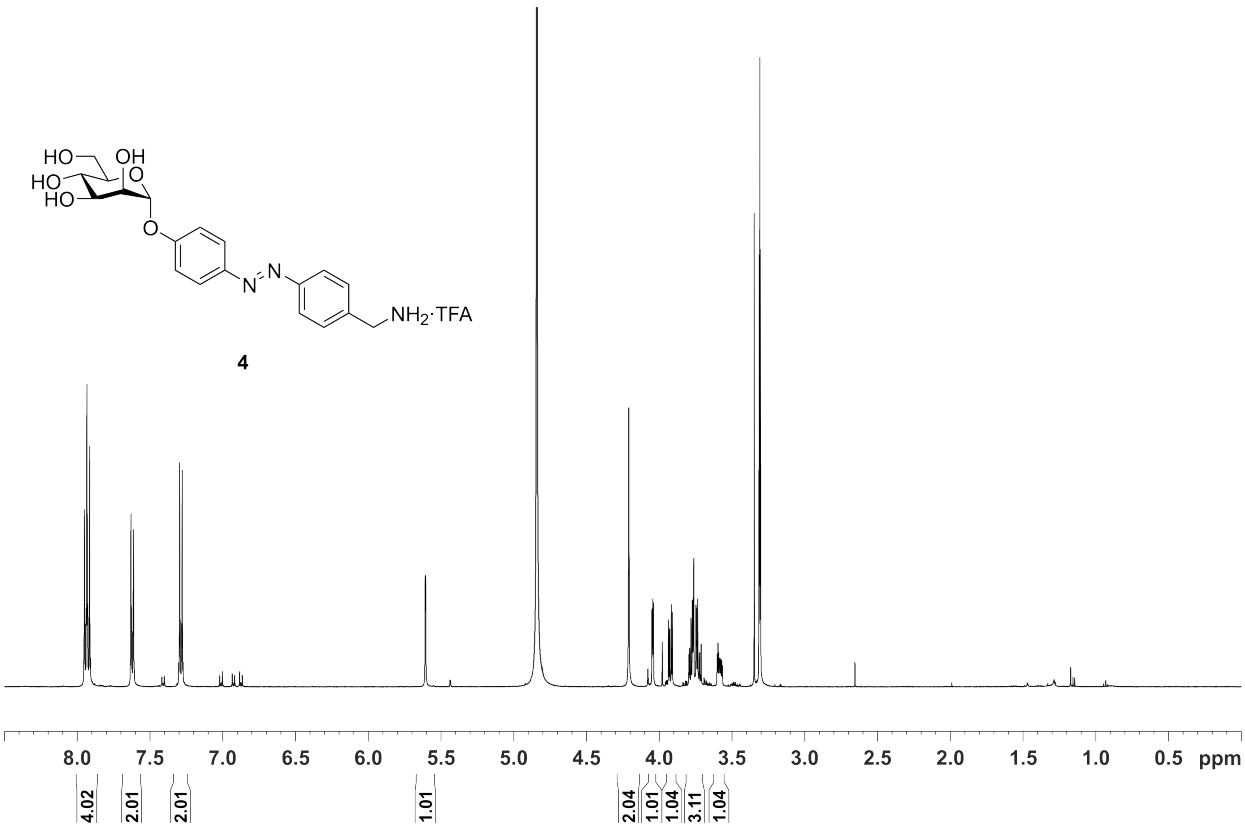

Figure 8.3. ^{1}H NMR spectrum of **4** (500 MHz, MeOH-d_4, 300 K).

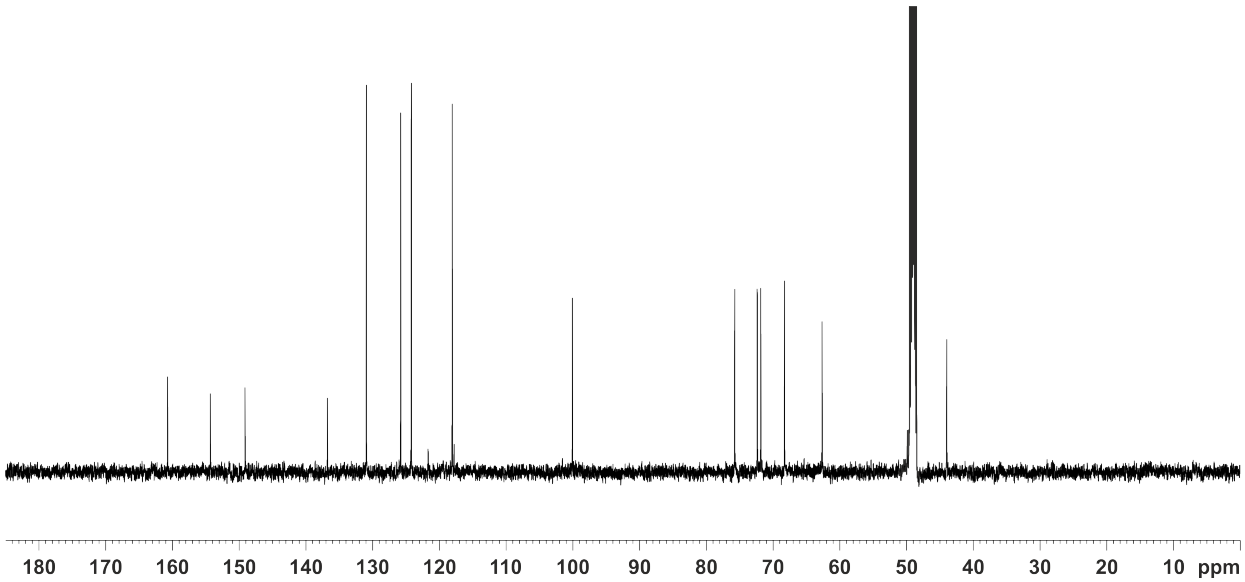

Figure 8.4. ^{13}C NMR spectrum of **4** (126 MHz, MeOH-d_4, 300 K).

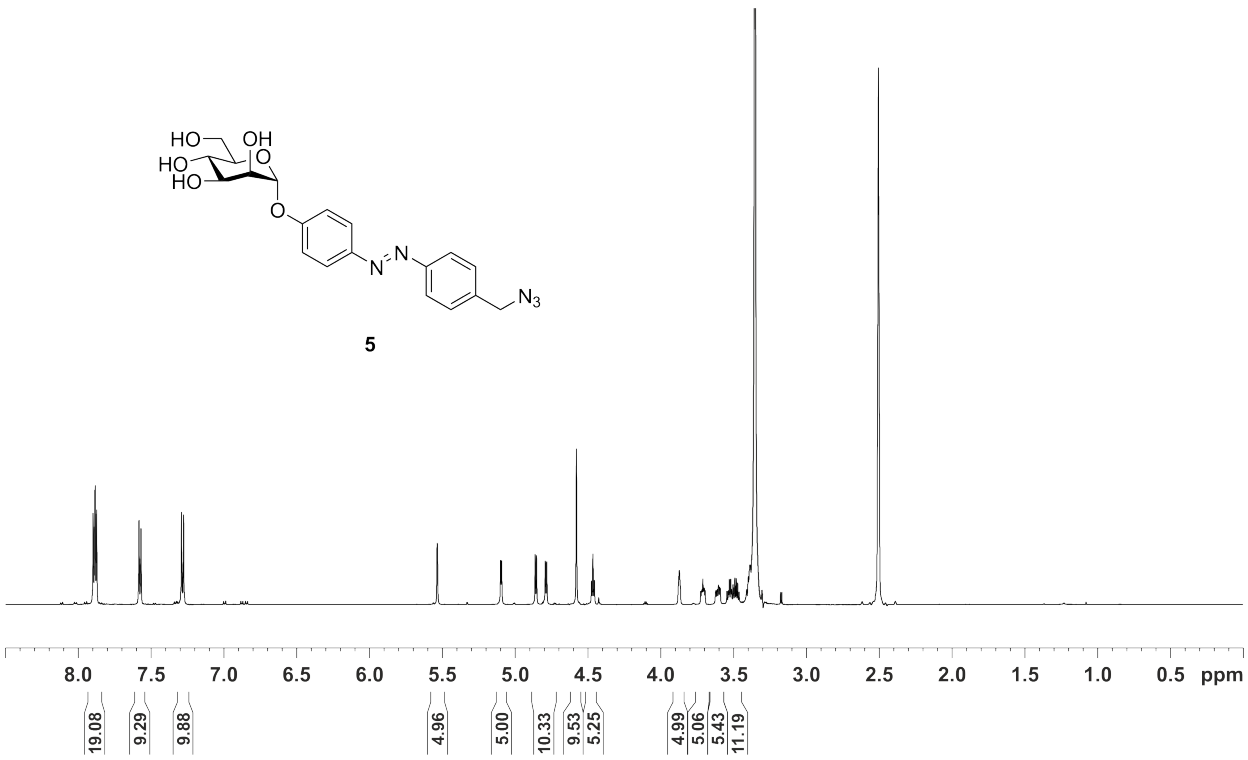

Figure 8.5. ^{1}H NMR spectrum of **5** (600 MHz, DMSO-d_6, 300 K).

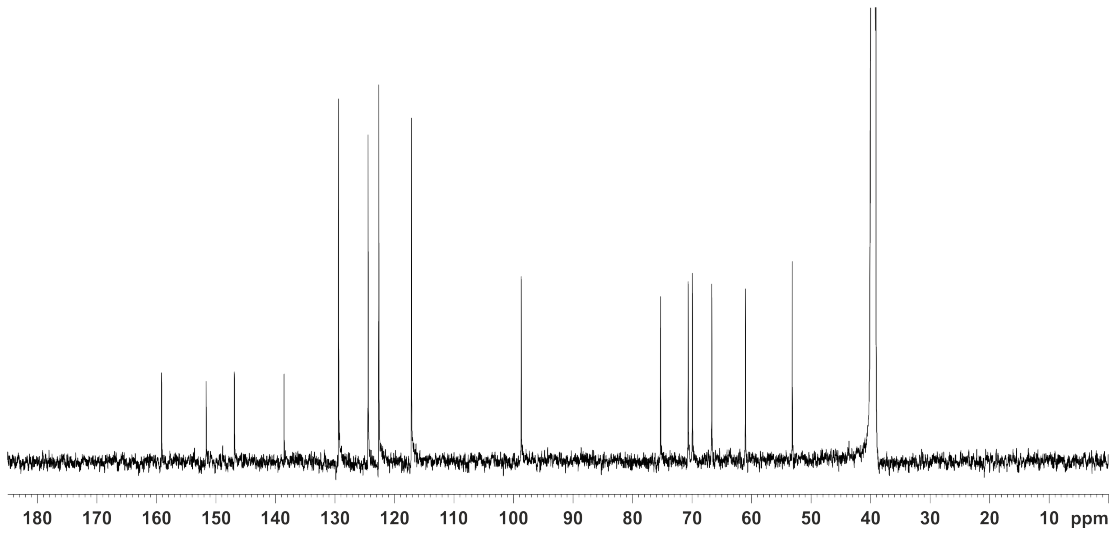

Figure 8.6. ^{13}C NMR spectrum of **5** (151 MHz, DMSO-d_6, 300 K).

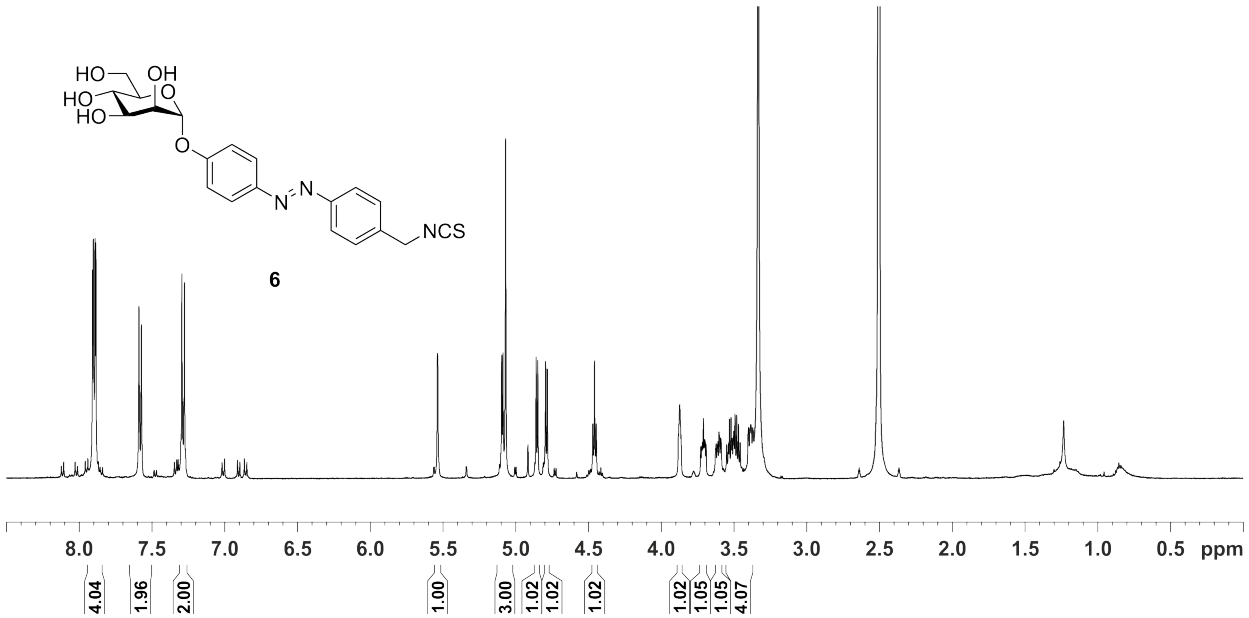

Figure 8.7. ^{1}H NMR spectrum of **6** (500 MHz, DMSO-d_6, 300 K).

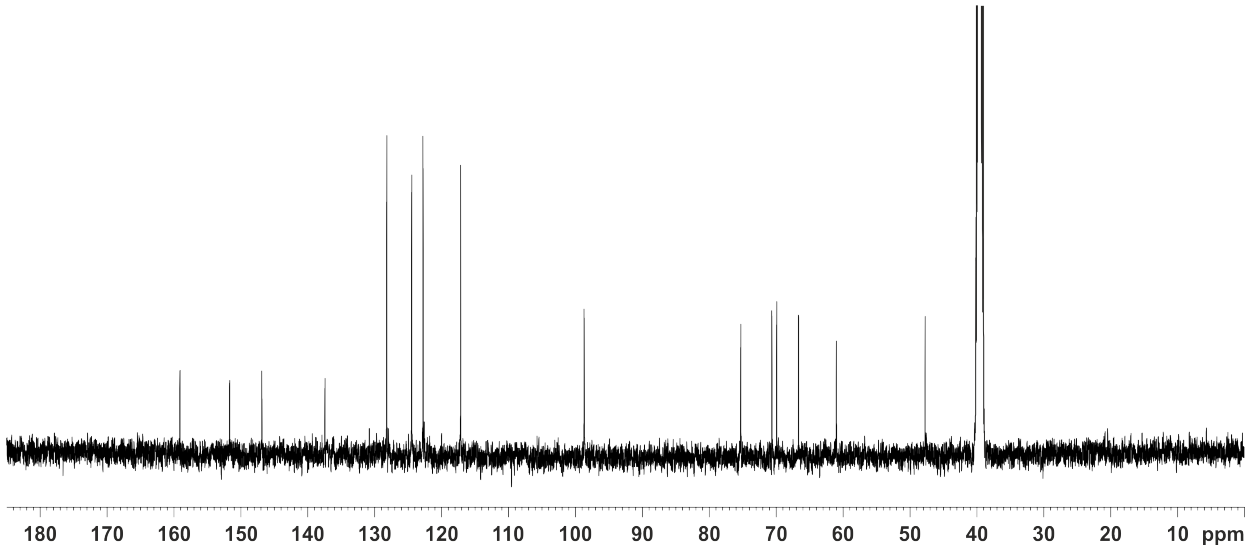

Figure 8.8. ^{13}C NMR spectrum of **6** (126 MHz, DMSO-d_6, 300 K).

UV-vis studies on azobenzene mannoside 6

For UV-vis spectroscopy, the *E*-configured azobenzene derivative **6** was dissolved in methanol and transfered to a UV cuvette, irradiated for 60 s with 365 nm light with a distance between LED and cuvette of ~5 cm. UV-vis spectra were recorded immediately afterwards. The absorption spectra showed an increase of the absorbance in the n-π* transition and simultaneous decrease in the π-π* transition, indicating the formation of the respective *Z* isomer. Extinction coefficients (ε) were deduced from UV-vis spectra measured at seven different concentrations (5 µM, 10 µM, 20 µM, 40 µM, 60 µM, 70 µM and 80 µM).

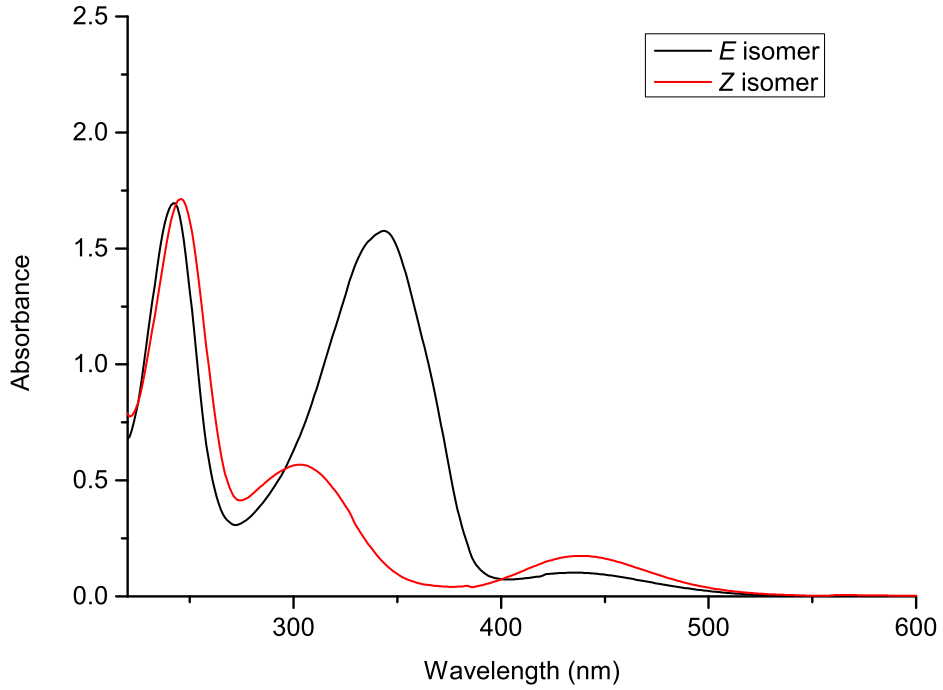

Figure 8.9. UV-vis spectra of **6**: *E* isomer in black, *Z* isomer in red; irradiation with 365 nm and 440 nm, respectively, in MeOH at 293 K.

Glass slide preparation

The mannoside **6** (43.0 mg, 100 µmol) was dried for 30 min in vacuum and afterwards dissolved in dry *N,N*-dimethylformamide (7 mL). Then molecular sieve 3 Å was added and the reaction mixture was stirred for 15 min at room temperature. Afterwards the silane **7** (30.0 mg, 100 µmol) was added and the reaction was again stirred for 16 h at room temperature. The silane **8** was diluted with *N,N*-dimethylformamide (13 mL) and immediately used for glass immobilization without purification.

Immobilization on quartz glass surfaces:

Quartz glass slides were cleaned using piranha solution (conc. sulfuric acid : 35% hydrogen peroxide, 3:1) for 16 h at room temperature. The slides were rinsed with water (2×) and methanol (2×) and dried under a nitrogen stream. Cleaned quartz slides were immersed in *N,N*-dimethylformamide (3 mL) and in the azobenzene silane coating solution (1 mL) for 16 h at 37 °C. Afterwards, the quartz slides were rinsed with *N,N*-dimethylformamide (2×) and methanol (2×) and then dried under a nitrogen stream.

UV-vis studies of the surface assembly

UV-vis measurements were carried out on dried quartz slides using a slide holder. Irradiations at 365 nm and at 440 nm were carried out in the dark at room temperature and without removing the slides from the holder.

For UV-vis spectroscopy, the functionalized glass slides were irradiated for 60 s at 365 nm with a distance between LED and the slide holder of ~5 cm. UV-vis spectra were recorded immediately afterwards. The absorption spectra showed an increase of the absorbance in the n-π^* transition and simultaneous decrease in the π-π^* transition, indicating the formation of the respective *Z* isomer.

The coverslips were irradiated in cycles at $\lambda = 365$ nm and at $\lambda = 440$ nm, respectively for 60 s. Changes in absorbance were measured at 350 nm.

Half-life determination of immobilized azobenzene mannoside **8**:

The kinetics of thermal $Z \rightarrow E$ relaxation process was determined using UV-vis spectroscopy at 20 °C in the dark. The half-life $\tau_{1/2}$ was determined as $\tau_{1/2} = \ln 2/k$. After irradiation with $\lambda = 365$ for 60 s, the UV-vis spectra of the quartz slide was recorded in regular intervals (30 min) over a period of 2 days. For the determination of the half-life the changes in absorbance at 350 nm were plotted and an exponential decay of first order fitted to the data.

Contact angle measurements

Contact angle measurements were recorded on a Drop shape analyser from Krüss GmbH and the contact angle was calculated using a Drop Shape Analysis DSA2 software.

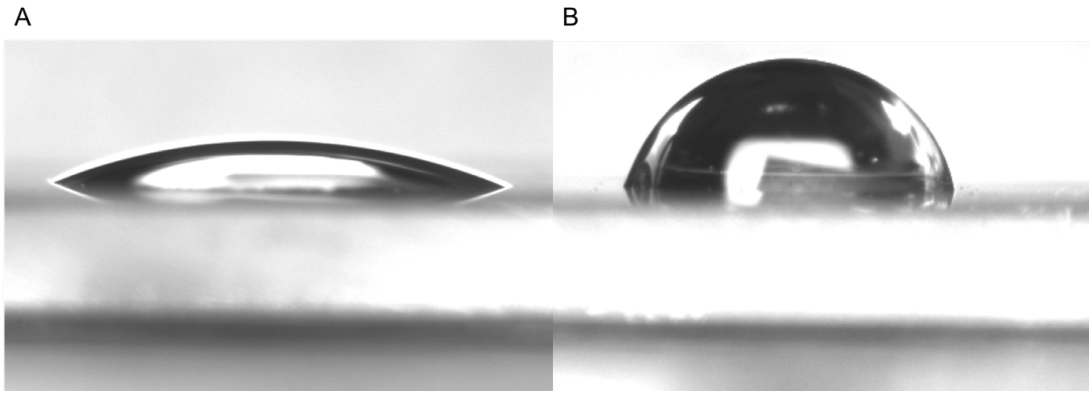

Figure 8.10. Contact angle measurements of the unfunctionalized quartz glass slide (A) compared to the azobenzene mannoside functionalized quartz glass slide (B). The contact angle increases from 26° up to 86°.

Bacterial adhesion studies

Irradiation setup for bacterial adhesion studies:

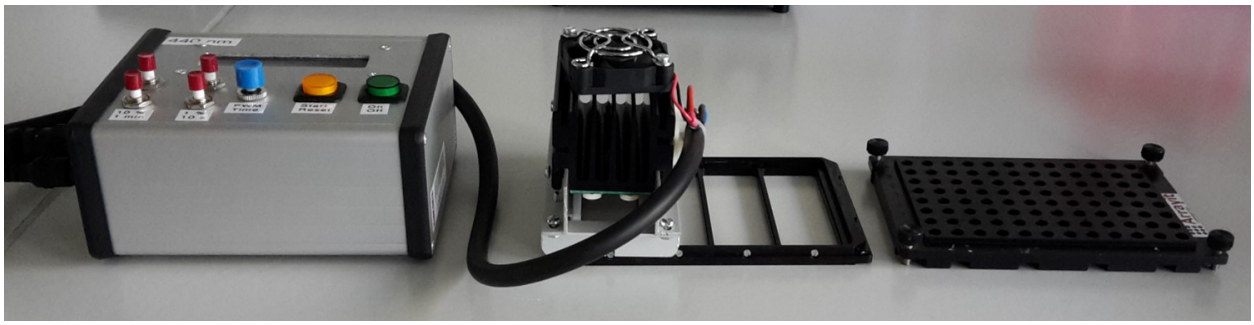

Figure 8.11. Setup for irradiation experiments. Glass slides were fixed in the microplate microarray cassette (Arrayit corporation, CA, USA). LEDs were arranged to exposure 1 quarter of the plate uniformly. Distance between glass slides and LED was 1 cm. Top of the plate (right) was added for adhesion of bacteria and the fluorescence read out in a microplate reader.

E. coli (strain PKL1162)[2] were inoculated in LB medium (10 mL) (Carl Roth, Karlsruhe, Germany) in presence of chloramphenicol (50 mg/L) and ampicillin (100 mg/L) (both Sigma-Aldrich) and grown at 37°C overnight at 175 rpm. Then, the bacteria were centrifuged and washed two times with PBS (Thermo Fisher Scientific, Waltham, MA), suspendend in PBS and the optical density at 600 nm was adjusted to 0.45 using a 7305 spectrophotometer from Jenway.

The prepared glass slides were clamped in a 96-well microarray platform (Arrayit, Sunnyvale, CA) and were exposed in two switching cycles with 365 nm and 440 nm. Every exposure was carried out for 1 min and 3750 mW (365 nm) or 2225 mW (440 nm). After every exposure one glass slide was taken away for analysis of bacterial adhesion.

The glass slides were incubated with 50 µL/well of the prepared bacterial suspension for 30 min at room temperature. Afterwards the slides were washed with PBS (3 x 100 µL/well) and the fluorescence read out (extinction 485 nm, emission 535 nm) was carried out.

Microscopic pictures of fluorescent *E. coli* bacteria

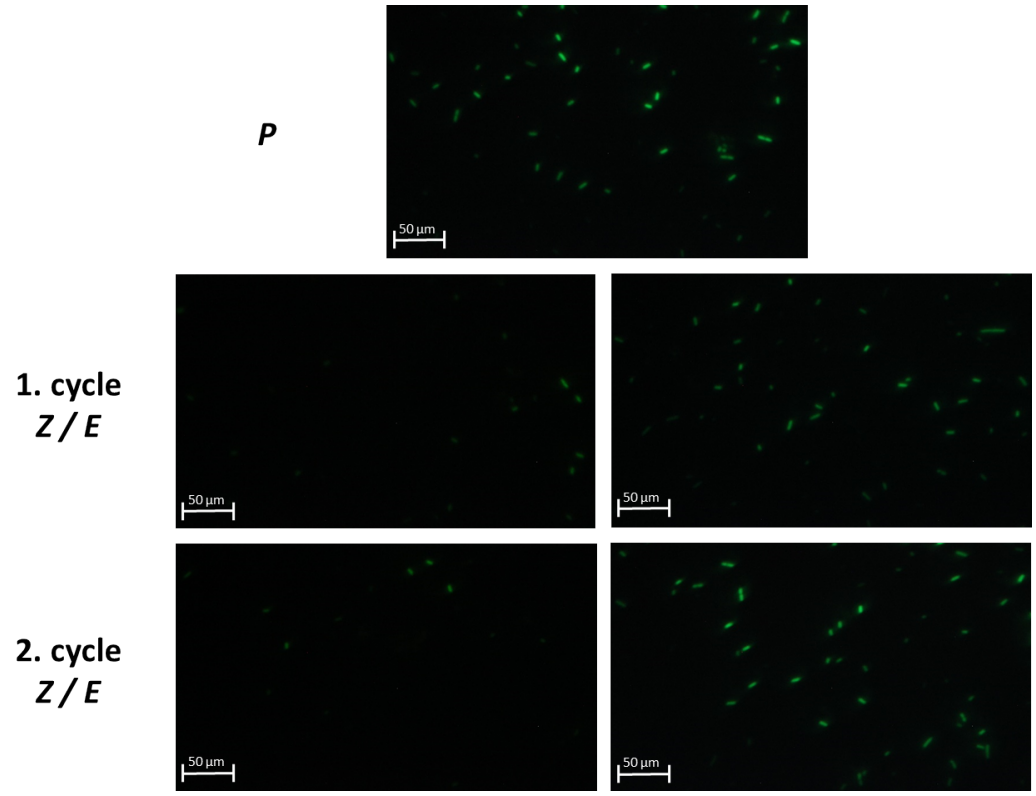

Figure 8.12. Adhesion of *E. coli* to *Z* and *E*-configured **8** on glass slides. Bacterial adhesion was additionally verified with fluorescence microscopy. The decrease of adhered *E. coli* can be seen in the left pictures in both switching cycles. Whereas in the right side the increased adhesion to *E*-configured **5** can be seen.

References

[1] B. Priewisch, K. Rück-Braun, *J. Org. Chem.* **2005**, *70*, 2350-2352.

[2] M. Hartmann, A. K. Horst, P. Klemm and T. K. Lindhorst, *Chem. Commun.* **2010**, *46*, 330-332.

[3] E. D. Goddard-Borger, R. V. Stick, *Org. Lett.* **2007**, *9*, 3797-3800.

8.2.2 Supporting Information for the Manuscript *Sweet and magnetic: A bead-based kit to study carbohydrate-specific adhesion of E. coli bacteria*

Supporting Information

for

Sweet and magnetic: A bead-based kit to study carbohydrate-specific adhesion of *E. coli* bacteria

A. Müller, Katharina Kolbe, Daniel Pussack, Laura Hartmann, T. K. Lindhorst

Methods and materials

Materials:

Materials: Tyramine hydrochloride (**1**) and D-arabinose were purchased from VWR International, anhydrous 2-(*N*-morpholino)ethanesulfonic acid (MES) BioChemica was purchased from Applichem, Fmoc-Lys(Boc)-OH was purchased from Iris Biotech GmbH, all other commercially available starting materials and reagents were purchased from either Alfa Aesar, Sigma Aldrich, Merck KGaA, Acros Organics or Thermo Fisher Scientific, respectively, and used without further purification. Moisture sensitive reactions were carried out in dry glassware and under a positive pressure of nitrogen. Acetonitrile and dichloromethane were dried over calcium hydride, pyridine was dried over potassium hydroxide and methanol was dried over magnesium under a nitrogen atmosphere. Dry *N*,*N*-dimethylformamide over molecular sieve was purchased from Acros Organics and used without further purification.

General methods:

Analytical thin layer chromatography (TLC) was performed on silica gel plates (GF 254, Merck) visualization was achieved by UV light and/or with 10% sulfuric acid in ethanol followed by heat treatment at ~180 °C. Flash chromatography was performed on silica gel 60 (Merck, 230-400 mesh, particle size 0.040-0.063 mm) by using distilled solvents. Melting points (mp) were determined on a Büchi M-56 apparatus. Optical rotations were measured with a Perkin-Elmer 241 polarimeter (sodium D-line: 589 nm, length of cell: 1 dm) in the solvents indicated. Proton (^{1}H) nuclear magnetic resonance spectra and carbon (^{13}C) nuclear magnetic resonance spectra were recorded on a Bruker DRX-500 and AV-600 spectrometer. Chemical shifts are referenced to the residual proton of the NMR solvent. Data are presented as follows: chemical shift, multiplicity (s=singlet, d=doublet, t=triplet, q=quartet, m=multiplet, and br=broad signal), coupling constant in hertz (Hz) and, integration. Full assignment of the peaks was achieved with the aid of 2D NMR techniques (^{1}H/^{1}H COSY and ^{1}H/^{13}C HSQC). Infrared (IR) spectra were measured with a Perkin Elmer FT-IR Paragon 1000 (ATR) spectrometer and were reported in cm^{-1}. ESI mass spectra were recorded on a LCQ Classic from Thermo Finnigan. Fluorescence read out was accomplished with a Infinite® 200 PRO multimode reader from Tecan.

Media and buffer solutions:

Carbonate buffer solution (pH 9.2): sodium carbonate (1.59 g) and sodium hydrogen carbonate (2.52 g) were dissolved in distilled deionized water. Phosphate-buffered saline (PBS) buffer solution (pH 7.2): sodium chloride (8.00 g), potassium chloride (200 mg), sodium hydrogen phosphate dihydrate (1.44 g), and potassium dihydrogen phosphate (200 mg) were dissolved in distilled deionized water (1.00 L). PBST buffer solution: PBS buffer + Tween® 20 (0.05% v/v). MES buffer solution (pH 6.3): MES (9.76 g) was dissolved in distilled deionized water (100 mL) and the buffer pH value was adjusted with sodium carbonate. Lectin binding buffer (LBB) solution (pH 7.0): 4-(2-hydroxyethyl)-1-piperazineethanesulfonic acid (HEPES) (238 mg), manganese chloride (12.6 mg) and calcium

chloride (11.1 mg) were dissolved in distilled deionized water (100 mL). Lysogeny broth (LB) medium: tryptone (10.0 g), sodium chloride (10.0 g), and yeast extract (5.00 g) were dissolved in distilled deionized water (1.00 L) and autoclaved, and ampicillin (100 mg) and chloramphenicol (50.0 mg) were added. The pH values of all buffer solutions were adjusted with aqueous HCl (1 M) and NaOH (1 M) unless indicated otherwise. All buffer and media were autoclaved prior use.

Covalent functionalization of magnetic PEG-COOH beads:

For glycosylated PEG bead preparation, magnetic beads (micromer®-M, polystyrol core, surface PEG-COOH, size: 2 µm; 600 µL, $7.2 \cdot 10^9$ particles) were incubated with an activation solution (1-ethyl-3-(3-dimethylaminopropyl)carbodiimide (EDC) (32.0 mg) and *N*-hydroxysuccinimide (NHS) (64.0 mg) in MES-buffer (1.00 mL); 100 µL) at ambient temperature and 600 rpm for 1 h. After washing the beads with PBS buffer (2 × 1 mL) they were partitioned (4 portions, each $1.8 \cdot 10^9$ beads). The respective glycosides **28**-**33** and the Fmoc-deprotected linker molecule (15 mM in carbonate buffer, 1.00 mL/portion) were incubated with the activated beads (1 portion, $1.8 \cdot 10^9$ particles) at ambient temperature and 600 rpm for 3 h. The beads were washed with PBS buffer (2 × 400 µL), subsequently blocked with ethanolamine (10 mM in carbonate buffer, 1.00 mL/portion) and incubated at ambient temperature and 600 rpm for 1 h. After washing with PBS buffer (2 × 1.00 mL) the functionalized beads were suspended in PBS buffer (1 mL/portion) and stored at 4 °C until use. As control one portion of beads was treated as described above without the addition of a substance to be immobilized. All steps were carried out in Eppendorf tubes® and a magnetic separation rack (DyneMag-2 magnet, Life technologies) was used for bead extraction.

Bacterial strain and cultivation of bacteria:

The employed GFP expressing *E. coli* strain pPKL1162[1] used for testing, is an *E. coli* mutant which exclusively expresses type 1 fimbriae as well as the green fluorescent protein (GFP) that allows for detection of adhered bacteria by read out of fluorescence intensity.[1] Construction of the *E. coli* strain pPKL1162 was accomplished by inserting the pPKL1174 plasmid into strain SAR18. The fim gene cluster, which is responsible for the expression of type 1 fimbriae, is contained in the pPKL1174 plasmid. The GFP gene is included in the genome of SAR18, controlled by a constitutive promoter. The GFP expressing *E. coli* bacteria (strain pPKL1162) were cultured from a frozen stock in LB medium and incubated overnight at 37 °C and 100 rpm. After centrifugation and washing twice with PBS buffer (2 mL), the bacteria pellet was resuspended in PBS buffer and the bacterial suspension was adjusted to an $OD_{600} = 0.4$ (2 mg/mL, $4 \cdot 10^8$ bac/mL) and $OD_{600} = 0.6$ (3 mg/mL, $6 \cdot 10^8$ bac/mL), respectively, with PBS using a 7305 spectrophotometer from Jenway.

Mannan coating of microtiter plates:

The published assay[1] was adapted and modified as follows: Black 96-well microtiter plates (Nunc™, MaxiSorp®) were incubated with a solution of mannan from Saccharomyces cerevisiae (1.2 mg/mL in carbonate buffer, 120 µL/well) and desiccated overnight at 37 °C and 100 rpm. Then the plates were washed with PBST (3 × 150 µL/well) and blocked with polyvinyl alcohol (PVA) (1% in PBS, 120 µL/well) at ambient temperature and 100 rpm for 2 h. In a subsequent step the microtiter plates were washed with PBST (2 × 150 µL/well) and PBS (150 µL/well).

Microtiter plate-based adhesion-inhibition assay with GFP-expressing *E. coli* bacteria:

Inhibitor solutions of the respective glycosides **28-33** (10 mM in PBS buffer) as well as MeMan (200 mM in PBS buffer) were prepared and serial dilutions of each solution added to the mannan-coated microtiter plates (50 µL/well). Subsequently, the prepared bacterial suspension (OD_{600} = 0.4, 50 µL/well) was added and the plates were incubated at 37 °C and 100 rpm for 1 h. After washing the microtiter plates with PBS (3 × 150 µL/well), the wells were filled with PBS (100 µL/well) and the fluorescence intensity (485 nm/535 nm) was determined. On each individual plate the standard inhibitor MeMan was tested simultaneously. Each compound was tested at least in triplicates.

Bead-based agglutination assay with *E. coli* bateria:

(a) Variation of beads concentration: Glycosylated beads of corresponding glycosides **28-33** were added to well 1 of a clear 96-well polystyrene conical bottom microWell™ plate (Thermo Scientific™, Nunc™) (50 µL/well of prepared beads suspension; $4.5 \cdot 10^7$ particles) and serially (1:2) diluted (starting with well 1). Then the prepared bacterial suspension (OD_{600} = 0.4, 50 µL/well) was added and the plates were incubated at ambient temperature and 600 rpm for 1 h. Carboxylic acid PEG beads blocked with ethanolamine and beads decorated with the Fmoc-deprotected linker molecule were tested as, well as controls in parallel on each individual plate. Results were optical evaluated. Each prepared beads suspension was tested at least in triplicates.

(b) Variation of bacteria concentration: Glycosylated beads of corresponding glycosides 28-33 (50 µL/well of prepared beads suspension; $9 \cdot 10^7$ particles) were added to clear 96-well V-bottom microtiter plates. Following this, the prepared bacterial suspension (OD_{600} = 0.4) was added in serial dilution (1:2, starting with a concentration of 100 µg/mL bacteria in PBS buffer; 50 µL/well) and the plates were incubated at ambient temperature and 600 rpm for 1 h. Carboxylic acid PEG-beads blocked with ethanolamine and beads decorated with the Fmoc-deprotected linker molecule were tested as well, as controls in parallel on each individual plate. Results were optical evaluated. Each prepared beads suspension was tested at least in triplicates.

Bead-based adhesion assay with GFP expressing *E. coli* bacteria:

To glycosylated beads of corresponding glycosides **28**-**33** (50 µL/well of prepared beads suspension; $9 \cdot 10^7$ particles) were transferred to an Eppendorf tube® PBS buffer (150 µL) and the prepared bacterial suspension ($OD_{600} = 0.4$, 100 µL/tube) were added. It was incubated at 37 °C and 250 rpm for 1 h. Then the beads were isolated subsequently washed with PBS buffer (500 µL/tube), resuspended in PBS buffer (100 µL/tube), transferred to a black 96-well microtiter plates (Nunc™, MaxiSorp®) and the fluorescence intensity (485 nm/535 nm) was determined. Carboxylic acid PEG-beads blocked with ethanolamine and beads decorated with the Fmoc-deprotected linker molecule were tested as well, as controls in parallel. Each prepared beads suspension was tested at least in triplicates. All steps were carried out in Eppendorf tubes® and a magnetic separation rack (DyneMag-2 magnet, Life technologies) was used for bead extraction.

Bead-based agglutination-inhibition assay with *E. coli* bacteria:

To inhibitor solutions of *p*APMan and MeMan in various concentrations (concentrations of used glycoside solutions in PBS buffer are indicated individually, see binding/inhibition figures; 50 µL/well) in clear 96-well V-bottom microtiter plates, glycosylated PEG beads decorated with **28** (50 µL/well of prepared beads suspension; $9 \cdot 10^7$ particles) were added. Subsequently, the prepared bacterial suspension ($OD_{600} = 0.4$, 50 µL/well) was added and the plates were incubated at ambient temperature and 600 rpm for 30 min. On each individual plate beads decorated with **28** were tested simultaneously without the addition of an inhibitor solution. Results were optical evaluated. Each compound was tested at least in duplicates.

Concanavalin A (Con A) assay:

Beads prepared from **28**, **29** and **32** ($1.20 \cdot 10^8$ particles) were washed with LBB medium (2 × 100 µL/tube) and resuspended in LBB medium (100 µL/tube). Subsequently, a solution of fluorescein isothiocyanate (FITC) labelled Con A from Canavalia ensiformis (Jack bean) in LBB medium (5.00 mg/mL; 5.00 µL) was added and incubated at ambient temperature and 600 rpm for 1 h. Then, beads were washed with LBB medium (3 × 100 µL/tube), resuspended in PBS buffer (100 µL/tube), transferred to a black 96-well microtiter plate (Nunc™, MaxiSorp®) and the fluorescence intensity (485 nm/535 nm) was determined. As a control blocked carboxylic acid PEG-beads were tested simultaneously on each individual plate. Each prepared beads suspension was tested at least in duplicates. All steps were carried out in Eppendorf tubes® and a magnetic separation rack (DyneMag-2 magnet, Life technologies) was used for bead extraction.

Synthesis of glycoconjugates

The Synthesis of abrabinofuranoside derivatives **9-18**, **24**, **25**, **30** and **31** can be found in the doctoral thesis of Katharina Kolbe.[402]

***p*-(2-Azidoethyl)phenyl 2,3,4,6-tetra-*O*-acetyl-α-D-mannopyranoside(4)**[2] was obtained by employing a new procedure: To a solution of the mannosyl donor **3**[3] (906 mg, 1.84 mmol) and **2**[4] (360 mg, 2.21 mmol) in dry dichloromethane (14 mL) $BF_3 \cdot Et_2O$ (350 µL, 2.76 mmol) was added under N_2 atmosphere at 0 °C. The reaction mixture was stirred at 0 °C for 30 min and for 16 h at room temperature. Then the reaction mixture was diluted with dichloromethane (30 mL) and washed with a saturated aq. $NaHCO_3$ solution (3 × 15 mL). The organic phase was dried over $MgSO_4$, it was filtered and the filtrate concentrated under reduced pressure. Purification of the crude product by column chromatography (cyclohexane/ethyl acetate, 3:1→2:1) gave mannoside **4** as colorless oil (632 mg, 1.28 mmol, 70%). R_f = 0.38 (cyclohexane/ethyl acetate, 2:1); m.p. 91 °C; $[\alpha]_D^{23}$ = +67.3 (c = 0.6 in dichloromethane); ^{1}H NMR (600 MHz, $CDCl_3$, 298 K): δ = 7.16-7.15 (m, 2H, Ar-H$_{meta}$), 7.05-7.03 (m, 2H, Ar-H$_{ortho}$), 5.56 (dd, $^3J_{2,3}$ = 3.5 Hz, $^3J_{3,4}$ = 10.0 Hz, 1H, H-3), 5.50 (d, $^3J_{1,2}$ = 1.7 Hz, 1H, H-1), 5.44 (dd, $^3J_{1,2}$ = 1.7 Hz, $^3J_{2,3}$ = 3.5 Hz, 1H, H-2), 5.37 (t~dd, $^3J_{3,4}$ = 10.0 Hz, $^3J_{4,5}$ = 10.0 Hz, 1H, H-4), 4.28 (dd, $^2J_{6,6'}$ = 11.9 Hz, $^3J_{5,6}$ = 4.9 Hz, 1H, H-6), 4.11-4.06 (m, 2H, H-5, H-6'), 3.47 (t, $^3J_{CH_2CH_2N_3,CH_2CH_2N_3}$ = 7.2 Hz, 2H, $CH_2CH_2N_3$), 2.85 (t, $^3J_{CH_2CH_2N_3,CH_2CH_2N_3}$= 7.2 Hz, 2H, $CH_2CH_2N_3$), 2.20, 2.05, 2.04, 2.04 (each s, each 3H, 4 $COCH_3$) ppm; ^{13}C NMR (151 MHz, $CDCl_3$, 298 K): δ = 170.5, 170.0, 170.0, 169.7 (4 $COCH_3$), 154.5 (C-Ar$_{ipso}$), 132.7 (C-Ar$_{para}$), 129.9 (C-Ar$_{meta}$), 116.7 (C-Ar$_{ortho}$), 95.9 (C-1), 69.4 (C-5), 69.1 (C-2), 68.9 (C-3), 66.0 (C-4), 62.1 (C-6), 52.5 ($CH_2CH_2N_3$), 34.5 ($CH_2CH_2N_3$), 20.9, 20.7 (2 $COCH_3$) ppm; IR (ATR): $\tilde{\nu}$ = 2900, 2113, 1743, 1510, 1365, 1213, 1034 cm^{-1}; ESI-MS: m/z calcd for $C_{22}H_{27}N_3O_{10}$: 516.2 $[M+Na]^+$; found 516.2.

***p*-(2-Azidoethyl)phenyl α-D-mannopyranoside (5):** To a solution of **4** (416 mg, 843 µmol) in dry methanol (3 mL), a sodium methoxide solution (1 M, 500 µl) was added under N_2 atmosphere. The reaction mixture was stirred for 16 h at room temperature. It was neutralized with Amberlite® IR 120, filtered and then the solvent was evaporated. Purification of the crude product by column chromatography (dichloromethane/methanol, 8:1) gave the mannoside **5** as a colorless amorphous solid (174 mg, 535 µmol, 63%). R_f = 0.36 (dichloromethane/methanol, 8:1); $[\alpha]_D^{23}$ = +77.3 (c = 0.5 in methanol); ^{1}H NMR (600 MHz, MeOH-d_4, 298 K): δ = 7.19-7.17 (m, 2H, Ar-H$_{meta}$), 7.07-7.05 (m, 2H, Ar-H$_{ortho}$), 5.44 (d, $^3J_{1,2}$ = 1.8 Hz, 1H, H-1), 3.99 (dd, $^3J_{1,2}$ = 1.8 Hz, $^3J_{2,3}$ = 3.4 Hz, 1H, H-2), 3.89 (dd, $^3J_{2,3}$ = 3.4 Hz, $^3J_{3,4}$ = 9.5 Hz, 1H, H-3), 3.77-3.70 (m, 2H, H-4, H-6, H-6'), 3.60 (ddd, $^3J_{4,5}$ = 9.8 Hz, $^3J_{5,6}$ = 5.1 Hz, $^3J_{5,6'}$ = 2.6 Hz, 1H, H-5), 3.47 (t, $^3J_{CH_2CH_2N_3,CH_2CH_2N_3}$ = 7.1 Hz, 2H, $CH_2CH_2N_3$), 2.82 (t, $^3J_{CH_2CH_2N_3,CH_2CH_2N_3}$ = 7.1 Hz, 2H, $CH_2CH_2N_3$) ppm; ^{13}C NMR (151 MHz, MeOH-d_4, 298 K): δ = 156.8 (C-Ar$_{ipso}$), 133.7 (C-Ar$_{para}$), 130.9 (C-Ar$_{meta}$), 117.9 (C-Ar$_{ortho}$), 100.3 (C-1), 75.3 (C-5), 72.4 (C-3), 72.0 (C-2), 68.4 (C-4), 62.6 (C-6), 53.7 ($CH_2CH_2N_3$), 35.6 ($CH_2CH_2N_3$) ppm; IR (ATR): $\tilde{\nu}$ = 3313, 2931, 2088, 1646, 1509, 1336, 1217, 831 cm^{-1}; ESI-MS: m/z calcd for $C_{14}H_{19}N_3O_6$: 326.1 $[M+H]^+$; found 326.8.

***p*-(2-Azidoethyl)phenyl 2,3,4,6-tetra-*O*-acetyl-β-D-glucopyranoside (7):** To a solution of glucose pentaacetate **6**[5] (1.06 g, 2.72 mmol) and **2**[4] (532 mg, 3.26 mmol) in dry dichloromethane (10 mL) $BF_3 \cdot Et_2O$ (1.85 mL, 15.0 mmol) was added under N_2 atmosphere at 0 °C. The reaction mixture was stirred at 0 °C for 30 min and for 16 h at room temperature. Then the reaction mixture

was diluted with dichloromethane (10 mL) and ice water (10 mL). The phases were separated and the aqueous phase extracted with dichloromethane (3 × 10 mL). The combined organic phases were washed with water (20 mL), a saturated aq. $NaHCO_3$ solution (20 mL), a saturated aq. NaCl solution (20 mL) and water (20 mL). It was dried over $MgSO_4$, filtered and the filtrate concentrated under reduced pressure. Purification of the crude product by column chromatography (cyclohexane/ethyl acetate, 3:1→2:1) gave glucoside **7** as colorless solid (931 mg, 1.89 mmol, 69%). R_f = 0.28 (cyclohexane/ethyl acetate, 2:1); m.p. 148 °C; $[\alpha]_D^{23}$ = -20.0 (c = 0.8 in dichloromethane); ^{1}H NMR (600 MHz, $CDCl_3$, 298 K): δ = 7.15-7.13 (m, 2H, Ar-H$_{meta}$), 6.95-6.94 (m, 2H, Ar-H$_{ortho}$), 5.31-5.24 (m, 2H, H-2, H-3), 5.16 (t~dd, $^3J_{3,4}$ = 9.5 Hz, $^3J_{4,5}$ = 9.5 Hz, 1H, H-4), 5.06 (d, $^3J_{1,2}$ = 7.4 Hz, 1H, H-1), 4.28 (dd, 1H, $^2J_{6,6'}$ = 12.3 Hz, $^3J_{5,6}$ = 5.3 Hz, 1H, H-6), 4.17 (dd, 1H, $^2J_{6,6'}$ = 12.3 Hz, $^3J_{5,6'}$ = 2.3 Hz, 1H, H-6'), 3.85 (ddd, $^3J_{4,5}$ = 9.5 Hz, $^3J_{5,6}$ = 5.3 Hz, $^3J_{5,6'}$ = 2.3 Hz, 1H, H-5), 3.47 (t, $^3J_{CH_2CH_2N_3,CH_2CH_2N_3}$= 7.1 Hz, 2H, $CH_2CH_2N_3$), 2.84 (t, $^3J_{CH_2CH_2N_3,CH_2CH_2N_3}$ = 7.1 Hz, 2H, $CH_2CH_2N_3$), 2.08, 2.06, 2.04, 2.03 (each s, each 3H, 4 $COCH_3$) ppm; ^{13}C NMR (151 MHz, $CDCl_3$, 298 K): δ = 170.7, 170.4, 169.5, 165.4 (4 *C*OCH_3), 155.9 (C-Ar$_{ipso}$), 133.2 (C-Ar$_{para}$), 130.0 (C-Ar$_{meta}$), 117.4 (C-Ar$_{ortho}$), 99.4 (C-1), 72.9 (C-3), 72.2 (C-5), 71.3 (C-2), 68.5 (C-4), 62.1 (C-6), 52.7 ($CH_2CH_2N_3$), 34.7 ($CH_2CH_2N_3$), 20.8, 20.8 (2 $COCH_3$) ppm; IR (ATR): $\tilde{\nu}$ = 2970, 2116, 2093, 1748, 1513, 1372, 1211, 1037 cm^{-1}; ESI-MS: m/z calcd for $C_{22}H_{27}N_3O_{10}$: 516.2 $[M+Na]^+$; found 516.2.

***p*-(2-Azidoethyl)phenyl β-D-glucopyranoside (8):** To a solution of **7** (453 mg, 918 µmol) in dry methanol (15 mL) a sodium methoxide solution (1 M, 3 mL) was added under N_2 atmosphere. The reaction mixture was stirred for 16 h at room temperature. It was neutralized with Amberlite® IR 120, filtered and then the solvent was evaporated. Purification of the crude product by column chromatography (dichloromethane/methanol, 10:1) gave the glucoside **8** as a colorless foam (257 mg, 790 µmol, 86%). R_f = 0.22 (dichloromethane/methanol, 9:1); m.p. 95 °C; $[\alpha]_D^{23}$ = -52.0 (c = 0.8 in methanol); ^{1}H NMR (500 MHz, MeOH-d_4, 300 K): δ = 7.19-7.16 (m, 2H, Ar-H$_{meta}$), 7.06-7.03 (m, 2H, Ar-H$_{ortho}$), 4.88-4.87 (m, 1H, H-1), 3.89 (dd, $^2J_{6,6'}$ = 12.1 Hz, $^3J_{5,6}$ = 2.2 Hz, 1H, H-6), 3.70 (dd, $^2J_{6,6'}$ = 12.1 Hz, $^3J_{5,6'}$ = 5.3 Hz, 1H, H-6'), 3.48 (m, 6H, H-2, H-3, H-4, H-5, $CH_2CH_2N_3$), 2.82 (t, $^3J_{CH_2CH_2N_3,CH_2CH_2N_3}$ = 7.1 Hz, 2H, $CH_2CH_2N_3$) ppm; ^{13}C NMR (126 MHz, MeOH-d_4, 300 K): δ = 158.0 (C-Ar$_{ipso}$), 133.7 (C-Ar$_{para}$), 130.8 (C-Ar$_{meta}$), 117.9 (C-Ar$_{ortho}$), 102.5 (C-1), 78.1 (C-3), 78.0 (C-5), 74.9 (C-2), 71.4 (C-4), 62.5 (C-6), 52.7 ($CH_2CH_2N_3$), 35.5 ($CH_2CH_2N_3$) ppm; IR (ATR): $\tilde{\nu}$ = 3285, 2927, 2095, 1612, 1511, 1229, 1010, 829 cm^{-1}; $C_{14}H_{19}N_3O_6$: 348.1 $[M+Na]^+$; found 348.3.

***N*$^\alpha$-(Fluoren-9-ylmethoxycarbonyl)-*N*$^\varepsilon$-(*tert*-butoxycarbonyl)-*N*-{[(4-(α-D-mannopyranosyloxy)-1-(ethyl)phenyl-1H-1,2,3-triazole-1-yl)methyl]}-L-lysinamide (22):** To a solution of the mannoside **5** (141 mg, 433 µmol) and the linker **19**[6] (219 mg, 433 µmol) in dimethylformamide (9 mL), a solution of copper sulfate pentahydrate (45.0 mg, 182 µmol) and a solution of sodium ascorbate (73.0 mg, 368 µmol) in water (each 0.75 mL) were added. The reaction mixture was stirred for 16 h at room temperature. Then water (10 mL) and a saturated aq. NH_4Cl solution (10 mL) were added and the aqueous phase extracted with ethyl acetate (4 × 20 mL). The combined organic phases were dried over $MgSO_4$, it was filtered and the filtrate concentrated under reduced pressure. Purification of the crude product by column chromatography (dichloromethane/methanol, 10:1) gave **22** as a colourless solid (302 mg, 357 µmol, 82%). R_f = 0.38 (dichloromethane/methanol,

9:1); m.p. 155 °C; $[\alpha]_D^{23}$ = +43.8 (c = 0.7 in methanol); ^{1}H NMR (600 MHz, MeOH-d_4, 300 K): δ = 7.78 (d, ^3J = 7.6 Hz, 2H, Ar-H$_{Fmoc}$), 7.66-7.63 (m, 3H, Ar-H$_{Triazole}$, Ar-H$_{Fmoc}$), 7.40-7.36 (m, 2H, Ar-H$_{Fmoc}$), 7.31-7.27 (m, 2H, Ar-H$_{Fmoc}$), 7.00-6.96 (m, 4H, Ar-H), 5.42 (s~d, 1H, H-1), 4.51-4.36 (m, 6H, CH_2CH Fmoc, CCH_2NHCO, ArCH$_2$CH_2N), 4.21 (t, $^3J_{CH_2CH\text{-Fmoc}, CH_2CH\text{-Fmoc}}$= 6.8 Hz, 1H, CH$_2$C*H*-Fmoc), 4.03 (dd, $^3J_{CH\text{NHFmoc},CHH'\text{CHNHFmoc}}$ = 8.6 Hz, $^3J_{CH\text{NHFmoc},CHH'\text{CHNHFmoc}}$ = 5.3 Hz, 1H, C*H*NHFmoc), 3.98 (dd, $^3J_{1,2}$ = 1.8 Hz, $^3J_{2,3}$ = 3.3 Hz, 1H, H-2), 3.88 (dd, $^3J_{2,3}$ = 3.3 Hz, $^3J_{3,4}$ = 9.4 Hz, 1H, H-3), 3.77-3.69 (m, 3H, H-4, H-6, H-6'), 3.58 (ddd, $^3J_{4,5}$ = 9.8 Hz, $^3J_{5,6}$= 5.3 Hz, $^3J_{5,6'}$ = 2.6 Hz, 1H, H-5), 3.06 (t, 2H, $^3J_{ArCH_2CH_2N,ArCH_2CH_2N}$= 7.2 Hz, ArC$H_2CH_2$N), 3.03-3.00 (m, 2H, C$H_2$NHBoc), 1.77-1.72 (m, 1H, C*H*H'CHNHFmoc), 1.66-1.60 (m, 1H, CH*H'*CHNHFmoc), 1.51-1.29 (m, 13H, CH_2CH$_2$NHBoc, CH$_2$CH_2CH$_2$NHBoc, C(CH$_3$)$_3$) ppm; ^{13}C NMR (151 MHz, MeOH-d_4, 300 K): δ = 175.1 (CCH$_2$NH*C*O), 158.6 (COO$_{Boc}$), 158.5 (COO$_{Fmoc}$), 156.5 (C-Ar), 146.2 (C-Ar), 145.3 (C-Ar$_{Triazole}$), 145.2 (C-Ar$_{Fmoc}$), 142.6 (C-Ar$_{Fmoc}$), 132.4 (C-Ar$_{Fmoc}$), 130.7 (C-Ar), 128.8 (C-Ar$_{Fmoc}$), 128.2 (C-Ar$_{Fmoc}$), 126.2 (C-Ar$_{Fmoc}$), 124.3 (C-Ar$_{Triazole}$), 121.0 (C-Ar$_{Fmoc}$), 118.0 (C-Ar), 100.2 (C-1), 79.9 (*C*(CH$_3$)$_3$), 75.3 (C-5), 72.4 (C-3), 72.0 (C-2), 68.4 (C-4), 67.9 (*C*H$_2$CH-Fmoc), 62.7 (C-6), 56.7 (*C*HNHFmoc), 52.7 (ArCH$_2$*C*H$_2$N), 48.4 (*C*H-Fmoc), 41.1 (*C*H$_2$NHBoc), 36.6 (ArCH$_2$*C*H$_2$N), 35.7 (*C*CH$_2$NHCO), 32.7 (*C*H$_2$CH$_2$NHBoc), 30.6 (*C*H$_2$CHNHFmoc), 28.8 (C(*C*H$_3$)$_3$), 24.2 (*C*H$_2$CH$_2$CH$_2$NHBoc) ppm; IR (ATR): $\tilde{\nu}$ =3308, 2930, 1657, 1510, 1450, 1228, 1010, 740 cm^{-1}; ESI-MS: m/z calcd for $C_{43}H_{54}N_6O_{11}$: 853.4 $[M+Na]^+$; found 853.4.

***N*$^\alpha$-(Fluoren-9-ylmethoxycarbonyl)-*N*$^\varepsilon$-(*tert*-butoxycarbonyl)-*N*-{[(4-(β-D-glucopyranosyloxy)-1-(ethyl)phenyl-1H-1,2,3-triazole-1-yl)methyl]}-L-lysinamide (23):** To a solution of the glucoside **8** (200 mg, 615 µmol) and the linker **19**[6] (311 mg, 615 µmol) in dimethylformamide (12 mL), a solution of copper sulfate pentahydrate (64.0 mg, 258 µmol) and a solution of sodium ascorbate (104 mg, 523 µmol) in water (each 1 mL) were added. The reaction mixture was stirred for 16 h at room temperature. Then water (15 mL) and a saturated aq. NH_4Cl solution (15 mL) were added and the aqueous phase extracted with ethyl acetate (4 × 30 mL). The combined organic phases were dried over $MgSO_4$, it was filtered and the filtrate concentrated under reduced pressure. Purification of the crude product by column chromatography (dichloromethane/methanol, 10:1) gave **23** as a colourless solid (404 mg, 486 µmol, 79%). R_f = 0.33 (dichloromethane/methanol, 9:1); m.p. 160 °C; $[\alpha]_D^{23}$ = -111 (c=0.9 in methanol); ^{1}H NMR (500 MHz, MeOH-d_4, 300 K): δ = 7.78 (d, ^3J = 7.5 Hz, 2H, Ar-H$_{Fmoc}$), 7.66-7.62 (m, 3H, Ar-H$_{Triazole}$, Ar-H$_{Fmoc}$), 7.40-7.36 (m, 2H, Ar-H$_{Fmoc}$), 7.31-7.27 (m, 2H, Ar-H$_{Fmoc}$), 6.99-6.96 (m, 4H, Ar-H), 4.86 (s~d, 1H, H-1), 4.56-4.35 (m, 6H, CH_2CH-Fmoc, CCH_2NHCO, ArCH$_2$CH_2N), 4.21 (t, $^3J_{CH2CH\text{-Fmoc}, CH2CH\text{-Fmoc}}$ = 6.5 Hz, 1H, CH$_2$C*H*-Fmoc), 4.03 (dd, $^3J_{CH\text{NHFmoc},CHH'\text{CHNHFmoc}}$ = 8.6 Hz, $^3J_{CH\text{NHFmoc},CHH'\text{CHNHFmoc}}$ = 5.2 Hz, 1H, C*H*NHFmoc), 3.88 (dd, $^2J_{6,6'}$ = 12.1 Hz, $^3J_{5,6}$ = 2.1 Hz, 1H, H-6), 3.69 (dd, $^2J_{6,6'}$ = 12.1 Hz, $^3J_{5,6'}$ = 5.5 Hz, 1H, H-6'), 3.48-3.36 (m, 4H, H 2, H 3, H-4, H-5), 3.08-3.00 (m, 4H, CH_2NHBoc, ArCH_2CH$_2$N), 1.77-1.71 (m, 1H, C*H*H'CHNHFmoc), 1.66-1.59 (m, 1H, CH*H'*CHNHFmoc), 1.47-1.29 (m, 13H, CH_2CH$_2$NHBoc, CH$_2$CH_2CH$_2$NHBoc, C(CH$_3$)$_3$) ppm; ^{13}C NMR (126 MHz, MeOH-d_4, 300 K): δ = 175.1 (CCH$_2$NH*C*O), 158.6 (COO$_{Boc}$), 158.5 (COO$_{Fmoc}$), 158.1 (C-Ar), 145.3 (C-Ar), 145.2 (C-Ar$_{Triazol}$e), 142.6 (C-Ar$_{Fmoc}$), 132.4 (C-Ar$_{Fmoc}$), 130.7 (C-Ar), 128.8 (C-Ar$_{Fmoc}$), 128.2 (C-Ar$_{Fmoc}$), 126.2 (C-Ar$_{Fmoc}$), 124.3 (C-Ar$_{Triazole}$), 121.0 (C-Ar$_{Fmoc}$), 118.0 (C-Ar), 102.4 (C-1), 79.9 (*C*(CH$_3$)$_3$), 78.1 (C-3), 78.0 (C-5), 74.9 (C-2), 71.4 (C-4), 67.9 (*C*H$_2$CH-Fmoc) 62.6 (C-6), 56.6 (*C*HNHFmoc),

52.7 ($ArCH_2\mathit{C}H_2N$), 48.4 (CH-Fmoc), 41.1 ($\mathit{C}H_2NHBoc$), 36.6 ($Ar\mathit{C}H_2CH_2N$), 35.7 ($C\mathit{C}H_2NHCO$), 32.7 ($\mathit{C}H_2CH_2NHBoc$), 30.5 ($\mathit{C}H_2CHNHFmoc$), 28.8 ($C(\mathit{C}H_3)_3$), 24.1 ($\mathit{C}H_2CH_2CH_2NHBoc$) ppm; IR (ATR): $\tilde{\nu}$ = 3303, 2932, 1662, 1511, 1450, 1233, 1043, 740 cm^{-1}; ESI-MS: m/z calcd for $C_{43}H_{54}N_6O_{11}$: 853.4 $[M+Na]^+$; found 853.4.

N^{α}-(Fluoren-9-ylmethoxycarbonyl)-N^{ε}-(*tert*-butoxycarbonyl)-*N*-{[(4-(2,3-di-*O*-acetyl-6-*O*-benzoyl-α-D-arabinofuranosyloxy)-1-(ethyl)phenyl-1H-1,2,3-triazole-1-yl)methyl]}-L-lysinamide (24): To a solution of the arabinoside **15** (171 mg, 354 µmol) and the linker **19**[6] (178 mg, 354 µmol) in dimethylformamide (6 mL), a solution of copper sulfate pentahydrate (37.0 mg, 149 µmol) and a solution of sodium ascorbate (60.0 mg, 301 µmmol) in water (each 1 mL) were added. The reaction mixture was stirred for 2 h at room temperature. Then water (20 mL) and a saturated aq. NH_4Cl solution (20 mL) were added and the aqueous phase extracted with ethyl acetate (4 × 30 mL). The combined organic phases were dried over $MgSO_4$, it was filtered and the filtrate concentrated under reduced pressure. Purification of the crude product by column chromatography (dichloromethane/methanol, 10:1) gave **24** as a colourless solid (404 mg, 486 µmol, 79%). R_f = 0.32 (dichloromethane/ethyl acetate/methanol, 5:5:1); $[\alpha]_D^{23}$ = +32.7 (c = 0.4 in dichloromethane); ^{1}H NMR (500 MHz, MeOH-d_4, 300 K): δ = 7.78 (d, ^3J = 7.5 Hz, 2H, Ar-H_{Fmoc}), 7.66-7.62 (m, 3H, Ar-$H_{Triazole}$, Ar-H_{Fmoc}), 7.40-7.36 (m, 2H, Ar-H_{Fmoc}), 7.31-7.27 (m, 2H, Ar-H_{Fmoc}), 6.99-6.96 (m, 4H, Ar-H), 4.86 (s~d, 1H, H-1), 4.56-4.35 (m, 6H, CH_2CH-Fmoc, CCH_2NHCO, $ArCH_2C\mathit{H_2}N$), 4.21 (t, $^3J_{CH2CH\text{-}Fmoc,\ CH2CH\text{-}Fmoc}$ = 6.5 Hz, 1H, $CH_2C\mathit{H}$-Fmoc), 4.03 (dd, $^3J_{C\mathit{H}NHFmoc,C\mathit{H}H'CHNHFmoc}$ = 8.6 Hz, $^3J_{C\mathit{H}NHFmoc,CH\mathit{H}'CHNHFmoc}$ = 5.2 Hz, 1H, CHNHFmoc), 3.88 (dd, $^2J_{6,6'}$ = 12.1 Hz, $^3J_{5,6}$ = 2.1 Hz, 1H, H-6), 3.69 (dd, $^2J_{6,6'}$ = 12.1 Hz, $^3J_{5,6'}$ = 5.5 Hz, 1H, H-6'), 3.48-3.36 (m, 4H, H 2, H 3, H-4, H-5), 3.08-3.00 (m, 4H, CH_2NHBoc, ArC$H_2$$CH_2N$), 1.77-1.71 (m, 1H, C$\mathit{H}$H'CHNHFmoc), 1.66-1.59 (m, 1H, CHH'CHNHFmoc), 1.47-1.29 (m, 13H, C$H_2$$CH_2$NHBoc, $CH_2C\mathit{H_2}CH_2$NHBoc, $C(CH_3)_3$) ppm; ^{13}C NMR (126 MHz, MeOH-d_4, 300 K): δ = 175.1 ($CCH_2NH\mathit{C}O$), 158.6 (COO_{Boc}), 158.5 (COO_{Fmoc}), 158.1 (C-Ar), 145.3 (C-Ar), 145.2 (C-$Ar_{Triazole}$), 142.6 (C-Ar_{Fmoc}), 132.4 (C-Ar_{Fmoc}), 130.7 (C-Ar), 128.8 (C-Ar_{Fmoc}), 128.2 (C-Ar_{Fmoc}), 126.2 (C-Ar_{Fmoc}), 124.3 (C-$Ar_{Triazole}$), 121.0 (C-Ar_{Fmoc}), 118.0 (C-Ar), 102.4 (C-1), 79.9 ($\mathit{C}(CH_3)_3$), 78.1 (C-3), 78.0 (C-5), 74.9 (C-2), 71.4 (C-4), 67.9 ($\mathit{C}H_2$CH-Fmoc) 62.6 (C-6), 56.6 (CHNHFmoc), 52.7 ($ArCH_2\mathit{C}H_2N$), 48.4 (CH-Fmoc), 41.1 ($\mathit{C}H_2$NHBoc), 36.6 ($Ar\mathit{C}H_2CH_2N$), 35.7 ($C\mathit{C}H_2NHCO$), 32.7 ($\mathit{C}H_2CH_2NHBoc$), 30.5 ($\mathit{C}H_2CHNHFmoc$), 28.8 ($C(\mathit{C}H_3)_3$), 24.1 ($\mathit{C}H_2CH_2CH_2NHBoc$) ppm; IR (ATR): $\tilde{\nu}$ = 3303, 2932, 1662, 1511, 1450, 1233, 1043, 740 cm^{-1}; ESI-MS: m/z calcd for $C_{28}H_{29}N_3O_{16}$: 622.1 $[M+Na]^+$; found 622.1.

N^{α}-(Fluoren-9-ylmethoxycarbonyl)-N^{ε}-(*tert*-butoxycarbonyl)-*N*-{[(4-(α-D-mannopyranosyloxy)ethyl-1H-1,2,3-triazole-1-yl)methyl]}-L-lysinamide (26): To a solution of the mannoside **20**[7] (519 mg, 2.08 mmol) and the linker **19**[6] (1.05 g, 2.08 mmol) in dimethylformamide (30 mL), a solution of copper sulfate pentahydrate (218 mg, 874 µmol) and a solution of sodium ascorbate (350 mg, 1.77 mmol) in water (each 5 mL) were added. The reaction mixture was stirred for 16 h at room temperature. Then water (50 mL) and a saturated aq. NH_4Cl solution (50 mL) were added and the aqueous phase extracted with ethyl acetate (4 × 100 mL). The combined organic phases were dried over $MgSO_4$, it was filtered and the filtrate concentrated under reduced pressure. Purification of the crude product by column chromatography (dichloromethane/methanol,

9:1) gave **26** as a colourless solid (1.39 g, 1.84 mmol, 89%). R_f = 0.31 (dichloromethane/methanol, 9:1); m.p. 93.7 °C; $[\alpha]_D^{23}$ = +17.3 (c = 0.6 in methanol); ^{1}H NMR (500 MHz, MeOH-d_4, 300 K): δ = 7.85 (s, 1H, Ar-H$_{Triazole}$), 7.80 (d, ^3J = 7.6 Hz, 2H, Ar-H$_{Fmoc}$), 7.69-7.66 (m, 2H, Ar-H$_{Fmoc}$), 7.40-7.37 (m, 2H, Ar-H$_{Fmoc}$), 7.32-7.29 (m, 2H, Ar-H$_{Fmoc}$), 4.68 (s~d, 1H, H-1), 4.60-4.36 (m, 6H, OCH$_2$CH_2N, CH_2CH-Fmoc, CCH_2NHCO), 4.22 (t, $^3J_{CH_2CH\text{-Fmoc, }CH_2CH\text{-Fmoc}}$ = 6.7 Hz, 1H, CH$_2$C*H*-Fmoc), 4.08-4.05 (m, 2H, OCH, C*H*NHFmoc), 3.83-3.74 (m, 3H, H-2, H-6, OCH'), 3.63 (dd, $^2J_{6,6'}$ = 12.0 Hz, $^3J_{5,6}$ = 6.0 Hz, 1H, H-6'), 3.58-3.51 (m, 2H, H-3, H-4), 3.12-3.10 (m, 1H, H-5), 3.02 ($^3J_{CH_2NHBoc,CH_2CH_2NHBoc}$ = 6.8 Hz, 2H, CH_2NHBoc), 1.81-1.75 (m, 1H, C*H*H'CHNHFmoc), 1.68-1.60 (m, 1H, CH*H'*CHNHFmoc), 1.51-1.32 (m, 13H, CH_2CH$_2$NHBoc, CH$_2$CH_2CH$_2$NHBoc, C(CH$_3$)$_3$) ppm; ^{13}C NMR (126 MHz, MeOH-d_4, 300 K): δ = 175.2 (CCH$_2$NH*C*O), 158.6 (COO$_{Boc}$), 158.5 (COO$_{Fmoc}$), 145.4 (C-Ar$_{Triazole}$), 145.2 (C-Ar$_{Fmoc}$), 142.6 (C-Ar$_{Fmoc}$), 128.8 (C-Ar$_{Fmoc}$), 128.2 (C-Ar$_{Fmoc}$), 126.2 (C-Ar$_{Fmoc}$), 125.1 (C-Ar$_{Triazole}$), 120.9 (C-Ar$_{Fmoc}$), 101.6 (C-1), 79.9 (*C*(CH$_3$)$_3$), 74.9 (C-5), 72.4 (C-3), 71.9 (C-2), 68.5 (C-4), 67.9 (*C*H$_2$CH-Fmoc), 66.6 (OCH$_2$), 62.8 (C-6), 56.6 (*C*HNHFmoc), 51.2 (OCH$_2$*C*H$_2$N), 48.5 (*C*H-Fmoc), 41.1 (*C*H$_2$NHBoc), 35.8 (*C*CH$_2$NHCO), 32.8 (*C*H$_2$CH$_2$NHBoc), 30.5 (*C*H$_2$CHNHFmoc), 28.8 (C(*C*H$_3$)$_3$), 24.2 (*C*H$_2$CH$_2$CH$_2$NHBoc) ppm; IR (ATR): $\tilde{\nu}$ = 3312, 2934, 1662, 1524, 1247, 1054, 740 cm^{-1}; ESI-MS: m/z calcd for $C_{37}H_{50}N_6O_{11}$: 777.3 $[M+Na]^+$; found 777.4.

***N*$^\alpha$-(Fluoren-9-ylmethoxycarbonyl)-*N*$^\varepsilon$-(*tert*-butoxycarbonyl)-*N*-{[(4-(α-D-glucopyranosyloxy)ethyl-1H-1,2,3-triazole-1-yl)methyl]}-L-lysinamide (27):** To a solution of the glucoside **21**[13] (578 mg, 2.32 mmol) and the linker **19**[11] (1.17 g, 1.33 mmol) in dimethylformamide (45 mL), a solution of copper sulfate pentahydrate (243 mg, 974 µmol) and a solution of sodium ascorbate (391 mg, 1.97 mmol) in water (each 3.75 mL) were added. The reaction mixture was stirred for 16 h at room temperature. Then water (55 mL) and a saturated aq. NH_4Cl solution (55 mL) were added and the aqueous phase extracted with ethyl acetate (4 × 110 mL). The combined organic phases were dried over $MgSO_4$, it was filtered and the filtrate concentrated under reduced pressure. Purification of the crude product by column chromatography (dichloromethane/methanol, 9:1) gave **27** as a colourless solid (1.00 g, 1.33 mmol, 57%). R_f = 0.15 (dichloromethane/methanol, 9:1); m.p. 140 °C; $[\alpha]_D^{23}$ = -8.4 (c = 0.6 in methanol); ^{1}H NMR (500 MHz, MeOH-d_4, 300 K): δ = 7.95 (s, 1H, Ar-H$_{Triazole}$), 7.79 (d, ^3J = 7.6 Hz, 2H, Ar-H$_{Fmoc}$), 7.68-7.66 (m, 2H, Ar-H$_{Fmoc}$), 7.40-7.37 (m, 2H, Ar-H$_{Fmoc}$), 7.32-7.28 (m, 2H, Ar-H$_{Fmoc}$), 4.57-4.36 (m, 6H, OCH$_2$CH_2N, CH_2CH-Fmoc, CCH_2NHCO), 4.26 (d, $^3J_{1,2}$ =7.8 Hz, 1H, H-1), 4.23-4.17 (m, 2H, OCH, CH$_2$C*H*-Fmoc), 4.05 (dd, $^3J_{CH\text{NHFmoc},CH\text{H'CHNHFmoc}}$ = 8.8 Hz, $^3J_{CH\text{NHFmoc},CH\text{H'CHNHFmoc}}$ = 5.2 Hz, 1H, C*H*NHFmoc), 3.97-3.93 (m, 1H, OCH'), 3.84 (dd, $^2J_{6,6'}$ = 11.9 Hz, $^3J_{5,6}$ = 1.9 Hz, 1H, H-6), 3.66-3.62 (m, 1H, H-6'), 3.35-3.23 (m, 3H, H 3, H-4, H-5), 3.19-3.16 (m, 1H, H-2), 3.03-3.00 (m, 2H, CH_2NHBoc), 1.80-1.73 (m, 1H, C*H*H'CHNHFmoc), 1.67-1.59 (m, 1H, CH*H'*CHNHFmoc), 1.51-1.28 (m, 13H, CH_2CH$_2$NHBoc, CH_2CH$_2$CH$_2$NHBoc, C(CH$_3$)$_3$) ppm; ^{13}C NMR (126 MHz, MeOH-d_4, 300 K): δ = 175.0 (CCH$_2$NH*C*O), 158.6 (COO$_{Fmoc}$, COO$_{Boc}$), 145.3 (C-Ar$_{Triazole}$), 145.2 (C-Ar$_{Fmoc}$), 142.6 (C-Ar$_{Fmoc}$), 128.8 (C-Ar$_{Fmoc}$), 128.2 (C-Ar$_{Fmoc}$), 126.2 (C-Ar$_{Fmoc}$), 125.5 (C-Ar$_{Triazole}$), 120.9 (C-Ar$_{Fmoc}$), 104.5 (C-1), 79.9 (*C*(CH$_3$)$_3$), 78.1 (C-3), 78.0 (C-5), 74.9 (C-2), 71.5 (C-4), 69.0 (OCH$_2$),

67.9 (*C*H_2CH-Fmoc), 62.7 (C-6), 56.6 (*C*HNHFmoc), 51.6 (OCH_2*C*H_2N), 48.5 (*C*H-Fmoc), 41.1 (*C*H_2NHBoc), 35.8 (*C*CH_2NHCO), 32.8 (*C*H_2CH_2NHBoc), 30.5 (*C*H_2CHNHFmoc), 28.8 (C(*C*H_3)$_3$), 24.0 (*C*H_2CH_2CH_2NHBoc) ppm; IR (ATR): $\tilde{\nu}$ = 3311, 2927, 1664, 1520, 1247, 1035, 740 cm^{-1}; ESI-MS: m/z calcd for $C_{37}H_{50}N_6O_{11}$: 777.3 $[M+Na]^+$; found 777.3.

N^{ε}-(*tert*-butoxycarbonyl)-*N*-{[(4-(α-D-mannopyranosyloxy)-1-(ethyl)phenyl-1H-1,2,3-triazole-1-yl)methyl]}-L-lysinamide (28): To a solution of the mannoside **22** (137 mg, 162 µmol) in dimethylformamide (1 mL), piperidine (0.25 mL) was added dropwise and the reaction mixture was stirred for 16 h at room temperature. Then the solvent was evaporated and the crude product resolved in water (10 mL) and dichloromethane (10 mL). The phases were separated and aqueous phase was washed with dichloromethane (3 × 10 mL). After lyophilisation the mannoside **28** was obtained as a colourless solid (42.0 mg, 67.2 µmol, 42%). R_f = 0.21 (dichloromethane/methanol/triethylamine, 5:1:0.05); m.p. 78.7 °C; $[\alpha]_D^{23}$ = -57.9 (c = 0.6 in methanol); ^{1}H NMR (600 MHz, MeOH-d_4, 300 K): δ = 7.66 (s, 1H, Ar-H*Triazole*), 7.06-7.01 (m, 4H, Ar-H), 5.43 (d, $^3J_{1,2}$ = 1.8 Hz, 1H, H-1), 4.59 (t, 2H, $^3J_{ArCH_2CH_2N,ArCH_2CH_2N}$ = 7.1 Hz, ArCH_2CH_2N), 4.44-4.38 (m, 2H,CCH_2NHCO), 3.98 (dd, $^3J_{1,2}$ = 1.8 Hz, $^3J_{2,3}$ = 3.3 Hz, 1H, H-2), 3.88 (dd, $^3J_{2,3}$ = 3.3 Hz, $^3J_{3,4}$ = 9.5 Hz, 1H, H-3), 3.76 (dd, $^2J_{6,6'}$ = 11.9 Hz, $^3J_{5,6}$ = 2.5 Hz, 1H, H-6), 3.74-3.69 (m, 2H, H-4, H-6'), 3.58 (ddd, $^3J_{4,5}$ = 9.8 Hz, $^3J_{5,6}$ = 5.4 Hz, $^3J_{5,6'}$ = 2.5 Hz, 1H, H-5), 3.14 (t, 2H, $^3J_{ArCH_2CH_2N,ArCH_2CH_2N}$ = 7.1 Hz, ArCH_2CH_2N), 3.02-2.99 (m, 2H, CH_2NHBoc), 1.76-1.62 (m, 1H, C*H*H'CHNH$_2$), 1.60-1.52 (m, 1H, CH*H'*CHNH$_2$), 1.49-1.30 (m, 13H, CH_2CH_2NHBoc, CH$_2$CH_2CH$_2$NHBoc, C(CH$_3$)$_3$) ppm; ^{13}C NMR (151 MHz, MeOH-d_4, 300 K): δ = 176.7 (CCH$_2$NH*C*O), 158.5 (COO*Boc*), 156.9 (C-Ar), 145.9 (C-Ar*Triazole*), 132.5 (C-Ar), 130.9 (C-Ar), 124.4 (C-Ar*Triazole*), 118.1 (C-Ar), 100.3 (C-1), 79.9 (C(CH$_3$)$_3$), 75.4 (C-5), 72.4 (C-3), 72.0 (C-2), 68.4 (C-4), 62.7 (C-6), 55.8 (*C*HNH$_2$), 52.8 (ArCH$_2$*C*H$_2$N), 41.1 (*C*H$_2$NHBoc), 36.7 (Ar*C*H$_2$CH$_2$N), 35.6 (*C*H$_2$CH$_2$NHBoc), 35.5 (C*C*H$_2$NHCO), 30.7 (*C*H$_2$CHNH$_2$), 28.8 (C(*C*H$_3$)$_3$), 23.9 (*C*H$_2$CH$_2$CH$_2$NHBoc) ppm; IR (ATR): $\tilde{\nu}$ =3288, 2930, 1681, 1511, 1450, 1229, 1012, 828 cm^{-1}; ESI-MS: m/z calcd for $C_{28}H_{44}N_6O$: 609.3 $[M+H]^+$; found 609.2.

N^{ε}-(*tert*-butoxycarbonyl)-*N*-{[(4-(α-D-glucopyranosyloxy)-1-(ethyl)phenyl-1H-1,2,3-triazole-1-yl)methyl]}-L-lysinamide (29): To a solution of the glucoside **23** (228 mg, 269 µmol) in dimethylformamide (2 mL), piperidine (500 µL) was added dropwise and the reaction mixture was stirred for 16 h at room temperature. Then the solvent was evaporated and the crude product resolved in water (10 mL) and dichloromethane (10 mL). The phases were separated and the aqueous phase was washed with dichloromethane (3 × 10 mL). After lyophilisation the glucoside **29** was obtained as a colourless solid (149 mg, 239 µmol, 89%). R_f = 0.42 (dichloromethane/methanol/triethylamine, 5:1:0.5); m.p. 304 °C; $[\alpha]_D^{23}$ = -18.0 (c = 0.5 in methanol); ^{1}H NMR (600 MHz, MeOH-d_4, 300 K): δ = 7.62 (s, 1H, Ar-H*Triazole*), 7.05-6.99 (m, 4H, Ar-H), 4.86 (s~d, 1H, H-1), 4.59 (t, 2H, $^3J_{ArCH_2CH_2N,ArCH_2CH_2N}$ = 7.1 Hz, ArCH_2CH_2N), 4.43-4.37 (m, 2H,CCH_2NHCO), 3.89 (dd, $^2J_{6,6'}$ = 12.1 Hz, $^3J_{5,6}$ = 2.1 Hz, 1H, H-6), 3.69 (dd, $^2J_{6,6'}$ = 12.1 Hz, $^3J_{5,6'}$ = 5.6 Hz, 1H, H-6'), 3.47-3.36 (m, 5H, H-2, H-3, H-4, H-5, C*H*NH$_2$), 3.14 (t, 2H, $^3J_{ArCH_2CH_2N,ArCH_2CH2N}$ = 7.1 Hz, ArCH_2CH_2N), 3.02-3.00 (m, 2H, CH_2NHBoc), 1.69-1.64 (m, 1H, C*H*H'CHNH$_2$), 1.57-1.51 (m, 1H, CH*H'*CHNH$_2$), 1.48-1.29 (m, 13H, CH_2CH_2NHBoc, CH$_2$CH_2CH$_2$NHBoc, C(CH$_3$)$_3$) ppm; ^{13}C NMR (151 MHz, MeOH-d_4, 300 K): δ = 177.1 (CCH$_2$NH*C*O), 158.6 (COO*Boc*), 158.1 (C-Ar), 145.9 (C-Ar*Triazole*), 132.5 (C-Ar), 130.8 (C-Ar), 124.5 (C-Ar*Triazol*e), 117.9 (C-Ar), 102.4 (C-1), 79.9 (C(CH$_3$)$_3$), 78.2

(C-3), 78.0 (C-5), 74.9 (C-2), 71.4 (C-4), 62.5 (C-6), 55.9 ($CHNH_2$), 52.8 ($ArCH_2CH_2N$), 41.1 (CH_2NHBoc), 36.7 ($ArCH_2CH_2N$), 35.7 (CCH_2NHCO), 35.5 (CH_2CH_2NHBoc), 30.8 (CH_2CHNH_2), 28.8 ($C(CH_3)_3$), 23.9 ($CH_2CH_2CH_2NHBoc$) ppm; IR (ATR): $\tilde{\nu}$ =3357, 2926, 1678, 1512, 1456, 1233, 1074, 835 cm-1; ESI-MS: m/z calcd for $C_{28}H_{44}N_6O_9$: 609.3 $[M+H]^+$; found 609.2.

N^{ε}-(*tert*-butoxycarbonyl)-*N*-{[(4-(α-D-mannpyranosyloxy)ethyl-1H-1,2,3-triazole-1-yl)methyl]}-L-lysinamide (32): To a solution of the mannoside **26** (1.09 g, 1.45 mmol) in dimethylformamide (10 mL), piperidine (2.5 mL) was added dropwise and the reaction mixture was stirred for 16 h at room temperature. Then the solvent was evaporated and the crude product resolved in water (10 mL) and dichloromethane (10 mL). The phases were separated and the organic phase extracted with water (10 mL). The combined aqueous phases were washed with dichloromethane (3 × 10 mL). After lyophilisation the mannoside **32** was obtained as a colourless solid (618 mg, 1.16 mmol, 85%). R_f = 0.29 (dichloromethane/methanol/triethylamine, 5:1:0.5); m.p. 104 °C; $[\alpha]_D^{23}$ = +37.8 (c = 0.9 in methanol); ^{1}H NMR (500 MHz, MeOH-d_4, 300 K): δ = 7.91 (s, 1H, Ar-H$_{Triazole}$), 4.69 (s, $^3J_{1,2}$ = 1.6 Hz, 1H, H-1), 4.63-4.57 (m, 2H, OCH_2CH_2N), 4.52-4.41 (m, 2H,CCH_2NHCO), 4.11-4.07 (m, 1H, OCH), 3.86-3.82 (m, 1H, OCH'), 3.76-3.73 (m, 2H, H-2, H-6), 3.63 (dd, $^2J_{6,6'}$ = 11.8 Hz, $^3J_{5,6}$ = 5.9 Hz, 1H, H-6'), 3.59-3.54 (m, 2H, H-3, H-4), 3.08 (ddd, $^3J_{4,5}$ = 9.4 Hz, $^3J_{5,6}$ = 5.9 Hz, $^3J_{5,6'}$ = 2.3 Hz, 1H, H-5), 3.02 (t, $^3J_{CH_2NHBoc,CH_2CH_2NHBoc}$ = 6.9 Hz, 2H, CH_2NHBoc), 1-78-1.64 (m, 1H, $CHH'CHNH_2$), 1.64-1.54 (m, 1H, $CHH'CHNH_2$), 1.50-1.30 (m, 13H, CH_2CH_2NHBoc, $CH_2CH_2CH_2NHBoc$, $C(CH_3)_3$) ppm; ^{13}C NMR (126 MHz, MeOH-d_4, 300 K): δ = 158.6 (COO_{Boc}), 146.1 (C-Ar$_{Triazole}$), 125.2 (C-Ar$_{Triazole}$), 101.6 (C-1), 79.9 ($C(CH_3)_3$), 74.9 (C-5), 72.4 (C-3), 71.9 (C-2), 68.4 (C-4), 66.7 (OCH_2), 62.8 (C-6), 51.3 (OCH_2CH_2N), 41.1 (CH_2NHBoc), 35.6 (CCH_2NHCO), 30.7 (CH_2CHNH_2), 28.8 ($C(CH_3)_3$), 23.9 ($CH_2CH_2CH_2NHBoc$) ppm; IR (ATR): $\tilde{\nu}$ = 3312, 2931, 1679, 1528, 1366, 1249, 1054 cm^{-1}; ESI-MS: m/z calcd for $C_{22}H_{40}N_6O_9$: 533.3 $[M+H]^+$; found 533.2.

N^{ε}-(*tert*-butoxycarbonyl)-*N*-{[(4-(α-D-glucopyranosyloxy)ethyl-1H-1,2,3-triazole-1-yl)methyl]}-L-lysinamide(33): To a solution of the glucoside **27** (851 mg, 1.13 mmol) in dimethylformamide (8 mL), piperidine (2 mL) was added dropwise and the reaction mixture was stirred for 16 h at room temperature. Then the solvent was evaporated and the crude product resolved in water (10 mL) and dichloromethane (10 mL). The phases were separated and the organic phase was extracted with water (10 mL). The combined aqueous phases were washed with dichloromethane (3 × 10 mL). After lyophilisation the glucoside **33** was obtained as a colourless solid (600 mg, 1.12 mmol, 99%). R_f = 0.29 (dichloromethane/methanol/triethylamine, 5:1:0.5); m.p. 140 °C; $[\alpha]_D^{23}$ = -4.4 (c=1.0 in methanol); ^{1}H NMR (500 MHz, MeOH-d_4, 300 K): δ = 8.02 (s, 1H, Ar-H$_{Triazole}$), 4.62 (t, 2H, $^3J_{OCH_2CH_2N,OCH_2CH_2N}$ = 5.2 Hz, OCH_2CH_2N), 4.50-4.41 (m, 2H,CCH_2NHCO), 4.29 (d, $^3J_{1,2}$ = 7.8 Hz, 1H, H-1), 4.24-4.20 (m, 1H, OCH), 4.02-3.97 (m, 1H, OCH'), 3.86 (dd, $^2J_{6,6'}$ = 11.8 Hz, $^3J_{5,6}$ = 1.6 Hz, 1H, H-6), 3.67-3.64 (m, 1H, H-6'), 3.36-3.26 (m, 4H, H 3, H-4, H-5, $CHNH_2$), 3.17 (dd, $^3J_{1,2}$ = 7.8 Hz, $^3J_{2,3}$ = 9.1 Hz, 1H, H-2), 3.02 (t, $^3J_{CH_2NHBoc,CH_2CH_2NHBoc}$ = 7.0 Hz, 2H, CH_2NHBoc), 1.72-1.65 (m, 1H, $CHH'CHNH_2$), 1.59-1.51 (m, 1H, $CHH'CHNH_2$), 1.49-1.29 (m, 13H, CH_2CH_2NHBoc, $CH_2CH_2CH_2NHBoc$, $C(CH_3)_3$) ppm; ^{13}C NMR (126 MHz, MeOH-d_4, 300 K): δ = 177.7 (CCH_2NHCO), 158.6 (COO_{Boc}), 145.9 (C-Ar$_{Triazole}$), 125.4 (C-Ar$_{Triazole}$), 104.5

(C-1), 79.9 ($C(CH_3)_3$), 78.1 (C-3), 78.0 (C-5), 75.0 (C-2), 71.5 (C-4), 69.1 (OCH_2), 62.7 (C-6), 56.0 ($CHNH_2$), 51.6 (OCH_2CH_2N), 41.1 (CH_2NHBoc), 35.9 (CCH_2NHCO), 35.6 (CH_2CH_2NHBoc), 30.7 (CH_2CHNH_2), 28.8 ($C(CH_3)_3$), 24.0 ($CH_2CH_2CH_2NHBoc$) ppm; IR (ATR): $\tilde{\nu}$ = 3336, 2938, 1677, 1523, 1243, 1165, 1054 cm^{-1}; ESI-MS: m/z calcd for $C_{22}H_{40}N_6O_9$: 555.3 $[M+Na]^+$; found 555.3.

^{1}H and ^{13}C NMR of target compounds

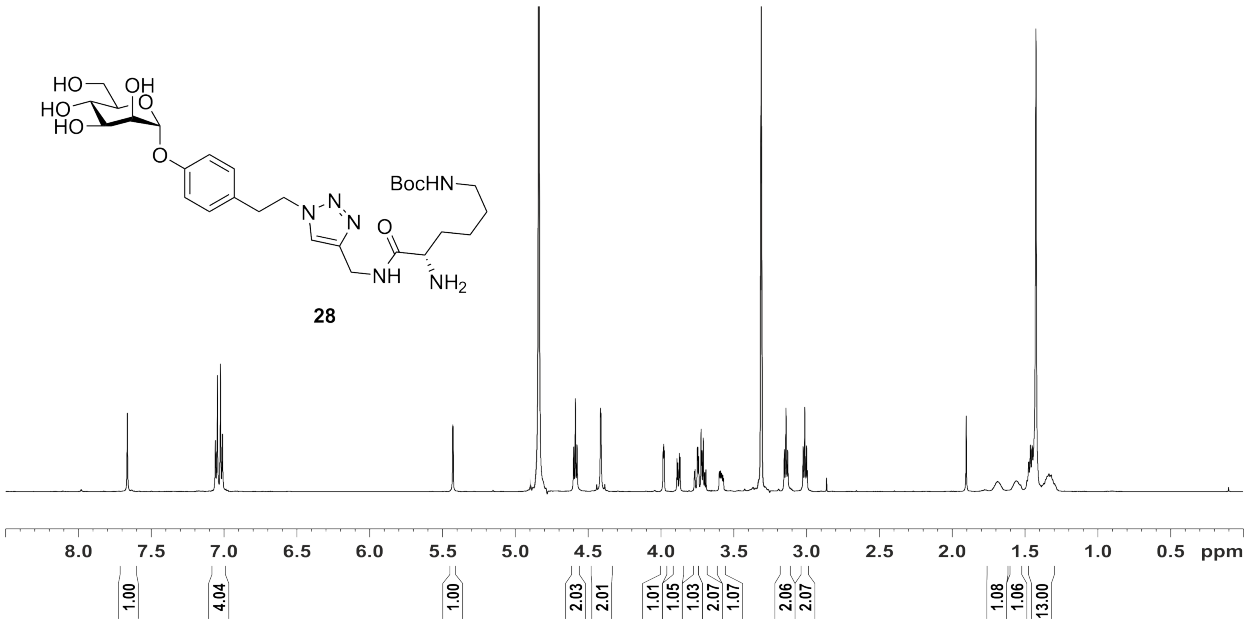

Figure 8.13. ^{1}H NMR spectrum of **28** (600 MHz, MeOH-d_4, 300 K).

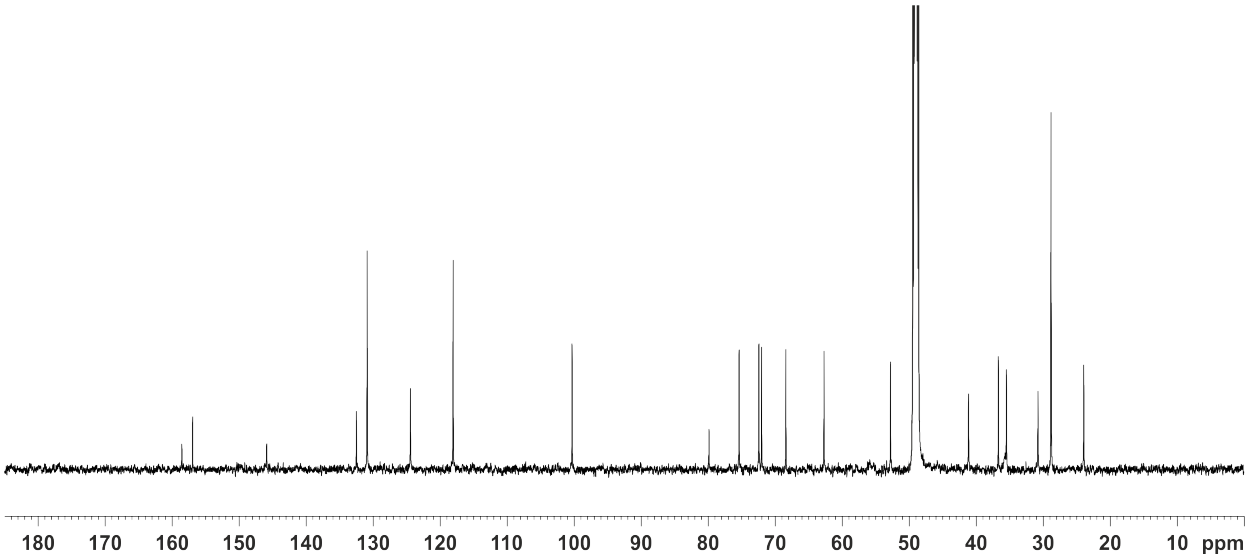

Figure 8.14. ^{13}C NMR spectrum of **28** (151 MHz, MeOH-d_4, 300 K).

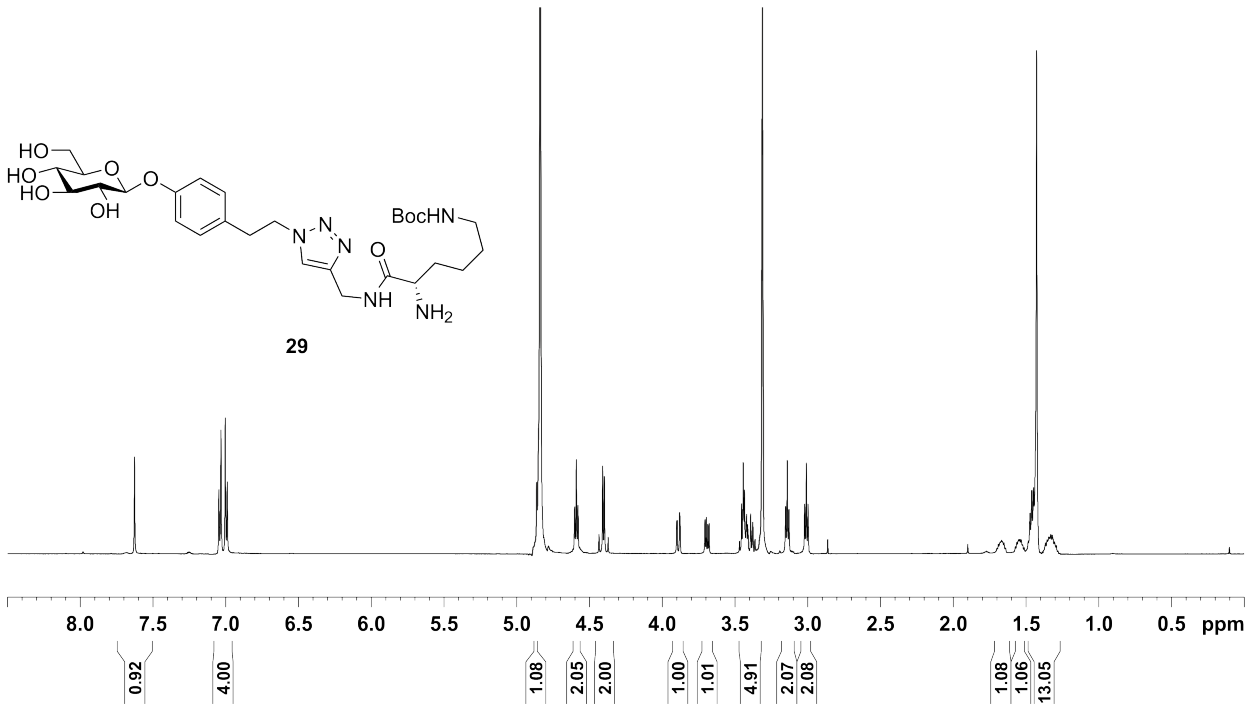

Figure 8.15. ^{1}H NMR spectrum of **29** (600 MHz, MeOH-d_4, 300 K).

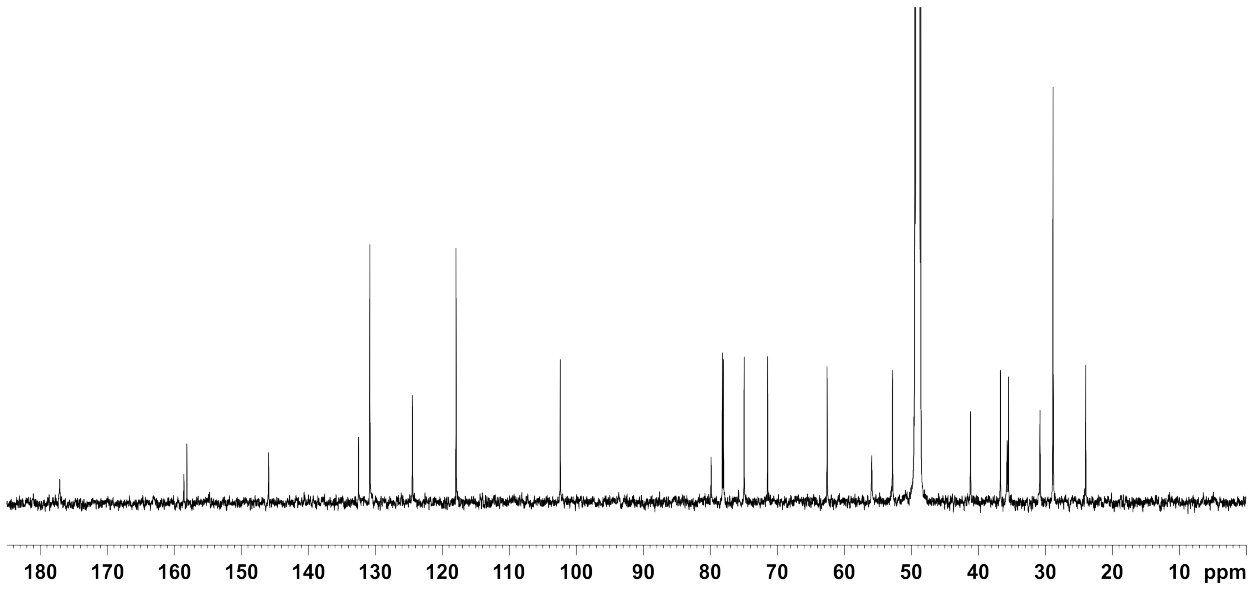

Figure 8.16. ^{13}C NMR spectrum of **29** (151 MHz, MeOH-d_4, 300 K).

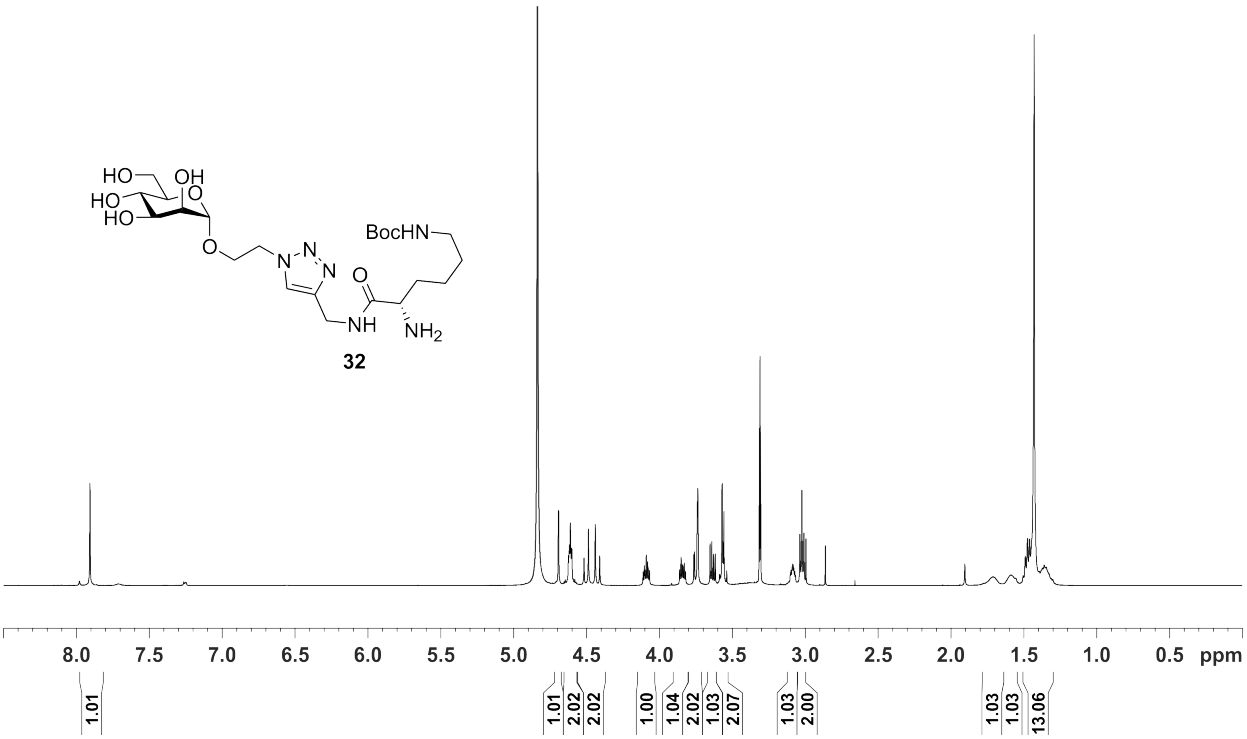

Figure 8.17. ^{1}H NMR spectrum of **32** (500 MHz, MeOH-d_4, 300 K).

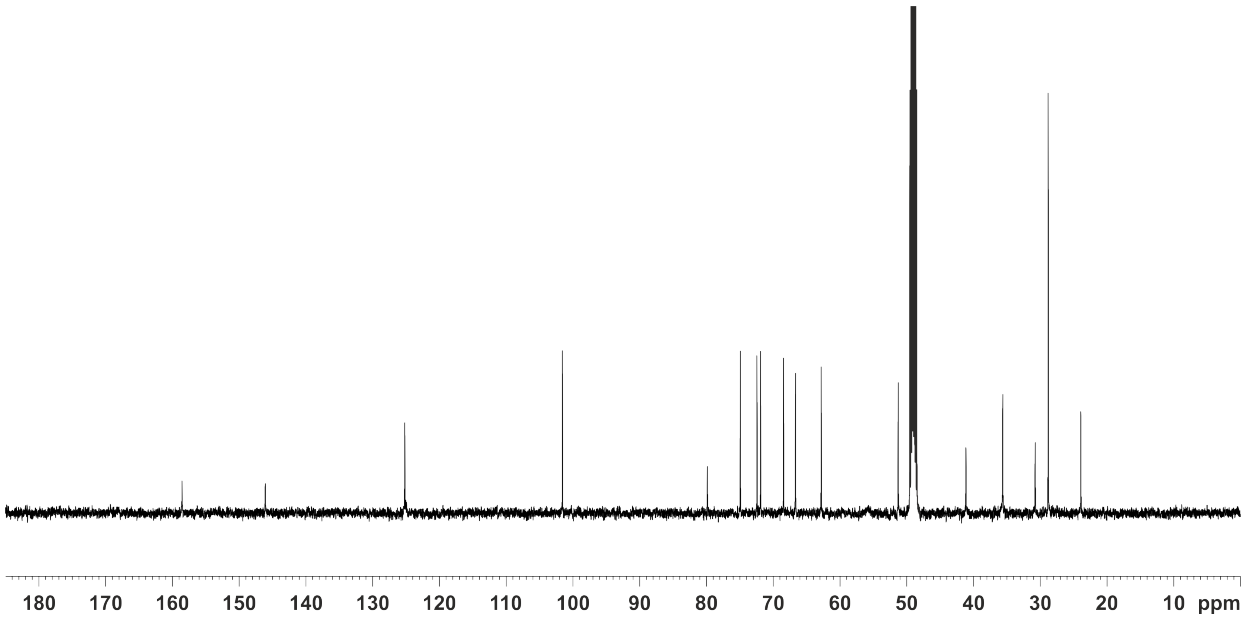

Figure 8.18. ^{13}C NMR spectrum of **32** (126 MHz, MeOH-d_4, 300 K).

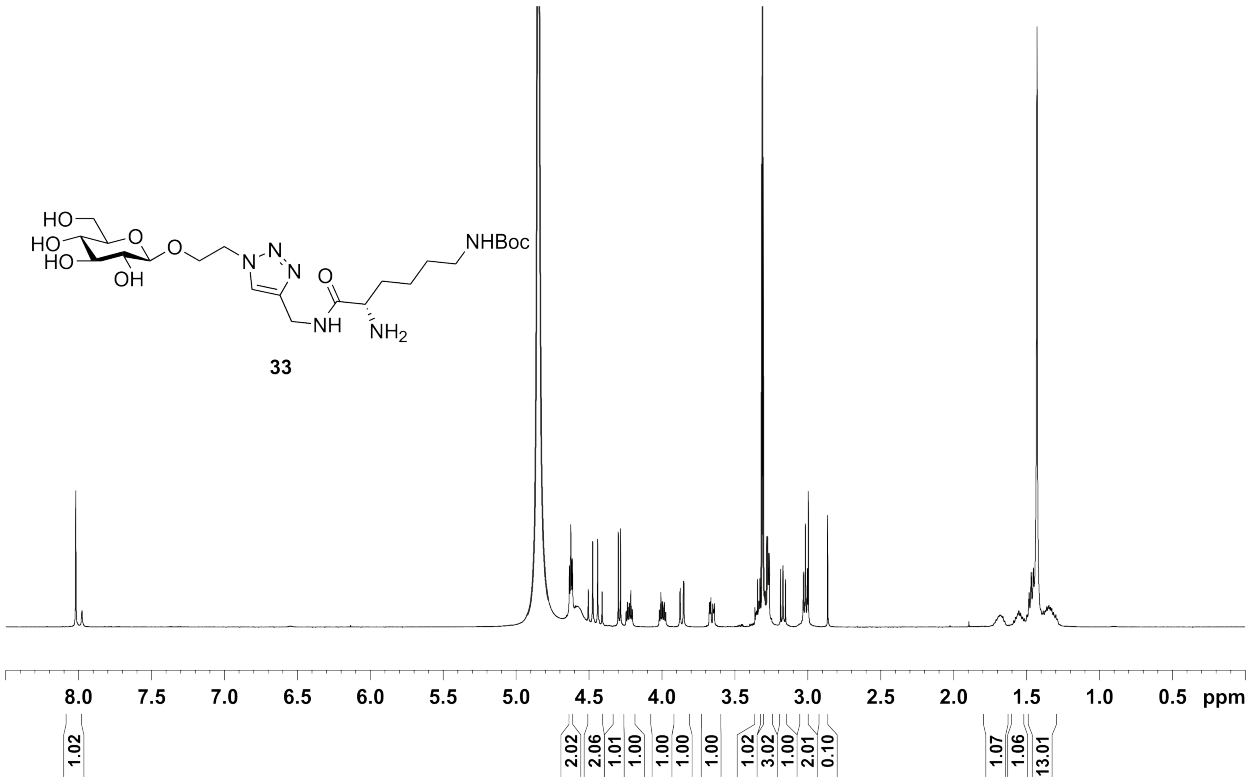

Figure 8.19. ^{1}H NMR spectrum of **33** (500 MHz, MeOH-d_4, 300 K).

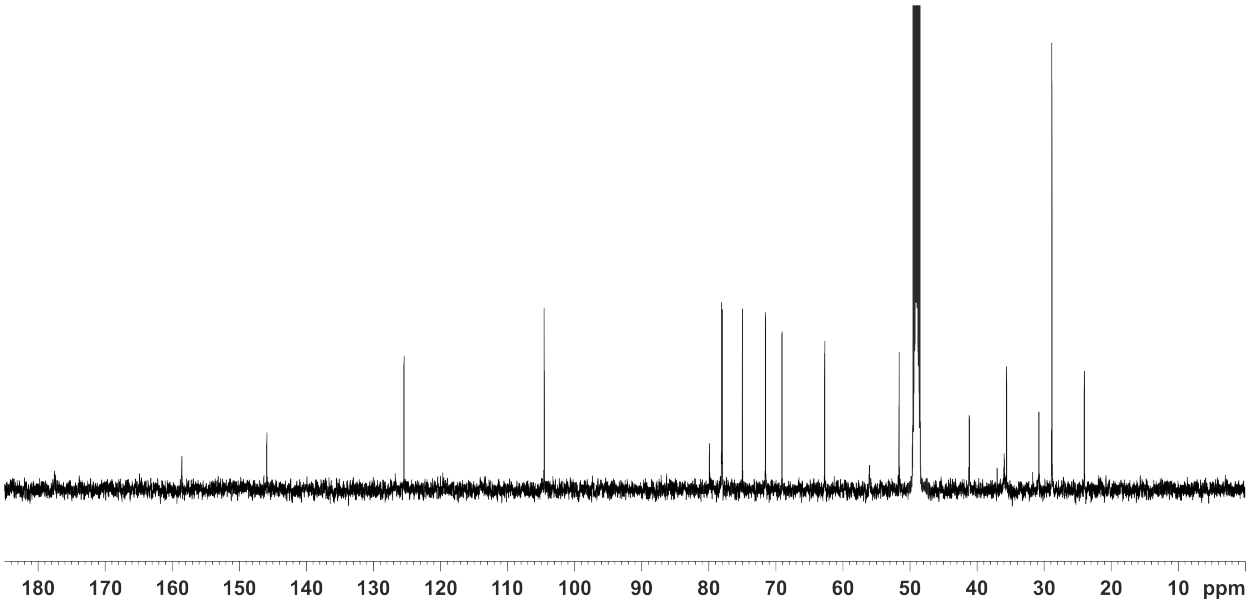

Figure 8.20. ^{13}C NMR spectrum of **33** (126 MHz, MeOH-d_4, 300 K).

Inhibition curves of adhesion-inhibition assay with GFP expressing *E. coli* bacteria

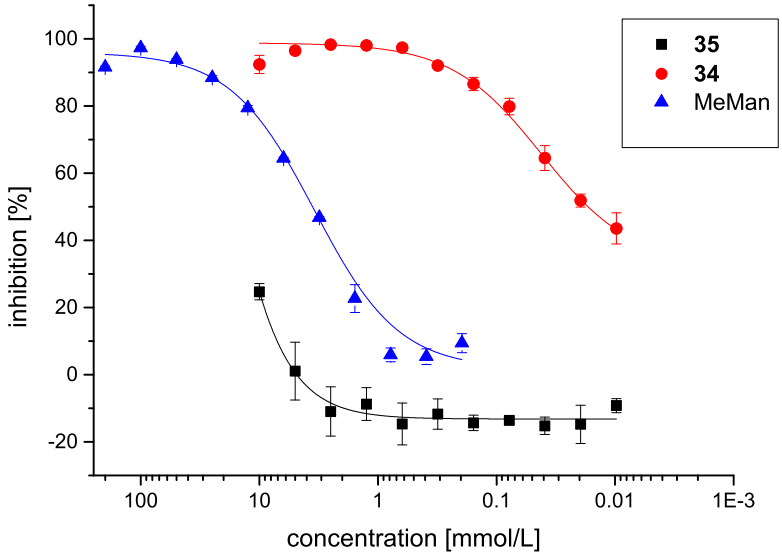

Figure 8.21. Inhibition curves obtained with manno- **34** and glucopyranoside **35** possessing an aromatic aglycon as inhibitors for type 1 fimbriae-mediated bacterial adhesion to mannan. The depicted inhibition curves are representative examples from two independent experiments. MeMan was tested simultaneously on each plate. Sigmoidal concentration-response curves were fitted by non-linear regression. Error bars are standard deviations from triplicate values on one plate.

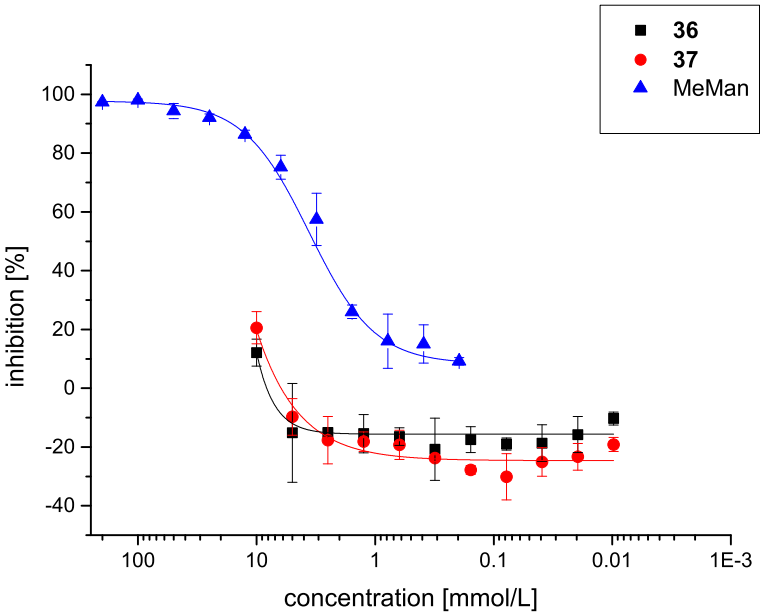

Figure 8.22. Inhibition curves obtained with arabinofuranosides **36** and **37** as inhibitors for type 1 fimbriae-mediated bacterial adhesion to mannan. The depicted inhibition curves are representative examples from two independent experiments. MeMan was tested simultaneously on each plate. Sigmoidal concentration-response curves were fitted by non-linear regression. Error bars are standard deviations from triplicate values on one plate.

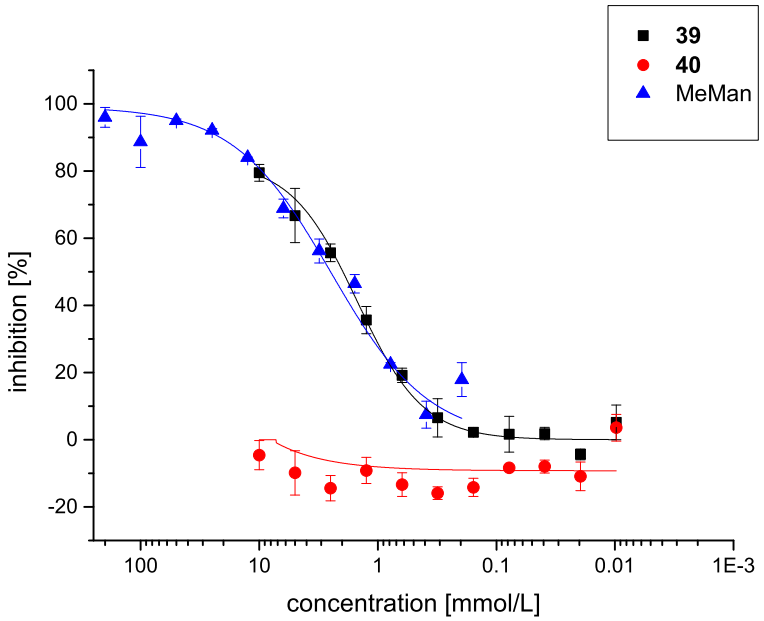

Figure 8.23. Inhibition curves obtained with manno- **39** and glucopyranoside **40** possessing an aliphatic aglycon as inhibitors for type 1 fimbriae-mediated bacterial adhesion to mannan. The depicted inhibition curves are representative examples from two independent experiments. MeMan was tested simultaneously on each plate. Sigmoidal concentration-response curves were fitted by non-linear regression. Error bars are standard deviations from triplicate values on one plate.

Agglutination assay with *E. coli* bacteria

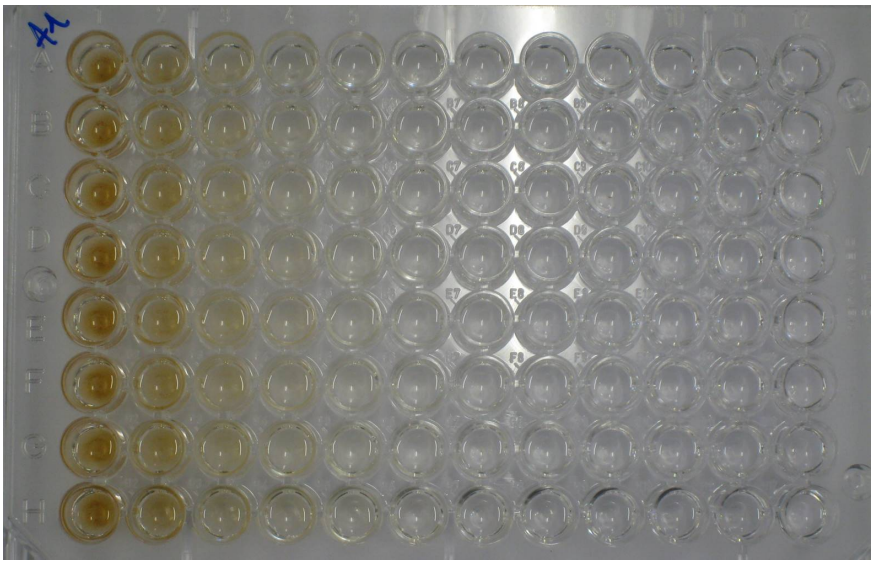

Figure 8.24. Agglutination of magnetic PEG beads in a serial dilution decorated with mannosides **30** or **31**; using type 1-fimbriated *E. coli* bacteria. The depicted figures are representative examples from at least three independent experiments. Carboxylic acid beads blocked with ethanolamine and beads decorated with the Fmoc-deprotected linker molecule were tested simultaneously on each plate.

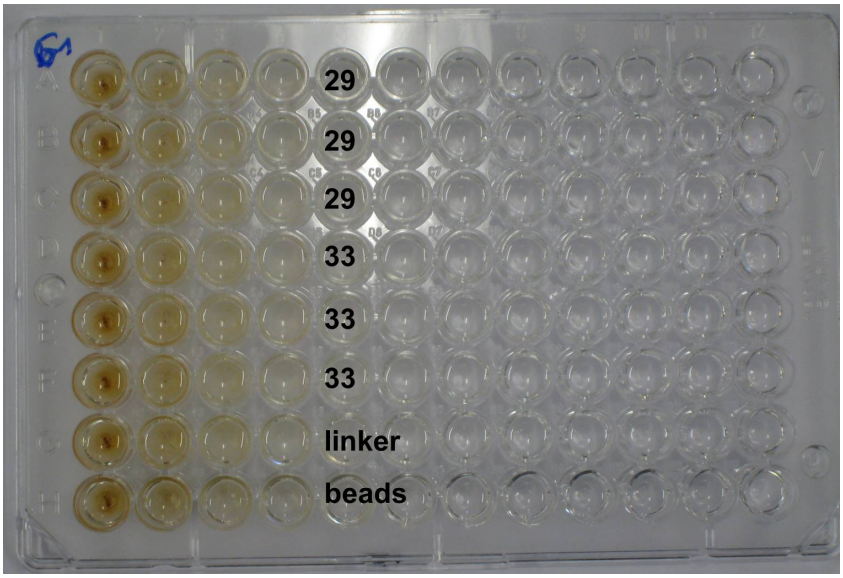

Figure 8.25. Agglutination of magnetic PEG beads in a serial dilution decorated with mannosides **29** or **33**; using type 1-fimbriated *E. coli* bacteria. The depicted figures are representative examples from at least three independent experiments. Carboxylic acid beads blocked with ethanolamine and beads decorated with the Fmoc-deprotected linker molecule were tested simultaneously on each plate.

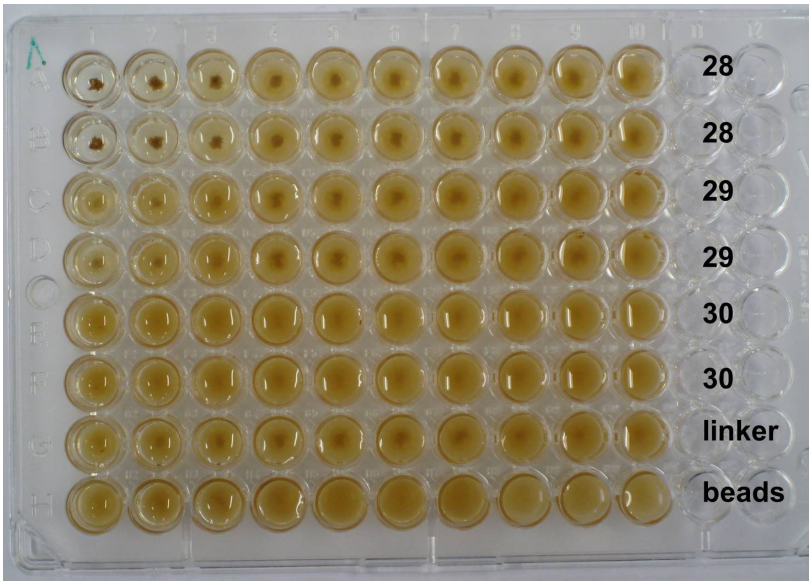

Figure 8.26. Agglutination of magnetic PEG beads with type 1-fimbriated *E. coli* bacteria which were added in serial dilution to the respective beads decorated with the corresponding glycosides **28** **29** and **30**. The depicted figures are representative examples from at least three independent experiments. Carboxylic acid beads blocked with ethanolamine and beads decorated with the Fmoc-deprotected linker molecule were tested simultaneously on each plate.

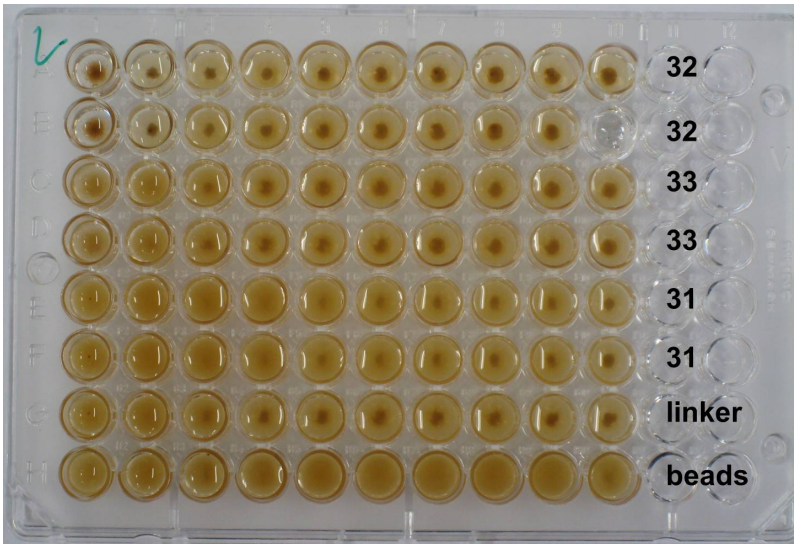

Figure 8.27. Agglutination of magnetic PEG beads with type 1-fimbriated *E. coli* bacteria which were added in serial dilution to the respective beads decorated with the corresponding glycosides **31**, **32** and **33**. The depicted figures are representative examples from at least three independent experiments. Carboxylic acid beads blocked with ethanolamine and beads decorated with the Fmoc-deprotected linker molecule were tested simultaneously on each plate.

References

[1] M. Hartmann, A. K. Horst, P. Klemm, T. K. Lindhorst, *Chem. Commun.* **2010**, *46*, 330–332.

[2] M. Touaibia, T. C. Shiao, A. Papadopoulos, J. Vaucher, Q. Wang, K. Benhamioud, R. Roy, *Chem. Commun.* **2007**, 380–382.

[3] K. H. Jung, M. Hoch, R. R. Schmidt, *Liebigs Ann. Chem.* **1989**, 1099–1106.

[4] C. Sibbersen, L. Lykke, N. Gregersen, K. A. Jørgensena, M. Johannsen, *Chem. Commun.* **2014**, *50*, 12098-12100.

[5] M. L. Wolfrom, A. Thompson, Meth. *Carbohydr. Chem.* **1963**, *2*, 211-215.

[6] S. Deshayes, V. Maurizot, M.-C. Clochard, C. Baudin, T. Berthelot, S. Esnouf, D. Lairez, M. Moenner G. Déléris, *Pharm. Res.* **2011**, *28*, 1631–1642.

[7] T. K. Lindhorst, S. Kötter, U. Krallmann-Wenzel, S. Ehlers, *J. Chem. Soc., Perkin Trans. 1* **2001**, 823–831.

[8] T. M. Tagmose, M. BoIs, *Chem. Eur. J.* **1997**, *3*, 453-462.

8.2.3 Further experimental data on chapter 4.4

Synthesis of azobenzene glycoconjugates:

***N*$^{\varepsilon}$-(*tert*-butoxycarbonyl)-*N*-{(*E*)-[*p*-[*p*'-(2,3,4,6-tetra-*O*-acetyl-α-D-mannopyranosyloxy)-phenylazo]benzyl-1H-1,2,3-triazole-1-yl)methyl]}-L-lysinamide (10):** To a solution of the mannoside **8** (68.0 mg, 117 µmol) and the linker **9**[403] (59.0 mg, 117 µmol) in dimethylformamide (3 mL), a solution of copper sulfate pentahydrate (12.0 mg, 49.1 µmol) and a solution of sodium ascorbate (20.0 mg, 99.5 µmol) in water (each 0.5 mL) were added. The reaction mixture was stirred for 16 h at room temperature. Then water (10 mL) and a saturated aq. NH_4Cl solution (10 mL) were added and the aqueous phase extracted with ethyl acetate (4 × 20 mL). The combined organic phases were dried over $MgSO_4$, it was filtered and the filtrate concentrated under reduced pressure. Purification of the crude product by column chromatography (cyclohexane/ethyl acetate/methanol, 1:1:0.1) gave **10** as an orange amorphous solid (101 mg, 92.7 µmol, 79%). R_f = 0.25 (cyclohexane/ethyl acetate/methanol, 1:1:0.1); $[\alpha]_D^{23}$ = +46.6 (c = 0.5 in methanol); ^{1}H NMR (500 MHz, MeOH-d_4, 300 K): δ = 7.89-7.75 (m, 9H, Ar-H$_{Fmoc}$, Ar-H$_{ortho}$, Ar H$_{ortho'}$, Ar-H$_{Triazole}$), 7.39-7.35 (m, 4H, Ar-H$_{meta'}$, Ar-H$_{Fmoc}$), 7.30-7.25 (m, 4H, Ar-H$_{meta}$, Ar-H$_{Fmoc}$), 5.76 (s~d, 1H, H-1), 5.63-5.32 (m, 6H, CH_2CH-Fmoc, ArCH_2N, H-2, H-3), 4.56-3.98 (m, 9H, C*H*NHFmoc, CCH_2NHCO, CH_2C*H*-Fmoc, H-4, H-5, H-6), 3.04-3.01 (m, 2H, CH_2NHBoc), 2.23, 2.09, 2.05, 1.98 (each s, each 3H, 4 $COCH_3$), 1.78-1.73 (m, 1H, C*H*H'CHNHFmoc), 1.70-1.59 (m, 1H, CH*H'*CHNHFmoc), 1.44-1.29 (m, 13H, CH_2CH_2NHBoc, CH_2CH_2CH_2NHBoc, C(CH_3)$_3$) ppm; ^{13}C NMR (126 MHz, MeOH-d_4, 300 K): δ = 175.2 (CCH_2NH*C*O), 172.2, 171.6, 171.5, 171.5 (4 *C*OCH_3), 159.4 (C-Ar$_{para}$), 158.5 (COO$_{Boc}$), 158.5 (COO$_{Fmoc}$), 153.8 (C-Ar$_{ipso'}$), 149.6 (C-Ar$_{ipso}$), 145.3 (C-Ar$_{Triazole}$), 145.2 (C-Ar$_{Fmoc}$), 142.6 (C-Ar$_{Fmoc}$), 139.9 (C-Ar$_{para'}$), 133.0 (C-Ar$_{Fmoc}$), 129.9 (C-Ar$_{meta'}$), 128.8 (C-Ar$_{Fmoc}$), 128.2 (C-Ar$_{Fmoc}$), 126.2 (C-Ar$_{Fmoc}$), 125.7 (C-Ar$_{ortho}$), 124.4 (C-Ar$_{Triazole}$), 124.1 (C-Ar$_{ortho'}$), 121.0 (C-Ar$_{Fmoc}$), 118.2 (C-Ar$_{meta}$), 97.0 (C-1), 79.9 (*C*(CH_3)$_3$), 70.9 (CH_2*C*H-Fmoc), 70.5 (C-2), 67.8 (*C*H_2CH-Fmoc), 67.0 (C-3), 63.3 (C-6), 56.7 (*C*HNHFmoc), 54.4 (C-4), 46.1 (C-5), 41.0 (*C*H_2NHBoc), 35.8 (C*C*H_2NHCO), 32.6 (*C*H_2CH_2NHBoc), 30.5 (*C*H_2CHNHFmoc), 28.8 (C(*C*H_3)$_3$), 24.1 (*C*$H_2CH_2CH_2$NHBoc), 20.6, 20.6 (2 CO*C*H_3) ppm; IR (ATR): $\tilde{\nu}$ = 2935, 1747, 1713, 1497, 1366, 1216, 1032, 740 cm^{-1}; ESI-MS: m/z calcd for $C_{56}H_{64}N_8O_{15}$: 1111.4 $[M+Na]^+$; found 1111.4.

***N*$^{\varepsilon}$-(*tert*-butoxycarbonyl)-*N*-{(*E*)-[*p*-[*p*'-(α-D-mannopyranosyloxy)phenylazo]benzyl-1H-1,2,3-triazole-1-yl)methyl]}-L-lysinamide (11):** To a solution of the mannoside **10** (65.0 mg, 59.7 µmol) in dimethylformamide (4 mL), piperidine (1 mL) was added dropwise and the reaction mixture was stirred for 16 h at room temperature. Then the solvent was evaporated and the crude product resolved in methanol (4 mL). Potassium carbonate (330 µg, 23.9 µmol) was added and the reaction mixture was stirred again for 16 h at room temperature. It was neutralized with Amberlite® IR 120, filtered and then the solvent was evaporated. Purification of the crude product by column chromatography (dichloromethane/methanol/triethylamine, 7:1:0.05→5:1:0.05) gave the azobenzene mannoside **11** as an orange amorphous solid (25.0 mg, 35.8 µmol, 60%). R_f = 0.22 (dichloromethane/methanol/triethylamine, 6:1:0.05); m.p. 78.7 °C; $[\alpha]_D^{23}$ = +38.9 (c = 0.5 in methanol); ^{1}H NMR (600 MHz, MeOH-d_4, 300 K): δ = 7.92-7.86 (m, 5H, Ar-H$_{ortho}$, Ar H$_{ortho'}$, Ar-H$_{Triazole}$), 7.49-7.46 (m, 2H, Ar-H$_{meta'}$), 7.29-7.27 (m, 2H, Ar H$_{meta}$), 5.68 (s, 2H, ArCH_2N), 5.61

(s~d, 1H, H-1), 4.47 (s, 2H, CC*H*$_2$NHCO), 4.05 (dd, $^3J_{1,2}$ = 1.8 Hz, $^3J_{2,3}$ = 3.3 Hz, 1H, H-2), 3.92 (dd, $^3J_{2,3}$ = 3.3 Hz, $^3J_{3,4}$ = 9.4 Hz, 1H, H-3), 3.79-3.74 (m, 2H, H-4, H-6'), 3.72 (dd, $^2J_{6,6'}$ = 12.0 Hz, $^3J_{5,6}$ = 5.5 Hz, 1H, H-6), 3.60-3.57 (m, 1H, H-5), 3.49-3.46 (m, 1H, C*H*NH$_2$), 2.99-2.96 (m, 2H, C*H*$_2$NHBoc), 1.74-1.69 (m, 1H, C*H*H'CHNH$_2$), 1.64-1.58 (m, 1H, CH*H'*CHNH$_2$), 1.49-1.26 (m, 13H, C*H*$_2$CH$_2$NHBoc, CH$_2$C*H*$_2$CH$_2$NHBoc, C(CH$_3$)$_3$) ppm; ^{13}C NMR (126 MHz, MeOH-d_4, 300 K): δ = 160.6 (C-Ar$_{para}$), 158.6 (COO$_{Boc}$), 153.9 (C-Ar$_{ipso'}$), 149.1 (C-Ar$_{ipso}$), 146.4 (C-Ar$_{Triazole}$), 139.2 (C-Ar$_{para'}$), 130.0 (C-Ar$_{meta'}$), 125.7 (C-Ar$_{ortho}$), 124.4 (C-Ar$_{Triazole}$), 124.1 (C-Ar$_{ortho'}$), 118.0 (C-Ar$_{meta}$), 100.1 (C-1), 79.8 (C(CH$_3$)$_3$), 75.7 (C-5), 72.4 (C-3), 71.8 (C-2), 68.3 (C-4), 62.7 (C-6), 55.4 (*C*HNH$_2$), 54.5 (ArC*H*$_2$N), 41.0 (*C*H$_2$NHBoc), 35.6 (C*C*H$_2$NHCO), 34.6 (*C*H$_2$CHNH$_2$), 30.7 (*C*H$_2$CH$_2$NHBoc), 28.8 (C(*C*H$_3$)$_3$), 23.6 (*C*H$_2$CH$_2$CH$_2$NHBoc) ppm; IR (ATR): $\tilde{\nu}$ = 2103, 1749, 1587, 1368, 1211, 1033, 844 cm^{-1}; ESI-MS: m/z calcd for $C_{28}H_{44}N_6O$: 609.3 $[M+H]^+$; found 609.2.

Irradiation of magnetic PEG beads and following binding assay with GFP-tagged *E. coli*:

Beads decorated with azobenzene mannoside **11** (4 × 50 µL/bowl of prepared beads suspension; $6 \cdot 10^7$ particles) were transferred to small plastic bowls and PBS buffer (900 µL/bowl) was added. Then, two sets of the beads were irradiated with UV light (365 nm) at ambient temperature and 100 rpm for 15 min. Whereas the other two sets of beads were shaken without irradiation at 100 rpm and ambient temperature for 15 min. Subsequently, the beads suspension was transferred to Eppendorf tubes®, washed with PBS buffer (400 µL/tube) and resuspended in PBS buffer (150 µL/tube). Following this, the prepared bacterial suspension (OD_{600} = 0.6, 50 µL/tube) was added and incubated at ambient temperature and 600 rpm for 30 min. Afterwards, beads were washed with PBS buffer (500 µL/tube), resuspended in PBS buffer (100 µL/tube), transferred to a black 96-well microtiter plates (Nunc, MaxiSorp®) and the fluorescence intensity (485 nm/535 nm) was determined. Each prepared beads suspension was tested at least in duplicates. As a control blocked carboxylic acid PEG-beads were tested as well to exclude bacterial binding caused by irradiation. Thus, unfunctionalized beads were treated as described above for beads prepared from **38**. A magnetic separation rack (DyneMag-2 magnet, Life technologies) was used for bead extraction.

8.3 Supporting Information on Chapter 5

8.3.1 Supporting Information for the Manuscript *Switching first contact: Photocontrol of E. coli adhesion to human cells*

Supporting Information

for

Switching first contact: Photocontrol of *E. coli* adhesion to human cells

L. Möckl, A. Müller, C. Bräuchle, T. K. Lindhorst

Electronic Supporting Information

Switching first contact: Photocontrol of *E. coli* adhesion to human cells

Leonhard Möckl, Anne Müller, Christoph Bräuchle* and Thisbe K. Lindhorst*

List of content

1. Materials and Methods

General methods

Analytical thin layer chromatography (TLC) was performed on silica gel plates (GF 254, Merck). Visualization was achieved by UV light and/or with 10% sulfuric acid in ethanol followed by heat treatment at ~180 °C. Flash chromatography was performed on silica gel 60 (Merck, 230-400 mesh, particle size 0.040-0.063 mm) by using distilled solvents. Melting points (mp) were determined on a Büchi M-56 apparatus. Optical rotations were measured with a Perkin-Elmer 241 polarimeter (sodium D-line: 589 nm, length of cell: 1 dm) in the solvents indicated. Proton (^{1}H) nuclear magnetic resonance spectra and carbon (^{13}C) nuclear magnetic resonance spectra were recorded on a Bruker DRX-500 and AV-600 spectrometer. Chemical shifts are referenced to the residual proton of the NMR solvent. Data are presented as follows: chemical shift, multiplicity (s=singlet, d=doublet, t=triplet, q=quartet, m=multiplet, and br=broad signal), coupling constant in hertz (Hz) and, integration. Full assignment of the peaks was achieved with the aid of 2D NMR techniques (^{1}H/^{1}H COSY and ^{1}H/^{13}C HSQC. All NMR spectra of the *E*-isomers of the azobenzene derivatives were recorded after they were kept for 16 h in the dark at 40 °C. Infrared (IR) spectra were measured with a Perkin Elmer FT-IR Paragon 1000 (ATR) spectrometer and were reported in cm^{-1}. ESI mass spectra were recorded on a LCQ Classic from Thermo Finnigan and HRMS ESI spectra on an Agilent 6224 ESI-TOF. UV-vis absorption spectra were performed on Perkin-Elmer Lambda-241 at a temperature of 20 °C ± 1 °C.

Bacterial Culture

E. coli (strain pPKL1162) were inoculated in LB medium (10 mL) (Sigma-Aldrich, St. Louis, MO) in presence of chloramphenicol (50 mg/L) and ampicillin (100 mg/L) (both Sigma-Aldrich) and grown at 37°C overnight under constant agitation. Then, the bacteria were centrifuged and washed two times with DPBS +Ca^{2+}/Mg^{2+} (Life Technologies, Carlsbad, St. Louis, MO) and once with cell medium. Then, the bacteria were resuspended in cell medium (10 mL) and the optical density at 600 nm was determined. For the experiments under static conditions, a 1:10 or 1:20 dilution of a suspension with OD_{600}=0.1 was used. Under flow conditions, the dilution was 1:50.

Cell Culture

HMEC-1 (CDC, Atlanta, GA) were seeded in collagen coated 8-well LabTekII-slides (Nunc, Rochester, NY) or in collagen coated Luer $I^{0.8}$ channels (IBIDI, Martinsried, Germany) and grown to confluency. The cells were cultured in MDCB-131 medium with 1% glutamax, 10% FBS, hEGF (10 ng/mL) (all Life Technologies), and hydocortisone (1 µg/mL) (Sigma-Aldrich) at 37°C in 5% CO_2-atmosphere.

Fluorescence Microscopy

Confocal fluorescence images were obtained with a commercially available spinning-disk inverted microscope (Zeiss).

Software

Images were analysed using ImageJ. For data visualization and analysis, OriginPro 8G was used. Figures were prepared with Corel Draw 12.

2. Synthesis of glycoconjugates

(*E*)-*p*-[*p'*-(Hydroxy)]phenylazophenyl α-D-mannopyranoside (3)[1] was obtained by employing a new procedure: To a solution of *p*-aminophenyl α-D-mannopyranoside[2] (**1**, 1.07 g, 3.94 mmol) in water (11 mL) 37% hydrochloric acid (310 µL, 3.94 mmol) was added and the reaction mixture was cooled to 0 °C. Then an ice-cold solution of sodium nitrite (272 mg, 3.94 mmol) in water (11 mL) was added dropwise at 0 °C. The reaction mixture was stirred for 2 h at 0 °C and then added dropwise to an ice cold solution of phenol (371 mg, 3.94 mmol), sodium hydroxide (158 mg, 3.94 mmol) and sodium carbonate (438 mg, 4.14 mmol) in water (11 mL). It was stirred for 2 h at 0 °C and afterwards the reaction mixture was acidified by adding hydrochloric acid. The precipitated solid was filtered off and washed with water. The crude product was recrystallised from water and methanol (4:1). The azobenzene mannoside **3** was obtained as an orange solid (737 mg, 1.98 mmol, 50%). R_f=0.09 (dichloromethane/methanol, 9:1); m.p. 259 °C; $[\alpha]_D^{23}$=+148.0 (*c*=0.6 in methanol); ^{1}H NMR (500 MHz, DMSO-d_6, 300 K): δ = 7.81-7.74 (m, 4H, Ar-H$_{ortho}$, Ar-H$_{ortho'}$), 7.25-7.22 (m, 2H, Ar-H$_{meta'}$), 6.94-6.91 (m, 2H, Ar-H$_{meta}$), 5.49 (d, $^3J_{1,2}$=1.8 Hz, 1H, H-1), 5.06 (d~br s, 1H, OH$_{C-2}$), 4.83 (d~br s, 1H, OH$_{C-4}$), 4.76 (d~br s, 1H, OH$_{C-3}$), 4.44 (t~br s, 1H, OH$_{C-6}$), 3.86 (m$_c$, 1H, H-2), 3.71-3.69 (m, 1H, H-3), 3.62-3.59 (m, 1H, H-6), 3.54-3.48 (m, 2H, H-4, H-6'), 3.41-3.37 (m, 1H, H-5) ppm; ^{13}C NMR (126 MHz, DMSO-d_6, 300 K): δ = 160.5 (C-Ar$_{para'}$), 158.1 (C-Ar$_{para}$), 147.0 (C-Ar$_{ipso}$), 145.2 (C-Ar$_{ipso'}$), 124.5 (C-Ar$_{ortho}$), 123.7 (C-Ar$_{ortho'}$), 117.1 (C-Ar$_{meta'}$), 115.9 (C-Ar$_{meta}$), 98.7 (C-1), 75.2 (C-5), 70.6 (C-3), 69.9 (C-2), 66.7 (C-4), 61.0 (C-6) ppm; IR (ATR): $\tilde{\nu}$ =3602, 3184, 2934, 1584, 1492, 1223, 1050, 953, 847 cm^{-1}; ESI-MS: *m/z* calcd for $C_{18}H_{20}N_2O_7$: 399.1 $[M+Na]^+$; found 399.2.

(*E*)-*p*-[*p'*-(Hydroxy)]phenylazophenyl β-D-glucopyranoside (4)[1] was obtained by employing a new procedure: To a solution of *p*-aminophenyl β-D-glucopyranoside[3] (**2**, 206 mg, 759 µmol) in water (5 mL) 37% hydrochloric acid (60.0 µL, 759 µmol) was added and the reaction mixture was cooled to 0 °C. Then an ice-cold solution of sodium nitrite (52.0 mg, 759 µmol) in water (5 mL) was added dropwise at 0 °C. The reaction mixture was stirred for 2 h at 0 °C and then added dropwise to an ice cold solution of phenol (71.0 mg, 759 µmol), sodium hydroxide (30.0 mg, 759 µmol) and sodium carbonate (84.0 mg, 797 µmol) in water (5 mL). It was stirred for 2 h at 0 °C and afterwards the reaction mixture was acidified by adding hydrochloric acid. The precipitated solid was filtered off and washed with water. The crude product was recrystallised from water. The azobenzene mannoside **4** was obtained as an orange solid (245 mg, 651 µmol, 86%). R_f=0.20 (dichloromethane/methanol, 9:1); m.p. 225 °C; $[\alpha]_D^{23}$=-56.0 (*c*=0.8 in methanol); ^{1}H NMR (600 MHz, MeOH-d_4, 300 K): δ = 7.83-7.77 (m, 4H, Ar-H$_{ortho}$, Ar-H$_{ortho'}$), 7.23-7.21 (m, 2H, Ar-H$_{meta'}$), 6.91-6.89 (m, 2H, Ar-H$_{meta}$), 5.03-4.99 (m, 1H, H-1), 3.92 (dd, $^2J_{6,6'}$=12.1 Hz, $^3J_{5,6}$=2.1 Hz, 1H, H-6), 3.73 (dd, $^2J_{6,6'}$=12.1 Hz, $^3J_{5,6'}$=5.7 Hz, 1H, H-6'), 3.52-3.48 (m, 3H, H-2, H-3, H-5), 3.44-3.40 (m, 1H, H-4) ppm; ^{13}C NMR (150 MHz, MeOH-d_4, 300 K): δ = 161.7 (C-Ar$_{para'}$), 160.8 (C-Ar$_{para}$), 149.4 (C-Ar$_{ipso}$), 147.5 (C-Ar$_{ipso'}$), 125.6 (C-Ar$_{ortho}$), 124.9 (C-Ar$_{ortho'}$), 117.9 (C-Ar$_{meta'}$), 116.7 (C-Ar$_{meta}$), 102.0 (C-1), 78.3 (C-3), 78.0 (C-5), 74.9 (C-2), 71.3 (C-4), 62.5 (C-6) ppm; IR (ATR): $\tilde{\nu}$ =3625, 3258, 2900, 1583, 1494, 1215, 1071, 1007, 843 cm^{-1}; ESI-MS: *m/z* calcd for $C_{18}H_{20}N_2O_7$: 399.1 $[M+Na]^+$; found 399.2.

(*E*)-*p*-[*p'*-(Propargyloxy)]phenylazophenyl α-D-mannopyranoside (5): To a suspension of azobenzene mannoside **3** (24.0 mg, 63.8 µmol) in a 1:1-mixture of acetonitrile and acetone (4 mL) potassium carbonate (35.0 mg, 255 µmol), potassium iodide (1.10 mg, 6.38 µmol) and propargyl bromide (80% in toluene, 6.00 µL, 63.8 µmol) were added. The reaction mixture was stirred for 6 h at 60 °C and for 16 h at room temperature. Then the solvent was evaporated. Purification of the crude product by

column chromatography (dichloromethane/methanol, 10:1→9:1→5:1) gave **5** as an orange solid (20.0 mg, 48.3 µmol, 76%). R_f=0.30 (ethyl acetate/methanol, 8:1); m.p. 227 °C; $[\alpha]_D^{23}$=+25.7 (*c*=0.5 in methanol); ^{1}H NMR (600 MHz, DMSO-d_6, 298 K): δ=7.87-7.82 (m, 4H, Ar-H$_{ortho}$, Ar-H$_{ortho'}$), 7.27-7.25 (m, 2H, Ar-H$_{meta'}$), 7.19-7.16 (m, 2H, Ar-H$_{meta}$), 5.51 (d, $^3J_{1,2}$=1.5 Hz, 1H, H-1), 5.09 (d, $^3J_{2,OH}$=4.4 Hz, 1H, OH$_{C-2}$), 4.92 (d, $^4J_{OCH2,C≡CH}$=2.3 Hz, 2H, OCH$_2$), 4.86 (d, $^3J_{3,OH}$=5.9 Hz, 1H, OH$_{C-3}$), 4.80 (d, $^3J_{4,OH}$=6.0 Hz, 1H, OH$_{C-4}$), 4.47 (t~dd, $^3J_{6,OH}$=6.0 Hz, $^3J_{6',OH}$=6.0 Hz, 1H, OH$_{C-6}$), 3.87-3.86 (m, 1H, H-2), 3.71 (ddd, $^3J_{3,4}$=9.3 Hz, $^3J_{3,OH}$=5.9 Hz, $^3J_{2,3}$=3.4 Hz, 1H, H-3), 3.64 (t, $^4J_{OCH2,C≡CH}$=2.3 Hz, 1H, C≡CH), 3.60 (ddd, $^2J_{6,6'}$=11.8 Hz, $^3J_{6,OH}$=6.0 Hz, $^3J_{5,6}$=2.0 Hz, 1H, H-6), 3.54-3.46 (m, 2H, H-4, H-6'), 3.40-3.37 (m, 1H, H-5) ppm; ^{13}C NMR (150 MHz, DMSO-d_6, 298 K): δ=159.4 (C-Ar$_{para'}$), 158.5 (C-Ar$_{para}$), 146.9 (C-Ar$_{ipso}$), 146.6 (C-Ar$_{ipso'}$), 124.1 (C-Ar$_{ortho}$), 124.0 (C-Ar$_{ortho'}$), 117.1 (C-Ar$_{meta'}$), 115.5 (C-Ar$_{meta}$), 98.7 (C-1), 78.9 (*C*≡CH), 78.7 (C≡*C*H), 75.2 (C-5), 70.6 (C-3), 69.9 (C-2), 66.6 (C-4), 61.0 (C-6), 55.8 (OCH$_2$) ppm; IR (ATR): $\tilde{\nu}$ =3400, 3291, 2939, 1580, 1493, 1227, 1123, 1008, 985, 840 cm^{-1}; UV-Vis (DMSO): λ^{max} (*ε*)=359 nm (21738 L mol^{-1} cm^{-1}); HRMS (ESI): *m/z* calcd for $C_{21}H_{22}N_2O_7$: 415.1505 [M+H]$^+$; found 415.1514.

(*E*)-*p*-[*p'*-(Propargyloxy)]phenylazophenyl β-D-glucopyranoside (6): To a suspension of azobenzene glucoside **4** (83.0 mg, 221 µmol) in acetone (5 mL) potassium carbonate (122 mg, 884 µmol), potassium iodide (4.00 mg, 22.1 µmol) and propargyl bromide (80% in toluene, 20.0 µL, 221 µmol) were added. The reaction mixture was stirred for 4 h at 60 °C and then the solvent was evaporated. Purification of the crude product by column chromatography (dichloromethane/methanol, 9:1) gave **6** as an orange solid (89.0 mg, 215 µmol, 97%). R_f=0.38 (dichloromethane/methanol, 9:1); m.p. 203 °C; $[\alpha]_D^{23}$=-46.7 (*c*=0.7 in methanol); ^{1}H NMR (600 MHz, DMSO-d_6, 300 K): δ=7.87-7.83 (m, 4H, Ar-H$_{ortho}$, Ar-H$_{ortho'}$), 7.21-7.19 (m, 2H, Ar-H$_{meta'}$), 7.18-7.16 (m, 2H, Ar-H$_{meta}$), 5.39 (d, $^3J_{2,OH}$=4.7 Hz, 1H, OH$_{C-2}$), 5.12 (d, $^3J_{3,OH}$=4.5 Hz, 1H, OH$_{C-3}$), 5.06 (d, $^3J_{4,OH}$=5.3 Hz, 1H, OH$_{C-4}$), 5.01 (d, $^3J_{1,2}$=7.3 Hz, 1H, H-1), 4.92 (d, $^4J_{OCH2,C≡CH}$=2.3 Hz, 2H, OCH$_2$), 4.60 (t~dd, $^3J_{6,OH}$=5.8 Hz, $^3J_{6',OH}$=5.8 Hz, 1H, OH$_{C-6}$), 3.73-3.70 (m, 1H, H-6), 6.63 (t, $^4J_{OCH2,C≡CH}$=2.3 Hz, 1H, C≡CH), 3.51-3.47 (m, 1H, H-6'), 3.41-3.38 (m, 1H, H-5), 3.32-3.26 (m, 2H, H-2, H-3), 3.22-3.18 (m, 1H, H-4) ppm; ^{13}C NMR (150 MHz, DMSO-d_6, 300 K): δ=159.6 (C-Ar$_{para'}$), 159.4 (C-Ar$_{para}$), 146.9 (C-Ar$_{ipso}$), 146.6 (C-Ar$_{ipso'}$), 124.1 (C-Ar$_{ortho}$), 124.0 (C-Ar$_{ortho'}$), 116.7 (C-Ar$_{meta'}$), 115.5 (C-Ar$_{meta}$), 100.1 (C-1), 78.9 (*C*≡CH), 78.7 (C≡*C*H), 77.2 (C-5), 76.6 (C-3), 73.2 (C-2), 69.7 (C-4), 61.0 (C-6), 55.8 (OCH$_2$) ppm; IR (ATR): $\tilde{\nu}$ =3250, 2920, 1583, 1495, 1232, 1012, 835 cm^{-1}; UV-Vis (DMSO): λ^{max} (*ε*)=359 nm (17123 L mol^{-1} cm^{-1}); HRMS (ESI): *m/z* calcd for $C_{21}H_{22}N_2O_7$: 415.1505 [M+H]$^+$; found 415.1517.

3. ^{1}H and ^{13}C NMR spectra of synthetic compounds

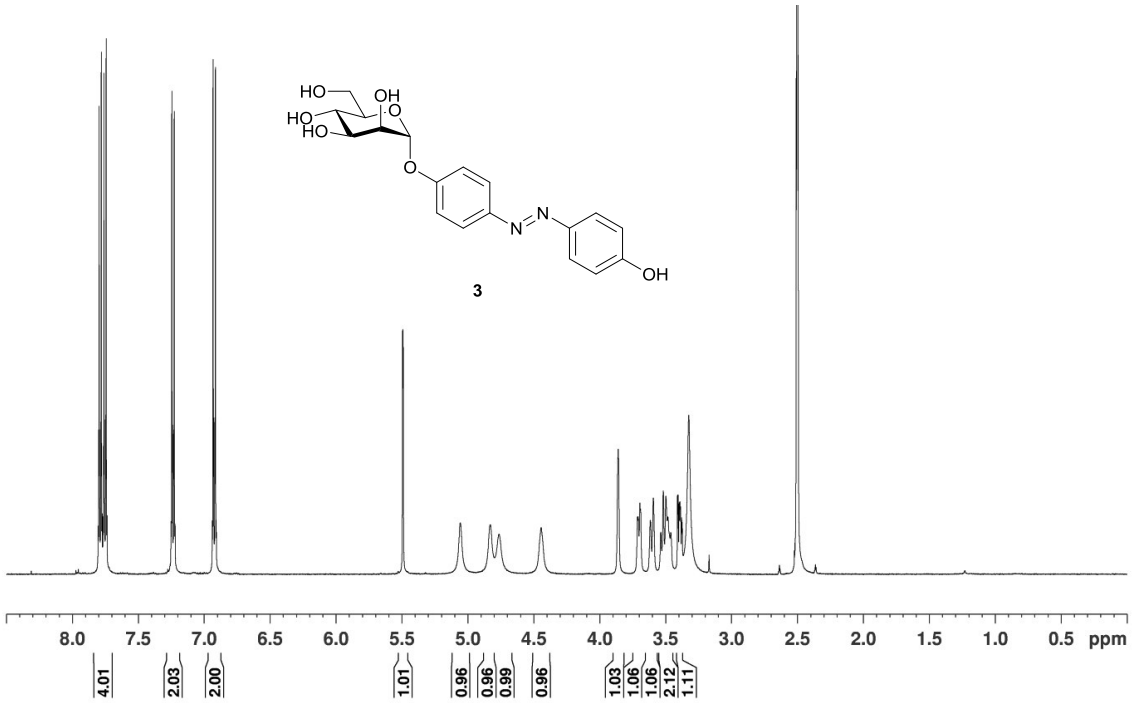

Figure S1. ^{1}H NMR spectrum of **3** (500 MHz, DMSO-d_6, 300 K).

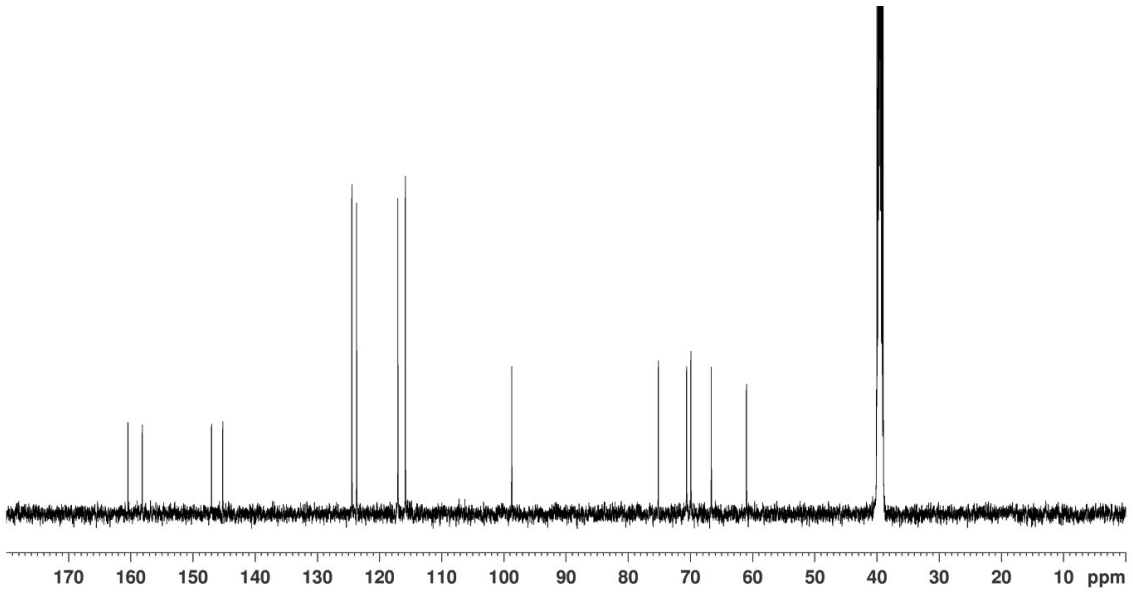

Figure S2. ^{13}C NMR spectrum of **3** (126 MHz, DMSO-d_6, 300 K).

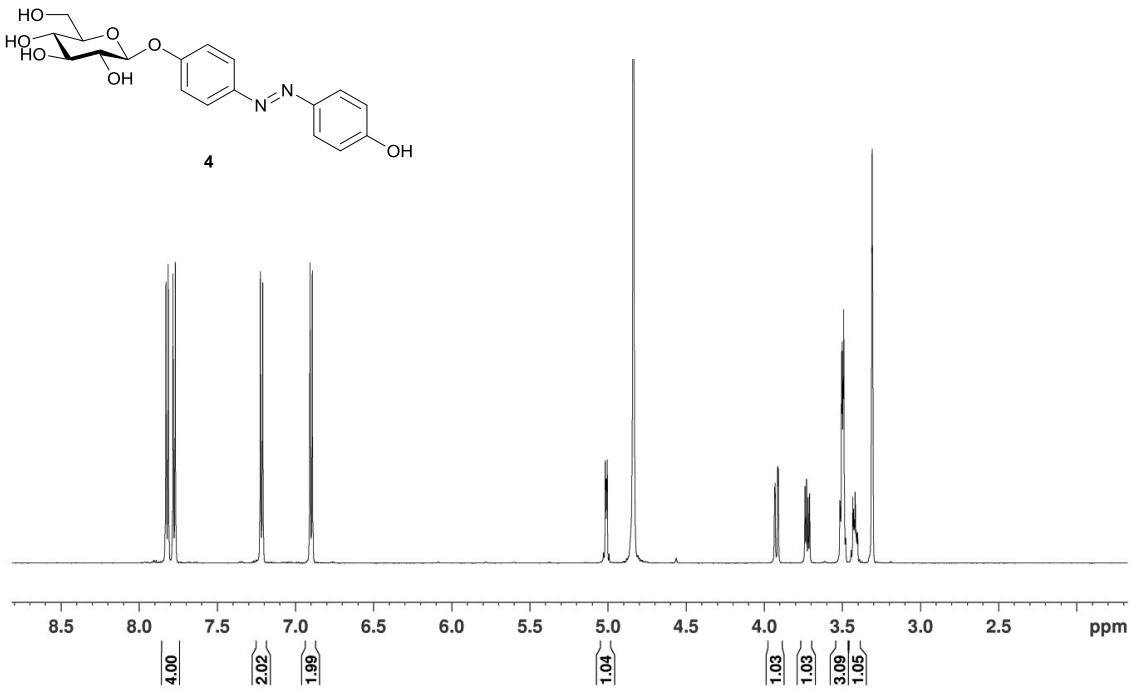

Figure S3. ^{1}H NMR spectrum of **4** (600 MHz, MeOH-d_4, 300 K).

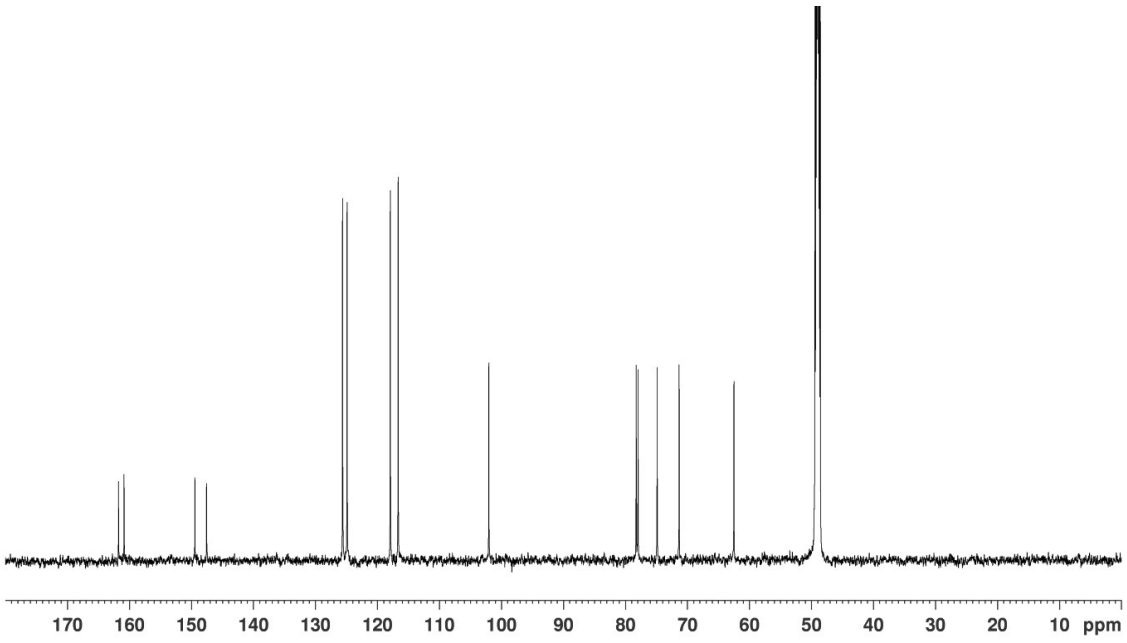

Figure S4. ^{13}C NMR spectrum of **4** (150 MHz, MeOH-d_4, 300 K).

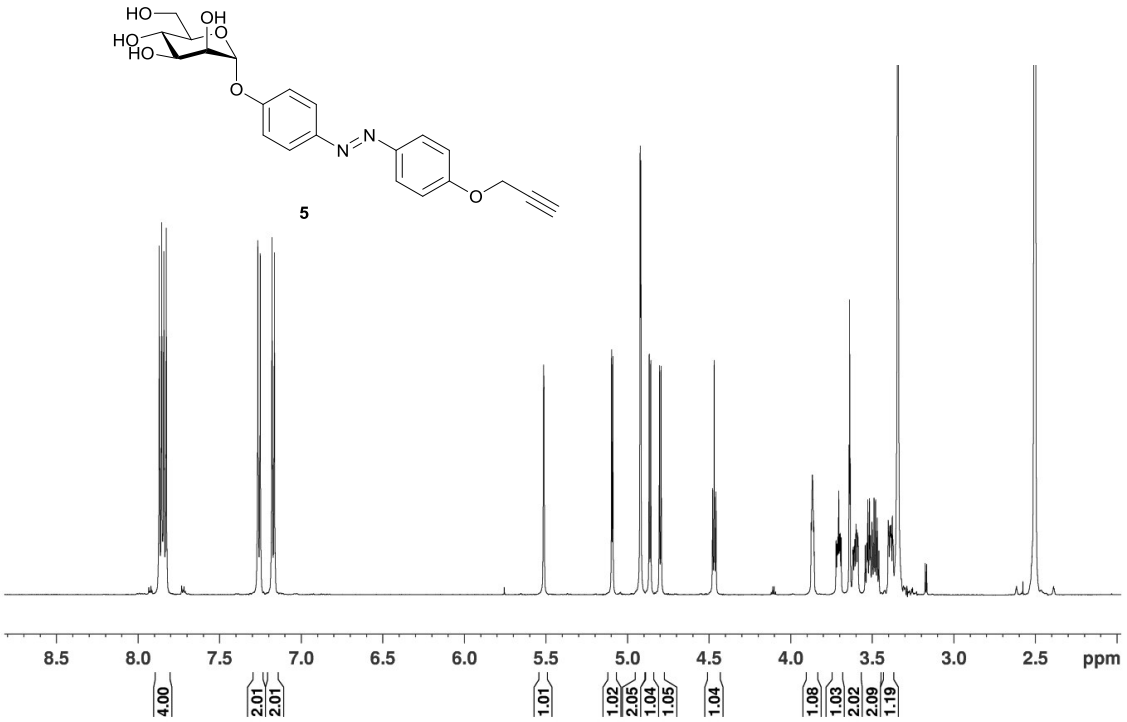

Figure S5. ^{1}H NMR spectrum of **5** (600 MHz, DMSO-d_6, 298 K).

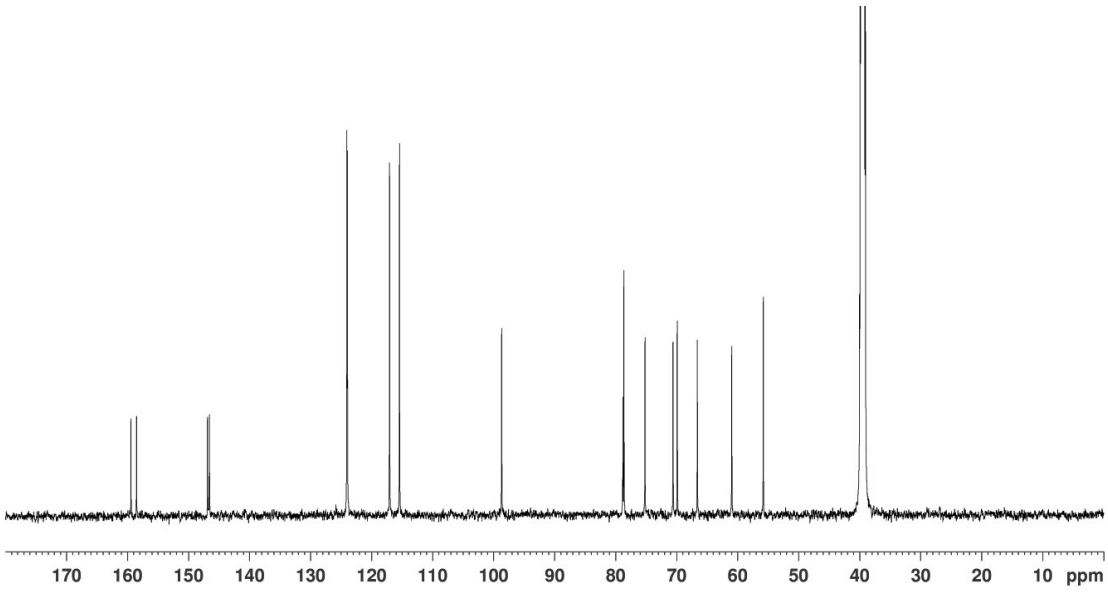

Figure S6. ^{13}C NMR spectrum of **5** (150 MHz, DMSO-d_6, 298 K).

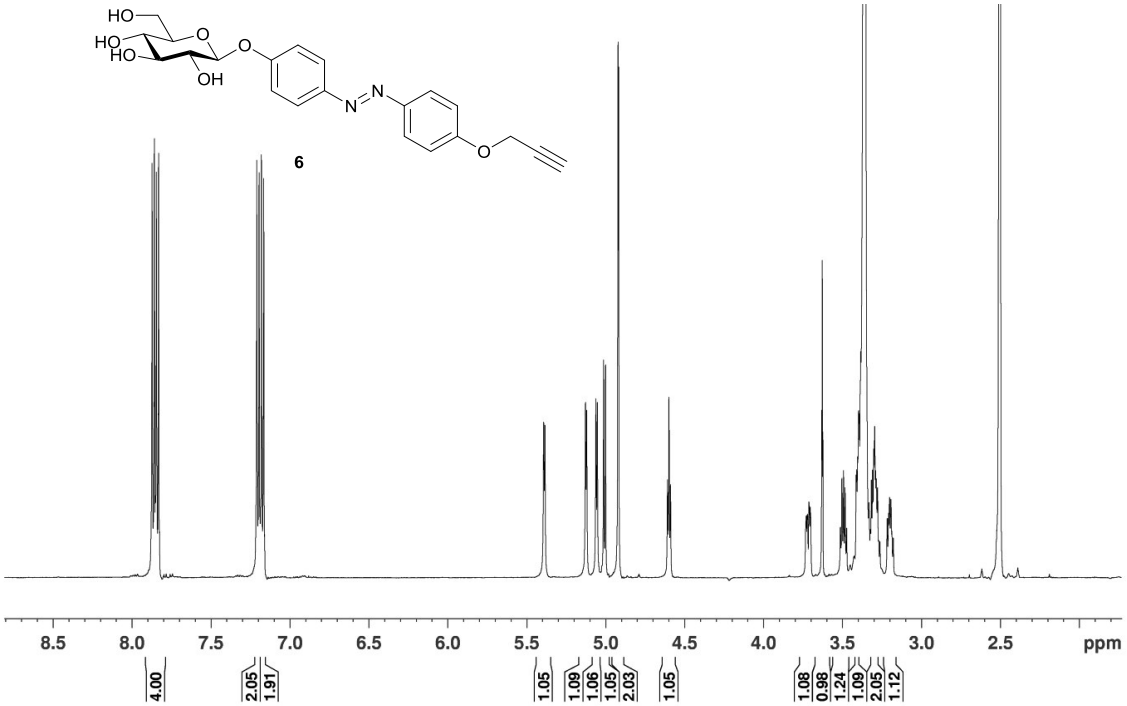

Figure S7. ^{1}H NMR spectrum of **6** (600 MHz, DMSO-d_6, 300 K).

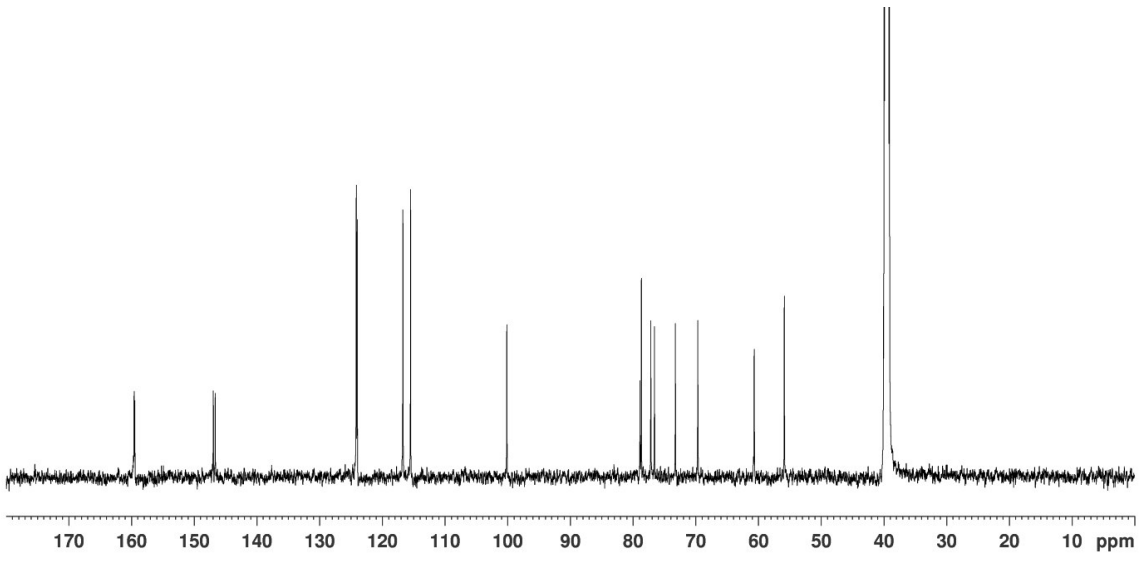

Figure S8. ^{13}C NMR spectrum of **6** (150 MHz, DMSO-d_6, 300 K).

4. Irradiation experiments

Irradiation was performed using a LED (emitting 365 nm light) from the Nichia Corporation (NC4U133A) with a FWHW of 9 nm and optical power output (P_O) ~1 W. *E*/*Z* ratios were determined by irradiating the sample in the NMR tube followed by ^{1}H NMR spectroscopy. The respective *E*-configured azobenzene (5-10 mg) was dissolved in DMSO-d_6 (500 µL) in a NMR tube and irradiated for 15 min at 365 nm. The distance between the LED and the sample in the NMR tube was about ~5 cm. Photostationary states (PSS) were reached after approx. 15 min. Then, the sample was kept in the dark, and ^{1}H NMR spectroscopy was performed immediately afterwards. The photostationary states (PSS) were determined by integration of the anomeric H-1 protons of the prepared compounds.

In analogy, for UV-vis spectroscopy, the *E*-configured azobenzene derivatives were dissolved in DMSO in a UV cuvette, irradiated for 15 min at 365 nm with a distance between LED and cuvette of ~5 cm. UV-vis spectra were recorded immediately afterwards. The absorption spectra showed an increase of the absorbance in the n-π* transition and simultaneous decrease in the π-π* transition, indicating the formation of the respective *Z* isomer. Extinction coefficients (ε) were deduced from UV-vis spectra measured at seven different concentrations (5 µM, 10 µM, 20 µM, 40 µM, 70 µM, 60 µM and 80 µM).

The kinetics of thermal *Z*→*E* relaxation process were determined by NMR spectroscopy in the dark. The half-life $\tau_{1/2}$ was determined as $\tau_{1/2} = \ln 2/k$. After irradiation, the ^{1}H NMR spectra of the samples were recorded in regular intervals (3 h) over a period of 5 to 6 days. For the determination of the half-life the *Z* and *E* signals of the respective azobenzene moiety were integrated. A signal that was not influenced by irradiation was set as reference. The decay of the integral of the *Z*- and the increase of the integral of the *E*-species were plotted and an exponential decay of first order fitted to the data.

NMR spectra of *Z*-configured compounds and UV-vis spectra

(*Z*)-*p*-[*p'*-(Propargyloxy)]phenylazophenyl α-D-mannopyranoside (5):

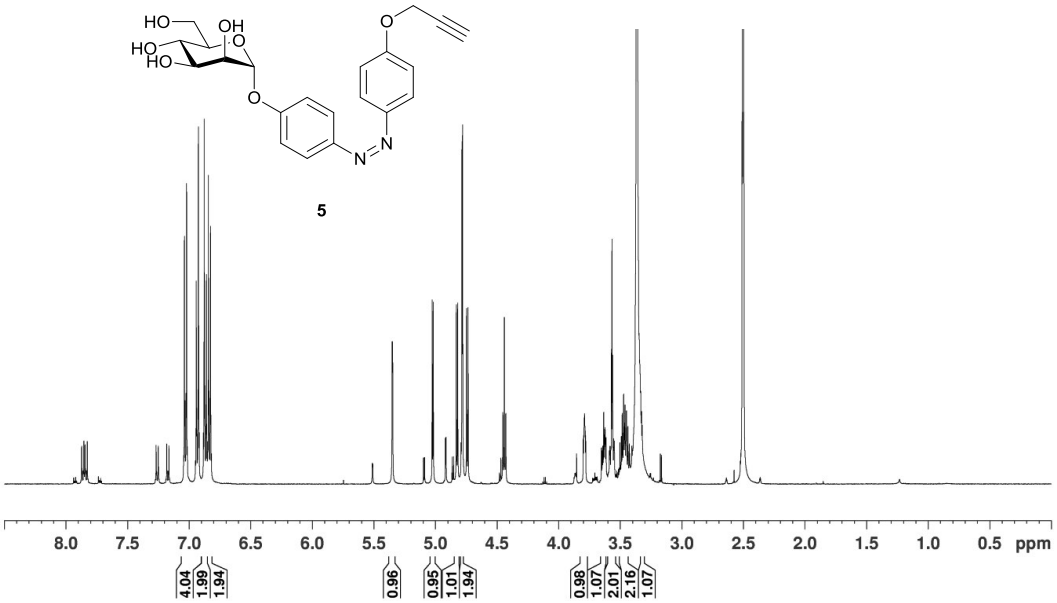

Figure S9. ^{1}H NMR spectrum of **5** (500 MHz, DMSO-d_6, 300 K).

^{1}H NMR (500 MHz, DMSO-d_6, 300 K): δ=7.04-6.91 (m, 4H, Ar-H$_{ortho}$, Ar-H$_{ortho'}$), 6.88-6.85 (m, 2H, Ar-H$_{meta'}$), 6.85-6.82 (m, 2H, Ar-H$_{meta}$), 5.35 (d, $^{3}J_{1,2}$=1.8 Hz, 1H, H-1), 5.02 (d, $^{3}J_{2,OH}$=4.5 Hz, 1H, OH$_{C-2}$), 4.83 (d, $^{3}J_{3,OH}$=5.7 Hz, 1H, OH$_{C-3}$), 4.78 (d, $^{4}J_{OCH2,C\equiv CH}$=2.4 Hz, 2H, OCH$_2$), 4.74 (d, $^{3}J_{4,OH}$=6.1 Hz, 1H, OH$_{C-4}$), 4.44 (t~dd, $^{3}J_{6,OH}$=6.0 Hz, $^{3}J_{6',OH}$=6.0 Hz, 1H, OH$_{C-6}$), 3.80-3.78 (m, 1H, H-2), 3.65-3.61 (m, 1H, H-3), 3.59-3.54 (m, 2H, C≡CH, H-6), 3.51-3.44 (m, 2H, H-4, H-6'), 3.35-3.32 (m, 1H, H-5) ppm.

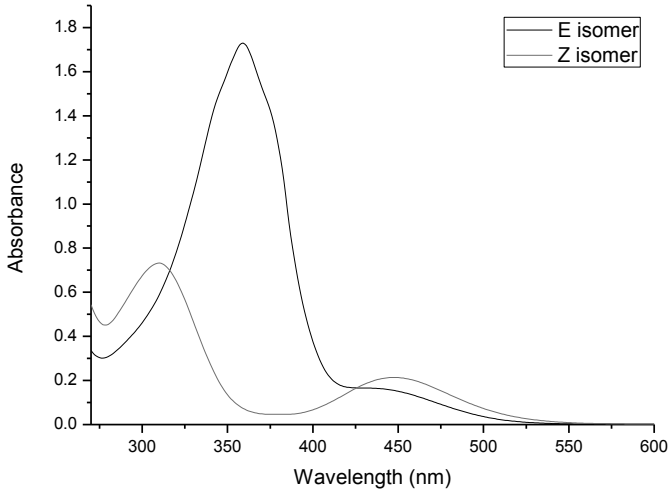

Figure S10. UV-Vis spectra of **5**: *E* isomer in black, *Z* isomer in red; irradiation with 365 nm and 440 nm, respectively, in DMSO at 293 K.

(*Z*)-*p*-[*p'*-(Propargyloxy)]phenylazophenyl β-D-glucopyranoside (6):

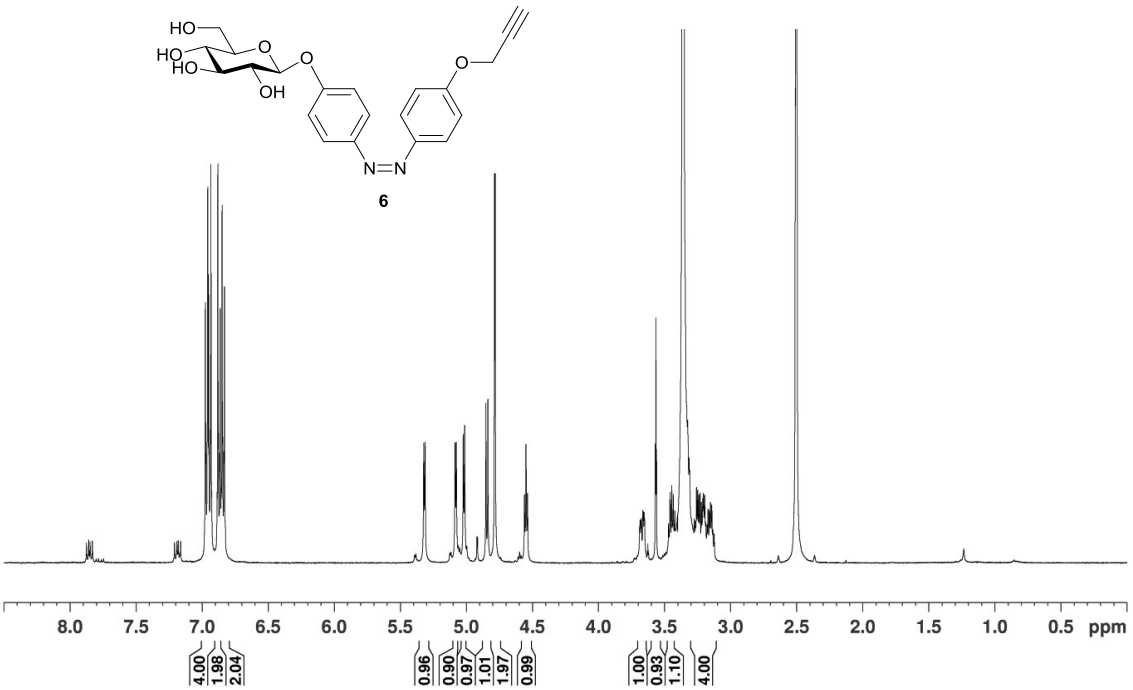

Figure S11. ^{1}H NMR spectrum of **6** (500 MHz, DMSO-d_6, 300 K).

^{1}H NMR (500 MHz, DMSO-d_6, 300 K): δ=6.98-6.93 (m, 4H, Ar-H$_{ortho}$, Ar-H$_{ortho'}$), 6.89-6.86 (m, 2H, Ar-H$_{meta'}$), 6.86-6.83 (m, 2H, Ar-H$_{meta}$), 5.32 (d, $^{3}J_{2,OH}$=5.0 Hz, 1H, OH$_{C-2}$), 5.08 (d, $^{3}J_{3,OH}$=4.8 Hz, 1H, OH$_{C-3}$), 5.02 (d, $^{3}J_{4,OH}$=5.3 Hz, 1H, OH$_{C-4}$), 4.85 (d, $^{3}J_{1,2}$=7.6 Hz, 1H, H-1), 4.78 (d, $^{4}J_{OCH2,C≡CH}$=2.4 Hz, 2H, OCH$_2$),4.55 (t~dd, $^{3}J_{6,OH}$=5.7 Hz, $^{3}J_{6',OH}$=5.7 Hz, 1H, OH$_{C-6}$), 3.69-3.65 (m, 1H, H-6), 6.57 (t, $^{4}J_{OCH2,C≡CH}$=2.4 Hz, 1H, C≡CH), 3.47-3.40 (m, 1H, H-6'), 3.30-3.12 (m, 4H, H-2, H-3, H-4, H-5) ppm.

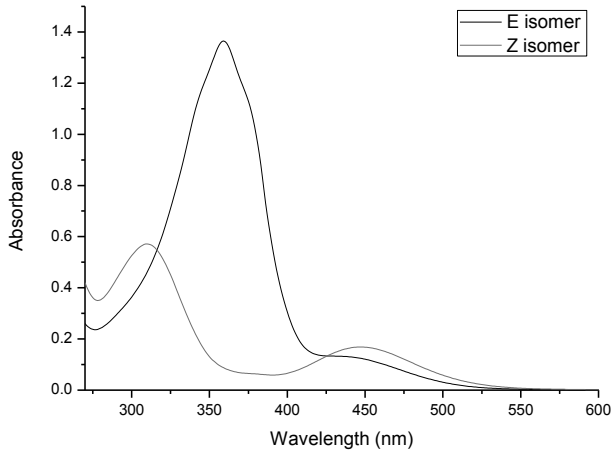

Figure S12. UV-Vis spectra of **6**: *E* isomer in black, *Z* isomer in red; irradiation with 365 nm and 440 nm, respectively, in DMSO at 293 K.

Table S1. Characterization of the *E* and *Z* isomer of the azobenzene derivatives **5** and **6**.

Azobenzene glycoconjugate	H-1 [ppm]	*E*/*Z* (PSS)[a]	λ_{max} [nm]	half-life, $\tau_{1/2}$ [h]
5	5.51 (*E*) 5.35 (*Z*)	1:99	359 (*E*) 310, 448 (*Z*)	30.9
6	5.01 (*E*) 4.85 (*Z*)	9:91	359 (*E*) 310, 447 (*Z*)	44.3

[a] According to the integration ratio of aromatic proton signals in the ^{1}H NMR spectra.

5. Required alkyne concentration for saturation

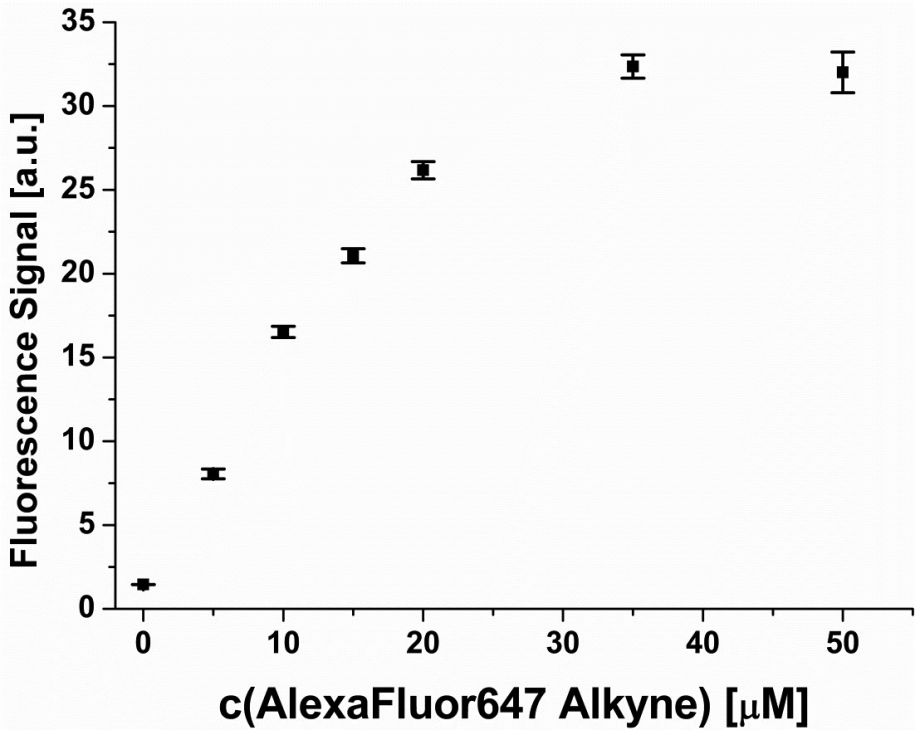

Figure S13. Required alkyne concentration for saturation. HMEC-1 were cultivated in presence of 50 µM Ac_4ManNAz for two days as described. Instead of an azobenzene derivate, a fluorescent alkyne was coupled at various concentrations to the incorporated azido groups under identical conditions. The membrane fluorescence was determined. It can be clearly seen that at 35 µM a plateau is reached. Hence, the concentration of 200 µM azobenzene derivate that we used in our experiment ensures that all available azido groups are tagged.

6. Experimental set up for bacterial adhesion experiments

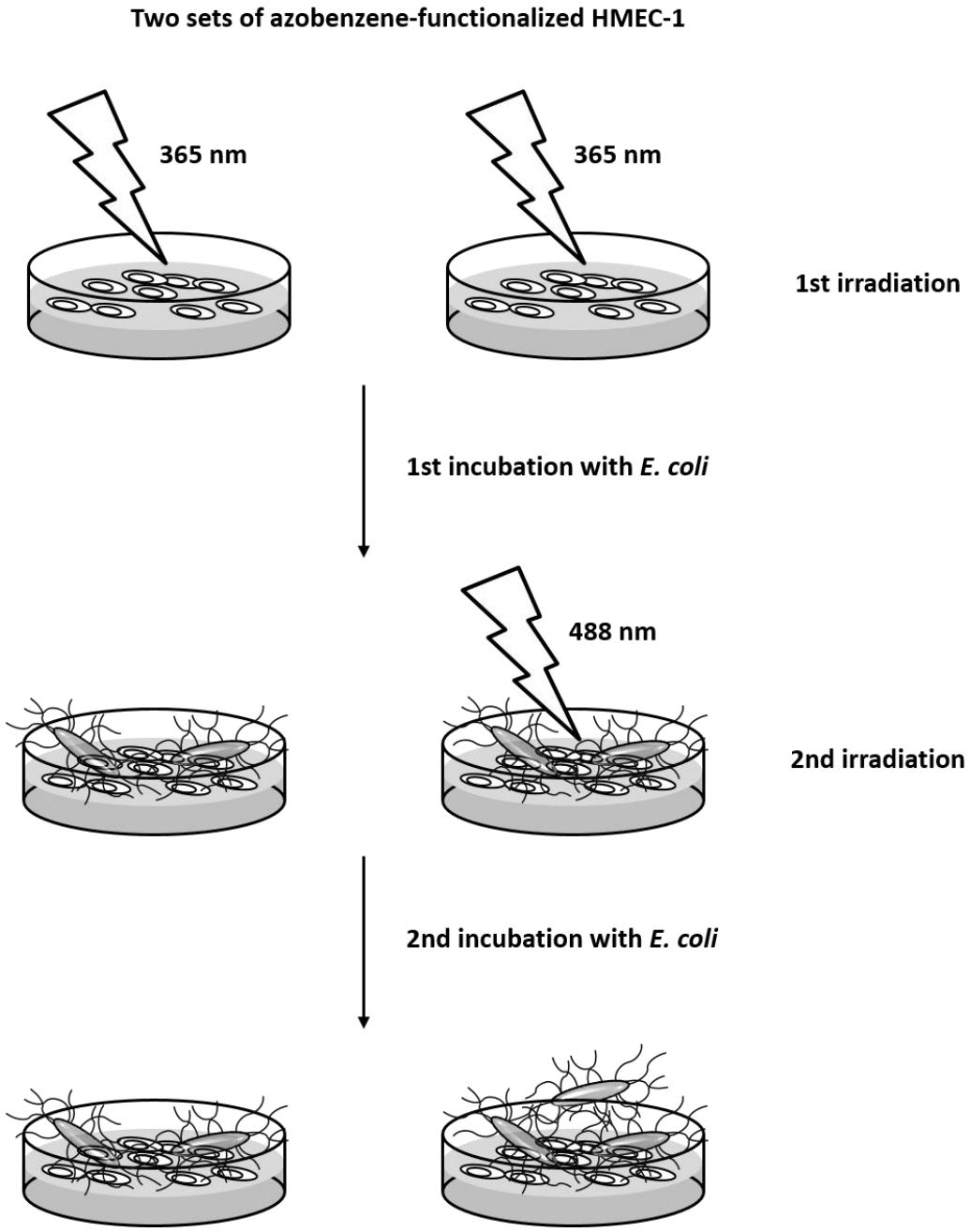

Figure S14. Experimental procedure for bacterial adhesion experiments. Two sets of azobenzene-functionalised HMEC-1 were first irradiated with UV light (365 nm) and then incubated with GFP fluorescent *E. coli* (PKL1162).[2] The number of adhered bacteria was counted employing high-resolution live-cell fluorescence microscopy. In the next step, only one set of cells was irradiated with green light (488 nm), whereas the other set of cells remained untreated. Afterwards, both sets of cells were again incubated with GFP-fluorescent *E. coli* (2^{nd} incubation) and adhesion was again quantified.

6. Microscopic pictures of fluorescent *E. coli* bacteria

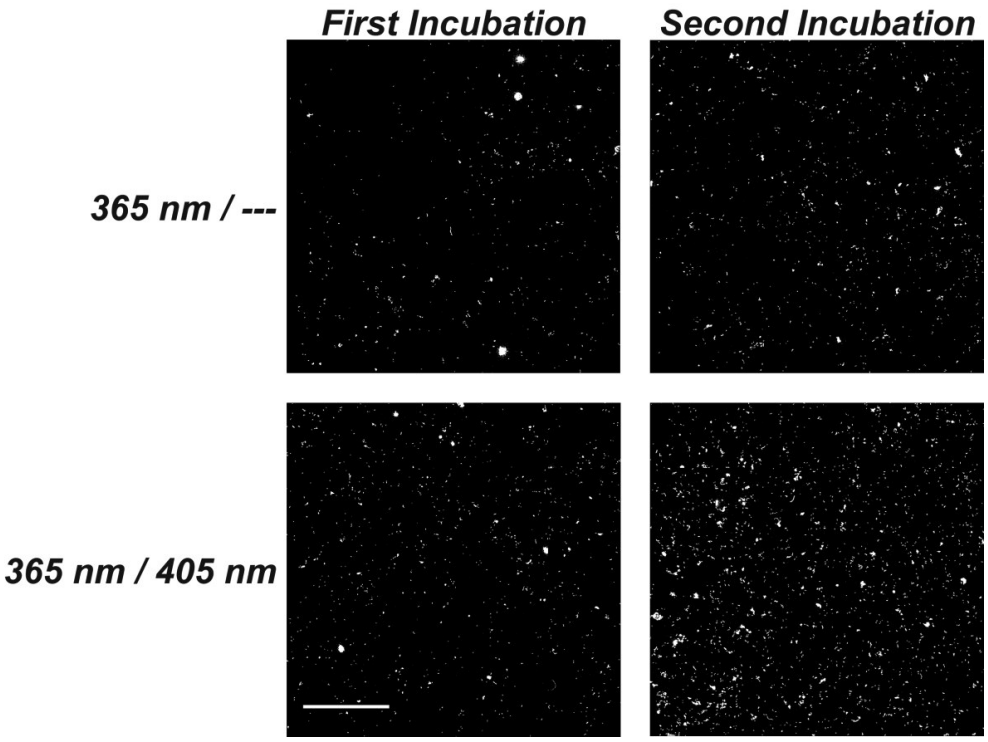

Figure S15. Adhesion of *E. coli* to *Z* and *E*-configured 5. Two sets of HMEC bearing sialic acid cell surface glycoconjugates, modified with *Z*-azobenzene mannoside **5**, were incubated with bacteria (after irradiation with light of 365) (left column). Next, one set of HMEC was irradiated with light of 405 nm to effect *Z*→*E* isomerisation of azobenzene mannoside. Then, both sets of HMEC were incubated again with bacteria. By high-resolution fluorescence microscopy it can be seen that the number of adhered bacteria increases strongly for HMEC in the *E*-state (bottom right), whereas it does not change significantly when HMEC were not irradiated with 405 nm light (leaving **5** in the *Z*-state) (top right). Scale bar = 250 µm.

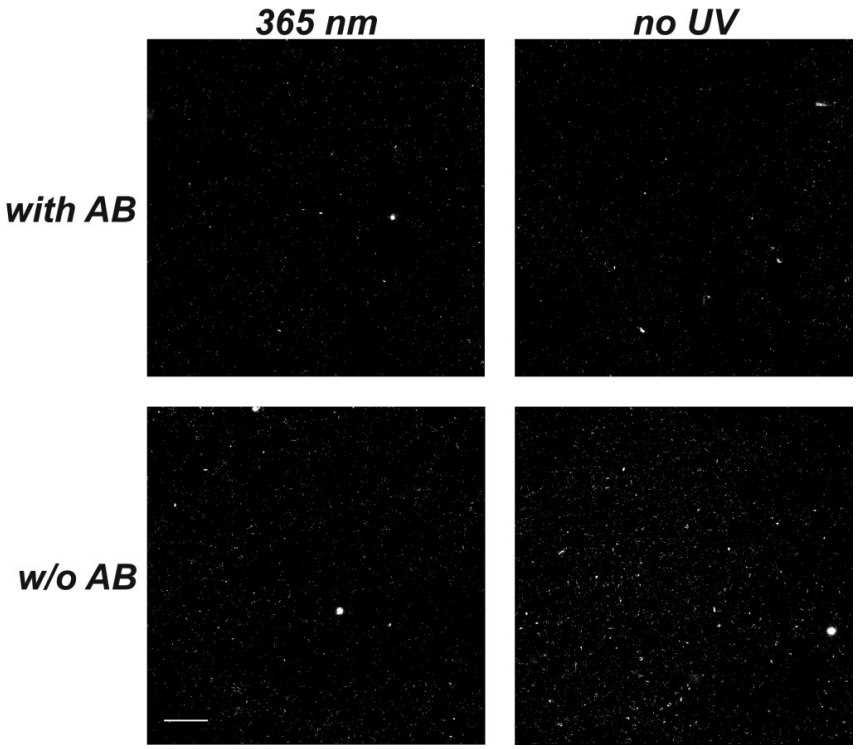

Figure S16. Adhesion of *E. coli* to *Z* and *E*-configured 7. HMEC were modified at their sialic acid cell surface glycoconjugates with either **7**, or remained untreated as control. Next, one set of cells was irradiated with 365 nm light in order to switch the azobenzene residues (AB) to the *Z*-state. The other set was not irradiated. After incubation with bacteria, fluorescence images were obtained. It can be clearly seen that the presence of **7** in both *Z*- and *E*-configuration reduced adhesion of bacteria. Scale bar = 250 µm.

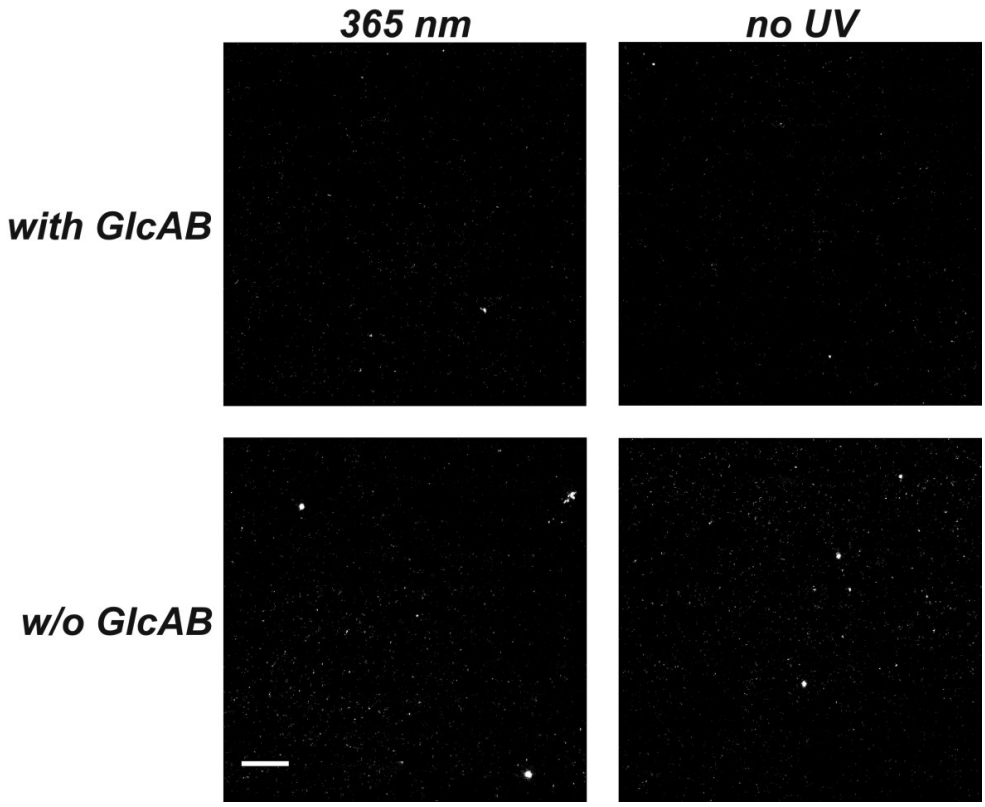

Figure S17. Adhesion of *E. coli* to *Z* and *E*-configured 6. HMEC were modified at sialic acids with **6** or remained untreated as control. Next, one set of cells was irradiated with 365 nm light in order to switch the azobenzene glucosides to the Z-state. The other set was not irradiated. After incubation with bacteria, fluorescence images were obtained. As for **7**, adhesion of bacteria was decreased. Therefore, the glucosyl moiety in **6** cannot serve as specific ligand. Also, unspecific interactions are not increased. Scale bar = 250 μm.

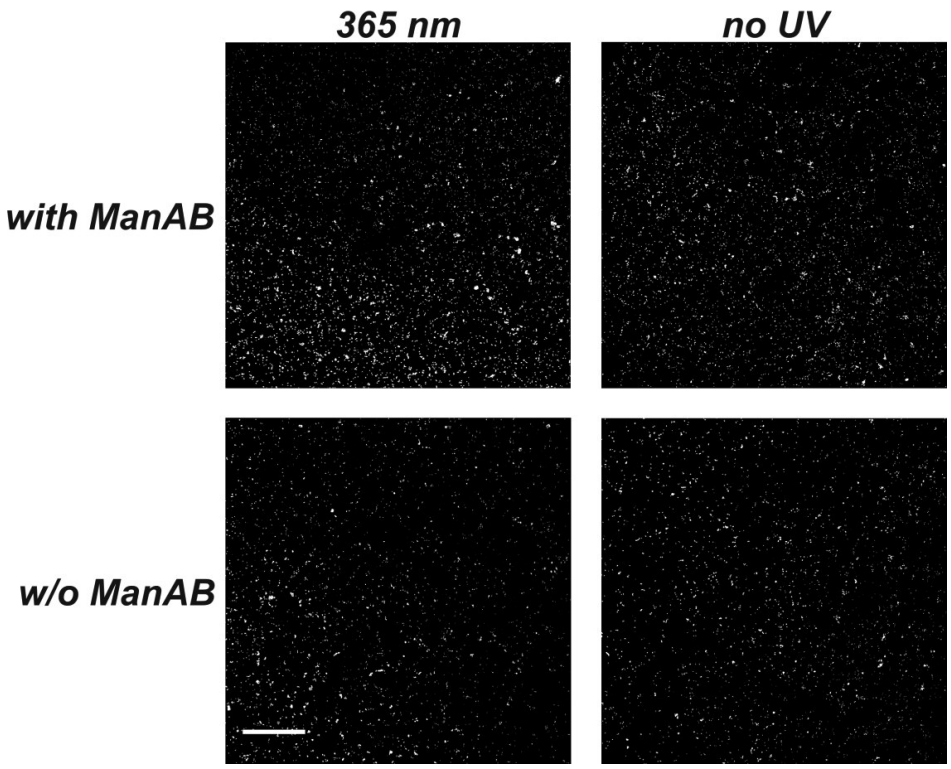

Figure S18. Adhesion of *E. coli* to *Z* and *E*-configured 5 linked to mucin-type proteins. HMEC were modified with **5** at mucin-type cell surface glycoproteins or remained untreated as control. In comparison to labelling of sialic acid glycoconjugates (cf. Fig. S15), this leads to attachment of **5** deeper within the glycan tree. Next, one set of HMEC was irradiated with 365 nm light in order to effect *E*→*Z* isomerisation of azobenzene mannosides. The other set was not irradiated. After incubation with bacteria, fluorescence images were obtained. It can be seen that the additional mannosyl residues increased adhesion in comparison to cells not treated with **5**, however, **E**/*Z* switching had no effect. This is reasonable since in this case, the change in orientation upon switching is small compared to the distance between conjugated azobenzene mannoside units and incoming. Scale bar = 250 µm.

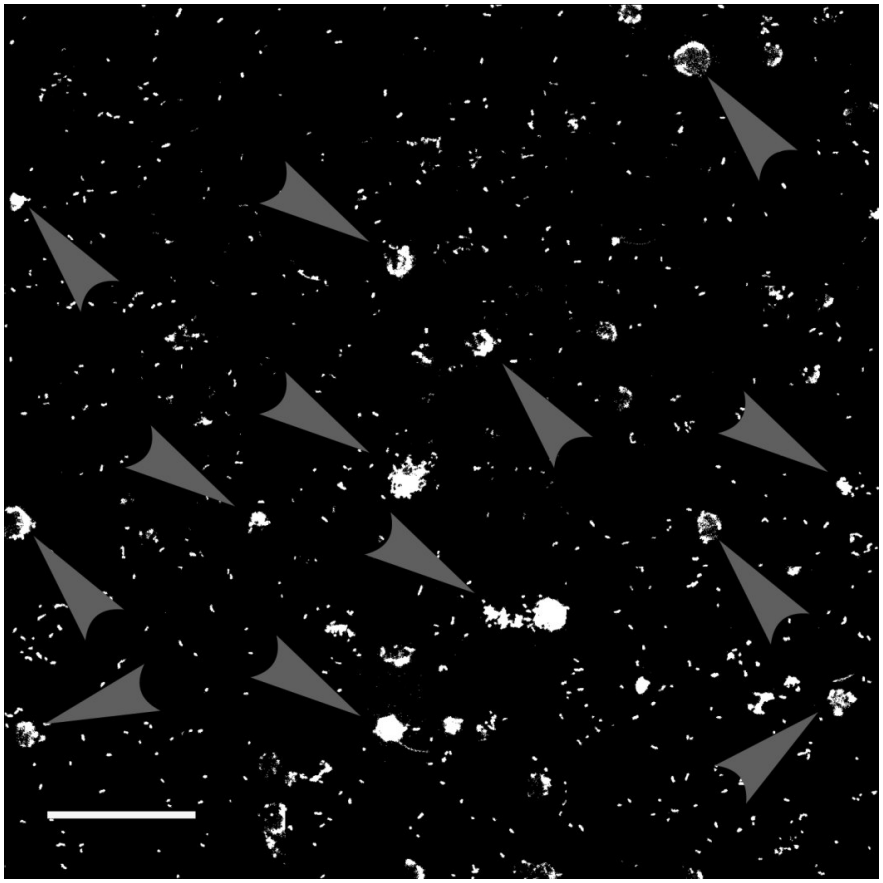

Figure S19. Formation of clumps of *E. coli* under flow conditions. With increasing time of flow, bacteria more and more adhere to already adhered bacteria and not to HMEC-1, forming clumps (some of them indicated by red arrow heads). Scale bar = 100 µm.

8. Literature

[1] V. Chandrasekaran, E. Johannes, H. Kobarg, F. D. Sönnichsen and T. K. Lindhorst, *ChemistryOpen*, 2014, **3**, 99-108.
[2] M. Hartmann, A. K. Horst, P. Klemm and T. K. Lindhorst, *Chem. Commun.*, 2010, **46**, 330-332.
[3] G. R. Gustafson, C. M. Baldino, M.-M. E. O'Donnell, A. Sheldon, R. J. Tarsa, C. J. Verni and D. L. Coffen, *Tetrahedron*, 1998, **54**, 4051-4065.

8.4 Supporting Information on Chapter 6

8.4.1 Supporting Information for the Manuscript *Synthesis of an orthogonal* trifunctional *carbohydrate scaffold for the preparation of azobenzene heteroglycoclusters*

Supporting Information

for

Synthesis of an orthogonal trifunctional carbohydrate scaffold for the preparation of azobenzene heteroglycoclusters

A. Müller, T. K. Lindhorst

Gerneral methods and Materials

All commercially available starting materials and reagents were purchased from either Alfa Aesar, Sigma Aldrich, Merck KGaA, Acros Organics or Thermo Fisher Scientific, respectively, and used without further purification. Moisture-sensitive reactions were carried out in dry glassware and under a positive pressure of nitrogen. Analytical thin layer chromatography (TLC) was performed on silica gel plates (GF 254, Merck). Visualization was achieved by UV light and/or with 10% sulfuric acid in ethanol followed by heat treatment at ~180 °C. Flash chromatography was performed on silica gel 60 (Merck, 230-400 mesh, particle size 0.040-0.063 mm) by using distilled solvents. Dry 1,4-dioxane and *N*,*N*-dimethylformamide over molecular sieves was purchased from Acros Organics and used without further purification. Melting points (mp) were determined on a Büchi M-56 apparatus. Optical rotations were measured with a Perkin-Elmer 241 polarimeter (sodium D-line: 589 nm, length of cell: 1 dm) in the solvents indicated. Proton (^{1}H) nuclear magnetic resonance spectra and carbon (^{13}C) nuclear magnetic resonance spectra were recorded on a Bruker DRX-500 and AV-600 spectrometer. Chemical shifts are referenced to the residual proton of the NMR solvent. Data are presented as follows: chemical shift, multiplicity (s=singlet, d=doublet, t=triplet, q=quartet, m=multiplet, and br=broad signal), coupling constant in hertz (Hz) and, integration. Full assignment of the peaks was achieved with the aid of 2D NMR techniques (^{1}H/^{1}H COSY and ^{1}H/^{13}C HSQC. All NMR spectra of the *E*-isomers of the azobenzene derivatives were recorded after they were kept for 16 h in the dark at 40 °C. Infrared (IR) spectra were measured with a Perkin Elmer FT-IR Paragon 1000 (ATR) spectrometer and were reported in cm^{-1}. ESI mass spectra were recorded on a LCQ Classic from Thermo Finnigan. UV-vis absorption spectra were performed on Perkin-Elmer Lambda-241 at a temperature of 20 °C ± 1 °C. For irradiation experiments with 365 nm an apparatus with 10 LEDs (Nichia NCSU276A U365) with a total power of 7500 W was used with 50 % (3750 W). For irradiation with 440 nm a similar apparatus with 10 LEDs (10 x Roithner VL440) with total power of 4500 W was used with 50 % (2250 W). Both apparatus were built from Sahlmann Photochemical Solutions. Fluorescence read out was accomplished with an Infinite® 200 PRO multimode reader from Tecan.

Synthesis of glycoconjugates

***N*-(Benzyloxycarbonyl)aminoethyl 3-*O*-(3-phthalimidopropyl-6-azido-6-deoxy-α-D-mannopyranoside (1):** To an ice-cold suspension of triphenylphosphin (1.25 g, 4.75 mmol) and sodium azide (702 mg, 10.8 mmol) in dry dimethylformamide (4 mL), a solution of tetrabromomethane (1.58 g, 4.75 mmol) in dry dimethylformamide (4 mL) was added at 0 °C. The reaction mixture was stirred for 15 min at 0 °C. Then a solution of the mannoside **5** (586 mg, 1.08 mmol) in dry dimethylformamide (4 mL) was added dropwise and the reaction mixture was stirred for 16 h at room temperature. Afterward methanol (25 mL) was added and it was again stirred for 1 h at room temperature. Then the solvent was evaporated and purification of the crude product by column chromatography (dichloromethane/ethyl acetate, 3:1→2:1→1:1) gave **1** as colourless foam (537 mg, 943 µmol, 87%). R_f = 0.17 (cyclohexane/ethyl acetate, 1:1); $[\alpha]_D^{23}$ = +15.0 (c = 0.7 in methanol); ^{1}H NMR (600 MHz, MeOH-d_4, 300 K): δ = 7.84-7.83 (m, 2H, Ar-H$_{Phth}$), 7.79-7.77 (m, 2H, Ar-H$_{Phth}$), 7.34-7.26 (m, 5H, Ar-H$_{Cbz}$), 5.07 (s, 2H, PhC*H*$_2$O), 4.80 (s~d, 1H, H-1), 4.03-4.00 (m, 1H, H-2), 3.86-3.77 (m, 3H, PhthNC*H*$_2$, CH*H'*CH$_2$NHCbz), 3.72-3.64 (m, 3H, H-4, H-5, PhthNCH$_2$CH$_2$CH*H'*), 3.55-3.40 (m, 5H, C*H*H'CH$_2$NHCbz, PhthNCH$_2$CH$_2$C*H*H', H-3, H-6, H-6'), 3.36-3.33 (m, 2H, C*H*$_2$NHCbz), 1.98-1.96 (m, 2H, PhthNCH$_2$C*H*$_2$CH$_2$) ppm; ^{13}C NMR (151 MHz, MeOH-d_4, 300 K): δ = 170.2 (C=O), 159.0 (OCONH), 138.4 (C-Ar$_{Cbz}$), 135.4 (C-Ar$_{Phth}$), 133.4 (C-Ar$_{Phth}$), 129.5 (C-Ar$_{Cbz}$), 129.0 (C-Ar$_{Cbz}$), 128.8 (C-Ar$_{Cbz}$), 124.1 (C-Ar$_{Phth}$), 101.5 (C-1), 80.8 (C-3), 73.9 (C-5), 69.8 (C-2), 68.7 (C-4), 67.9 (PhthNCH$_2$CH$_2$*C*H$_2$), 67.7 (*C*H$_2$CH$_2$NHCbz), 67.5 (Ph*C*H$_2$O), 52.9 (C-6), 41.7 (*C*H$_2$NHCbz), 36.1 (PhthN*C*H$_2$), 30.1 (PhthNCH$_2$*C*H$_2$CH$_2$) ppm; IR (ATR): $\tilde{\nu}$ = 2924, 2099, 1698, 1397, 1252, 1041, 720 cm^{-1}; ESI-MS: m/z calcd for $C_{27}H_{31}N_5O_9$: 592.2 $[M+Na]^+$; found 592.2.

***N*-(Benzyloxycarbonyl)aminoethyl 3-*O*-(3-phthalimidopropyl)α-D-mannopyranoside (5)**[1]: To a solution of the benzyloxycarbonyl protected mannoside **4**[2] (3.29 g, 9.19 mmol) in dry methanol (90 mL), dibutyltin oxide (2.40 g, 9.65 mmol) was added and refluxed for 2 h. Then the solvent was evaporated and the crude product resolved in dry dimethylformamide (90 mL). *N*-(3-bromopropyl)phthalimide (9.12 g, 34.0 mmol) and caesium fluoride (1.40 g, 9.19 mmol) were added and the reaction mixture was stirred for 3 d at room temperature. Afterwards the solvent was evaporated and purification of the crude product by column chromatography (dichloromethane/ethyl acetate/methanol, 10:5:1→5:5:1) gave **5** as colourless foam (1.87 g, 3.44 mmol, 37%). R_f = 0.32 (dichloromethane/ethyl acetate/methanol, 5:5:1); $[\alpha]_D^{23}$ = +32.7 (c = 0.4 in dichloromethane); ^{1}H NMR (600 MHz, DMSO-d_6, 298 K): δ = 7.87-7.82 (m, 4H, Ar-H$_{Phth}$), 7.37-7.29 (m, 6H, NH, Ar-H$_{Cbz}$), 5.02 (s, 2H, PhC*H*$_2$O), 4.73 (d, ^3J = 5.7 Hz, 1H, OH), 4.65 (s~d, 1H, H-1), 4.61 (d, ^3J = 4.7 Hz, 1H, OH), 4.46 (t, ^3J = 6.0 Hz, 1H, OH), 3.82-3.80 (m, 1H, H-2), 3.72-3.62 (m, 3H, PhthNC*H*$_2$, H-6), 3.61-3.56 (m, 2H, C*H*$_2$CH$_2$NHCbz), 3.51-3.48 (m, 1H, H-4), 3.47-3.40 (m, 3H, PhthNCH$_2$CH$_2$C*H*$_2$, H-6'), 3.38-3.35 (m, 1H, H-5), 3.27 (dd, $^3J_{2,3}$ = 3.0 Hz, $^3J_{3,4}$ = 9.2 Hz, 1H, H-3), 3.24-3.14 (m, 2H, C*H*$_2$NHCbz), 1.85 (p, $^3J_{OCH_2CH_2CH_2N,OCH_2CH_2CH_2CH_2N}$=6.7 Hz, $^3J_{OCH_2CH_2CH_2N,OCH_2CH_2CH_2CH_2N}$=6.7 Hz, 2H, PhthNCH$_2$C*H*$_2CH_2$) ppm; ^{13}C NMR (150 MHz, DMSO-d_6, 298 K): δ = 168.0 (C=O), 156.2 (OCONH), 137.2 (C-Ar$_{Cbz}$), 134.3 (C-Ar$_{Phth}$), 131.7 (C-Ar$_{Phth}$), 128.3 (C-Ar$_{Cbz}$), 127.7 (C-Ar$_{Cbz}$),

123.0 (C-Ar$_{Phth}$), 99.9 (C-1), 79.6 (C-3), 74.0 (C-5), 66.8 (C-2), 66.4 (*C*H$_2$CH$_2$NHCbz), 65.7 (C-4), 65.5 (PhthNCH$_2$CH$_2$*C*H$_2$), 65.2 (Ph*C*H$_2$O), 61.1 (C-6), 40.1 (*C*H$_2$NHCbz), 35.1 (PhthN*C*H$_2$), 28.7 (PhthNCH$_2$*C*H$_2$CH$_2$) ppm; IR (ATR): $\tilde{\nu}$ = 3386, 2924, 1770, 1699, 1397, 1371, 1259, 1113, 1042, 721 cm^{-1}; ESI-MS: m/z calcd for $C_{27}H_{32}N_2O_{10}$: 567.2 $[M+Na]^+$; found 567.5.

(*E*)-*p*-[*p*'-(*N*-*tert*-Butoxycarbonyl-aminomethyl)phenylazo]phenyl α-D-mannopyranoside (12): Crude 7[3] (51% purity, 541 mg, 1.55 mmol) and *p*-aminophenyl α-D-mannopyranoside (**9**[4], 420 mg, 1.55 mmol) were dissolved in a mixture of dimethyl sulfoxide and acetic acid (1:1, 14 mL). The reaction mixture was stirred for 16 h at room temperature. The product was precipitated by addition of water, filtered off and washed with water. Purification of the crude product by column chromatography (dichloromethane/methanol, 9:1→8:1) gave **12** as an orange solid (640 mg, 1.31 mmol, 84%). R$_f$ = 0.38 (ethyl acetate/methanol, 10:1); m.p. 137 °C; $[\alpha]_D^{23}$ = +114.6 (c = 0.4 in methanol); ^{1}H NMR (600 MHz, MeOH-d_4, 300 K): δ = 7.90-7.83 (m, 4H, Ar-H$_{ortho}$, Ar H$_{ortho'}$), 7.44-7.42 (m, 2H, Ar-H$_{meta'}$), 7.30-7.27 (m, 2H, Ar H$_{meta)}$, 5.60 (d, $^3J_{1,2}$ = 1.8 Hz, 1H, H-1), 4.31 (s, 2H, C*H*$_2$NHBoc), 4.04 (dd, $^3J_{1,2}$ = 1.8 Hz, $^3J_{2,3}$ = 3.3 Hz, 1H, H-2), 3.93 (dd, $^3J_{2,3}$ = 3.4 Hz, $^3J_{3,4}$ =9.5 Hz, 1H, H-3), 3.80-3.71 (m, 3H, H-4, H-6, H-6'), 3.59 (ddd, $^3J_{4,5}$ = 9.7 Hz, $^3J_{5,6}$ = 5.4 Hz, $^3J_{5,6'}$ = 2.5 Hz, 1H, H-5), 1.47 (s, 9H, C(CH$_3$)$_3$) ppm; ^{13}C NMR (126 MHz, MeOH-d_4, 300 K): δ = 160.3 (C-Ar$_{para}$), 158.6 (C=O$_{Boc}$), 153.1 (C-Ar$_{ipso'}$), 149.2 (C-Ar$_{ipso}$), 144.0 (C-Ar$_{para'}$), 128.8 (C-Ar$_{meta'}$), 125.5 (C-Ar$_{ortho}$), 123.7 (C-Ar$_{ortho'}$), 118.0 (C-Ar$_{meta}$), 100.1 (C-1), 80.3 (*C*(CH$_3$)$_3$), 75.7 (C-5), 72.4 (C-3), 71.9 (C-2), 68.3 (C-4), 62.7 (C-6), 44.8 (*C*H$_2$NHBoc), 28.8 (C(*C*H$_3$)$_3$) ppm; IR (ATR): $\tilde{\nu}$ = 3281, 2922, 1683 1600, 1581, 1470, 1363, 1339, 1228, 1098, 1017, 846 cm^{-1}; ESI-MS: m/z calcd for $C_{24}H_{31}N_3O_8$: 512.2 $[M+Na]^+$; found 512.2.

(*E*)-*p*-[*p*'-(*N*-*tert*-Butoxycarbonyl-aminomethyl)phenylazo]phenyl β-D-glucopyranoside (13): Crude 7[3] (46% purity, 345 mg, 1.04 mmol) and *p*-aminophenyl β-D-glucopyranoside (**10**[5], 284 mg, 1.04 mmol) were dissolved in a mixture of dimethyl sulfoxide and acetic acid (1:1, 10 mL). The reaction mixture was stirred for 16 h at room temperature. The product was precipitated by addition of water, filtered off and washed with water. Purification of the crude product by column chromatography (dichloromethane/methanol, 9:1) gave **13** as an orange solid (393 mg, 776 µmol, 75%). R$_f$ = 0.23 (dichloromethane/methanol, 9:1); m.p. 153 °C; $[\alpha]_D^{23}$ = -46.1 (c = 0.4 in methanol); ^{1}H NMR (600 MHz, MeOH-d_4, 300 K): δ = 7.90-7.88 (m, 2H, Ar H$_{ortho}$), 7.84-7.83 (m, 2H, Ar-H$_{ortho'}$), 7.44-7.42 (m, 2H, Ar-H$_{meta'}$), 7.25-7.23 (m, 2H, Ar H$_{meta}$), 5.03 (d, $^3J_{1,2}$ = 7.4 Hz, 1H, H-1), 4.31 (s, 2H, C*H*$_2$NHBoc), 3.93 (dd, $^2J_{6,6'}$ = 12.1 Hz, $^3J_{5,6}$ = 2.1 Hz, 1H, H-6), 3.73 (dd, $^2J_{6,6'}$ = 12.1 Hz, $^3J_{5,6'}$ = 5.7 Hz, 1H, H-6'), 3.53-3.48 (m, 3H, H-2, H-3, H-5), 3.44-3.40 (m, 1H, H-4), 1.47 (s, 9H, C(CH$_3$)$_3$) ppm; ^{13}C NMR (151 MHz, MeOH-d_4, 300 K): δ = 161.5 (C-Ar$_{para}$), 158.6 (C=O$_{Boc}$), 153.1 (C-Ar$_{ipso'}$), 149.3 (C-Ar$_{ipso}$), 144.0 (C-Ar$_{para'}$), 128.8 (C-Ar$_{meta'}$), 125.4 (C-Ar$_{ortho}$), 123.7 (C-Ar$_{ortho'}$), 118.0 (C-A$_{rmeta}$), 102.0 (C-1), 80.3 (*C*(CH$_3$)$_3$), 78.3 (C-3), 78.0 (C-5), 74.9 (C-2), 71.3 (C-4), 62.5 (C-6), 44.7 (*C*H$_2$NHBoc), 28.8 (C(*C*H$_3$)$_3$) ppm; IR (ATR): $\tilde{\nu}$ = 3353, 2917, 1682, 1601, 1499, 1392, 1365, 1235, 1162, 1078, 933, 810 cm^{-1}; ESI-MS: m/z calcd for $C_{24}H_{31}N_3O_8$: 490.2 $[M+H]^+$; found 490.1.

(*E*)-*p*-[*p*'-(*N*-*tert*-Butoxycarbonyl-aminomethyl)phenylazo]phenyl α-D-glucopyranoside (14): Crude 7[3] (48% purity, 336 mg, 976 µmol) and *p*-aminophenyl α-D-glucopyranoside (**11**[6], 264 mg, 976 µmol) were dissolved in a mixture of dimethyl sulfoxide and acetic acid (1:1, 20 mL). The reaction mixture was stirred for 16 h at room temperature. Then water was added (40 mL) and the aqueous phase extracted with ethyl acetate (3 × 50 mL). The combined organic phases were washed with saturated aq. $NaHCO_3$ solution (2 × 50 mL). The organic phase was dried over $MgSO_4$, it was filtered and the filtrate concentrated under reduced pressure. Purification of the crude product by column chromatography (dichloromethane/methanol, 9:1) gave **14** as an orange solid (374 mg, 740 µmol, 76%). R_f = 0.38 (dichloromethane/methanol, 9:1); m.p. 177 °C; $[\alpha]_D^{23}$ = +154.3 (c = 0.2 in methanol); ^{1}H NMR (500 MHz, MeOH-d_4, 300 K): δ = 7.90-7.88 (m, 2H, Ar-H$_{ortho}$), 7.84-7.83 (m, 2H, Ar-H$_{ortho'}$), 7.44-7.42 (m, 2H, Ar-H$_{meta'}$), 7.34-7.31 (m, 2H, Ar-H$_{meta}$), 5.61 (d, $^3J_{1,2}$ = 3.6 Hz, 1H, H-1), 4.31 (s, 2H, CH_2NHBoc), 3.90-3.87 (m, 1H, H-3), 3.76 (dd, $^2J_{6,6'}$ = 12.0 Hz, $^3J_{5,6}$ = 2.4 Hz, 1H, H-6), 3.71 (dd, $^2J_{6,6'}$ = 12.0 Hz, $^3J_{5,6'}$ = 5.0 Hz, 1H, H-6'), 3.65 (ddd, $^3J_{4,5}$ = 9.9 Hz, $^3J_{5,6}$ = 5.0 Hz, $^3J_{5,6'}$ = 2.4 Hz, 1H, H-5), 3.62 (dd, $^3J_{1,2}$ = 3.6 Hz, $^3J_{2,3}$ = 9.8 Hz, 1H, H-2), 3.45 (dd, $^3J_{3,4}$ = 9.2 Hz, $^3J_{4,5}$ = 9.8 Hz, 1H, H-4), 1.47 (s, 9H, C(CH_3)$_3$) ppm; ^{13}C NMR (151 MHz, MeOH-d_4, 300 K): δ = 161.0 (C-Ar$_{para}$), 158.6 (C=O$_{Boc}$), 153.1 (C-Ar$_{ipso'}$), 149.3 (C-Ar$_{ipso}$), 144.0 (C-Ar$_{para'}$), 128.8 (C-Ar$_{meta'}$), 125.4 (C-Ar$_{ortho}$), 123.7 (C-Ar$_{ortho'}$), 118.3 (C-Ar$_{meta}$), 99.2 (C-1), 80.3 (*C*(CH$_3$)$_3$), 74.9 (C-3), 74.7 (C-5), 73.2 (C-2), 71.4 (C-4), 62.4 (C-6), 44.8 (*C*H$_2$NHBoc), 28.8 (C(*C*H$_3$)$_3$) ppm; IR (ATR): $\tilde{\nu}$ = 3354, 2930, 1679, 1600, 1581, 1499, 1365, 1233, 1079, 1021, 841 cm^{-1}; ESI-MS: m/z calcd for $C_{24}H_{31}N_3O_8$: 490.2 $[M+H]^+$; found 490.2.

(*E*)-*p*-[*p*'-(Aminomethyl)phenylazo]phenyl α-D-mannopyranoside · TFA(15): To a suspension of the mannoside **12** (832 mg, 1.70 mmol) in dichloromethane (20 mL), trifluoroacetic acid (2 mL) was added. The reaction mixture was stirred for 1.5 h at room temperature. Then the solvent was evaporated and **15** was obtained as an orange solid (850 mg, 1.68 mmol, 99%). The TFA salt was used in the next step without further purification. R_f = 0.15 (ethyl acetate/methanol, 5:1); m.p. 259 °C; $[\alpha]_D^{23}$ = -4.50 (c=0.6 in methanol); ^{1}H NMR (500 MHz, MeOH-d_4, 300 K): δ = 7.95-7.91 (m, 4H, Ar-H$_{ortho}$, Ar H$_{ortho'}$), 7.64-7.61 (m, 2H, Ar-H$_{meta'}$), 7.30-7.27 (m, 2H, Ar H$_{meta}$), 5.61 (d, $^3J_{1,2}$ = 1.8 Hz, 1H, H-1), 4.21 (s, 2H, CH_2NH$_2$), 4.05 (dd, $^3J_{1,2}$ = 1.8 Hz, $^3J_{2,3}$ = 3.5 Hz, 1H, H-2), 3.92 (dd, $^3J_{2,3}$ = 3.5 Hz, $^3J_{3,4}$ = 9.5 Hz, 1H, H-3), 3.80-3.71 (m, 3H, H-4, H-6, H-6'), 3.59 (ddd, $^3J_{4,5}$ = 9.7 Hz, $^3J_{5,6}$ = 5.3 Hz, $^3J_{5,6'}$ = 2.6 Hz, 1H, H-5) ppm; ^{13}C NMR (126 MHz, MeOH-d_4, 300 K): δ = 160.7 (C-Ar$_{para}$), 154.3 (C-Ar$_{ipso'}$), 149.1 (C-Ar$_{ipso}$), 136.8 (C-Ar$_{para'}$), 130.9 (C-Ar$_{meta'}$), 125.8 (C-Ar$_{ortho}$), 124.2 (C-Ar$_{ortho'}$), 118.1 (C-Ar$_{meta}$), 100.1 (C-1), 75.7 (C-5), 72.4 (C-2), 71.8 (C-3), 68.3 (C-4), 62.6 (C-6), 44.0 (CH_2NH_2) ppm; IR (ATR): $\tilde{\nu}$ = 2929, 1663, 1494, 1233, 1188, 1000, 845 cm^{-1}; ESI-MS: m/z calcd for $C_{19}H_{23}N_3O_6$: 412.2 $[M+Na]^+$; found 412.2.

(*E*)-*p*-[*p*'-(Aminomethyl)phenylazo]phenyl β-D-glucopyranoside · TFA (16): To a suspension of the mannoside **13** (300 mg, 593 µmol) in dichloromethane (10 mL), trifluoroacetic acid (2 mL) was added. The reaction mixture was stirred for 45 min at room temperature. Then the solvent was evaporated and 16 was obtained as an orange solid (332 mg, quant.). The TFA salt was used in the next step without further purification. R_f = 0.02 (ethyl acetate/methanol, 10:1); m.p. 114 °C; $[\alpha]_D^{23}$ = -47.8 (c=0.5 in methanol); ^{1}H NMR (500 MHz, MeOH-d_4, 300 K): δ = 7.95-7.91 (m, 4H, Ar-H$_{ortho}$, Ar H$_{ortho'}$), 7.63-7.61 (m, 2H, Ar-H$_{meta'}$), 7.27-7.24 (m, 2H, Ar H$_{meta}$), 5.05-5.04 (m,

1H, H-1), 4.21 (s, 2H, CH_2NH$_2$), 3.93 (dd, $^2J_{6,6'}$ = 12.1 Hz, $^3J_{5,6}$ = 2.3 Hz, 1H, H-6), 3.73 (dd, $^2J_{6,6'}$ = 12.1 Hz, $^3J_{5,6'}$ = 5.7 Hz, 1H, H-6'), 3.53-3.48 (m, 3H, H-2, H-3, H-5), 3.44-3.40 (m, 1H, H-4) ppm; ^{13}C NMR (126 MHz, MeOH-d_4, 300 K): δ = 161.9 (C-Ar$_{para}$), 154.3 (C-Ar$_{ipso'}$), 149.2 (C-Ar$_{ipso}$), 136.7 (C-Ar$_{para'}$), 130.9 (C-Ar$_{meta'}$), 125.7 (C-Ar$_{ortho}$), 124.2 (C-Ar$_{ortho'}$), 118.0 (C-Ar$_{meta}$), 101.9 (C-1), 78.3 (C-3), 78.0 (C-5), 74.8 (C-2), 71.3 (C-4), 62.5 (C-6), 43.9 (CH_2NH_2) ppm; IR (ATR): $\tilde{\nu}$ = 3090, 2925, 2361, 1667, 1602 1497, 1378, 1190, 1138, 1037, 844 cm^{-1}; ESI-MS: m/z calcd for $C_{19}H_{23}N_3O_6$: 390.2 $[M+H]^+$; found 389.9.

(*E*)-*p*-[*p'*-(Aminomethyl)phenylazo]phenyl α-D-glucopyranoside · TFA (17): To a suspension of the mannoside **14** (345 mg, 682 µmol) in dichloromethane (10 mL), trifluoroacetic acid (1 mL) was added. The reaction mixture was stirred for 45 min at room temperature. Then the solvent was evaporated and **17** was obtained as an orange solid (360 mg, quant.). The TFA salt was used in the next step without further purification. R_f = 0.02 (ethyl acetate/methanol, 10:1); m.p. 102.1 °C; $[\alpha]_D^{23}$ = +129.6 (c=0.6 in methanol); ^{1}H NMR (600 MHz, MeOH-d_4, 300 K): δ = 7.95-7.92 (m, 4H, Ar-H$_{ortho}$, Ar H$_{ortho'}$), 7.63-7.62 (m, 2H, Ar-H$_{meta'}$), 7.35-7.34 (m, 2H, Ar H$_{meta}$), 5.63 (d, $^3J_{1,2}$ = 3.5 Hz, 1H, H-1), 4.21 (s, 2H, CH_2NH$_2$), 3.89 (t~dd, $^3J_{2,3}$ = 9.3 Hz, $^3J_{3,4}$ = 9.3 Hz, 1H, H-3), 3.76 (dd, $^2J_{6,6'}$ = 12.0 Hz, $^3J_{5,6}$ = 2.4 Hz, 1H, H-6), 3.71 (dd, $^2J_{6,6'}$ = 12.0 Hz, $^3J_{5,6'}$ = 5.0 Hz, 1H, H-6'), 3.65-3.62 (m, 2H, H-2, H-5), 3.46 (t~dd, $^3J_{3,4}$ = 9.3 Hz, $^3J_{4,5}$ = 9.3 Hz, 1H, H-4) ppm; ^{13}C NMR (151 MHz, MeOH-d_4, 300 K): δ = 161.4 (C-Ar$_{para}$), 154.3 (C-Ar$_{ipso'}$), 149.1 (C-Ar$_{ipso}$), 136.7 (C-Ar$_{para'}$), 130.9 (C-Ar$_{meta'}$), 125.7 (C-Ar$_{ortho}$), 124.2 (C-Ar$_{ortho'}$), 118.3 (C-Ar$_{meta}$), 99.1 (C-1), 74.9 (C-3), 74.8 (C-5), 73.2 (C-2), 71.4 (C-4), 62.3 (C-6), 44.0 (CH_2NH_2) ppm; IR (ATR): $\tilde{\nu}$ = 3286, 2926, 2365, 1672, 1598, 1498, 1421, 1380, 1201, 1131, 1002, 839 cm^{-1}; ESI-MS: m/z calcd for $C_{19}H_{23}N_3O_6$: 412.2 $[M+Na]^+$; found 412.2.

(*E*)-*p*-[*p'*-(Azidomethyl)phenylazo]phenyl 2,3,4,6-tetra-*O*-acetyl-α-D-mannopyranoside (18): To a suspension of the amine **15** (310 mg, 597 µmol), potassium carbonate (165 mg, 1.19 mmol) and $CuSO_4 \cdot 5\ H_2O$ (1.50 mg, 5.97 µmol) in methanol (4 mL), imidazole-1-sulfonyl azide hydrochloride[7] (200 mg, 955 µmol) was added. The reaction mixture was stirred for 4 h at room temperature. Then the solvent was evaporated and the crude product was dissolved in pyridine (4 mL). Acetic anhydride (400 µL, 4.18 mmol) was added and the reaction mixture was stirred for 16 h at room temperature. Then water (10 mL) was added and the aqueous phase extracted with dichloromethane (3 × 10 mL). The combined organic phases were washed with hydrochloric acid (1M, 2 × 10 mL) and a saturated aq. NaCl solution (10 mL). The organic phase was dried over $MgSO_4$, it was filtered and the filtrate concentrated under reduced pressure. Purification of the crude product by column chromatography (cyclohexane/ethyl acetate, 2:1) gave **18** as an orange solid (244 mg, 418 µmol, 70% over two steps). R_f = 0.31 (cyclohexane/ethyl acetate, 2:1); m.p. 50.4 °C; $[\alpha]_D^{23}$ = +63.4 (c=0.8 in dichloromethane); ^{1}H NMR (500 MHz, $CDCl_3$, 300 K): δ = 7.94-7.90 (m, 4H, Ar-H$_{ortho}$, Ar H$_{ortho'}$), 7.47-7.45 (m, 2H, Ar-H$_{meta'}$), 7.25-7.22 (m, 2H, Ar-H$_{meta}$), 5.63 (d, $^3J_{1,2}$ = 1.8 Hz, 1H, H-1), 5.58 (dd, $^3J_{2,3}$ = 3.5 Hz, $^3J_{3,4}$ = 10.0 Hz, 1H, H-3), 5.48 (dd, $^3J_{1,2}$ = 1.8 Hz, $^3J_{2,3}$ = 3.5 Hz, 1H, H-2), 5.39 (t~dd, $^3J_{3,4}$ = 10.0 Hz, $^3J_{4,5}$ = 10.0 Hz, 1H, H-4), 4.43 (s, 2H, CH_2N$_3$), 4.32-4.28 (m, 1H, H-6), 4.13-4.08 (m, 2H, H-5, H-6'), 2.22, 2.06, 2.05, 2.03 (each s, each 3H, 4 $COCH_3$) ppm; ^{13}C NMR (126 MHz, $CDCl_3$, 300 K): δ = 170.6, 170.1, 170.1, 169.8 (4 $COCH_3$), 157.9 (C-Ar$_{para}$), 152.5 (C-Ar$_{ipso'}$), 148.5 (C-Ar$_{ipso}$), 138.1 (C-Ar$_{para'}$), 129.0 (C-Ar$_{meta'}$),

124.8 (C-Ar$_{ortho}$), 123.3 (C-Ar$_{ortho'}$), 116.9 (C-Ar$_{meta}$), 95.8 (C-1), 69.6 (C-5), 69.4 (C-2), 68.9 (C-3), 66.0 (C-4), 62.2 (C-6), 54.6 (CH_2N_3), 21.0, 20.8 (2 $COCH_3$) ppm; IR (ATR): $\tilde{\nu}$ = 2361, 2099, 1743, 1497, 1367, 1209, 1125, 1030, 844 cm^{-1}; ESI-MS: m/z calcd for $C_{27}H_{29}N_5O_10$: 606.2 $[M+Na]^+$; found 606.0.

(*E*)-*p*-[*p*'-(Azidomethyl)phenylazo]phenyl 2,3,4,6-tetra-*O*-acetyl-β-D-glucopyranoside (19): To a suspension of the amine **16** (296 mg, 570 µmol), potassium carbonate (157 mg, 1.14 mmol) and $CuSO_4 \cdot 5\ H_2O$ (1.40 mg, 5.70 µmol) in methanol (4 mL), imidazole-1-sulfonyl azide hydrochloride[7] (191 mg, 912 µmol) was added. The reaction mixture was stirred for 16 h at room temperature. Then the solvent was evaporated and the crude product was dissolved in pyridine (4 mL). Acetic anhydride (800 µL, 7.98 mmol) was added and the reaction mixture was stirred for 16 h at room temperature. Then water (10 mL) was added and the aqueous phase extracted with dichloromethane (3 × 10 mL). The combined organic phases were washed with hydrochloric acid (1M, 2 × 10 mL) and a saturated aq. NaCl solution (10 mL). The organic phase was dried over $MgSO_4$, it was filtered and the filtrate concentrated under reduced pressure. Purification of the crude product by column chromatography (cyclohexane/ethyl acetate, 2:1) gave **19** as an orange solid (229 mg, 393 µmol, 69% over two steps). R_f = 0.31 (cyclohexane/ethyl acetate, 2:1); m.p. 169 °C; $[\alpha]_D^{23}$ = -4.20 (c=0.4 in dichloromethane); ^{1}H NMR (500 MHz, $CDCl_3$, 300 K): δ = 7.92-7.90 (m, 4H, Ar-H$_{ortho}$, Ar H$_{ortho'}$), 7.47-7.45 (m, 2H, Ar-H$_{meta'}$), 7.14-7.10 (m, 2H, Ar H$_{meta}$), 5.34-5.30 (m, 2H, H-2, H-3), 5.25-5.17 (m, 2H, H-1, H-4), 4.43 (s, 2H, CH_2N_3), 4.31 (dd, $^2J_{6,6'}$ = 12.3 Hz, $^3J_{5,6}$ = 5.5 Hz, 1H, H-6), 4.20 (dd, $^2J_{6,6'}$ = 12.3 Hz, $^3J_{5,6'}$ = 2.4 Hz, 1H, H-6'), 3.93 (ddd, $^3J_{4,5}$ = 10.0 Hz, $^3J_{5,6}$ = 5.5 Hz, $^3J_{5,6'}$ = 2.4 Hz, 1H, H-5), 2.09, 2.08, 2.06, 2.05 (each s, each 3H, 4 $COCH_3$) ppm; ^{13}C NMR (126 MHz, $CDCl_3$, 300 K): δ = 170.7, 170.4, 169.5, 169.4 (4 $COCH_3$), 159.1 (C-Ar$_{para}$), 152.5 (C-Ar$_{ipso'}$), 148.7 (C-Ar$_{ipso}$), 138.2 (C-Ar$_{para'}$), 129.0 (C-Ar$_{meta'}$), 124.8 (C-Ar$_{ortho}$), 123.3 (C-Ar$_{ortho'}$), 117.2 (C-Ar$_{met}$a), 98.8 (C-1), 72.8 (C-3), 72.4 (C-5), 71.3 (C-2), 68.4 (C-4), 62.1 (C-6), 54.6 (CH_2N_3), 20.8, 20.8, 20.8, 20.7 (4 $COCH_3$) ppm; IR (ATR): $\tilde{\nu}$ = 2935, 2091, 1745, 1597, 1496, 1367, 1216, 1042, 844 cm^{-1}; ESI-MS: m/z calcd for $C_{27}H_{29}N_5O_10$: 606.2 $[M+Na]^+$; found 606.1.

(*E*)-*p*-[*p*'-(Azidomethyl)phenylazo]phenyl 2,3,4,6-tetra-*O*-acetyl-α-D-glucopyranoside (20): To a suspension of the amine **17** (354 mg, 682 µmol), potassium carbonate (189 mg, 1.36 mmol) and $CuSO_4 \cdot 5\ H_2O$ (1.70 mg, 6.82 µmol) in methanol (4.5 mL), imidazole-1-sulfonyl azide hydrochloride[7] (229 mg, 1.09 mmol) was added. The reaction mixture was stirred for 16 h at room temperature. Then the solvent was evaporated and the crude product was dissolved in pyridine (4.5 mL). Acetic anhydride (450 µL, 4.77 mmol) was added and the reaction mixture was stirred for 16 h at room temperature. Then water (11 mL) was added and the aqueous phase extracted with dichloromethane (3 × 11 mL). The combined organic phases were washed with hydrochloric acid (1M, 2 × 11 mL) and a saturated aq. NaCl solution (11 mL). The organic phase was dried over $MgSO_4$, it was filtered and the filtrate concentrated under reduced pressure. Purification of the crude product by column chromatography (cyclohexane/ethyl acetate, 2:1) gave **20** as an orange solid (315 mg, 540 µmol, 79% over two steps). R_f = 0.36 (cyclohexane/ethyl acetate, 2:1); m.p. 85.8 °C; $[\alpha]_D^{23}$ = +454.6 (c=0.6 in methanol); ^{1}H NMR (600 MHz, $CDCl_3$, 300 K): δ = 7.94-7.90 (m, 4H, Ar-H$_{ortho}$, Ar H$_{ortho'}$), 7.47-7.46 (m, 2H, Ar-H$_{meta'}$), 7.24-7.22 (m, 2H, Ar H$_{meta}$), 5.84 (d, $^3J_{1,2}$ = 3.6 Hz, 1H, H-1), 5.73 (t~dd, $^3J_{2,3}$ = 10.3 Hz, $^3J_{3,4}$ = 10.3 Hz, 1H, H-3), 5.18 (t~dd, $^3J_{3,4}$ = 10.3 Hz, $^3J_{4,5}$ = 10.3 Hz,

1H, H-4), 5.09 (dd, $^{3}J_{1,2}$ = 3.6 Hz, $^{3}J_{2,3}$ = 10.3 Hz, 1H, H-2), 4.43 (s, 2H, CH_2N_3),), 4.26 (dd, $^{2}J_{6,6'}$ = 12.4 Hz, $^{3}J_{5,6}$ = 4.6 Hz, 1H, H-6), 4.12 (ddd, $^{3}J_{4,5}$ = 10.3 Hz, $^{3}J_{5,6}$ = 4.6 Hz, $^{3}J_{5,6'}$ = 2.1 Hz, 1H, H-5), 4.07 (dd, $^{2}J_{6,6'}$ = 12.4 Hz, $^{3}J_{5,6'}$ = 2.1 Hz, 1H, H-6'), 2.09, 2.07, 2.05, 2.05 (each s, each 3H, 4 $COCH_3$) ppm; ^{13}C NMR (151 MHz, $CDCl_3$, 300 K): δ = 170.7, 170.3, 169.7 (3 $COCH_3$), 158.4 (C-Ar_{para}), 152.5 (C-$Ar_{ipso'}$), 148.5 (C-Ar_{ipso}), 138.1 (C-$Ar_{para'}$), 129.0 (C-$Ar_{meta'}$), 124.9 (C-Ar_{ortho}), 123.3 (C-$Ar_{ortho'}$), 117.0 (C-Ar_{meta}), 94.3 (C-1), 70.5 (C-2), 70.1 (C-3), 68.5 (C-5), 68.4 (C-4), 61.7 (C-6), 54.6 (CH_2N_3), 20.9, 20.8, 20.8, 20.7 (4 $COCH_3$) ppm; IR (ATR): $\tilde{\nu}$ = 3751, 3249, 2334, 2252, 2096, 1741, 1597, 1497, 1365, 1216, 1033, 843 cm^{-1}; ESI-MS: m/z calcd for $C_{27}H_{29}N_5O_{10}$: 606.2 $[M+Na]^+$; found 606.1.

(*E*)-*p*-[*p*'-(Isothiocyanatomethyl)phenylazo]phenyl 2,3,4,6-tetra-*O*-acetyl-α-D-mannopyranoside (21): To a solution of the azide **18** (233 mg, 400 µmol) in chloroform (5 mL), first carbon disulfide (1.00 mL, 16.0 mmol) and then triphenylphosphin (420 mg, 1.60 mmol) were added. The reaction mixture was stirred for 16 h at room temperature. Then the solvent was evaporated and purification of the crude product by column chromatography (cyclohexane/ethyl acetate, 3:1→2:1) gave **21** as an orange solid (225 mg, 375 µmol, 94%). R_f = 0.36 (cyclohexane/ethyl acetate, 2:1); m.p. 117 °C; $[\alpha]_D^{23}$ = +70.0 (c=0.2 in methanol); ^{1}H NMR (500 MHz, $CDCl_3$, 300 K): δ = 7.94-7.90 (m, 4H, Ar-H_{ortho}, Ar $H_{ortho'}$), 7.47-7.45 (m, 2H, Ar-$H_{meta'}$), 7.25-7.22 (m, 2H, Ar H_{meta}), 5.63 (d, $^{3}J_{1,2}$ = 1.8 Hz, 1H, H-1), 5.58 (dd, $^{3}J_{2,3}$ = 3.5 Hz, $^{3}J_{3,4}$ = 10.0 Hz, 1H, H-3), 5.48 (dd, $^{3}J_{1,2}$ = 1.8 Hz, $^{3}J_{2,3}$ = 3.5 Hz, 1H, H-2), 5.39 (t~dd, $^{3}J_{3,4}$ = 10.0 Hz, $^{3}J_{4,5}$ = 10.0 Hz, 1H, H-4), 4.80 (s, 2H, CH_2NCS), 4.32-4.28 (m, 1H, H-6), 4.12-4.08 (m, 2H, H-5, H-6'), 2.22, 2.06, 2.05, 2.04 (each s, each 3H, 4 $COCH_3$) ppm; ^{13}C NMR (126 MHz, $CDCl_3$, 300 K): δ = 170.6, 170.1, 170.1, 169.8 (4 $COCH_3$), 158.0 (C-Ar_{para}), 152.6 (C-$Ar_{ipso'}$), 148.4 (C-Ar_{ipso}), 136.8 (C-$Ar_{para'}$), 127.7 (C-$Ar_{meta'}$), 124.9 (C-Ar_{ortho}), 123.4 (C-$Ar_{ortho'}$), 116.9 (C-Ar_{meta}), 95.8 (C-1), 69.6 (C-5), 69.4 (C-2), 68.9 (C-3), 66.0 (C-4), 62.2 (C-6), 48.6 (*C*H_2NCS), 21.0, 20.8 (2 $COCH_3$) ppm; IR (ATR): $\tilde{\nu}$ = 2972, 2069, 1743, 1597 1496, 1365, 1213, 1126, 1026, 976, 851 cm-1; ESI-MS: m/z calcd for $C_{28}H_{29}N_3O_{10}S$: 622.1 $[M+Na]^+$; found 622.1.

(*E*)-*p*-[*p*'-(Isothiocyanatomethyl)phenylazo]phenyl 2,3,4,6-tetra-*O*-acetyl-β-D-glucopyranoside (22): To a solution of the azide **19** (195 mg, 334 µmol) in chloroform (4.5 mL), first carbon disulfide (810 µL, 13.4 mmol) and then triphenylphosphin (351 mg, 1.34 mmol) were added. The reaction mixture was stirred for 16 h at room temperature. Then the solvent was evaporated and purification of the crude product by column chromatography (cyclohexane/ethyl acetate, 3:1→2:1) gave **22** as an orange solid (169 mg, 282 µmol, 84%). R_f = 0.27 (cyclohexane/ethyl acetate, 2:1); m.p. 175 °C; $[\alpha]_D^{23}$ = -3.40 (c=0.5 in dichloromethane); ^{1}H NMR (500 MHz, $CDCl_3$, 300 K): δ = 7.97-7.91 (m, 4H, Ar-H_{ortho}, Ar-$H_{ortho'}$), 7.47-7.43 (m, 2H, Ar-$H_{meta'}$), 7.12-7.10 (m, 2H, Ar-H_{meta}), 5.36-5.30 (m, 2H, H-2, H-3), 5.23-5.16 (m, 2H, H-1, H-4), 4.80 (s, 2H, CH_2NCS), 4.31 (dd, $^{2}J_{6,6'}$ = 12.3 Hz, $^{3}J_{5,6}$ = 4.5 Hz, 1H, H-6), 4.20 (dd, $^{2}J_{6,6'}$ = 12.3 Hz, $^{3}J_{5,6'}$ = 2.4 Hz, 1H, H-6'), 3.93 (ddd, $^{3}J_{4,5}$ = 10.0 Hz, $^{3}J_{5,6}$ = 4.5 Hz, $^{3}J_{5,6'}$ = 2.4 Hz, 1H, H-5), 2.09, 2.08, 2.06, 2.05 (each s, each 3H, 4 $COCH_3$) ppm; ^{13}C NMR (126 MHz, $CDCl_3$, 300 K): δ = 170.7, 170.4, 169.5, 169.4 (4 $COCH_3$), 159.2 (C-Ar_{para}), 152.6 (C-$Ar_{ipso'}$), 148.6 (C-Ar_{ipso}), 136.8 (C-$Ar_{para'}$), 127.7 (C-$Ar_{meta'}$),

124.8 (C-Ar$_{ortho}$), 123.4 (C-Ar$_{ortho'}$), 117.2 (C-Ar$_{meta}$), 98.7 (C-1), 72.8 (C-3), 72.4 (C-5), 71.3 (C-2), 68.4 (C-4), 62.1 (C-6), 48.6 (*C*H$_2$NCS), 20.8, 20.8, 20.8, 20.7 (4 COCH$_3$) ppm; IR (ATR): $\tilde{\nu}$ = 2365, 2072, 1741, 1597 1499, 1366, 1218, 1034, 840 cm^{-1}; ESI-MS: m/z calcd for $C_{28}H_{29}N_3O_{10}S$: 622.1 $[M+Na]^+$; found 622.1.

(*E*)-*p*-[*p'*-(Isothiocyanatomethyl)phenylazo]phenyl 2,3,4,6-tetra-*O*-acetyl-α-D-glucopyranoside (23): To a solution of the azide **20** (259 mg, 444 µmol) in chloroform (6 mL), first carbon disulfide (1.07 mL, 17.8 mmol) and then triphenylphosphin (465 mg, 1.77 mmol) were added. The reaction mixture was stirred for 16 h at room temperature. Then the solvent was evaporated and purification of the crude product by column chromatography (cyclohexane/ethyl acetate, 3:1→2:1) gave **23** as an orange oil (225 mg, 375 µmol, 85%). R$_f$ = 0.09 (dichloromethane/methanol, 9:1); $[\alpha]_D^{23}$ = +158.7 (c=0.7 in dichloromethane); ^{1}H NMR (500 MHz, $CDCl_3$, 300 K): δ = 7.94-7.91 (m, 4H, Ar-H$_{ortho}$, Ar H$_{ortho'}$), 7.47-7.46 (m, 2H, Ar-H$_{meta'}$), 7.25-7.22 (m, 2H, Ar H$_{meta}$), 5.85 (d, $^3J_{1,2}$ = 3.6 Hz, 1H, H-1), 5.73 (t~dd, $^3J_{2,3}$ = 9.8 Hz, $^3J_{3,4}$ = 9.8 Hz, 1H, H-3), 5.18 (t~dd, $^3J_{3,4}$ = 9.8 Hz, $^3J_{4,5}$ = 9.8 Hz, 1H, H-4), 5.09 (dd, $^3J_{1,2}$ = 3.6 Hz, $^3J_{2,3}$ = 10.3 Hz, 1H, H-2), 4.81 (s, 2H, CH$_2$NCS), 4.26 (dd, $^2J_{6,6'}$ = 12.3 Hz, $^3J_{5,6}$ = 4.6 Hz, 1H, H-6), 4.12 (ddd, $^3J_{4,5}$ = 10.2 Hz, $^3J_{5,6}$ = 4.6 Hz, $^3J_{5,6'}$ = 2.2 Hz, 1H, H-5), 4.07 (dd, $^2J_{6,6'}$ = 12.3 Hz, $^3J_{5,6'}$ = 2.2 Hz, 1H, H-6'), 2.09, 2.07, 2.05, 2.05 (each s, each 3H, 4 COCH$_3$) ppm; ^{13}C NMR (126 MHz, $CDCl_3$, 300 K): δ = 170.7, 170.3, 169.7 (3 COCH$_3$), 158.5 (C-Ar$_{para}$), 152.6 (C-Ar$_{ipso'}$), 148.5 (C-Ar$_{ipso}$), 136.8 (C-Ar$_{para'}$), 127.7 (C-Ar$_{meta'}$), 124.9 (C-Ar$_{ortho}$), 123.4 (C-Ar$_{ortho'}$), 117.0 (C-Ar$_{meta}$), 94.3 (C-1), 70.5 (C-2), 70.1 (C-3), 68.5 (C-5), 68.4 (C-4), 61.7 (C-6), 48.6 (*C*H$_2$NCS), 20.9, 20.8, 20.8, 20.7 (4 COCH$_3$) ppm; IR (ATR): $\tilde{\nu}$ = 2962, 2363, 2076, 1749, 1602 1497, 1366, 1210, 1036, 840 cm^{-1}; ESI-MS: m/z calcd for $C_{28}H_{29}N_3O_{10}S$: 622.1 $[M+Na]^+$; found 622.1.

***N*-(Benzyloxycarbonyl)aminoethyl 3-*O*-(3-aminopropyl)-6-azido-6-deoxy-α-D-mannopyranoside, Acetate salt (24):** To solution of the mannoside **1** (227 mg, 399 µmol) in ethanol (10 mL), hydrazine hydrate (30.0 µL, 676 µmol) was added. The reaction mixture was stirred for 16 h at room temperature. Then it was filtered through a bed of celite®, the solvent was removed in vacuo and the residual syrup was co-evaporated with ethanol (3 × 20 mL). Afterwards water was added and the pH was adjusted to 5.0 with acetic acid. The aqueous phase was extracted with ethyl acetate (3 × 40 mL). After lyophilisation mannoside **24** was obtained as colourless oil (195 mg, 390 µmmol, 97%). R$_f$ = 0.09 dichloromethane/methanol/triethylamine, 10:1:0.1); $[\alpha]_D^{23}$ = +8.36 (c=0.5 in methanol); ^{1}H NMR (500 MHz, MeOH-d_4, 300 K): δ = 7.35-7.29 (m, 5H, Ar-H$_{Cbz}$), 5.08 (s, 2H, PhC*H*$_2$O), 4.83 (s~d, overlap with HDO, H 1), 4.05-4.04 (m, 1H, H-2), 3.87-3.76 (m, 2H, CH*H'*CH$_2$NHCbz, NH$_2$CH$_2$CH$_2$CH*H'*), 3.74-3.63 (m, 3H, H-4, H-5, C*H*H'CH$_2$NHCbz), 3.57-3.33 (m, 6H, NH$_2$CH$_2$CH$_2$C*H*H', C*H*$_2$NHCbz, H-3, H-6, H-6'), 3.13-3.10 (m, 2H, NH$_2$C*H*$_2$), 1.98-1.90 (m, 5H, NH$_2$CH$_2$C*H*$_2$CH$_2$, COCH$_3$) ppm; ^{13}C NMR (126 MHz, MeOH-d_4, 300 K): δ = 129.5 (C-Ar$_{Cbz}$), 129.0 (C-Ar$_{Cbz}$), 128.8 (C-Ar$_{Cbz}$), 101.5 (C-1), 80.8 (C-3), 73.9 (C-5), 68.9 (NH$_2$CH$_2$CH$_2$*C*H$_2$), 68.2 (C-2), 68.0 (C-4), 67.8 (*C*H$_2$CH$_2$NHCbz), 67.5 (Ph*C*H$_2$O), 52.7 (C-6), 41.6 (*C*H$_2$NHCbz), 40.2 (NH$_2$*C*H$_2$), 28.2 (NH$_2$CH$_2$*C*H$_2$CH$_2$), 22.8 (CO*C*H$_3$) ppm; IR (ATR): $\tilde{\nu}$ = 3386, 2924, 1770, 1699, 1397, 1371, 1259, 1113, 1042, 721 cm^{-1}.

***N*-(Benzyloxycarbonyl)aminoethyl 3-*O*-{(*E*)-*p*-[*p*'-(2,3,4,6-tetra-*O*-acetyl-α-D-mannopyranosyloxy)phenylazo](benzyl)thioureidopropyl}-6-azido-6-deoxy-α-D-mannopyranoside (25):** To solution of the mannoside **24** (179 mg, 358 µmol) in dry dimethylformamide (24 mL), molecular sieve 3 Å and ethyldiisopropylamine (60.0 µL, 362 µmol) were added. The reaction mixture was stirred for 15 min at room temperature and then a solution of the azobenzene mannoside **21** (215 mg, 358 µmol) in dry dimethylformamide (24 mL) was added. It was stirred for 16 h at room temperature, then the solvent was evaporated and purification of the crude product by column chromatography (dichloromethane/ethyl acetate, 1:1→1:2→1:3) gave **25** as an orange solid (230 mg, 221 µmol, 62%). R_f = 0.12 (dichloromethane/ethyl acetate, 1:1); m.p. 66.1 °C; $[\alpha]_D^{23}$ = +56.8 (c=0.5 in methanol); ^{1}H NMR (500 MHz, MeOH-d_4, 300 K): δ = 7.93-7.91 (m, 2H, Ar-H$_{ortho}$), 7.85-7.84 (m, 2H, Ar-H$_{ortho'}$), 7.49-7.47 (m, 2H, Ar-H$_{meta'}$), 7.33-7.28 (m, 7H, Ar-H$_{Cbz}$, Ar H$_{meta}$), 5.75 (s~d, 1H, H-1a), 5.51-5.50 (m, 2H, H-2a, H-3a), 5.34 (t~dd, $^3J_{3a,4a}$ = 9.9 Hz, $^3J_{4a,5a}$ = 9.9 Hz, 1H, H-4a), 5.06 (s, 2H, PhCH_2O), 4.77 (s~d, 1H, H-1b), 4.27-4.23 (m, 1H, H-6a), 4.12-4.06 (m, 2H, H-5a, H-6a'), 4.76 (s~d, 1H, H-2b), 3.81-3.35 (m, 11H, H-3b, H-4b, H-5b, H-6b, H-6b', CH_2NHCbz, CHH'CH$_2$NHCbz, CHH'CH$_2$NHCbz, NHCH$_2$CH$_2$CHH', NHCH$_2$CH$_2$CHH'), 2.19, 2.06, 2.01, 1.96 (each s, each 3H, 4 COCH$_3$), 1.91-1.83 (m, 2H, NHCH$_2$CH_2CH$_2$) ppm; ^{13}C NMR (126 MHz, MeOH-d_4, 300 K): δ = 172.2, 171.5, 171.5 (3 COCH$_3$), 159.2 (OCONH), 158.9 (C-Ar$_{para}$), 153.1 (C-Ar$_{ipso'}$), 149.7 (C-Ar$_{ipso}$), 138.3 (C-Ar$_{para'}$,C-Ar$_{Cbz}$), 129.5 (C-Ar$_{Cbz}$), 129.2 (C-Ar$_{meta'}$), 129.0 (C-Ar$_{Cbz}$), 128.8 (C-Ar$_{Cbz}$), 125.6 (C-Ar$_{ortho}$), 123.8 (C-Ar$_{ortho'}$), 118.2 (C-Ar$_{meta}$), 101.6 (C-1b), 97.0 (C-1a), 80.6 (C-3b), 73.9 (C-5b), 70.9 (C-5a), 70.5 (C-3a), 70.3 (C-2a), 68.5 (C-2b), 68.2 (C-4b), 68.2 (NHCH$_2$CH$_2$CH_2), 67.7 (CH_2CH$_2$NHCbz), 67.5 (PhCH_2O), 67.0 (C-4a), 63.3 (C-6a), 52.8 (C-6b), 41.7 (CH_2NHCbz), 30.2 (NHCH$_2$CH_2CH$_2$), 20.6, 20.6 (2 COCH$_3$) ppm; IR (ATR): $\tilde{\nu}$ = 2924, 2100, 1746, 1660, 1497, 1368, 1214, 1031, 1026, 843 cm^{-1}; UV-vis (MeOH): $\lambda_{max}(\varepsilon)$ = 342 nm (20979 L mol^{-1} cm^{-1}).

***N*-(Benzyloxycarbonyl)aminoethyl 3-*O*-{(*E*)-*p*-[*p*'-(2,3,4,6-tetra-*O*-acetyl-α-D-mannopyranosyloxy)phenylazo](benzyl)thioureidopropyl}-6-amino-6-deoxy-α-D-mannopyranoside(26):** To solution of the mannoside **25** (71.0 mg, 68.3 µmol) in dry dimethylformamide (3.5 mL), triphenylphosphine (20.0 mg, 75.1 µmol) was added. The reaction mixture was stirred for 16 h at room temperature. Then water (350 µL) was added and it was stirred for 3 d at room temperature. Afterwards the solvent was evaporated and purification of the crude product by column chromatography (dichloromethane/methanol/triethylamine, 10:0.5:0.1→10:1:0.1) gave **26** as an orange oil (56.0 mg, 55.3 µmol, 81%). R_f = 0.15 dichloromethane/methanol/triethylamine, 10:1:0.1); $[\alpha]_D^{23}$ = +44.6 (c=0.5 in methanol); ^{1}H NMR (500 MHz, MeOH-d_4, 300 K): δ = 7.94-7.92 (m, 2H, Ar-H$_{ortho}$), 7.86-7.84 (m, 2H, Ar H$_{ortho'}$), 7.50-7.48 (m, 2H, Ar-H$_{meta'}$), 7.33-7.29 (m, 7H, Ar-H$_{Cbz}$, Ar H$_{meta}$), 5.76 (s~d, 1H, H-1a), 5.51-5.49 (m, 2H, H-2a, H-3a), 5.35 (t~dd, $^3J_{3a,4a}$ = 9.9 Hz, $^3J_{4a,5a}$ = 9.9 Hz, 1H, H-4a), 5.22 (s, 2H, PhCH$_2$O), 4.83 (s~d, overlap with HDO, H-1b), 4.27-4.23 (m, 1H, H-6a), 4.12-4.07 (m, 2H, H-5a, H-6a'), 4.03 (br s~d, 1H, H-2b), 3.77-3.39 (m, 11H, H-3b, H-4b, H-5b, H-6b, CH_2NHCbz, CHH'CH$_2$NHCbz, CHH'CH$_2$NHCbz, , NHSNHCH_2CH$_2$CH$_2$, NHSNHCH$_2$CH$_2$), 3.05 (dd, $^2J_{6b,6b'}$ = 13.3 Hz, $^3J_{6b',5b}$ = 8.3 Hz, 1H, H-6b'), 2.20, 2.06, 2.02, 1.96 (each s, each 3H, 4 COCH3), 1.91-1.85 (m, 2H, NHCH$_2$CH_2CH$_2$) ppm; ^{13}C NMR (126 MHz, MeOH-d_4, 300 K): δ = 172.1 (COCH$_3$), 129.5 (C-Ar$_{Cbz}$), 129.2 (C-Ar$_{meta'}$), 129.1 (C-Ar$_{Cbz}$), 128.8 (C-Ar$_{Cbz}$),

125.6 (C-Ar$_{ortho}$), 123.8 (C-Ar$_{ortho'}$), 118.2 (C-Ar$_{meta}$), 101.9 (C-1b), 97.1 (C-1a), 80.4 (C-3b), 70.9 (C-5b), 70.5 (C-5a), 70.5 (C-3a), 70.3 (C-2a), 68.7 (C-2b), 68.3 (C-4b), 68.3 (NHCH$_2$CH$_2$*C*H$_2$), 67.8 (*C*H$_2$CH$_2$NHCbz), 67.8 (Ph*C*H$_2$O), 67.0 (C-4a), 63.3 (C-6a), 48.0 (C-6b), 41.6 (*C*H$_2$NHCbz), 30.8 (NH$_2$CH$_2$CH$_2$CH$_2$), 20.6, 20.6 (2 COCH$_3$) ppm; IR (ATR): $\tilde{\nu}$ =2972, 2069, 1743, 1597 1496, 1365, 1213, 1126, 1026, 976, 851 cm^{-1}.

***N*-(Benzyloxycarbonyl)aminoethyl 3-*O*-{(*E*)-*p*-[*p*'-(2,3,4,6-tetra-*O*-acetyl-α-D-mannopyranosyloxy)-6-{(*E*)-*p*"-[*p*"'-(2,3,4,6-tetra-*O*-acetyl-α-D-glucopyranosyloxy)phenylazo(benzyl)thioureidopropyl}-6-deoxy-α-D-mannopyranoside (27):** To solution of the mannoside **26** (54.0 mg, 53.3 µmol) in dry dimethylformamide (9 mL), molecular sieve 3 Å and ethyldiisopropylamine (9.10 µL, 53.8 µmol) were added. The reaction mixture was stirred for 15 min at room temperature and then a solution of the azobenzene glucoside **22** (32.0 mg, 53.3 µmol) in dry dimethylformamide (9 mL) was added. It was stirred for 2 d at room temperature, and then the solvent was evaporated. Purification of the crude product by column chromatography (dichloromethane/ethyl acetate, 1:3→ dichloromethane/ethyl acetate/methanol, 1:3:0.5) gave **27** as an orange solid (43.0 mg, 26.7 µmol, 50%). R*f* = 0.17 (dichloromethane/ethyl acetate, 1:1); m.p. 66.1 °C; $[\alpha]_D^{23}$ = +16.4 (c = 1.1 in methanol); ^{1}H NMR (600 MHz, MeOH-d_4, 300 K): δ = 7.88-7.79 (m, 8H, Ar-H$_{ortho}$, Ar H$_{ortho'}$, Ar-H$_{ortho"}$, Ar H$_{ortho"'}$), 7.48-7.43 (m, 4H, Ar-H$_{meta}$, Ar-H$_{meta"}$), 7.31-7.24 (m, 7H, Ar-H$_{Cbz}$, Ar H$_{meta'}$), 7.16-7.14 (m, 2H, Ar-H$_{meta"'}$), 5.72 (d, $^3J_{1a,2a}$ = 1.4 Hz, 1H, H-1a), 5.51-5.48 (m, 2H, H-2a, H-3a), 5.45 (d, $^3J_{1b,2b}$ = 7.9 Hz, 1H, H-1b), 5.42 (t~dd, $^3J_{2b,3b}$ = 9.5 Hz, $^3J_{3b,4b}$ = 9.5 Hz, 1H, H-3b), 5.35-5.32 (m, 1H, H-4a), 5.22 (dd, $^3J_{1b,2b}$ = 7.9 Hz, $^3J_{3b,4b}$ = 9.5 Hz, 1H, H-2b), 5.14 (dd, $^3J_{3b,4b}$ = 9.5 Hz, $^3J_{4b,5b}$ = 9.9 Hz, 1H, H-4b), 5.02 (s, 2H, PhC*H*$_2$O), 4.72 (s~d, 1H, H-1c), 4.32 (dd, $^2J_{6b,6b'}$ = 12.4 Hz, $^3J_{6b,5b}$ = 5.3 Hz, 1H, H-6b), 4.23 (dd, $^2J_{6a,6a'}$ = 11.9 Hz, $^3J_{6a,5a}$ = 5.1 Hz, 1H, H-6a), 4.18 (dd, $^2J_{6b,6b'}$ = 12.4 Hz, $^3J_{6b',5b}$ = 2.3 Hz, 1H, H-6b'), 4.14 (ddd, $^3J_{4b,5b}$ = 9.9 Hz, $^3J_{6b,5b}$ = 5.3 Hz, $^3J_{6b',5b}$ = 2.4 Hz, 1H, H-5b), 4.09-4.04 (m, 2H, H-5a, H-6a'), 3.96 (s~d, 1H, H-2c), 3.80-3.40 (m, 11H, H-3c, H-4c, H-5c, H-6c, H-6c', NHSNHCH$_2$CH$_2$C*H*$_2$, NHSNHCH$_2$C*H*$_2$, CH*H'*CH$_2$NHCbz, C*H*H'CH$_2$NHCbz,), 3.26-3.21 (m, 2H, CH$_2$NHCbz), 2.20, 2.05, 2.04, 2.02, 2.01, 1.94 (each s, 24 H, 8 COCH$_3$), 1.94-1.83 (m, 2H, NHCH$_2$C*H*$_2$CH$_2$) ppm; ^{13}C NMR (151 MHz, MeOH-d_4, 300 K): δ = 172.3, 172.2, 171.6, 171.5, 171.5, 171.2, 171.1 (7 COCH$_3$), 160.4 (O*C*ONH), 159.1 (C-A$_{rpara'}$), 158.9 (C-Ar$_{para"'}$), 153.1 (C-Ar$_{ipso}$), 153.1 (C-Ar$_{ipso"}$), 149.7 (C-Ar$_{ipso'}$), 149.6 (C-Ar$_{ipso"'}$), 138.3 (C-Ar$_{Cbz}$), 129.5 (C-Ar$_{Cbz}$), 129.3 (C-Ar$_{meta"}$), 129.2 (C-Ar$_{meta}$), 129.0 (C-Ar$_{Cbz}$), 128.8 (C-Ar$_{Cbz}$), 125.6 (C-Ar$_{ortho'}$), 125.6 (C-Ar$_{ortho"'}$), 123.9 (C-Ar$_{ortho}$), 123.9 (C-Ar$_{ortho"}$), 118.2 (C-Ar$_{meta'}$), 118.0 (C-Ar$_{meta"'}$), 101.7 (C-1c), 99.2 (C-1b), 97.1 (C-1a), 80.2 (C-3c), 74.1 (C-3b), 73.1 (C-5b), 73.1 (C-5c), 72.6 (C-2b), 70.8 (C-5a), 70.5 (C-3a), 70.3 (C-2a), 69.7 (C-4b), 68.5 (C-2c), 68.2 (C-4c), 67.5 (PhthNCH$_2$CH$_2$*C*H$_2$), 67.5 (*C*H$_2$CH$_2$NHCbz), 67.5 (Ph*C*H$_2$O), 67.0 (C-4a), 63.3 (C-6a), 63.1 (C-6b), 41.7 (*C*H$_2$NHCbz), 30.1 (NHCH$_2$*C*H$_2$CH$_2$), 20.7, 20.6, 20.6 (3 COCH$_3$) ppm; IR (ATR): $\tilde{\nu}$ = 2972, 2069, 1743, 1597 1496, 1365, 1213, 1126, 1026, 976, 851 cm-1; UV-Vis (MeOH): $\lambda_{max}(\varepsilon)$ = 342 nm (47973 L mol^{-1} cm^{-1}); ESI-MS: m/z calcd for $C_{28}H_{29}N_3O_{16}S$: 1634.5 $[M+Na]^+$; found 1634.2.

***N*-(Benzyloxycarbonyl)aminoethyl 3-*O*-(3-phthalimidopropyl)-6-amino-6-deoxy-α-D-mannopyranoside (28):** To solution of the mannoside **1** (100 mg, 176 µmol) in dry dimethylformamide (10 mL), triphenylphosphine (50.0 mg, 193 µmol) was added. The reaction mixture was stirred for 16 h at room temperature. Then water (1 mL) was added and it was again stirred for 16 h at room temperature. Afterwards the solvent was evaporated and purification of the crude product by column chromatography (dichloromethane/methanol/triethylamine, 10:0:1:0.05→9:1:0.05) gave **28** as a colourless oil (45.0 mg, 82.8 µmol, 47%). R_f = 0.21 (dichloromethane/methanol/triethylamine, 9:1:0.05); $[\alpha]_D^{23}$ = +7.92 (c=0.5 in dimethylsulfoxide); ^{1}H NMR (500 MHz, MeOH-d_4, 300 K): δ = 7.90-7.81 (m, 4H, Ar-H$_{Phth}$), 7.37-7.29 (m, 5H, Ar-H$_{Cbz}$), 5.11 (s, 2H, PhCH_2O), 4.84 (s~d, overlap with HDO, H-1), 4.09 (dd, $^3J_{1,2}$ = 1.9 Hz, $^3J_{2,3}$ = 2.9 Hz, 1H, H-2), 3.87-3.35 (m, 12H, H-3, H-4, H-5, H-6, PhthNCH_2, PhthNCH$_2$CH$_2$CHH', PhthNCH$_2$CH$_2$CHH', CHH'CH$_2$NHCbz, CHH'CH$_2$NHCbz, CH_2NHCbz), 3.05 (dd, $^2J_{6,6'}$ = 13.1 Hz, $^3J_{6',5}$ = 8.1 Hz, 1H, H-6'), 2.04-1.99 (m, 2H, PhthNCH$_2$CH_2CH$_2$) ppm; ^{13}C NMR (126 MHz, MeOH-d_4, 300 K): δ = 170.2 (C=O), 159.1 (OCONH), 138.3 (C-Ar$_{Cbz}$), 135.4 (C-Ar$_{Phth}$), 133.4 (C-Ar$_{Phth}$), 129.5 (C-Ar$_{Cbz}$), 129.0 (C-Ar$_{Cbz}$), 128.8 (C-Ar$_{Cbz}$), 124.2 (C-Ar$_{Phth}$), 101.8 (C-1), 80.5 (C-3), 70.4 (C-5), 68.7 (C-2), 68.4 (C-4), 67.9 (PhthNCH$_2$CH$_2$CH_2), 67.5 (CH_2CH$_2$NHCbz), 67.5 (PhCH_2O), 42.1 (C-6), 41.6 (CH_2NHCbz), 36.1 (PhthNCH_2), 30.0 (PhthNCH$_2$CH_2CH$_2$) ppm; IR (ATR):$\tilde{\nu}$ = 2924, 1702, 1636, 1398, 1257, 1111, 1041, 722 cm-1.

***N*-(Benzyloxycarbonyl)aminoethyl 3-*O*-(3-phthalimidopropyl)-6-{(*E*)-*p*-[*p*'-(2,3,4,6-tetra-*O*-acetyl-*β*-D-glucopyranosyloxy)phenylazo](benzyl)thioureido}-6-deoxy-α-D-mannopyranoside (29):** To solution of the mannoside **28** (40.0 mg, 73.6 µmol) in dry dimethylformamide (5 mL), molecular sieve 3 Å and ethyldiisopropylamine (12.0 µL, 74.3 µmol) were added. The reaction mixture was stirred for 15 min at room temperature and then a solution of the azobenzene glucoside **22** (44.0 mg, 73.6 µmol) in dry dimethylformamide (5 mL) was added. It was stirred for 16 h at room temperature, and then the solvent was evaporated. Purification of the crude product by column chromatography (dichloromethane/ethyl acetate, 1:1→1:2→1:3) gave **29** as an amorphous orange solid (20.0 mg, 17.5 µmol, 24%). R_f = 0.12 (dichloromethane/ethyl acetate, 1:1); $[\alpha]_D^{23}$ = -5.19 (c=0.6 in metahnol); ^{1}H NMR (600 MHz, MeOH-d_4, 300 K): δ = 7.87-7.76 (m, 8H, Ar-H$_{ortho}$, Ar H$_{ortho'}$, Ar-H$_{Phth}$), 7.50-7.49 (m, 2H, Ar-H$_{meta}$), 7.31-7.14 (m, 7H, Ar-H$_{Cbz}$, Ar H$_{meta'}$), 5.46 (d, $^3J_{1a,2a}$= 7.9 Hz, 1H, H-1$_{Glc}$), 5.42 (t~dd, $^3J_{2a,3a}$ = 9.5 Hz, $^3J_{3a,4a}$ = 9.5 Hz, 1H, H-3$_{Glc}$), 5.21 (dd, $^3J_{1a,2a}$ = 7.9 Hz, $^3J_{3a,4a}$ = 9.5 Hz, 1H, H-2$_{Glc}$), 5.14 (t~dd, , $^3J_{3a,4a}$ = 9.5 Hz, $^3J_{4a,5a}$ = 9.5 Hz, 1H, H-4$_{Glc}$), 5.03 (s, 2H, PhCH$_2$O), 4.75 (s~d, 1H, H 1b), 4.33 (dd, $^2J_{6a,6a'}$ = 12.6 Hz, $^3J_{6a,5a}$ = 5.2 Hz, 1H, H-6$_{Glc}$), 4.22-4.14 (m, 4H, H-6$_{Glc'}$, H-5$_{Glc}$, H-6b, H-6b'), 4.00 (s~dd, 1H, H-2b), 3.85-3.75 (m, 3H, PhthNCH_2, CHH'CH$_2$NHCbz), 3.68-3.42 (m, 8H, H-3b, H-4b, H-5b, CHH'CH$_2$NHCbz, PhCH_2NHSNH, PhthNHCH$_2$CH$_2$CHH', PhthNCH$_2$CH$_2$CHH'), 3.32-3.24 (m, overlap with MeOH-d_4, CH$_2$NHCbz), 2.06 (s, 6H, 2 COCH$_3$), 2.05, 2.01 (each s, each 3H, 2 COCH$_3$), 1.99-1.93 (m, 2H, PhthNCH$_2$CH_2CH$_2$) ppm; ^{13}C NMR (151 MHz, MeOH-d_4, 300 K): δ = 172.3, 171.6, 171.3, 171.1 (4 COCH$_3$), 170.2, 169.4 (2 C=O$_{Phth}$), 160.4 (OCONH), 159.0 (C-Ar$_{para'}$), 153.1 (C-Ar$_{ipso}$), 149.7 (C-Ar$_{ipso'}$), 138.3 (C-Ar$_{Cbz}$), 135.4 (C-Ar$_{Phth}$), 132.4 (C-Ar$_{Phth}$), 129.9 (C-Ar$_{Cbz}$), 129.5 (C-Ar$_{meta'}$), 129.3 (C-Ar$_{meta}$), 129.0 (C-Ar$_{Cbz}$), 128.8 (C-Ar$_{Cbz}$), 125.5 (C-Ar$_{ortho'}$), 124.2 (C-Ar$_{Phth}$), 123.9 (C-Ar$_{ortho}$), 118.0 (C-Ar$_{meta'}$), 101.6 (C-1b), 99.2 (C-1$_{Glc}$), 80.5 (C-3b), 74.1

(C-3$_{Glc}$), 73.1 (C-5$_{Glc}$), 73.1 (C-5b), 72.7 (C-2$_{Glc}$), 69.7 (C-4$_{Glc}$), 68.7 (C-2b), 68.5 (C-4b), 68.0 (PhthNCH$_2$CH$_2$*C*H$_2$), 67.5 (*C*H$_2$CH$_2$NHCbz), 67.5 (Ph*C*H$_2$O), 63.1 (C-6$_{Glc}$), 40.2 (*C*H$_2$NHCbz), 35.1 (PhthN*C*H$_2$), 30.1 (PhthNCH$_2$*C*H$_2$CH$_2$), 20.7, 20.6 (2 COCH$_3$) ppm; UV-vis (MeOH): $\lambda_{max}(\varepsilon)$ = 342 nm (20979 L mol^{-1} cm^{-1}); ESI-MS: m/z calcd for $C_{55}H_{62}N_6O_{19}S$: 1165.4 $[M+Na]^+$; found 1165.4.

^{1}H and ^{13}C NMR spectra of target compounds

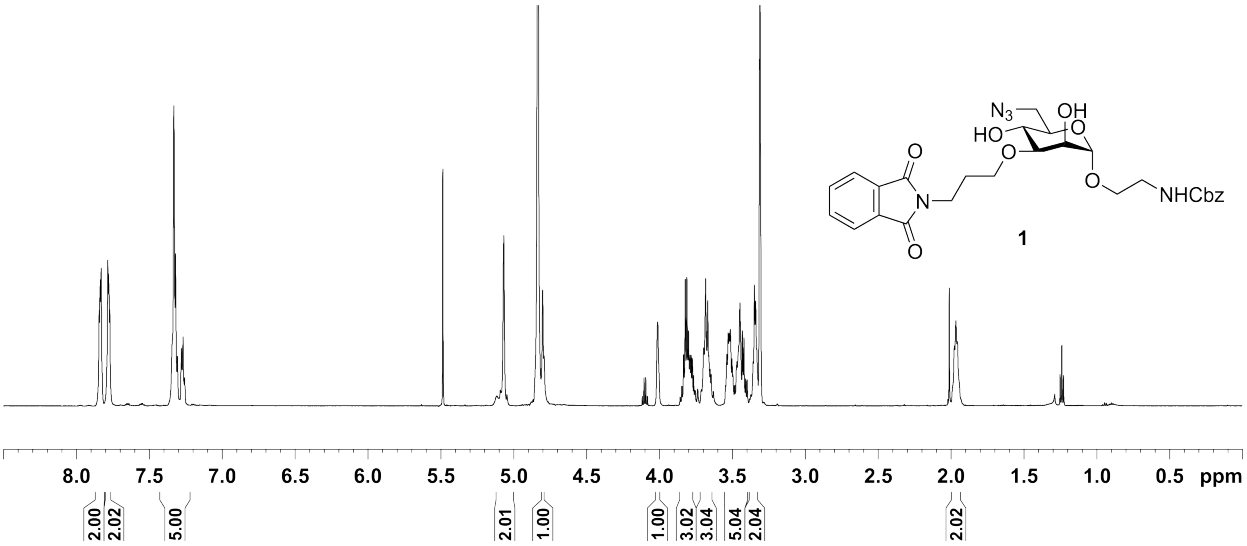

Figure 8.28. ^{1}H NMR spectrum of **1** (600 MHz, MeOH-d_4, 300 K).

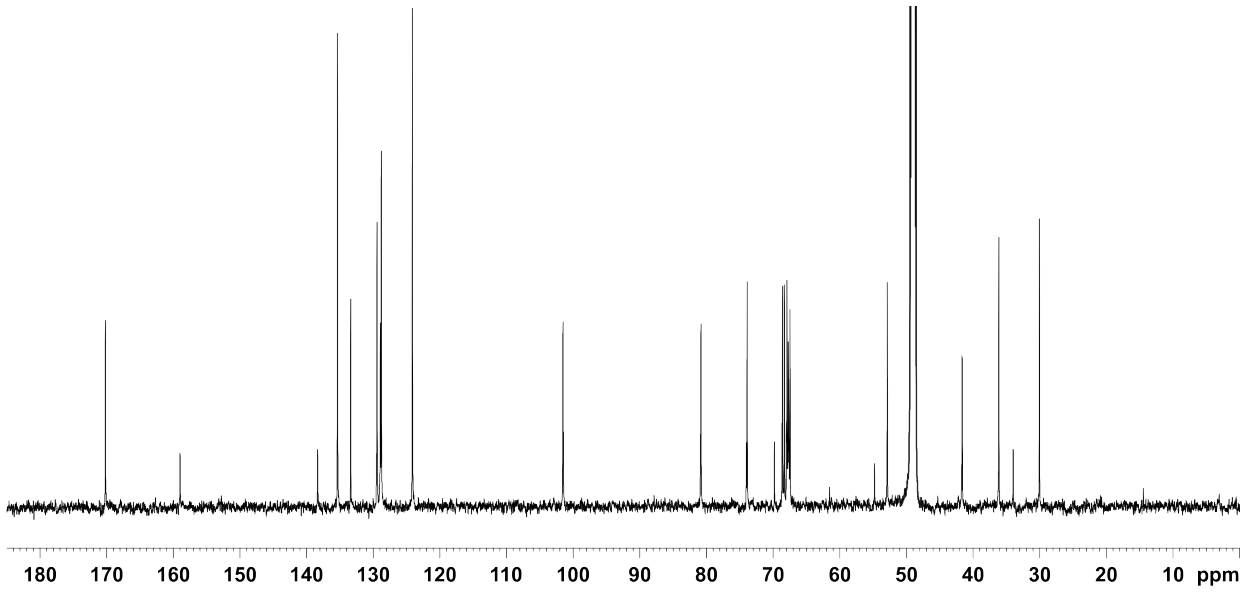

Figure 8.29. ^{13}C NMR spectrum of **1** (151 MHz, MeOH-d_4, 300 K).

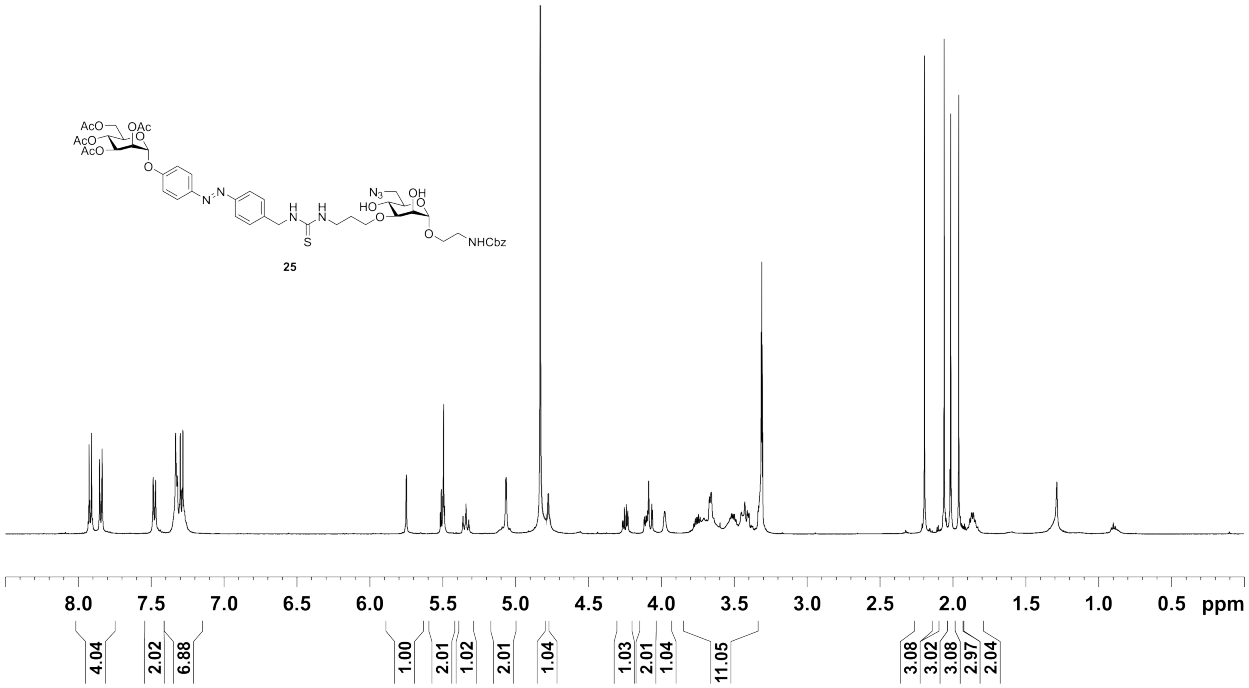

Figure 8.30. ^{1}H NMR spectrum of **25** (500 MHz, MeOH-d_4, 300 K).

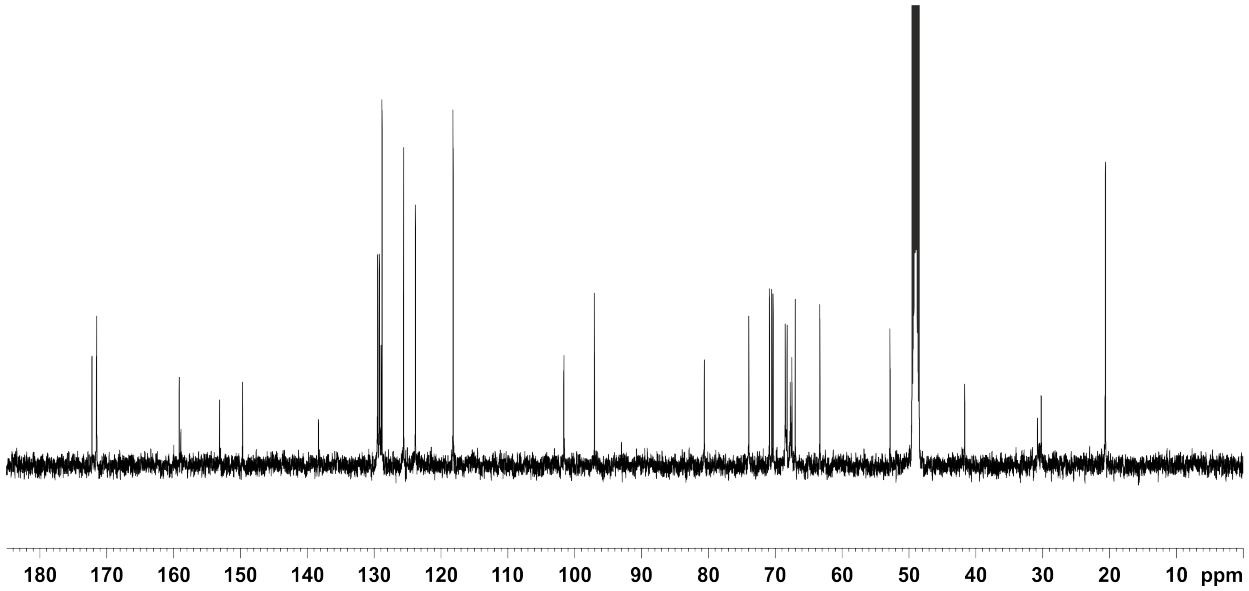

Figure 8.31. ^{13}C NMR spectrum of **25** (126 MHz, MeOH-d_4, 300 K).

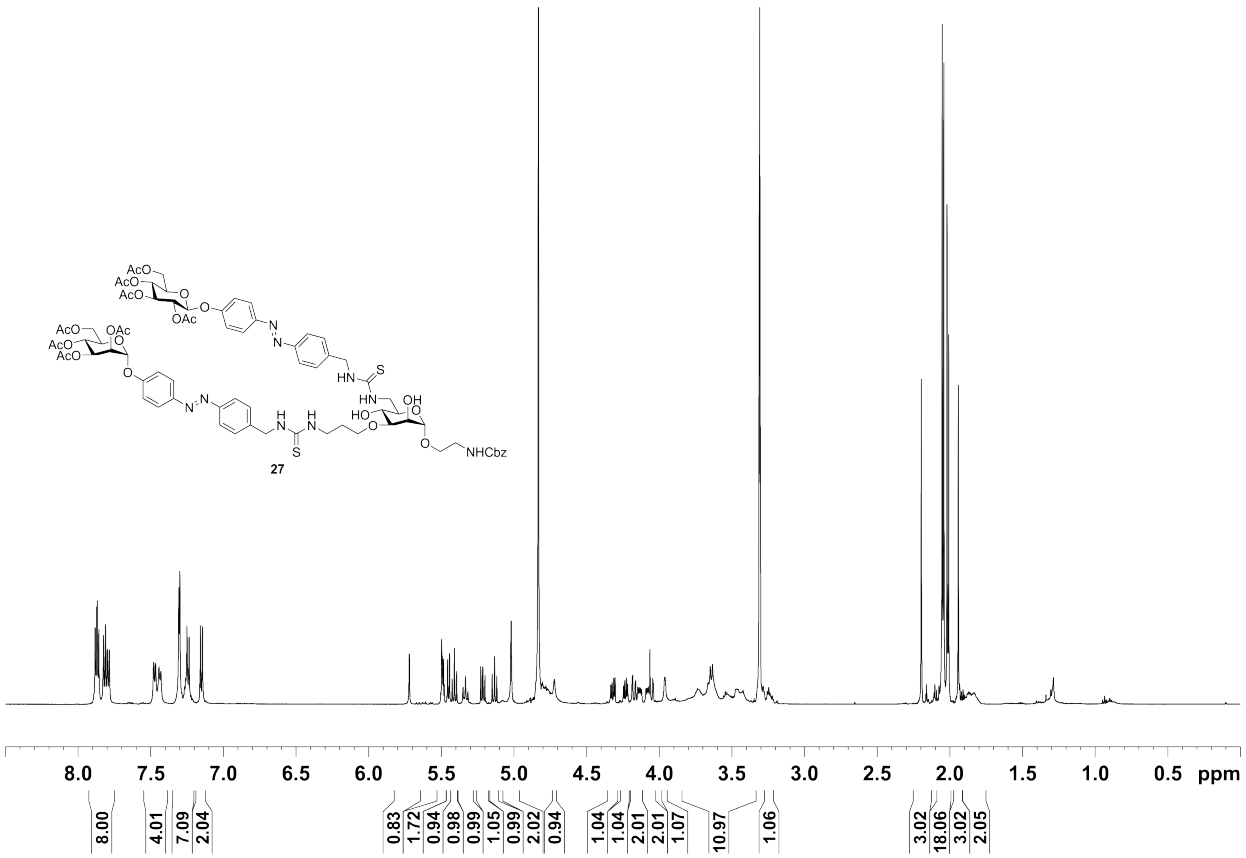

Figure 8.32. ^{1}H NMR spectrum of **27** (600 MHz, MeOH-d_4, 300 K).

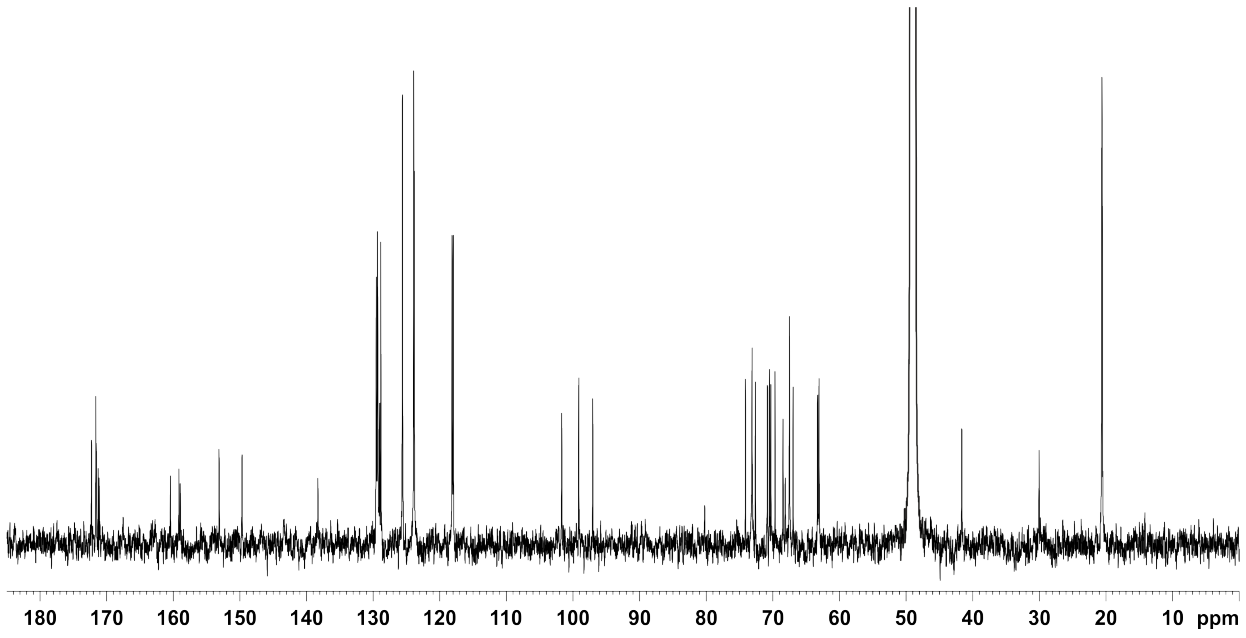

Figure 8.33. ^{13}C NMR spectrum of **27** (151 MHz, MeOH-d_4, 300 K).

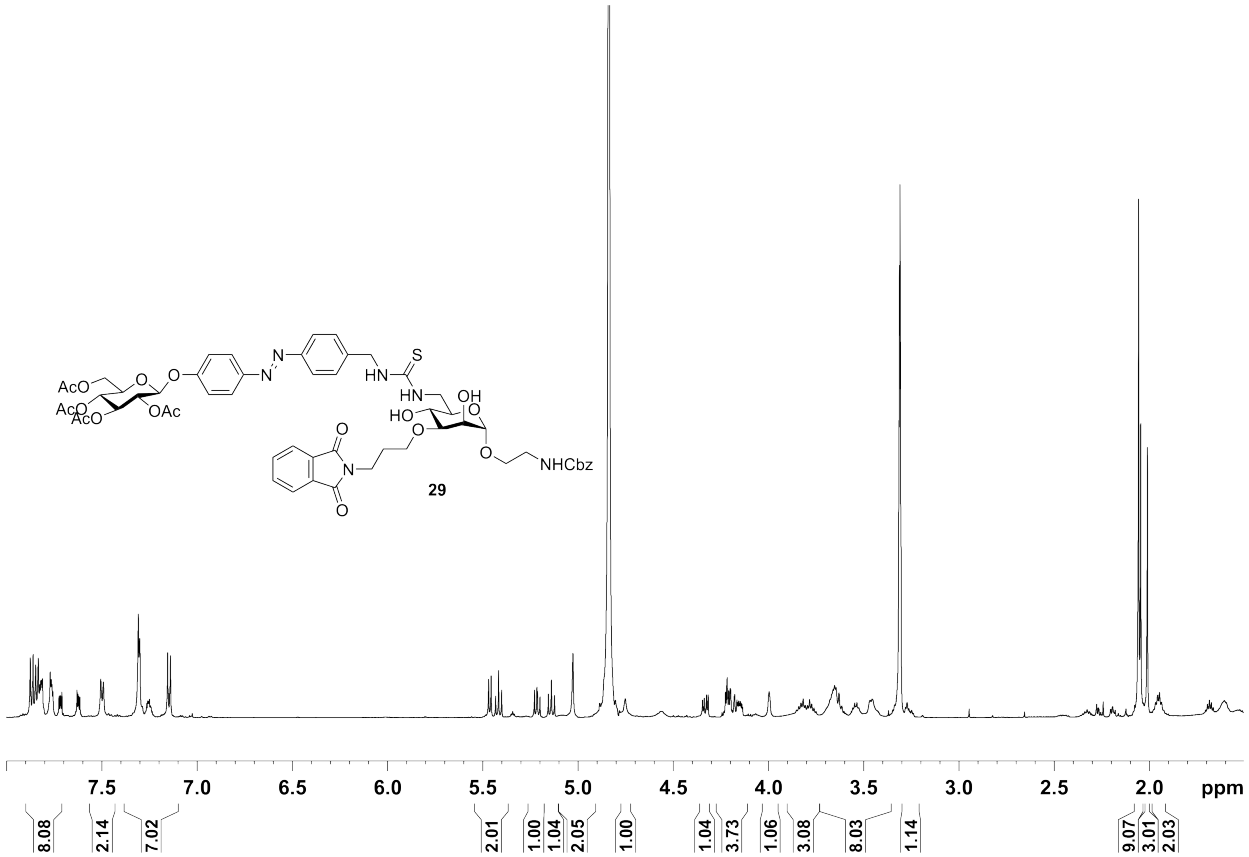

Figure 8.34. ^{1}H NMR spectrum of **29** (600 MHz, MeOH-d_4, 300 K).

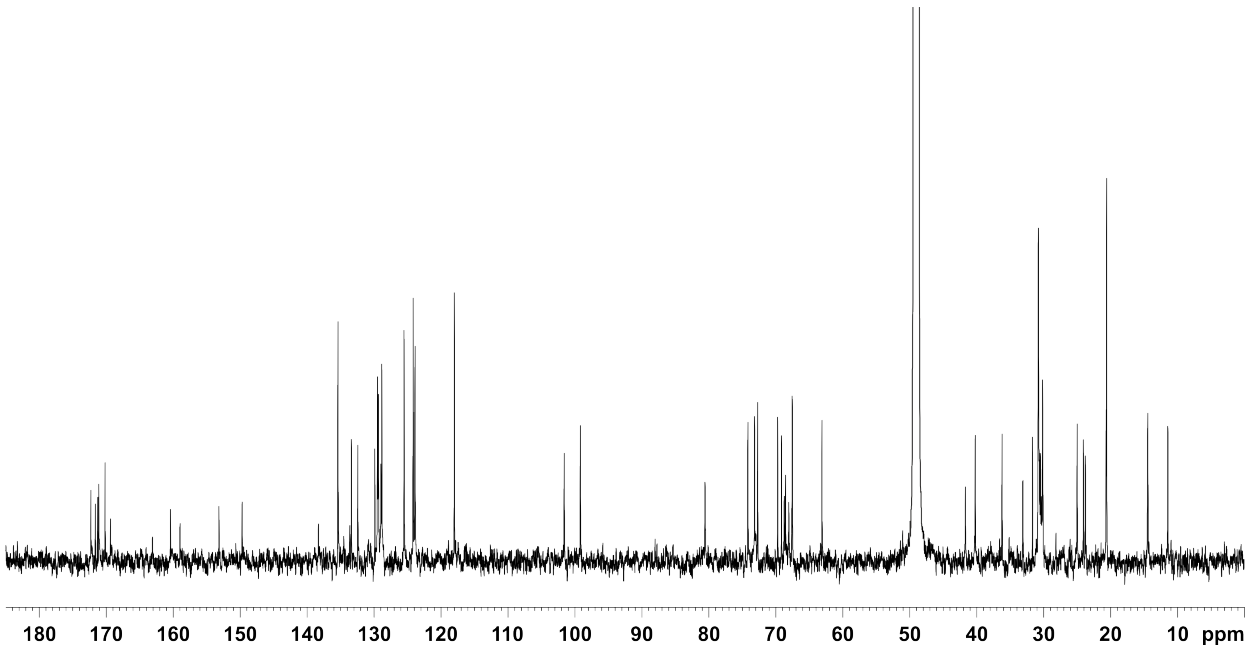

Figure 8.35. ^{13}C NMR spectrum of **29** (151 MHz, MeOH-d_4, 300 K).

Irradiation experiments

Irradiation experiments Irradiation was performed using a LED (emitting 365 nm light) from the Nichia Corporation (NC4U133A) with a FWHW of 9 nm and optical power output (P_0) ~1 W. E/Z ratios were determined by irradiating the sample in the NMR tube followed by ^{1}H NMR spectroscopy. The respective *E*-configured azobenzene (5-10 mg) was dissolved in MeOH-d_4 (500 µL) in a NMR tube and irradiated for 15 min at 365 nm. The distance between the LED and the sample in the NMR tube was about ~5 cm. Photostationary states (PSS) were reached after approx. 15 min. Then, the sample was kept in the dark, and ^{1}H NMR spectroscopy was performed immediately afterwards. The photostationary states (PSS) were determined by integration of the anomeric H-1 protons of the prepared compounds. In analogy, for UV-vis spectroscopy, the *E*-configured azobenzene derivatives were dissolved in DMSO in a UV cuvette, irradiated for 15 min at 365 nm with a distance between LED and cuvette of ~5 cm. UV-vis spectra were recorded immediately afterwards. The absorption spectra showed an increase of the absorbance in the n-π^* transition and simultaneous decrease in the π-π^* transition, indicating the formation of the respective *Z* isomer. Extinction coefficients (ε) were deduced from UV-vis spectra measured at seven different concentrations (5 µM, 10 µM, 20 µM, 40 µM, 70 µM, 60 µM and 80 µM). The kinetics of thermal $Z \rightarrow E$ relaxation process were determined by NMR spectroscopy in the dark. The half-life $\tau_{1/2}$ was determined as $\tau_{1/2} = \ln 2/k$. After irradiation, the ^{1}H NMR spectra of the samples were recorded in regular intervals (3 h) over a period of 5 to 6 days. For the determination of the half-life the *Z* and *E* signals of the respective azobenzene moiety were integrated. A signal that was not influenced by irradiation was set as reference. The decay of the integral of the *Z*- and the increase of the integral of the *E*-species were plotted and an exponential decay of first order fitted to the data.

NMR spectra of *Z*-configured compounds and UV-vis spectra

_N_-(Benzyloxycarbonyl)aminoethyl 3-_O_-{(_Z_)-_p_-[_p_'-(2,3,4,6-tetra-_O_-acetyl-α-D-mannopyranosyloxy)phenylazo](benzyl)thioureidopropyl}-6-azido-6-deoxy-α-D-mannopyranoside

^{1}H NMR (500 MHz, MeOH-d_4, 300 K): δ = 7.34-7.26 (m, 7H, Ar-H$_{ortho}$, Ar-H$_{Cbz}$), 7.06-7.04 (m, 2H, Ar H$_{ortho'}$), 6.91-6.89 (m, 2H, Ar-H$_{meta'}$), 6.84-6.82 (m, 2H, Ar-H$_{meta}$), 5.59 (s~d, 1H, H-1a), 5.44-5.40 (m, 2H, H-2a, H-3a), 5.30 (t~dd, $^3J_{3a,4a}$ = 9.7 Hz, $^3J_{4a,5a}$ = 9.7 Hz, 1H, H-4a), 5.07 (s, 2H, PhCH_2O), 4.79 (s~d, 1H, H 1b), 4.69 (br s, 2H, PhCH_2NHCS), 4.24-4.20 (m, 1H, H-6a), 4.05-3.99 (m, 2H, H-5a, H-6a', H-2b), 3.80-3.33 (m, 13H, H-3b, H-4b, H-5b, H-6b, H-6b', CH_2NHCbz, C*H*H'CH$_2$NHCbz, CH*H'*CH$_2$NHCbz, NHCH$_2$CH$_2$CH_2, NHCH$_2$CH$_2$CH*H'*, NHCH$_2$CH$_2$C*H*H'), 2.16, 2.04, 1.98, 1.96 (each s, each 3H, 4 COCH$_3$), 1.91-1.79 (m, 2H, NHCH$_2$CH$_2$CH$_2$) ppm.

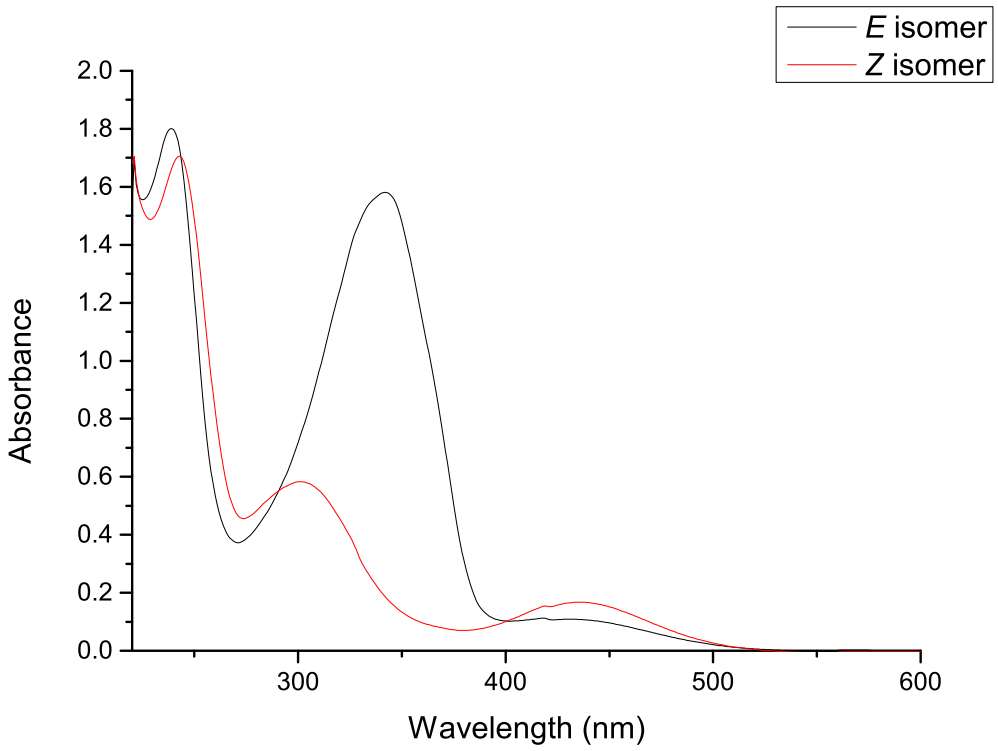

Figure 8.36. UV-vis spectra of **25**: *E* isomer in black, *Z* isomer in red; irradiation with 365 nm and 440 nm, respectively, in MeOH at 293 K.

_N_-(Benzyloxycarbonyl)aminoethyl 3-_O_-{(_Z_)-_p_-[_p_'-(2,3,4,6-tetra-_O_-acetyl-α-D-mannopyranosyloxy)-6-{(_Z_)-_p_"-[_p_"'-(2,3,4,6-tetra-_O_-acetyl-α-D-glucopyranosyloxy)phenylazo(benzyl)thioureidopropyl}-6-deoxy-α-D-mannopyranoside

^{1}H NMR (600 MHz, MeOH-d_4, 300 K): δ = 7.88-7.79 (m, 8H, Ar-H$_{ortho}$, Ar H$_{ortho'}$, Ar-H$_{ortho"}$, Ar H$_{ortho"'}$), 7.48-7.43 (m, 4H, Ar-H$_{meta}$, Ar-H$_{meta"}$), 7.31-7.24 (m, 7H, Ar-HCbz, Ar H$_{meta'}$), 7.16-7.14 (m, 2H, Ar-H$_{meta"'}$), 5.72 (d, $^3J_{1a,2a}$ = 1.4 Hz, 1H, H-1a), 5.51-5.48 (m, 2H, H-2a, H-3a), 5.45 (d, $^3J_{1b,2b}$ = 7.9 Hz, 1H, H-1b), 5.42 (t~dd, $^3J_{2b,3b}$ = 9.5 Hz, $^3J_{3b,4b}$ = 9.5 Hz, 1H, H-3b), 5.35-5.32 (m, 1H, H-4a), 5.22 (dd, $^3J_{1b,2b}$ = 7.9 Hz, $^3J_{3b,4b}$ = 9.5 Hz, 1H, H-2b), 5.14 (dd, $^3J_{3b,4b}$ = 9.5 Hz, $^3J_{4b,5b}$ = 9.9 Hz, 1H, H-4b), 5.02 (s, 2H, PhCH$_2$O), 4.72 (s~d, 1H, H 1c), 4.32 (dd, $^2J_{6b,6b'}$ = 12.4

Hz, $^{3}J_{6b,5b}$ = 5.3 Hz, 1H, H-6b), 4.23 (dd, $^{2}J_{6a,6a'}$ = 11.9 Hz, $^{3}J_{6a,5a}$ = 5.1 Hz, 1H, H-6a), 4.18 (dd, $^{2}J_{6b,6b'}$ = 12.4 Hz, $^{3}J_{6b',5b}$ = 2.3 Hz, 1H, H-6b'), 4.14 (ddd, $^{3}J_{4b,5b}$ = 9.9 Hz, $^{3}J_{6b,5b}$ = 5.3 Hz, $^{3}J_{6b',5b}$ = 2.4 Hz, 1H, H-5b), 4.09-4.04 (m, 2H, H-5a, H-6a'), 3.96 (s~d, 1H, H-2c), 3.80-3.40 (m, 11H, H-3c, H-4c, H-5c, H-6c, H-6c', NHSNHCH$_2$CH$_2$C*H*$_2$, NHSNHCH$_2$C*H*$_2$, CH*H*'CH$_2$NHCbz, C*H*H'CH$_2$NHCbz,), 3.26-3.21 (m, 2H, C*H*$_2$NHCbz), 2.20, 2.05, 2.04, 2.02, 2.01, 1.94 (each s, 24 H, 8 COCH$_3$), 1.94-1.83 (m, 2H, NHCH$_2$CH$_2$CH$_2$) ppm.

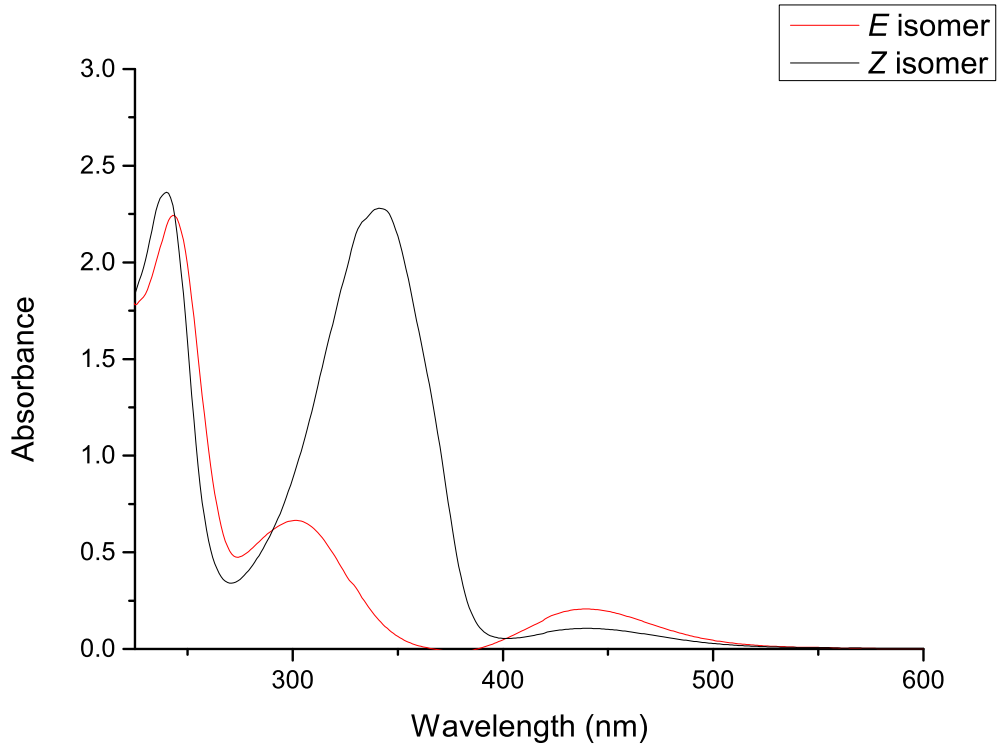

Figure 8.37. UV-vis spectra of **27**: *E* isomer in black, *Z* isomer in red; irradiation with 365 nm and 440 nm, respectively, in MeOH at 293 K.

_N_-(Benzyloxycarbonyl)aminoethyl 3-_O_-(3-phthalimidopropyl)-6-{(_Z_)-_p_-[_p_'-(2,3,4,6-tetra-_O_-acetyl-_β_-D-glucopyranosyloxy)phenylazo](benzyl)thioureido}-6-deoxy-α-D-mannopyranoside

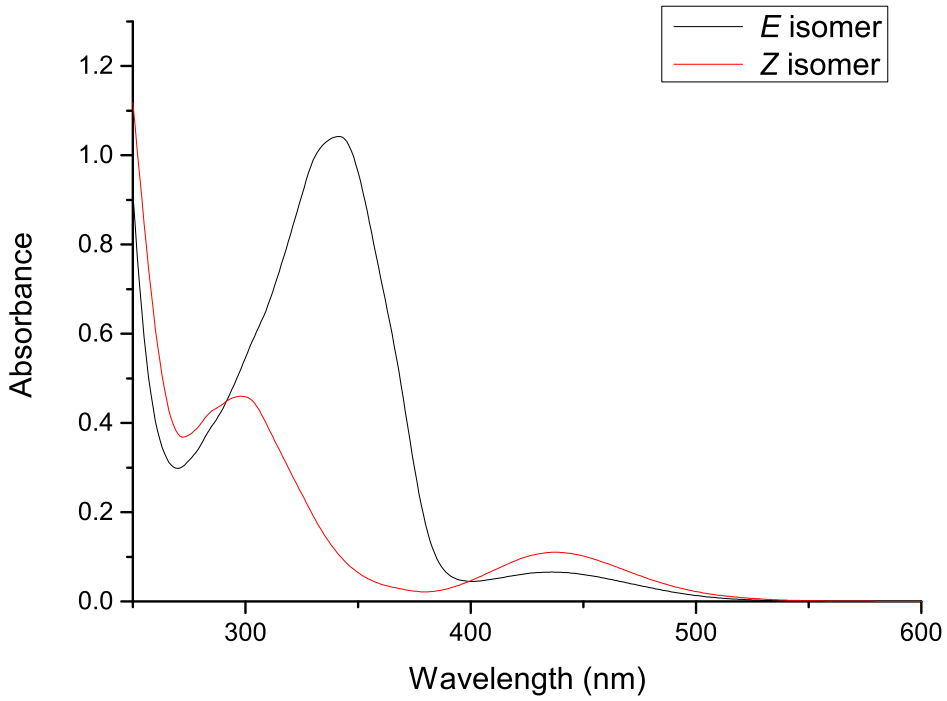

Figure 8.38. UV-vis spectra of **29**: _E_ isomer in black, _Z_ isomer in red; irradiation with 365 nm and 440 nm, respectively, in MeOH at 298 K.

References

[1] C. Hojnik, A. Müller, T.-E. Gloe, T. K. Lindhorst, T. M. Wrodnigg, *Eur. J. Org. Chem.* **2016**, *2016*, 43284337.

[2] N. Jayaraman, J. F. Stoddart, *Tetrahedron Letters* **1997**, *38*, 6767-6770.

[3] B. Priewisch, K. Rück-Braun, *J. Org. Chem.* **2005**, *70*, 2350-2352.

[4] M. Hartmann, A. K. Horst, P. Klemm and T. K. Lindhorst, *Chem. Commun.* **2010**, *46*, 330-332.

[5] G. R. Gustafson, C. M. Baldino, M.-M. E. O'Donnell, A. Sheldon, R. J. Tarsa, C. J. Verni and D. L. Coffen, *Tetrahedron* **1998**, *54*, 4051-4065.

[6] C. Grabosch, M. Hartmann, J. Schmidt-Lassen, T. K. Lindhorst, *ChemBioChem* **2011**, *12*, 1066-1074.

[7] E. D. Goddard-Borger, R. V. Stick, *Org. Lett.* **2007**, *9*, 3797-380.

References

[1] B. Alberts, A. Johnson, J. Lewis, M. Raff, K. Roberts, P. Walter, *Molecular Biology of the Cell*, 4th Ed., Taylor & Francis Ltd., New York, **2002**.

[2] R. Apweiler, H. Hermjakob, N. Sharon, *Biochim. Biophys. Acta* **1999**, *1473*, 4–8.

[3] T. W. Rademacher, R. B. Parekh, R. A. Dwek, *Annu. Rev. Biochem.* **1988**, *57*, 785–838.

[4] A. Varki, R. D. Cummings, J. D. Esko, H. H. Freeze, P. Stanley, C. R. Bertozzi, G. W. Hart, M. E. Etzler, *Essentials of Glycobiology*, 2nd edition, Cold Spring Harbor Laboratory Press, New York, **2009**.

[5] http://www.functionalglycomics.org/.

[6] Y. D. Vankar, R. R. Schmidt, *Chem. Soc. Rev.* **2000**, *29*, 201–216.

[7] S. Degroote, J. Wolthoorn, G. van Meer, *Semin. Cell Dev. Biol.* **2004**, *15*, 375–387.

[8] T. K. Lindhorst, *Essentials of Carbohydrate Chemistry and Biochemistry*, 2nd edition, Wiley-VCH, Weinheim, **2007**.

[9] N. Sharon, H. Lis, *Science* **1989**, *246*, 227–234.

[10] N. Sharon, H. Lis, *Sci. Am.* **1993**, *268*, 82–89.

[11] I. Ofek, D. L. Hasty, N. Sharon, *FEMS Immunol. Med. Mic.* **2003**, *38*, 181–191.

[12] I. Eggens, B. Fenderson, T. Toyokuni, B. Dean, M. Stroud, S. Hakomori, *J. Biol. Chem.* **1989**, *264*, 9476–9484.

[13] N. Kojima, S. Hakomori, *J. Biol. Chem.* **1991**, *266*, 17552–17558.

[14] I. Bucior, S. Scheuring, A. Engel, M. M. Burger, *J. Cell Biol.* **2004**, *165*, 529–537.

[15] I. Bucior, M. M. Burger, *Curr. Opin. Struct. Biol.* **2004**, *14*, 631–637.

[16] H. Lis, N. Sharon, *Chem. Rev.* **1998**, *98*, 637–674.

[17] M. Ambrosi, N. R. Cameron, B. G. Davis, *Org. Biomol. Chem.* **2005**, *3*, 1593–1608.

[18] D. Kilpatrick, *Biochim. Biophys. Acta* **2002**, *1572*, 187–197.

[19] H.-J. Gabius, H.-C. Siebert, S. André, J. Jiménez-Barbero, H. Rüdiger, *ChemBioChem* **2004**, *5*, 740–764.

[20] H. Stillmark, phdthesis, Dorpat, **1888**.

[21] J. B. Sumner, S. F. Howell, *J. Bacteriol.* **1936**, *32*, 227–237.

[22] N. Sharon, H. Lis, *Lectins*, Chapman and Hall, London, **1989**.

[23] I. E. Liener, N. Sharon, I. J. Goldstein, *The Lectins: Properties, Functions and Applications in Biology and Medicine*, Academic Press, Orlando, **1986**.

[24] K. Drickamer, *J. Biol. Chem.* **1988**, *263*, 9557–9560.

[25] N. Sharon, *Glycobiology* **2004**, *14*, 53R–62R.

[26] D. C. Wiley, J. J. Skehel, *Annu. Rev. Biochem.* **1987**, *56*, 365–394.

[27] N. Sharon, *FEBS Lett.* **1987**, *217*, 145–157.

[28] T. K. Lindhorst, *In Carbohydrate-Modifying Biocatalysts*, chapter Oligosaccharides and Glycoconjugates in Recognition Processes, p. 147–215, 2nd Ed., Pan Stanford Publishing, New Jersey, London, Singapore, **2016**.

[29] T. J. Wiles, R. R. Kulesus, M. A. Mulvey, *Exp. Mol. Pathol.* **2008**, *85*, 11–19.

[30] M. Kukkonen, T. Raunio, R. Virkola, K. Lähteenmäki, P. H. Mäkelä, P. Klemm, S. Clegg, T. K. Korhonen, *Mol. Microbiol.* **1993**, *7*, 229–237.

[31] E. V. Sokurenko, V. Chesnokova, R. J. Doyle, D. L. Hasty, *J. Biol. Chem.* **1997**, *272*, 17880–17886.

[32] B. Madison, I. Ofek, S. Clegg, S. N. Abraham, *Infect. Immun.* **1994**, *62*, 843–848.

[33] D. Choudhury, A. Thompson, V. Stojanoff, S. Langermann, J. Pinkner, S. J. Hultgren, S. D. Knight, *Science* **1999**, *285*, 1061–1066.

[34] M. Vetsch, C. Puorger, T. Spirig, U. Grauschopf, E. U. Weber-Ban, R. Glockshuber, *Nature* **2004**, *431*, 329–333.

[35] C.-S. Hung, J. Bouckaert, D. Hung, J. Pinkner, C. Widberg, A. deFusco, C. G. Auguste, R. Strouse, S. Langermann, G. Waksman, S. J. Hultgren, *Mol. Microbiol.* **2002**, *44*, 903–915.

[36] J. Bouckaert, J. Berglund, M. Schembri, E. de Genst, L. Cools, M. Wuhrer, C.-S. Hung, J. Pinkner, R. Slättegård, A. Zavialov, D. Choudhury, S. Langermann, S. J. Hultgren, L. Wyns, P. Klemm, S. Oscarson, S. D. Knight, H. de Greve, *Mol. Microbiol.* **2004**, *55*, 441–455.

[37] N. Firon, S. Ashkenazi, D. Mirelman, I. Ofek, N. Sharon, *Infect. Immun.* **1987**, *55*, 472–476.

[38] M. Hartmann, T. K. Lindhorst, *Eur. J. Org. Chem.* **2011**, *2011*, 3583–3609.

[39] S. Sattin, A. Bernardi, *Trends Biotechnol.* **2016**, *34*, 483–495.

[40] N. Sharon, I. Ofek, *Glycoconjugate J.* **2000**, *17*, 659–664.

[41] K.-A. Karlsson, *Mol. Microbiol.* **1998**, *29*, 1–11.

[42] A. Bernardi, J. Jiménez-Barbero, A. Casnati, C. de Castro, T. Darbre, F. Fieschi, J. Finne, H. Funken, K.-E. Jaeger, M. Lahmann, T. K. Lindhorst, M. Marradi, P. Messner, A. Molinaro, P. V. Murphy, C. Nativi, S. Oscarson, S. Penadés, F. Peri, R. J. Pieters, O. Renaudet, J.-L. Reymond, B. Richichi, J. Rojo, F. Sansone, C. Schäffer, W. B. Turnbull, T. Velasco-Torrijos, S. Vidal, S. Vincent, T. Wennekes, H. Zuilhof, A. Imberty, *Chem. Soc. Rev.* **2013**, *42*, 4709–4727.

[43] X. Jiang, D. Abgottspon, S. Kleeb, S. Rabbani, M. Scharenberg, M. Wittwer, M. Haug, O. Schwardt, B. Ernst, *J. Med. Chem.* **2012**, *55*, 4700–4713.

[44] A. Khalili, M. Ahmad, *Int. J. Mol. Sci.* **2015**, *16*, 18149–18184.

[45] M. E. Taylor, K. Drickamer, *Curr. Opin. Cell Biol.* **2007**, *19*, 572–577.

[46] C. R. Bertozzi, L. L. Kiessling, *Science* **2001**, *291*, 2357–2364.

[47] J. W. Wehner, M. Hartmann, T. K. Lindhorst, *Carbohydr. Res.* **2013**, *371*, 22–31.

[48] T. Horlacher, P. H. Seeberger, *Chem. Soc. Rev.* **2008**, *37*, 1414–1422.

[49] P. Tompa, *Chem. Soc. Rev.* **2016**, *45*, 4252–4284.

[50] P. A. Hargrave, J. H. McDowell, *FASEB J.* **1992**, *6*, 2323–2331.

[51] P. A. Hargrave, J. H. McDowell, D. R. Curtis, J. K. Wang, E. Juszczak, S.-L. Fong, J. K. M. Rao, P. Argos, *Biophys. Struct. Mechanism* **1983**, *9*, 235–244.

[52] I. M. Pepe, *Prog. Retin. Eye Res.* **2001**, *20*, 733–759.

[53] W. M. Oldham, H. E. Hamm, *Nat. Rev. Mol. Cell Biol.* **2008**, *9*, 60–71.

[54] H. R. Bourne, E. C. Meng, *Science* **2000**, *289*, 733–734.

[55] K. D. Ridge, K. Palczewski, *J. Biol. Chem.* **2007**, *282*, 9297–9301.

[56] T. Ebrey, Y. Koutalos, *Prog. Retin. Eye Res.* **2001**, *20*, 49–94.

[57] S. Jähnichen, „3D structure model of bovine rhodopsin. Derived from the 2.6 Å crystal stucture of rhodopsin (1L9H) with covalently linked retinal and palmityl residues (grey). Structural informations were obtained from pdb.org and rendered using PyMol 0.99“, online material, **2010**, requested at 05.09.2016, https://upload.wikimedia.org/wikipedia/commons/2/2d/Rhodopsin.jpg.

[58] S. A. Tatulian, *Biochemistry* **2015**, *54*, 5523–5532.

[59] J. Lee, P. F. Pilch, S. E. Shoelson, S. F. Scarlata, *Biochemistry* **1997**, *36*, 2701–2708.

[60] C. W. Ward, M. C. Lawrence, *Bioessays* **2009**, *31*, 422–434.

[61] V. Baron, P. Kaliman, N. Gautier, E. van Obberghen, *J. Biol. Chem.* **1992**, *267*, 23290–23294.

[62] L. L. Kiessling, J. E. Gestwicki, L. E. Strong, *Angew. Chem.* **2006**, *118*, 2408–2429; *Angew. Chem. Int. Ed.* **2006**, *45*, 2348-2368.

[63] J. W. Dennis, I. R. Nabi, M. Demetriou, *Cell* **2009**, *139*, 1229–1241.

[64] N. Strömberg, P. G. Nyholm, I. Pascher, S. Normark, *Proc. Natl. Acad. Sci. USA* **1991**, *88*, 9340–9344.

[65] S. i. Hakomori, *Proc. Natl. Acad. Sci. USA* **2002**, *99*, 225–232.

[66] S. itiroh Hakomori, *FEBS Lett.* **2009**, *584*, 1901–1906.

[67] I. Willner, *Acc. Chem. Res.* **1997**, *30*, 347–356.

[68] B. L. Feringa, W. R. Browne, *Molecular Switches*, Wiley-VCH, Weinheim, **2011**.

[69] W. Szymański, J. M. Beierle, H. A. V. Kistemaker, W. A. Velema, B. L. Feringa, *Chem. Rev.* **2013**, *113*, 6114–6178.

[70] C. Dugave, L. Demange, *Chem. Rev.* **2003**, *103*, 2475–2532.

[71] G. S. Hartley, *Nature* **1937**, *140*, 281.

[72] H. Rau, *Angew. Chem.* **1973**, *85*, 248–258; *Angew. Chem. Int. Ed.* **1973**, *12*, 224-235.

[73] A. Mostad, C. Rømming, *Acta Chem. Scand.* **1971**, *25*, 3561–3568.

[74] J. J. de Lange, J. M. Robertson, I. Woodward, *J. Chem. Soc.* **1939**, *171*, 398–410.

[75] G. C. Hampson, J. M. Robertson, *J. Chem. Soc.* **1941**, 409–413.

[76] W. Horspool, F. Lenci, *CRC Handbook of Organic Photochemistry and Photobiology Vol. 1 & 2*, 2nd Edition, CRC Press, London, New York, Washington DC, **1989**.

[77] R. Turanský, M. Konôpka, N. L. Doltsinis, I. Štich, D. Marx, *Phys. Chem. Chem. Phys.* **2010**, *12*, 13922–13932.

[78] J. Henzl, M. Mehlhorn, H. Gawronski, K.-H. Rieder, K. Morgenstern, *Angew. Chem.* **2006**, *118*, 617–621; *Angew. Chem. Int. Ed.* **2006**, *45*, 603-606.

[79] G. S. Hartley, *J. Chem. Soc.* **1938**, 633–642.

[80] X. Tong, M. Pelletier, A. Lasia, Y. Zhao, *Angew. Chem.* **2008**, *120*, 3652–3655; *Angew. Chem. Int. Ed.* **2008**, *47*, 3596-3599.

[81] Z. F. Liu, K. Hashimoto, A. Fujishima, *Nature* **1990**, *347*, 658–660.

[82] J. L. Magee, W. Shand, H. Eyring, *J. Am. Chem. Soc.* **1941**, *63*, 677–688.

[83] D. Y. Curtin, E. J. Grubbs, C. G. McCarty, *J. Am. Chem. Soc.* **1966**, *88*, 2775–2786.

[84] H. M. D. Bandara, S. C. Burdette, *Chem. Soc. Rev.* **2012**, *41*, 1809–1825.

[85] T. Sueyoshi, N. Nishimura, S. Yamamoto, S. Hasegawa, *Chem. Lett.* **1974**, *3*, 1131–1134.

[86] T. Schultz, J. Quenneville, B. Levine, A. Toniolo, T. J. Martínez, S. Lochbrunner, M. Schmitt, J. P. Shaffer, M. Z. Zgierski, A. Stolow, *J. Am. Chem. Soc.* **2003**, *125*, 8098–8099.

[87] E. W.-G. Diau, *J. Phys. Chem. A* **2004**, *108*, 950–956.

[88] D. M. Shin, D. G. Whitten, *J. Am. Chem. Soc.* **1988**, *110*, 5206–5208.

[89] B. Marcandalli, L. P.-D. Liddo, C. D. Fede, I. R. Bellobono, *J. Chem. Soc., Perkin Trans. 2* **1984**, 589–593.

[90] C.-W. Chang, Y.-C. Lu, T.-T. Wang, E. W.-G. Diau, *J. Am. Chem. Soc.* **2004**, *126*, 10109–10118.

[91] T. Fujino, S. Y. Arzhantsev, T. Tahara, *J. Phys. Chem. A* **2001**, *105*, 8123–8129.

[92] P. Bortolus, S. Monti, *J. Phys. Chem.* **1979**, *83*, 648–652.

[93] L. Wang, W. Xu, C. Yi, X. Wang, *J. Mol. Graph. Model.* **2009**, *27*, 792–796.

[94] E. Fischer, M. Frankel, R. Wolovsky, *J. Chem. Phys.* **1955**, *23*, 1367.

[95] N. Siampiringue, G. Guyot, S. Monti, P. Bortolus, *J. Photochem.* **1987**, *37*, 185–188.

[96] H. Rau, E. Lueddecke, *J. Am. Chem. Soc.* **1982**, *104*, 1616–1620.

[97] C. R. Crecca, A. E. Roitberg, *J. Phys. Chem. A* **2006**, *110*, 8188–8203.

[98] D. Gegiou, K. A. Muszkat, E. Fischer, *J. Am. Chem. Soc.* **1968**, *90*, 12–18.

[99] S. Malkin, E. Fischer, *J. Phys. Chem.* **1962**, *66*, 2482–2486.

[100] E. Fischer, *J. Am. Chem. Soc.* **1960**, *82*, 3249–3252.

[101] T. Asano, T. Yano, T. Okada, *J. Am. Chem. Soc.* **1982**, *104*, 4900–4904.

[102] E. Merino, M. Ribagorda, *Beilstein J. Org. Chem.* **2012**, *8*, 1071–1090.

[103] A. A. Beharry, G. A. Woolley, *Chem. Soc. Rev.* **2011**, *40*, 4422–4437.

[104] F. Hamon, F. Djedaini-Pilard, F. Barbot, C. Len, *Tetrahedron* **2009**, *65*, 10105–10123, and articels cited therein.

[105] V. Chandrasekaran, K. Kolbe, F. Beiroth, T. K. Lindhorst, *Beilstein J. Org. Chem.* **2013**, *9*, 223–233.

[106] V. Chandrasekaran, T. K. Lindhorst, *Chem. Commun.* **2012**, *48*, 7519–7521.

[107] T. Weber, V. Chandrasekaran, I. Stamer, M. B. Thygesen, A. Terfort, T. K. Lindhorst, *Angew. Chem.* **2014**, *126*, 14812–14815; *Angew. Chem. Int. Ed.* **2014**, *53*, 14583-14586.

[108] V. Chandrasekaran, H. Jacob, F. Petersen, K. Kathirvel, F. Tuczek, T. K. Lindhorst, *Chem. Eur. J.* **2014**, *20*, 8744–8752.

[109] J. Hain, V. Chandrasekaran, T. K. Lindhorst, *Isr. J. Chem.* **2015**, *55*, 383–386.

[110] V. Chandrasekaran, E. Johannes, H. Kobarg, F. D. Sönnichsen, T. K. Lindhorst, *ChemistryOpen* **2014**, *3*, 99–108.

[111] V. V. Rostovtsev, L. G. Green, V. V. Fokin, K. B. Sharpless, *Angew. Chem.* **2002**, *114*, 2708–2711; *Angew. Chem. Int. Ed.* **2002**, *41*, 2596-2599.

[112] C. W. Tornøe, C. Christensen, , M. Meldal, *J. Org. Chem.* **2002**, *67*, 3057–3064.

[113] M. Hartmann, A. K. Horst, P. Klemm, T. K. Lindhorst, *Chem. Commun.* **2010**, *46*, 330–332.

[114] M. Hartmann, H. Papavlassopoulos, V. Chandrasekaran, C. Grabosch, F. Beiroth, T. K. Lindhorst, C. Röhl, *FEBS Lett.* **2012**, *586*, 1459–1465.

[115] K. Dąbrowa, P. Niedbała, J. Jurczak, *J. Org. Chem.* **2016**, *81*, 3576–3584.

[116] M. K. Adam, J. S. Poisson, Y. Hu, G. Prasannakumar, M. J. Pottage, R. N. Ben, B. L. Wilkinson, *RSC Adv.* **2016**, *6*, 39240–39244.

[117] Y. Hu, R. F. Tabor, B. L. Wilkinson, *Org. Biomol. Chem.* **2015**, *13*, 2216–2225.

[118] News, *Science* **2010**, *330*, 1612–1613.

[119] S. Spörlein, H. Carstens, H. Satzger, C. Renner, R. Behrendt, L. Moroder, P. Tavan, W. Zinth, J. Wachtveitl, *Proc. Natl. Acad. Sci. USA* **2002**, *99*, 7998–8002.

[120] J. A. Ihalainen, J. Bredenbeck, R. Pfister, J. Helbing, L. Chi, I. H. M. van Stokkum, G. A. Woolley, P. Hamm, *Proc. Natl. Acad. Sci. USA* **2007**, *104*, 5383–5388.

[121] A. Mourot, M. A. Kienzler, M. R. Banghart, T. Fehrentz, F. M. E. Huber, M. Stein, R. H. Kramer, D. Trauner, *ACS Chem. Neurosci.* **2011**, *2*, 536–543.

[122] A. A. Beharry, O. Sadovski, G. A. Woolley, *J. Am. Chem. Soc.* **2011**, *133*, 19684–19687.

[123] M. Dong, A. Babalhavaeji, S. Samanta, A. A. Beharry, G. A. Woolley, *Acc. Chem. Res.* **2015**, *48*, 2662–2670.

[124] D. B. Konrad, J. A. Frank, D. Trauner, *Chem. Eur. J.* **2016**, *22*, 4364–4368.

[125] H. A. Wegner, *Angew. Chem.* **2012**, *124*, 4869–4871; *Angew. Chem. Int. Ed.* **2012**, *51*, 4787-4788.

[126] C. Knie, M. Utecht, F. Zhao, H. Kulla, S. Kovalenko, A. M. Brouwer, P. Saalfrank, S. Hecht, D. Bléger, *Chem. Eur. J.* **2014**, *20*, 16492–16501.

[127] D. Bléger, S. Hecht, *Angew. Chem.* **2015**, *127*, 11494–11506; *Angew. Chem. Int. Ed.* **2015**, *54*, 11338-11349.

[128] C. Poloni, W. Szymański, L. Hou, W. R. Browne, B. L. Feringa, *Chem. Eur. J.* **2014**, *20*, 946–951.

[129] V. Blanco, D. A. Leigh, V. Marcos, *Chem. Soc. Rev.* **2015**, *44*, 5341–5370.

[130] Z. Yu, S. Hecht, *Chem. Commun.* **2016**, *52*, 6639–6653.

[131] M.-M. Russew, S. Hecht, *Adv. Mater.* **2010**, *22*, 3348–3360.

[132] J. Broichhagen, J. A. Frank, D. Trauner, *Acc. Chem. Res.* **2015**, *48*, 1947–1960.

[133] G. Mayer, A. Heckel, *Angew. Chem.* **2006**, *118*, 5020–5042; *Angew. Chem. Int. Ed.* **2006**, *45*, 4900-4921.

[134] S. Keiper, J. S. Vyle, *Angew. Chem.* **2006**, *118*, 3384–3387; *Angew. Chem. Int. Ed.* **2006**, *45*, 3306-3309.

[135] M. Liu, H. Asanuma, M. Komiyama, *J. Am. Chem. Soc.* **2006**, *128*, 1009–1015.

[136] S. Roy, R. Nagarajan, P. Wu, K. Yang, F. F. Bruno, V. S. Parmar, S. K. Tripathy, J. Kumar, L. A. Samuelson, *J. Macromol. Sci., Pure Appl. Chem.* **2001**, *38*, 1383–1392.

[137] F. Wang, X. Liu, I. Willner, *Angew. Chem.* **2014**, *127*, 1112–1144; *Angew. Chem. Int. Ed.* **2014**, *54*, 1098-1129.

[138] S. P. Graether, C. M. Slupsky, P. L. Davies, B. D. Sykes, *Biophys. J.* **2001**, *81*, 1677–1683.

[139] P. L. Davies, *Trends Biochem. Sci.* **2014**, *39*, 548–555.

[140] H. Chao, C. I. DeLuca, P. L. Davies, B. D. Sykes, F. D. Sönnichsen, *Protein Sci.* **1994**, *3*, 1760–1769.

[141] F. D. Sönnichsen, P. L. Davies, B. D. Sykes, *Biochem. Cell Biol.* **1998**, *76*, 284–293.

[142] P. L. Davies, B. D. Sykes, *Curr. Opin. Struct. Biol.* **1997**, *7*, 828–834.

[143] J. Bang, J. Lee, R. Murugan, S. Lee, H. Do, H. Koh, H.-E. Shim, H.-C. Kim, H. Kim, *Mar. Drugs* **2013**, *11*, 2013–2041.

[144] C. Renner, L. Moroder, *ChemBioChem* **2006**, *7*, 868–878.

[145] L. Ulysse, J. Chmielewski, *Bioorg. Med. Chem. Lett.* **1994**, *4*, 2145–2146.

[146] L. Ulysse, J. Cubillos, J. Chmielewski, *J. Am. Chem. Soc.* **1995**, *117*, 8466–8467.

[147] R. Behrendt, C. Renner, M. Schenk, F. Wang, J. Wachtveitl, D. Oesterhelt, L. Moroder, *Angew. Chem.* **1999**, *111*, 2941–2943; *Angew. Chem. Int. Ed.* **1999**, *38*, 2771-2774.

[148] R. Behrendt, M. Schenk, H.-J. Musiol, L. Moroder, *J. Pept. Sci.* **1999**, *5*, 519–529.

[149] A. Aemissegger, D. Hilvert, *Nat. Protoc.* **2007**, *2*, 161–167.

[150] C. Hoppmann, P. Schmieder, P. Domaing, G. Vogelreiter, J. Eichhorst, B. Wiesner, I. Morano, K. Rück-Braun, M. Beyermann, *Angew. Chem.* **2011**, *123*, 7841–7845; *Angew. Chem. Int. Ed.* **2011**, *50*, 7699-7702.

[151] G. A. Woolley, *Acc. Chem. Res.* **2005**, *38*, 486–493.

[152] J. R. Kumita, O. S. Smart, G. A. Woolley, *Proc. Natl. Acad. Sci. USA* **2000**, *97*, 3803–3808.

[153] Z. Zhang, D. C. Burns, J. R. Kumita, O. S. Smart, G. A. Woolley, *Bioconjugate Chem.* **2003**, *14*, 824–829.

[154] D. C. Burns, F. Zhang, G. A. Woolley, *Nat. Protoc.* **2007**, *2*, 251–258.

[155] J. M. Scholtz, R. L. Baldwin, *Annu. Rev. Biophys. Biomol. Struct.* **1992**, *21*, 95–118.

[156] D. C. Burns, D. G. Flint, J. R. Kumita, H. J. Feldman, L. Serrano, Z. Zhang, O. S. Smart, G. A. Woolley, *Biochemistry* **2004**, *43*, 15329–15338.

[157] D. G. Flint, J. R. Kumita, O. S. Smart, G. A. Woolley, *Chem. Biol.* **2002**, *9*, 391–397.

[158] J. R. Kumita, D. G. Flint, O. S. Smart, G. A. Woolley, *Protein Eng.* **2002**, *15*, 561–569.

[159] S. Kneissl, E. J. Loveridge, C. Williams, M. P. Crump, R. K. Allemann, *ChemBioChem* **2008**, *9*, 3046–3054.

[160] L. Guerrero, O. S. Smart, G. A. Woolley, R. K. Allemann, *J. Am. Chem. Soc.* **2005**, *127*, 15624–15629.

[161] L. Guerrero, O. S. Smart, C. J. Weston, D. C. Burns, G. A. Woolley, R. K. Allemann, *Angew. Chem.* **2005**, *117*, 7956–7960; *Angew. Chem. Int. Ed.* **2005**, *44*, 7778-7782.

[162] R. J. Mart, P. Wysoczański, S. Kneissl, A. Ricci, A. Brancale, R. K. Allemann, *ChemBioChem* **2012**, *13*, 515–519.

[163] A. M. Ali, M. W. Forbes, G. A. Woolley, *ChemBioChem* **2015**, *16*, 1757–1763.

[164] L. Nevola, A. Martín-Quirós, K. Eckelt, N. Camarero, S. Tosi, A. Llobet, E. Giralt, P. Gorostiza, *Angew. Chem.* **2013**, *125*, 7858–7862; *Angew. Chem. Int. Ed.* **2013**, *52*, 7704-7708.

[165] A. Martín-Quirós, L. Nevola, K. Eckelt, S. Madurga, P. Gorostiza, E. Giralt, *Chem. Biol.* **2015**, *22*, 31–37.

[166] B. Schierling, A.-J. Noël, W. Wende, L. T. Hien, E. Volkov, E. Kubareva, T. Oretskaya, M. Kokkinidis, A. Römpp, B. Spengler, A. Pingoud, *Proc. Natl. Acad. Sci. USA* **2009**, *107*, 1361–1366.

[167] F. Zhang, K. A. Timm, K. M. Arndt, G. A. Woolley, *Angew. Chem.* **2010**, *122*, 4035–4038; *Angew. Chem. Int. Ed.* **2010**, *49*, 3943-3946.

[168] A. A. Beharry, L. Wong, V. Tropepe, G. A. Woolley, *Angew. Chem.* **2011**, *123*, 1361–1363; *Angew. Chem. Int. Ed.* **2011**, *50*, 1325-1327.

[169] C. Hoppmann, P. Schmieder, N. Heinrich, M. Beyermann, *ChemBioChem* **2011**, *12*, 2555–2559.

[170] C. Hoppmann, I. Maslennikov, S. Choe, L. Wang, *J. Am. Chem. Soc.* **2015**, *137*, 11218–11221.

[171] C. Hoppmann, R. Kühne, M. Beyermann, *Beilstein J. Org. Chem.* **2012**, *8*, 884–889.

[172] C. Hoppmann, V. K. Lacey, G. V. Louie, J. Wei, J. P. Noel, L. Wang, *Angew. Chem.* **2014**, *126*, 4013–4017; *Angew. Chem. Int. Ed.* **2014**, *53*, 3932-3936.

[173] T. Fehrentz, M. Schönberger, D. Trauner, *Angew. Chem.* **2011**, *123*, 12362–12390; *Angew. Chem. Int. Ed.* **2011**, *50*, 12156-12182.

[174] P. Gorostiza, E. Y. Isacoff, *Science* **2008**, *322*, 395–399.

[175] R. H. Kramer, J. J. Chambers, D. Trauner, *Nat. Chem. Biol.* **2005**, *1*, 360–365.

[176] B. Horstmann, M. Korbus, T. Friedmann, C. Wolff, C. M. Thiele, F.-J. Meyer-Almes, *Bioorg. Chem.* **2014**, *57*, 155–161.

[177] D. M. Barber, M. Schönberger, J. Burgstaller, J. Levitz, C. D. Weaver, E. Y. Isacoff, H. Baier, D. Trauner, *Chem. Sci.* **2016**, *7*, 2347–2352.

[178] J. Levitz, A. T. Popescu, A. Reiner, E. Y. Isacoff, *Front. Mol. Neurosci.* **2016**, *9*, 1–15.

[179] A. A. John, C. P. Ramil, Y. Tian, G. Cheng, Q. Lin, *Org. Lett.* **2015**, *17*, 6258–6261.

[180] C. Wyart, F. D. Bene, E. Warp, E. K. Scott, D. Trauner, H. Baier, E. Y. Isacoff, *Nature* **2009**, *461*, 407–410.

[181] M. Volgraf, P. Gorostiza, R. Numano, R. H. Kramer, E. Y. Isacoff, D. Trauner, *Nat. Chem. Biol.* **2005**, *2*, 47–52.

[182] M. Banghart, K. Borges, E. Isacoff, D. Trauner, R. H. Kramer, *Nat. Neurosci.* **2004**, *7*, 1381–1386.

[183] A. Reiner, J. Levitz, E. Y. Isacoff, *Curr. Opin. Pharmacol.* **2015**, *20*, 135–143.

[184] A. Rullo, A. Reiner, A. Reiter, D. Trauner, E. Y. Isacoff, G. A. Woolley, *Chem. Commun.* **2014**, *50*, 14613–14615.

[185] J. P. van der Berg, W. A. Velema, W. Szymański, A. J. M. Driessen, B. L. Feringa, *Chem. Sci.* **2015**, *6*, 3593–3598.

[186] L. Schweighauser, H. A. Wegner, *ChemBioChem* **2015**, *16*, 1709–1711.

[187] L. L. Kiessling, R. A. Splain, *Annu. Rev. Biochem.* **2010**, *79*, 619–653.

[188] Z. Zhang, I. R. Ollmann, X.-S. Ye, R. Wischnat, T. Baasov, C.-H. Wong, *J. Am. Chem. Soc.* **1999**, *121*, 734–753.

[189] B. G. Davis, *J. Chem. Soc., Perkin Trans. 1* **2000**, 2137–2160.

[190] P. H. Seeberger, W.-C. Haase, *Chem. Rev.* **2000**, *100*, 4349–4394.

[191] O. J. Plante, E. R. Palmacci, P. H. Seeberger, *Science* **2001**, *291*, 1523–1527.

[192] P. H. Seeberger, *Acc. Chem. Res.* **2015**, *48*, 1450–1463.

[193] N. V. Ganesh, K. Fujikawa, Y. H. Tan, K. J. Stine, A. V. Demchenko, *Org. Lett.* **2012**, *14*, 3036–3039.

[194] B. Fiege, S. Rabbani, R. C. Preston, R. P. Jakob, P. Zihlmann, O. Schwardt, X. Jiang, T. Maier, B. Ernst, *ChemBioChem* **2015**, *16*(8), 1235–1246.

[195] M. del C. Fernández-Alonso, D. Díaz, M. . Berbis, F. Marcelo, J. Ca ñada, J. Jiménez-Barbero, *Curr. Protein Pept. Sci.* **2012**, *13*, 816–830.

[196] L. P. Calle, B. Echeverria, A. Franconetti, S. Serna, M. C. Fernández-Alonso, T. Diercks, F. J. Cañada, A. Ardá, N.-C. Reichardt, J. Jiménez-Barbero, *Chem. Eur. J.* **2015**, *21*, 11408–11416.

[197] A. El-Hawiet, E. N. Kitova, J. S. Klassen, *Biochemistry* **2012**, *51*, 4244–4253.

[198] S. J. North, P. G. Hitchen, S. M. Haslam, A. Dell, *Curr. Opin. Struct. Biol.* **2009**, *19*, 498–506.

[199] Y. Yao, K. Shams-Ud-Doha, R. Daneshfar, E. N. Kitova, J. S. Klassen, *J. Am. Soc. Mass Spectrom.* **2014**, *26*, 98–106.

[200] H.-J. Gabius, S. André, J. Jiménez-Barbero, A. Romero, D. Solís, *Trends Biochem. Sci.* **2011**, *36*, 298–313.

[201] A. Geissner, P. H. Seeberger, *Annual Rev. Anal. Chem.* **2016**, *9*, 223–247.

[202] N. Laurent, J. Voglmeir, S. L. Flitsch, *Chem. Commun.* **2008**, 4400–4412.

[203] M. T. Puvirajesinghe, E. J. Turnbull, „Glycoarray Technologies: Deciphering Interactions from Proteins to Live Cell Responses“, **2016**.

[204] J. Hirabayashi, *Lectins*, Springer, New York, **2014**.

[205] G. K. Hirst, *J. Exp. Med.* **1942**, *75*, 49–64.

[206] E. Spackman, *Animal Influenza Virus*, Springer, New York, **2014**.

[207] J. McCoy, J. Varani, I. J. Goldstein, *Anal. Biochem.* **1983**, *130*, 437–444.

[208] J. McCoy, J. Varani, I. J. Goldstein, *Exp. Cell Res.* **1984**, *151*, 96–103.

[209] C. Maierhofer, K. Rohmer, V. Wittmann, *Bioorg. Med. Chem.* **2007**, *15*, 7661–7676.

[210] T. K. Dam, C. F. Brewer, *Chem. Rev.* **2002**, *102*, 387–430.

[211] S. Leavitt, E. Freire, *Curr. Opin. Struct. Biol.* **2001**, *11*, 560–566.

[212] G. Safina, *Anal. Chim. Acta* **2012**, *712*, 9–29.

[213] G. Safina, I. B. Duran, M. Alasel, B. Danielsson, *Talanta* **2011**, *84*, 1284–1290.

[214] C. Wang, V. K. Yadavalli, *Micron* **2014**, *60*, 5–17.

[215] S. Fukui, T. Feizi, C. Galustian, A. M. Lawson, W. Chai, *Nat. Biotech.* **2002**, *20*, 1011–1017.

[216] B. T. Houseman, M. Mrksich, *Cell Chem. Biol.* **2002**, *9*, 443–454.

[217] S. Park, I. Shin, *Angew. Chem.* **2002**, *114*, 3312–3314; *Angew. Chem. Int. Ed.* **2002**, *41*, 3180-3182.

[218] D. Wang, S. Liu, B. J. Trummer, C. Deng, A. Wang, *Nat. Biotech.* **2002**, *20*, 275–281.

[219] W. G. T. Willats, S. E. Rasmussen, T. Kristensen, J. D. Mikkelsen, J. P. Knox, *PROTEOMICS* **2002**, *2*, 1666–1671.

[220] F. Fazio, M. C. Bryan, O. Blixt, J. C. Paulson, C.-H. Wong, *J. Am. Chem. Soc.* **2002**, *124*, 14397–14402.

[221] A. Beloqui, J. Calvo, S. Serna, S. Yan, I. B. H. Wilson, M. Martin-Lomas, N. C. Reichardt, *Angew. Chem.* **2013**, *125*, 7625–7629; *Angew. Chem. Int. Ed.* **2013**, *52*, 7477-7481.

[222] M. J. Weissenborn, J. W. Wehner, C. J. Gray, R. Šardzik, C. E. Eyers, T. K. Lindhorst, S. L. Flitsch, *Beilstein J. Org. Chem.* **2012**, *8*, 753–762.

[223] A. R. de Boer, C. H. Hokke, A. M. Deelder, M. Wuhrer, *Glycoconjugate J.* **2008**, *25*, 75–84.

[224] M. Fais, R. Karamanska, S. Allman, S. A. Fairhurst, P. Innocenti, A. J. Fairbanks, T. J. Donohoe, B. G. Davis, D. A. Russell, R. A. Field, *Chem. Sci.* **2011**, *2*, 1952–1959.

[225] S. Park, J. C. Gildersleeve, O. Blixt, I. Shin, *Chem. Soc. Rev.* **2013**, *42*, 4310–4326.

[226] C. D. Rillahan, J. C. Paulson, *Annu. Rev. Biochem.* **2011**, *80*, 797–823.

[227] Y. Liu, A. S. Palma, T. Feizi, *Biol. Chem.* **2009**, *390*, 647–656.

[228] N. Laurent, R. Haddoub, J. Voglmeir, S. C. C. Wong, S. J. Gaskell, S. L. Flitsch, *ChemBioChem* **2008**, *9*, 2592–2596.

[229] M. D. Disney, P. H. Seeberger, *Chem. Biol.* **2004**, *11*, 1701–1707.

[230] O. Blixt, S. Head, T. Mondala, C. Scanlan, M. E. Huflejt, R. Alvarez, M. C. Bryan, F. Fazio, D. Calarese, J. Stevens, N. Razi, D. J. Stevens, J. J. Skehel, I. van Die, D. R. Burton, I. A. Wilson, R. Cummings, N. Bovin, C.-H. Wong, J. C. Paulson, *Proc. Natl. Acad. Sci. USA* **2004**, *101*, 17033–17038.

[231] P.-H. Liang, S.-K. Wang, C.-H. Wong, *J. Am. Chem. Soc.* **2007**, *129*, 11177–11184.

[232] J. L. de Paz, C. Noti, P. H. Seeberger, *J. Am. Chem. Soc.* **2006**, *128*, 2766–2767.

[233] M. Kleinert, T. Winkler, A. Terfort, T. K. Lindhorst, *Org. Biomol. Chem.* **2008**, *6*, 2118–2132.

[234] C. Grabosch, M. Kleinert, T. Lindhorst, *Synthesis* **2009**, *2010*, 828–836.

[235] C.-Y. Huang, D. A. Thayer, A. Y. Chang, M. D. Best, J. Hoffmann, S. Head, C.-H. Wong, *Proc. Natl. Acad. Sci. USA* **2005**, *103*, 15–20.

[236] Y. Zhang, S. Luo, Y. Tang, L. Yu, K.-Y. Hou, J.-P. Cheng, X. Zeng, P. G. Wang, *Anal. Chem.* **2006**, *78*, 2001–2008.

[237] B. T. Houseman, E. S. Gawalt, M. Mrksich, *Langmuir* **2003**, *19*, 1522–1531.

[238] J. W. Wehner, M. J. Weissenborn, M. Hartmann, C. J. Gray, R. Šardzik, C. E. Eyers, S. L. Flitsch, T. K. Lindhorst, *Org. Biomol. Chem.* **2012**, *10*(44), 8919–8926.

[239] E. W. Adams, D. M. Ratner, H. R. Bokesch, J. B. McMahon, B. R. O. Keefe, P. H. Seeberger, *Chem. Biol.* **2004**, *11*, 875–881.

[240] M. A. Brun, M. D. Disney, P. H. Seeberger, *ChemBioChem* **2006**, *7*, 421–424.

[241] S. Park, M.-R. Lee, S.-J. Pyo, I. Shin, *J. Am. Chem. Soc.* **2004**, *126*, 4812–4819.

[242] M.-R. Lee, I. Shin, *Angew. Chem.* **2005**, *117*, 2941–2944; *Angew. Chem. Int. Ed.* **2005**, *44*, 2881-2884.

[243] M.-R. Lee, S. Park, I. Shin, *Methods Mol. Biol.* **2012**, *808*, 103–116.

[244] M. Shipp, R. Nadella, H. Gao, V. Farkas, H. Sigrist, A. Faik, *Glycoconjugate J.* **2007**, *25*, 49–58.

[245] H. S. G. Beckmann, A. Niederwieser, M. Wiessler, V. Wittmann, *Chem. Eur. J.* **2012**, *18*, 6548–6554.

[246] O. Roling, A. Mardyukov, S. Lamping, B. Vonhören, S. Rinnen, H. F. Arlinghaus, A. Studer, B. J. Ravoo, *Org. Biomol. Chem.* **2014**, *12*, 7828–7835.

[247] S. Angeloni, *Glycobiology* **2004**, *15*, 31–41.

[248] M. ryul Lee, I. Shin, *Org. Lett.* **2005**, *7*, 4269–4272.

[249] S. Park, M.-R. Lee, I. Shin, *Bioconjugate Chem.* **2009**, *20*, 155–162.

[250] E. L. Shipp, L. C. Hsieh-Wilson, *Chem. Biol.* **2007**, *14*, 195–208.

[251] M. C. Bryan, O. Plettenburg, P. Sears, D. Rabuka, S. Wacowich-Sgarbi, C.-H. Wong, *Chem. Biol.* **2002**, 713–720.

[252] T. Feizi, M. S. Stoll, C.-T. Yuen, W. Chai, A. M. Lawson, „Neoglycolipids: Probes of oligosaccharide structure, antigenicity, and function“ in *Methods. in Enzymol.*, Elsevier, **1994**, p. 484–519.

[253] L. Zou, H.-L. Pang, P.-H. Chan, Z.-S. Huang, L.-Q. Gu, K.-Y. Wong, *Carbohydr. Res.* **2008**, *343*, 2932–2938.

[254] C. Grabosch, K. Kolbe, T. K. Lindhorst, *ChemBioChem* **2012**, *13*, 1874–1879.

[255] F. Fazio, M. C. Bryan, H.-K. Lee, A. Chang, C.-H. Wong, *Tetrahedron Lett.* **2004**, *45*, 2689–2692.

[256] M. B. Biskup, J. U. Müller, R. Weingart, R. R. Schmidt, *ChemBioChem* **2005**, *6*, 1007–1015.

[257] C. I. Biggs, S. Edmondson, M. I. Gibson, *Biomater. Sci.* **2015**, *3*, 175–181.

[258] G. Nan, H. Yan, G. Yang, Q. Jian, C. Chen, Z. Li, *Current Pharm. Biotechnol.* **2009**, *10*, 138–146.

[259] Z. liang Zhi, A. K. Powell, J. E. Turnbull, *Anal. Chem.* **2006**, *78*, 4786–4793.

[260] Z.-L. Zhi, N. Laurent, A. K. Powell, R. Karamanska, M. Fais, J. Voglmeir, A. Wright, J. M. Blackburn, P. R. Crocker, D. A. Russell, S. Flitsch, R. A. Field, J. E. Turnbull, *ChemBioChem* **2008**, *9*, 1568–1575.

[261] A. Sanchez-Ruiz, S. Serna, N. Ruiz, M. Martin-Lomas, N.-C. Reichardt, *Angew. Chem.* **2011**, *123*, 1841–1844; *Angew. Chem. Int. Ed.* **2011**, *50*, 1801-1804.

[262] D. J. Scurr, T. Horlacher, M. A. Oberli, D. B. Werz, L. Kroeck, S. Bufali, P. H. Seeberger, A. G. Shard, M. R. Alexander, *Langmuir* **2010**, *26*, 17143–17155.

[263] M. Kind, C. Wöll, *Prog. Surf. Sci.* **2009**, *84*, 230–278.

[264] B. Vonhören, O. Roling, C. Buten, M. Körsgen, H. F. Arlinghaus, B. J. Ravoo, *Langmuir* **2016**, *32*, 2277–2282.

[265] C. Grabosch, M. Kind, Y. Gies, F. Schweighöfer, A. Terfort, T. K. Lindhorst, *Org. Biomol. Chem.* **2013**, *11*, 4006–4015.

[266] N. P. Pera, R. J. Pieters, *Med. Chem. Commun.* **2014**, *5*, 1027–1035.

[267] M. Hartmann, P. Betz, Y. Sun, S. N. Gorb, T. K. Lindhorst, A. Krueger, *Chem. Eur. J.* **2012**, *18*, 6485–6492.

[268] C. Fessele, S. Wachtler, V. Chandrasekaran, C. Stiller, T. K. Lindhorst, A. Krueger, *Eur. J. Org. Chem.* **2015**, *2015*, 5519–5525.

[269] A. K. Adak, H.-J. Lin, C.-C. Lin, *Org. Biomol. Chem.* **2014**, *12*, 5563–5573.

[270] A. K. Adak, B.-Y. Li, C.-C. Lin, *Carbohydr. Res.* **2015**, *405*, 2–12.

[271] M. Delbianco, P. Bharate, S. Varela-Aramburu, P. H. Seeberger, *Chem. Rev.* **2016**, *116*, 1693–1752.

[272] T. Kaufmann, C. Wendeln, M. T. Gokmen, S. Rinnen, M. M. Becker, H. F. Arlinghaus, F. D. Prez, B. J. Ravoo, *Chem. Commun.* **2013**, *49*, 63–65.

[273] M. Marradi, F. Chiodo, I. García, S. Penadés, *Chem. Soc. Rev.* **2013**, *42*, 4728–4745.

[274] R. M. Fratila, M. Moros, J. M. de la Fuente, *Anal. Bioanal.Chem.* **2015**, *408*, 1783–803.

[275] X.-L. Sun, W. Cui, C. Haller, E. L. Chaikof, *ChemBioChem* **2004**, *5*, 1593–1596.

[276] P. Babu, S. Sinha, A. Surolia, *Bioconjugate Chem.* **2007**, *18*, 146–151.

[277] J. M. de la Fuente, A. G. Barrientos, T. C. Rojas, J. Rojo, J. Cañada, A. Fernández, S. Penadés, *Angew. Chem.* **2001**, *113*, 2317–2321; *Angew. Chem. Int. Ed.* **2001**, *40*, 2257-2261.

[278] P. D. Rye, *Nat. Biotech.* **1996**, *14*, 155–157.

[279] M. D. Disney, J. Zheng, T. M. Swager, P. H. Seeberger, *J. Am. Chem. Soc.* **2004**, *126*, 13343–13346.

[280] J. Heimburg-Molinaro, M. Tappert, X. Song, Y. Lasanajak, G. Air, D. F. Smith, R. D. Cummings, „Probing Virus Glycan Interactions Using Glycan Microarrays“ in *Methods Mol. Biol.*, Springer Science Business Media, **2011**, p. 251–267.

[281] Y. Chevolot (Ed.:), *Carbohydrate Microarrays*, Humana Press, **2012**.

[282] K. Schwekendiek, H. Kobarg, L. Daumlechner, F. D. Sönnichsen, T. K. Lindhorst, *Chem. Commun.* **2011**, *47*, 9399–9401.

[283] H. Fernando, Phdthesis, CAU Kiel, **2013**.

[284] K. Schwekendiek, phdthesis, CAU Kiel, **2010**.

[285] A. K. Ciuk, T. K. Lindhorst, *Beilstein J. Org. Chem.* **2015**, *11*, 668–674.

[286] J. Auernheimer, C. Dahmen , U. Hersel , A. Bausch, , H. Kessler, *J. Am. Chem. Soc.* **2005**, *127*, 16107–16110.

[287] D. Liu, Y. Xie, H. Shao, X. Jiang, *Angew. Chem.* **2009**, *121*, 4470–4472; *Angew. Chem. Int. Ed.* **2009**, *48*, 4406-4408.

[288] Y.-H. Gong, C. Li, J. Yang, H.-Y. Wang, R.-X. Zhuo, X.-Z. Zhang, *Macromolecules* **2011**, *44*, 7499–7502.

[289] L. F. Kadem, M. Holz, K. G. Suana, Q. Li, C. Lamprecht, R. Herges, C. Selhuber-Unkel, *Adv. Mater.* **2016**, *28*, 1799–1802.

[290] J. Voskuhl, S. Sankaran, P. Jonkheijm, *Chem. Commun.* **2014**, *50*, 15144–15147.

[291] C. Poloni, W. Szymański, B. L. Feringa, *Chem. Commun.* **2014**, *50*, 12645–12648.

[292] H. S. Lim, J. T. Han, D. Kwak, M. Jin, , K. Cho, *J. Am. Chem. Soc.* **2006**, *128*, 14458–14459.

[293] G. Wang, J. Zhang, *J. Photochem. Photobiol., C* **2012**, *13*, 299–309.

[294] J. Robertus, W. R. Browne, B. L. Feringa, *Chem. Soc. Rev.* **2010**, *39*, 354–378.

[295] P. M. Mendes, *Chem. Soc. Rev.* **2008**, *37*, 2512–2529.

[296] A. Goulet-Hanssens, K. L. W. Sun, T. E. Kennedy, C. J. Barrett, *Biomacromolecules* **2012**, *13*, 2958–2963.

[297] E. Vaselli, C. Fedele, S. Cavalli, P. A. Netti, *ChemPlusChem* **2015**, *80*, 1547–1555.

[298] C.-G. Qin, C.-X. Lu, G.-W. Ouyang, K. Qin, F. Zhang, H.-T. Shi, X.-H. Wang, *Chin. J. Anal. Chem.* **2015**, *43*, 433–443.

[299] M. A. Cole, N. H. Voelcker, H. Thissen, H. J. Griesser, *Biomaterials* **2009**, *30*, 1827–1850.

[300] K. Rafal, *Pure Appl. Chem.* **2010**, *82*, 2247–2279.

[301] O. Nachtigall, C. Kördel, L. H. Urner, R. Haag, *Angew. Chem.* **2014**, *126*, 9824–9828; *Angew. Chem. Int. Ed.* **2014**, *53*, 9669-9673.

[302] Y. Huang, H. Kang, G. Li, C. Wang, Y. Huang, R. Liu, *RSC Advances* **2013**, *3*, 15909–15916.

[303] O. Roling, L. Stricker, J. Voskuhl, S. Lamping, B. J. Ravoo, *Chem. Commun.* **2016**, *52*, 1964–1966.

[304] B. Priewisch, K. Rück-Braun, *J. Org. Chem.* **2005**, *70*, 2350–2352.

[305] E. D. Goddard-Borger, R. V. Stick, *Org. Lett.* **2007**, *9*, 3797–3800.

[306] D. H. Dube, C. R. Bertozzi, *Curr. Opin. Chem. Biol.* **2003**, *7*, 616–625.

[307] J. Du, M. A. Meledeo, Z. Wang, H. S. Khanna, V. D. P. Paruchuri, K. J. Yarema, *Glycobiology* **2009**, *19*, 1382–1401.

[308] O. T. Keppler, R. Horstkorte, M. Pawlita, C. Schmidt, W. Reutter, *Glycobiology* **2001**, *11*, 11R–18R.

[309] O. T. Keppler, P. Stehling, M. Herrmann, H. Kayser, D. Grunow, W. Reutter, M. Pawlita, *J. Biol. Chem.* **1995**, *270*, 1308–1314.

[310] L. K. Mahal, K. J. Yarema, C. R. Bertozzi, *Science* **1997**, *276*, 1125–1128.

[311] E. Saxon, C. R. Bertozzi, *Science* **2000**, *287*, 2007–2010.

[312] H. Kayser, R. Zeitler, C. Kannicht, D. Grunow, R. Nuck, W. Reutter, *J. Biol. Chem.* **1992**, *267*, 16934–16938.

[313] H. C. H. C. R. Bertozzi, *J. Am. Chem. Soc.* **2001**, *123*, 1242–1243.

[314] H. C. Hang, C. Yu, D. L. Kato, C. R. Bertozzi, *Proc. Natl. Acad. Sci. USA* **2003**, *100*(25), 14846–14851.

[315] D. J. Vocadlo, H. C. Hang, E.-J. Kim, J. A. Hanover, C. R. Bertozzi, *Proc. Natl. Acad. Sci. USA* **2003**, *100*, 9116–9121.

[316] J. A. Prescher, C. R. Bertozzi, *Nat .Chem. Biol.* **2005**, *1*, 13–21.

[317] H. C. H. C. R. Bertozzi, *Acc. Chem. Res.* **2001**, *34*, 727–736.

[318] E. M. Sletten, C. R. Bertozzi, *Acc. Chem. Res.* **2011**, *44*, 666–676.

[319] E. M. Sletten, C. R. Bertozzi, *Angew. Chem.* **2009**, *121*, 7108–7133; *Angew. Chem. Int. Ed.* **2009**, *48*, 6974-6998.

[320] D. M. Patterson, J. A. Prescher, *Curr. Opin. Chem. Biol.* **2015**, *28*, 141–149.

[321] R. K. V. Lim, Q. Lin, *Chem. Commun.* **2010**, *46*, 1589–1600.

[322] M. F. Debets, J. C. M. van Hest, F. P. J. T. Rutjes, *Org. Biomol. Chem.* **2013**, *11*, 6439–6455.

[323] C. P. Ramil, Q. Lin, *Chem. Commun.* **2013**, *49*, 11007–11022.

[324] B. Zödl, M. Zeiner, W. Marktl, I. Steffan, C. Ekmekcioglu, *Biol. Trace Elem. Res.* **2003**, *96*, 143–152.

[325] L. M. Gaetke, C. K. Chow, *Toxicology* **2003**, *189*, 147–163.

[326] G. Wittig, A. Krebs, *Chem. Ber.* **1961**, *94*, 3260–3275.

[327] N. J. Agard, J. A. Prescher, C. R. Bertozzi, *J. Am. Chem. Soc.* **2004**, *126*, 15046–15047.

[328] J. M. Baskin, J. A. Prescher, S. T. Laughlin, N. J. Agard, P. V. Chang, I. A. Miller, A. Lo, J. A. Codelli, C. R. Bertozzi, *Proc. Natl. Acad. Sci. USA* **2007**, *104*, 16793–16797.

[329] X. Zhang, Y. Zhang, *Molecules* **2013**, *18*, 7145–7159.

[330] M. L. Blackman, M. Royzen, J. M. Fox, *J. Am. Chem. Soc.* **2008**, *130*, 13518–13519.

[331] N. K. Devaraj, R. Upadhyay, J. B. Haun, S. A. Hilderbrand, R. Weissleder, *Angew. Chem.* **2009**, *121*, 7147–7150; *Angew. Chem. Int. Ed.* **2009**, *48*, 7013-7016.

[332] N. K. Devaraj, R. Weissleder, S. A. Hilderbrand, *Bioconjugate Chem.* **2008**, *19*, 2297–2299.

[333] D. N. Kamber, L. A. Nazarova, Y. Liang, S. A. Lopez, D. M. Patterson, H.-W. Shih, K. N. Houk, J. A. Prescher, *J. Am. Chem. Soc.* **2013**, *135*, 13680–13683.

[334] M. Yang, J. Li, P. R. Chen, *Chem. Soc. Rev.* **2014**, *43*, 6511–6526.

[335] C. D. Spicer, T. Triemer, B. G. Davis, *J. Am. Chem. Soc.* **2012**, *134*, 800–803.

[336] S. V. Chankeshwara, E. Indrigo, M. Bradley, *Curr. Opin. Chem. Biol.* **2014**, *21*, 128–135.

[337] M. Zheng, L. Zheng, P. Zhang, J. Li, Y. Zhang, *Molecules* **2015**, *20*, 3190–3205.

[338] P. V. Chang, J. A. Prescher, M. J. Hangauer, C. R. Bertozzi, *J. Am. Chem. Soc.* **2007**, *129*, 8400–8401.

[339] F. Liu, A. J. Aubry, I. C. Schoenhofen, S. M. Logan, M. E. Tanner, *ChemBioChem* **2009**, *10*, 1317–1320.

[340] B. M. Swarts, C. M. Holsclaw, J. C. Jewett, M. Alber, D. M. Fox, M. S. Siegrist, J. A. Leary, R. Kalscheuer, C. R. Bertozzi, *J. Am. Chem. Soc.* **2012**, *134*, 16123–16126.

[341] A. Dumont, A. Malleron, M. Awwad, S. Dukan, B. Vauzeilles, *Angew. Chem.* **2012**, *124*, 3197–3200; *Angew. Chem. Int. Ed.* **2012**, *51*, 3143-3146.

[342] C. T. Saeui, E. Urias, L. Liu, M. P. Mathew, K. J. Yarema, *Glycoconjugate J.* **2015**, *32*, 425–441.

[343] S. T. Laughlin, J. M. Baskin, S. L. Amacher, C. R. Bertozzi, *Science* **2008**, *320*, 664–667.

[344] D. S. del Amo, W. Wang, H. Jiang, C. Besanceney, A. C. Yan, M. Levy, Y. Liu, F. L. Marlow, P. Wu, *J. Am. Chem. Soc.* **2010**, *132*, 16893–16899.

[345] J. A. Prescher, D. H. Dube, C. R. Bertozzi, *Nature* **2004**, *430*, 873–877.

[346] D. H. Dube, J. A. Prescher, C. N. Quang, C. R. Bertozzi, *Proc. Natl. Acad. Sci. USA* **2006**, *103*, 4819–4824.

[347] M. Mammen, S.-K. Choi, G. M. Whitesides, *Angew. Chem.* **1998**, *110*, 2908–2953; *Angew. Chem. Int. Ed.* **1998**, *37*, 2754-2794.

[348] C. Fasting, C. A. Schalley, M. Weber, O. Seitz, S. Hecht, B. Koksch, J. Dernedde, C. Graf, E.-W. Knapp, R. Haag, *Angew. Chem.* **2012**, *124*, 10622–10650; *Angew. Chem. Int. Ed.* **2012**, *51*, 10472-10498.

[349] N. Jayaraman, *Chem. Soc. Rev.* **2009**, *38*, 3463–3483.

[350] Y. C. Lee, R. T. Lee, *Acc. Chem. Res.* **1995**, *28*, 321–327.

[351] J. J. Lundquist, E. J. Toone, *Chem. Rev.* **2002**, *102*, 555–578.

[352] C. Müller, G. Despras, T. K. Lindhorst, *Chem. Soc. Rev.* **2016**, *45*, 3275–3302.

[353] Y. M. Chabre, R. Roy, *Chem. Soc. Rev.* **2013**, *42*, 4657–4708.

[354] R. Roy, T. C. Shiao, *Chem. Soc. Rev.* **2015**, *44*, 3924–3941.

[355] R. T. Lee, Y. C. Lee, *Glycoconjugate J.* **1987**, *4*, 317–328.

[356] R. T. Lee, Y. C. Lee, *Bioconjugate Chem.* **1997**, *8*, 762–765.

[357] S. Cecioni, A. Imberty, S. Vidal, *Chem. Rev.* **2015**, *115*, 525–561.

[358] N. Spinelli, E. Defrancq, F. Morvan, *Chem. Soc. Rev.* **2013**, *42*, 4557–4573.

[359] M. M. K. Boysen, K. Elsner, O. Sperling, T. K. Lindhorst, *Eur. J. Org. Chem.* **2003**, *2003*, 4376–4386.

[360] M. A. Abramov, R. Shukla, D. B. Amabilino, W. Dehaen, *J. Org. Chem.* **2002**, *67*, 1004–1007.

[361] M. Ortega-Muñoz, F. Perez-Balderas, J. Morales-Sanfrutos, F. Hernandez-Mateo, J. Isac-García, F. Santoyo-Gonzalez, *Eur. J. Org. Chem.* **2009**, *2009*, 2454–2473.

[362] P. Langer, S. J. Ince, S. V. Ley, *J. Chem. Soc., Perkin Trans. 1* **1998**, 3913–3916.

[363] T. K. Lindhorst, M. Dubber, U. Krallmann-Wenzel, S. Ehlers, *Eur. J. Org. Chem.* **2000**, *2000*, 2027–2034.

[364] G. R. Newkome, R. K. Behera, C. N. Moorefield, G. R. Baker, *J. Org. Chem.* **1991**, *56*, 7162–7167.

[365] M. Gómez-García, J. M. Benito, R. Gutiérrez-Gallego, A. Maestre, C. O. Mellet, J. M. G. Fernández, J. L. J. Blanco, *Org. Biomol. Chem.* **2010**, *8*, 1849–1860.

[366] I. Velter, B. L. Ferla, F. Nicotra, *J. Carbohydr. Chem.* **2006**, *25*, 97–138.

[367] C. Kieburg, M. Dubber, T. K. Lindhorst, *Synlett* **1997**, *12*, 1447–1449.

[368] M. Dubber, T. K. Lindhorst, *Carbohydr. Res.* **1998**, *310*, 35–41.

[369] M. M. K. Boysen, T. K. Lindhorst, *Org. Lett.* **1999**, *1*, 1925–1927.

[370] D. Solomon, P. I. Kitov, E. Paszkiewicz, G. A. Grant, J. M. Sadowska, , D. R. Bundle, *Org. Lett.* **2005**, *7*, 4369–4372.

[371] M. Dubber, T. K. Lindhorst, *J. Org. Chem.* **2000**, *65*, 5275–5281.

[372] M. Dubber, T. K. Lindhorst, *Org. Lett.* **2001**, *3*, 4019–4022.

[373] M. Dubber, A. Patel, K. Sadalapure, I. Aumüller, T. K. Lindhorst, *Eur. J. Org. Chem.* **2006**, *2006*, 5357–5366.

[374] T. K. Lindhorst, M. Dubber, *Carbohydr. Res.* **2015**, *403*, 90–97.

[375] M. Köhn, J. M. Benito, C. Ortiz Mellet, T. K. Lindhorst, J. M. García Fernández, *ChemBioChem* **2004**, *5*, 771–777.

[376] R. P. McGeary, I. Jablonkai, I. Toth, *Tetrahedron* **2001**, *57*, 8733–8742.

[377] J. Brask, K. J. Jensen, *J. Pept. Sci.* **2000**, *6*, 290–299.

[378] J. Ni, H. Song, Y. Wang, N. M. Stamatos, , L.-X. Wang, *Bioconjugate Chem.* **2006**, *17*, 493–500.

[379] W. Zhong, M. Skwarczynski, P. Simerska, M. F. Good, I. Toth, *Tetrahedron* **2009**, *65*, 3459–3464.

[380] V. Fagan, I. Toth, P. Simerska, *Beilstein J. Org. Chem.* **2014**, *10*, 1741–1748.

[381] O. Sperling, M. Dubber, T. K. Lindhorst, *Carbohydr. Res.* **2007**, *342*, 696–703.

[382] A. A. Kulkarni, A. A. Weiss, S. S. Iyer, *Anal. Chem.* **2010**, *82*, 7430–7435.

[383] T. C. Shiao, R. Rej, M. Rose, G. M. Pavan, R. Roy, *Molecules* **2016**, *21*, 448–464.

[384] T.-E. Gloe, A. Müller, A. Ciuk, T. M. Wrodnigg, T. K. Lindhorst, *Carbohydr. Res.* **2016**, *425*, 1–9.

[385] C. Kieburg, K. Sadalapure, T. Lindhorst, *Eur. J. Org. Chem.* **2000**, *2000*, 2035–2040.

[386] K. Sadalapure, T. K. Lindhorst, *Angew. Chem.* **2000**, *112*, 2066–2069; *Angew. Chem. Int. Ed.* **2000**, *41*, 2596-2599.

[387] A. Patel, T. K. Lindhorst, *J. Org. Chem.* **2001**, *66*, 2674–2680.

[388] M. Dubber, O. Sperling, T. K. Lindhorst, *Org. Biomol. Chem.* **2006**, *4*, 3901–3912.

[389] A. Patel, T. Lindhorst, *Eur. J. Org. Chem.* **2002**, *2002*, 79–86.

[390] T. Ogawa, M. Matsui, *Carbohydr. Res.* **1977**, *56*, C1–C6.

[391] T. Ogawa, M. Matsui, *Carbohydr. Res.* **1978**, *62*, C1–C4.

[392] S. Hanessian (Ed.:), *Preparative Carbohydrate Chemistry*, Marcel Dekker, New York, **1997**, 73-74.

[393] C. D. Heidecke, T. K. Lindhorst, *Chem. Eur. J.* **2007**, *13*, 9056–9067.

[394] N. Moitessier, C. Henry, N. Aubert, Y. Chapleur, *Tetrahedron Lett.* **2005**, *46*, 6191–6194.

[395] T. Opatz, C. Kallus, T. Wunberg, W. Schmidt, S. Henke, H. Kunz, *Eur. J. Org. Chem.* **2003**, *2003*, 1527–1536.

[396] G. T. Le, G. Abbenante, B. Becker, M. Grathwohl, J. Halliday, G. Tometzki, J. Zuegg, W. Meutermans, *Drug Discovery Today* **2003**, *8*, 701–709.

[397] U. Hünger, J. Ohnsmann, H. Kunz, *Angew. Chem.* **2004**, *116*, 1125–1128; *Angew. Chem. Int. Ed.* **2004**, *43*, 1104-1107.

[398] O. Srinivas, N. Mitra, A. Surolia, N. Jayaraman, *J. Am. Chem. Soc.* **2002**, *124*, 2124–2125.

[399] O. Srinivas, N. Mitra, A. Surolia, N. Jayaraman, *Glycobiology* **2005**, *15*, 861–873.

[400] T.-E. Gloe, Phdthesis, CAU Kiel, **2016**.

[401] S. O. Jaeschke, Bachelor thesis, CAU Kiel, **2014**.

[402] K. Kolbe, Phdthesis, CAU Kiel, **2016**.

[403] S. Deshayes, V. Maurizot, M.-C. Clochard, C. Baudin, T. Berthelot, S. Esnouf, D. Lairez, M. Moenner, G. Déléris, *Pharm. Res.* **2011**, *28*, 1631–1642.

Appendix

Abbreviations

E. coli	*Escherichia coli*
AB	azobenzene
Ac	acetyl
Ac_2O	acetic anhydride
AcOH	acetic acid
AFM	atomic force microscopy
AFP	antifreeze proteins
AIBN	azobisisobutyronitrile
aq.	aqueous
Asn	asparagine
ATR	attenuated total reflection
Boc	*tert*-butyloxycarbonyl
Boc_2O	di-*tert*-butyl dicarbonate
br	broad (NMR)
Bu	butyl
calcd	calculated
CD	cyclodextrines
CFG	Consortium for Functional Glycomics
CMP	cytidine-5'-monophospho
Con A	Concanavalin A
conc	concentrated
COSY	correlation spectroscopy

CRD	carbohydrate recognition domain
Cys	cysteine
d	doublet (NMR)
DBU	1,8-diazabicycloundec-7-ene
DCM	dichloromethane
DDQ	2,3-dichloro-5,6-dicyano-1,4-benzoquinone
DIC	*N*,*N'*-Diisopropylcarbodiimide
DIPEA	*N*,*N*-Diisopropylethylamine
DMAP	4-dimethylaminopyridine
DMF	*N*,*N*-dimethylformamide
DMSO	dimethyl sulfoxide
EDC	1-ethyl-3-(3-dimethylaminopropyl)carbodiimide
ELLA	enzyme-linked lectin assay
ER	endoplasmic reticulum
ESI	electrospray ionization
Et	ethyl
FITC	fluorescein isothiocyanate
Fmoc	fluorenylmethyloxycarbonyl
Fuc	fucose
Gal	galactose
GalNAc	*N*-acetylgalactosamine
GalNAz	*N*-azidoacetylgalactosamine
GFP	green fluorescent protein
Glc	glucose
GlcNAc	*N*-acetylglucosamine
GlcNAz	*N*-azidoacetylglucosamine
HAI	hemagglutination inhibition assay
HATU	1-[Bis(dimethylamino)methylene]-1H-1,2,3-triazolo[4,5-b]pyridinium 3-oxid hexafluorophosphate

HEPES	4-(2-hydroxyethyl)-1-piperazineethanesulfonic acid
HI	hemagglutination inhibition assay
HMEC	human mammary epithelial cells
HR	high resolution
IM	inner membrane
IR	infrared
IRRAS	infrared reflection-absorption spectroscopy
ITC	isothermal titration calorimetry
LB	lysogeny broth
LBB	lectin binding buffer
LED	light emitting diod
Lys	lysine
m	multiplet (NMR)
MALDI-MS	Matrix-assisted laser desorption ionization mass spectroscopy
Man	mannose
ManNAc	*N*-acetylmannosamine
ManNAc-6-P	*N*-Acetylmannosamine-6-phosphate
Me	methyl
MeMan	methyl α-D-mannopyranoside
MeOH	methanol
MES	2-(*N*-morpholino)ethanesulfonic acid
MOE	metabolic oligosaccharide engineering
mp	melting point
MS	mass spectrometry
NCS	isothiocyanate
Neu5Ac	*N*-acetylneuraminic acid
Neu5Ac-9-P	*N*-acetylneuraminic acid-9-phosphate
NHS	*N*-hydroxysuccinimide
NMR	nuclear magnetic resonance spectroscopy

OD	optical density
OM	outer membrane
PBS	phosphate-buffered saline
PCR	polymerase chain reaction
PEG	polyethylene glycol
PG	protecting group
Ph	phenyl
PMB	4-methoxybenzyl chloride
PS	polystyrene
PSS	photostationary state
PVA	polyvinyl alcohol
QS	quorum sensing
quant.	quantitative
R_f	retardation factor
RIP	relative inhibitory potencies
RP	reverse phase
rt	room temperature
s	singlet (NMR)
SAM	self-assembled monolayer
SD	standard deviation
SEM	standard error of the mean
Ser	serine
SPAAC	strain promoted azide-alkyne cycloaddition
SPR	surface plasmon resonance
t	triplet (NMR)
TBAI	tetrabutylammonium iodide
TBDMS	*tert*-butyldimethylsilyl
TFA	trifluoroacetic acid
THF	tetrahydrofuran

Thr	threonine
TLC	thin layer chromatography
TMS	tetramethylsilane
TOF	time of flight
Tos	*para*-tolylsulfony
Tyr	tyrosine
UDP	uridine diphosphate
UPEC	uropathogenic *Escherichia coli*
UV	ultraviolet
E. coli	*Escherichia coli*
m	*meta*
o	*ortho*
*p*APMan	*p*-aminophenyl mannoside
p	*para*